

Mechanistic Studies of Orthogonal Transformations of Bis-Vinyl Ethers:
Modular Access to Complex Small Molecules

by

Natasha Felicia O'Rourke
B.Sc., St. Francis Xavier University, 2008

A Dissertation Submitted in Partial Fulfillment
of the Requirements for the Degree of

DOCTOR OF PHILOSOPHY

in the Department of Chemistry

© Natasha Felicia O'Rourke, 2014
University of Victoria

All rights reserved. This dissertation may not be reproduced in whole or in part, by
photocopy or other means, without the permission of the author.

Supervisory Committee

Mechanistic Studies of Orthogonal Transformations of Bis-Vinyl Ethers:
Modular Access to Complex Small Molecules

by

Natasha Felicia O'Rourke
B.Sc., St. Francis Xavier University, 2008

Supervisory Committee

Dr. Jeremy E. Wulff, Department of Chemistry
Supervisor

Dr. Thomas Fyles, Department of Chemistry
Departmental Member

Dr. Fraser Hof, Department of Chemistry
Departmental Member

Dr. Perry L. Howard, Department of Biochemistry and Microbiology
Outside Member

Abstract

Supervisory Committee

Dr. Jeremy E. Wulff, Department of Chemistry

Supervisor

Dr. Thomas Fyles, Department of Chemistry

Departmental Member

Dr. Fraser Hof, Department of Chemistry

Departmental Member

Dr. Perry L. Howard, Department of Biochemistry and Molecular Biology

Outside Member

Efficient access to molecular complexity and diversity is important for the development of small-molecule screening libraries designed to identify highly specific modulators of disease relevant macromolecular interactions. We envisioned the use of iteratively synthesized bis-vinyl ether substrates for cascade-type transformations to gain rapid access to several different classes of stereochemically rich, linear or polycyclic scaffolds. To evaluate their utility in this context, mechanistic investigations were undertaken to understand the chemical reactivity of bis-vinyl ethers in radical cyclization reactions and [3,3]-sigmatropic rearrangements.

Radical cyclization across bis-vinyl ethers proceeded through an apparent *6-endo-trig/5-exo-trig* ring closure to afford functionalized hexahydro-*2H*-furo[3,4-*b*]pyrans in good yield, with high diastereoselectivity and excellent regiocontrol. Combination of two electron-withdrawing substituents on the bis-vinyl ether backbone resulted in the trapping of a *5-exo-trig*/ β -scission product, prompting us to investigate the mechanism for cyclization. Formation of the hexahydrofuropyrans was found to be the result of a *5-exo-*

trig/3-exo-trig/retro-3-exo-trig pathway to afford a “formal” 6-*endo* pyranosyl radical that could participate in a second 5-*exo-trig* cyclization to secure the two ring system.

From this earlier study, we found certain combinations of substituents on the bis-vinyl ether backbone increased the propensity for these substrates to undergo Claisen rearrangement at remarkably low temperatures. Kinetic investigations of the substituent effects influencing bis-vinyl ether stability found that electron-releasing substituents on the γ -allyloxy fragment increased the rate of rearrangement as a result of stabilization of a cationic allyl fragment in the transition state. Thermochemical data derived from the earlier kinetic investigations also indicated that the Claisen rearrangement of bis-vinyl ether substrates occurred through a dissociative mechanism, characterised by an ΔS^\ddagger of $+2.3 \text{ cal K}^{-1} \text{ mol}^{-1}$.

A palladium-catalyzed auxiliary-controlled diastereoselective Claisen rearrangement of bis-vinyl ethers to access aldol-type products is currently under development. Preliminary results indicate that a modest degree of diastereoselectivity can be achieved in this reaction, provided that the steric burden at the stereogenic element is close enough to the pericyclic framework to exert an influence on facial selectivity.

Table of Contents

| | |
|---|-------|
| Supervisory Committee | ii |
| Abstract | iii |
| Table of Contents | v |
| List of Tables | x |
| List of Figures | xii |
| List of Schemes | xv |
| List of Abbreviations and Symbols | xxi |
| Acknowledgments | xxiii |
| Dedication | xxv |
| | |
| Chapter 1 Introduction | 1 |
| 1.1 Prologue | 1 |
| 1.2 The Medicinal Chemist's Toolbox and its Limitation on Drug Discovery | 2 |
| 1.3 Discovering NCEs by Emulating Natural Product Structure..... | 6 |
| 1.4 Developing Synthetic Methodologies to Access Molecular Complexity | 7 |
| 1.4.1 Iterative Synthesis of Reactive Polymers | 8 |
| 1.5 Known Chemical Reactivity of Bis-Vinyl Ethers..... | 12 |
| 1.5.1 The Ester-Enolate (Ireland) Claisen Rearrangement | 12 |
| 1.5.2 Stereocontrol in the Ester-Enolate (Ireland) Claisen Rearrangement..... | 14 |
| 1.5.3 Stereoselective Enolate Formation | 15 |
| 1.5.4 Effect of Enolate Geometry on Product Distribution for Acyclic Substrates .. | 17 |
| 1.6 Ireland Claisen Rearrangement: Effect of the C6 Oxygen for Acyclic Substrates. | 18 |
| 1.7 Ireland Claisen Rearrangement: Effect of the C6 Oxygen for Cyclic Substrates... | 25 |
| 1.7.1 Ester-Enolate Claisen Rearrangement of Glycal Derivatives: TS Geometry .. | 25 |
| 1.7.2 Ester-Enolate Claisen Rearrangement of Glycal Derivatives: Rate of Rearrangement | 34 |
| 1.8 The Vinylogous Anomeric Effect..... | 39 |
| 1.9 Electronic Structure of the Transition State..... | 40 |
| 1.10 Degree of Charge Separation in the Transition State..... | 41 |

| | |
|--|------------|
| | vi |
| 1.11 Summary | 46 |
| 1.12 Thesis Objectives | 48 |
| Chapter 2 Radical Cyclization Across Bis-Vinyl Ethers | 51 |
| 2.1 Foreword | 52 |
| 2.2 Identifying a Mechanism to Access Polycyclic Ethers | 52 |
| 2.3 Predicting the Mode of Cyclization in Radical Reactions | 53 |
| 2.3.1 Baldwin's Rules | 54 |
| 2.3.2 Beckwith's Rules | 56 |
| 2.3.3 Radical Philicity and Polar Effects | 57 |
| 2.4 Factors to Consider for Cyclization of (Poly)Vinyl Ethers | 59 |
| 2.4.1 Protecting the Alkyne Carbon | 61 |
| 2.5 Initial Radical Cyclization Attempts | 62 |
| 2.6 Alkynes as a Precursor to Vinyl Radicals | 69 |
| 2.7 Cyclization of Alkene Radicals onto a Bis-Vinyl Ether | 73 |
| 2.7.1 Assignment of Relative Configuration and Rationale for Observed Diastereoselectivity: | 76 |
| 2.8 Mechanistic Studies Pertaining to the Apparent 6-endo/5-exo Radical Cascade ... | 78 |
| 2.8.1 Probing the Mechanism for Radical Cyclization Using Radical Clocks | 83 |
| 2.8.2 Identifying Sites of Radical Character Through Cyclopropane Ring Opening | 91 |
| 2.9 Validation of a 5-exo/3-exo/retro-3-exo Pathway | 95 |
| 2.10 Vinyl Halides as an Alkyne Surrogate | 99 |
| 2.11 Theoretical Analyses Pertaining to Product Distribution | 106 |
| 2.11.1 Effect of Phenyl Substitution on Product Distribution | 106 |
| 2.11.2 Effect of Substitution on the Vinyl Ether | 107 |
| 2.12 Behaviour of Intermediate Radicals: Hydrogen Atom Transfer in Bis-Vinyl Ethers | 110 |
| 2.13 Summary | 114 |
| Chapter 3 Thermal Aliphatic Claisen Rearrangement | 117 |
| 3.1 The Aliphatic Claisen Rearrangement | 118 |

| | |
|---|------------|
| 3.2 Motivation for a Mechanistic Investigation of the Claisen Rearrangement | 119 |
| 3.3 Design of Substrates for VT-NMR Study..... | 124 |
| 3.4 Synthesis of Substrates for VT-NMR Studies: | 126 |
| 3.4.1 Part I: Synthetic Building Blocks | 126 |
| 3.4.2 Part II: Bis-Vinyl Ethers | 127 |
| 3.5 Nature of Transition-State Structure: Linear Free-Energy Relationships..... | 130 |
| 3.5.1 Quantitative Determination of the Rate of Claisen Rearrangement | 130 |
| 3.5.2 Interpretation of Kinetic Data for Bis-Vinyl Ethers 3.8a—3.8g: | 133 |
| 3.5.3 Determination of ΔS^\ddagger for Claisen Rearrangements of Bis-Vinyl Ethers 3.8 . | 139 |
| 3.6 Claisen Rearrangement of Bis-Vinyl Ethers Lacking an Aryl Substituent..... | 144 |
| 3.7 Extent of Polarization in the Transition State | 146 |
| 3.8 Substituent Effects on the Rate of Claisen Rearrangement at C1, C2 and C4..... | 149 |
| 3.8.1 Reduction of the Ester at C1 | 149 |
| 3.8.2 Electronically Neutral Substituent at C2..... | 150 |
| 3.8.3 Electron-Withdrawing Substituent at C4 | 151 |
| 3.8.4 Secondary Deuterium Kinetic Isotope Effects..... | 156 |
| 3.9 Cross Over Experiments | 158 |
| 3.10 Summary | 159 |
| | |
| Chapter 4 En Route to a Diastereoselective Claisen Rearrangement of Bis-Vinyl | |
| Ethers | 162 |
| 4.1 Introduction..... | 162 |
| 4.2 Diastereoselective Claisen Rearrangement of Bis-Vinyl Ethers | 166 |
| 4.2.1 Early Diastereoselective Claisen Rearrangements of γ -Allyloxy Vinyl Ethers | |
| | 167 |
| 4.3 Accessing Aldol-Type Products Using the Claisen Rearrangement..... | 173 |
| 4.4 Developing Conditions for an Asymmetric Claisen Rearrangement..... | 175 |
| 4.5 Evaluation of Auxiliary-Controlled Diastereoselective Claisen Rearrangements | 182 |
| 4.6 Method A: Incorporation of a Chiral Auxiliary at C1 | 182 |
| 4.6.1 Synthesis of Oxazolidinone Building Blocks | 182 |

| | |
|--|------------|
| 4.6.2 Synthesis of Bis-Vinyl Ethers Containing Oxazolidinone-Based Chiral Auxiliaries..... | 184 |
| 4.6.3 [3,3]-Sigmatropic Rearrangements of Bis-Vinyl Ether 4.29d..... | 186 |
| 4.6.4 Delineation of Mechanistic Possibilities for By-Product Formation..... | 189 |
| 4.6.5 [3,3]-Sigmatropic Rearrangements of Bis-Vinyl Ether 4.29a–c..... | 191 |
| 4.6.6 Synthesis of Thiazolidinethione Building-Block 4.28d..... | 195 |
| 4.6.7 Oppolzer’s Camphorsultam Auxiliary at C1..... | 198 |
| 4.7 Method B: Incorporation of a Chiral Auxiliary at C6..... | 202 |
| 4.7.1 Synthesis of Bis-Vinyl Ethers Containing Benzyl-Derived Chiral Auxiliaries..... | 205 |
| 4.7.2 Optimization of the Palladium-Mediated Claisen Rearrangement..... | 207 |
| 4.7.3 [3,3]-Sigmatropic Rearrangements of Bis-Vinyl Ethers 4.53..... | 210 |
| 4.8 Summary..... | 212 |
| 4.9 Future Work..... | 214 |
| Chapter 5 Experimental..... | 220 |
| 5.1 General Experimental Remarks..... | 220 |
| 5.2 Materials..... | 220 |
| 5.3 Instrumentation..... | 221 |
| 5.4 General Experimental Procedures for Chapter 2..... | 222 |
| 5.4.1 General Procedure for Conjugate Addition..... | 222 |
| 5.4.2 General Procedure for LiAlH ₄ /LiAlD ₄ Reduction..... | 222 |
| 5.4.3 General Procedure for Methylation..... | 222 |
| 5.4.4 General Procedure for IBX Oxidation..... | 223 |
| 5.4.5 General Procedure for the Wittig Olefination..... | 223 |
| 5.4.6 General Procedure for Cyclopropanation Reaction..... | 224 |
| 5.4.7 General Procedure for the Sonogashira Coupling..... | 224 |
| 5.4.8 General Procedure for the Hydrozirconation Reaction..... | 225 |
| 5.4.9 Procedure for Acetal Protection of 2.110c..... | 226 |
| 5.4.10 Procedure for the Acetal Deprotection of 2.111c..... | 226 |
| 5.4.11 General Procedure for the Radical-Mediated Cyclization Reaction..... | 226 |

| | |
|---|---------|
| 5.5 General Experimental Procedures for Chapter 3 | 227 |
| 5.5.1 General Procedure for the Sonogashira Coupling(329)..... | 227 |
| 5.5.2 General Procedure for TBAF Deprotection..... | 227 |
| 5.5.3 General Procedure for Acylation of Aryl Alkynes(207)..... | 228 |
| 5.5.4 General Procedure for Conjugate Addition | 228 |
| 5.5.5 General Procedure for DIBAL-H Reduction | 228 |
| 5.5.6 Procedure for the Methylation of Alcohol 3.17 | 229 |
| 5.5.7 Procedure for the Preparation of 3.21b(221) | 229 |
| 5.5.8 Synthesis of 1,1,1-trifluoro-4-methoxy-4-(4-methylphenyl)-3-butene-2-ol (3.22b)..... | 230 |
| 5.5.9 General Procedure for Kinetic Measurements | 230 |
| 5.6 General Experimental Procedures for Chapter 4 | 232 |
| 5.6.1 General Procedure for Conjugate Addition (Method A) | 232 |
| 5.6.2 General Procedure for Conjugate Addition (Method B)..... | 232 |
| 5.6.3 General Procedure for Conjugate Addition (Method C)..... | 232 |
| 5.6.4 General Procedure for DIBAL-H Reduction | 233 |
| 5.6.5 General Procedure for the Microwave-Promoted Claisen Rearrangement.... | 233 |
| 5.6.6 General Procedure for Palladium-Mediated Claisen Rearrangements | 234 |
| 5.7 Compounds Pertaining to Chapter 2..... | 235 |
| 5.8 Compounds Pertaining to Chapter 3 | 256 |
| 5.9 Compounds Pertaining to Chapter 4..... | 276 |
| Bibliography | 289 |
| Appendix A Chapter 2 Spectral Data..... | i |
| Appendix B Chapter 3 Eyring and Arrhenius Plots..... | xxxviii |
| Appendix C Chapter 3 Spectral Data..... | xlv |

List of Tables

| | |
|--|-----|
| Table 1.1 Reaction types used in pharmaceutical R&D for the construction of small molecules that constitute chemical libraries. ^a | 3 |
| Table 1.2 Enolization of methyl esters. ^a | 16 |
| Table 1.3 Ester-enolate Claisen rearrangement of parent and C6 alkoxy-substituted allyl propionates. ^a | 21 |
| Table 1.4 Ester-enolate Claisen rearrangement of furanoid and pyranoid glycols. ^a | 27 |
| Table 1.5 Ester-enolate rearrangement of carbocycles and cyclic glycols.(45) | 31 |
| Table 1.6 Kinetic data for tandem ester-enolate Claisen rearrangements of pyranoid glycols. | 37 |
| Table 1.7 Rate of the Claisen rearrangement of C6-substituted silyl ketene acetals. ^a | 39 |
| Table 1.8 Changes in Mulliken charges and dipole moments for the parent and C6-hydroxy substituted allyl vinyl ether | 43 |
| Table 1.9 The effect of C6-alkoxy substitution on the Claisen rearrangement.(69) | 44 |
| Table 1.10 Bond lengths (Å) calculated for optimized transition structures of the parent and C6-hydroxy substituted allyl vinyl ethers at the RHF/6-31G* level of theory.(72) .. | 45 |
| Table 2.1 Stannyl-mediated radical cyclization across bis-vinyl ethers ^a | 75 |
| Table 2.2 Optimization of cyclopropanation conditions on diene 2.74. | 88 |
| Table 2.3 Change in Product Distribution with Addition Rate ^a | 103 |
| Table 2.4 Cyclization of Deuterated Substrates | 114 |
| Table 3.1 Synthesis of aryl alkynoates. ^a | 127 |
| Table 3.2 Synthesis of bis-vinyl ether substrates for VT-NMR studies. ^a | 129 |
| Table 3.3 Rate constants, relative rates and activation parameters for rearrangement of bis-vinyl ethers in bromobenzene- <i>d</i> ₅ | 135 |
| Table 3.4 Kinetic data and activation parameters for the rearrangement of allyl vinyl ethers with oxygen substitution at the 4-, 5- or 6-position. | 140 |
| Table 3.5 Entropy of activation, determined by Eyring plot analysis. | 141 |
| Table 3.6 Solvent effects for the Claisen rearrangement of 3.16 and the effect of reduction at C1 (3.18). | 148 |
| Table 3.7 Substituent effects at C2 and C4. | 151 |

| | |
|--|-----|
| Table 4.1 Survey of Lewis acids. ^e | 176 |
| Table 4.2 Synthesis of bis-vinyl ethers 4.29. | 186 |
| Table 4.3 Effect of ligand addend on product distribution. | 190 |
| Table 4.4 Claisen rearrangement of bis-vinyl ethers 4.29a–c. | 192 |
| Table 4.5 Auxiliary-directed ester-enolate Claisen rearrangement of substituted allyl glycolates.(311)..... | 203 |
| Table 4.6 Synthesis of allyl alcohols 4.56a–d..... | 205 |
| Table 4.7 Synthesis of bis-vinyl ethers 4.53. | 207 |
| Table 4.8 Product distribution in the Claisen rearrangement of bis-vinyl ether 4.53a using Pd(PhCN) ₂ Cl ₂ or Pd(CH ₃ CN) ₂ Cl ₂ as the Lewis acid catalyst. | 208 |
| Table 4.9 Effect of solvent polarity on the Pd-mediated Claisen rearrangement. | 210 |
| Table 4.10 Claisen rearrangement of bis-vinyl ethers 4.53a–d. | 212 |

List of Figures

| | |
|---|-----|
| Figure 1.1 Marrying iterative sequences with orthogonal transformations to access molecular complexity..... | 9 |
| Figure 1.2 Lasalocid A..... | 25 |
| Figure 1.3 Non-bonding interactions present in the transition state for the ester-enolate Claisen rearrangement of ester 6..... | 29 |
| Figure 1.4 Conformational constraints and electronic repulsive interactions for trapped ester-enolates of cyclohexene and pyranoid glycol derivatives. Steric interactions between the silyloxy and C1-CH ₃ with the ring system are reduced for cyclopentene and furanoid glycol derivatives (not shown), exhibiting a preference for the chair- and boat-geometry in the transition state when X = CH ₂ and O, respectively. | 33 |
| Figure 1.5 Vinylogous anomeric effect. | 40 |
| Figure 1.6 Mechanistic options for the aliphatic Claisen rearrangement: diyl (A), diradical (B), dipolar (C) and ion-pair (D)..... | 40 |
| Figure 2.1 Synthetic strategy for efficient access to architecturally rich small-molecules from a common linear precursor..... | 52 |
| Figure 2.2 Patterns for ring closure for 3- to 6-membered rings. Reactions predicted to be favoured (green) or disfavoured (red) by Baldwin are highlighted. The radical (or anion) center initiating the reaction is designated as “X” while the atom center bearing the radical (or anion) post cyclization is designated as “Z.” | 56 |
| Figure 2.3 Frontier molecular orbital interactions for radical species. | 58 |
| Figure 2.4 DFT calculations investigating the effect of substitution on the aromatic ring | 107 |
| Figure 2.5 Effect of substitution on the vinyl ether | 109 |
| Figure 3.1 Mechanistic options for the aliphatic Claisen rearrangement, and summary of known substituent effects..... | 119 |
| Figure 3.2 Iterative synthesis of oligo-vinyl ethers. | 119 |
| Figure 3.3 Synthetic application of bis-vinyl ethers in the development of juvenile hormone III mimics..... | 121 |

| | |
|---|-----|
| Figure 3.4 Cascade radical cyclization across bis-vinyl ether to afford architecturally-rich, complex small-molecules..... | 121 |
| Figure 3.5 Summary of substituent effects on the rate of Claisen rearrangement, observed from our earlier bis-vinyl ether studies. | 122 |
| Figure 3.6 Two possible mechanistic possibilities for the observed increase in the rate of Claisen rearrangement for bis-vinyl ethers with an electron-withdrawing group on the oxyallyl fragment. | 123 |
| Figure 3.7 Compounds 3.8a–3.8g and the criterion (red) they satisfy..... | 126 |
| Figure 3.8 Relevant signals monitored in the ^1H NMR spectrum during the course of Claisen rearrangement (at 145 °C) for bis-vinyl ether 3.8g..... | 132 |
| Figure 3.9 Measurement of the consumption of bis-vinyl ether 3.8g at 145 °C over time (A) and determination of the corresponding rate constant from a plot of the natural logarithm of this data (B)..... | 133 |
| Figure 3.10 Hammett plots for the rate of rearrangement of compounds 3.8, plotted against different σ values (derived from either radical or polar reactions) to probe the electronic nature of the transition state structure. Hammett parameters in plots A–C are derived from radical reactions, while those in plots D–E are derived from polar reactions. | 137 |
| Figure 3.11 Change in ΔG^\ddagger with temperature for bis-vinyl ethers 3.8 and 3.16. Inset plot shows the change in ΔG^\ddagger (kcal mol^{-1}) for all aryl-substituted compounds, relative to the measured ΔG^\ddagger at 130 °C. The standard error for the slope of this line (<i>i.e.</i> , inset) is $2.3 \text{ cal K}^{-1} \text{ mol}^{-1}$, thus the true value for ΔS^\ddagger may be said to lie between 0 and $5 \text{ cal K}^{-1} \text{ mol}^{-1}$ | 143 |
| Figure 3.12 Possible resonance contributors for a dissociative transition state provide rationale for the increase in rate of Claisen rearrangement when a CF_3 substituent is at C4..... | 155 |
| Figure 3.13 Representative cationic fragments of TS-IV leading from 3.8c and 3.27 (A) with calculated electronic potential maps (B). The neopentoxy-group in 3.8c was simplified to a methoxy-substituent for the purpose of carrying out DFT calculations. | 156 |
| Figure 3.14 Proposed deuterated analogues for measuring kinetic isotope effects (A) and difficulties associated with introduction of deuterium label at C6 (B). | 158 |

Figure 3.15 Mechanistic proposal to account for the observed differences in reactivity in the Claisen rearrangement with different substitution on the allyl- and oxyallyl-fragments (at C6 and C1, respectively)..... 160

List of Schemes

| | |
|--|----|
| Scheme 1.1 Iterative conjugate addition/reduction sequence to access (poly)vinyl ethers. | 10 |
| Scheme 1.2 Several possible avenues for orthogonal transformation of oligo-vinyl ethers. | 11 |
| Scheme 1.3 Formation of a stable ester-enolate intermediate and its subsequent transformation in an alkylation reaction (A) or Claisen rearrangement (B). | 13 |
| Scheme 1.4 Geometric isomers at C1–C2 yield diastereomeric products when passing through the same transition state structure (<i>e.g.</i> , chair-like transition state, shown). | 15 |
| Scheme 1.5 Ester-enolate formation in THF (A) and 23% HMPA in THF (B). | 16 |
| Scheme 1.6 Stereocontrol in the ester-enolate Claisen rearrangement. | 18 |
| Scheme 1.7 Ester-enolate Claisen rearrangement offers access to tertiary alcohols, resembling aldol-type products, with high stereocontrol. | 19 |
| Scheme 1.8 Alkoxy substituent at C6 leads to allylic rearrangement in the presence of a catalytic amount of acid. | 19 |
| Scheme 1.9 Kinetic enrichment of the <i>E</i> -enolate, when C4 = CH ₃ , leads to erosion in diastereoselectivity for the ester-enolate Claisen rearrangement. | 23 |
| Scheme 1.10 A “loose” (A) or dissociative (B) transition state may be responsible for the observed loss of stereocontrol in the ester-enolate Claisen rearrangement when C6 bears two electron donating substituents. | 24 |
| Scheme 1.11 Ester-enolate Claisen rearrangement of furanoid or pyranoid glycols. | 26 |
| Scheme 1.12 Ester-enolate Claisen rearrangement of 6 in 23% HMPA-THF (A) or THF (B) afforded ester 7, rather than the expected epimeric products at C α | 28 |
| Scheme 1.13 Chemical differentiation of the pendant carbohydrate hydroxyl functionality through chemoselective ester-enolate Claisen rearrangement. Carbohydrate numbering is shown in blue, while allyl vinyl ether numbering is in red. | 34 |
| Scheme 1.14 Pseudomonic acids A, B, C and D. | 35 |
| Scheme 1.15 Tandem ester-enolate Claisen rearrangement. | 38 |
| Scheme 1.16 Allyl vinyl ether units bearing EDGs at C6 and EWG at C1 within the oligovinyl ether framework. | 47 |

| | |
|--|----|
| Scheme 1.17 Acid catalyzed allylic rearrangement of bis-vinyl ether. | 48 |
| Scheme 1.18 Destabilization of the alkene HOMO can result in unwanted intermolecular (A) or intramolecular (B) side reactions with electrophilic species. | 48 |
| Scheme 2.1 Cascading 6- <i>endo-trig</i> cyclization along acyclic poly(ene) precursor. | 59 |
| Scheme 2.2 Potential cyclization pathways for oligo-vinyl ether substrates. | 60 |
| Scheme 2.3 Protection of the alkyne carbon for installation of hydrogen atoms at R. | 61 |
| Scheme 2.4 Results for the conjugate addition of an alcohol to silyl-masked propiolates. | 62 |
| Scheme 2.5 Retrosynthetic analysis to gain access to an acyl radical precursor. | 63 |
| Scheme 2.6 PDC oxidation of alcohol 2.19 results in an intramolecular rearrangement. | 63 |
| Scheme 2.7 Synthesis of phenyl selenyl esters. | 65 |
| Scheme 2.8 Initial cyclization attempt from an acyl radical precursor. | 65 |
| Scheme 2.9 Preference for <i>exo</i> -cyclization when a vinyl ether is conjugated to an electron withdrawing group. | 66 |
| Scheme 2.10 Steric bias at R ² leads to formation of the larger ring product after cyclization. | 67 |
| Scheme 2.11 Acyl radical cyclization in the presence of tert-dodecanethiol and ACCN. | 68 |
| Scheme 2.12 Early installation of the acyl radical precursor as a masked aldehyde. | 69 |
| Scheme 2.13 Retrosynthetic analysis for generation of an alkenyl radical. | 70 |
| Scheme 2.14 Synthesis of vinyl ethers. | 71 |
| Scheme 2.15 Substitution dictates regioselectivity in the cyclization of mono-vinyl ethers. | 72 |
| Scheme 2.16 Protodestannylation of 2.43a. | 73 |
| Scheme 2.17 Protodestannylation of representative cyclized products to determine the relative stereochemistry of 2.49. | 77 |
| Scheme 2.18 Rational for the diastereoselectivity observed in the cyclization of bis-vinyl ethers. | 78 |
| Scheme 2.19 Mechanistic possibilities for radical cyclization onto bis-vinyl ethers. | 80 |
| Scheme 2.20 Divergent reactivity with trifluoromethyl substituted vinyl ethers. | 82 |
| Scheme 2.21 Mechanistic probes for identifying the presence of a radical at the 5-position (A) and the 6-position (B), relative to the approaching radical. | 84 |

| | |
|--|-----|
| Scheme 2.22 Synthesis of cyclopropane 2.61..... | 85 |
| Scheme 2.23 Synthesis of dienyl ether 2.70. | 85 |
| Scheme 2.24 Conditions for performing a [2+1] using diazo-compounds..... | 87 |
| Scheme 2.25 Attempted cyclopropanation of 2.70..... | 89 |
| Scheme 2.26 Synthesis of Cyclopropane 2.65..... | 90 |
| Scheme 2.27 Identification of radical character at the anomeric carbon..... | 91 |
| Scheme 2.28 Possible competing processes for radical cyclization of 2.65..... | 93 |
| Scheme 2.29 Formation of 2.68 confirms initial 5- <i>exo</i> mode of cyclization..... | 94 |
| Scheme 2.30 Cyclization of substrate 2.70..... | 94 |
| Scheme 2.31 Faster addition of triphenyltin hydride precludes cyclization onto the vinyl ether due to the faster, competing hydrogen atom transfer..... | 96 |
| Scheme 2.32 Proposed trapping of monocyclic products originating from an initial cyclization event onto a vinyl ether. | 97 |
| Scheme 2.33 Proposed route to probe the intermediacy of 2.102. | 98 |
| Scheme 2.34 Vinyl bromides as precursors to alkenyl radicals..... | 100 |
| Scheme 2.35 Synthesis of vinyl bromides 2.104a and 2.104b..... | 101 |
| Scheme 2.36 Synthesis of vinyl bromide 2.104c..... | 102 |
| Scheme 2.37 Plausible scaffolds for development of medicinal chemistry programs using our radical cascade methodology. All substrates are amenable to further functionalization. For example: vinyl stannanes can be used in palladium-mediated couplings, while exocyclic olefins can participate in [3+2] cycloaddition reactions with substituted allenes. | 110 |
| Scheme 2.38 Synthesis of deuterated substrates for evaluation of premature quenching of radical intermediates by hydrogen atom transfer reactions. | 112 |
| Scheme 2.39 Efficient access to molecular complexity by marrying iterative synthesis to radical cascade cyclizations. | 114 |
| Scheme 2.40 Use of a cyclopropane ring as a radical trapping agent to indicate those positions where radical character is developed during the cyclization of mono-vinyl ether substrates..... | 115 |
| Scheme 3.1 Synthesis of 3.16 and 3.18 for VT-NMR studies..... | 145 |
| Scheme 3.2 Proposed synthesis of CF ₃ -analogue..... | 152 |

| | |
|---|-----|
| Scheme 3.3 Synthesis of C4 analogue 3.27. | 153 |
| Scheme 3.4 Crossover experiment with 3.8h and 3.8d. | 159 |
| Scheme 4.1 Thermal Claisen rearrangement of acyclic, aliphatic allyl vinyl ethers preferentially pass through a chair-type transition state to afford a single diastereomer of product as a mixture of enantiomers. | 163 |
| Scheme 4.2 Asymmetric versions of the Claisen rearrangement. | 164 |
| Scheme 4.3 Claisen rearrangement of cyclic (A) and acyclic (B) γ -allyloxy vinyl ethers. | 167 |
| Scheme 4.4 Auxiliary-controlled diastereoselective Claisen rearrangement of a γ -allyloxy allyl vinyl ether. | 168 |
| Scheme 4.5 Rationale for formation of (R)-4.14 as the major enantiomer.(76)..... | 169 |
| Scheme 4.6 Serine-derived oxazolidinone used to control the diastereoselectivity in the Ireland Claisen rearrangement of β -alkoxy and β -aryloxy enol ethers..... | 170 |
| Scheme 4.7 Ireland Claisen rearrangement of alkoxyallyl glycinates..... | 171 |
| Scheme 4.8 Diastereocontrolled Ireland Claisen rearrangement of allyl β -amino esters. | 171 |
| Scheme 4.9 Hydrogen-bonding catalysts (A) and oxophilic Lewis acids (B) may not be suitable stereocontrol agents. The extent of bond lengthening at C4—O3 makes the ethereal oxygen more accessible for coordination; this could result in fission of the vinyl ether, in which case [3,3]-rearranged products would be produced with poor diastereoselectivity, [1,3]-rearranged products could become possible, or the two fragments may fail to recombine entirely. | 173 |
| Scheme 4.10 A general aldol addition reaction. | 174 |
| Scheme 4.11 Transformation of bis-vinyl ether 4.24 into aldol-type product 4.26..... | 174 |
| Scheme 4.12 Incorporation of a remote chiral element into the bis-vinyl ether scaffold. | 179 |
| Scheme 4.13 Auxiliary-controlled diastereoselective Carroll rearrangement, using (S)-1-amino-2-methoxymethylpyrrolidine as the chiral auxiliary. | 180 |
| Scheme 4.14 Synthetic plan for incorporating oxazolidinone-auxiliaries into our alkyne building-blocks for the conjugate addition sequence..... | 181 |
| Scheme 4.15 Incorporation of a chiral auxiliary at C1. | 182 |

| | |
|--|-----|
| Scheme 4.16 Synthesis of chiral building blocks to act as a remote auxiliary off bis-vinyl ethers of type 4.29..... | 183 |
| Scheme 4.17 Synthesis of allyl alcohol 4.38a and 4.38b..... | 184 |
| Scheme 4.18 Thermal induced Claisen rearrangement of 4.29d. | 187 |
| Scheme 4.19 Unexpected formation of oxazolidinone 4.40. | 188 |
| Scheme 4.20 Mechanistic possibilities for the unexpected chemical reactivity of 4.29d when treated with Pd(PhCN) ₂ Cl ₂ | 189 |
| Scheme 4.21 Evaluation of a possible retro-aldol reaction with prolonged exposure to palladium..... | 191 |
| Scheme 4.22 Product distribution, after removal of the chiral auxiliary, can determine whether the rearrangement is diastereoselective (A) or whether competing transition-state geometries lead to good overall enantioselectivity but poor diastereoselectivity (B). ... | 193 |
| Scheme 4.23 Retrosynthetic plan for the synthesis of thiazolidinethione 4.28d. | 194 |
| Scheme 4.24 Synthesis Crimmins' auxiliary 4.32d and its use in an acylation reaction. | 195 |
| Scheme 4.25 Crimmins' auxiliary 4.32d and its use in an acylation reaction. | 196 |
| Scheme 4.26 DCC-coupling between tetrolic acid and Crimmins' auxiliary..... | 197 |
| Scheme 4.27 An attempt to take advantage of hard-soft acid-base concept to overcome unwanted reactivity of the thiocarbonyl. | 197 |
| Scheme 4.28 Alternate route to access compound 4.28d..... | 198 |
| Scheme 4.29 An asymmetric Claisen rearrangement of allyl vinyl ether 4.46 using Oppolzer's camphorsultam as a remote chiral auxiliary at C1. | 199 |
| Scheme 4.30 Rotamers of oxazolidinone-based auxiliaries. | 200 |
| Scheme 4.31 Attack of the preferred conformation for non-chelate (A) and chelate (B) reactions, with camphor-derived auxiliaries, occurs on the <i>Re</i> -face to produce the same stereoisomers under either set of conditions. | 201 |
| Scheme 4.32 Incorporation of Oppolzer's auxiliary into the bis-vinyl ether scaffold.... | 201 |
| Scheme 4.33 Modest diastereoselectivity can be achieved in the Claisen rearrangement of allyl glycolates with use of 1-phenylethanol as a remote auxiliary at C1.(311)..... | 202 |
| Scheme 4.34 Ester-enolate Claisen rearrangement of substituted allyl glycinates.(80). | 204 |
| Scheme 4.35 Incorporation of a benzyl-derived auxiliary at C6. | 204 |

| | |
|---|-----|
| Scheme 4.36 Determination of relative stereochemistry by stereoablation at C α , where each result is arbitrarily referenced to compound "A". | 215 |
| Scheme 4.37 Including an allyl scavenger (<i>e.g.</i> , SvH ₂) as a reagent in the deallylcarbonylation reaction may circumvent the competing decarboxylative allylation of 4.57. | 216 |
| Scheme 4.38 Asymmetric synthesis of bis-vinyl ether 4.53f and its subsequent transformations. | 218 |
| Scheme 4.39 Proposed synthesis of Mosher ester for determination of absolute configuration at the stereogenic carbinol. | 219 |
| Scheme 4.40 Synthesis of (<i>R</i>)-4.62. | 219 |

List of Abbreviations and Symbols

| | |
|---------------------|--|
| $^1\text{H NMR}$ | proton nuclear magnetic resonance |
| $^{13}\text{C NMR}$ | carbon-13 nuclear magnetic resonance |
| AVE | allyl vinyl ether |
| Å | angstroms |
| Ac | acetyl |
| acac | acetylacetonate |
| ACCN | 1,1'-azobis(cyclohexanecarbonitrile) |
| AcOH | acetic acid |
| AIBN | 2,2'-azobisisobutyronitrile |
| °C | degrees Celcius |
| calcd | calculated |
| cat | catalytic |
| cm^{-1} | wavenumbers |
| ΔG^\ddagger | Gibbs free energy of activation |
| ΔH^\ddagger | enthalpy of activation |
| ΔS^\ddagger | entropy of activation |
| dba | dibenzylideneacetone |
| DCC | <i>N,N'</i> -dicyclohexylcarbodiimide |
| DIBAL-H | diisobutylaluminum hydride |
| DMAP | 4-methylaminopyridine |
| DMP | Dess-Martin periodinane |
| DOS | diversity oriented synthesis |
| EDG | electron donating group |
| e.g. | for example |
| EWG | electron withdrawing group |
| F_{sp^3} | fraction of sp^3 hybridized centers in a molecule |
| h | hours |
| HMPA | hexamethylphosphoramide |
| HOMO | highest occupied molecular orbital |

| | |
|----------|--|
| HRMS | high resolution mass spectrometry |
| HTS | high throughput screening |
| Hz | Hertz, s ⁻¹ |
| IBX | 2-iodoxybenzoic acid |
| IR | infrared |
| <i>J</i> | coupling constant |
| JH | juvenile hormone |
| LiICA | lithium <i>N</i> -isopropylcyclohexylamine |
| LRMS | low resolution mass spectrometry |
| LUMO | lowest unoccupied molecular orbital |
| M | molar |
| mg | milligrams |
| mmol | millimoles |
| <i>n</i> | straight chain |
| NCE | new chemical entity |
| PPI | protein-protein interaction |
| R&D | research and development |
| r.t. | room temperature |
| SAR | structure activity relationship |
| SOMO | singly occupied molecular orbital |
| SPS | solvent purification system |
| TBAF | tetrabutylammonium fluoride |
| TBS | <i>tert</i> -butyldimethylsilyl |
| TMS | trimethylsilyl |
| TS | transition state |
| UV | ultraviolet |
| VAE | vinyllogous anomeric effect |
| vs | versus |
| ~ | approximately |

Acknowledgments

*We, as humans, are merely a blip on the scale of evolutionary time. In retrospect, one might ask how six years could surmount to anything meaningful. But if we consider that my time in Graduate School constitutes 21% of my days since birth (and will make up ca. 7.5% of my entire life's journey, assuming I live to the ripe old age of 80), then this time spent amongst my colleagues, my mentors, and my friends effectively amounts to the most significant years of my life. I say this because for every individual I have encountered, whether I have mentioned you by name or not, I want you to know: **you matter, you are significant, and you have worth.***

First and foremost, I would like to extend my gratitude to my supervisor, Dr. Jeremy Wulff (*aka*, “the Boss”), for providing me with the opportunity to study under his tutelage for the past six years. When I became a member of his research group, he had been an Assistant Professor for just over a year and was still working in the lab in order to establish the foundation for a number of projects that would see to the growth of the research group in the years to come. It is a rare privilege to work for a Professor in these earliest stages of becoming an academic. You bear witness to the seemingly insurmountable number of challenges that must be faced in attaining an independent research career, and one becomes acutely aware of the unrelenting determination and commitment required to succeed in such endeavours. Jeremy, your struggle, in some small way, became ours (the Graduate student's), and we were forced to collectively evolve. Through this I have acquired a greater knowledge about who I am as an individual, and as a scientist. I thank you for allowing me to be part of that. The experience has taught me to have greater confidence in my own abilities, and to arise to the challenge...because at the end of the day, you must learn to survive.

It is only fitting that I next acknowledge those of you who have been on this journey with me. Jason Davy, you are one of the most gifted individuals I have ever had the privilege of meeting. I have learned so much from you over the years; I thank you for your *time* which you invested so selflessly. Mike Brant, you speak the *truth*, little buddy. You've been my

bench-mate the entire time. Thank you for the laughs, the frustration, and for being you. Kevin Allen, anything I say here will be *irrelephant*. You've been the ringleader for a number of pranks. Thank you for keeping me on my toes and for being a great *friend*. Emma Nicholls-Allison, the tremendous amount of work that you have invested in your life's passion has truly been an *inspiration* that has provided the spark to ignite the flame for pursuing my own future endeavours. Amanda Whiting, I would be nowhere if not for your *advice*. Krystyn Dubicki, thank you for taking time with me to stop and enjoy *life* (or coffee, or dance). Katherine Davies, Caleb Bromba, Ronan Hanley, and Jun Chen – thank you for the memories, and for being part of this crazy *family*.

I would also like to thank the technical, administrative and teaching staff (and people at Stores!) in the Chemistry Department at University of Victoria for all of their help throughout the years. A special thank you is extended to Chris Barr for his helpful discussions of all things NMR-related, and for the countless hours he allowed me to log on the 500 MHz.

Last, but not least, I would like to thank my family for their endless support and encouragement in what truly have been the most arduous but rewarding years of my life.

Dedication

In loving memory of my grandfather, John William O'Rourke (1925 – 2013).

Chapter 1 Introduction

1.1 Prologue

Despite significant synthetic advancements over the last half century, the productivity of pharmaceutical research efforts, as measured by the number of new drugs that have been approved each year, has dropped off considerably.⁽¹⁾ Attempts to rationalize the obvious disparity between the number of newly synthesized compounds with approved therapeutics has revealed that the types of molecular scaffolds medicinal chemists utilize for drug development (and consequently the types of molecules that populate chemical libraries for high throughput screening (HTS) technologies) exhibit poor physicochemical properties and fail to adequately explore chemical space.⁽²⁾ As result of this deficiency, small molecules capable of modulating key protein-protein interactions¹ involved in complex pathologies (*e.g.*, cancer and Alzheimer's disease) have largely not been identified, and targets of this nature are widely perceived as being “undruggable.”

But, as Eric Lander⁽³⁾ stated, “druggable is merely a description of the current state of our abilities.” As organic chemists, it is our responsibility to continue to redefine the current state within the medical community not by offering one solution to a single problem, but to understand the problem on a grander scale and to set forth with an arsenal of new technologies and innovations in order to overcome it.

¹ Unlike enzymes, which function through binding of primary metabolites in well-defined pockets, PPIs are mediated through flat, extended contact surfaces that make them difficult to target using a small molecule.

1.2 The Medicinal Chemist's Toolbox and its Limitation on Drug Discovery

Given the pressure to identify, develop and deliver small-molecule new chemical entities (NCEs) for prevention or treatment of disease, it is not surprising that medicinal chemists rely heavily upon a small set of robust and reliable synthetic procedures designed to incorporate molecular diversity in (a) a few number of steps and (b) in the presence of pendant functional groups, while (c) simultaneously alleviating bottlenecks during target synthesis. Many of these reactions, discussed below, take advantage of commercially available reagents that are amenable to parallel synthetic methodologies for rapid diversification intended for screening structure-reactivity relationships (SAR).

In recent years, however, the types of reactions utilized in pharmaceutical R&D laboratories have come under scrutiny. Many believe that the modular design techniques adopted by medicinal chemists has limited the structural diversity of the molecular frameworks available for screening, primarily yielding flat molecules that consequently have poor physicochemical properties. A recent review published by Roughley and Jordan⁽⁴⁾ examined this purported stereotype, wherein they report on the types of reactions utilized in large pharmaceutical companies around the globe (**Table 1.1**).

Table 1.1 Reaction types used in pharmaceutical R&D for the construction of small molecules that constitute chemical libraries.^a

| Reaction Type | % Subtype ^b | % Total ^c |
|-------------------------------------|------------------------|----------------------|
| Heteroatom Alkylation and Arylation | | 23.1 |
| <i>N</i> -arylation with Ar-X | 27.1 | |
| <i>N</i> -substitution with alkyl-X | 23.1 | |
| reductive amination | 22.9 | |
| Acylation and Related Processes | | 22.4 |
| <i>N</i> -acylation to amide | 71.3 | |
| <i>N</i> -sulfonylation | 9.9 | |
| <i>N</i> -acylation to urea | 9.5 | |
| C-C Bond Formation | | 11.5 |
| Suzuki coupling | 40.2 | |
| Sonogashira reaction | 18.4 | |
| ester condensation | 5.5 | |
| Grignard reaction | 5.6 | |
| Heterocycle Formation | | 8.2 |
| <i>N</i> -containing | 89.4 | |
| <i>O</i> -containing | 8.9 | |
| <i>S</i> -containing | 1.7 | |
| Protection / Deprotection | | 3.1 / 18.0 |
| Reduction / Oxidation | | 5.6 / 1.5 |
| Functional Group Interconversions | | 5.6 |
| Functional Group Additions | | 1.0 |

^aTaken from data set in Ref (4). ^bTaken from the top three contributors for reaction type. ^cFrom a total of 7315 reactions used to prepare 3566 compounds.

While it is not surprising that heteroatom-carbon bond forming reactions top the list, accounting for the largest percentage (45.5%) of reactions utilized by medicinal chemists, the formation of heterocycles (a common feature of many therapeutics) surprisingly accounts for a mere 8.2% of all reaction classes. The types of molecules contained within the data set possess, on average, three ring systems with *N*-containing heterocycles being most prevalent. This observation suggests that the development of NCEs for screening is biased towards commercially available starting materials that are then later functionalized and/or incorporated into the core scaffold.

Similarly, carbon-carbon bond forming reactions were found to be dominated by palladium-mediated couplings. The Sonogashira and Suzuki couplings, for which the Nobel Prize was awarded in 2010, are responsible for the formation of approximately 60% of all new carbon-carbon bonds. It is of importance to note that both the Suzuki coupling and Sonogashira reaction are primarily utilized for coupling of unsaturated systems. Roughley and Jordan(4) are also keen to point out that while the Suzuki and Sonogashira reactions can afford aromatic or acetylenic moieties, respectively, these functional groups are rarely reduced or altered in the final product. Additional transformations, such as functional group additions, were also found to be aimed at installation of halogens, as would be anticipated in light of the prevalence of palladium-mediated cross couplings.

The reliance on these latter reactions is, in part, due to the difficulty associated with formation of Csp^3-Csp^3 bonds. Introduction of new stereocenters needs to be highly controlled as enantiomers of a given drug molecule may have detrimental effects on patient health (*e.g.*, (*S*)-naproxen is an anti-inflammatory drug while (*R*)-naproxen is a liver toxin). Installation of new stereogenic centers often requires use of chiral auxiliaries and very specific reaction conditions that may not be well tolerated in the presence of other pendant functionality. In fact, only 1093 of the 3566 compounds (less than 1/3) that appear in the survey by Roughley and Jordan had at least one stereogenic center with defined configuration, and only 13% of these were accessed through enantioselective processes rather than commercially available, enantiopure starting materials. Palladium-mediated couplings, on the other hand, not only offer efficient access to Csp^2-Csp^2 bonds with high chemoselectivity and functional group tolerability, but are amenable to parallel synthesis

for rapid exploration of structure-activity relationships. This process is made more convenient by commercial suppliers which provide diverse libraries of readily available, cost effective reagents to be used for these types of synthetic strategies.

Other key reactions, listed in **Table 1.1**, are concerned with functional group manipulations. Despite the high cost, poor efficiency and lower yield, use of protecting groups in synthesis is still quite prevalent. Protecting group removal, in particular, accounts for approximately 1/5th of all reactions examined in the data set. Many commercially available building blocks now have masked pendant functionality, accounting for the disparity between the removal of protecting groups (18%) from the scaffold and the complementary protection of pendant functionality (1.1%). Oxidation and reduction reactions are generally less common and are mainly utilized to gain access to an amine or alcohol (*via* reduction), with the later generally being oxidized to the corresponding reactive aldehyde for use in heteroatom-carbon or carbon-carbon bond forming reactions.

Considering that these NCEs are accessed in 3-5 synthetic steps, the high reliance on so few reactions types that fail to introduce three-dimensional architectural elements is concerning. The NCEs being produced intrinsically lack new stereogenic elements that aid with specificity of binding, and are inherently large with flat chemical landscapes chiefly comprised of at least three ring systems – a feature that can greatly affect the physicochemical properties of a molecule(5) and its probability for further development into a viable drug candidate for clinical trials.

1.3 Discovering NCEs by Emulating Natural Product Structure

Most compounds found in screening libraries have been designed to incorporate drug-like attributes as defined by a set of guidelines established by Lipinski(6) and Veber.(7) These guidelines in no way dictate the type of structural features or molecular architecture required for a given molecule to be biologically active, nor do they provide a concrete framework for dictating a compound's molecular properties. For example, natural products and natural product-like compounds frequently fall outside these specifications; nonetheless, they are taken up by cellular organisms and often possess potent activity. Having said that, there are a number of structural elements found in natural products that confer advantage when compared to the types of compounds found in combinatorial libraries:(8)

- (a) Natural products contain a large number of stereogenic elements that can improve substrate-target interaction due to the high degree of stereospecificity that is naturally present within protein-interaction domains and substrate binding pockets.
- (b) They have a high F_{sp^3} count,(9) permitting greater occupancy of chemical space without significantly increasing the molecular weight of the molecule. This higher degree of saturation is accompanied by
- (c) Fewer degrees of conformational freedom embodied by fused-, bridged- and spiro-ring systems, providing a thermodynamic advantage with fewer entropic losses upon engagement with the mechanistic target.
- (d) The types of ring systems that are present in natural products contain heteroatoms that are largely accounted for by oxygen (rather than nitrogen and sulfur found in combinatorial compounds). Cyclic ethers,(10) in particular, improve drug

developability by decreasing metabolic lability while simultaneously improving aqueous solubility.

- (e) Incorporation of heteroatoms (with non-protonatable nitrogen) into a rigid, but still flexible, saturated framework also improves drug bioavailability by decreasing non-specific binding to human serum albumin and hERG.
- (f) Their three-dimensional architecture provides an attachment point for out-of-plane substituents, possibly increasing receptor ligand complementarity.

As is made evident by the above list, natural products are more amenable to exploration of chemical space. Movement toward the development of natural product-like molecules could increase the chances of finding bioactive compounds.(11) The ability to generate such leads in a flexible manner, however, is a synthetic feat which is quite difficult to achieve since the number of steps required to access such complex synthetic targets leaves little material available for exploration of SAR.

1.4 Developing Synthetic Methodologies to Access Molecular Complexity

The efficient synthesis of natural product-like derivatives remains a daunting synthetic challenge that, in recent years, has begun to garner increased attention with the need to develop new types of molecular scaffolds for therapeutic intervention.

Given that natural products (or natural product-like substrates) are not easily synthesized, nor are they isolated in any sufficient quantity from a living organism that is suitable for clinical development,(12) it has fallen unto the synthetic chemist to develop new methods

to access highly complex, three-dimensional, polycyclic scaffolds that emulate the desirable features of natural products and their derivatives, whilst affording the ease of synthesis required for pharmaceutical development.(11)

Synthetic chemists often utilize convergent approaches to achieve this type of molecular complexity (*e.g.*, diversity oriented synthesis(13, 14) and multicomponent reactions), whereas Nature has elegantly gained her efficiency by relying on iterative, linear syntheses followed by cascade- or tandem-type transformations to incorporate a high degree of stereochemical complexity and functionality into a natural product molecule. We therefore sought to emulate Nature's approach by developing new synthetic methodologies that would enable efficient access to different classes of complex small-molecules from a common, iteratively synthesized linear precursor.

1.4.1 Iterative Synthesis of Reactive Polymers

For the past number of years, we have been developing an iterative protocol for the synthesis of highly functionalized, reactive polymeric substrates that have untapped chemical potential. The ease of incorporating a number of different types of functionality through repetition of simple, high-yielding synthetic operations, using easily accessible building blocks, without the need for chromatographic purification, makes this method particularly attractive for the development of automated processes in organic synthesis (**Figure 1.1A**).

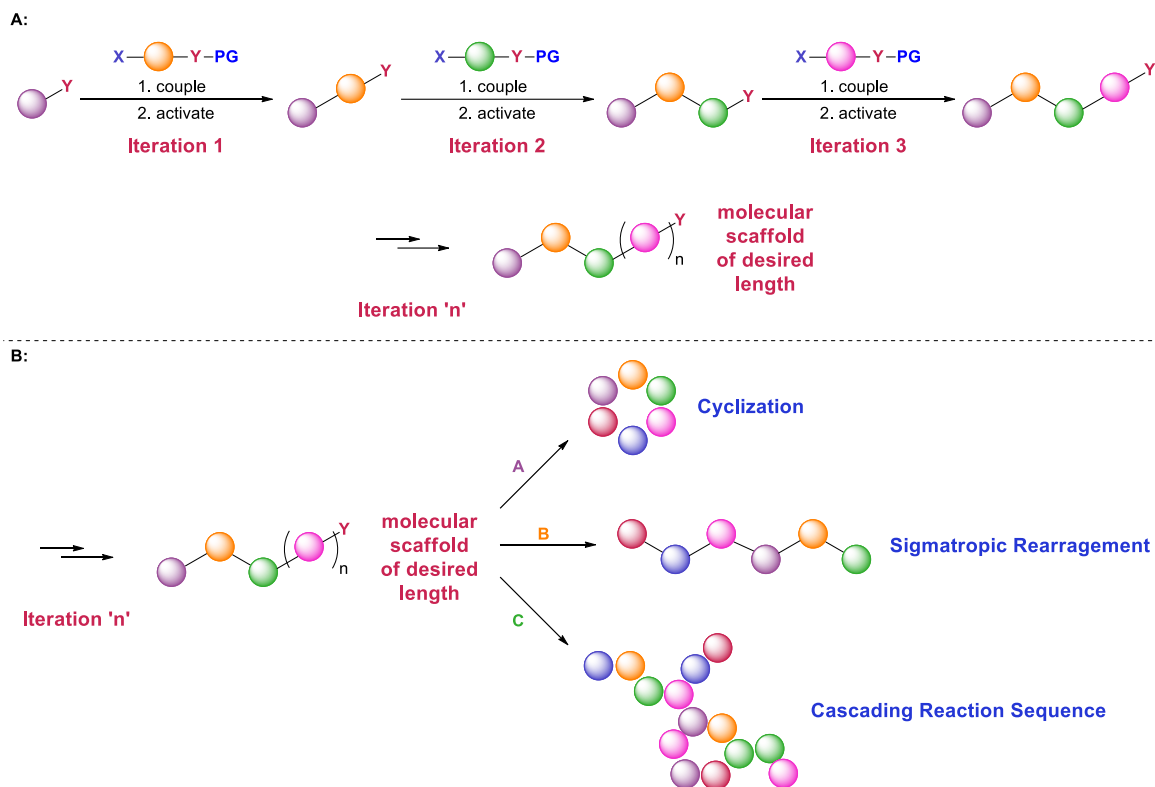
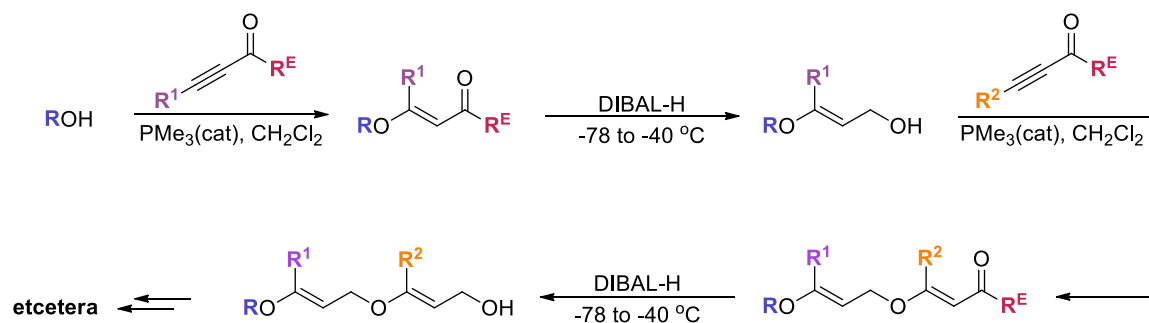


Figure 1.1 Marrying iterative sequences with orthogonal transformations to access molecular complexity.

If one could imagine taking these reactive polymers and have them be amenable to further chemical elaboration, *via* orthogonal cascade-type transformations, access to several different classes of stereochemically rich, linear and polycyclic scaffolds could be achieved in as little as one synthetic operation (**Figure 1.1B**).

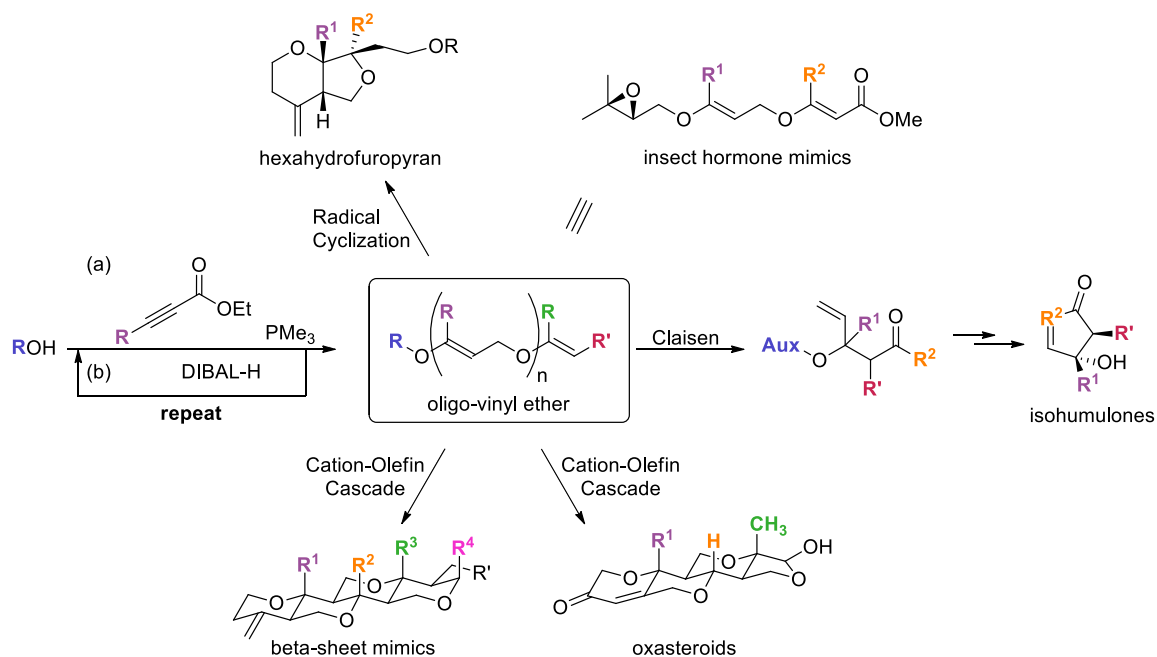
The first milestone of this project has already been realised with the development and optimization of an iterative conjugate addition/reduction sequence to access poly(vinyl) ether scaffolds. These reactions are reproducibly high yielding (>90%), tolerant of a wide

variety of functionality, and the selectivity for the conjugate addition favors formation of the *E*-olefin, unless **R** becomes too sterically encumbering in which case an erosion in this selectivity is observed (**Scheme 1.1**).



Scheme 1.1 Iterative conjugate addition/reduction sequence to access (poly)vinyl ethers.

Having explored the scope of the conjugate addition/reduction sequence, we envisioned access to a variety of different biologically interesting molecular scaffolds through radical mediated cyclizations, [3,3]-sigmatropic rearrangements and cation-olefin cascades (**Scheme 1.2**).



Scheme 1.2 Several possible avenues for orthogonal transformation of oligo-vinyl ethers.

Thus, the primary goal for this work was to evaluate the chemical reactivity of these (poly)viny ethers through systematic examination of substrates with additional monomeric units. While much is known about the chemical reactivity of mono-vinyl ethers, the prevalence of those compounds with the same bond connectivity bearing two, three or four of these functional units drops off significantly. In fact, little is known about bis-vinyl ethers outside a few experimental and theoretical investigations pertaining to their influence on the rate of Claisen rearrangement (discussed later in Chapter 1). Even then, there are few reports for their use in organic synthesis, owing to the highly reactive nature of these substrates. At three functional units, these compounds become virtually non-existent outside our own work. For these reasons, we have focused our attention on evaluating bis-vinyl ether reactivity in order to gauge the limitations of this system and to

endeavor in the development of new reactions that could ultimately see use for our proposed methodology.

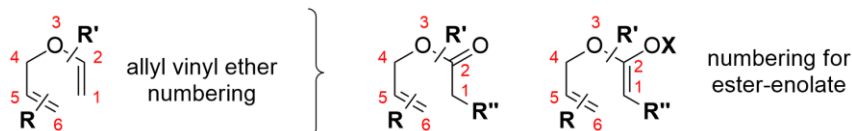
1.5 Known Chemical Reactivity of Bis-Vinyl Ethers

The pre-existing literature pertaining to the reactivity of bis-vinyl ether substrates is almost exclusively derived from investigations of substituent effects in the thermal- and ester-enolate Claisen rearrangement. For this reason, it is pertinent to compare the reactivity of the parent system (for these reactions) to that of the C6-alkoxy variant to delineate the differences in reactivity imparted by this substitution.²

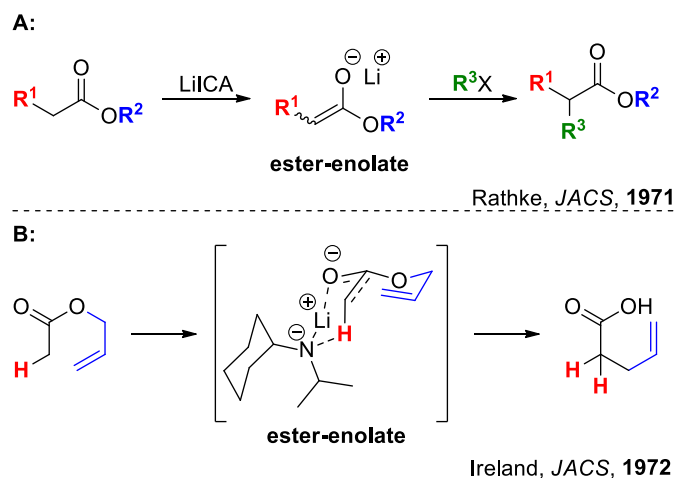
1.5.1 The Ester-Enolate (Ireland) Claisen Rearrangement

The ester-enolate Claisen rearrangement was developed by Robert Ireland in the early 1970s. Rathke's(15) investigations on the quantitative formation of ester enolates in the presence of lithium *N*-isopropylcyclohexyl amide (LiICA), without competing self-condensation, led Ireland to speculate that successful application of this methodology to the generation of enolate anions of allyl esters would result in the formation of a transient

² The following “review” is not intended to be an exhaustive account of the known literature on this subject, but is meant to highlight the key trends that will later complement the findings of our own investigations. Extensive use of allyl vinyl ether numbering (which is mirrored in the substrates for the ester-enolate Claisen rearrangement) will be used throughout the text and is understood as follows:



species that could undergo a Claisen-type rearrangement to afford γ,δ -unsaturated carboxylic acids under mild reaction conditions (**Scheme 1.3**).



Scheme 1.3 Formation of a stable ester-enolate intermediate and its subsequent transformation in an alkylation reaction (A) or Claisen rearrangement (B).

The success of Ireland's [3,3]-sigmatropic rearrangement(16) continues to expand the scope and general applicability of the Claisen rearrangement(17) to the preparation of acyclic and macromolecular systems rich in stereochemical elements including, but not limited to, polyether antibiotics,(18-23) secondary metabolites, marine natural products, amino acids,(24) C-glycosides (*see Section 1.7*), chiral stannanes(25) and allyl silanes.(26)

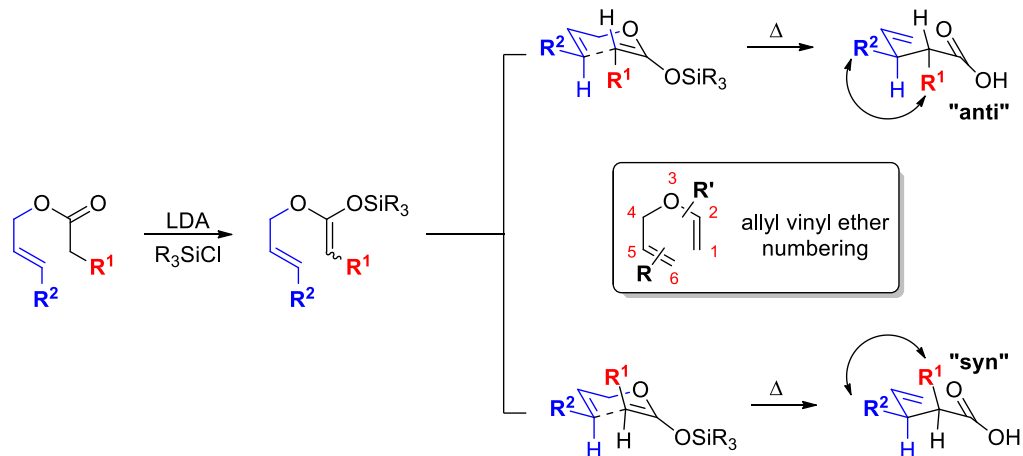
The inclusion of the silyloxy functionality at C2, accessed *via* the trapping of the ester-enolate, has also been shown to accelerate the rate of the aliphatic Claisen rearrangement to such an extent that γ,δ -unsaturated carboxylic acids can be accessed at temperatures below 32 °C. Alternative procedures employing the rearrangement of vinyl, orthoester or amide acetal congeners generally requires heating in excess of 100 °C, making this a

particularly attractive attribute in instances where there may be undesirable, competing thermal rearrangements due to latent reactivity within the substrate of interest.(27)

This approach to carbon-carbon bond formation (*i.e.*, the Claisen rearrangement) remains an area of research interest in the chemical community, as is evident by a recent theoretical investigation on the origin of stereoselectivity in the rearrangement of pyranoid glucals,(28) its use in the construction of complex molecular architecture bearing contiguous stereocenters(29-31) and the continued development of new variants of this reaction (*i.e.*, Ireland-Claisen rearrangement of alkenylboronates as a masked alcohol functionality) in order to access β -hydroxy acids without the inherent loss in diastereoselectivity imparted by alkoxy-substitution at C6.(32)

1.5.2 Stereocontrol in the Ester-Enolate (Ireland) Claisen Rearrangement

The Ireland Claisen rearrangement is generally achieved *via* two synthetic operations: (1) the generation of the ester-enolate, with subsequent trapping to form a silylketene acetal, followed by (2) a thermally induced [3,3]-sigmatropic rearrangement. The first of these synthetic operations is important for relaying stereochemical information, *via* the geometry about the olefin at C1–C2 in the silyl-ketene acetal, to the newly formed C1–C6 bond in the γ,δ -unsaturated carboxylic acid. The significance of this first synthetic transformation is only realised when the nature of the transition state structure (be it chair- or boat-like in nature) for the Claisen rearrangement has been defined for a given system (**Scheme 1.4**).

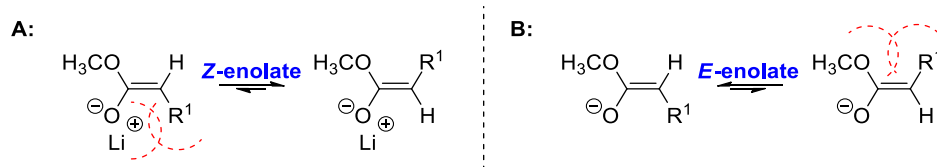


Scheme 1.4 Geometric isomers at C1–C2 yield diastereomeric products when passing through the same transition state structure (*e.g.*, chair-like transition state, shown).

The ability to control the olefin geometry and to predict the transition-state structure enables one to choose the optimal set of reaction conditions required to obtain the desired (relative) configuration at the newly formed C1–C6 bond in the target molecule. It should be noted that no one set of rules enables accurate prediction of product distribution in the Claisen rearrangement (or variants thereof), as changes to the size and/or electronic properties of substituents, or conformational degrees of freedom in the system ultimately lead to changes in the reaction trajectory.

1.5.3 Stereoselective Enolate Formation

Unique to Ireland's system is the ability to alter the geometry about the resultant olefin, generated from the ester *in situ*, through preferential enolization to the *E*- or *Z*-isomer (**Scheme 1.5**).



Scheme 1.5 Ester-enolate formation in THF (A) and 23% HMPA in THF (B).

When enolization is achieved in tetrahydrofuran (THF) formation of the *Z*-enolate is observed, while in a more polar solvent system (*i.e.*, 23% hexamethylphosphoramide in tetrahydrofuran) formation of the *E*-enolate is preferred (**Table 1.2**).⁽²⁷⁾

Table 1.2 Enolization of methyl esters.^a

| Entry | R ¹ | Solvent | <i>E</i> : <i>Z</i> Enolate ^b |
|-------|-----------------------------------|--------------|--|
| 1 | CH ₃ CH ₂ | THF | 9 : 91 |
| 2 | CH ₃ CH ₂ | 23% HMPA-THF | 84 : 16 |
| 3 | C ₆ H ₅ | THF | 71 : 29 |
| 4 | C ₆ H ₅ | 23% HMPA-THF | 95 : 5 |
| 5 | (CH ₃) ₃ C | THF | 3 : 97 |
| 6 | (CH ₃) ₃ C | 23% HMPA-THF | 91 : 9 |

^aConditions: Enolization with 1.1 equiv. LDA at -78 °C, followed by trapping with TBSCl. ^bRatio determined by NMR analysis of crude isolate.⁽²⁷⁾

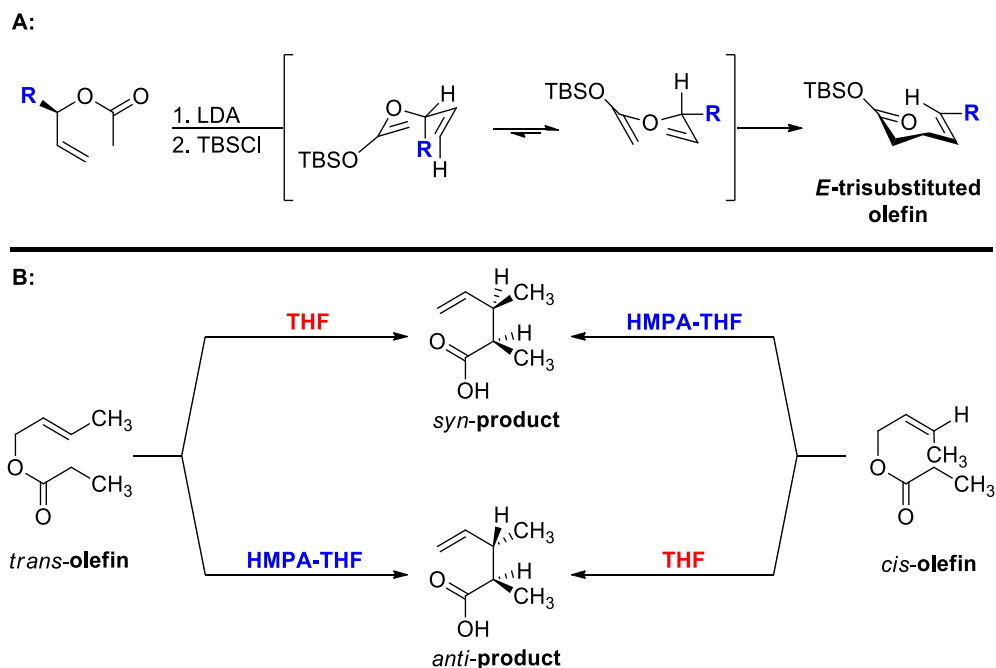
This inherent stereochemical bias, described above, is believed to be the kinetic result of steric requirements for enolization of the ester (**Scheme 1.5**). When the reaction is performed in a more weakly coordinating solvent, like THF, coordination of the carbonyl oxygen to the lithium ion is important. The enolate oxygen is now considerably more

sterically encumbered than the corresponding naked ion, thus preferring to minimize unfavourable, non-bonding interactions through formation of the less sterically congested *Z*-enolate (**Scheme 1.5A**). Alternatively, generation of the enolate in the presence of HMPA leads to sequestering of lithium ions, shifting the product distribution in favour of the *E*-enolate (**Scheme 1.5B**).⁽²⁷⁾ It is worth noting that this relationship begins to erode with inclusion of substituents at **R**¹ that are capable of stabilizing the resultant enolate through resonance, in which case the *E*-enolate predominates regardless of the solvent condition employed (entry 3 and 4, **Table 1.2**).

1.5.4 Effect of Enolate Geometry on Product Distribution for Acyclic Substrates

Ireland's variant on the traditional aliphatic Claisen rearrangement maintains the same reaction trajectory as that found for the analogous acyclic allyl vinyl ether system, namely being that it passes through a chair-like transition-state structure *en route* to the rearranged product.^(33, 34) The stereochemical consequence of a chair-type transition-state structure is two-fold:

- (1) Firstly, the presence of the (pseudo)axial hydrogen atom at C6 imparts a stereochemical preference for formation of the *E*-trisubstituted olefin when a substituent is present at C4, (**Scheme 1.6A**).
- (2) Secondly, assuming substitution at C1 and/or C6, the relative stereochemistry at the newly generated carbon-carbon single bond can be discerned based on the geometry found within the original 1,5-diene framework (**Scheme 1.6B**).⁽²⁷⁾

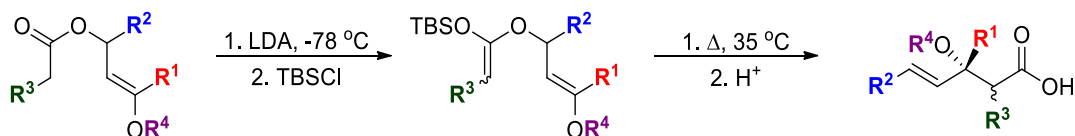


Scheme 1.6 Stereocontrol in the ester-enolate Claisen rearrangement.

1.6 Ireland Claisen Rearrangement: Effect of the C6 Oxygen for Acyclic Substrates

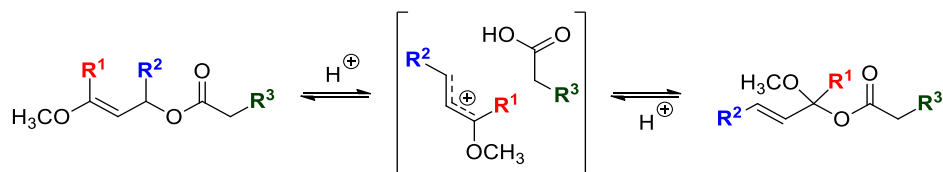
The inherent stereoselectivity in the ester-enolate Claisen rearrangement, coupled with the mild conditions for which the reaction is performed, makes it an attractive synthetic technique for construction of aldol-type products that may not be easily accessed using traditional methods (*see Chapter 4*).⁽³⁵⁾

Employing the ester-enolate Claisen rearrangement to access β -alkoxy acids required careful introduction of a masked hydroxyl substituent at C6 (**Scheme 1.7**) – marking the first appearance of bis-vinyl ethers, to the best of our knowledge, in the chemical literature.⁽³⁶⁾



Scheme 1.7 Ester-enolate Claisen rearrangement offers access to tertiary alcohols, resembling aldol-type products, with high stereocontrol.

Incorporation of this new functionality into the allyl backbone was not found to be trivial. Such substrates displayed a marked increase in lability compared to the parent system, particularly when $R^2 \neq H$ (**Scheme 1.8**), and were found to be susceptible to decomposition upon aqueous workup.⁽³⁶⁾ While the products of the decomposition pathway were not elucidated in this earlier work, a later report discussed the propensity of these compounds to undergo allylic rearrangement in the presence of a catalytic amount of acid (**Scheme 1.8**).⁽³⁷⁾



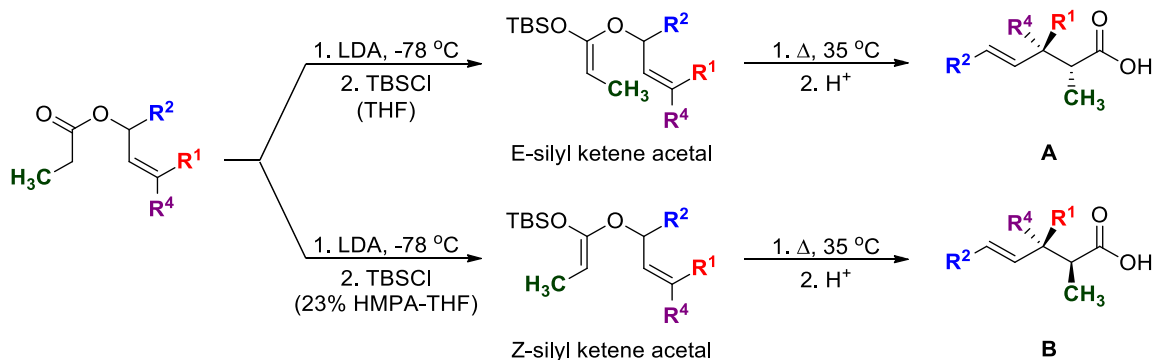
Scheme 1.8 Alkoxy substituent at C6 leads to allylic rearrangement in the presence of a catalytic amount of acid.

These findings were the first to indicate that alkoxy substituents at C6, in an acyclic system, could result in a significant weakening of the C4–O3 bond adjacent the enol-ether. If one considers that the backbone of allyl ester in **Scheme 1.8** strongly resembles the bond connectivity found in furanoid or pyranoid glycals (discussed in **Section 1.7**), then this

latent reactivity is not entirely unexpected and is, in fact, a well-documented phenomenon that has been described by other research groups in the carbohydrate literature.(38, 39) Formation of the undesirable, [1,3]-rearranged by-product can be suppressed by washing the crude ester with base prior to purification by distillation,(37) or through immediate trapping of the crude enolate as the corresponding silyl ketene acetal.(36)

Assuming a chair type transition-state structure, where deprotonation of the ester is the kinetic determinant for the geometry the enolate,(17) the distribution of products was found to be reversed upon changes to solvent polarity (**Table 1.3**). Introduction of the alkoxy functionality at **R⁴** led to slight erosion in the diastereoselectivity of this transformation (entry 5 and 6) when compared to the parent system (entry 1 and 2), although not to any significant extent.

Table 1.3 Ester-enolate Claisen rearrangement of parent and C6 alkoxy-substituted allyl propionates.^a

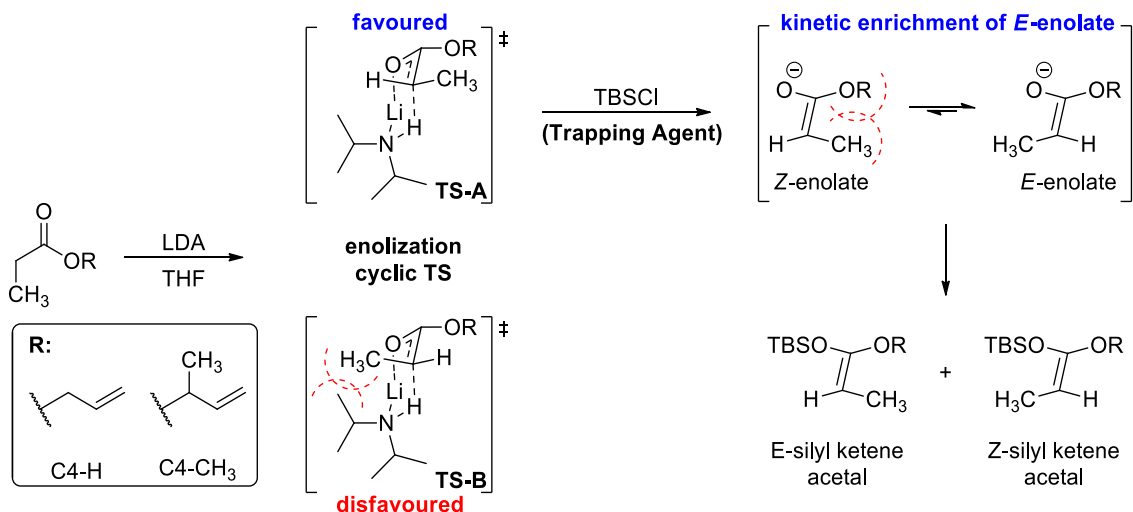


| Entry | R ¹ | R ² | R ⁴ | Solvent | Yield (%) | A : B ^c | t _{1/2} ^d |
|----------------|-------------------------------|-----------------|------------------|--------------|-----------|--------------------|-------------------------------|
| 1 ^b | CH ₃ | H | H | THF | 75 | 89 : 11 | - |
| 2 ^b | CH ₃ | H | H | 23% HMPA-THF | 75 | 14 : 86 | - |
| 3 | H | H | OCH ₃ | THF | 80 | 82 : 18 | ≤ 5.0 |
| 4 | H | H | OCH ₃ | 23% HMPA-THF | 75 | 20 : 80 | ≤ 5.0 |
| 5 | CH ₃ | H | OCH ₃ | THF | 76 | 83 : 17 | 9 ± 2 |
| 6 | CH ₃ | H | OCH ₃ | 23% HMPA-THF | 80 | 23 : 77 | 9 ± 2 |
| 7 ^e | C ₆ H ₅ | H | OCH ₃ | THF | 67 | 53 : 47 | 42 ± 8 |
| 8 ^e | C ₆ H ₅ | H | OCH ₃ | 23% HMPA-THF | 72 | 48 : 52 | 42 ± 8 |
| 9 | CH ₃ | CH ₃ | OCH ₃ | THF | 60 | 70 : 30 | 10 ± 2 |
| 10 | CH ₃ | CH ₃ | OCH ₃ | 23% HMPA-THF | 59 | 22 : 78 | 10 ± 2 |

^aData from references (36) and (37). ^bData from reference (27). ^cRatio of diastereomers A and B as determined by NMR analysis. ^dHalf-life, in minutes, at 35 °C for Claisen rearrangement, as determined by NMR analysis. ^eIsolated as the methyl ester.

The most intriguing results were those that were found to originate from a combination of alkoxy-substitution at R⁴ with additional substitution at R¹ or R². Substitution at R² (or

formally C4) in this series appears to only impact the diastereoselectivity when enolization of the ester is performed in THF (**Table 1.3**, entry 9). Assuming a chair-type transition state is favoured, the ratio of A:B should correspond to the amount of *E*- and *Z*-silyl ketene acetal generated in the first synthetic operation. Recall that, in a weakly coordinating solvent, ester enolization occurs through one of two cyclic (or expanded cyclic) transition states, **TS-A** or **TS-B**, where lithium is coordinated to the enolate oxygen (**Scheme 1.9**). **TS-B** is higher in energy, relative to **TS-A**, due to a 1,3-diaxial interaction that exists between the C1 methyl and the isopropyl chain of LDA. It is expected that the *Z*-enolate predominates under these conditions and is formed in the same ratio as that exhibited for those substrates where \mathbf{R}^2 (C4) = H. Addition of a trapping agent (*e.g.*, TBSCl) leads to disruption of **TS-A**, at which point some of the liberated enolate can isomerize to the lower energy *E*-conformer just prior to silylation. When $\mathbf{R}^2 = \text{H}$, the $A_{1,3}$ strain is not as substantial as when $\mathbf{R}^2 = \text{CH}_3$ and so the observed kinetic enrichment of the *Z*-silyl ketene acetal is only apparent in the latter case, as is made evident by the significant erosion in diastereoselectivity for this substrate (**Table 1.3**, entry 9).

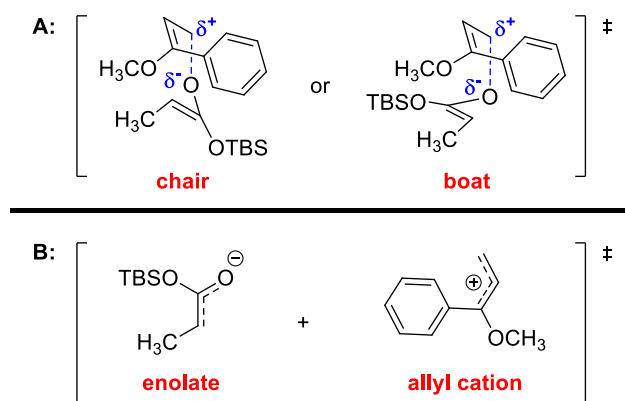


Scheme 1.9 Kinetic enrichment of the *E*-enolate, when C4 = CH₃, leads to erosion in diastereoselectivity for the ester-enolate Claisen rearrangement.

Unlike in the former example, the complete loss of diastereoselectivity when $R^1 = C_6H_5$ is not so easily explained (entry 7 and 8, **Table 1.3**). In the absence of an alkoxy substituent at R^4 , aryl substitution at C6 has no deleterious effect on the stereoselectivity of the reaction (*i.e.*, the reported *dr* in such cases can range anywhere from 6:1 to 20:1).⁽⁴⁰⁻⁴⁴⁾ The absence of such an effect when $R^4 = OCH_3$ and $R^1 = CH_3$ may suggest that the resulting diastereomeric ratio is the result of the specific combination of substituents at C6.

Two possible explanations exist for the change in diastereoselectivity for the reaction pictured in **Scheme 1.10**. The first is that the presence of the C6 oxygen may lead to an increase in O3–C4 bond breaking, resulting in a much more “loose,” dipolar transition-state structure (**Scheme 1.10A**).⁽⁴⁵⁾ This effect would be exacerbated in the presence of two donor groups at C6 through additional resonance stabilization of the resulting allyl cation. The “loose” nature of the transition state would also lend itself to lowering the

energy of the boat-conformer by greatly diminishing any unfavourable steric interactions that exist between C2 and C5 to the point where passing through a boat- or chair-TS structure become equally probable reaction trajectories. The second possibility, put forth by Ireland, is that the rearrangement for this substrate may be the result of a non-concerted pathway (**Scheme 1.10B**),⁽³⁶⁾ where an allyl cation and a silyloxy enolate are generated during the course of the reaction and recombine to afford a 1:1 mixture of diastereomers.



Scheme 1.10 A “loose” (A) or dissociative (B) transition state may be responsible for the observed loss of stereocontrol in the ester-enolate Claisen rearrangement when C6 bears two electron donating substituents.

The implication of the bond lengthening at O3–C4 will be the subject of greater discussion in later sections. While these two postulates are related, differing only by the extent to which O3–C4 bond breaking occurs in the transition state, they have drastically different ramifications for understanding and controlling the distribution of products. As the Claisen rearrangement is one of high synthetic utility in forging new carbon-carbon bonds, it goes without saying that much time has been devoted to trying to understand the mechanism of this reaction, particularly when the system bears a γ -alkoxy allylic substituent.

1.7 Ireland Claisen Rearrangement: Effect of the C6 Oxygen for Cyclic

Substrates

1.7.1 Ester-Enolate Claisen Rearrangement of Glycol Derivatives: TS Geometry

As an extension of the methodology outlined in **Section 1.6**, for which the acyclic substrates served as a model system, Ireland developed a general, stereoselective approach to accessing structural analogues of polyether antibiotics *via* the ester-enolate Claisen rearrangement of furanoid and pyranoid glycols.(37)

Two characteristic structural features, present in nearly all polyether antibiotics, originate from differences in stereospecific attachment of a chiral carbon residue to C1 of the saturated oxygen-containing heterocycle: the first appears as an aldol-type structure with a 1,3 relationship for carbon-oxygen attachment (red) while the second provides a glycol diether through a 1,2-attachment of the carbon-oxygen bond (blue) (**Figure 1.2**).

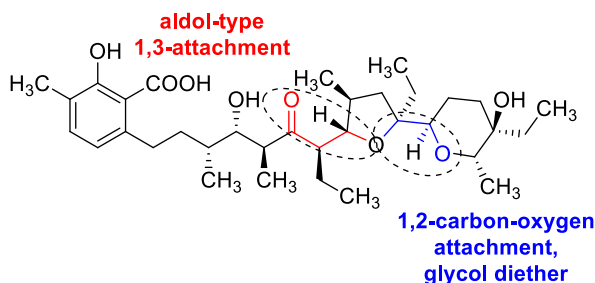
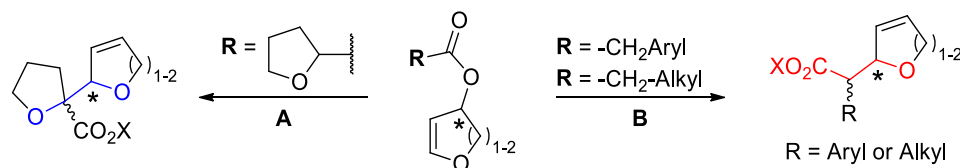


Figure 1.2 Lasalocid A.

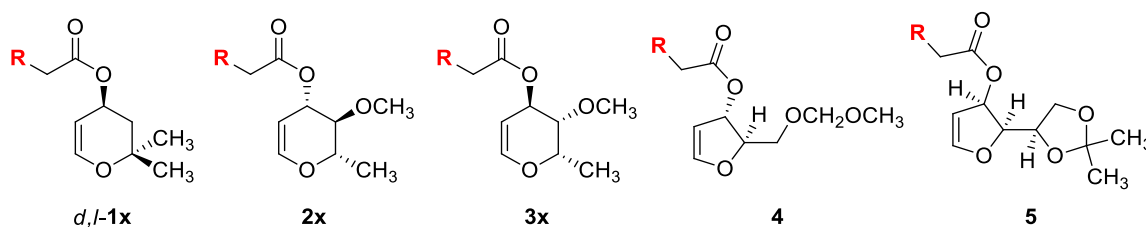
Due to the inherent stereoselectivity of the ester-enolate Claisen rearrangement, one can envision utilizing the aforementioned reaction to specifically generate the distinguishing carbon-carbon bond connections found in naturally occurring ionophores, **Scheme 1.11**,

simply by varying the identity of the α -substituents between aliphatic (**B**, to form the aldol-type structural unit) and α -alkoxy (**A**, to form the glycol diether congener) functionality.



Scheme 1.11 Ester-enolate Claisen rearrangement of furanoid or pyranoid glycols.

Much like their acyclic counterparts (**Section 1.6**), preparation of cyclic esters derived from furanoid or pyranoid glycols were found to be susceptible to unwanted acid-catalyzed rearrangements, albeit to a greater extent (an attribute that will become important later in the document). Again, this reactivity could be mitigated through preparation of the ester without isolation prior to use. Generation of the silylketene acetal was found to provide the expected reversal in diastereoselectivity upon changes to solvent polarity, while products formed in the ester-enolate Claisen rearrangement were found to generally be of higher yield than the analogous acyclic series (**Table 1.4**).

Table 1.4 Ester-enolate Claisen rearrangement of furanoid and pyranoid glycols.^a

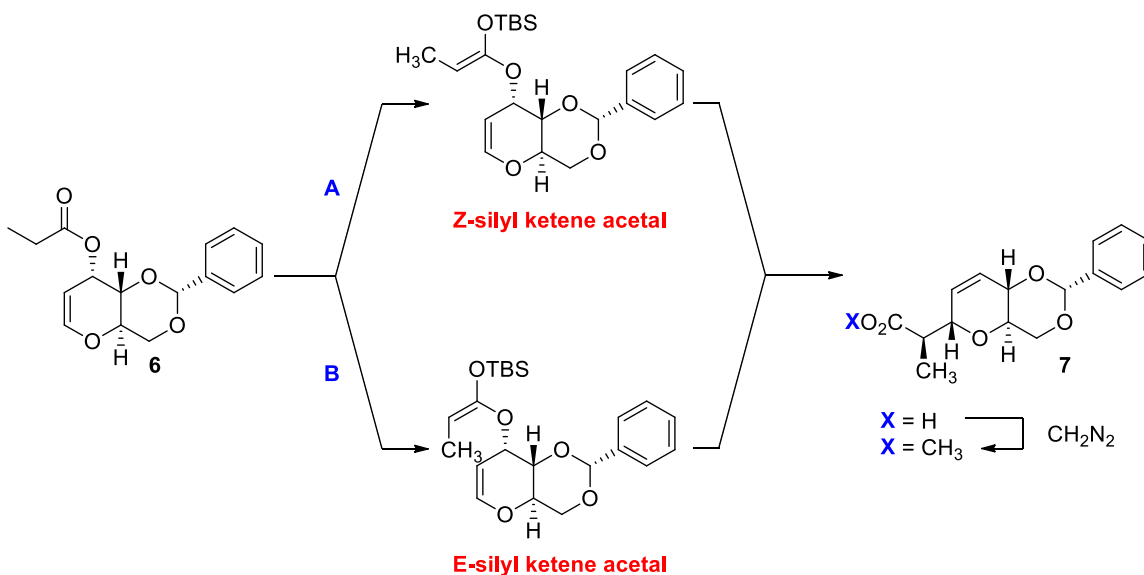
| Entry | Substrate | R | Solvent ^b | Yield (%) | a : b ^c |
|-------|----------------|-------------------------------|----------------------|-----------|--------------------|
| 1 | <i>dl</i> -1 | CH ₃ | 23% HMPA-THF | 79 | 1 : 11 |
| 2 | 2 | CH ₃ | THF | 73 | 4 : 1 |
| 3 | 2 | CH ₃ | 23% HMPA-THF | 71 | 1 : 4 |
| 4 | 2 ^d | CH ₃ | THF | 79 | 4 : 1 |
| 5 | 3 ^d | CH ₃ | THF | 69 | 4 : 1 |
| 6 | 3 ^d | CH ₃ | 23% HMPA-THF | 74 | 1 : 4 |
| 7 | 4 ^d | C ₂ H ₅ | THF | 73 | 4 : 1 ^e |
| 8 | 4 ^d | C ₂ H ₅ | 23% HMPA-THF | 60 | 1 : 4 ^e |
| 9 | 5 ^d | CH ₃ | THF | 52 | 4 : 1 |
| 10 | 5 ^d | CH ₃ | 23% HMPA-THF | 54 | 1 : 1 |

^aData taken from reference (37). ^bSolvent employed during deprotonation of the ester. ^cDetermined by ¹H NMR analysis, where the high field resonance for the α -proton is designated as “a” and the low field resonance for the α -proton is designated as “b” for two diastereomers produced. ^dEster was prepared from the corresponding allyl alcohol just prior to use and was not isolated. ^eDetermined by GC analysis of the hydrogenated methyl ester.

It is worth noting that Ireland refrained from assigning the relative configuration for the two resulting diastereomeric products, “a” and “b,” in **Table 1.4**. While the Claisen rearrangement of acyclic substrates is expected to pass through a chair-like transition state,

the stereochemical assignment of the cyclic derivatives (derived from pyranoid or furanoid glycols) is more difficult to assign. The inherently reduced conformational flexibility of cyclic substrates makes the nature of the transition state rather elusive. Ill-defined non-bonding interactions may actually lead to preferential formation of a boat-type TS-structure.(46)

A rather anomalous result, in a later report, prompted Ireland to address this very question. While investigating the ester-enolate Claisen rearrangement of propionate esters, *en route* to the Prelog-Djerassi lactone,(20) it was discovered that the major rearranged product that resulted from the enolate generated in either THF (**B**) or 23% HMPA-THF (**A**) was ester **7**, rather than the expected epimeric products at C α that should have formed under the complementary set of reaction conditions (**Scheme 1.12**).



Scheme 1.12 Ester-enolate Claisen rearrangement of **6** in 23% HMPA-THF (**A**) or THF (**B**) afforded ester **7**, rather than the expected epimeric products at C α .

Seeing that the stereochemical outcome of the enolization for these substrates had been firmly established in both cyclic- and acyclic-derivatives of glycols of this type, it was suggested that ester **7** had to be the result of differing nature of the transition state structure (**Figure 1.3**).

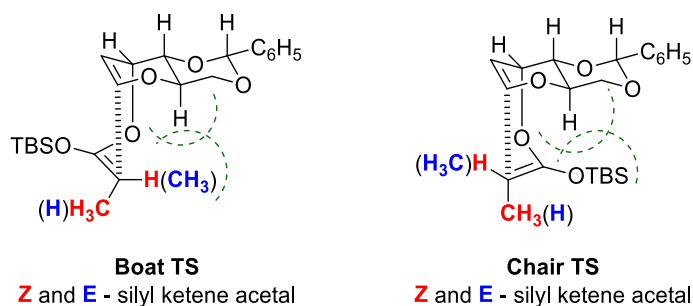


Figure 1.3 Non-bonding interactions present in the transition state for the ester-enolate Claisen rearrangement of ester **6**.

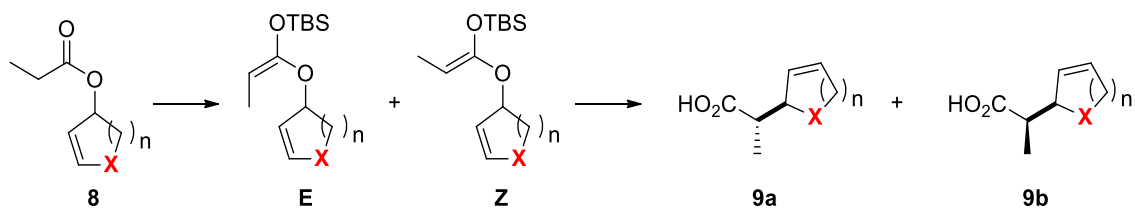
Under the complementary set of reaction conditions used for the [3,3]-sigmatropic rearrangement of ester **6**, it appeared that the chair-type transition state for either the *E*- or *Z*-silyl ketene acetal would be destabilized by the presence of the bulky *tert*-butyldimethylsilyloxy substituent at C2. The *E*-silyl ketene acetal, however, would suffer similar steric encumbrance in the boat-type transition state as result of the methyl at C1. Thus, the *E*-enolate would have preference for a boat-type transition state, producing a 9:1 mixture of diastereomers,³ while the *Z*-enolate suffers from diminished stereocontrol

³ A more recent report by Kishi (*Org. Lett.* **2009**, 409) on the ester-enolate Claisen rearrangement of pyranoid glycols provides an alternate explanation for the observed loss in stereocontrol for this reaction. In this Letter, Kishi reports that both the *E*- and *Z*-silyl ketene acetal pass through a boat-like transition state but, due to a larger degree of steric congestion, the *E*-isomer rearranges more slowly. Upon heating the *E*-silylketene acetal undergoes a thermally induced isomerization to the *Z*-isomer, leading to a shift in product distribution towards a single diastereomeric product under the complementary set of reactions conditions (*i.e.*, enolization in THF versus 23% HMPA-THF).

during the course of the reaction ($dr = 35:65$), with preference for the chair conformation. Subsequent work, from the Ireland laboratory, for the synthesis of (+) - and (-)-nonactic acids provided similar results, where a preference for a boat-type transition state for either the *E*- or *Z*-conformer, in the absence of any outstanding steric constraints, was observed for the rearrangement of glycal silyl ketene acetals.(18, 22, 47)

In a later investigation it became clear that the C6 oxygen played a significant role in influencing the reaction trajectory for the Claisen rearrangement in cyclic systems (**Table 1.5**).(45) While the differences in steric and conformational flexibility should be minor for exchange of a methylene ($X = \text{CH}_2$) for an oxygen atom ($X = \text{O}$) at C6, the inclusion of the C6 oxygen in compound **8** was found to afford a relatively high stabilization of the boat transition-state structure, relative to a chair, by approximately 1.0–2.2 kcal.mol⁻¹.

Table 1.5 Ester-enolate rearrangement of carbocycles and cyclic glycols.(45)



| Entry | X | n | Solvent ^a | E : Z | 9a : 9b | Favored TS |
|-------|---|---|----------------------|--------------|---------|------------|
| 1 | C | 1 | THF | ^b | 75 : 25 | chair |
| 2 | C | 1 | THF / 23% HMPA | ^c | 40 : 60 | chair |
| 3 | O | 1 | THF | ^b | 43 : 57 | boat |
| 4 | O | 1 | THF / 23% HMPA | ^c | 80 : 20 | boat |
| 5 | C | 2 | THF | 83 : 17 | 84 : 16 | chair |
| 6 | C | 2 | THF / 45% DMPU | 4 : 96 | 72 : 28 | boat |
| 7 | C | 2 | THF / 23% HMPA | 14 : 86 | 73 : 27 | boat |
| 8 | O | 2 | THF | ^b | 29 : 71 | boat |
| 9 | O | 2 | THF / 45% DMPU | ^c | 86 : 14 | boat |

^aSolvent employed for enolization of the ester. ^bEnolization in THF forms predominantly the *E*-silyl ketene acetal. ^cEnolization in the presence of DMPU or HMPA forms predominantly the *Z*-silyl ketene acetal.

Since the difference in energy for the chair and boat transition states in the carbocyclic series is quite small (*ca.* 1 kcal.mol⁻¹), the additional stabilization afforded to the boat-transition state when X = O must be electronic in nature. Two rationales were put forth to explain the inherent change in preference on the basis of disparate stereoelectronic stabilization of the two transition-state geometries:

1. In **Figure 1.4**, both the *E*- and *Z*-silyl ketene acetal exhibit slight preference for the boat geometry due to fewer destabilizing steric and/or electronic-repulsive interactions between the silyloxy substituent and the ring $-\mathbf{XCH}_2-$. Relative to the parent allyl vinyl ether, silyloxy substitution at C2 leads to a significant degree of homolytic O3–C4 bond cleavage through stabilization of the π -bond of the developing oxyallyl radical species, lowering the energy of activation by 9 kcal.mol⁻¹.(27, 48) The boat-geometry is considered to be the more “loose” of the two conformations, and so the tipping point for lowering the energy of the boat-geometry relative to the chair would rely upon an electronic effect that would offer greater stabilization of the allyl fragment in the more “loosely” held conformation, where the allyl radical would be developed to a greater extent. The presence of an electron-donating group at C6 would accomplish this, a result made all the more dramatic when the substituent is capable of affording this additional stabilization through resonance (*i.e.*, when $\mathbf{X} = \text{O}$).
2. An alternate explanation, which differs from the former on the basis of the nature of the transition state species (diradical *versus* dipolar), is the vinylogous anomeric effect. Discussed in **Section 1.9**, the vinylogous anomeric effect would lead to an increase in the dipolar character of the transition state through lengthening of the O3–C4 bond, thus relying on a C6-substituent’s ability to stabilize the cationic allyl fragment in the transition-state structure. Preference for one transition state geometry over another, in this case, would be derived from the number of contacts made between the two fragments of the molecule. Coulombic attraction between the two ends of the dipole for the “allyl-oxyallyl” pair would be greater in the boat-shaped transition state (where 6-atom overlap can be achieved), as opposed to the chair (4-atom overlap), leading to

an observed reaction trajectory where the stereochemical outcome in the product is found to originate from a boat-like TS. While the vinylogous anomeric effect would also be operative in acyclic systems, the effect would be diminished by the rotational flexibility of the C6–O bond, whereas in the furanoid and pyranoid glycal series the C6-oxygen is stereoelectronically locked – affording the necessary orbital overlap required for greater stabilization of the allyl cation.

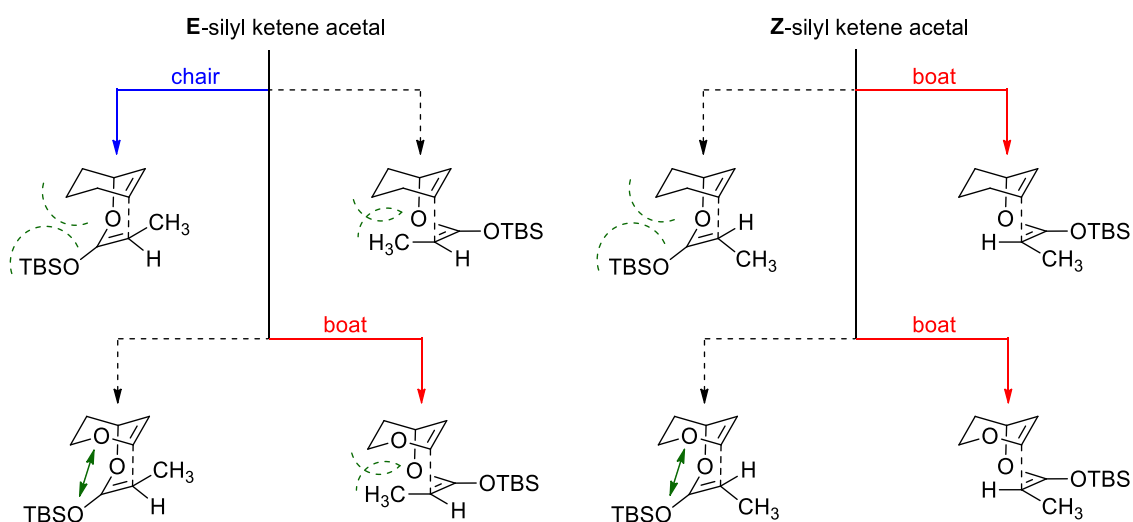
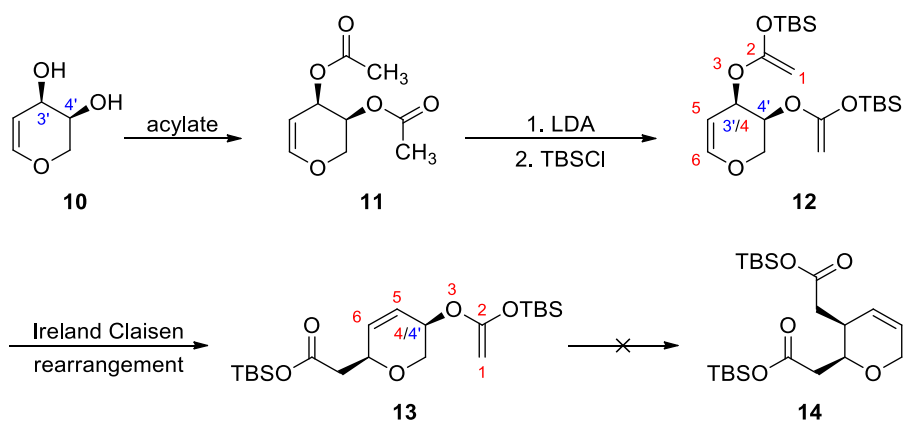


Figure 1.4 Conformational constraints and electronic repulsive interactions for trapped ester-enolates of cyclohexene and pyranoid glycal derivatives. Steric interactions between the silyloxy and C1-CH₃ with the ring system are reduced for cyclopentene and furanoid glycal derivatives (not shown), exhibiting a preference for the chair- and boat-geometry in the transition state when X = CH₂ and O, respectively.

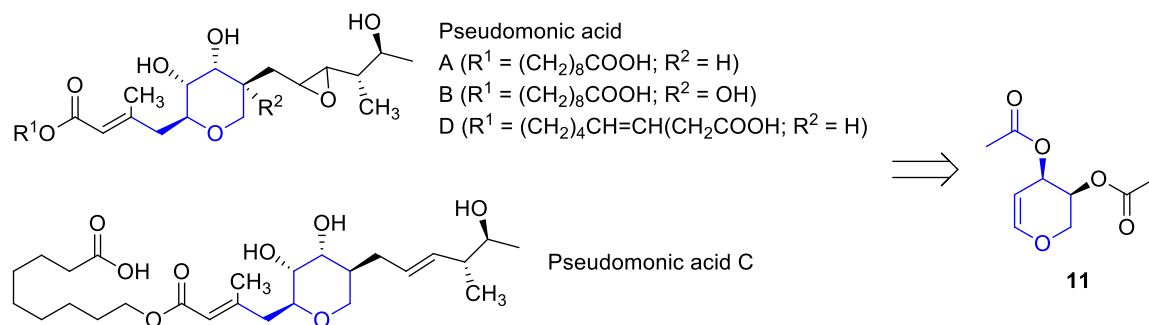
1.7.2 Ester-Enolate Claisen Rearrangement of Glycol Derivatives: Rate of Rearrangement

While Ireland's work on the ester-enolate Claisen rearrangement of glycol substrates clearly highlighted the utility of his "building block" approach to the synthesis of natural products and biologically relevant C-glycosyl compounds, the extensive protection-deprotection sequences that are perceived to be required to chemically differentiate between the remaining hydroxyl groups on the carbohydrate ultimately detracted from the synthetic utility of this otherwise generally useful methodology.⁽⁴⁹⁾ In an effort to overcome these limitations, Curran sought to develop a protecting-group free protocol that would enable chemical differentiation of the pendant hydroxyl groups on the basis of a chemoselective Claisen rearrangement of a bis(ketenesilyl) acetal (**12**) derived from **10**, **Scheme 1.13**, where the *mono*-Claisen rearranged product (**13**), resulting from acylation of the hydroxyl functionality at C3', would predominate without succumbing to further reactivity through a second possible rearrangement of this type (*i.e.*, to afford **13**, but not **14**).⁽⁴⁹⁻⁵¹⁾



Scheme 1.13 Chemical differentiation of the pendant carbohydrate hydroxyl functionality through chemoselective ester-enolate Claisen rearrangement. Carbohydrate numbering is shown in blue, while allyl vinyl ether numbering is in red.

This work⁽⁵⁰⁾ led into a series of publications examining the selectivity of a *mono*-Claisen rearrangement as it was applied to the synthesis of a class of C-glycoside antimicrobial agents known as pseudomonic acids (**Scheme 1.14**).



Scheme 1.14 Pseudomonic acids A, B, C and D.

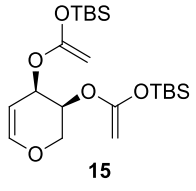
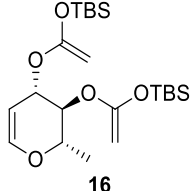
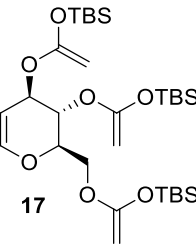
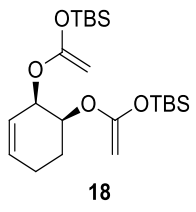
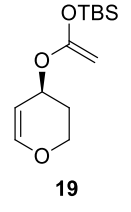
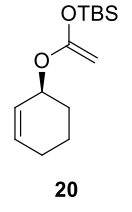
At the time of this discovery, substituent effects on the rate of Claisen rearrangement had not been extensively quantified,⁽⁵²⁾ although theoretical predictions by Carpenter⁽⁵³⁾ purported that an electron donating substituent at C6 would lead to an increase in the enthalpy of activation, ΔH^\ddagger , a result that clearly contradicts the experimental outcome of the investigation discussed above (*i.e.*, the C6 oxygen appears to lower the barrier to activation). Intrigued by the apparent disparity between the theoretical and experimental results, Curran performed a series of kinetic investigations to ascertain origin of acceleration for the first Claisen rearrangement.^(51, 54)

A selection of the key results of this kinetic investigation are summarized in **Table 1.6**. All rate constants were measured over several half-lives and were found to obey first order kinetic approximations, where the rate of the first Claisen rearrangement (k_1) was found to be 20-575 times faster than the rate of the second Claisen rearrangement (k_2) (entries 1-

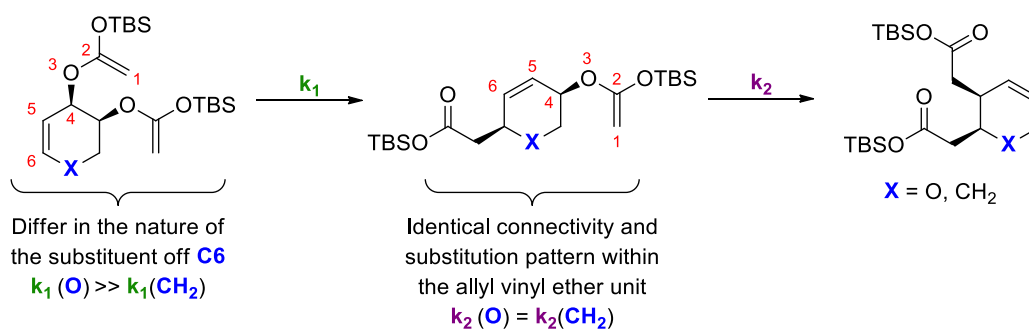
3).(51) Interestingly, exchange of the pyranoid backbone for an all carbon analogue revealed little discrepancy between its k_1 and k_2 (entry 4).(51, 54) In addition, cross comparison of the rate constants for substrates **15** and **18** (entry 1 vs. entry 4) clearly demonstrate that the rate enhancement of the first Claisen rearrangement is a direct result of the γ -allylic oxygen present in **15** (*i.e.*, $k_1(\mathbf{15})$ is much larger than $k_1(\mathbf{18})$, with no observable difference in k_2 between either substrate; **Scheme 1.15**).⁴

⁴ The rate constant for the [3,3]-sigmatropic rearrangement of pyranoid glycal **15** and its cyclohexene analogue (**18**) were measured at 70 °C and 65 °C, respectively. Assuming differences in conformational and/or steric preferences are negligible, the expectation is that the reaction performed at a higher temperature should be accompanied by a larger rate constant. As such, the 1.5-fold increase in k_2 for **15** is likely an artifact arising from the alteration to the condition for which the experiments were conducted. For all intents and purposes, k_2 is considered to be equal in magnitude in both the pyranoid and cyclohexene substrate.

Table 1.6 Kinetic data for tandem ester-enolate Claisen rearrangements of pyranoid glycols.

| Entry | Substrate | k_1 (sec ⁻¹) ^{a,b} | k_2 (sec ⁻¹) ^{a,b} | Temperature ^c | k_1/k_2 |
|-------|---|---|---|--------------------------|-----------|
| 1 |  | 48 | 2.5 | 70 | 20 |
| 2 |  | 200 | 0.35 | 60 | 575 |
| 3 |  | 160 | 0.71 | 60 | 225 |
| 4 |  | 3.3 | 1.7 | 65 | 2 |
| 5 |  | 44 | - | 60 | 10 |
| 6 |  | - | 4.8 | 60 | |

^aRate as determined by integration of ¹H NMR resonances in *d*₆-benzene, under an inert atmosphere of N₂, over several half-lives. ^bRate × 10⁻⁵ s⁻¹. ^cTemperature in °C.

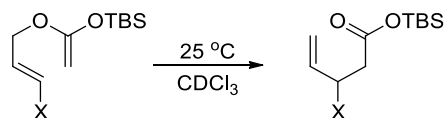


Scheme 1.15 Tandem ester-enolate Claisen rearrangement.

Attempts to rationalize the difference in the rate of tandem Claisen rearrangement for these substrates on the basis of steric or conformational arguments was superseded by the observation that **19** and **20**, which should possess similar steric and conformational preferences, underwent [3,3]-sigmatropic rearrangement at significantly different rates (**Table 1.6**, entries 5 and 6).

While these cyclic examples are known to proceed through a boat-type transition state, and are thus predicted to be more sensitive to electronic effects at C6 relative to their acyclic counterparts, the same general trend was also observed in an acyclic series, shown in **Table 1.7**, and was later rationalized on the basis of a stereoelectronic argument that Curran dubbed the “vinylogous anomeric effect.”^(54, 55)⁵

⁵ The vinylogous anomeric effect was first coined in 1984 by Denmark to describe the axial preference of α -chloro-substituted ketoximes (prepared from α -chlorocyclohexanone) as a result of $n\text{-}\sigma^*$ interaction of the lone pair of electrons on the chlorine being transmitted through the $\pi^*\text{C=N}$.

Table 1.7 Rate of the Claisen rearrangement of C6-substituted silyl ketene acetals.^a

| Entry | X | k^b | k_{rel} |
|-------|------------------|-------|------------------|
| 1 | H | 1.4 | 1 |
| 2 | CH ₃ | 1.7 | 1.2 |
| 3 | OCH ₃ | 48 | 35.5 |

^aData from reference (54). ^bRate $\times 10^{-5} \text{ s}^{-1}$.

1.8 The Vinylogous Anomeric Effect

As was evidenced in the previously described study by Curran, the inclusion of a substituent that is electron donating by resonance, but not by induction, at C6 leads to a significant increase in the rate of Claisen rearrangement for both cyclic and acyclic allyl vinyl ethers (Section 1.7.2, Table 1.6 and 1.7).(54) The stereoelectronic enhancement ascribed to the C6-oxygen, known as the vinylogous anomeric effect, is described as a molecular orbital π - σ^* stabilization of the vinyl ether, the consequence of which is a weakening of the O3–C4 bond as a result of populating an antibonding orbital (Figure 1.5A).(54) While stabilization of the vinyl ether, *via* the γ -allylic oxygen, would be expected to lower the energy of the ground state of **21** (and therefore decrease the rate of reaction), the alternate resonance “double-bond – no-bond” depiction(51) of this effect (Figure 1.5B) highlights the chemical consequence of the increase bond length at O3–C4 – namely that the TS structure is stabilized to a greater extent by the vinylogous anomeric effect than is the ground-state, with an overall net acceleration being expected.(51)

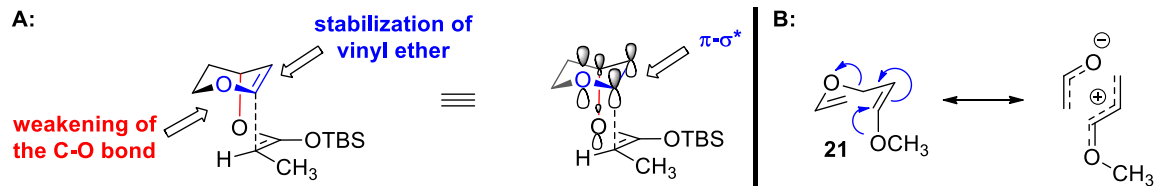


Figure 1.5 Vinylogous anomeric effect.

1.9 Electronic Structure of the Transition State

If one returns to the two postulates in **Section 1.7.1**, proffered as an explanation for the observed preference for a boat-type transition state on the basis of a stereoelectronic argument, where the purpose of the C6-oxygen is to stabilize the developing (electron deficient) allyl fragment, and combine these with the role of the C6-oxygen operative in the vinylogous anomeric effect (where the $\pi\text{-}\sigma^*$ interaction results in a decrease in bond order for O3–C4) then all three explanations are related – if based solely on the extent to which the O3–C4 bond is lengthened in the transition state. This single feature imparted by the C6-oxygen has serious implications on the mechanistic picture that has been envisaged for the Claisen rearrangement (**Figure 1.6**).

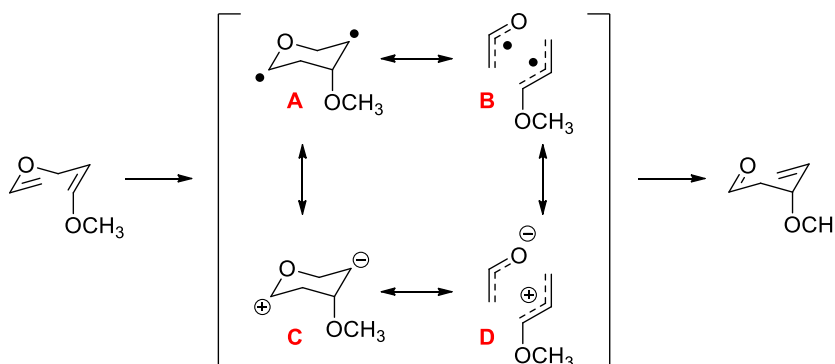


Figure 1.6 Mechanistic options for the aliphatic Claisen rearrangement: diyl (A), diradical (B), dipolar (C) and ion-pair (D).

Traditionally, the Claisen rearrangement has been accepted to occur through a concerted, albeit asynchronous,(56-58) bond reorganization process *via* a six-membered cyclic transition state,(59, 60) although many details of the reaction trajectory remain elusive. In particular, the precise electronic structure for the reaction is difficult to interpret. Depending on the substitution pattern off the allyl vinyl ether scaffold, the transition-state structure may lie anywhere on a continuum between a diradical(48, 61-68) (**Figure 1.6, A** or **B**) or dipolar(68-70) species (**Figure 1.6, C**), although theoretically it should be possible to access an enolate-allyl ion-pair (**Figure 1.6, D**) provided the right combination of substituents are present on the molecule or that the conditions for rearrangement are conducive to a two-step mechanism. It is thus conceivable that the extent of bond-lengthening imparted by alkoxy-substitution at C6 is capable of significantly altering the reaction trajectory towards a more polar, even dissociative, mechanism.

1.10 Degree of Charge Separation in the Transition State

The nature of the transition state can be derived through careful examination of solvent effects on the rate of reaction upon moving from non-polar (small dielectric constant, ϵ) to polar, protic media (large dielectric constant, ϵ). If the reaction under scrutiny were to be accelerated with increasing solvent polarity, this would be indicative of the development of a charged species in the transition state, where the magnitude of the observed solvent effect would correlate to the degree of charge separation/ionic character for a purported dipolar species.

Like many pericyclic reactions,(71) the Claisen rearrangement generally passes through a relatively non-polar transition state with considerable cyclic delocalization. Secondary kinetic isotopic studies on the aliphatic Claisen rearrangement have shown that the transition state occurs “early” with bond breaking well in advance of bond making.(58) While theoretical investigations do show some enolate/allyl cation character in the transition state, with charge separation calculated to be approximately 0.31 electron (**Table 1.8**)(72) for the parent system (**22**), this is too small to be signified by any extensive change in rate of rearrangement upon moving from benzene ($\epsilon_{\text{benzene}} = 2.3$) to acetonitrile ($\epsilon_{\text{acetonitrile}} = 37.5$; **Table 1.9**, entry 1).(69) The measured increase in the rate of rearrangement for the unsubstituted allyl vinyl ether (**22**) in polar, protic solvents such as methanol(69) ($\epsilon_{\text{methanol}} = 32.7$, **Table 1.9**) and water ($\epsilon_{\text{water}} = 80.1$, data not shown) (73, 74) is somewhat misleading; the origin of this reactivity has largely been attributed to enhanced hydrogen-bonding(75) in the transition state, entropic acceleration due to hydrophobic effects,(76, 77) and electronic polarization within the oxyallyl fragment(77) rather than stabilization of the putative charge separated allyl-allyloxy species suggested by Carpenter.(68) In addition, Gajewski’s(66) examination of secondary kinetic isotope effects for the rearrangement of allyl vinyl ether in solvents ranging from the relatively non-polar *m*-xylene ($\epsilon_{m\text{-xylene}} = 2.4$) to 75% aqueous methanol support this argument, as no significant changes in the extent of bond breaking in the transition state were observed.

Table 1.8 Changes in Mulliken charges and dipole moments for the parent and C6-hydroxy substituted allyl vinyl ether.

| | Δ charges | | | | | | | | ΔD^d |
|-------------------------|------------------|--------|--------|--------|--------|-------|----------------|-----------------|--------------|
| | C1 | C2 | O3 | C4 | C5 | C6 | O ^b | TS ^c | |
| AVE^a | 0.033 | -0.007 | 0.006 | -0.071 | -0.070 | 0.108 | - | ± 0.306 | 1.60 |
| 6-OH^e | -0.034 | -0.006 | -0.017 | -0.065 | 0.011 | 0.076 | 0.037 | ± 0.398 | 1.89 |

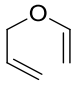
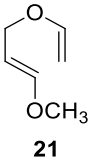
^aRef (61) and (67). ^bOxygen of OH. ^cCharge separation in the TS. ^dChange in dipole moment. ^eData taken from reference (72), calculated at the RHF/6-31G* level of theory for C6-OH substitution on the allyl vinyl ether (AVE).

The above description would thus seem to favour a transition state that more closely resembles a diradical (**Figure 1.6B**) species, without complete homolytic cleavage of O3–C4 bond. While it has been stated that this mechanistic picture may change with substitution of the allyl vinyl ether scaffold, the description of the transition state for substituents that are expected to aid in O3–C4 bond breaking (such as a γ -allylic oxygen) have been subject to much debate. No concrete evidence for the presence of the oxyallyl-allyl pair (**Figure 1.6D**), which should exist at the other end of this continuum, has been unambiguously identified.

At the heart of this debate is the study from Coates and Curran on the effect of alkoxy-substitution on the rate of Claisen rearrangement.⁽⁶⁹⁾ Quantitative assessment of the role of the C6-oxygen has undoubtedly affirmed its accelerating influence (**Table 1.9**)⁽⁶⁹⁾ which, in the absence of any additional substitution, results in a 9.5-fold enhancement for the rate of rearrangement of **21** in benzene, relative to the parent allyl vinyl ether (**22**). More importantly, a moderate solvent effect was observed for **21** upon moving from

benzene to acetonitrile, while little difference was exhibited for the parent compound, **22**. While this rate enhancement may be modest at best – and in no way is indicative of a charge separated species – it does nonetheless suggest the existence of a dipolar contributor to the transition state structure.

Table 1.9 The effect of C6-alkoxy substitution on the Claisen rearrangement.⁽⁶⁹⁾

| Entry | Substrate | k^c | k_{rel} | ΔH^\ddagger^d | ΔS^\ddagger^e | Solvent | T (°C) | k_{rel}^f |
|-------|--|----------------------|------------------|------------------------------|-------------------------------|-------------------------------------|--------|--------------------|
| 1 |  22 | 0.649 ^{a,b} | 1.0 | 25.4 ^a (± 0.7) | -15.9 ^a (± 1.5) | benzene- <i>d</i> ₆ | 134 | 1.0 |
| | | | | | | acetonitrile- <i>d</i> ₃ | 134 | 1.5 |
| | | | | | | methanol- <i>d</i> ₄ | 134 | 1.7 |
| 2 |  21 | 6.12 | 9.5 | 24.7 (± 0.3) | -12.8 (± 0.7) | benzene- <i>d</i> ₆ | 80 | 1.0 |
| | | | | | | acetone- <i>d</i> ₆ | 80 | 1.5 |
| | | | | | | acetonitrile- <i>d</i> ₃ | 80 | 3.2 |
| | | | | | | methanol- <i>d</i> ₄ | 80 | 68 |

^aData taken from Carpenter and Burrows(52). ^bStudy performed in di-*n*-butyl ether rather than in benzene. ^cRate $\times 10^{-6}$, s⁻¹ at 80 °C. ^dEnthalpy of activation expressed in kcal/mol. ^eEntropy of activation expressed in eu. ^fRelative to the rate of rearrangement for the compound in benzene.

In contrast to the parent compound, **22**, compound **21** is accompanied by a marked increase in the rate of Claisen rearrangement in methanol, with the rate of reaction proceeding 68 times faster than in benzene (**Table 1.9**). This appears to be much more substantial effect than the meager 1.7-fold rate enhancement observed for **22**, reinforcing the notion that the C6-oxygen contributes to the formation of a more “loosely” held transition-state structure.

Theoretical investigations support this observation, concluding that the C6-alkoxy substituent lengthens the C4–O3 bond by ~0.08–0.10 Å while bond making has been found to occur to a lesser extent than the parent system, with an increase in C1–C6 bond length of ~0.06–0.07 Å (**Table 1.10**).⁽⁷²⁾ Experimental secondary kinetic isotope effects are not available for compound **21**, however the computed charge separation predicted for the transition state, which has increased by approximately 0.1e compared to the parent system, is not large enough to indicate formation of the enolate-oxonium ion-pair.⁽⁷²⁾ It is entirely possible that the substantial increase in the rate of rearrangement is merely the result of greater accessibility of the enolate-oxygen in the TS due to an increase in O3–C4 bond length.^(66, 75) This is not an unreasonable assumption considering hydrogen-bond donating catalysts, such as Curran’s urea⁽⁷⁸⁾ and Jacobsen’s guanidinium derivative,⁽⁷⁹⁾ accelerate the rate of Claisen rearrangement when added to the reaction performed in benzene or hexanes, respectively. Curran also dismisses the formation of **D**, **Figure 1.6**, on the basis of experimental evidence that the entropy of activation is quite similar for **21** and the parent system (**22**), **Table 1.9**, with a large, negative ΔS^\ddagger that is characteristic of a transition state with a high degree of ordering.⁽⁶⁹⁾

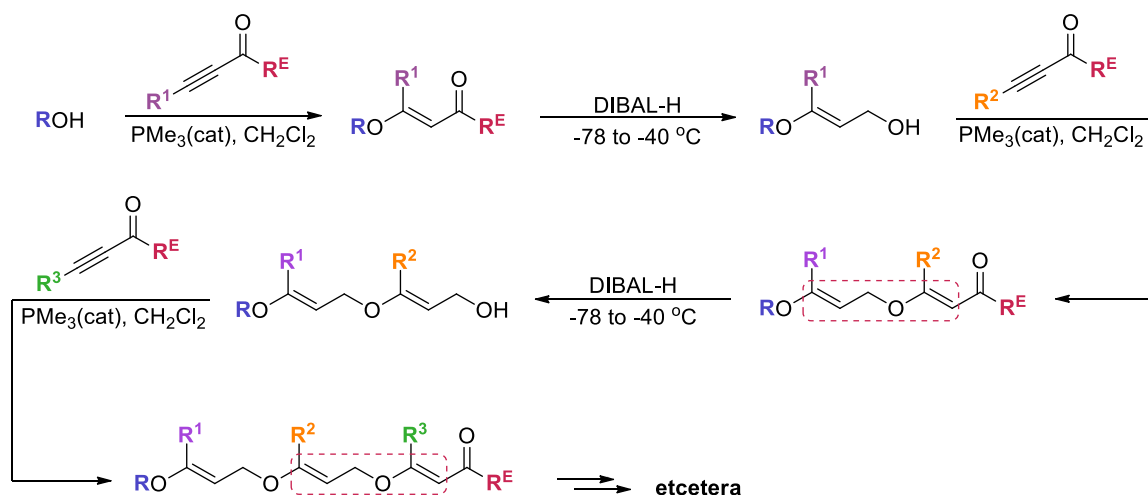
Table 1.10 Bond lengths (Å) calculated for optimized transition structures of the parent and C6-hydroxy substituted allyl vinyl ethers at the RHF/6-31G* level of theory.⁽⁷²⁾

| | C1-C2 | C2-O3 | O3-C4 | C4-C5 | C5-C6 | C6-C1 |
|--------------|-------|-------|-------|-------|-------|-------|
| AVE | 1.374 | 1.262 | 1.918 | 1.390 | 1.376 | 2.266 |
| C6-OH | 1.375 | 1.256 | 2.016 | 1.373 | 1.390 | 2.330 |

Despite the complete lack of experimental evidence for **D**, prior to our own investigations discussed in Chapter 3, there is a general consensus that a charge separated enolate-allyl cation transition state is not unreasonable – provided the parent structure be suitably decorated with a sufficiently good electron-donating group at either C4 or C6 and an electron-withdrawing group at C1 or C2.^(66, 73) Access to such compounds, however, is often thwarted by the profoundly enhanced rate at which these substrates undergo Claisen rearrangement, often precluding kinetic investigation.⁽⁶⁹⁾ Recent literature in the field provides subtle clues to suggest that the mechanism of Claisen rearrangement for such substrates (decorated as described above) may not be concerted, an inference very much in line with this earlier supposition.^(80, 81)

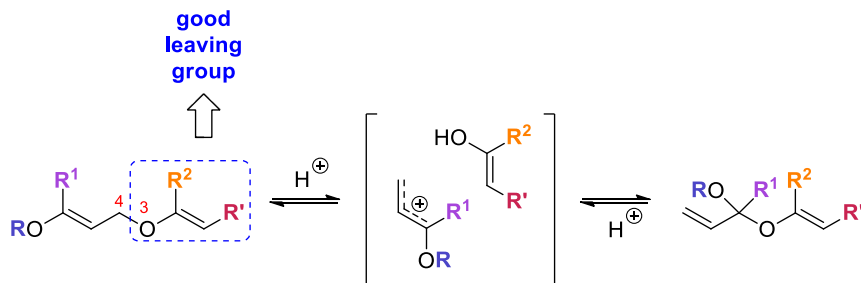
1.11 Summary

The most obvious conclusion that can be drawn about the chemical reactivity of bis-vinyl ether substrates is that they are highly prone to [3,3]-sigmatropic rearrangements, even at ambient temperature. If we consider our own proposed scaffold, upon which we intend to perform a variety of orthogonal transformations, at every other intermediary stage (*i.e.*, at every operational conjugate addition after the first) the molecule is set up to rapidly degrade due to a destabilized HOMO at the acting allyl fragment and a stabilized LUMO at the acting oxyallyl fragment (**Scheme 1.16**). The pendant functionality at the acting C2 (**R²**) and C6 (**R¹**) will undoubtedly contribute to this increase in reactivity, however certain combinations of substituents could possibly serve to mitigate unwanted Claisen rearrangements as well.



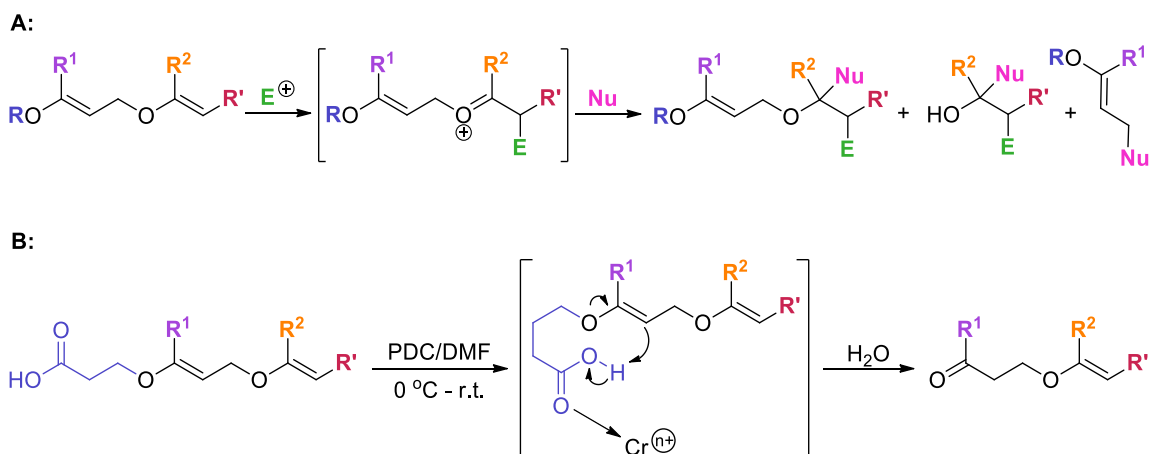
Scheme 1.16 Allyl vinyl ether units bearing EDGs at C6 and EWG at C1 within the oligovinyl ether framework.

Provided that the Claisen rearrangement in our own system can be understood, and even controlled, there are a number of additional concerns regarding the stability of our materials. Bis-vinyl ethers, and higher order congeners, are stabilized in the ground state by the vinylogous anomeric effect (see **Section 1.8, Figure 1.5**). The molecular orbital π - σ^* stabilization that results in population of the antibonding orbital will lead to some indiscernible decrease in C4–O3 bond order, ultimately placing additional electron density on the vinyl ether oxygen. As a direct result of an increase in the energy of the HOMO of the olefin (of the vinyl ether), these substrates will be more prone to react with acids and other electrophilic species – putting these compounds at greater risk for participating in unwanted side reactions (*e.g.*, **Scheme 1.17**).



Scheme 1.17 Acid catalyzed allylic rearrangement of bis-vinyl ether.

Selection of reagents for performing chemical transformations – particularly at the “orthogonal transformation” stage, as well as intramolecular functional group tolerability, will need to be considered when planning synthetic routes (**Scheme 1.18**).



Scheme 1.18 Destabilization of the alkene HOMO can result in unwanted intermolecular (A) or intramolecular (B) side reactions with electrophilic species.

1.12 Thesis Objectives

Our group has previously established an efficient, iterative protocol for synthesizing reactive (oligo)vinyl ether substrates. We hope to use this foundation to build in additional, complex architecture through cascade-type transformations. To achieve this goal, we will

need to acquire a better understanding of the chemical reactivity of our vinyl ether substrates.

Earlier work from our group established that bis-vinyl ether/alkyne conjugates are capable of participating in stannyl-mediated radical cascade cyclization reactions to afford functionalized hexahydro-2*H*-furo[3,4-*b*]pyrans through an apparent 6-*endo-trig*/5-*exo-trig* pathway.⁽⁸²⁾ While exploring substrate scope, it was discovered that the presence of two electron-withdrawing CF₃ substituents (at **R**¹ and **R**²) on the vinyl ether backbone resulted in the trapping of a 5-*exo-trig*/β-scission product. This result placed the purported 6-*endo-trig*/5-*exo-trig* cyclization under scrutiny. Was the difference in the electronic contributors, imparted by CF₃ substitution, affecting the mode of ring closure? Or did all substrates undergo an initial 5-*exo-trig* cyclization event where β-scission was favoured when **R**² = CF₃, while in all other cases a neophenyl rearrangement yielded the formal 6-*endo* intermediate? These questions are addressed in a thorough mechanistic study of the radical cyclization across bis-vinyl ethers in **Chapter 2**.

These earlier studies also found that certain combinations of substituents at **R**¹ and **R**² increased the propensity of bis-vinyl ethers to undergo Claisen rearrangement at remarkably low temperatures. If we intend to use bis-vinyl ethers as a reactive precursor for molecular complexity, we need to better understand the substituent effects governing their stability (**Chapter 3**). To this end, we chose to investigate the quantitative structure-reactivity relationship for a number of aryl-substituted bis-vinyl ethers in order to obtain a better picture of the nature of the transition state for the reported Claisen rearrangement.

This would, by extension, provide an understanding of the electronic contributors that promote (and impede) formation of β -alkoxy- γ,δ -unsaturated- β -ketoesters.

Finally, since our substrates are susceptible to Claisen rearrangement, we wanted to determine whether we could exploit this reaction for the development of an auxiliary-controlled diastereoselective variant to gain access to linear, aldol-type products containing highly congested, tertiary and quaternary vicinal stereocenters (**Chapter 4**).

Chapter 2 Radical Cyclization Across Bis-Vinyl Ethers

Adapted from:

Katherine A. Davies¹ and Jeremy E. Wulff¹

Organic Letters (2011) 13, 5552 – 5555

and

Natasha F. O'Rourke,¹ Katherine A. Davies¹ and Jeremy E. Wulff¹

Journal of Organic Chemistry (2012), 77, 8634 – 8647.

¹Department of Chemistry, University of Victoria, Victoria, BC, Canada

NFO performed all syntheses and investigations for the development of masked acyl radical precursors and protecting group strategies for ethyl propiolate. Work performed by KAD was the primary feature of the earlier communication published in *Organic Letters*.

NFO developed the research, performed syntheses, and collected and analyzed data for the full paper published in the *Journal of Organic Chemistry*. Writing of the manuscript was completed by JEW and NFO. KAD was responsible for the synthesis and collection of data for deuterium labeled substrates and all reactions leading to the synthesis (and subsequent cyclization of) compound **2.61**.

2.1 Foreword

As outlined in Chapter 1, our group is interested in developing new synthetic strategies that permit efficient access to chemical complexity through pairing of iterative synthetic protocols with chemoselective tandem or cascade type sequences.(82-84)

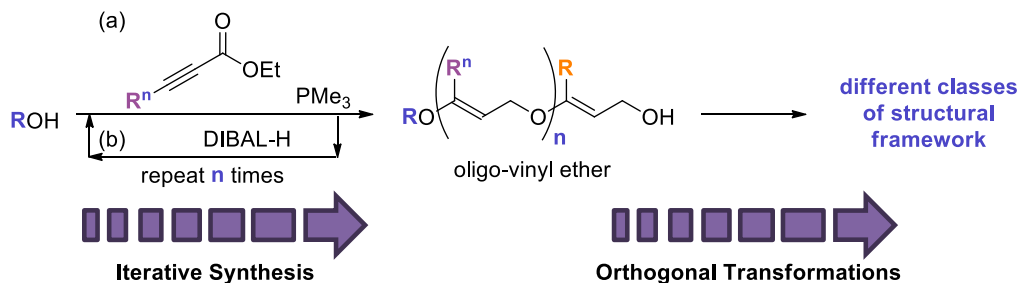


Figure 2.1 Synthetic strategy for efficient access to architecturally rich small-molecules from a common linear precursor.

Specific to our program has been the development and optimization of an iterative conjugate addition/reduction sequence to provide a variety of functionalized oligo-vinyl ethers from easily accessible or commercially available starting materials (**Figure 2.1**). (82, 84, 85) We envision that this common linear precursor can undergo a diverse range of selective, orthogonal transformations to generate new, stereochemically rich, linear- or (poly)cyclic-targets that have medicinal utility. In order to harness the chemical potential of this substrate, a fundamental understanding of the chemical reactivity of bis-vinyl ethers (and larger congeners thereof) must be acquired.

2.2 Identifying a Mechanism to Access Polycyclic Ethers

Our objective in this work was to investigate cascade cyclization strategies that would permit access to fused, polycyclic products. A number of useful methodologies have been

explored in the literature for invoking such chemical transformations for the analogous polyene precursor (including transition-metal catalyzed cyclization, cation-olefin cyclizations and radical initiated cyclizations).(86-92) We chose to avoid any strategy that would require use of Lewis acids in order to mitigate any destructive interaction that they may have with our electron-rich vinyl ethers. The earliest of our investigations, therefore, sought to invoke a radical-initiated cascade to gain access to these desired end-products.

Radical reactions are relatively “mild” in that they are generally tolerant of a wide variety of functionality appended to a given substrate. Furthermore, carbon-(93, 94), oxygen-(95, 96) and nitrogen-(97-99) centred radicals are all known to participate in radical addition reactions with vinyl ethers, presenting themselves as possible initiators for our projected intramolecular cascade.

Given the types of products that we were generating from our iterative protocol, we decided to focus our attention on carbon-centered radicals. Radical precursors of this type could be easily accessed from a diverse range of functionality (*e.g.*, alkyl halides, nitro compounds, acyl species, vinyl halides, or by addition of another species to an alkyne), providing us the opportunity to evolve this portion of the molecule to suit the chemical reactivity (or functional group tolerability) of our substrates.

2.3 Predicting the Mode of Cyclization in Radical Reactions

Having identified a preliminary synthetic platform (incorporation of carbon-centered radical precursor) for our oligo-vinyl ether substrates, we now wanted to be able to predict

the types of products that could result from our cyclization strategy. With virtually no record of cascading cyclizations across systems similar to ours to which analogies could be drawn, we looked to the set of rules developed by Baldwin(100) and Beckwith(101) to predict the most plausible mode of cyclization of a carbon-centered radical onto a vinyl ether.

2.3.1 Baldwin's Rules

Baldwin's Rules(100) are a set of empirically-derived guidelines based on stereoelectronic considerations that predict the favourable regiochemical outcome in the ring closure of acyclic reactive intermediates (**Figure 2.2**). The factors that govern the trajectory of incipient radicals ("X", **Figure 2.2**) onto a tethered functionality at the point of ring closure ("Y", **Figure 2.2**) are (i) chain length, (ii) the hybridization at the bond being broken (red solid line, **Figure 2.2**) and (iii) the relative position of the bond during ring closure.

The ring forming process is characterized by three prefixes (*e.g.*, 5-*exo-trig* cyclization). The first is a number that describes the number of atoms constituting the size of the skeleton of the cycle and can adopt any value ≥ 3 . The second descriptor, *endo* vs. *exo*, refers to the position of the bond that has to be broken in the event of cyclization. *Endo* indicates that the bond that is broken resides within the new ring system, while *exo* indicates that the bond to be broken resides outside of the newly formed ring system (**Figure 2.2**). The third descriptor indicates the hybridization at the point of ring closure: *tet*- (tetrahedral) for sp^3 , *trig*- (trigonal) for sp^2 and *dig*- (digonal) for sp -hybridization.

Taken together, these classifications for ring closure describe the reaction trajectory two terminal atoms must take *en route* to cycle formation. To clarify, the length of the tether that dictates ring size *also* restricts the motion of **X** and **Y** (**Figure 2.2**), whereas the hybridization at the bond to be broken determines the angle of the interacting nuclei. These factors are a determinant as to whether the transition-state geometry will obtain the required orbital overlap necessary for ring closure.

These guidelines do not predict the absolute probability that a reaction will (or will not) take place, but they do describe whether or not a reaction is favourable or unfavourable in a relative sense. That is, unfavourable reactions generally occur at a rate that is not capable of competing with more “favourable” processes, but may in fact be observed if no other pathway is available.

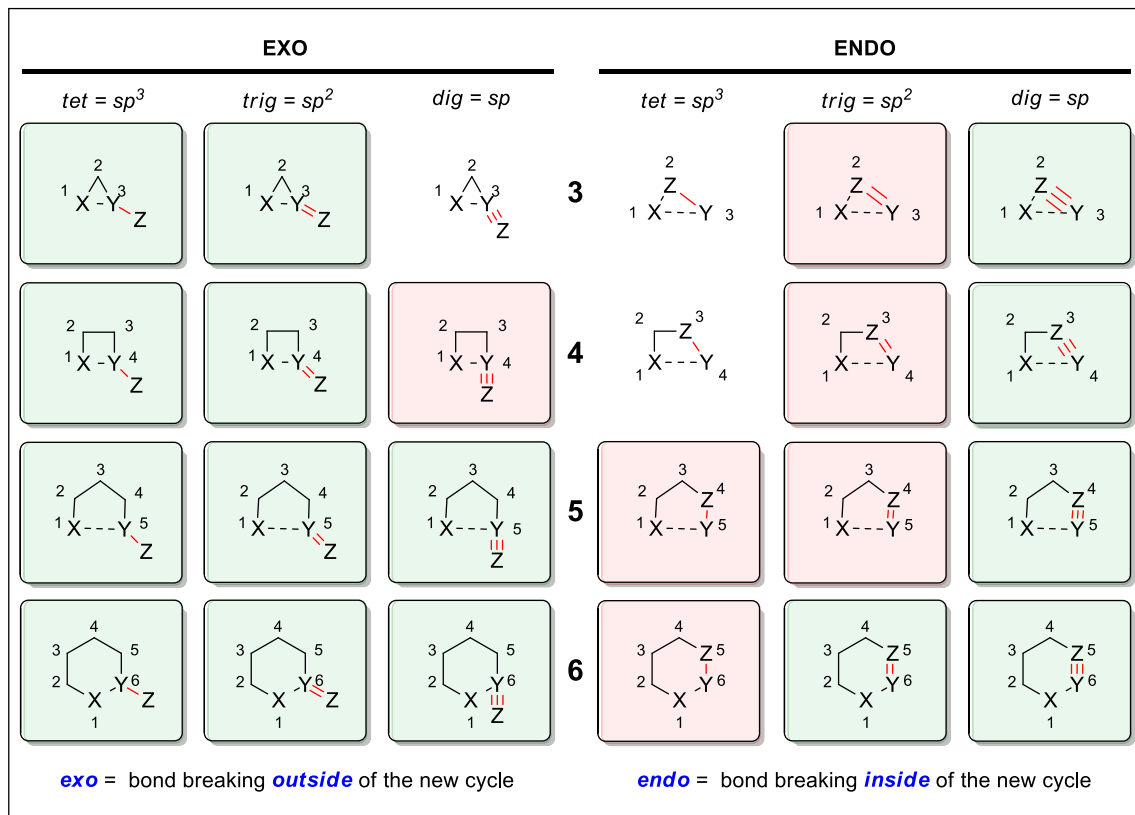


Figure 2.2 Patterns for ring closure for 3- to 6-membered rings. Reactions predicted to be favoured (green) or disfavoured (red) by Baldwin are highlighted. The radical (or anion) center initiating the reaction is designated as “X” while the atom center bearing the radical (or anion) post cyclization is designated as “Z.”

2.3.2 Beckwith's Rules

Beckwith's rules⁽¹⁰¹⁾ serve to complement those of Baldwin (*above*) by looking at both steric and stereoelectronic factors that enable prediction of favourable radical ring closures.

These rules are as follows:

- (i) *Intramolecular addition under kinetic control in lower alkenyl and alkynyl radicals and related species occurs preferentially in the exo-mode.* In unsaturated systems where the interacting termini are connected by five (or fewer) carbon atoms, the *exo-mode* for ring closure is kinetically favoured over the *endo* process.

- (ii) *Substituents on an olefinic bond disfavour homolytic addition at the substituted center.* The preference of an *exo*-ring closure can be overridden by substitution at the internal position of the alkene.
- (iii) *Homolytic cleavage is favoured when the bond concerned lies close to the plane of an adjacent semi-occupied orbital or of an adjacent filled non-bonding or π -orbital.* *Exo*-radicals can readily acquire the required orbital overlap for ring closure, whereas *endo*-radicals often cannot due to ring constraints.
- (iv) *1,5-Ring closures of substituted hex-5-enyl and related radicals are stereoselective: 1- or 3-substituted systems afford mainly cis-disubstituted products, whereas 2- or 4-substituted systems give mainly trans-products.* The stereoselectivity observed in 2-, 3- and 4-substituted 5-hexenyl radicals reflects a conformational preference for a chair-type transition state(101) where substituents preferentially occupy pseudo-equatorial positions to minimize unfavourable non-bonding interactions.(102-104)

2.3.3 Radical Philicity and Polar Effects

Although steric and stereoelectronic effects are considered to be primary indicators for determining the favourability for ring formation from an acyclic precursor, the philicity of the reactive radical species can explain the differences for the rate at which a given reaction will occur, and provides rationale for the observed regioselectivity when more than one reaction pathway is possible.

Simply stated, the frontier molecular orbital for a radical species (*i.e.*, the singly occupied molecular orbital, SOMO) can interact with either the HOMO or the LUMO of the

molecule it is reacting with (**Figure 2.3**). Identifying the philicity of the reacting radical enables one to predict which orbital interaction is stronger: a nucleophilic radical (*e.g.*, alkyl, acyl, stannyl radicals) will have a high lying SOMO and therefore interact more strongly with the LUMO of the reacting species. This reaction becomes even faster when the radical acceptor is stabilized by an electron-withdrawing group (**Figure 2.3A**). Conversely, an electrophilic radical (*e.g.*, oxygen-centered radical, carbon-centered radical alpha to a carbonyl) will have a low lying SOMO and therefore be closer in energy with the HOMO of the reacting partner. The presence of an electron-donating group on the reacting partner will decrease the SOMO-HOMO gap, thereby increasing the rate at which this reaction takes place (**Figure 2.3B**).

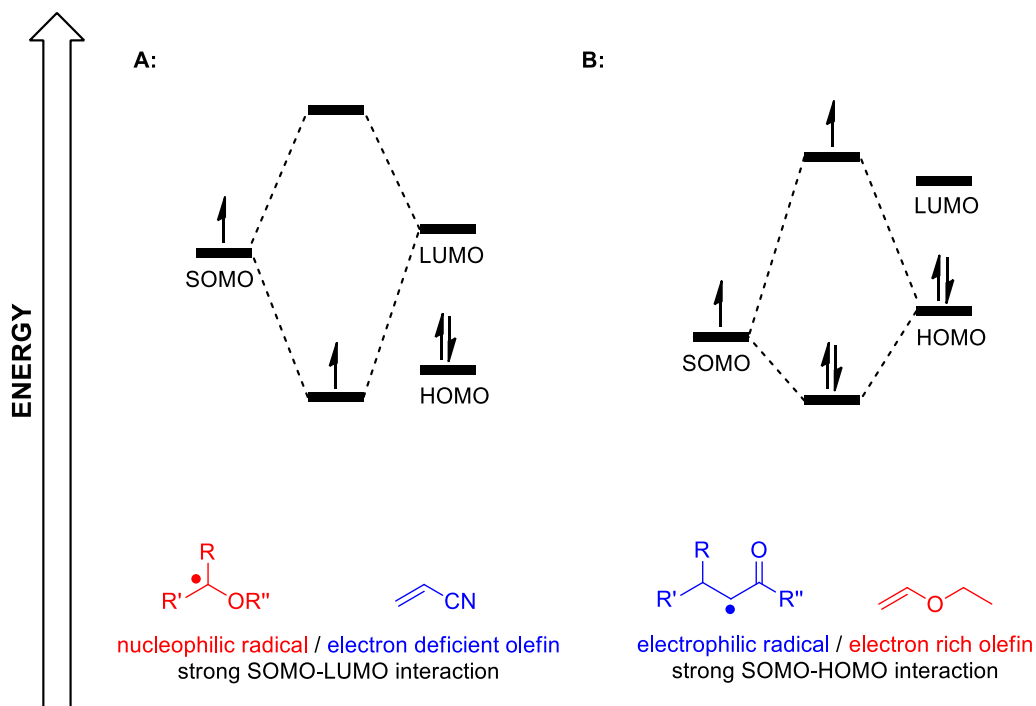
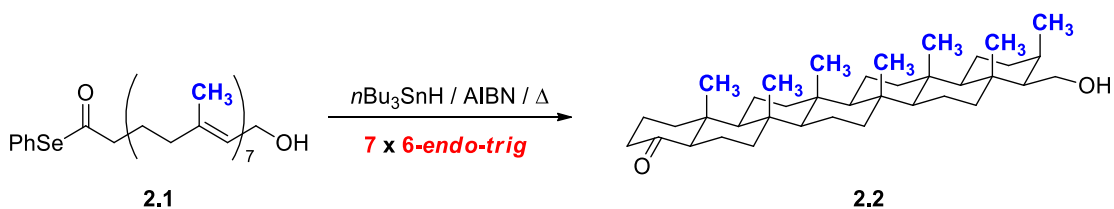


Figure 2.3 Frontier molecular orbital interactions for radical species.

2.4 Factors to Consider for Cyclization of (Poly)Vinyl Ethers

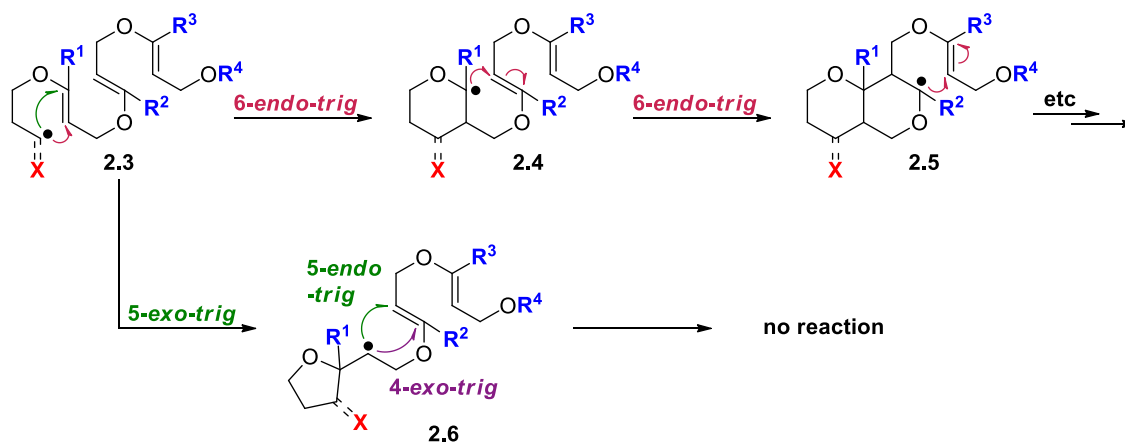
There is a strong interplay between electronic and steric effects that govern the mode of radical cyclization for complex, fused ring systems. One example, which is relevant to our own work, comes from Pattenden's mechanistically related radical cascade cyclization along polyene substrate **2.1** (Scheme 2.1). Subjecting **2.1** to standard conditions for tin-mediated radical cyclization was found to afford fused-heptacycle **2.2** in approximately 20% overall yield.⁽¹⁰⁵⁾ In theory, cyclization *via* a 5-*exo* pathway should have been favoured, but as Beckwith indicated, this can be overridden by the presence of a substituent on the internal position of the alkene.⁽¹⁰¹⁾



Scheme 2.1 Cascading 6-*endo-trig* cyclization along acyclic poly(ene) precursor.

For our own vinyl ether substrates, two cyclization pathways would likewise be possible:

(i) 6-*endo-trig* cyclization or (ii) 5-*exo-trig* cyclization pathway (Scheme 2.2).



Scheme 2.2 Potential cyclization pathways for oligo-vinyl ether substrates.

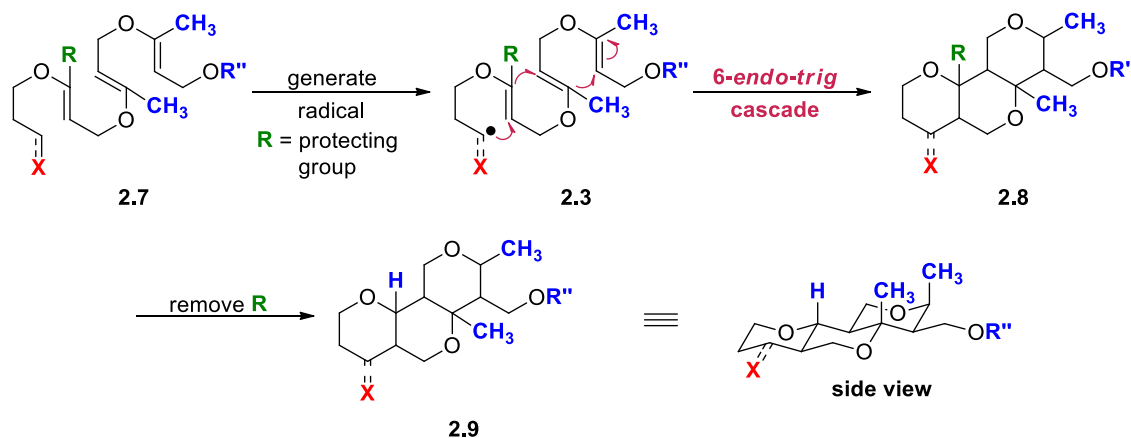
We had hoped that we would be able to emulate the steric control found in Pattenden's(105) (and Boger's(106)) system, whereby substitution on the proximal alkene would lead to a kinetic deceleration of the 5-*exo-trig* cyclization. That said, the 6-*endo-trig* cyclization could, in theory, propagate along the vinyl ether framework (*i.e.*, **2.3** → **2.4** → **2.5** → *etc*) resulting in successful cascade reaction to afford the desired fused polycyclic ether scaffold.

It was also quite possible that the incorporation of heteroatoms along the backbone of our polymer would sufficiently decelerate the rate for 6-*endo-trig* ring closure. The corresponding 5-*exo-trig* cyclization (*i.e.*, **2.3** → **2.6**) would likely terminate, however, after the first ring-forming event as the subsequent 5-*endo-trig* cyclization would be disfavoured. While a 4-*exo-trig* cyclization would be allowed (in principle) by both Baldwin's and Beckwith's guidelines, we predicted that the strain associated with the introduction of a four-ring system would prevent this reaction from occurring at a rate sufficient to permit a cascade cyclization to take place.

Nevertheless, we were interested in determining whether introduction of substituents (at positions marked as **R**, **Scheme 2.2**) on the vinyl ether would bias the system towards the *6-endo-trig* (over the *5-exo-trig*) reaction trajectory.

2.4.1 Protecting the Alkyne Carbon

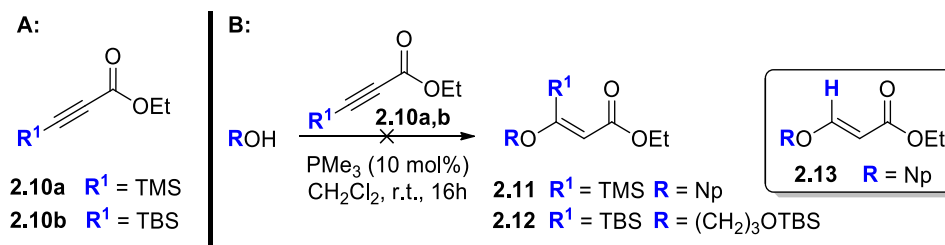
We recognised that, in our attempt to bias our system towards the *6-endo-trig* pathway, we limit our ability to introduce functionality where **R** = H. In order to maintain the inherent steric bias, we sought to install functionality along the vinyl ether framework that could be later removed to unveil **R** = H post-cyclization (**Scheme 2.3**).



Scheme 2.3 Protection of the alkyne carbon for installation of hydrogen atoms at **R**.

To this end, we synthesized alkyneates **2.10a** and **2.10b** to be used as a substitute for ethyl propiolate in our conjugate addition/reduction methodology (**Scheme 2.4**). We found that alkyneate **2.10a** afforded vinyl ether **2.13** as the sole isolable product (99% yield) from this reaction. By contrast, reaction with **2.10b** primarily resulted in recovery of starting materials and comparatively smaller quantities of an analogue of **2.13**. This later

observation suggested to us that addition of the phosphine to **2.10b** is hindered by steric encumbrance imposed by R^1 , while the silyl-functionality is not compatible with the conditions used to invoke the intended transformation.

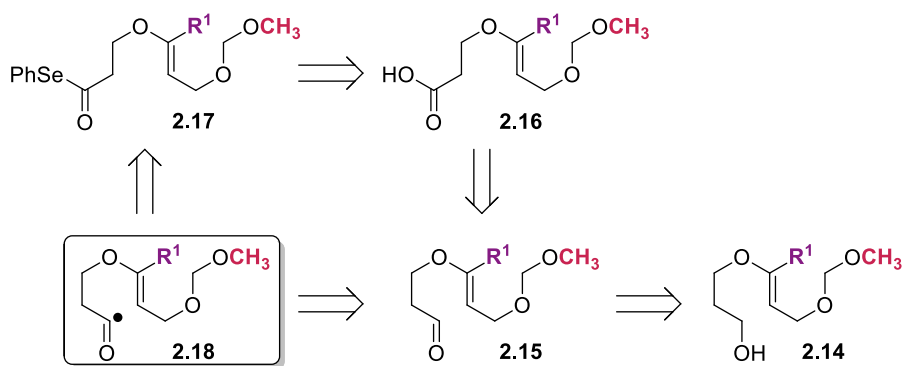


Scheme 2.4 Results for the conjugate addition of an alcohol to silyl-masked propiolates.

2.5 Initial Radical Cyclization Attempts

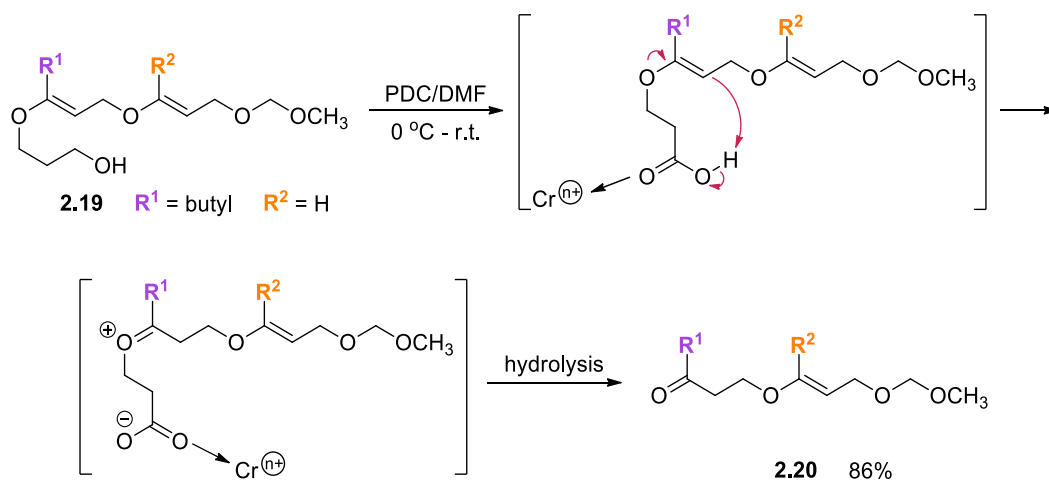
Prior to our work, there were no examples of cascading radical cyclizations across bis-vinyl ether substrates. As such, we opted for a systematic approach to identify a suitable cyclization strategy for our system, with optimization of the identified conditions being performed on the simpler mono-vinyl ether before being taken forward for evaluation on larger polymeric substrates.

The earliest of our attempts to initiate the radical cyclization sequence was through generation of an acyl radical precursor (**Scheme 2.5**, **2.18**) from either aldehyde **2.15** or acyl selenide **2.17**. We had envisioned that these substrates could be conveniently accessed through a common scaffold, **2.14**, permitting simultaneous evaluation of both methods.



Scheme 2.5 Retrosynthetic analysis to gain access to an acyl radical precursor.

As shown in the retrosynthetic analysis, access to the acyl selenide **2.17** would require oxidation of alcohol **2.14** to carboxylic acid **2.16**, followed by selenylation to afford phenyl selenylate **2.17**. Such synthetic manipulations proved to be non-trivial. Direct oxidation of alcohol **2.19** to the corresponding acid was found to result in an intramolecular rearrangement that led to decomposition of the bis-vinyl ether employed (**Scheme 2.6**).



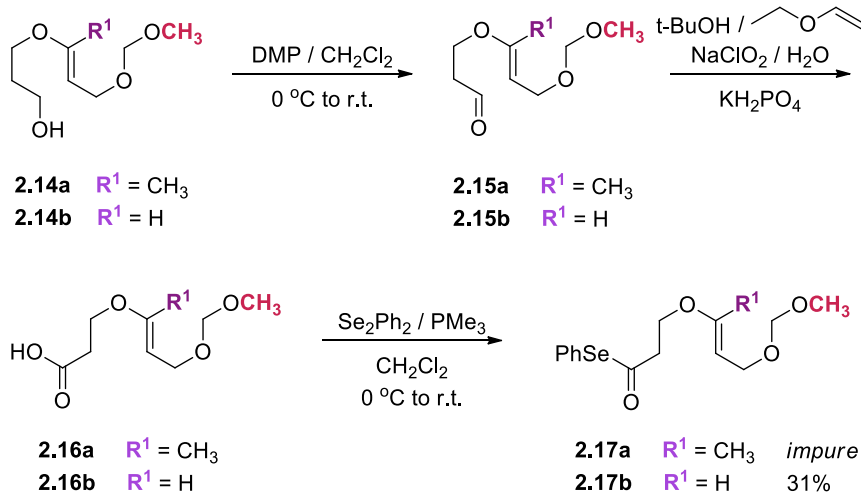
Scheme 2.6 PDC oxidation of alcohol 2.19 results in an intramolecular rearrangement.

It comes as no surprise that vinyl ethers would be prone to decomposition *via* the pathway outlined in **Scheme 2.6**. While we have employed similar reaction conditions as

Pattenden(107) for the analogous transformation of an all carbon polyene system,⁶ oxygen substitution of the olefin (in our system) raises the energy of the HOMO, comparatively. This means that our substrates are inherently more sensitive to the presence of acids or electrophilic species – particularly in the presence of metals that can act as good Lewis acids.

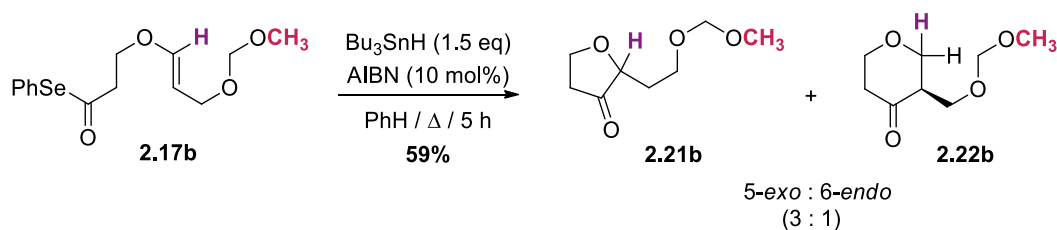
A stepwise oxidation was also investigated as an alternative approach to acid **2.16**. Oxidation of alcohol **2.14** first to aldehyde (**2.15**) using Dess-Martin periodinane(108) was a particularly attractive method, since periodinane is known to be unreactive towards vinyl ethers(109) and the work-up for this reaction can be done under basic conditions. Likewise, access to acid **2.16** could be achieved through Pinnick oxidation(110) of **2.15**, provided that the reaction protocol was slightly modified. Replacement of the traditional sacrificial alkene, 2-methyl-2-butene, with a more electron rich alkene (*i.e.*, ethyl vinyl ether) would aid in sequestering any hypochlorite ions (HOCl) that may be produced during the course of the reaction – thereby avoiding deleterious reactivity of this byproduct with our own vinyl ethers (**Scheme 2.7**).

⁶ Due to the sensitive nature of our substrates, oxidation of alcohol **2.19** to the corresponding acid was attempted with pyridinium dichromate (PDC), rather than pyridinium chlorochromate (PCC) that was featured in Pattenden's work for the analogous transformation of the all carbon polyene system.



Scheme 2.7 Synthesis of phenyl selenyl esters.

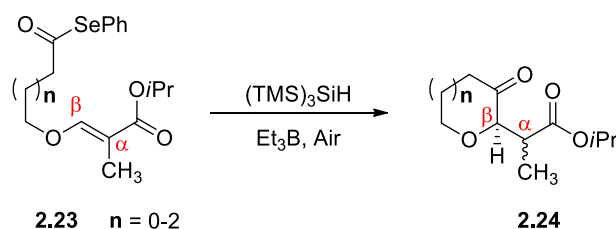
When $R^1 = \text{H}$, alcohol **2.14b** could be successfully converted to the desired oxidation products (**2.15b**, then **2.16b**) under the conditions described in **Scheme 2.7**. Isolation of **2.16b** permitted further derivatization to selenyl ester(111) **2.17b**, which was then taken forward to be evaluated in our proposed cyclization strategy. Generation and cyclization of the acyl radical, in the presence of azobisisobutyronitrile and tributyltin hydride, provided cyclic ethers **2.21b** and **2.22b** in a 3:1 ratio (**Scheme 2.8**).



Scheme 2.8 Initial cyclization attempt from an acyl radical precursor.

All previously reported cyclizations of this type (*i.e.*, generation of an acyl radical followed by addition onto a vinyl ether) were found to occur through a 5-*exo* cyclization

pathway.(112) It should be duly noted, however, that the vinyl ether examined in these earlier examples was conjugated to an electron withdrawing group (*i.e.*, ester). Even in examples where the alkyl tether (**Scheme 2.9**) is extended by one carbon atom, a preference for ring closure is found to occur *via* an *exo*-cyclization pathway.(113) Thus, a clear electronic bias is found to be operative for all these previous reports, where the larger LUMO coefficient at C β (of the acrylate) favours nucleophilic(114, 115) attack at this position from the acyl radical.

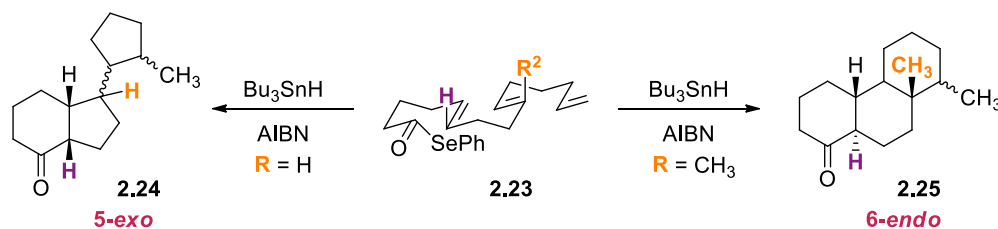


Scheme 2.9 Preference for *exo*-cyclization when a vinyl ether is conjugated to an electron withdrawing group.

While the *5-exo* pathway is still favoured by our system, the fact that we obtained any *6-endo* product, **2.22b**, is quite unusual. Nevertheless, it did suggest to us that this later mode of cyclization was available (although it is equally probable that **2.22b** was formed through an initial formation of the 5-membered ring, followed by rearrangement to yield the more thermodynamically stable product(106)).

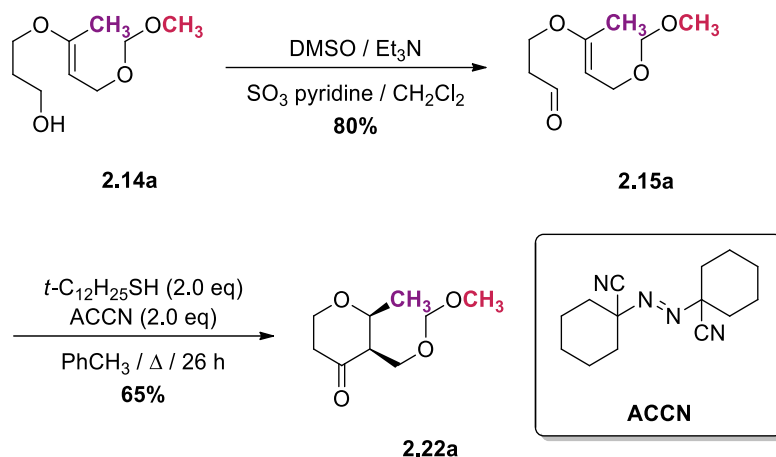
Our intention now was to attempt to further skew product distribution in favour of the larger (*6-endo*) ring size. Surrounding literature for similar transformations suggested that

this, in accordance with Beckwith's rules, could be accomplished through the introduction of additional steric bulk at R^1 (or C5 in our substrate) (**Scheme 2.10**). (107, 116)



Scheme 2.10 Steric bias at R^2 leads to formation of the larger ring product after cyclization.

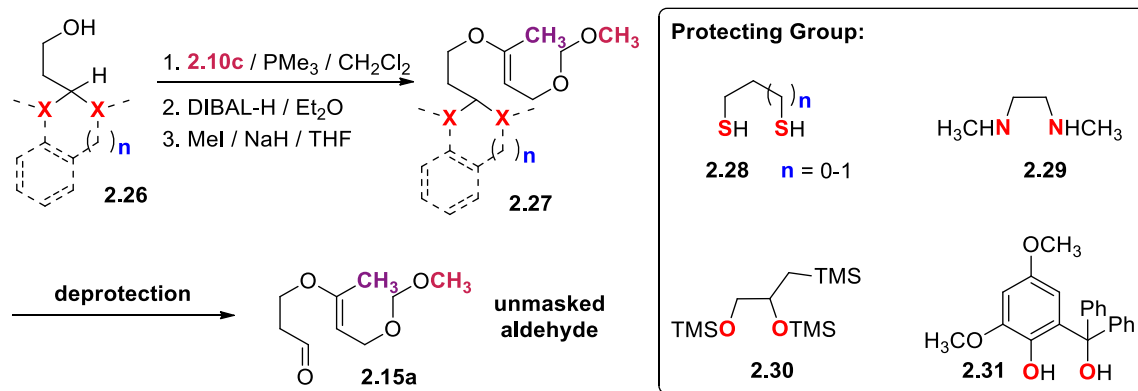
Optimization of the conditions for the oxidation of **2.14a** to the corresponding aldehyde or acid, where $R^1 = CH_3$, proved to be more difficult. Application of the same reaction conditions as seen for **2.14b** were found to result in product mixtures due to the additional electron density on the olefin. Katherine Davies found that Parikh-Doering oxidation(117) (rather than the periodinane oxidation) to aldehyde **2.15a** afforded the best conversion, although access to the acid was still not achievable. For this reason, a cyclization attempt using the aldehyde as the acyl radical precursor was explored (**Scheme 2.11**).



Scheme 2.11 Acyl radical cyclization in the presence of *tert*-dodecanethiol and ACCN.

Using modified reaction conditions based on the work of Tomioka *et al.*,⁽¹¹⁸⁾ **2.15a** was reacted in the presence of an excess of *tert*-dodecanethiol and ACCN in refluxing toluene to afford the 6-*endo* cyclized product **2.22a** in moderate yield. This initial result proved to be quite promising, however we would soon find that we were unable to successfully apply the conditions for the Parikh-Doering oxidation to our larger, bis-vinyl ether substrates.

In order to circumvent the need for this late-stage oxidation to the aldehyde, an alternate strategy was envisioned. We prepared a number of masked acyl-radical precursors, incorporating a variety of protecting groups on the aldehyde, that could, in principle, be removed under mild (**2.28** and **2.29**),^(119, 120) basic (**2.30**)⁽¹²¹⁾ or photochemical (**2.31**)^(122, 123) reaction conditions thereby allowing us to unmask the pre-requisite aldehyde just prior to cyclization (**Scheme 2.12**).



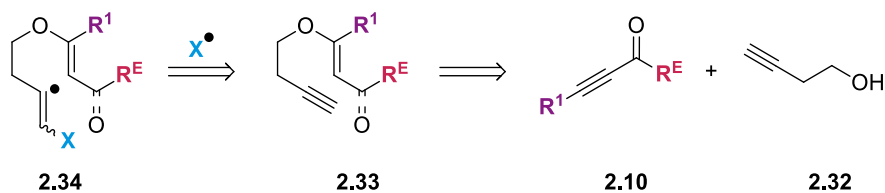
Scheme 2.12 Early installation of the acyl radical precursor as a masked aldehyde.

In practice, the protecting groups were either cumbersome to synthesize (**2.31**, 6 steps), proved to be too labile (**2.29**) or were not easily removed without significant decomposition of the vinyl ether (**2.28** and **2.30**). In light of the fact that our vinyl ethers did not tolerate early⁷ or late stage introduction of an acyl radical precursor, we decided to pursue other strategies for initiating the radical cascade cyclization sequence.

2.6 Alkynes as a Precursor to Vinyl Radicals

We next decided to examine alkynes as precursors to carbon-centered alkenyl radicals (**Scheme 2.13**). The utility of this approach is twofold: (1) the alkyne is easily incorporated into our iterative protocol using 3-butyne-1-ol (**2.32**) as the starting alcohol for the conjugate addition / reduction sequence, and (2) there is good literature precedent for the cyclization of alkenyl radicals onto mono-vinyl ethers.(124-127)

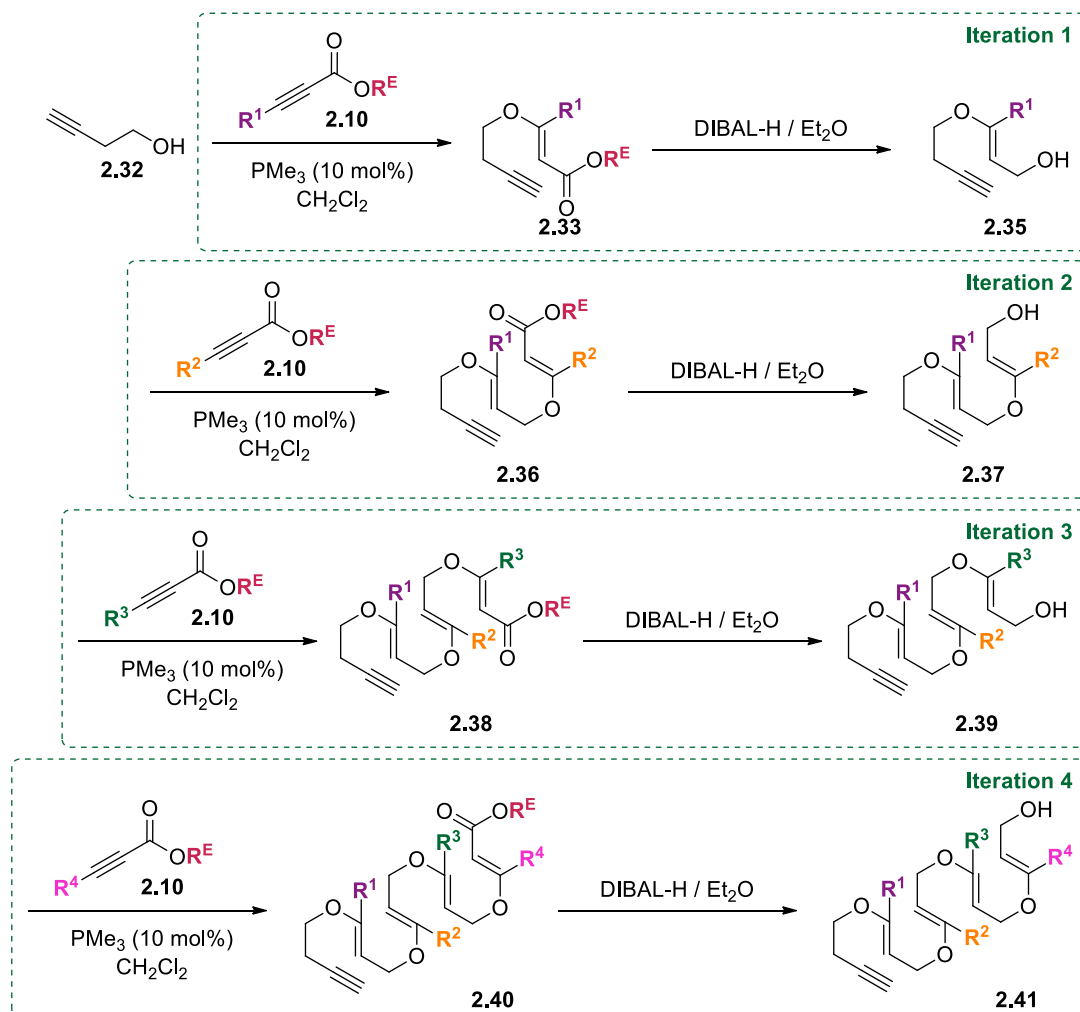
⁷ Also investigated was the early installation of a phenyl selenyl ester (not shown) from either 3-((tert-butyldimethylsilyl)oxy)propanoic acid or 3-(benzyloxy)propanoic acid. Deprotection of the alcohol, in either case, resulted in lactone formation.



Scheme 2.13 Retrosynthetic analysis for generation of an alkenyl radical.

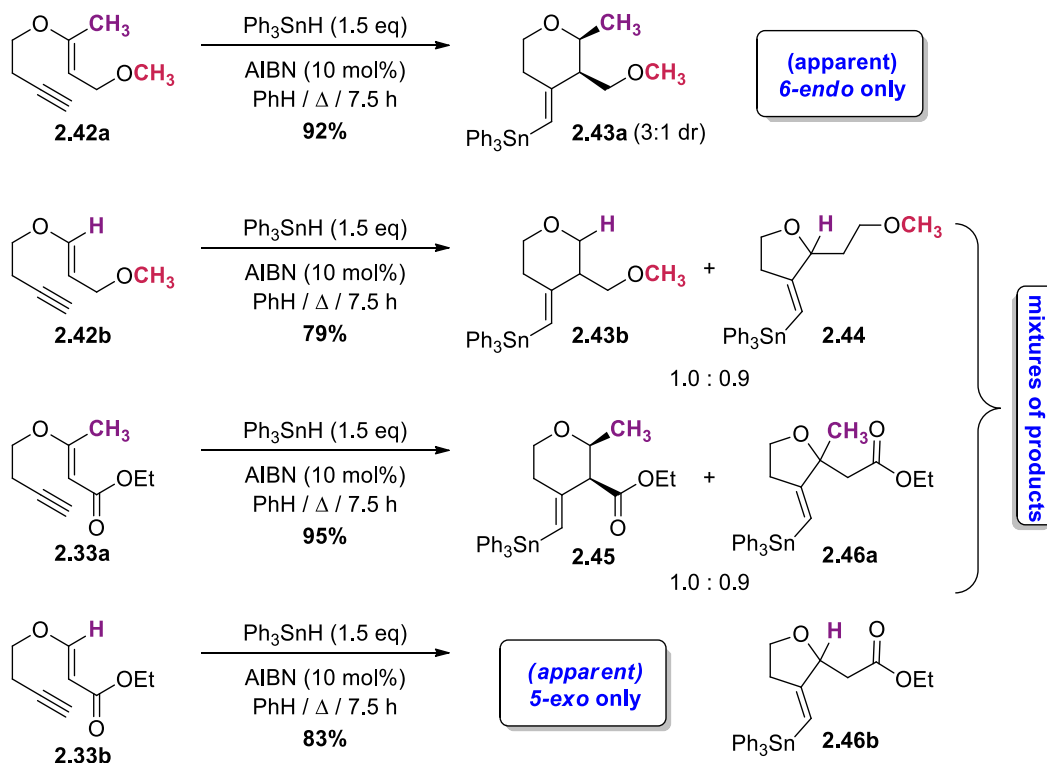
Synthesis of the substrates was straightforward, with conjugate addition and reduction steps yielding relatively pure crude isolates that could be readily purified over triethylamine-treated silica gel to afford product ($\geq 95\%$ purity) in good to excellent yields (**Scheme 2.14**).⁽⁸²⁾ Katherine Davies found that the *E/Z*-stereoselectivity for the conjugate addition could be improved⁸ if the reaction were carried out at 0 °C followed by gradual warming of the reaction mixture to room temperature over the course of a 16 hour period. To ensure that our iterative protocol could be applied in excess of two iterations, Ms. Davies also generated tris- and tetrakis-vinyl ethers (where $\mathbf{R}^1 = \text{CH}_3$, $\mathbf{R}^2 = \mathbf{R}^3 (= \mathbf{R}^4) = \text{H}$) in yields comparable with that of our smaller congeners.

⁸ Phosphine mediated conjugate addition of 3-butyn-1-ol (**2.32**) to ethyl-2-butynoate (**2.10c**) at room temperature afforded **2.33a** ($\mathbf{R}^1 = \text{CH}_3$; $\mathbf{R}^E = \text{OEt}$) as a 4:1 of *E:Z* isomers (**Scheme 2.14**). When the same reaction was performed at 0 °C, with subsequent warming to ambient temperature overnight, **2.33a** was produced with an improved *E:Z* ratio of greater than 20:1.



Scheme 2.14 Synthesis of vinyl ethers.

The stannyl-mediated radical cyclization for our new class of substrates was investigated in a systematic manner. We first chose to determine what effect steric encumbrance would have on the product distribution for the cyclization of mono-vinyl ethers. To this extent, we synthesized mono-vinyl ethers **2.42a** and **2.42b**, protecting the alcohol functionality as a methyl ether to prevent any unwanted reactivity from the alcohol during the cyclization process (**Scheme 2.15**).

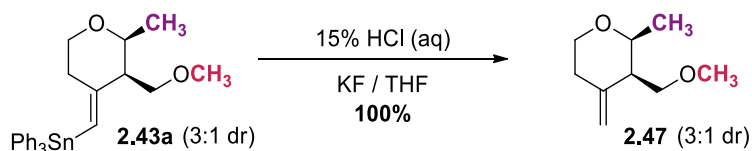


Scheme 2.15 Substitution dictates regioselectivity in the cyclization of mono-vinyl ethers.

We had predicted that the strong nucleophilic nature of the vinyl radical in combination with reduced steric burden at **R**¹ would favour cyclization through the 5-*exo* pathway for substrate **2.42b**. The result from this cyclization afforded near equimolar quantities of both the 5-*exo* (**2.44**) and 6-*endo* (**2.43b**) cyclized products, with slight preference given for the 6-*endo* pathway. Replacing **R**¹ with a methyl substituent led to formation of the tetrahydropyran (**2.43a**), as would be anticipated from attack of the radical at the less sterically hindered carbon of the olefin.⁹ Protodestannylation of **2.43a**, using 15% HCl and potassium fluoride

⁹ Katherine Davies noted that a low *E:Z* ratio for **2.43a** (*i.e.*, higher levels of the *Z*-isomer are present) resulted in poor conversion to the cyclized product. This suggests that the *Z*-isomer either does not cyclize, or that it does so at a rate that is much slower than hydride abstraction by the alkene radical.

in THF, afforded the corresponding alkene in quantitative yield as a 3:1 mixture of diastereomers (major diastereomer shown, **Scheme 2.16**).



Scheme 2.16 Protodestannylation of **2.43a**.

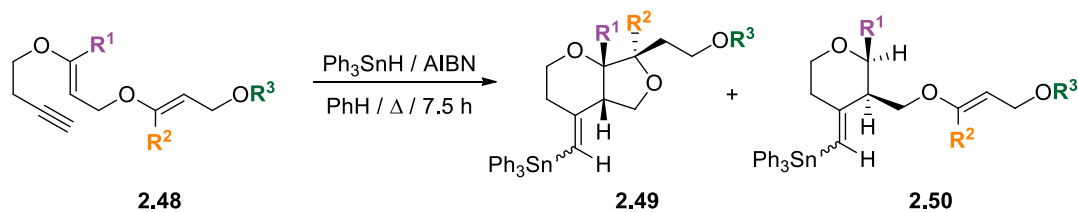
For consistency, we also elected to examine the product distribution for those vinyl ethers where the oxygen containing carbon was in conjugation with an electron withdrawing group (**2.33a** and **2.33b**, **Scheme 2.15**). As stated earlier, the nucleophilic nature of the vinyl radical would be expected to interact strongly (and hence, react quickly) with the lower energy LUMO of the acrylate. Cyclization of **2.33b**, where $R^1 = H$, predictably afforded tetrahydrofuran **2.46b** as the sole isolable product for the reaction while compound **2.33a**, where $R^1 = CH_3$, under the same conditions yielded the anticipated mixture of regioisomers resulting from the additional steric bias that methyl substitution would impose at C3 (**2.45** and **2.46a**, **Scheme 2.15**).

2.7 Cyclization of Alkene Radicals onto a Bis-Vinyl Ether

In accordance with the direction of our intended purpose, we decided to pursue subsequent cascading cyclizations of bis-vinyl ether substrates with exclusive alkyl or aryl substitution

at **R**¹ to ensure formation of the desired 6-membered ring system. The results are summarized in **Table 2.1**.¹⁰

¹⁰ Bis-vinyl ethers of type **2.36** were prone to facile Claisen rearrangement at temperatures as low as ambient. Reduction of the ester was found to mitigate this reactivity.

Table 2.1 Stannyl-mediated radical cyclization across bis-vinyl ethers^a

| Entry | Substrate | R ¹ | R ² | R ³ | Yield (<i>dr</i>) ^b | |
|-------|-----------|----------------------|-----------------|----------------|------------------------------------|------------------------------------|
| | | | | | 2.49 | 2.50 |
| 1 | 2.48a | Me | H | Me | a 77% (4:1) | – ^c |
| 2 | 2.48b | Me | Me | Me | b 33% (5:1) | b 54% (4:1) |
| 3 | 2.48b | Me | Me | Me | b 55% (5:1) ^d | b 27% (3:1) ^d |
| 4 | 2.48c | Me | H | H | c 81% (1.4:1) | – ^c |
| 5 | 2.48d | Me | H | Bn | d 74% (2.7:1) | – ^c |
| 6 | 2.48e | Et | H | Me | e 76% (8:1) | – ^c |
| 7 | 2.48f | Et | Et | Me | – ^c | f 67% (2:1) |
| 8 | 2.48g | Ph | H | Me | g 80% (4:1) | – ^c |
| 9 | 2.48h | Ph | Me | Me | – ^c | h 72% (12:1) |
| 10 | 2.48i | CF ₃ | H | Me | i 64% (7:1) | – ^c |
| 11 | 2.48j | CF ₃ | CF ₃ | Me | – ^e | – ^e |
| 12 | 2.48k | CH ₂ OTHP | H | Me | k 67% (2:1) | – ^c |

^aConditions: A solution of Ph₃SnH (1.5 eq) and AIBN (0.1 eq) was added over a 6 h period to a refluxing solution of alkyne **2.48** in deoxygenated benzene to a final concentration of 8 mM. Heating was continued for 1.5 h prior to work-up. The major diastereomers are shown for **2.49** and **2.50**. ^bReported values refer to the major observed product and the second most abundant species. ^cProduct was not observed in >10% yield. ^dReaction performed at 1.6 mM final concentration. ^eFormation of the expected products was not observed.

Our initial attempt at forming a fused bicycle was performed on **2.48a** (Table 2.1, entry 1). After the initial cyclization onto the first vinyl ether the substrate proceeded to react further, adding across the second available vinyl ether in the molecule. Examination of the substrate scope found that when **R**² was a hydrogen the cascade cyclization went exclusively through an apparent *6-endo-trig* / *5-exo-trig* ring closure to afford functionalized hexahydro-2H-furo[3,4-*b*]pyrans **2.49** in moderate yield.

Furthermore, when **R**² was a methyl, the reaction produced a significant quantity of **2.49b**, setting three contiguous stereocenters and two adjacent quaternary centers in one synthetic operation. Monocycle **2.50b** was also observed in this reaction, likely resulting from the increased steric burden associated with closure of the second ring. These steric effects were found to dictate product distribution. As the size of **R**² (or **R**¹, when **R**² was of equal or greater size than methyl) was increased, product distribution was shifted in favour of the formation of **2.50**.

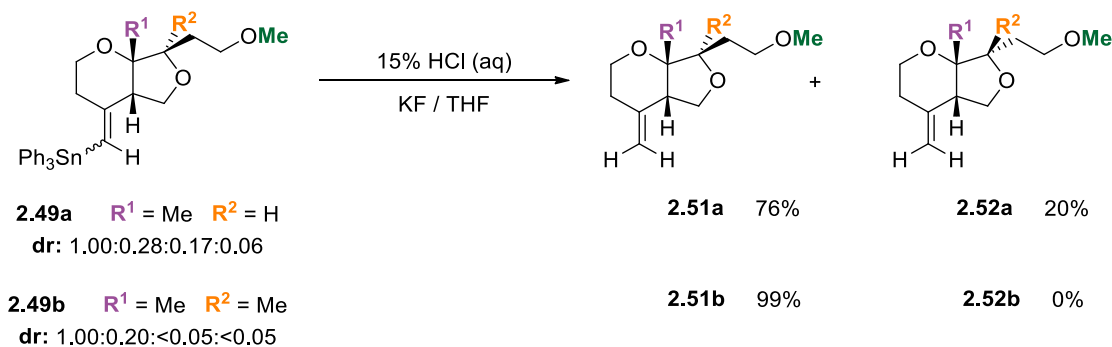
Exchange of the methyl ether at **R**³ for either the free (entry 4) or benzyl-protected (entry 5) alcohol did not adversely affect formation of the bicycle, although a significant decrease in the diastereoselectivity of the reaction was observed (Table 2.1).

2.7.1 Assignment of Relative Configuration and Rationale for Observed

Diastereoselectivity:

Assignment of the relative configuration for **2.49** was found to be complicated by the presence of minor isomers in the ¹H NMR spectral data. In order to simplify this

assignment, representative compounds (**2.49a** and **2.49b**) were subjected to the earlier described conditions for protodestannylation (**Scheme 2.17**). Structures of the exocyclic alkene products were then analyzed by 2D NMR, with assignment of all other species **2.49** made by analogy.

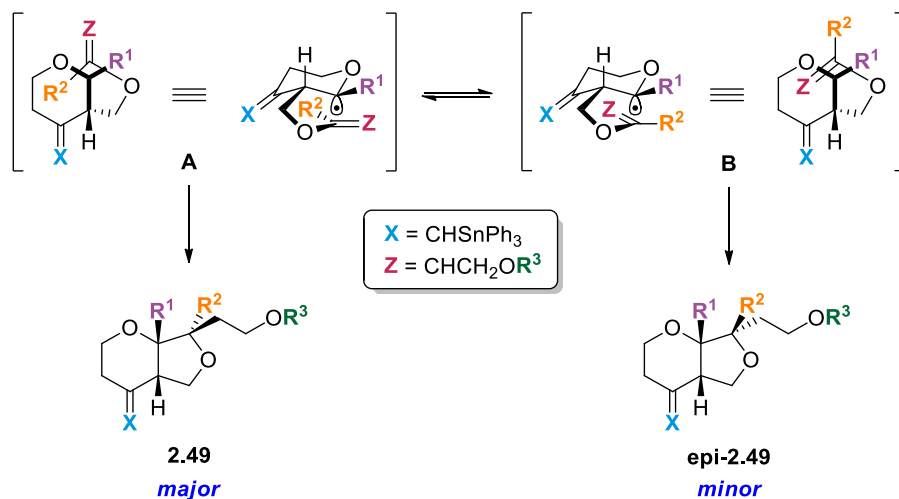


Scheme 2.17 Protodestannylation of representative cyclized products to determine the relative stereochemistry of **2.49**.

Destannylation of **2.49a** (an approximate 4:1 mixture of major diastereomers) afforded products **2.51a** and **2.52a** in *ca.* 4:1 ratio, indicating that for those substrates (**2.49**) where $R^2 = \text{H}$, this ratio corresponds to a mixture of epimers at the carbon bearing R^2 . In contrast, removal of the tin from **2.49b** afforded a single diastereomer, indicating that the minor species was the result of geometrical isomers at the olefin.

The high level of diastereoselectivity observed for this cyclization process was attributed to preferential orientation of the allylic chain away from the tetrahydro-2*H*-pyran core (*i.e.*, *anti* to R^1) during the second cyclization event (**Scheme 2.18**). Evidence in support of this proposal came from the observed erosion in diastereoselectivity for **2.49k**, where the tetrahydropyranyl ether at R^1 was likely too large to be accommodated by conformer **A**,

and **B** becomes an equally probable pathway for addition of the anomeric radical onto the distal vinyl ether residue.



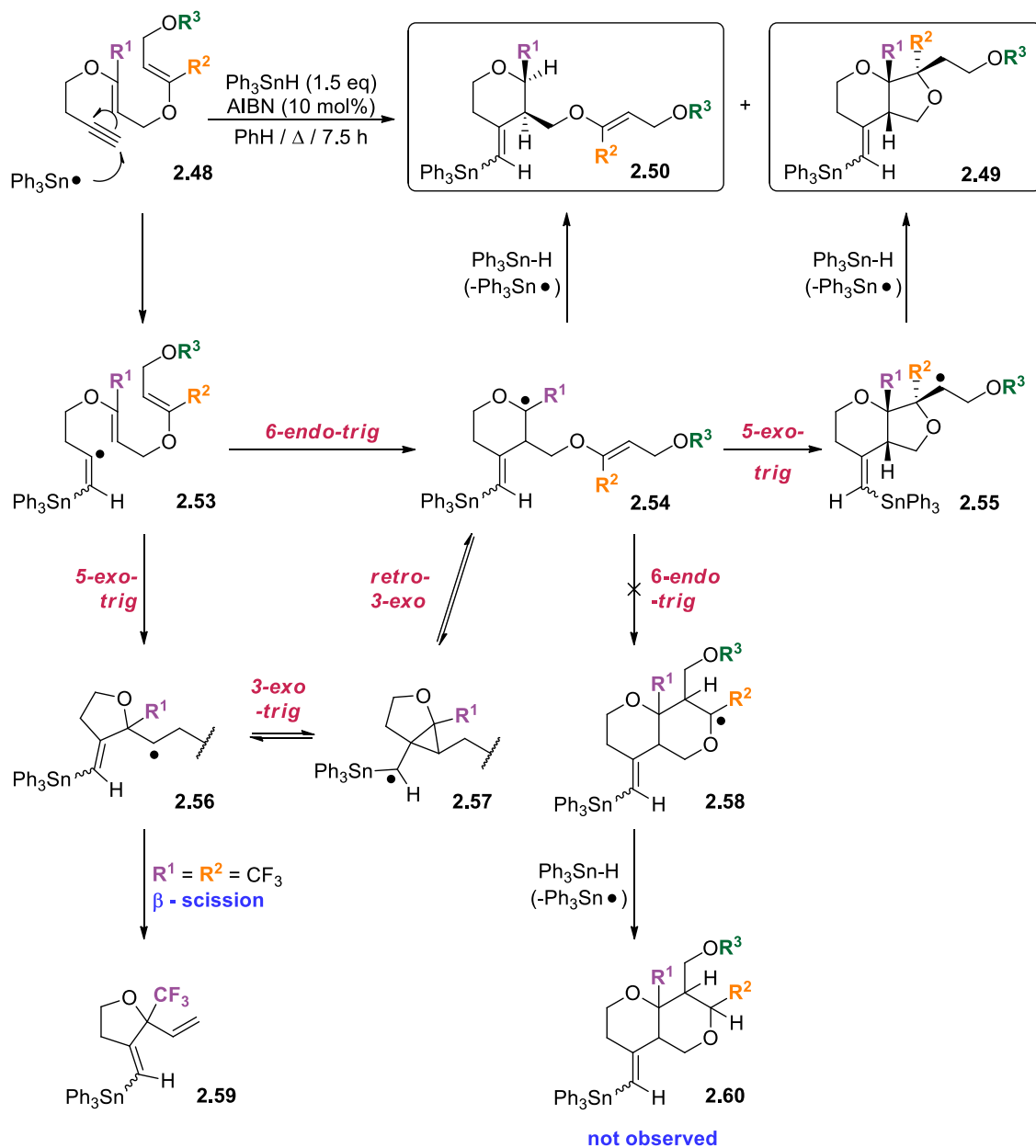
Scheme 2.18 Rational for the diastereoselectivity observed in the cyclization of bis-vinyl ethers.

2.8 Mechanistic Studies Pertaining to the Apparent 6-endo/5-exo Radical Cascade

Hexahydro-2H-furo[3,4-*b*]pyrans of the type described herein (and oxidized forms thereof) have been utilized in medicinal chemistry programs(128-132) and are found to be contained within the core scaffold for several natural products.(133-144) The potential for biological applications of this class of molecules makes these attractive targets for the development of synthetic strategies (113, 145) that would permit rapid generation of analogues for exploration of structure-activity relationships. As such, the factors governing the regio- and stereochemical outcome of our radical cascade cyclization, across bis-vinyl

ethers, must be firmly established if we hope to apply this methodology to matters of biological importance.

The Pattenden group has published extensively on the development of synthetic methodologies to transform all-carbon polyene systems, which are structurally related to our oligo-vinyl ethers, to steroidal-like molecules.^(105, 107, 116, 146) Generation of molecular complexity is achieved through intramolecular addition of an acyl radical to an alkene, resulting in the propagation of a series of successive *6-endo-trig* cyclization events to generate fused, polycyclic scaffolds. The regiocontrol for this chemical transformation has been attributed to steric influences which lead to preferential addition of the radical to the less sterically hindered carbon of the nearest alkene. Since cyclization of **2.42b** provided 1.00:0.89 *6-endo-trig*:*5-exo-trig* cyclized products, while **2.42a** afforded exclusive formation of the *6-endo-trig* cyclized product, it would appear that steric control is similarly important in our system. Unlike Pattenden's polyene, we do not observe a successive *6-endo-trig* cyclization across our bis-vinyl ethers, but an unusual *6-endo/5-exo-trig* route. We therefore cannot discount the possibility that the difference in the electronic contributors affecting ring closure, in our system, may lead to an altogether different reaction trajectory. In order to fully understand the mechanism for rearrangement, all modes for cyclization must first be considered (**Scheme 2.19**).



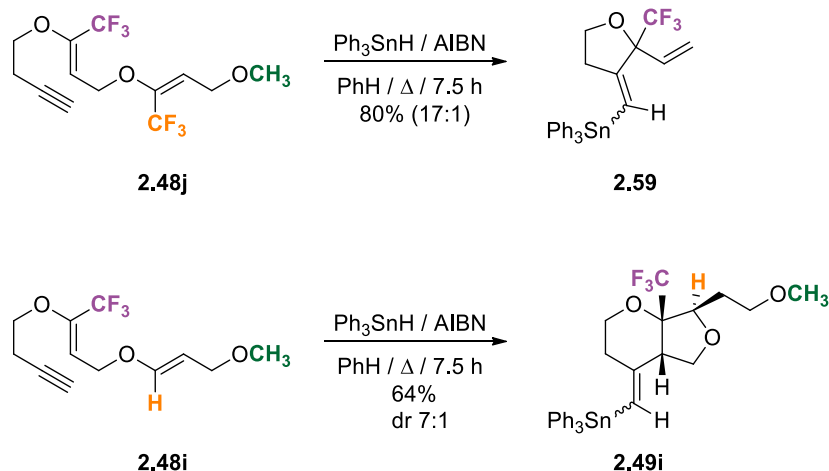
Scheme 2.19 Mechanistic possibilities for radical cyclization onto bis-vinyl ethers.

It would appear at first glance that after the first cyclization event, electron donation from the oxygen adjacent the radical-bearing carbon increases the energy of the SOMO, thereby increasing the nucleophilicity of intermediate **2.54**. While it is theoretically possible that the steric influence of a substituent at \mathbf{R}^2 could direct a second *6-endo* cyclization event of

this type (to yield **2.60** via **2.58**), it is electronically disfavoured as it would require interaction of a high energy SOMO with the largest coefficient in the HOMO of the electron rich vinyl ether. Instead, there is an apparent regiochemical “switch” that lends itself to preferential interaction with the less nucleophilic end of the second alkene via a 5-*exo* route (to yield **2.49** via **2.55**).

But if this last statement (above) were true, the mechanism for the first ring closure should fall under scrutiny, as the nucleophilic nature of the β -stannyl alkene radical(125) would present the same electronic bias as in the latter case. The doubts surrounding the mechanism for the first ring closure were confirmed when exposure of vinyl ether **2.48j** to a source of stannyl radicals resulted not in the anticipated 6-*endo* / 5-*exo* cascade (or 6-*endo-trig* ring closure to yield the monocycle, due to the increased steric bulk at **R**²), but in the exclusive generation of compound **2.59**.

Compound **2.59** appears to originate from an initial 5-*exo* attack on the olefin at the carbon bearing **R**¹, followed by a β -scission event. In contrast, vinyl ether **2.48i**, possessing a single trifluoromethyl substituent at **R**¹, cyclized to give the usual hexahydrofuropyran in good yield (**Scheme 2.20**).



Scheme 2.20 Divergent reactivity with trifluoromethyl substituted vinyl ethers.

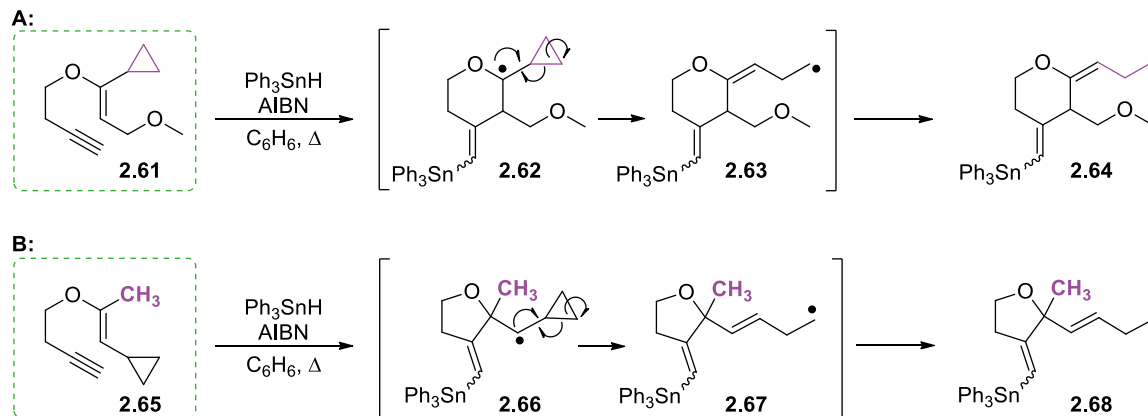
The first vinyl ether group to participate in a radical cyclization is the same for both **2.48i** and **2.48j**, thus a change in the regioselectivity on the basis of a distal substituent at **R**² would seem unlikely. A more realistic interpretation for the divergent reactivity of **2.48i** and **2.48j** is that both substrates react through an initial 5-*exo* attack, but that the presence of the second trifluoromethyl substituent at **R**² (in **2.48j**) favours a fast β -scission event trapping intermediate **2.56** (Scheme 2.19). This interpretation would imply, then, that **2.48i** undergoes a neophenyl-type rearrangement to eventually yield what is now a formal 6-*endo* intermediate, **2.54**.

While this explanation seems plausible, we cannot discount the fact that trifluoromethyl substitution at **R**² and/or **R**¹ significantly alters the electronic factors governing ring closure and consequently may not be representative of simpler alkyl-substituted vinyl-ethers.

2.8.1 Probing the Mechanism for Radical Cyclization Using Radical Clocks

Given the ambiguity surrounding the formation of the pyranosyl radical (**2.54**) when \mathbf{R}^1 = alkyl or aryl, we sought to install cyclopropane(147) groups into our structures as probes for the presence of radical character(148-151) at both the 5- and 6-positions (relative to the approaching radical) throughout the cyclization of the 6-membered ring. In this way, we would be able to delineate between the two mechanistic possibilities for the first ring closure event: either (1) a direct *6-endo-trig* cyclization to generate intermediate **2.54**, or (2) an initial *5-exo-trig* cyclization followed by a *3-exo/retro-3-exo* rearrangement sequence to afford intermediate **2.54**.

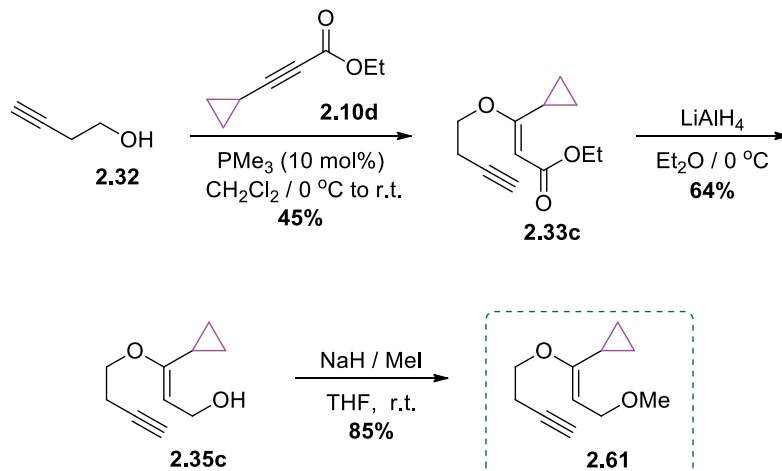
In designing our reactivity probes, we recognised that we could simplify our system to examine the pathway for formation of the pyranosyl radical in our mono-vinyl ethers, as these substrates (*e.g.*, **2.42a**) were also found to afford exclusively the six-membered ring product (*e.g.*, **2.43a**) when \mathbf{R}^1 was something other than a hydrogen and the alkene was not conjugated to an electron-withdrawing function (**Scheme 2.15**). We chose first to synthesize targets **2.61** and **2.65** as simple cyclopropane derivatives, since these would be less prone to spontaneous ring opening (compared to the much more facile ring opening of diphenylcyclopropane) in the absence of a radical intermediate (**Scheme 2.21**).(152)



Scheme 2.21 Mechanistic probes for identifying the presence of a radical at the 5-position (A) and the 6-position (B), relative to the approaching radical.

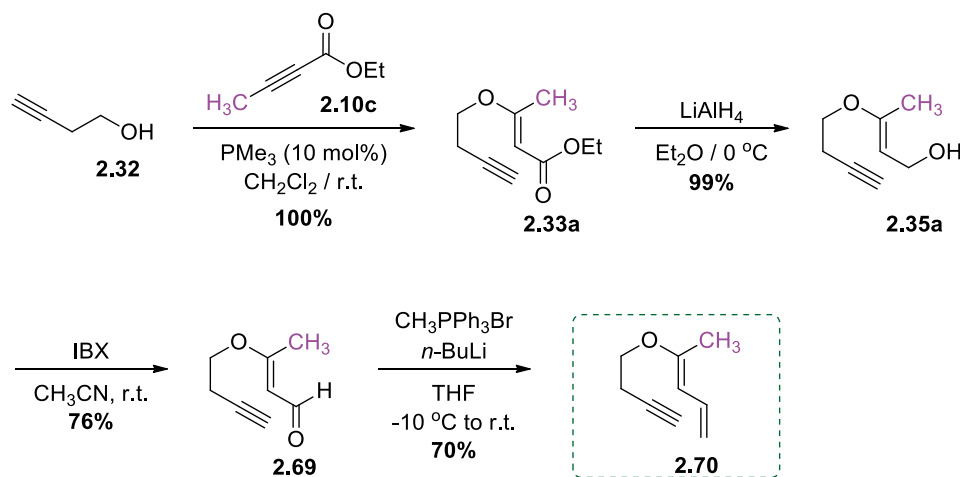
Compound **2.61**,¹¹ incorporating a cyclopropane at **R**¹ (oxygen bearing carbon) of the vinyl ether was accessed by conjugate addition of alcohol **2.32** to known ethyl-3-cyclopropyl propiolate **2.10d** (Scheme 2.22). The yield for this reaction was poor owing to the instability of the cyclopropane function in both alkynoate **2.10d** and vinyl ether **2.33c**. Reduction of **2.33c** to alcohol **2.35c** was performed using lithium aluminum hydride in place of our standard protocol (*i.e.*, DIBAL-H) in order to circumvent the decomposition of **2.35c** that was found to result from extended reaction times. Immediate methylation of **2.35c** afforded our first mechanistic probe (**2.61**) to be used in our radical cyclization protocol.

¹¹ Synthesis, characterization and cyclization of target **2.61** as a probe for the presence of radical character at the anomeric carbon was performed by Katherine Davies.



Scheme 2.22 Synthesis of cyclopropane **2.61**.

Synthesis of compound **2.65**, incorporating a cyclopropane on the non-oxygen bearing carbon of the vinyl ether, proved to be more challenging. Due to the high reactivity of our vinyl ethers, we opted for mild conditions that would permit selective installation of the required functionality at the terminus of dienyl ether **2.70** (**Scheme 2.23**). Fortuitously, literature precedent for a related system suggested that this could possibly be accomplished using transition metal-mediated decomposition of diazo-compounds.⁽¹⁵³⁾

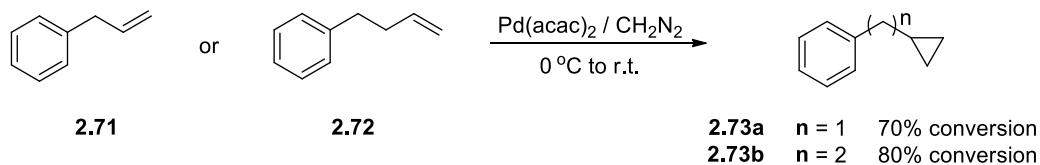


Scheme 2.23 Synthesis of dienyl ether **2.70**.

The success of these types of [2+1] cycloaddition reactions onto alkenes hinges upon the appropriate choice of reagents.(154-156) The reactivity of the carbenic carbon is significantly affected by the nature of the transition-metal used for decomposition of diazocompounds which, by extension, affects the chemoselectivity of the activated complex towards the olefinic substrate.

While rhodium(157) and chromium(158) catalysts typically exhibit the reactivity profile required for reacting with electron-rich olefins, palladium(II) species have been reported to be the only metal that reliably generates cyclopropanes using diazomethane as a carbene source.(159, 160) Furthermore, palladium(II) catalysts demonstrate a high degree of regioselectivity for cyclopropanation of dienes, with preferential reactivity occurring at the less substituted, terminal olefin.(153, 161-163) The vast majority of reports on these reactions, however, focus on the [2+1] cycloaddition of metal carbenoids to electron deficient alkenes,(159, 164-166) indicating that installation of our desired mechanistic probe onto **2.70** would require significant optimization of reaction conditions.

Due to the cost associated with production of our vinyl ether substrates, coupled with their propensity to decompose in the presence of certain of Lewis acids, we decided to first optimize the conditions for our cyclopropanation using commercially available allyl benzene (**2.71**) and 4-phenyl-1-butene (**2.72**) (**Scheme 2.24**).



Scheme 2.24 Conditions for performing a [2+1] using diazo-compounds.

Several palladium catalysts were screened (data not shown) for their ability to generate **2.73** in the presence of excess diazomethane or diphenyldiazomethane. Successful conversion of either substrate could be achieved by reacting 2.0 equivalents of diazomethane in the presence of a catalytic amount of palladium(II) acetylacetonate (5 mol%) in diethyl ether at $0\text{ }^\circ\text{C}$, followed by warming to room temperature over the course of one hour.

Having determined a set of reaction conditions for inducing the [2+1] cycloaddition onto non-conjugated mono-alkenes, we wanted to examine whether this reactivity was transferrable to our electron-rich vinyl ethers. Given the lack of close literature precedent, and the competing functionality in **2.70** (*i.e.*, the alkyne), compound **2.74** was identified as a suitable analogue for which the conditions for cyclopropanation could be developed before tackling the more challenging substrate, **2.70** (Table 2.2).

While the reaction was expected to be fairly clean, we could not ensure the chemoselectivity of the transformation, and acknowledged that cyclopropanation could result at either (1) the internal olefin (**2.75**), (2) the terminal olefin (**2.76**) or (3) both (**2.77**). As such, **2.74** additionally afforded a non-volatile, synthetic handle to enable

chromatographic purification and complete removal of all solvents so that the products of the reaction could be unambiguously identified.

Table 2.2 Optimization of cyclopropanation conditions on diene 2.74.

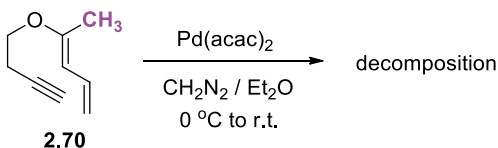
| Equivalents of Reagent | | | | |
|------------------------|-----------------------|--------------------------------|----------------|----------------|
| Entry | Pd(acac) ₂ | CH ₂ N ₂ | Product | Conversion (%) |
| 1 | 0.10 | 2.0 | — ^a | — ^a |
| 2 | 0.10 | 8.0 | 2.76 | 48% |
| 3 ^b | 0.30 | 24 | 2.76 | 90% |

^aRecovered unreacted starting material. ^bPd(acac)₂ (10 mol%) and an ethereal solution of CH₂N₂ (8.0 eq) were added to **2.74** (1.0 eq) at 0 °C at which point the reaction was warmed to room temperature. After 40 minutes, the reaction mixture was again cooled to 0 °C and this procedure was repeated twice more before finally stirring at room temperature overnight.

When compound **2.74** was reacted with diazomethane, in the presence of 10 mol% catalyst loading of Pd(acac)₂, we observed no reaction of the diene (**Table 2.2**, entry 1). Given that palladium-carbenoids react much more slowly with electron rich olefins, significant decomposition of the diazomethane may have occurred before the cycloaddition had a chance to take place. Fortunately, by increasing the number of equivalents of diazomethane, **2.74** could be transformed into **2.76**, but never in more than *ca.* 50% conversion (entry 2).¹² Further attempts to optimize the reaction for dienyl ether **2.74** by increasing the catalyst loading (data not shown) also failed to improve upon these results.

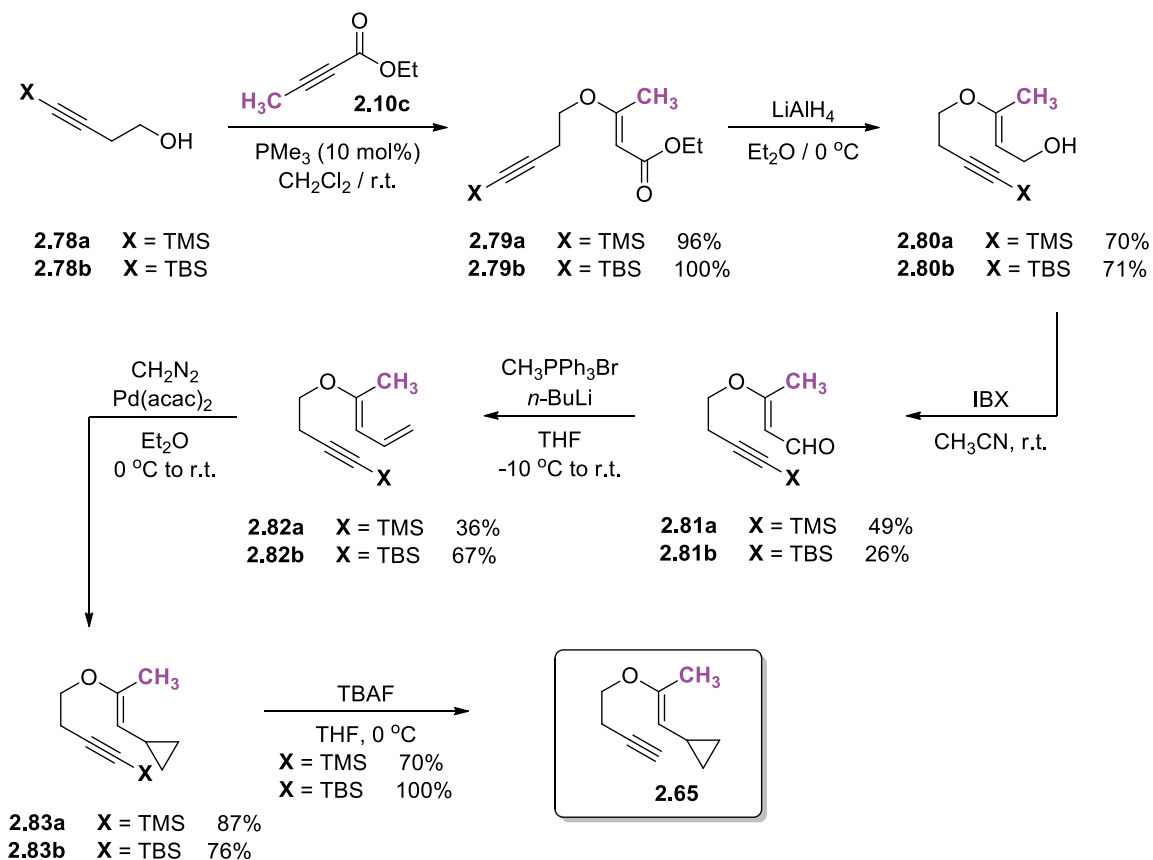
¹² It was also possible that the electron rich diene was coordinating to the Pd-catalyst, precluding formation of the metal-carbenoid or limiting catalyst turnover.

The possibility that the palladium catalyst was forming unreactive adducts *in situ* was confirmed when we discovered that tandem addition of the catalyst and diazomethane, in three portions over the course of 2 hours, provided a significantly higher conversion for **2.74** (Table 2.2, entry 3; unoptimized).



Scheme 2.25 Attempted cyclopropanation of **2.70**.

Attempted conversion of **2.70** to **2.65** under these optimized cyclopropanation conditions resulted in extensive decomposition of the substrate (**Scheme 2.25**). In order to alleviate the obvious cross-reactivity of the cyclopropanating reagents with the terminal alkyne, we elected to protect this functionality (**Scheme 2.26**). Silyl protected alkynes **2.78a** and **2.78b** were prepared following literature protocols(167) and subjected to the usual conjugate addition/reduction sequence to afford alcohols **2.80a** and **2.80b**. Oxidation was complicated by a competing side reaction which led to an inseparable mixture of compounds. The crude isolate could not be effectively purified and was taken forward to the Wittig olefination step, at which point diene **2.82a** and **2.82b** could be cleanly isolated.



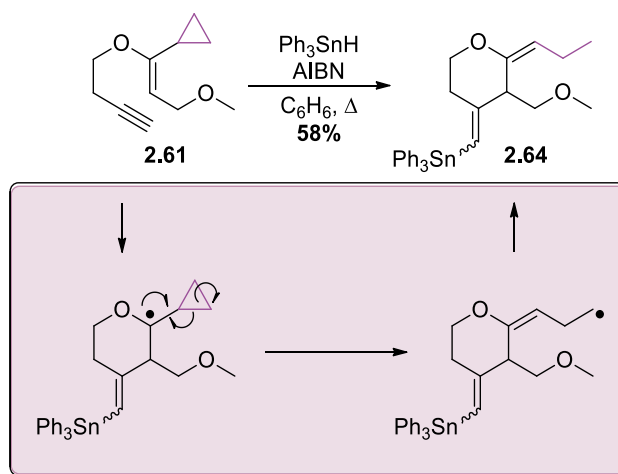
Scheme 2.26 Synthesis of Cyclopropane **2.65**.

We were pleased to find that **2.82a** and **2.82b** were much better substrates for cyclopropanation, relative to unprotected alkyne **2.70**. Treatment with 30 equivalents of freshly generated diazomethane, in the presence of a catalytic amount of palladium(II) acetylacetonate(168) (7 mol%), administered in 6 portions over the course of 8 hours, resulted in 90% conversion to the corresponding cyclopropane, without inducing decomposition. Removal of the silyl protecting group at 0 °C using tetrabutylammonium fluoride yielded **2.65** (containing 10% diene **2.70** as an impurity).

2.8.2 Identifying Sites of Radical Character Through Cyclopropane Ring Opening

With our mechanistic probes (**2.61** and **2.65**) now in hand, we performed the radical cyclization under routine conditions to determine whether the product distribution afforded by these substrates would give a clear picture of the mode of ring closure.

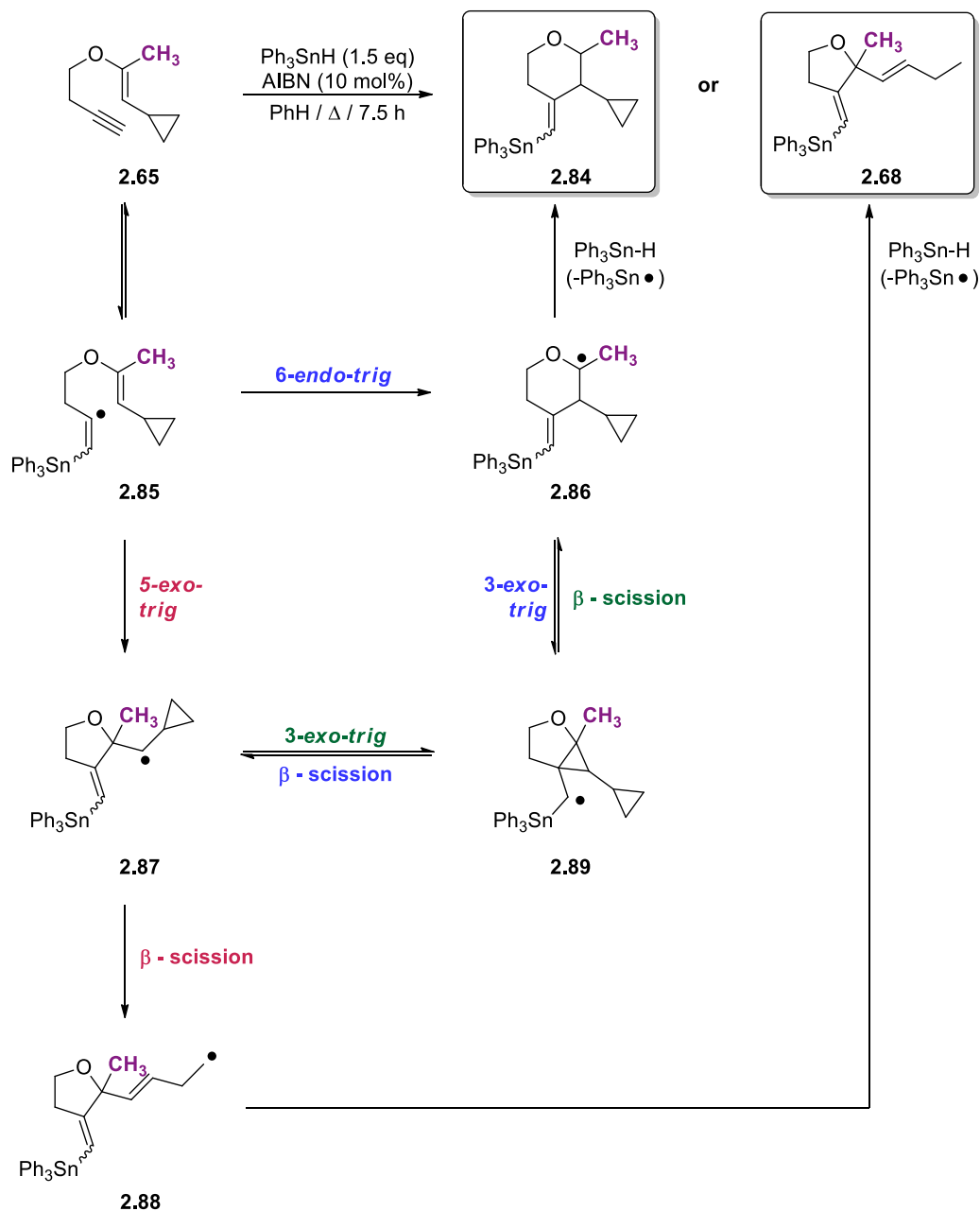
As expected, cyclization of compound **2.61** yielded exclusively the cyclopropane-opened 6-*endo* derivative **2.64** in 58% yield (**Scheme 2.27**). While this result offered no new information pertaining to the mode of cyclization, it nonetheless reaffirmed that at some point during the reaction a pyranosyl radical was formed.



Scheme 2.27 Identification of radical character at the anomeric carbon.

We next wanted to evaluate the product distribution for the radical cyclization of compound **2.65**. Addition of the stannyl radical to an unsaturated C-C bond is known to be reversible (169, 170), but once **2.85** is formed it can be trapped through one of two possible cyclization events (**Scheme 2.28**):

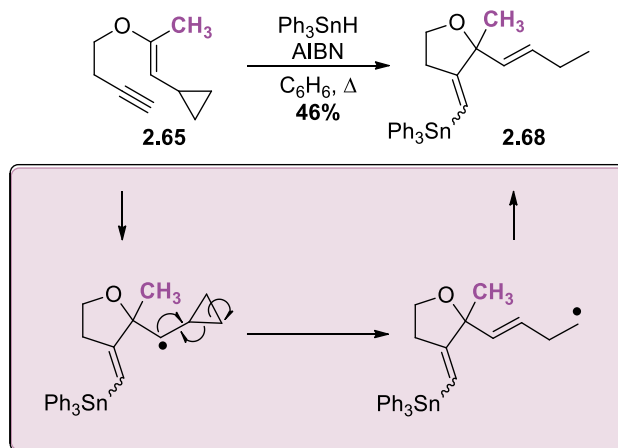
1. The first of these is that the β -stannyl alkene radical (**2.85**) would be trapped through an initial *6-endo-trig* addition onto the vinyl ether. Intermediate **2.86** should be a relatively persistent species since the carbon-centered radical is stabilized by both increased substitution at this position and through hyperconjugative effects with the α -oxygen. Rearrangement to **2.87** (*via* **2.86** \rightarrow **2.89** \rightarrow **2.87**) would proceed much more slowly than the corresponding quench, thus, one would expect exclusive isolation of compound **2.84** where the cyclopropane is left intact (**Scheme 2.28**).
2. If the formation of the tetrahydropyran occurs through an indirect mechanism *via* an initial *5-exo-trig* cyclization event then, after ring closure, cyclopropylcarbinyl radical **2.87** would result. Two fates are possible for this reactive intermediate: (a) the cyclopropane ring will open (at a rate of *ca.* 10^8 s^{-1}) to yield **2.88**. Subsequent quenching of the homoallylcarbinyl radical (the rate for the reverse reaction, k_C , has been determined to be *ca.* 10^4 s^{-1})(171) would give rise to product **2.68**, offering support to the thesis statement for which this work was undertaken; or, (b) intermediate **2.87** could undergo a *3-exo-trig*/ β -*scission* event to yield **2.86** (and eventually **2.84**), although this is rather unlikely.



Scheme 2.28 Possible competing processes for radical cyclization of 2.65.

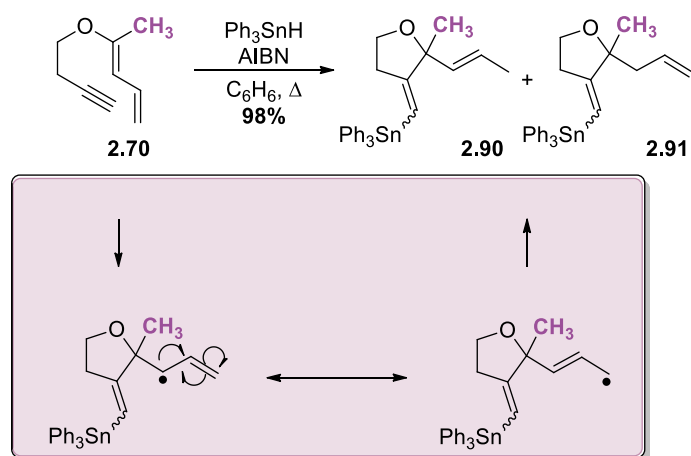
Given that a significant amount of time and effort had been invested in the synthesis of **2.65**, and it would not be trivial to introduce alkyl- or aryl-substituted cyclopropanes into our scaffold, we were most delighted to find that radical cyclization of **2.65** resulted in exclusive formation of the cyclopropane-ring opened furan derivative **2.68**, lending

considerable support that a *5-exo-trig* cyclization process is the initial step in the overall reaction sequence (**Scheme 2.29**).



Scheme 2.29 Formation of **2.68** confirms initial *5-exo* mode of cyclization.

This result was further supported when diene **2.70** also cyclized to give only 5-membered ring products **2.90** and **2.91**, as a mixture of inseparable isomers (**Scheme 2.30**, **2.90:2.91**, 4:1).



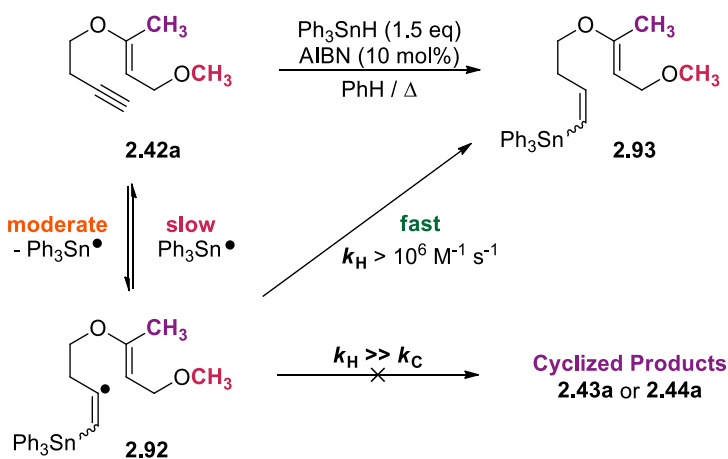
Scheme 2.30 Cyclization of substrate **2.70**.

While the results in **Scheme 2.29** and **Scheme 2.30** offer support to a mechanism where trapping of the alkenyl radical occurs through an initial *5-exo-trig* cyclization, the possibility that the *5-exo-trig*/ β -*scission* products **2.59** and **2.68** could arise from an initial *6-endo-trig* cyclization, followed by isomerization to a formal *5-exo-trig* intermediate, which then undergoes β -*scission*, could not be discounted. While it is unlikely that this is the case, the reversibility of the *3-exo-trig*/*retro-3-exo-trig* rearrangement (**2.56** \rightarrow **2.57** \rightarrow **2.54** vs. **2.54** \rightarrow **2.57** \rightarrow **2.56**, **Scheme 2.19**) and the steric hindrance afforded by the alkyl substitution at **R**¹ (which should disfavour attack of the alkenyl radical at the 5-position relative to the approaching radical) requires that we find solid grounds with which to disprove this possibility.

2.9 Validation of a 5-exo/3-exo/retro-3-exo Pathway

Several possibilities presented themselves as a means to validate our earlier findings. The most obvious approach was to determine whether the product ratio (5- to 6- membered ring) was dependant on the concentration of hydrogen donor available during the course of the reaction.^(172, 173) Unfortunately, our system was found to be incompatible with this type of experiment as attempts to increase the rate at which the triphenyltin hydride and AIBN were added to a solution of refluxing alkyne, **2.42a**, resulted in reduction of the β -stannyl alkene radical (**2.92**) affording **2.93** as the major product (**Scheme 2.31**).

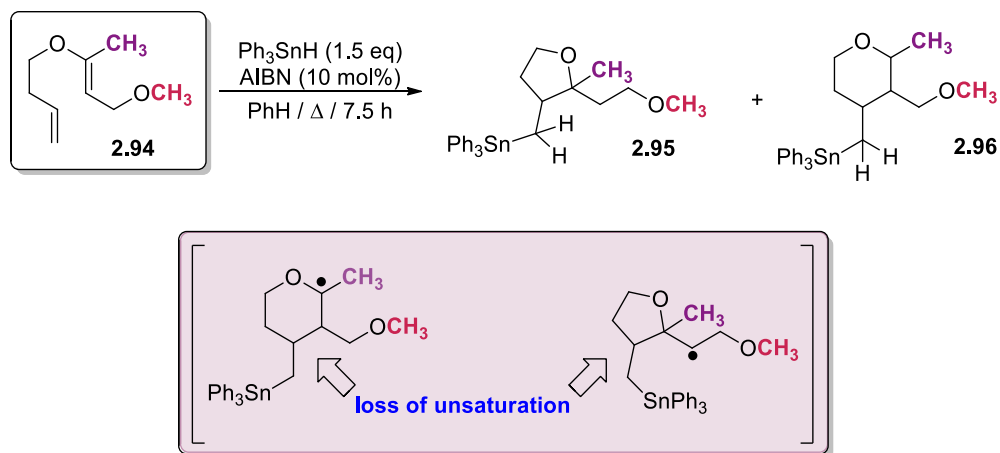
As stated previously, addition of stannyl radicals to π -systems is a reversible process.¹³ In most systems, once a β -stannyl alkene radical is formed the forward reaction tends to be much faster than fragmentation into alkynes and Sn-radicals.⁽¹⁷⁴⁾ Having said that, alkenyl radicals possess a high lying SOMO, effectively increasing the energy barrier to cyclization onto our electron-rich vinyl ether. The competing hydrogen abstraction from triphenyltin hydride,⁽¹⁷⁵⁾ which occurs at a rate greater than $10^6 \text{ M}^{-1}\text{s}^{-1}$, precludes formation of any significant quantities of cyclized product (**Scheme 2.31**).



Scheme 2.31 Faster addition of triphenyltin hydride precludes cyclization onto the vinyl ether due to the faster, competing hydrogen atom transfer.

As an alternative approach, we elected to disrupt the reversibility of 3-*exo* ring closure by removing the intermediacy of the homoallyl radical (**Scheme 2.32**).

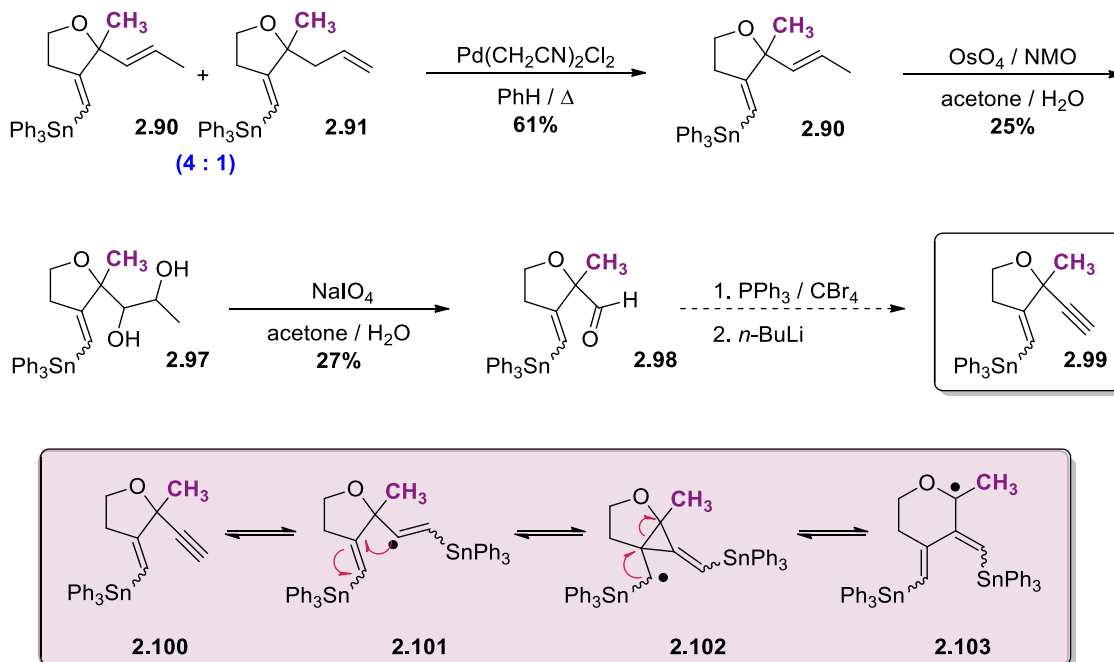
¹³ No absolute rate coefficients have been determined for the addition of a stannyl radical to unsaturated carbon systems (*i.e.* $\text{C}\equiv\text{C}$ and $\text{C}=\text{C}$), however it is known that addition to the alkyne is considerably slower compared to addition to the corresponding alkene system.



Scheme 2.32 Proposed trapping of monocyclic products originating from an initial cyclization event onto a vinyl ether.

Such an approach seemed to be a good idea at the time. In hindsight, changing the radical precursor would lead to several consequences that would manifest themselves as a failed attempt at cyclization. In contrast to alkyne **2.42a**, addition of the tin radical to alkene **2.94** should proceed more quickly, however the lower reactivity of the resulting alkyl radical would render it more susceptible to β -elimination ($k_f > 10^6 \text{ M}^{-1}\text{s}^{-1}$).¹⁴ We had hoped that the overall lower concentration of tin hydride available in solution, at a given time, would compensate for this poor reactivity, but after several attempts to cyclize **2.94** we found that we could only recover unreacted starting materials with no evidence of cyclized product. Therefore, we decided to revisit the products resulting from radical cyclization of diene **2.70** (Scheme 2.33).

¹⁴ In *Comprehensive Organic Synthesis*, Trost, B. M.; Flemming, I.; Paquette, L. E. Pergamon: Oxford, 1991; Vol. 4, p. 744.



Scheme 2.33 Proposed route to probe the intermediacy of **2.102**.

One way to prove the intermediacy of **2.102** would be to subject furan derivative **2.99** to our conditions for tin-mediated radical cyclization. Access to the ring expansion product (from **2.103**) from this substrate would support the proposed rearrangement mechanism (**Scheme 2.33**).

We envisioned synthesizing target **2.99** through elaboration of our isolated cyclic products **2.90** and **2.91**. Isomerization of the olefin to the more thermodynamically stable isomer was accomplished using bis(acetonitrile)palladium(II) dichloride(176) with heating in benzene to afford **2.90** as primarily one regioisomer (**2.90:2.91** > 10:1). The low yield obtained from this reaction was attributed to transmetalation of the stannane, where the resulting volatile furan was lost upon concentrating under reduced pressure.

Dihydroxylation using Upjohn conditions(177) followed by oxidative cleavage gave aldehyde **2.98**.

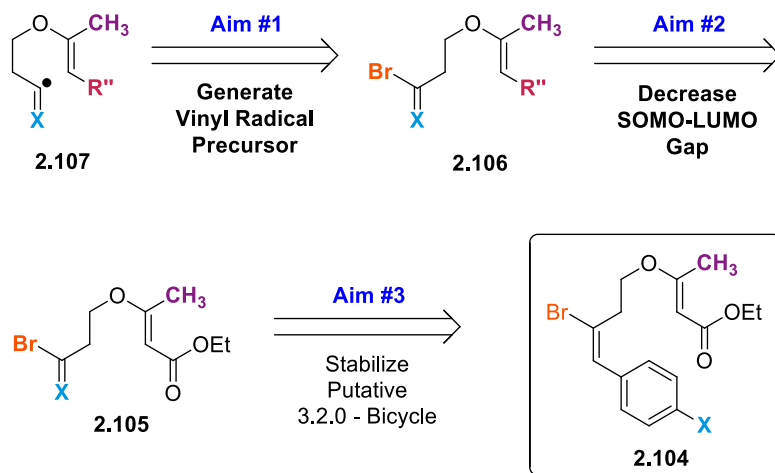
Although we were able to access the required intermediate **2.98** for conversion to **2.99**, the low yields for its formation resulted in the decision to forego the Corey-Fuchs alkynylation and instead we opted to explore the mechanism for rearrangement using a modified scaffold that would exhibit similar reactivity to the parent system.

2.10 Vinyl Halides as an Alkyne Surrogate

To resolve the issues encountered in **Section 2.9**, and to permit further study of the radical cascade reaction, we decided to instead target compound **2.104** as a synthetic equivalent to alkyne **2.42a**.(126, 127, 172, 178, 179) We imagined that irreversible abstraction of the vinyl bromide by a stannyl radical *via* this route would be comparatively fast (with respect to formation of the alkenyl radical in **2.42a**) — thus depleting the available pool of unreacted Ph_3SnH (**Scheme 2.34**).

Secondly, our mono-vinyl ether / alkyne conjugates generally afforded only a single product after each cyclization attempt (*e.g.*, **2.42a** yielded either the 6-*endo* ring system or the product resulting from direct Sn-H addition across the alkyne **2.93**, depending on the rate of addition of Ph_3SnH and AIBN). A brief survey of alternative reaction conditions failed to yield any other cyclized products that we could use for the basis of comparison. To address this problem, and ensure trapping of the nucleophilic vinyl radical, an electron-withdrawing group conjugated to the vinyl ether was maintained in **2.104**. The advantage

of this approach was that a discernable mixture of products should result, the concentrations of which might vary in response to applied cyclization conditions. Also, by decreasing the SOMO-LUMO gap we ensure that at least some of the alkenyl radical will be trapped by addition onto the olefin.

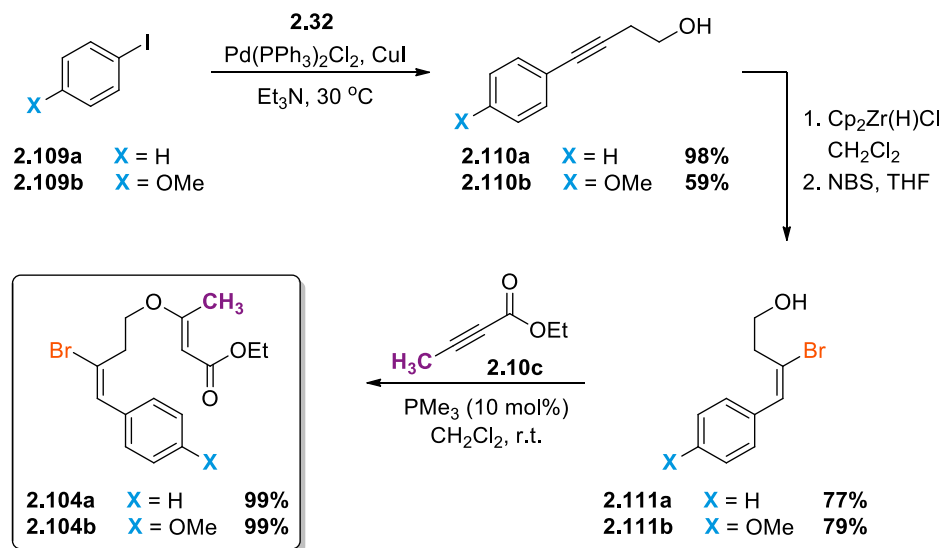


Scheme 2.34 Vinyl bromides as precursors to alkenyl radicals.

In keeping with our original synthetic platform, we decided to elaborate alcohol **2.32** for easy incorporation of this substrate into our conjugate addition sequence (**Scheme 2.35**). We decided to also install phenyl substituents with electron-donating (**X** = OCH₃), electron-neutral (**X** = H) and electron withdrawing (**X** = C(O)CH₃) functionality at the *para*-position. The rationale behind this later modification was twofold:

1. First, we had hoped that we would be able to obtain some additional information about the energetic barrier associated with the *3-exo/retro-3-exo* isomerization process.
2. Secondly, another research group⁽¹⁷⁹⁾ reported successful isolation of the putative *3-exo* intermediate from a related isomerization using similarly substituted vinyl bromide precursors. Benzylic stabilization afforded to the radical intermediate likely

enabled its trapping in the presence of tributyltin hydride. We reckoned that the increase in hydrogen donor capability of triphenyltin hydride may enable us to, likewise, trap our 3.2.0.-bicycle in order to prove its intermediacy in the reaction pathway.

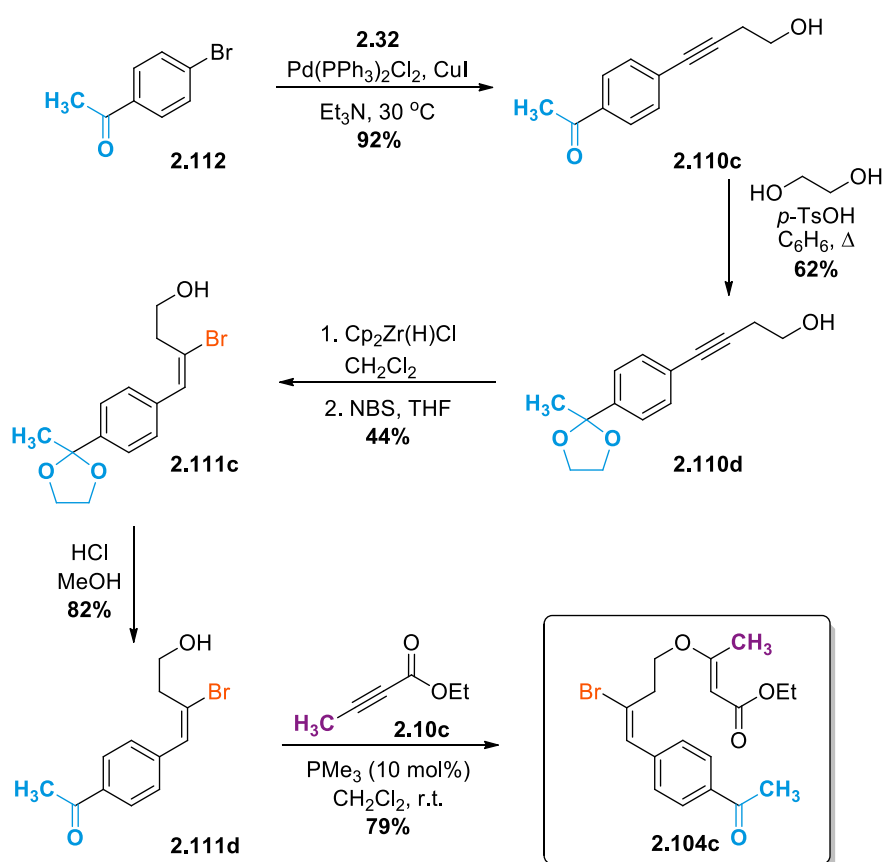


Scheme 2.35 Synthesis of vinyl bromides **2.104a** and **2.104b**.

Compounds **2.104a** and **2.104b** were synthesized as shown in **Scheme 2.35**. The appropriate aryl halide was coupled to 3-butyn-1-ol in a Sonogashira reaction to afford **2.110**. The cross-coupled product, **2.110**, was then subjected to a hydroxyl-directed hydrozirconation,⁽¹⁸⁰⁾ followed by electrophilic trapping with *N*-bromosuccinimide to afford the vinyl bromide (**2.111**) as a single regio- and stereoisomer. Conjugate addition proceeded in high yields to afford the desired cyclization substrates **2.104a** and **2.104b**.¹⁵

¹⁵ Chromatographic purification was found to be insufficient for removal of residual halides from the previous reaction steps in this sequence. The success of the conjugate addition therefore required that alcohol **2.111a** and **2.111b** be washed with an aqueous solution of sodium thiosulfate prior to use.

A slightly modified approach was required for the synthesis of **2.104c**. The procedure required that the carbonyl group be unmasked during the Sonogashira coupling (where an electron deficient substrate is advantageous) but be protected for the hydrozirconation step (where a more nucleophilic alkene was required for electrophilic trapping). An acetal protection / deprotection sequence was therefore included in the synthesis of this substrate (Scheme 2.36).



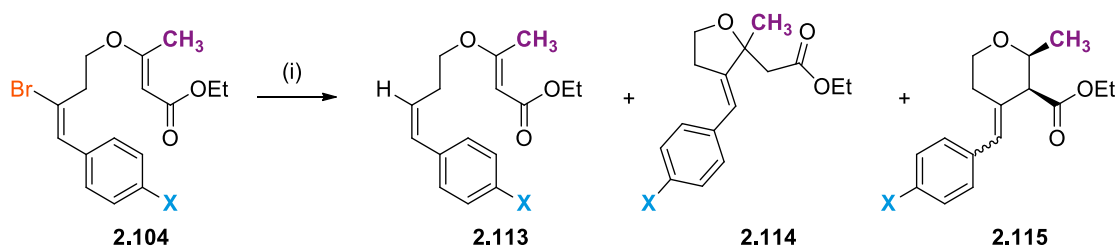
Scheme 2.36 Synthesis of vinyl bromide **2.104c**.

Vinyl bromides **2.104a–c** were then subjected to our standard radical cyclization protocol. We were pleased to discover that cyclization of **2.104a** and **2.104b** afforded an approximate 1:1 ratio of 5- and 6-membered ring products, along with some reduced substrate when

triphenyltin hydride and AIBN were added over a 6.25 hour period (entry 1 and 2, **Table 2.3**). The ratio of cyclized products was found to be in good agreement with the cyclization of **2.33a** (**Scheme 2.15**) which was carried out under identical reaction conditions. Furthermore, these compounds could be effectively separated by flash column chromatography on silica gel to provide clean samples of **2.113**, **2.114** and **2.115** for characterization with excellent combined, overall yield.

Surprisingly, compound **2.104c** did not react under these conditions (entry 3, **Table 2.3**). This result was attributed to the presence of the electron-withdrawing ketone conjugated to the vinyl halide, which presumably made the bromide more difficult to abstract.

Table 2.3 Change in Product Distribution with Addition Rate^a



| Entry | Substrate | X | Addition Time, h | 2.113 / 2.114 / 2.115 ^b |
|-------|---------------|---------------------|------------------|------------------------------------|
| 1 | 2.104a | H | 6.25 | 0.5 / 1.0 / 1.0 |
| 2 | 2.104b | OCH ₃ | 6.25 | 0.8 / 1.2 / 1.0 |
| 3 | 2.104c | C(O)CH ₃ | 6.25 | — ^c |
| 4 | 2.104a | H | 2.50 | 1.0 / 1.5 / 1.0 |
| 5 | 2.104b | OCH ₃ | 2.50 | 1.3 / 1.5 / 1.0 |

^aConditions: (i) Ph₃SnH (1.5 eq) and AIBN (0.1 eq) were added to a refluxing solution of **2.104** (final concentration of 8 mM) in benzene. Heating was continued for 1.5 h prior to work-up. ^bCompound **2.115** was formed as an approximate 1:1 mixture of geometrical isomers. ^cOnly recovered starting material was observed.

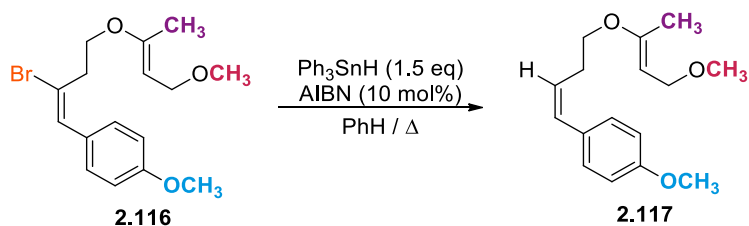
Since ring closure of vinyl bromide **2.104a** and **2.104b** competes with direct reduction by triphenyltin hydride, the yield of the acyclic product is expected to increase with a faster addition of Ph₃SnH and AIBN. With respect to the ratios of the cyclic products, however, the faster addition of these reagents will manifest itself differently for each of the three mechanistic possibilities that are under investigation:

1. If the formation of **2.114** and **2.115** are independent of one another the overall yield of cyclic product will decrease, but the ratio of **2.114** to **2.115** will remain unchanged.
2. If the formation of **2.115** does not occur through a direct *6-endo-trig* cyclization, but through an initial *5-exo-trig* cyclization followed by rapid rearrangement *via* a reversible *3-exo-trig*/ β -*scission* process, then the *5-exo*:*6-endo* ratio will appear as a function of tin hydride concentration (with higher concentrations favouring the kinetic *5-exo* product).
3. If the formation of **2.115** occurs through a direct *6-endo-trig* cyclization, but then rearranges *via* a reversible *3-exo-trig*/ β -*scission* process, then the *5-exo*:*6-endo* ratio will, again, appear as a function of tin hydride concentration (with higher concentrations favouring the *6-endo* product).

Changing to a faster addition rate for **2.104a** and **2.104b** (entries 4 and 5, **Table 2.3**) resulted in a significant increase in the amount of **2.114** relative to **2.115**. This result unambiguously confirmed that the *5-exo-trig* cyclization is the first step in the cascade.¹⁶

¹⁶ Attempts to conduct the same reaction with a longer addition time (17.6 h) failed to yield any measurable quantity of **2.113**, **2.114** or **2.115**. Premature formation of hexaphenyldistannane precluded halide abstraction.

To ensure that these results were in no way altered by electronic factors governing the mode of cyclization (and that the same mechanism is operative in the reduced system) we also performed the reaction on substrate **2.116** (Scheme 2.37).



Scheme 2.37: Attempted cyclization of 2.116.

Access to ether **2.116** was complicated by inherent differences in the reactivity profile of **2.104b** towards reduction and subsequent methylation (when compared to all other vinyl ethers described in this Chapter). Nevertheless, enough material was obtained to explore the result of radical cyclization using this substrate.

Using identical conditions to those employed for cyclization of **2.104a–c** (Table 2.3), **2.116** reacted to form **2.117** as the major product. This result was not surprising, given the larger energy barrier towards cyclization. Further analysis of the crude reaction mixture by thin layer chromatography did indicate that there were additional, minor compounds present in the sample. Purification of the crude oil revealed that minute amounts of both 5-membered and 6-membered ring products were formed during the course of the reaction. This result provides additional evidence to support the notion that, even in the absence of a conjugated electron-withdrawing group off the vinyl ether, the reaction proceeds through

an initial 5-*exo-trig* cyclization followed by rapid rearrangement to yield the formal 6-*endo*-product.

2.11 Theoretical Analyses Pertaining to Product Distribution

2.11.1 Effect of Phenyl Substitution on Product Distribution

Returning to **2.104a** and **2.104b**, we were surprised to find that both the methoxy-substituted (**2.104b**) and the unsubstituted aryl vinyl bromide (**2.104a**) gave a very similar ratio of 5-*exo* and 6-*endo* product. We had anticipated that inclusion of an electron-donating group on the phenyl ring would provide stabilization to the intermediate formed after 3-*exo*-cyclization (analogous to **2.57**, **Scheme 2.19**), thereby reducing the overall barrier to isomerization and favouring the six-membered ring product **2.115**. To explain why this did not occur, we turned to DFT calculations to evaluate the relative heats of formation for the various intermediate radical species pictured in **Figure 2.4**.¹⁷

¹⁷ All calculations were performed by supervisor Dr. Jeremy Wulff at the B3LYP/6-31G* level using the Spartan 06 Molecular Modeling package.

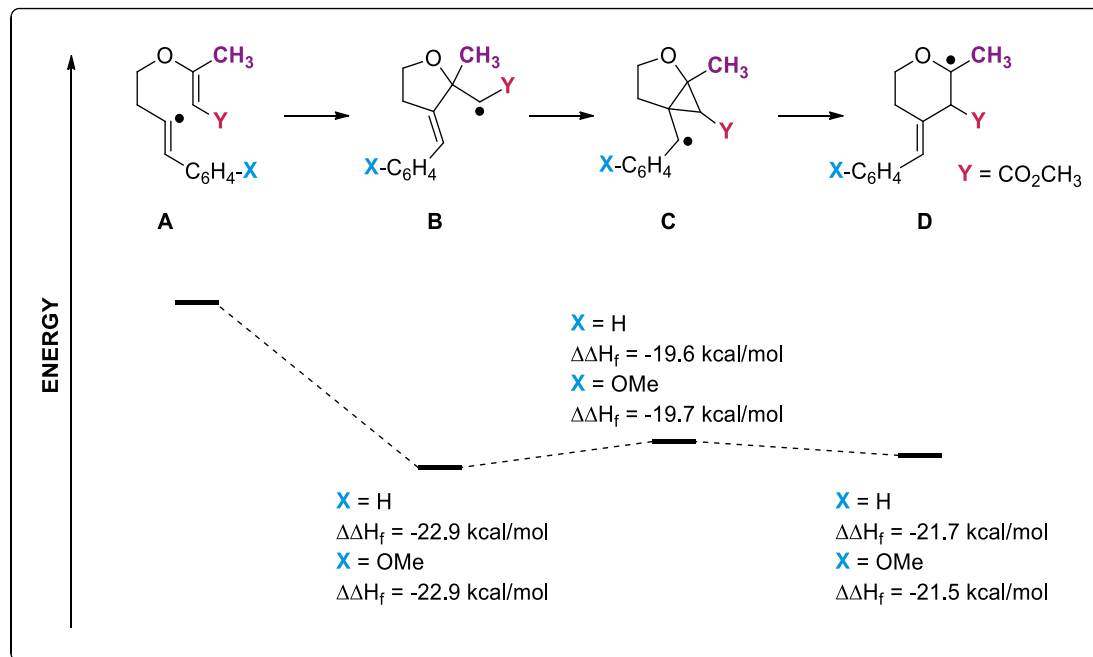


Figure 2.4 DFT calculations investigating the effect of substitution on the aromatic ring

As shown in **Figure 2.4**, methoxy-substitution of the phenyl ring does not substantially change the relative energies of the 3-*exo* product (**B**). In fact, the calculated energies for **B**, **C** and **D** (relative to **A**) are essentially identical between the two series. It is interesting to note that the calculated energies for **B** and **D** are also quite close together (within approximately 2 kcal/mol) favouring an almost eqimolar product mixture of the five- and six-membered ring radical intermediates. This picture is consistent with the experimental results reported in **Table 2.3** in which compounds **2.114** and **2.115** were observed in similar quantities when triphenyltin hydride was added over a 6.25 hour period (entry 1 and 2).

2.11.2 Effect of Substitution on the Vinyl Ether

Having established that all of our cyclizations do indeed occur through an initial 5-*exo-trig* addition onto the vinyl ether, the results presented earlier in the chapter for the cyclization

of mono-vinyl ether / alkyne conjugates are somewhat puzzling. The enhanced preference for the formation of the six-membered ring product for methyl-substituted vinyl ethers **2.33a** and **2.42a** (relative to **2.33b** and **2.42b**) appears, at first glance, to be the result of a classic kinetically controlled regioselectivity bias, where the incoming radical has been directed away from the more sterically encumbered end of the vinyl ether function. We know, however, that this cannot be the case since all of our cyclizations proceed through an initial 5-*exo* attack on the olefin.

The regiochemical control observed for this system, when $\mathbf{R}^1 = \text{CH}_3$ versus H, must be due to either a change in the rate for isomerization leading to the 6-membered ring (analogous to **2.56** \rightarrow **2.57** \rightarrow **2.54**) or a difference in the thermodynamic preference for **2.54** vs. **2.56** (**Scheme 2.19**). To provide an answer to this question, we again turned to DFT calculations to evaluate the relative heats of formation for the intermediate radical species leading to compounds analogous to **2.43a** (when $\mathbf{R}^1 = \text{CH}_3$) versus those leading to **2.43b** and **2.44** (when $\mathbf{R}^1 = \text{H}$). To avoid relativistic effect problems associated with the tin atom, we replaced the triphenyltin substituent with a methyl group.

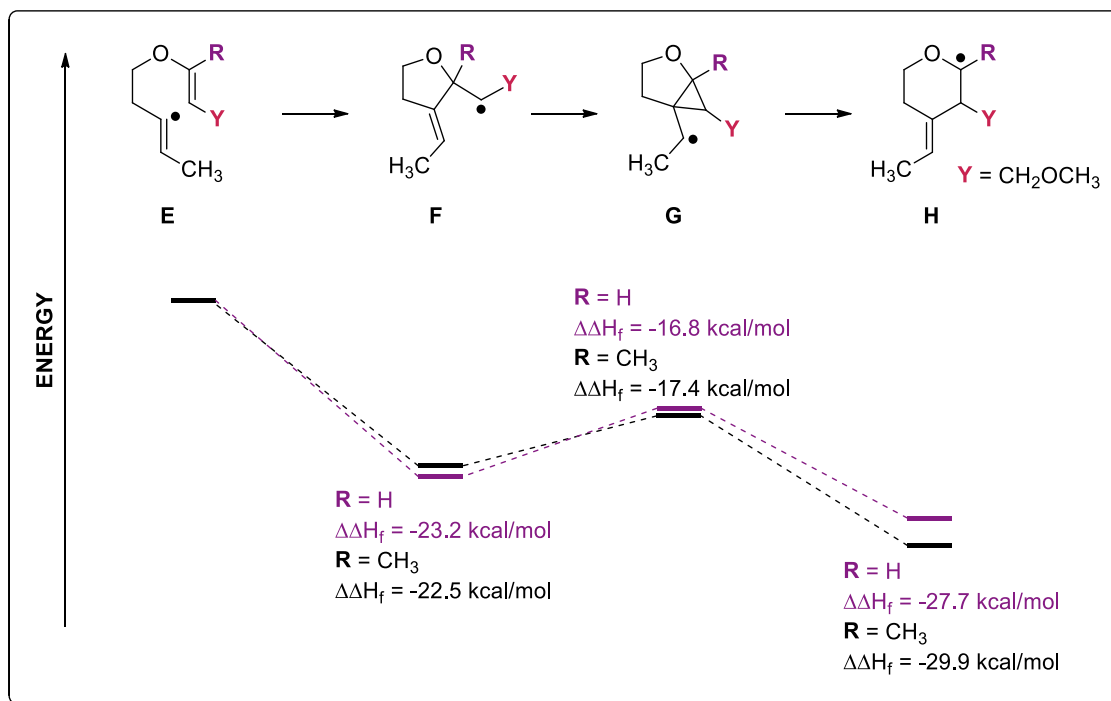
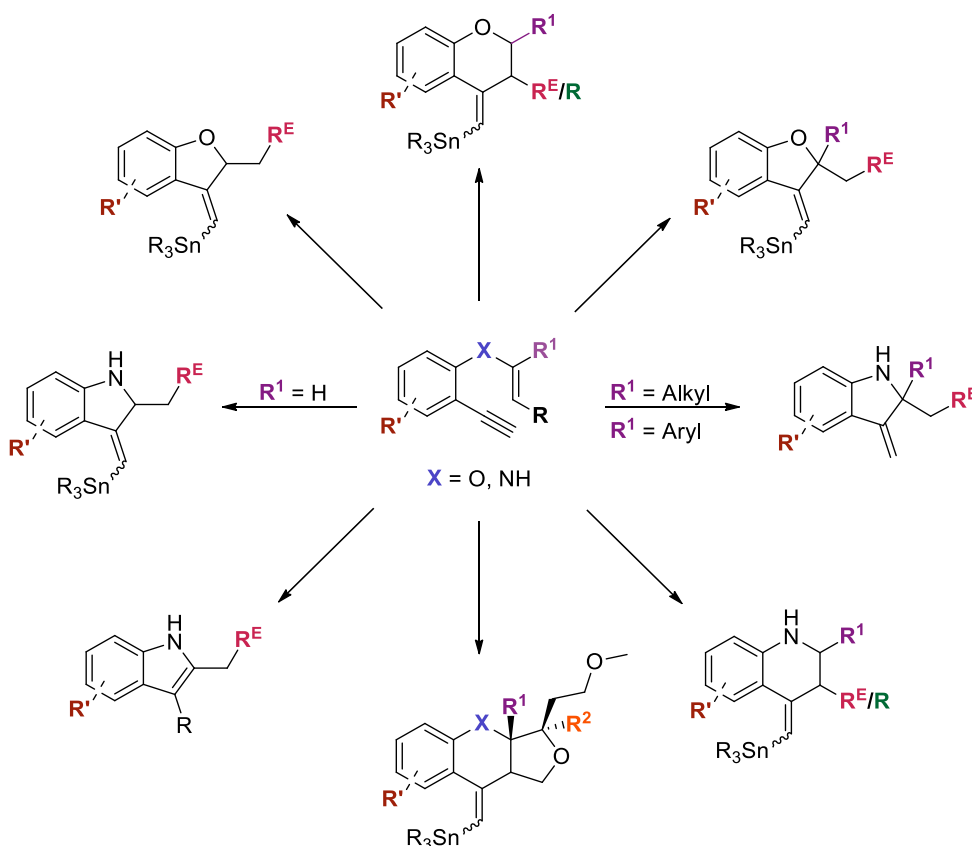


Figure 2.5 Effect of substitution on the vinyl ether

As depicted in **Figure 2.5**, alkyl substitution at the **R¹** position is found to destabilize the 5-*exo* radical intermediate **F** due to steric strain associated with formation of the new quaternary center. This same substitution in 6-*endo* radical intermediate **H**, on the other hand, stabilizes the anomeric radical by incorporating a greater degree of substitution at this electron deficient center. The combination of these two effects nearly double the degree to which the pyranosyl radical is favoured (7.4 kcal/mol when **R¹** = CH₃ vs. 4.5 kcal/mol when **R¹** = H). While this analysis omits discussion of the rate for which these species (**F** and **H**) may be quenched by the incoming hydride donor, it does provide some rationale for the extent to which substitution on the vinyl ether can control the regiochemical outcome of the reaction without changing the site of initial attack.

2.12 Behaviour of Intermediate Radicals: Hydrogen Atom Transfer in Bis-Vinyl Ethers

The exhaustive detailing of the mechanism developed thus far for the conversion of **2.48** to **2.49** should be useful in designing future radical cascades leading to alternatively fused bicycles and polycycles that may have utility in a number of medicinal chemistry programs (*e.g.*, **Scheme 2.37**).

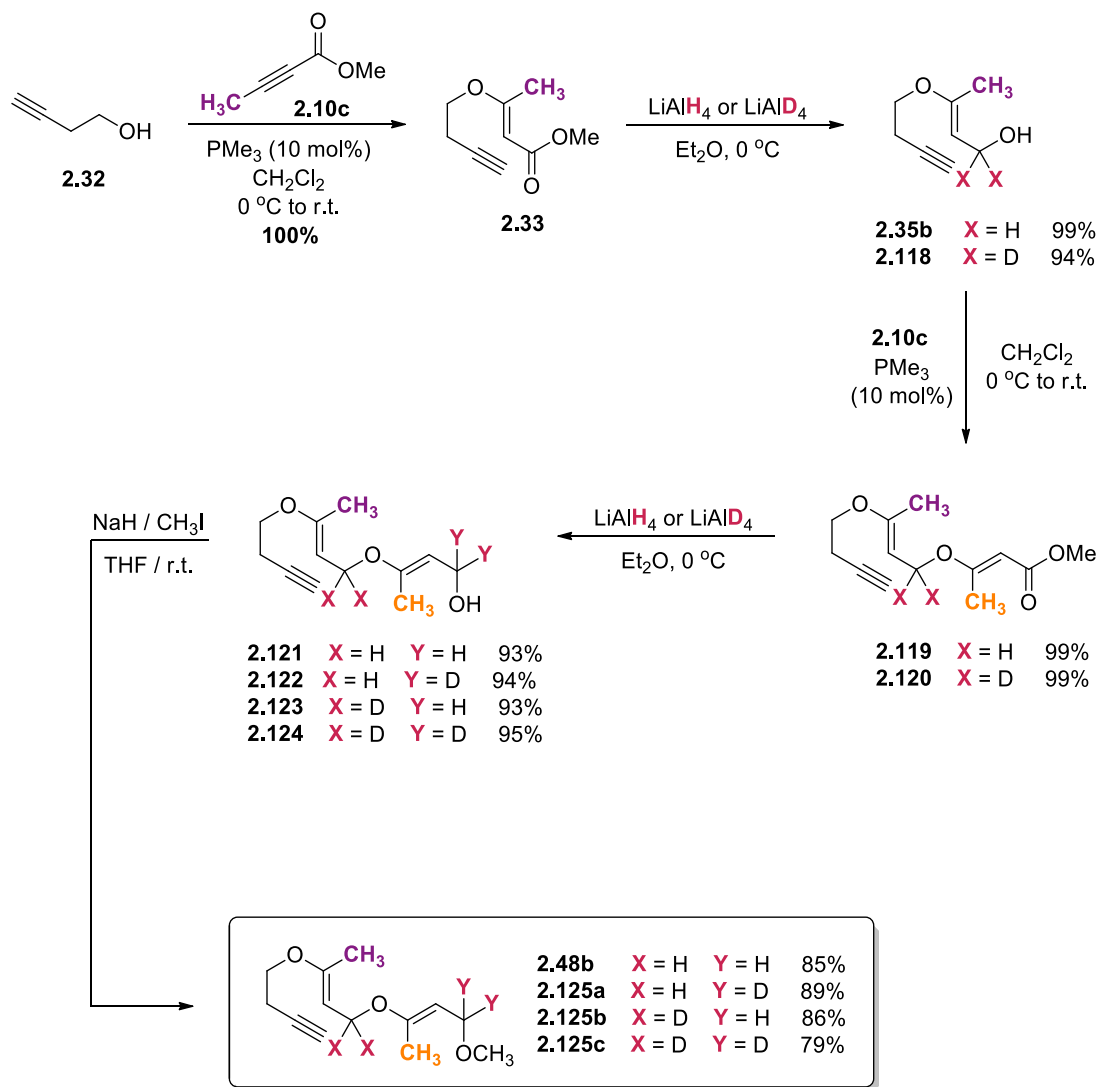


Scheme 2.37 Plausible scaffolds for development of medicinal chemistry programs using our radical cascade methodology. All substrates are amenable to further functionalization. For example: vinyl stannanes can be used in palladium-mediated couplings, while exocyclic olefins can participate in [3+2] cycloaddition reactions with substituted allenes.

This former statement, however, can only be true if the various radical intermediates (**2.54**–**2.56**, **Scheme 2.19**) are well-behaved and do not participate in hydrogen atom

transfers with other positions on the substrate. In particular, we recognised that two carbon centers on bis-vinyl ether **2.48** were positioned between an oxygen and an alkene, effectively decreasing the bond dissociation energy associated with the C-H bonds at these positions (*i.e.*, the resulting radicals would be highly stabilized). If hydrogen atom abstraction from these positions occurred, and resulted in the quenching of late stage radicals such as **2.56**, **2.54** or **2.55** (**Scheme 2.19**), prior to quenching with the desired hydride source (Ph_3SnH), then the potential utility of these substrates in future radical cascades would be undermined by their inability to persist long enough to engage in additional cyclization steps (should they be desired).

To evaluate the likelihood of these unwanted side reactions, Katherine Davies synthesized a number of deuterated analogues, using LiAlD_4 in place of our usual reducing agent (DIBAL-H or LiAlH_4) in the conjugate addition / reduction sequence (**Scheme 2.38**).



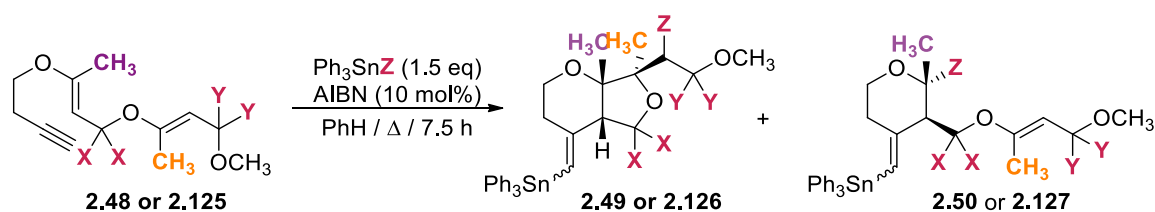
Scheme 2.38 Synthesis of deuterated substrates for evaluation of premature quenching of radical intermediates by hydrogen atom transfer reactions.

In designing these substrates, we intentionally chose bis-vinyl ether **2.48b** as our model system (where $\mathbf{R}^1 = \mathbf{R}^2 = \text{CH}_3$) as we knew from previous studies(82) that this construct provided both the monocyclic and bicyclic products (**2.49b** and **2.50b**) when subjected to the conditions for our radical cyclization. This provided us with a method by which to fully probe the stability of each intermediate, since we would be able to isolate and characterize two distinct products from each deuterated substrate. Evaluation of the monocyclic

substrates was of particular interest to us since we reasoned that **2.54** would be the most persistent of the cyclic radical intermediates, making it the most probable to participate in any unwanted hydrogen (or deuterium) transfers. If no deuteration were detected at the anomeric position of product **2.54**, following cyclization, we could confidently assert that the likelihood of premature quenching by hydrogen atom transfer was quite low.

Gratifyingly, cyclization of **2.48** and **2.125a–c** led to no detectable migration of the deuterium label(s) in either the fully cyclized (**2.49** or **2.126**) or partially cyclized (**2.50** or **2.127**) products (**Table 2.4**, entries 1–4). No partial deuteration of undeuterated positions could be detected by NMR integration of the purified products, nor did we observe any degree of deuterium erosion at the deuterated position by MS analysis. To complete this series of investigations, Katherine Davies also synthesized triphenyltin deuteride (Ph_3SnD)⁽¹⁸¹⁾ and used this (in place of Ph_3SnH) in the cyclization of the non-deuterated substrate **2.48b** (**Table 2.4**, entry 5). As anticipated, we observed complete deuteration at the anomeric position of **2.50**, along with 50% deuteration at each of the two diastereotopic positions in **2.49**.

Table 2.4 Cyclization of Deuterated Substrates

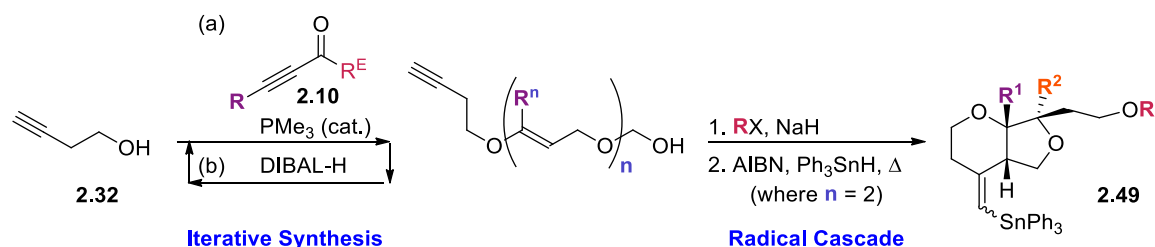


| Entry | Substrate | 2.49 or 2.126 | | | 2.50 or 2.127 | | |
|----------------|--------------------|----------------|----------------|----------------|----------------|----------------|----------------|
| | | X ^a | Y ^a | Z ^a | X ^a | Y ^a | Z ^a |
| 1 ^b | 2.48b | H (>90) | H (>90) | H (>90) | H (>90) | H (>90) | H (>90) |
| 2 ^b | 2.125a | H (>90) | D (>90) | H (>90) | H (>90) | D (>90) | H (>90) |
| 3 ^b | 2.125b | D (>90) | H (>90) | H (>90) | D (>90) | H (>90) | H (>90) |
| 4 ^b | 2.125c | D (>90) | D (>90) | H (>90) | D (>90) | D (>90) | H (>90) |
| 5 ^c | 2.48b ^d | H (>90) | H (>90) | D (>90) | H (>90) | H (>90) | D (>90) |

^aPercent incorporation is given in parentheses. ^bReaction was performed using Ph₃SnH. ^cReaction was performed using Ph₃SnD. ^dFor **2.49**, two diastereotopic hydrogen atoms can be replaced by deuterium; approximately 50% deuteration was observed at each position.

2.13 Summary

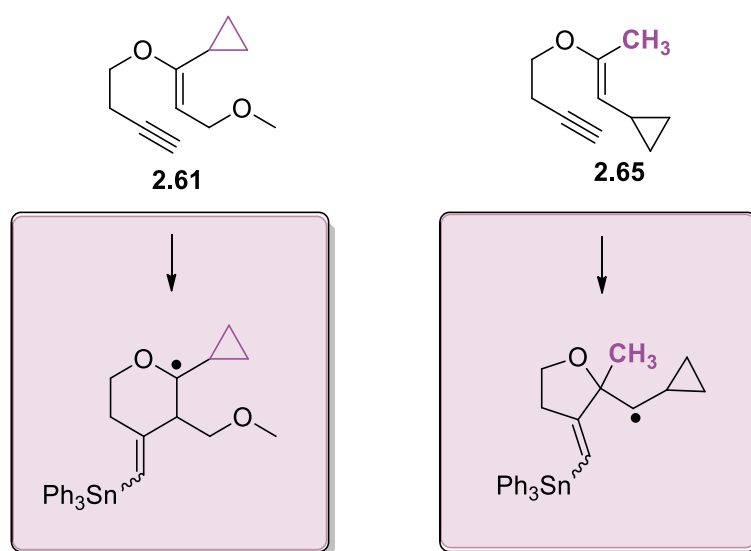
This chapter details our efforts towards developing new synthetic methodology to invoke a radical cascade cyclization across bis-vinyl ether / alkyne conjugates, allowing us to access architecturally rich, bicyclic structures (**Scheme 2.39**).



Scheme 2.39 Efficient access to molecular complexity by marrying iterative synthesis to radical cascade cyclizations.

Substrates **2.48** are readily synthesized from simple building blocks using our established conjugate addition / reduction protocol. Exploration of substrate scope was performed by Katherine Davies, and the system was found tolerant of a wide range of substituents at \mathbf{R}^1 ($\mathbf{R}^1 = \text{H}$, alkyl or aryl) and \mathbf{R}^2 ($\mathbf{R}^2 = \text{H}$ or alkyl). Stannyl-mediated radical cyclization across bis-vinyl ethers furnished bicyclic products **2.49**, setting three contiguous stereocenters and up to two adjacent quaternary centers in one synthetic operation with high yield and good overall diastereoselectivity (**Scheme 2.39**).

Mechanistic investigations were performed to determine the mode of cyclization leading to formation of **2.49**. Radical trapping agents (*i.e.*, cyclopropanes, **Scheme 2.40**) were incorporated into the vinyl ether scaffold to probe the location of radical character during the course of the reaction. The results from these trapping experiments indicated that radical character is formed at both the anomeric carbon and the methylene carbon.



Scheme 2.40 Use of a cyclopropane ring as a radical trapping agent to indicate those positions where radical character is developed during the cyclization of mono-vinyl ether substrates.

In order to determine whether the formation of the six-membered- and five-membered-ring systems were independent of one another (or whether the six-membered ring was formed indirectly through an initial *5-exo* attack on the olefin followed by rearrangement), the rate of stannane addition was varied in the reaction with a series of vinyl bromides (**Table 2.3**). Product distribution was found to be dependent on the rate at which the hydride donor was added to the reaction flask, providing unambiguous evidence that the formation of the bicyclic product occurs through an initial *5-exo-trig* addition, followed by a *3-exo-trig*/ β -scission sequence to indirectly afford the pyranosyl radical, which can then undergo a second *5-exo-trig* cyclization yield **2.49**. Finally, we discovered that the last step in our cascade cycle is the direct delivery of a hydride from Ph_3SnH .

Chapter 3 Thermal Aliphatic Claisen Rearrangement

Adapted from:

Natasha F. O'Rourke¹ and Jeremy E. Wulff¹

Organic and Biomolecular Chemistry (2014) 12, 1292-1308

with permission of The Royal Society of Chemistry.

¹Department of Chemistry, University of Victoria, Victoria, BC, Canada

NFO designed and conducted all research that appeared in the full manuscript published in *Organic and Biomolecular Chemistry*. This includes the synthesis and characterization of all substrates, analysis of all spectroscopic data, interpretation of results, and writing of the manuscript (edited by Dr. Jeremy E. Wulff) and accompanying supporting information.

3.1 The Aliphatic Claisen Rearrangement

The development of the Claisen rearrangement (and variants thereof) over the past century has unambiguously demonstrated the power and synthetic utility of this deceptively simple transformation.⁽¹⁸²⁻¹⁸⁷⁾ While the regio- and stereoselective formation of new carbon-carbon bonds in this manner has been widely accepted to occur through a concerted, albeit asynchronous,^(56-58, 188) bond reorganization process *via* a six-membered cyclic transition state,^(59, 60) many details about the reaction trajectory remain elusive (**Figure 3.1**). Most notably, substituent effects on the rate of Claisen rearrangement have often afforded contradictory interpretations of what the transition-state structure may look like (be it diradical^(48, 61-68) or dipolar⁽⁶⁸⁻⁷⁰⁾ in nature) and theoretical predictions are not always consistent with experimental results.^(48, 53, 63) For these reasons, substituent^(27, 48, 52, 54, 65, 69, 72, 189-201) and solvent effects^(73, 75, 190, 202) have been thoroughly investigated over the past three decades in order to elucidate the mechanistic details of the rearrangement and, more specifically, the nature and geometry of the transition-state structure. Although the precise electronic structure of the transition state presumably varies somewhat with changing substitution patterns on the allyl vinyl ether scaffold, there is general consensus as to the highly organized nature of the transition structure itself, consistent with a significant negative ΔS^\ddagger (*vide infra*).

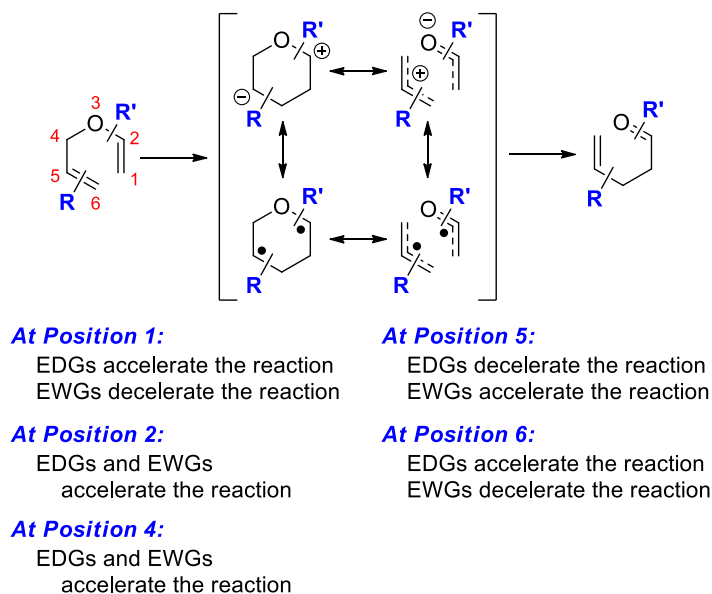


Figure 3.1 Mechanistic options for the aliphatic Claisen rearrangement, and summary of known substituent effects.

3.2 Motivation for a Mechanistic Investigation of the Claisen Rearrangement

For the past number of years, our research group has been interested in the development of chemo-orthogonal cascade transformations of reactive, oligo-vinyl ethers to enable efficient access to variously functionalized, complex small-molecules.(82, 83, 85)

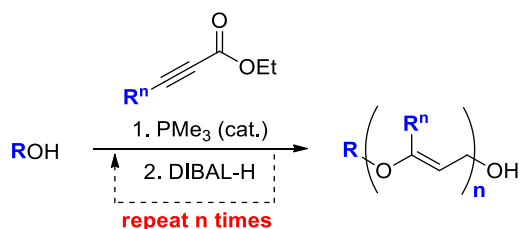


Figure 3.2 Iterative synthesis of oligo-vinyl ethers.

During the course of our studies, we have had ample opportunity to observe the propensity (or lack thereof) for these substrates to undergo Claisen rearrangement. Bis-vinyl ethers, by virtue of their bond-connectivity, are structurally related to allyl vinyl ethers, differing only by the presence of an additional oxygen atom at C6 (**Figure 3.1**). The influence of substitution, in addition to the C6 oxygen, on these substrate's ability to undergo Claisen rearrangement has not been extensively studied, notwithstanding some significant earlier contributions published by the laboratories of Curran(49-51, 54, 69, 78) and Augé(76, 203) (see also: the general trends highlighted in **Chapter 1** regarding the effect of the C6 oxygen in the Ireland-Claisen rearrangement).

In our earlier investigation in this area, we were surprised to discover that the substituent effects for our bis-vinyl ethers differed from those in the pre-existing literature for the analogous rearrangement of allyl vinyl ethers. For instance, in a series of compounds prepared by Katherine Davies as mimics of juvenile hormone III (**Figure 3.3**) we found that the presence of an electron-withdrawing ester function at the terminus of the bis-vinyl ether (effectively C1, **Figure 3.3**) system enabled the compounds to undergo facile Claisen rearrangement at remarkably low temperatures.(85) This, in addition to the ability of the Claisen products to undergo further decomposition (primarily through elimination) to afford volatile by-products, led us to propose the utility of such compounds as ecologically degradable insect control agents.(85)

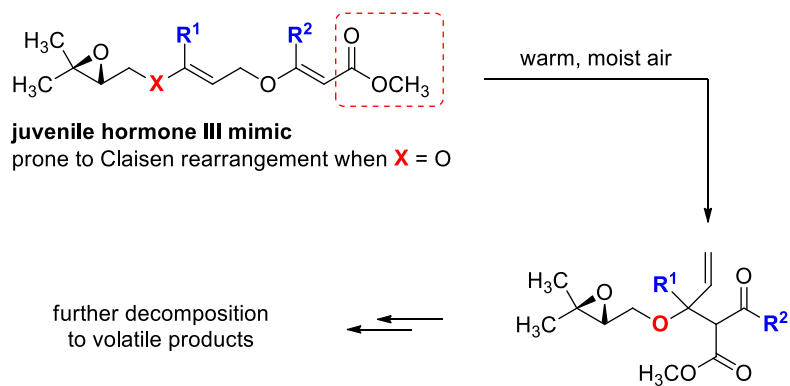


Figure 3.3 Synthetic application of bis-vinyl ethers in the development of juvenile hormone III mimics.

By contrast, substrates where the electron-withdrawing group was absent (at C1) were found to be relatively resistant to Claisen rearrangement, such that they could be used in high-temperature radical cascade reactions without any obvious signs of decomposition (**Figure 3.4**).^(82, 83)

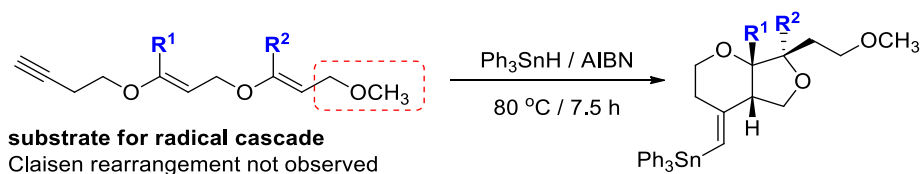


Figure 3.4 Cascade radical cyclization across bis-vinyl ether to afford architecturally-rich, complex small-molecules.

The fact that an electron withdrawing-group at C1 resulted in such a dramatic increase in the rate of Claisen rearrangement is surprising, given that previous studies of allyl vinyl ether systems had determined that electron-donating groups at C1 increase the rate of Claisen rearrangement,^(190, 193-195, 199) while electron-withdrawing groups stabilize the substrates.^(52, 69, 198)

The supposition that bis-vinyl ethers may undergo Claisen rearrangement through a fundamentally different mechanism than most other allyl vinyl ethers was additionally supported by observation that the rate of Claisen rearrangement (for JH-III mimics, **Figure 3.3**) was found to be greatly enhanced by the addition of an electron-withdrawing CF_3 group at C2 (or R^2) to such an extent that most bis-vinyl ethers of this type could not be cleanly isolated.⁽⁸⁵⁾ This propensity to undergo Claisen rearrangement could be mitigated by installation of a second CF_3 group at C6 (or R^1) to the point where <20% Claisen rearranged product was observed after 14 days of heating at 37 °C (in a carbon dioxide incubator at >90% relative humidity).

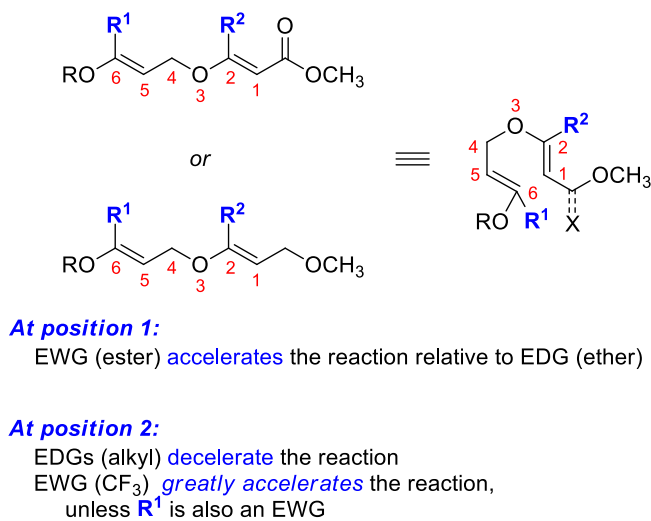


Figure 3.5 Summary of substituent effects on the rate of Claisen rearrangement, observed from our earlier bis-vinyl ether studies.

This data, summarized in **Figure 3.5**, suggested to us that the rearrangement was promoted by a “push-pull” mechanism, whereby the electron-rich half of the bis-vinyl ether system (*i.e.*, the allyl fragment, C4 to C6) serves to stabilize a developing (partial) positive charge, while the more electron-deficient half of the system (*i.e.*, the oxyallyl fragment, C1 to O3)

acts to stabilize a developing (partial) negative charge in the transition-state structure (Figure 3.6).

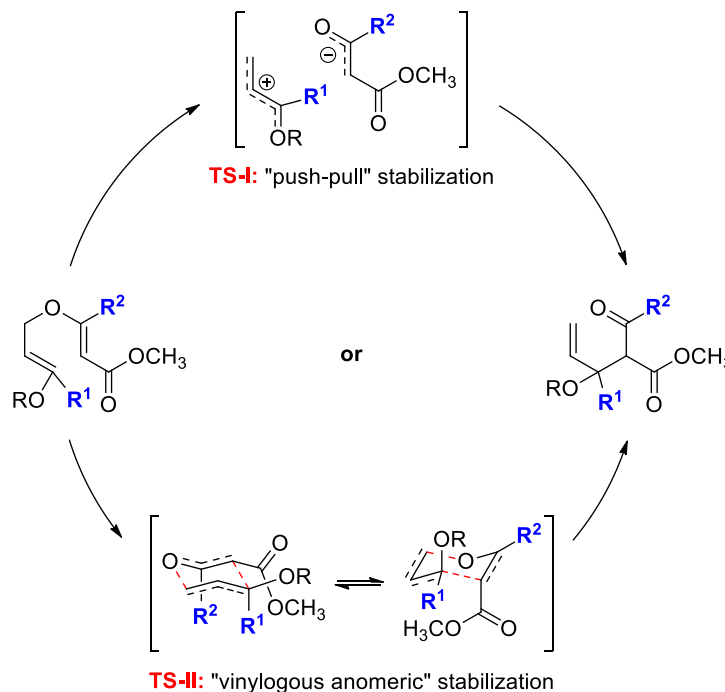


Figure 3.6 Two possible mechanistic possibilities for the observed increase in the rate of Claisen rearrangement for bis-vinyl ethers with an electron-withdrawing group on the oxyallyl fragment.

This description of the reactivity of bis-vinyl ethers is similar to Curran's postulated "vinylogous anomeric effect" used to ascribe the role of the C6 oxygen,(51, 54) but goes further in rationalizing substituent effects at C1 and C2 (or R^2).¹⁸

¹⁸ In order to rationalize the unusually fast Claisen rearrangement of α -ethoxyallyl enol ethers with nitrile substitution at C1, Curran invoked a possible bidentate ion-pair that could be stabilized by simultaneous interactions at all four termini. No further investigations were performed to unambiguously determine the nature of the transition state structure. See Coates, R. M. *et al. J. Am. Chem. Soc.* **1987**, 1160.

The implication that our bis-vinyl ethers may rearrange through a “push-pull” mechanism is significant. While all four hypothetical transition states, shown in **Figure 3.1**, are theoretically attainable (given the right combination of electron-withdrawing and electron-donating substituents),^(204, 205) a fully dissociated dipolar mechanism is distinct from that observed for all other allyl vinyl ethers. If our substrates do pass through a full charge separated transition-state structure, it should have implications for the thermodynamic properties associated with the rearrangement, particularly for the entropy of activation (ΔS^\ddagger). To better understand the mechanism by which our substituted bis-vinyl ethers rearrange to afford δ,γ -unsaturated- β -ketoesters, we undertook a more extensive study of the thermally induced aliphatic Claisen rearrangement using variable-temperature NMR methods.

3.3 Design of Substrates for VT-NMR Study

In order to analyze the thermodynamic properties of our system using variable-temperature NMR methods, we had to first design a scaffold that satisfied the following criteria:

1. at least one of the vinyl ether motifs (**R¹** or **R²**) in our bis-vinyl ether system had to be amenable to systematic variation of its electronic properties to permit Hammett-type analysis in order to probe the electronic nature of the transition state;
2. substrates would undergo Claisen rearrangement within a specified temperature range that would be consistent with study by variable-temperature NMR spectroscopy, in order to measure the ΔS^\ddagger for the rearrangement;
3. few overlapping signals would be present in the ¹H NMR spectrum, to permit accurate acquisition of data for quantifying the rate of rearrangement for our substrates; and

4. all compounds should be accessible using our existing iterative protocols, and be stable enough to isolate and characterize prior to their use in NMR studies.

We recognised that an aromatic substituent at C6 (**R**¹) or C2 (**R**²) would be ideal for the purpose of systematically varying the electronic properties of our substrates. Since we knew from previous studies that aromatic groups were not well-tolerated at **R**², we elected to install a series of *para*-substituted aromatic rings at **R**¹. In hindsight, it would have been beneficial to also examine *meta*-substitution of the phenyl rings, as analysis of both *meta*- and *para*-substituted aryl systems (at **R**¹) would have enabled further evaluation of the extent of resonance stabilization in the reactive species, provided an allylic-carbocation was formed, using the Yukawa-Tsuno equation.(206)

Qualitative assessment of substituent effects of our juvenile III hormone mimics(85) also indicated that aryl substitution at **R**¹ would result in an increase in the Gibbs free energy of activation, relative to an alkyl group at this position. This, in combination with the lack of any apparent Claisen rearrangement product for an alkyl group at C1 in the radical cyclization described by **Figure 3.4**, led us to believe that this particular combination of substituents would require exceedingly high temperatures for reaction, rendering them incompatible with our intended method of analysis. Thus, to satisfy our second criterion, we chose to focus on bis-vinyl ether systems that were terminated in an ester, as we knew these to rearrange within a more accessible temperature range that could be accommodated with using bromobenzene-*d*₅ as the solvent for our NMR studies (as per criterion #2 and #3).

Lastly, we chose 2,2-dimethylpropanol as the alcohol used to initiate the iterative synthesis of our substrates (**ROH**, **Figure 3.2**), since the neopentyl group (Np) has few signals to complicate the ^1H NMR spectra, yet contains sufficient mass to render the various intermediates and products non-volatile. Compounds **3.8a–3.8g** (**Figure 3.7**) therefore became our primary targets for synthesis.

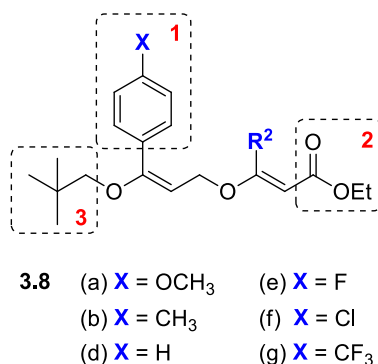
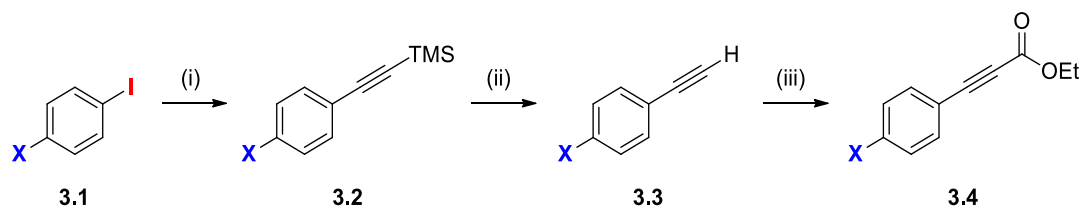


Figure 3.7 Compounds **3.8a–3.8g** and the criterion (**red**) they satisfy.

3.4 Synthesis of Substrates for VT-NMR Studies:

3.4.1 Part I: Synthetic Building Blocks

Alkynoates **3.4a–3.4g** were readily accessed from commercially available, *para*-substituted aryl iodides. The appropriate aryl halide (**3.1**) was reacted in a Sonogashira coupling with trimethylsilyl acetylene to afford known alkynylsilanes (**3.2**) in good to excellent yield after chromatographic purification (**Table 3.1**). Deprotection of the alkyne, followed by acylation(207) in the presence of ethyl (or methyl) chloroformate afforded our desired building blocks (**3.4**) to be used in our established iterative protocol.

Table 3.1 Synthesis of aryl alkynoates.^a

| Entry | X | Sonogashira | | Aryl acetylene | | Alkynoate | |
|-------|-------------------|----------------|-----|----------------|-----|-------------------|-----|
| | | Product | | | | | |
| 1 | CH ₃ O | 3.2a | 98% | 3.3a | 88% | 3.4a | 93% |
| 2 | CH ₃ | 3.2b | 99% | 3.3b | 95% | 3.4b | 95% |
| 3 | H | — ^b | | — ^b | | 3.4d ^c | 88% |
| 4 | F | 3.2e | 99% | 3.3e | 84% | 3.4e | 96% |
| 5 | Cl | 3.2f | 84% | 3.3f | 99% | 3.4f | 80% |
| 6 | CF ₃ | 3.2g | 99% | 3.3g | 99% | 3.4g | 84% |

^aConditions: (i) Pd(PPh₃)₂Cl₂ (2 mol%), CuI (4 mol%), trimethylsilylacetylene (1.2 equiv), Et₃N, 60 °C, 5 h. (ii) TBAF (1.1 equiv), THF, 0 °C, 20 min. (iii) *n*-BuLi (1.05 equiv), ethyl chloroformate (1.2 equiv), THF, -78 °C to r.t., 19h. ^bCompound 3.4d was synthesized from commercially available phenyl acetylene. ^cMethyl chloroformate was used in place of ethyl chloroformate.

3.4.2 Part II: Bis-Vinyl Ethers

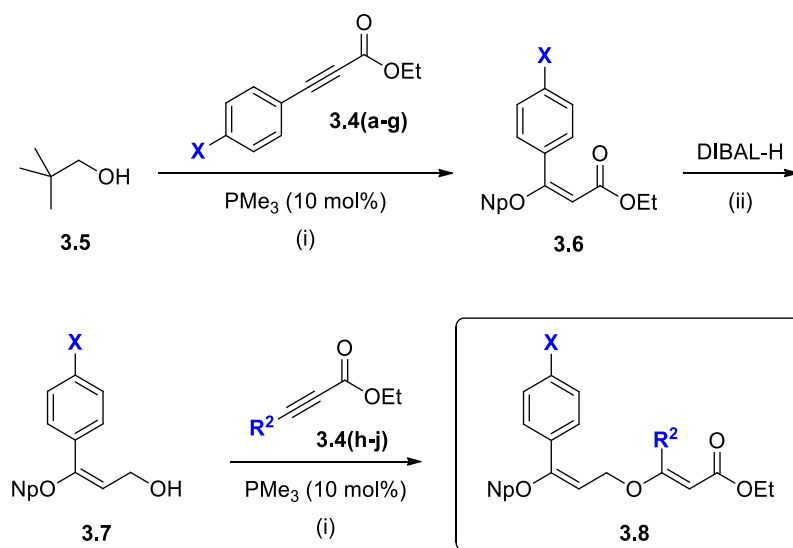
Each of our synthetic targets (bis-vinyl ethers **3.8a–3.8g**) was accessed efficiently, using the conjugate addition/reduction/conjugate addition sequence that we developed previously. A broad selection of functional groups (X) on the aryl ring were well-tolerated, allowing us to access substrates ranging from very electron-rich (*e.g.*, *p*-CH₃O, entry 1) to very electron-poor (*e.g.*, *p*-CF₃, entry 9). While it would be possible to prepare substrates with electron-withdrawing (CF₃),¹⁹ electron-neutral (H),²⁰ and electron-releasing (CH₃)

¹⁹ Incorporation of the CF₃ at C2 would inevitably lead to a mixture of *E*- and *Z*-isomers at the second olefin, require chromatographic separation prior to their use in VT-NMR studies. More importantly, the instability of this class of compounds negated their synthesis for this mechanistic investigation.

²⁰ We did, in fact, prepare the entire series where R² = H. These substrates were found to be more difficult to follow by ¹H NMR spectroscopy, resulting in the accumulation of larger errors within a given data set.

functionality at \mathbf{R}^2 , we chose to focus our studies mostly on those substrates that had a methyl substituent placed at C2, although we did prepare **3.8c** (entry 3), lacking this functionality for comparative purposes (**Table 3.2**). In addition to our standard substrates, we also synthesized a deuterated analogue (**3.8b-*d*₂**, entry 4) with which to carry kinetic isotope experiments.²¹

²¹ We considered synthesizing an alkyl series (where $\mathbf{R}^1 = \text{H}$ and $\mathbf{R}^2 = \text{CH}_3$) with deuterated analogues at the C4 and C6 position in order to gauge the extent of bond breaking and bond making in the TS. This will be discussed later in the Chapter.

Table 3.2 Synthesis of bis-vinyl ether substrates for VT-NMR studies.^a

| Entry | X | R ² | 1 st Addition Yield (<i>E:Z</i>) | Reduction Yield (<i>E:Z</i>) | 2 nd Addition Yield (<i>E:Z</i>) ^b |
|----------------|-------------------|-----------------|---|--------------------------------------|--|
| 1 | CH ₃ O | CH ₃ | 3.6a 94% (15:1) | 3.7a 97% (18:1) | 3.8a 99% (9:1) |
| 2 | CH ₃ | CH ₃ | 3.6b 99% (17:1) | 3.7b 82% (20:1) | 3.8b 100% (9:1) |
| 3 | CH ₃ | H | " " | " " | 3.8c 100% (9:1) |
| 4 ^c | CH ₃ | CH ₃ | " " | 3.7b-d₂ 75% (14:1) | 3.8b-d₂ 97% (8:1) |
| 5 | H | CH ₃ | 3.6d^d 94% (>20:1) | 3.7d 98% (>20:1) | 3.8d 98% (9:1) |
| 6 | F | CH ₃ | 3.6e 82% (13:1) | 3.7e 88% (14:1) | 3.8e 87% (7:1) |
| 7 | F | Et | " " | " " | 3.8h 88% (6:1) |
| 8 | Cl | CH ₃ | 3.6f 89% (13:1) | 3.7f 99% (15:1) | 3.8f 82% (8:1) |
| 9 | CF ₃ | CH ₃ | 3.6g 78% (>20:1) | 3.7g 86% (>20:1) | 3.8g 99% (11:1) |

^aConditions: (i) CH₂Cl₂, 0 to 23 °C, 16 h. (ii) Et₂O, -78 °C to -40 °C, 4h. ^bFor compounds with more than one vinyl ether, the *E:Z* ratio refers to the ratio of all *E*-product to all other adducts. ^cCompound **3.8b** was deuterated at the 4-position by employing LiAlD₄ in place of DIBAL-H in the reduction step. ^dThe methyl ester was used in place of the ethyl ester for this step.

3.5 Nature of Transition-State Structure: Linear Free-Energy Relationships

In keeping with the objective stated in our first criterion, **Section 3.3**, we wanted to determine whether altering the electronic properties at **R¹** (C6) would affect the rate at which compounds **3.8a–3.8g** would undergo Claisen rearrangement. Furthermore, we wanted to know whether or not we could fit observed substituent effects (if any) to a set of Hammett parameters that would enable us to define the nature of the transition-state structure for our substrates. To this end, we studied the rate of Claisen rearrangement by variable-temperature NMR spectroscopy.

3.5.1 Quantitative Determination of the Rate of Claisen Rearrangement

Each bis-vinyl ether (**3.8a–3.8g**) was prepared as a 0.020 M solution in bromobenzene-*d*₅ containing 0.005 M hexamethylbenzene as an internal standard. Prior to performing kinetic experiments, the spin-lattice relaxation time (T_1) was determined (at elevated temperature) for each sample by the inversion-recovery Fourier transform method and the delay time set to $5T_1$ to permit quantitative acquisition of data. The rate of rearrangement for **3.8a–3.8g** was then monitored by ¹H NMR spectroscopy over time at 500 MHz in an instrument pre-equilibrated to 130 °C (for a direct point of comparison for Hammett plot analysis) and at three additional temperatures that were chosen to provide an analytically meaningful data set for Eyring plot analysis. Plots of $[A]_t/[A]_0$ versus t were obtained (**Figure 3.9**), where $[A]_t$ is the integral for the observed vinyl ether protons in **3.8** (the average of the $\sum(\mathbf{Ha} + \mathbf{Hb})$)²² for all isomers) normalized to the internal standard (*i.e.*, hexamethylbenzene), $[A]_0$

²² Bis-vinyl ether **3.8g**, **Figure 3.8**, is a well-behaved system and not truly representative of the behaviour for all other compounds examined (**3.8**). Depending on the substitution at **X**,

is defined as the sum of the normalized integrals for the starting bis-vinyl ether (**3.8**, **Ha** and **Hb**) and the relevant signals in the rearrangement product **3.9** (using the ΣHc for both diastereomers produced)²³ and t is time of spectral acquisition (**Figure 3.8**). In some instances by-products were generated²⁴ in the reaction, these were accounted for in the calculation of $[A]_0$. First order-rate constants, k , for bis-vinyl ethers **3.8a–3.8g** were then obtained by fitting the data to the equation $[A]_t = [A]_0 e^{-kt} + B$ using linear least squares analysis (**Figure 3.9**). For first-order reactions (*i.e.*, Claisen rearrangement) B should be equal to zero, however it is customary to allow B to float as a way to account for small experimental errors within the data set (*e.g.*, geometric isomers other than the major E , E -species will undergo reaction at a different rate,^(59, 60) or may not rearrange at all; the sample may not be at a single homogeneous temperature at the start of the reaction; and other minor experimental departures from ideality).^(84, 200) The activation energy was then directly calculated from k using the Eyring equation:

$$\Delta G^\ddagger = RT \left[\ln \left(\frac{k_B}{h} \right) - \ln \left(\frac{k}{T} \right) \right]$$

where R is defined as the ideal gas constant, T the temperature at which the experiment was conducted (in Kelvin), k_B the Boltzmann constant, h is Planck's constant and k is the rate constant for the reaction at given temperature (T). Eyring parameters were also

E,E-**3.8** may be prone to isomerization at either olefin. In such cases, a second pair of signals (that mirror **Ha** and **Hb**) appear upfield from those in *E,E*-**3.8**.

²³ Protons **Hd/Hd'**, and to a lesser extent **He/Hf**, could also be used to monitor the appearance of the Claisen rearrangement product (**3.9**). The choice of monitoring **Hc/Hc'** is based on the ease of integration for these protons, since they are relatively isolated from other resonances in the ¹H NMR spectrum, and they span a smaller range than **Hd/Hd'**.

²⁴ For substrates that possess electron-releasing substituents (by resonance) at **X**, the second set of terminal olefinic protons appear further downfield in the ¹H NMR spectrum and correspond to formation of the elimination product.

generated from the resulting values of k (temperature ranges used for this analysis are listed in **Table 3.3**) and the associated error in the thermodynamic properties determined on the basis of error associated with the slope (from which ΔH^\ddagger is derived) and intercept (from which ΔS^\ddagger is derived) for the data set were obtained using the XLfit statistical analysis package (data for the analysis of Eyring and Arrhenius plots can be found in **Appendix B**).

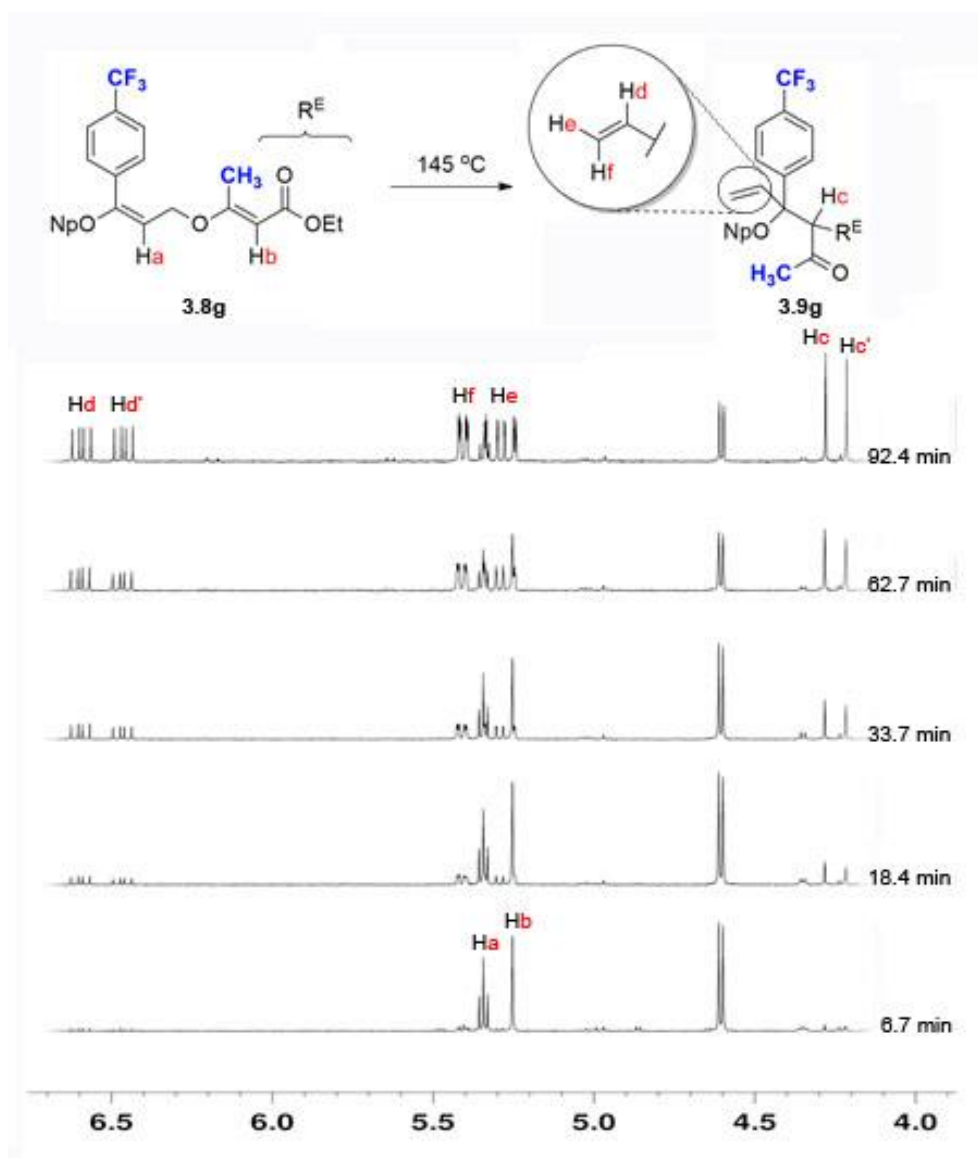


Figure 3.8 Relevant signals monitored in the ^1H NMR spectrum during the course of Claisen rearrangement (at $145\text{ }^\circ\text{C}$) for bis-vinyl ether **3.8g**.

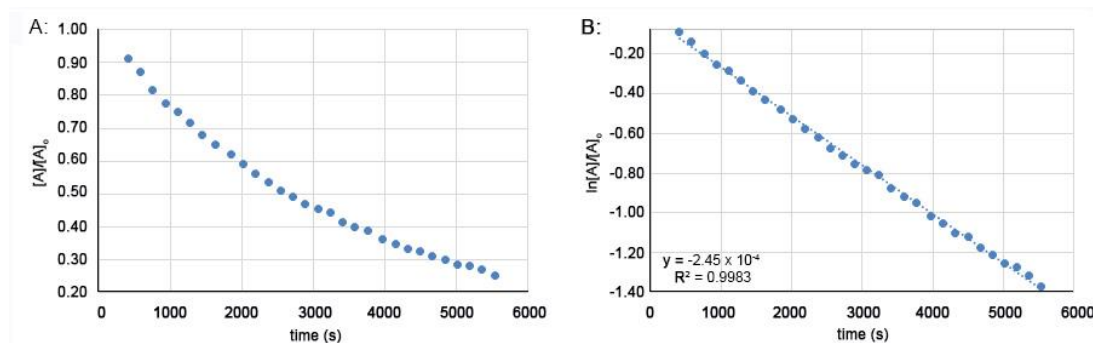


Figure 3.9 Measurement of the consumption of bis-vinyl ether **3.8g** at 145 °C over time (A) and determination of the corresponding rate constant from a plot of the natural logarithm of this data (B).

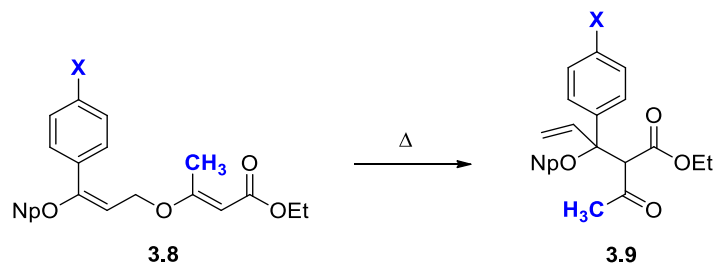
3.5.2 Interpretation of Kinetic Data for Bis-Vinyl Ethers **3.8a–3.8g**:

The first notable piece of evidence that our rearrangement may be proceeding through a fundamentally different mechanism (*i.e.*, dissociative) to that reported in the literature for the analogous thermal rearrangement of simpler allyl vinyl ethers was that each substrate examined in our aryl-series (**3.8**) produced a *ca.* 1:1 ratio of diastereomeric products. While we recognise the possibility that, under the reaction conditions employed, epimerization at the α -position of the Claisen product **3.9** could occur, this initial result was consistent with our mechanistic hypothesis.

As was stated in the previous section, analysis of the rate of [3,3]-sigmatropic rearrangement was complicated somewhat by the fact that *E,E*-**3.8** can undergo partial isomerization to afford mixtures of *E,E*; *E,Z*; *Z,E*; and *Z,Z* isomers at the temperature used to promote chemical transformation. This effect was particularly problematic for substrates that possessed electron-donating substituents (by resonance) at the **X** position. At first glance, this result may appear to provide a rationale to account for the mixture of

diastereomeric products obtained in this reaction. However, if we consider that the normalized integration for *Z*-containing isomers of **3.8g** is maintained throughout the course of the reaction, but still provides a 1:1 mixture of diastereomers as products, we then find that this result precludes any contribution that bond isomerization may have with respect to product distribution as only *E,E*-**3.8g** is expected to undergo rearrangement at any appreciable rate. These same substrates (*i.e.*, when **X** is an electron-releasing group) when rearranged were found to be prone to further decomposition *via* elimination of neopentyl alcohol. Nonetheless, when these factors were appropriately accounted for, the rates and energies of activation for the rearrangement of **3.8a–3.8g** could be accurately calculated (**Table 3.3**).

Table 3.3 Rate constants, relative rates and activation parameters for rearrangement of bis-vinyl ethers in bromobenzene-*d*₅.



| Entry | Compound | X | T (°C) ^a | <i>k</i> at 130 °C ^b (× 10 ⁻⁶ s ⁻¹) | <i>k</i> _{rel} | Δ <i>G</i> ^{‡c,d} (kcal.mol ⁻¹) |
|-------|----------|-------------------|---------------------|--|-------------------------|---|
| 1 | 3.8a | CH ₃ O | 100-130 | 783 | 3.3 | 29.5 |
| 2 | 3.8b | CH ₃ | 110-140 | 373 | 1.6 | 30.1 |
| 3 | 3.8d | H | 115-130 | 237 | 1.0 | 30.5 |
| 4 | 3.8e | F | 115-140 | 212 | 0.9 | 30.6 |
| 5 | 3.8f | Cl | 120-145 | 114 | 0.5 | 31.1 |
| 6 | 3.8g | CF ₃ | 130-145 | 51.0 | 0.2 | 31.7 |

^aTemperature range of kinetic measurements (± 1 °C); a range of 25–30 °C was used, except in cases where this led to problematic decomposition, or where the solvent could not accommodate such a large range. ^bThe rate of rearrangement of compounds **3.8b**, **3.8c**, **3.8b-*d*₂** and **3.25** was measured multiple times at a fixed temperature (see **Table 3.7**); in each case the standard deviation was less than 10%. A maximum error of $\pm 10\%$ is therefore assigned to all rates. ^cΔ*G*[‡] at 130 °C, calculated using the Eyring equation from the observed rate of rearrangement. ^dA maximum error of $\pm 10\%$ in the rate of the reaction corresponds to a maximum error of ± 0.1 kcal.mol⁻¹ in the Δ*G*[‡].

As shown in **Table 3.3**, the presence of electron-donating substituents on the aromatic ring were found to enhance the rate of rearrangement (relative to phenyl-substituted compound **3.8d**), while electron-withdrawing groups impeded the reaction. In order to further quantify the influence of this substituent effect on the rearrangement, the rate data in **Table 3.3** were plotted against a variety of Hammett parameters derived from both radical reactions (which report a substituents' ability to stabilize a radical-type transition state) and polar reactions (which report a substituents' ability to stabilize a polar transition state). By performing this exercise, we had hoped to find large differences in the quality of fit to our experimental

data, therefore providing important information about the nature (and relative spin-density) of the transition state for the system under study.

To this end, $\log(k_{\mathbf{X}}/k_{\mathbf{H}})$ was plotted against: (1) Arnold's $\sigma_{\alpha}^{\bullet}$ parameters based on ESR hyperfine coupling of benzyl radicals (**Figure 3.10A**);(208) (2) Creary's $\sigma_{\mathbf{C}}^{\bullet}$ parameters taken from the thermal rearrangement of substituted methylenecyclopropane systems (**Figure 3.10B**);(209, 210) (3) Jiang and Ji's $\sigma_{\text{jj}}^{\bullet}$ parameters measured from the thermal cyclodimerization of α,β,β -trifluorostyrenes (**Figure 3.10C**);(211, 212) (4) Hammett's original σ_{p} parameters based on the ionization of *para*-substituted benzoic acids (**Figure 3.10D**);(213) and Brown's σ_{p}^{+} parameters based on the solvolysis of substituted *t*-cumyl chlorides (**Figure 3.10E**).(214)

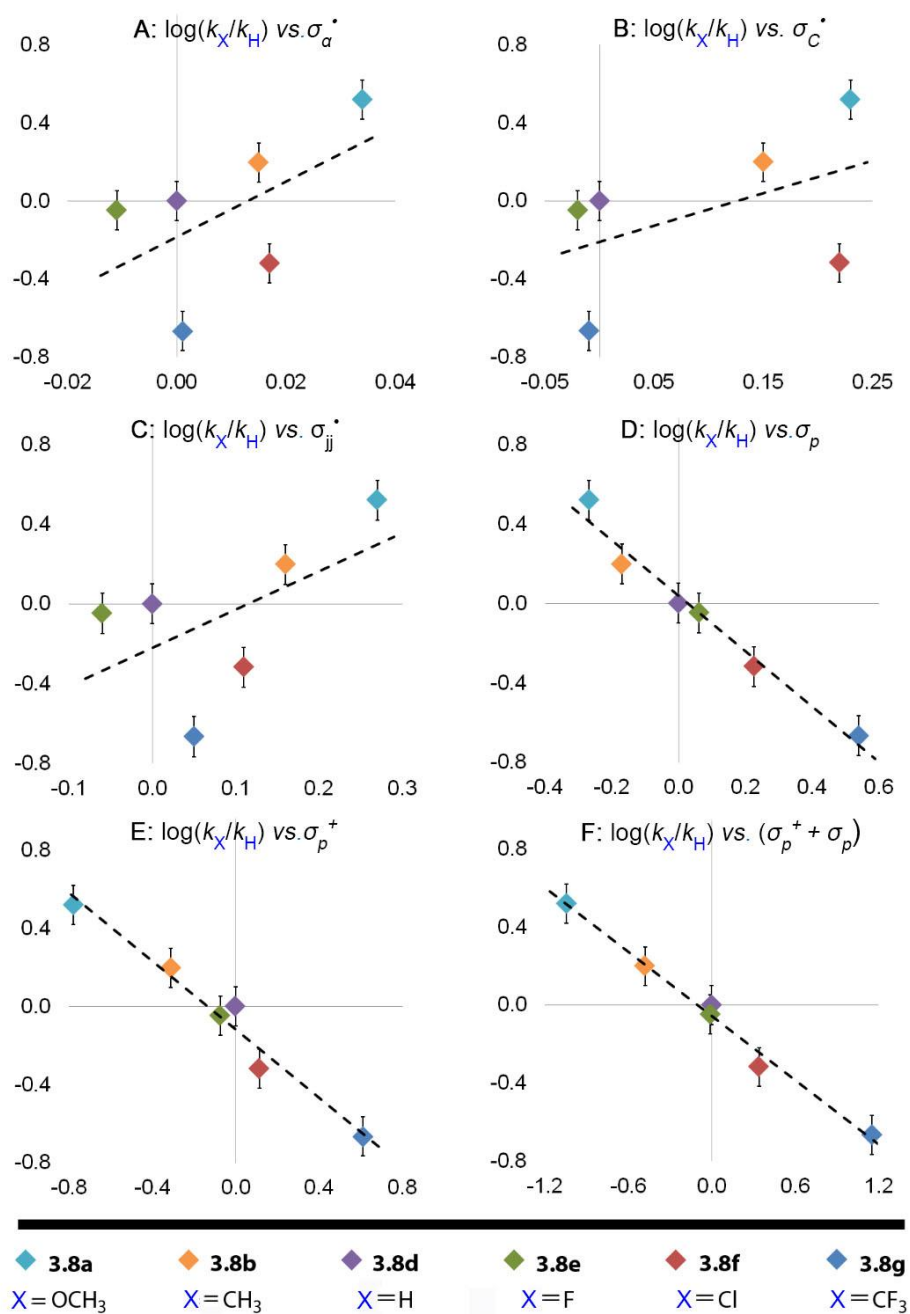


Figure 3.10 Hammett plots for the rate of rearrangement of compounds 3.8, plotted against different σ values (derived from either radical or polar reactions) to probe the electronic nature of the transition state structure. Hammett parameters in plots A–C are derived from radical reactions, while those in plots D–E are derived from polar reactions.

All radical-based Hammett parameters provided a very poor correlation ($R^2 < 0.5$) to the data obtained for the rate of rearrangement of bis-vinyl ethers **3.8** at 130 °C. By contrast, σ -values derived from polar reactions (σ_p or σ_p^+) provided an excellent fit to the data ($R^2 = 0.97$ in both cases).²⁵ Attempts to use dual correlations incorporating both radical- and polar-stabilizing effects, as described by Kim,⁽²¹⁵⁾ were found to only worsen the degree of fit. This suggested to us that the stabilization offered in the transition state by electron-releasing substituents (**X**) was not due to a polarized diradical species, but the development of carbocation character on the allyl fragment. Interestingly, the best fit for our data came from plotting our rate against the sum of σ_p and σ_p^+ ($R^2 = 0.99$, **Figure 3.10F**). While this data is not necessarily any more meaningful than that appearing in **Figure 3.10D** and **3.10E**, it may be justified if one considers that the original Hammett values over-emphasize inductive effects at the expense of resonance contributions,⁽²¹⁶⁾ while the values calculated by Brown are likely to incorporate resonance effects to a greater degree than might be reasonable in this case (see below).⁽²¹⁷⁾

The measured ρ values (reaction constants) obtained for Hammett substituent constants derived from polar reactions are -1.4 and -0.87 for σ_p and σ_p^+ , respectively (**Figure 3.10D** and **3.10E**). These values indicate that a substantial degree of positive charge is associated with the C6 carbon atom in the transition state. However, they do not necessarily indicate whether or not the reaction is fully dissociative. That is to say, the σ -values used to describe electrophilic reactions (*e.g.*, Brown's σ_p^+) may vary depending on the nature and steric requirements of the reaction mechanism. While the value of ρ derived from such plots is

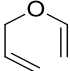
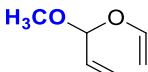
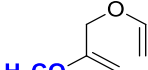
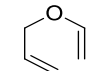
²⁵ Correlations to Hammett parameters are considered to be real when $R^2 \geq 0.95$.

expected to be a measure of the degree of charge build-up in the transition-state structure, the magnitude of such values is not necessarily a true indication of the extent of ionization for the activated species. For example, ρ -values of -1.7 to -6.7 have been reported for electrophilic reactions involving a full positive charge localized to a single benzylic center.⁽²¹⁸⁾ For the rearrangement of compounds **3.8**, several factors would be expected to reduce this value, although the magnitude of this reduction is difficult to predict. These factors include: (1) substantial delocalization of the positive charge onto the neighbouring oxygen atom and C4 (as illustrated in **Figure 3.12**); (2) structural constraints in the transition state that disrupt coplanarity of the aryl system with the developing carbocation; and (3) the existence of a closely associated counter-ion – all of which decrease the “electrophilic pull” the carbocation-center has on the electron-releasing substituent. In order to corroborate the extent of carbocation formation, we decided to probe the degree of organization in the transition state, since a more dissociative mechanism for rearrangement would be reflected by an atypically positive (*i.e.*, less negative) ΔS^\ddagger .

3.5.3 Determination of ΔS^\ddagger for Claisen Rearrangements of Bis-Vinyl Ethers **3.8**

A survey of the literature for the aliphatic Claisen rearrangement of simpler allyl vinyl ethers (*e.g.*, **3.10–3.13**, **Table 3.4**) demonstrates that the rearrangement of such compounds proceeds with a significantly negative entropy of activation (ΔS^\ddagger), indicative of a highly ordered, associative transition state. Particularly noteworthy is that alkoxy substitution at C6 is predicted to result in a “looser” transition-state⁽⁵¹⁾ structure. This is not reflected in the experimentally obtained ΔS^\ddagger for compound **3.13**, and instead the highly ordered nature of the transition state was found to be maintained.

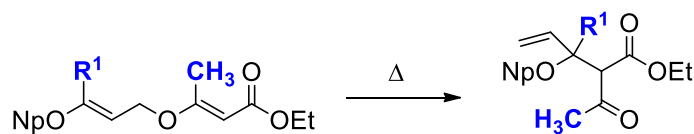
Table 3.4 Kinetic data and activation parameters for the rearrangement of allyl vinyl ethers with oxygen substitution at the 4-, 5- or 6-position.

| Compound | k^a ($\times 10^{-6} \text{ s}^{-1}$) | k_{rel} | ΔH^\ddagger (kcal mol $^{-1}$) | ΔS^\ddagger (cal K $^{-1}$ mol $^{-1}$) |
|--|--|------------------|--|---|
|  3.10 | 0.649 ^{b,c} | 1.0 | 25.4 ^c | -15.9 ^c |
|  3.11 | 62.1 ^d | 96 | 22.4 ^d | -14.7 ^d |
|  3.12 | 0.0161 ^d | 0.025 | 30.9 ^d | -7.0 ^d |
|  3.13 | 6.12 ^d | 9.2 | 24.7 ^d | -12.8 ^d |

^aRate in benzene-*d*₆ at 80 °C. ^bStudy performed in di-*n*-butyl ether rather than in benzene. ^cValues taken from reference (52). ^dValues taken from reference (69).

By contrast, determination of the ΔS^\ddagger for our substrates (**3.8**) using Eyring analysis revealed that our system passes through a transition state that (on average) possessed a small *positive* ΔS^\ddagger (Table 3.5, entries 1–6).

Table 3.5 Entropy of activation, determined by Eyring plot analysis.



| Entry | Compound | R ¹ | Product <i>dr</i> | $\Delta S^{\ddagger a}$ (cal K ⁻¹ mol ⁻¹) |
|----------------|----------|----------------|-------------------|---|
| 1 ^b | 3.8a | | 1:1 | -4.5 ± 7.6 |
| 2 ^b | 3.8b | | 1:1 | +1.8 ± 7.6 |
| 3 | 3.8d | | 1:1 | +4.8 ± 3.7 |
| 4 | 3.8e | | 1:1 | +2.8 ± 4.6 |
| 5 ^b | 3.8f | | 1:1 | -4.1 ± 8.7 |
| 6 | 3.8g | | 1:1 | +4.9 ± 3.6 |
| 7 | 3.16 | | 3:1 | -13.5 ± 3.2 |

^aCalculated uncertainties are based on the standard error of the intercept, as determined by the XLFit statistical analysis package. ^bThe line of best fit for Eyring plot analysis had an $R^2 < 0.99$.

Good quality data sets could be obtained for compounds **3.8d**, **3.8e** and **3.8g**. For each of these substrates, high-quality Eyring plots ($R^2 > 0.99$) could be generated, thereby limiting the degree of uncertainty in the measurement of ΔS^{\ddagger} . For the remaining three of our aryl-substituted substrates, however, we found rather large errors associated with determination of the ΔS^{\ddagger} using this method of analysis. Derivation of the rate constants for **3.8a**, **3.8b** and **3.8f** was complicated by overlap of characteristic ¹H NMR signals used for kinetic analysis,

thereby preventing accurate integration. The small uncertainties associated with the obtained rates necessarily led to Eyring plots (and Arrhenius plots, **Appendix B**) with less than perfect fits ($R^2 = 0.98$ or below). Since determination of ΔS^\ddagger by this method requires that one extrapolate far outside of one's data points to obtain the intercept, this led to unsatisfactory errors in determining the activation entropy. Nonetheless, the calculated range for ΔS^\ddagger encompasses $0 \text{ cal K}^{-1} \text{ mol}^{-1}$, suggesting that the actual value for the ΔS^\ddagger is small.

In order to include the measurements associated with those substrates that possess more electron-rich aromatic rings, we devised an alternate method to probe the ΔS^\ddagger for our system. We reasoned that if we were to examine the change in ΔG^\ddagger (derived directly from k , using the Eyring equation) as a function of temperature, we would be able to obtain a data set where the slope of the resulting line of best fit would correspond to $-\Delta S^\ddagger$.

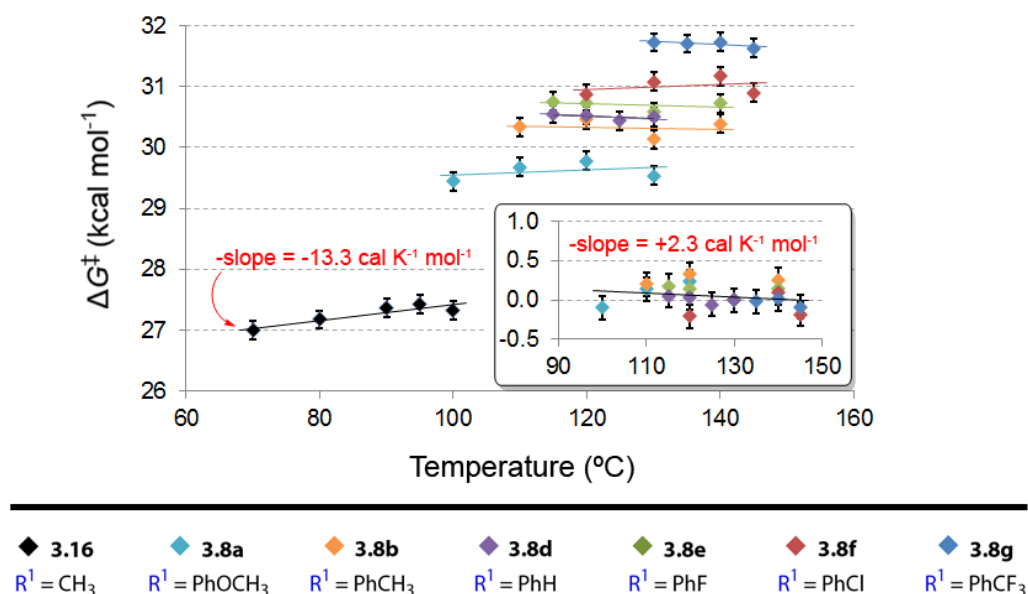


Figure 3.11 Change in ΔG^\ddagger with temperature for bis-vinyl ethers 3.8 and 3.16. Inset plot shows the change in ΔG^\ddagger (kcal mol⁻¹) for all aryl-substituted compounds, relative to the measured ΔG^\ddagger at 130 °C. The standard error for the slope of this line (*i.e.*, inset) is 2.3 cal K⁻¹ mol⁻¹, thus the true value for ΔS^\ddagger may be said to lie between 0 and 5 cal K⁻¹ mol⁻¹.

As shown in **Figure 3.11**, for each of the bis-vinyl ether substrates examined, the ΔG^\ddagger remains constant (within experimental error). Since the slope of each of these lines is essentially near-zero, the ΔS^\ddagger must be correspondingly small. If one assumes that compounds 3.8a–3.8g have approximately the same entropy of activation (*i.e.*, that the differences in rates are due to enthalpic factors associated with electron-releasing or -withdrawing groups), then one can normalize this data by shifting the 130 °C data to the same, arbitrary point on the graph (see inset to **Figure 3.11**). All of the data in the resulting plot can then be used to fit a single line, the slope of which (multiplied by -1) corresponds to the ΔS^\ddagger for bis-vinyl ethers 3.8. When this method of analysis is applied to our data set,

we find that the consensus value for the ΔS^\ddagger is $+2.3 \pm 2.4 \text{ cal K}^{-1} \text{ mol}^{-1}$, suggesting the true value for the entropy of activation may lie somewhere between 0 and $5 \text{ cal K}^{-1} \text{ mol}^{-1}$.

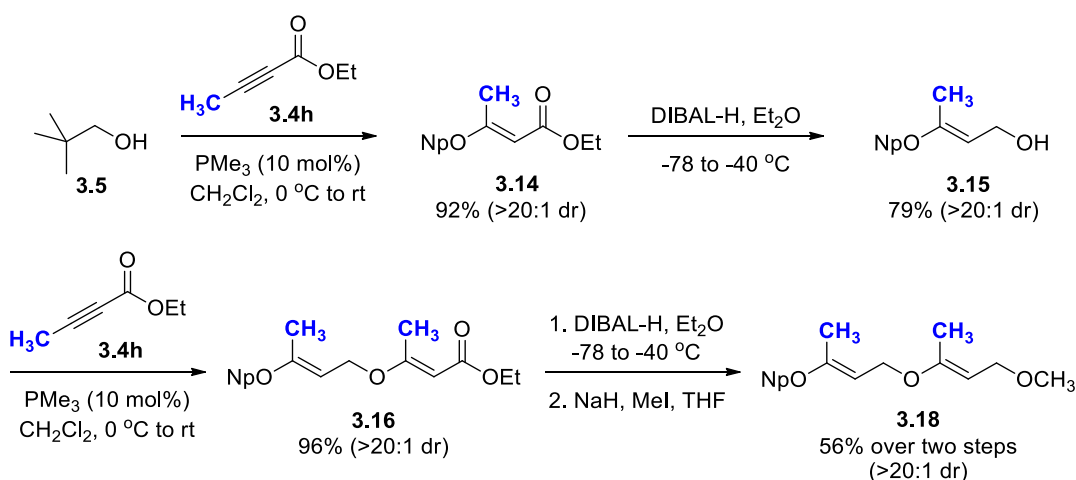
To the best of our knowledge, this is the least negative ΔS^\ddagger ever reported for the aliphatic Claisen rearrangement of any allyl vinyl ether substrate.²⁶ This result provides compelling evidence for the formation of Claisen products *via* a two-step mechanism marked by a dissociative transition state.

3.6 Claisen Rearrangement of Bis-Vinyl Ethers Lacking an Aryl Substituent

Incorporation of *para*-substituted aryl systems at **R¹** for substrates **3.8a–3.8g** provided an opportunity to examine how electronic effects influenced the rate of Claisen rearrangement. The entropy of activation obtained from this data indicated that there was an increase in disorder, compared to simpler allyl vinyl ethers, signifying that our substrates pass through a more dissociative transition-state structure. That said, an aromatic substituent at C6 (**R¹**) likely influenced the stability of the transition-state structure through conjugation with the allyl fragment. To this end, we elected to repeat the temperature study with alkyl-substituted bis-vinyl ether **3.16** in order to evaluate the effect of the aromatic functionality itself.

²⁶ The presence of *gem*-dialkyl substituents at C4 can also lead to a significantly reduced ΔS^\ddagger by providing a higher degree of organization in the ground state. See *J. Org. Chem.* **1990**, *55*, 1813.

Substrate **3.16** was synthesized as shown in **Scheme 3.1**, and subsequently prepared as a 0.020 M solution in bromobenzene-*d*₅ spiked with 0.010 M 1,4-dioxane as an internal standard. This substrate was similarly allowed to rearrange at five different temperatures and the energy of activation was calculated in an identical manner to compounds **3.8** (*i.e.*, directly from *k*, using the Eyring equation).²⁷ For a qualitative comparison to the aryl series, the ΔG^\ddagger for this data was plotted as a function of temperature, where the ΔS^\ddagger can be said to correspond to the negative slope of the line of best fit (**Figure 3.11**). The data was also treated by Eyring analysis and appears, with product ratio, in **Table 3.5** (entry 7).



Scheme 3.1 Synthesis of **3.16** and **3.18** for VT-NMR studies.

The alkyl-substituted compound, **3.16**, was found to possess significantly different behaviour than the corresponding aryl-substituted analogues **3.8**. The ΔG^\ddagger for **3.16** was found to be *ca.* 90% that of phenyl-substituted bis-vinyl ether **3.8d**, with the alkyl-

²⁷ Alkyl-substituted bis-vinyl ether **3.16** was found to rearrange considerably faster than compounds **3.8**, necessitating the use of a lower temperature range in order to obtain a good-quality data set.

derivative rearranging approximately 28 times faster than its aryl-substituted counterpart (data at 130 °C for **3.16** was extrapolated from the Eyring equation).

While the aryl series of compounds (**3.8**) was found to undergo Claisen rearrangement to afford a 1:1 mixture of diastereomers, **3.16** instead produced a 3:1 ratio of products. Moreover, the calculated ΔS^\ddagger for **3.16** was *ca.* $-13 \text{ cal K}^{-1} \text{ mol}^{-1}$.²⁸ This ΔS^\ddagger differs significantly from the one obtained for substrates **3.8** and is within experimental error of Curran's C6 methoxy-substituted allyl vinyl ether **3.13** (Table 3.4). These results indicate that the transition state for the rearrangement of **3.16** is less dissociative than that for compounds **3.8**.

3.7 Extent of Polarization in the Transition State

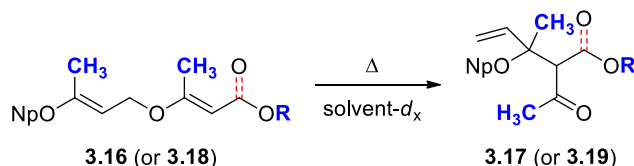
To further probe the electronic nature of the transition state, we sought to determine whether or not our substrates exhibit solvent-dependent behaviour during reaction. The evidence accumulated thus far suggested that the presence of the oxygen substituent at C6, in combination with an electron-withdrawing substituent at C1, was resulting in heterolytic cleavage of the C4—O3 bond (*i.e.*, rather than the commonly perceived homolytic cleavage). If this were the case, then the resulting ionic fragments should be much more sensitive to changes in solvent polarity.

²⁸ The entropy of activation for compound **3.16** obtained using the method described in Figure 3.10 (*i.e.*, plotting ΔG^\ddagger versus temperature; $-13.3 \text{ cal K}^{-1} \text{ mol}^{-1}$) was found to be in good agreement with that derived from Eyring plot analysis ($-13.5 \text{ cal K}^{-1} \text{ mol}^{-1}$), suggesting the validity of such an approach.

We recognised that **3.16** likely followed a different reaction trajectory than compounds **3.8**, but the lower temperature required for the rearrangement of **3.16** made it an ideal substrate for carrying out these studies since a broader range of polar, aprotic solvents could be employed. To this end, we monitored the rate of Claisen rearrangement of **3.16** in less polar (benzene-*d*₆) and more polar, aprotic (dichloroethane-*d*₄, acetonitrile-*d*₃) NMR solvents (**Table 3.6**). The results showed a substantial increase in the reaction rate with increasing dielectric constant. Attempts to repeat the same experiments with polar, protic solvents (*i.e.*, methanol-*d*₄ and D₂O) were unsuccessful as the rearrangement (and subsequent decomposition) occurred much too rapidly to follow by NMR spectroscopy, even at 30 °C.²⁹

²⁹ The solvent effect imposed by use of polar, protic solvents is not diagnostic of the extent of charge formation in the transition-state structure. Compound **3.13** does exhibit a pronounced solvent effect in methanol-*d*₄ (*i.e.*, 68 times faster than in benzene-*d*₆). This has been attributed to the greater accessibility of the vinyl ether oxygen to hydrogen-bonding interactions by virtue of greater C4—O3 bond length in the transition-state and to destabilization of the ground state for **3.13**. We therefore cannot read too heavily into the acceleration imparted by polar, protic solvents on our own system.

Table 3.6 Solvent effects for the Claisen rearrangement of 3.16 and the effect of reduction at C1 (3.18).



| Entry | Compound | Solvent (ϵ) | T ($^{\circ}\text{C}$) ^a | k at 70 $^{\circ}\text{C}$ ($\times 10^{-6} \text{ s}^{-1}$) | k_{rel} ^b | $\Delta G^{\ddagger c}$ (kcal mol ⁻¹) |
|-------|-------------|---|---------------------------------------|---|-------------------------------|--|
| 1 | 3.16 | C ₆ D ₆ (2.3) | 70 | 20.3 | 0.5 | 27.5 |
| 2 | 3.16 | C ₆ D ₅ Br (5.2) | 70-100 | 44.1 | 1.0 | 27.0 |
| 3 | 3.16 | (CD ₂ Cl) ₂ (10.4) | 70 | 207 | 4.7 | 25.9 |
| 4 | 3.16 | CD ₃ CN (37.5) | 70 | 393 | 8.9 | 25.5 |
| 5 | 3.18 | C ₆ D ₅ Br (5.2) | 110 | — ^d | — ^d | — ^d |

^aTemperature range of kinetic measurements (± 1 $^{\circ}\text{C}$). ^bRelative to the rate of rearrangement for **3.16** in bromobenzene-*d*₅. ^cCalculated from the observed rate of Claisen rearrangement using the Eyring equation. ^dAttempts to measure the rate of rearrangement for compound **3.18** revealed an autocatalytic process that did not display first order kinetics.

By contrast, the aliphatic Claisen rearrangement of less substituted allyl vinyl ethers is known to be relatively unaffected by changes in solvent polarity. Even Curran's C6 alkoxyallyl vinyl ether, **3.13**, only experiences a 3.2-fold rate enhancement for rearrangement at 80 $^{\circ}\text{C}$ upon moving from benzene-*d*₆ to acetonitrile-*d*₃ (compared to the 19.4-fold increase for **3.16**).⁽⁶⁹⁾

The fact that **3.16** is much more sensitive to solvent effects than **3.13** strongly suggests that **3.16** rearranges through a more highly polarized transition state. This would be consistent with a greater degree of O3—C4 heterolytic cleavage prior to formation of the new bond

between C1 and C6. While the magnitude of the solvent effect (coupled with a typically large, negative ΔS^\ddagger characteristic a more ordered transition state) is not sufficient to suggest a zwitterionic intermediate, its transition state appears to be much more fragmented than **3.13**.

3.8 Substituent Effects on the Rate of Claisen Rearrangement at C1, C2 and C4

3.8.1 Reduction of the Ester at C1

The lower temperature required for the rearrangement of **3.16**, relative to **3.8**, provided us with the opportunity to investigate the rearrangement of bis-vinyl ether **3.18**, without an electron withdrawing group at C1. We knew from previous studies that reduction of the ester (at C1) would stabilize the substrate to Claisen rearrangement (**Figure 3.4**). Using our existing experimental platform we were already working at the extent of our instrumental capabilities with bis-vinyl ether esters **3.8**. Reduced analogues of this substrate were not expected to rearrange at accessible temperatures, and so these substrates were not pursued. However, since **3.16** rearranged more easily, we had hoped that the corresponding methyl ester (**3.18**) would provide a tractable target for study. We therefore prepared compound **3.18** (as shown in **Scheme 3.1**) and attempted to study its rearrangement by NMR spectroscopy.

Compound **3.18** was found to undergo rearrangement at an appreciable rate at temperatures above 100 °C (in bromobenzene-*d*₅) to afford 5:1 (or better) mixtures of diastereomeric products. Unfortunately, we were unable to derive the rate of rearrangement for this substrate as it was found to deviate from linear behaviour. We attributed this to an

autocatalytic process, whereby the rearrangement product from **3.18** undergoes decomposition under the conditions of the experiment and one of the resulting by-products serves to promote the initial rearrangement. This observation would appear to be supported by the fact that the diastereoselectivity of the reaction was found to change over time (*i.e.*, the major diastereomer produced in the initial (slow) stages becomes the minor product as the reaction progresses; prolonged heating affords only one diastereomer by ^1H NMR analysis). This data suggests that, in the absence of an electron-withdrawing group at C1, compound **3.18** is unable to stabilize the formation of a negatively-charged oxyallyl fragment, and must therefore proceed through a higher-energy, associative transition state that is better described by Curran's "vinylogous anomeric" model.

3.8.2 Electronically Neutral Substituent at C2

Returning to aromatic substrates **3.8**, we next wanted to compare the rate of rearrangement for **3.8b** (bearing an electron-donating methyl substituent at R^2) to that for **3.8c** (bearing an electron-neutral substituent at R^2). Using our earlier described protocol, both substrates were rearranged in bromobenzene- d_5 and their rate constant determined as an average over three to four measurements, **Table 3.7**. Compound **3.8c** was found to rearrange *ca.* 1.5 times slower than **3.8b**. This result is found to contradict earlier observations from Katherine Davies' study of juvenile III hormone mimics, where the rate of rearrangement was found to decrease from hydrogen > methyl > ethyl at R^2 (**Figure 3.3**). Several explanations for the difference in reactivity may include: (a) a slight change in the mechanism for solvated *versus* adsorbed samples, (b) additional substitution at R^2 can better accommodate the negative charge build-up on the oxyallyl-fragment by having it

spread over a larger number of atoms, and (c) the presence of a larger substituent in place of hydrogen, in this case, can restrict the number of conformations in the reactant upon moving to the transition state, thereby decreasing the entropy of the system, resulting in a net acceleration. In any event, the change in the rate of rearrangement for **3.8c**, relative to **3.8b**, is small and a larger sample set (varying the size of the substituent at **R**²) would be required to provide ample evidence for entropic acceleration.

Table 3.7 Substituent effects at C2 and C4.

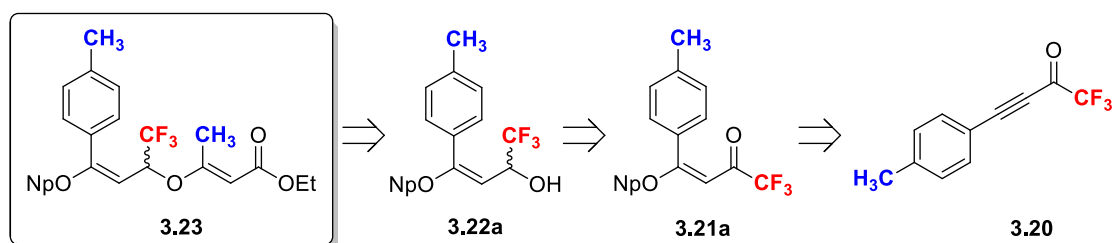
| Entry | Compound | k at 130 °C ($\times 10^{-6} \text{ s}^{-1}$) | k_{rel} | Notes |
|-------|---------------------------|--|------------------|---|
| 1 | 3.8b | $373 \pm 8^{\text{a}}$ | 1.00 | |
| 2 | 3.8c | $253 \pm 24^{\text{b}}$ | 0.68 ± 0.08 | |
| 3 | 3.8b-d₂ | $251 \pm 10^{\text{a}}$ | 0.67 ± 0.04 | $k_{\text{H}}/k_{\text{D}} = 1.48 \pm 0.10$ |
| 4 | 3.27 | $251 \pm 2^{\text{b}}$ | 1.21 ± 0.03 | $k_{3.27}/k_{3.8c} = 1.79 \pm 0.20$ |

^aStandard deviation over 4 measurements. ^bStandard deviation over 3 measurements.

3.8.3 Electron-Withdrawing Substituent at C4

As a mechanistic probe we elected to install a CF₃-substituent at the C4 position of **3.8**. In what appears to be a dipolar, dissociative-type mechanism, we reasoned that incorporation of this functionality would likely reduce the rate of Claisen rearrangement (*via* destabilization the developing carbocation on the allyl-fragment) thereby affording additional information about the extent of ionization in the transition state.⁽²¹⁹⁾ Since we expected that the CF₃ analogue would rearrange much more slowly than the corresponding C4-H₂ bis-vinyl ether, we had envisioned modifying our existing synthetic protocol to gain access to an analogue of **3.8b**. The rationale behind the choice of substituent at **R**¹ followed logically from the fact that the parent compound, **3.8b**, undergoes reaction at a lower

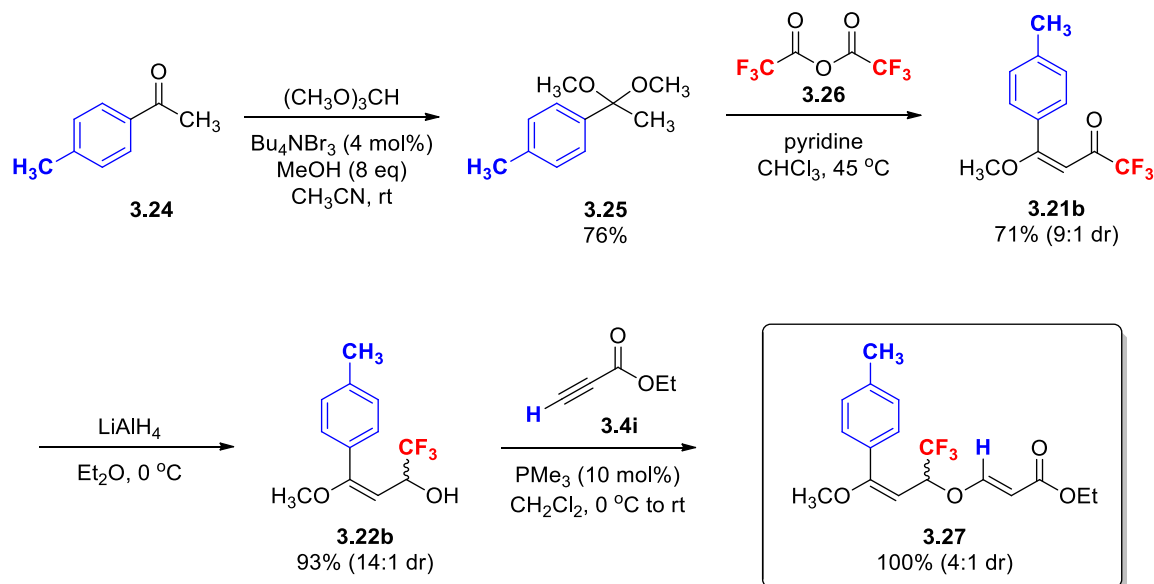
temperature-range (than that observed for other bis-vinyl ethers in the aryl-series) and is additionally less prone to olefin-isomerization (than **3.8a**). We had hoped that these features would make **3.23** a tractable target for monitoring the rate of reaction for the CF₃-congener.



Scheme 3.2 Proposed synthesis of CF₃-analogue.

In an attempt to make use of our existing synthetic platform, we envisioned reacting neopentyl alcohol (**3.5**) with 4-(tolyl)-1,1,1-trifluorobut-3-yn-2-one (**3.20**)⁽²²⁰⁾ in the first conjugate addition for our reaction sequence (see **Scheme 3.2**). Unfortunately, the trifluoromethyl ketone was far too reactive to provide the expected mono-vinyl ether (**3.21a**), necessitating the use of an alternate route to our desired mechanistic probe.

Following the procedure reported by Bonacorso,⁽²²¹⁾ we were able to efficiently access trifluoroketone **3.21b** from commercially available 4'-methylacetophenone (**3.24**) in good yield over two steps. The ketone function was then selectively reduced using LiAlH₄ to provide alcohol **3.22b** as primarily one geometric isomer (*E:Z*, 14:1; **Scheme 3.3**).



Scheme 3.3 Synthesis of C4 analogue **3.27**.

As per our original synthetic proposal (outlined in **Scheme 3.2**) we sought to perform the second conjugate addition with ethyl 2-butynoate (**3.4h**), however **3.22b** was too sterically encumbered for this to occur. This synthetic shortcoming was easily overcome through swapping **3.4h** for ethyl propiolate (**3.4i**) to furnish **3.27** as a 4:1 mixture of diastereomers (major isomer shown).

The rearrangement of **3.27** was monitored under the usual conditions and found to proceed nearly twice as fast as the closest related analogue, **3.8c** (see **Table 3.7** for data).³⁰ This is a larger rate enhancement than reported for the analogous (C4)-trifluoromethylated allyl vinyl ether reported by Gajewski ($k_{\text{rel}} = 1.3$ compared to **3.10**).⁽⁶⁵⁾ Although unexpected, the faster rate of rearrangement for **3.27** (relative to

³⁰ The relative rate of rearrangement for **3.27** is likely underestimated (relative to **3.8c**, prepared as a 9:1 mixture of diastereomers) since *E,Z*; *Z,E*; and *Z,Z*-allyl vinyl ethers are known to rearrange more sluggishly than the corresponding *E,E*-isomer.

3.8c) is understandable if one considers that the CF₃ group has a significant destabilizing influence on only one of the three representations of the allylic carbocation proposed fully-dissociative transition state (**TS-V**, **Figure 3.12**). For the other two possible resonance structures (*i.e.*, **TS-III** and **TS-IV**) the CF₃ substituent may actually be stabilizing as the enthalpic cost of migrating the olefin is compensated by additional substitution for the resulting olefin at C4–C5 (**Figure 3.12**).³¹

³¹ The resonance structures pictured in **Figure 3.12** are different representations of the same molecule. The use of “stabilizing” and “destabilizing” effects, with respect to the CF₃ substituent, are used only to describe which resonance structure affords a better description of the observed chemical reactivity for this system.

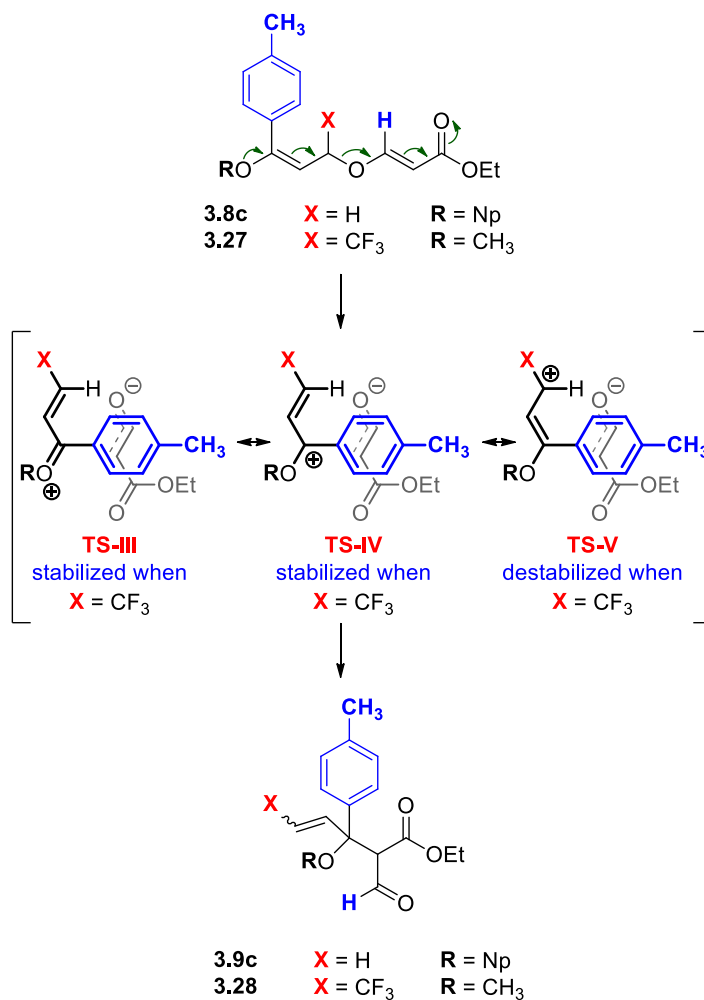


Figure 3.12 Possible resonance contributors for a dissociative transition state provide rationale for the increase in rate of Claisen rearrangement when a CF_3 substituent is at C4.

This analysis was further supported by DFT calculations (performed by Dr. J. E. Wulff at the B3LYP/6-31G* level of theory), which confirmed that most of the positive charge for the cationic fragment, for our proposed dissociative transition state, is located at C6 (Figure 3.13).

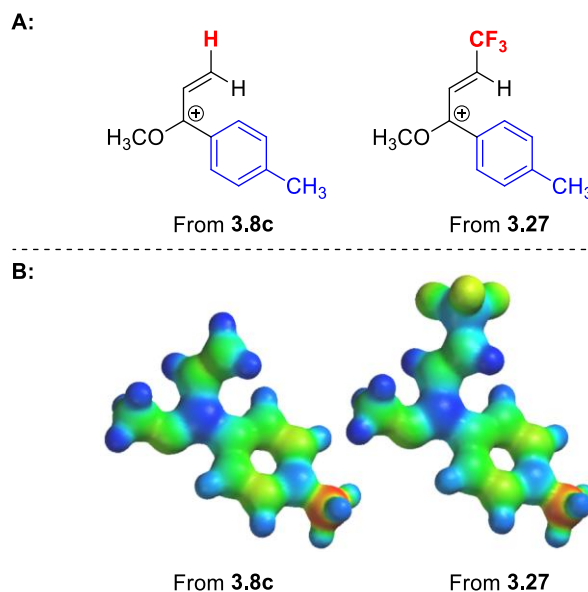


Figure 3.13 Representative cationic fragments of TS-IV leading from **3.8c** and **3.27** (A) with calculated electronic potential maps (B). The neopentoxy-group in **3.8c** was simplified to a methoxy-substituent for the purpose of carrying out DFT calculations.

3.8.4 Secondary Deuterium Kinetic Isotope Effects

Our original objective for preparing compound **3.27** was to measure the extent of carbocation formation in the transition state (qualitatively) by observing a change in the rate of rearrangement relative to **3.8c**. While this effort was marred by the lack of electronic influence exhibited by having a CF_3 -substituent at the C4 position, we could get at this data through examination of secondary deuterium kinetic isotope effects.

By measuring the rate of reaction of allyl vinyl ethers and their deuterated counterparts (which have been labeled at the C4 or C6 position) one can quantify the extent of C1–C6

bond-making and C4—O3 bond-breaking³² in the transition-state structure with changes to substitution off the pericyclic framework.(48, 56, 57, 65)

To measure the extent of bond breaking in our system, we compared the rate of rearrangement of **3.8b** to **3.8b-d₂** (see **Table 3.7**). The deuterated analogue (**3.8b-d₂**) was found to react considerably slower, relative to the parent molecule, resulting in a large secondary kinetic isotope effect of 1.48. We were unable to calculate the precise extent of bond breaking for this system, due to the nature of our substrate³³ but this value is consistent with a large degree of bond-breaking early in the reaction pathway (*e.g.*, the simpler allyl vinyl ether **3.10** produces a k_H/k_D of 1.09 with a BB = 0.42).

For purpose of comparison, we also tried to prepare an analogue containing a deuterium label at C6 (**Figure 3.14**). Since we proposed that the mechanism for rearrangement of the alkyl-substituted bis-vinyl ethers (like **3.29**) lies somewhere between allyl vinyl ether **3.10** and those in our aryl-series (**3.8**), we reasoned that the kinetic isotope effect measured for this substrate would inform us whether there was more (or less) bond-making in the transition state for compounds **3.8**. This idea was soon discarded when we discovered that **3.4k** reacted in the conjugate addition to afford deuterium scrambled products (**Figure 3.14B**).

³² When compared to the calculated equilibrium isotope effect (EIE), the ratio of (the logarithms of) the KIE and the EIE provide a measure of the progress of the transition state along a reaction coordinate between the reactants and products.

³³ The maximum secondary kinetic effect for our system is difficult to predict, since the precise electronic role of the C6 oxygen is not perfectly understood. It is possible that hyperconjugative effects owing to the C6 alkoxy group lead to inflation of the value reported.

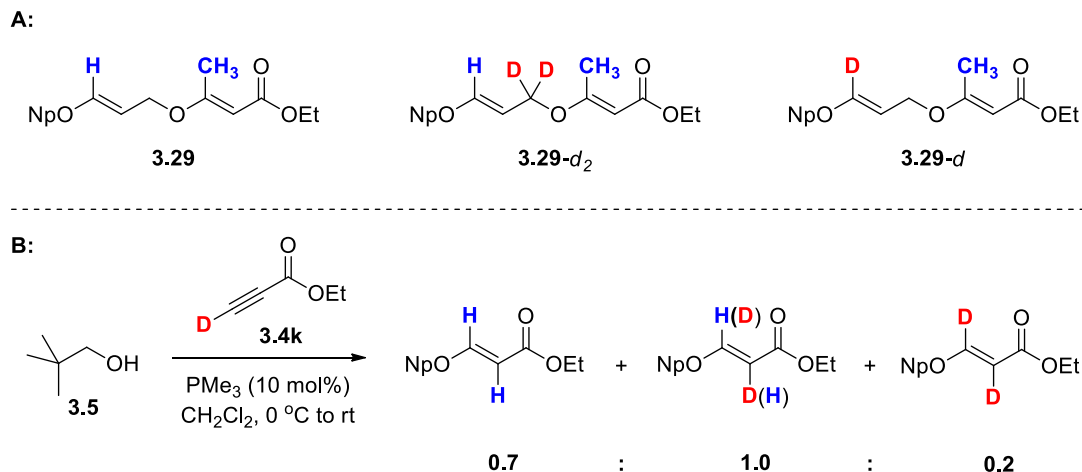
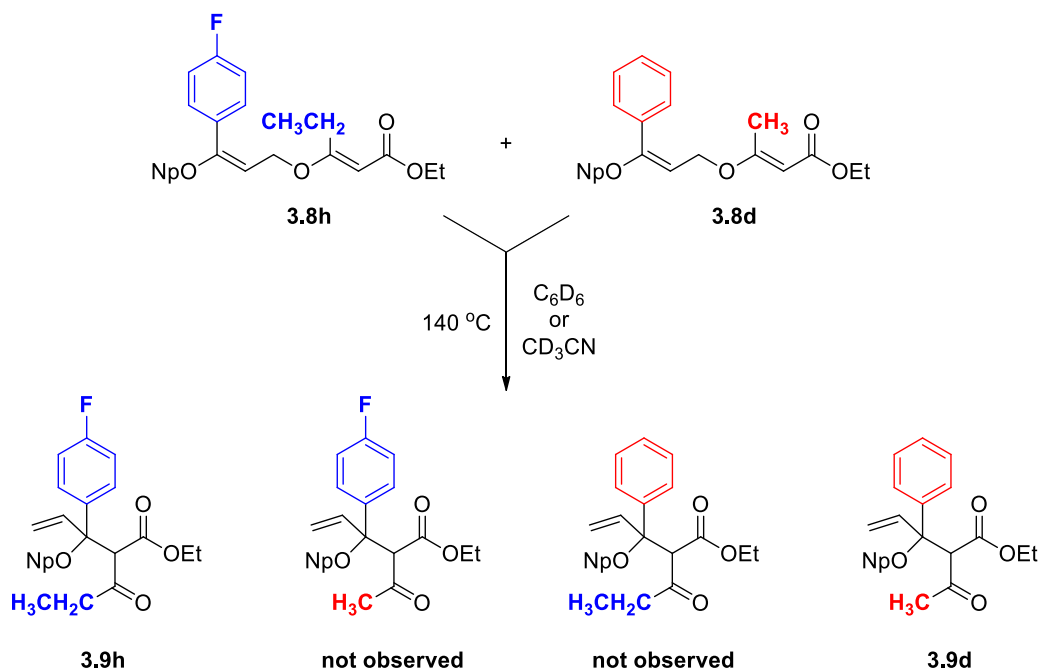


Figure 3.14 Proposed deuterated analogues for measuring kinetic isotope effects (A) and difficulties associated with introduction of deuterium label at C6 (B).

3.9 Cross Over Experiments

At this stage in our investigation, we have uncovered significant evidence supporting a largely dissociative transition state for bis-vinyl ethers like **3.8** and **3.27** that contain an electron-withdrawing group at C1 as well as additional conjugation at C6. In an effort to characterize the extent of dissociation (which differs from the extent of bond breaking), we conducted a cross-over experiment with substrates **3.8d** and **3.8h** - chosen for their ability to undergo reaction at identical rates (within experimental error) (**Scheme 3.4**).



Scheme 3.4 Crossover experiment with 3.8h and 3.8d.

Both compounds were allowed to react in solution together in both non-polar and polar, aprotic solvents. Only products originating from intramolecular reaction of **3.8d** and **3.8h** were observed. No intermolecular (*i.e.*, cross-over) products could be detected by LRMS analysis. This indicated that the fragments depicted in **Figure 3.12** are tightly associated with one another. While they can presumably react with different reaction trajectories, they maintain extended contact and are not free to diffuse through solution.

3.10 Summary

Several lines of evidence described herein support the mechanistic hypothesis illustrated in **Figure 3.15**. The aliphatic Claisen rearrangement of bis-vinyl ethers can be thought to take place on a continuum between two mechanistic extremes: **TS-I** (“push-pull”

mechanism that we have principally focused on here) and **TS-II** (Curran's "vinylogous anomeric" model).

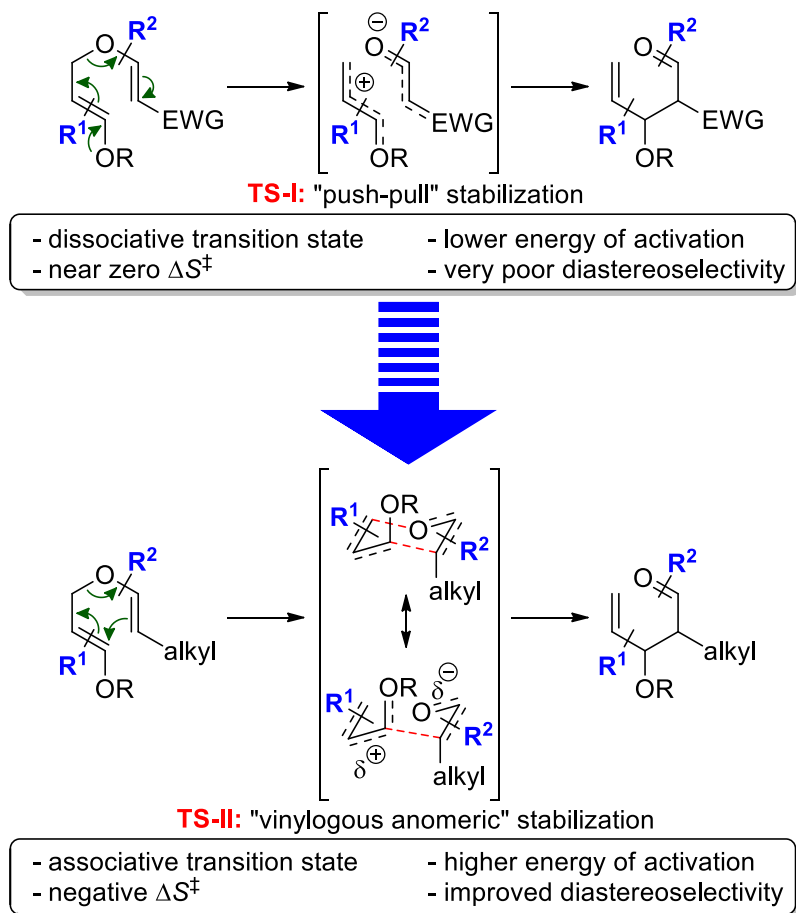


Figure 3.15 Mechanistic proposal to account for the observed differences in reactivity in the Claisen rearrangement with different substitution on the allyl- and oxyallyl-fragments (at C6 and C1, respectively).

Bis-vinyl ethers like **3.8a–g** and **3.27**, containing both an electron-withdrawing group at C1 and additional conjugation at C6, are best described as rearranging through **TS-I**. This model explains the lack of diastereoselectivity for these reactions, the observed rate acceleration with electron-donating substituents on the allyl-fragment, the near-zero

entropy of activation and the large secondary kinetic isotope effect. The ΔS^\ddagger is particularly noteworthy; at $+2.3 \text{ cal K}^{-1} \text{ mol}^{-1}$ it is the largest (*i.e.*, least negative) entropy of activation ever reported for a non-catalyzed aliphatic Claisen rearrangement. While others have speculated(81) that a dissociative transition-state may exist, we have provided the first conclusive evidence of this phenomenon.

Compounds lacking an electron-withdrawing function at C1 (*e.g.*, **3.10** and **3.18**) are not capable of stabilizing an anionic oxyallyl fragment, and appear to undergo Claisen rearrangement through a more associative pathway, as described by Curran. This would explain the improved diastereoselectivity observed for the rearrangement of **3.18**, although non-linear effects make it more difficult to assess the thermodynamic properties for this rearrangement.

Substrate **3.16**, which has the ester function at C1 to stabilize formation of an anionic oxyallyl fragment, but lacks additional conjugation at C6 for stabilization of the carbocation fragment (in **TS-I**), might be said to occupy mechanistic space somewhere in the middle of this continuum. This compound rearranged with a substantial negative entropy of activation, but nonetheless afforded modest diastereoselectivity and a pronounced solvent effect – both of which are hallmarks of a more polarized transition state than those compounds lacking the ester at C1.

Chapter 4 En Route to a Diastereoselective Claisen Rearrangement of Bis-Vinyl Ethers

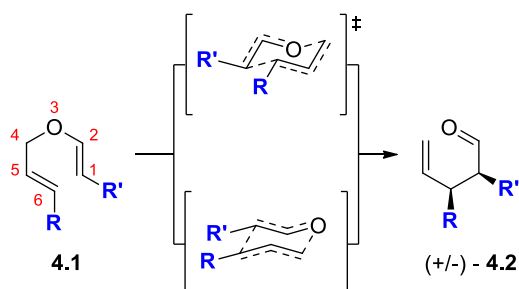
4.1 Introduction

The efficient synthesis of complex natural products and enantiomerically enriched, pharmaceutically important small-molecules is an important challenge in preparative organic chemistry.⁽²²²⁾ New synthetic strategies for the direct, enantioselective formation of carbon-carbon bonds to provide vicinal tertiary or quaternary stereocenters need to be developed.⁽²²²⁻²²⁶⁾ Not surprisingly, [3,3]-sigmatropic rearrangements have been found to be a reliable class of reactions for the development of such synthetic methodologies as they enable the assembly of such sterically congested structures in a single synthetic operation.^(227, 228)

The general irreversibility (for *retro*-Claisen rearrangements see references (229-238)),³⁴ and synthetic utility of the aliphatic Claisen rearrangement has rendered it one of the most powerful pericyclic reactions for the construction of new carbon-carbon σ -bonds with high stereocontrol.^(182-187, 228, 239-242) For acyclic allyl vinyl ethers that bear substituents at prochiral carbon atoms C1 and C6, the relative configuration of the newly formed, adjacent stereogenic centers can be reliably predicted from the olefin geometry in the original structure (assuming a reaction trajectory where a chair-type transition state predominates).^(59, 60) This implies, however, that achiral substrates (*e.g.*, **4.1** in **Scheme**

³⁴ The Claisen rearrangement is generally considered to be irreversible. Exceptions do exist, but in all cases the reverse reaction appears to be driven by the release of strain associated with highly constrained ring systems in the γ,δ -unsaturated carbonyl compound.

4.1) proceed through two enantiomeric transition states that result in formation of racemic product (*e.g.*, (+/-) - **4.2**).



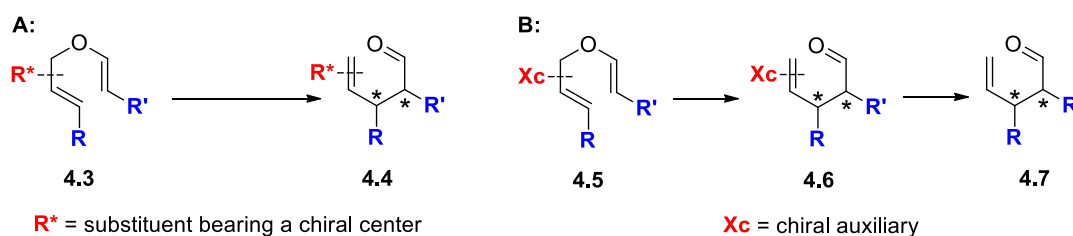
Scheme 4.1 Thermal Claisen rearrangement of acyclic, aliphatic allyl vinyl ethers preferentially pass through a chair-type transition state to afford a single diastereomer of product as a mixture of enantiomers.

The potential for this reaction to rapidly generate molecular complexity (*i.e.*, two new contiguous stereocenters as well as a geometrically-defined olefin) from simple, linear substrates in an asymmetric fashion has consequently engendered considerable interest from the synthetic community.(239, 243-245) Despite the many efforts in this pursuit, development of an asymmetric variant of the Claisen rearrangement has proven to be a non-trivial task.

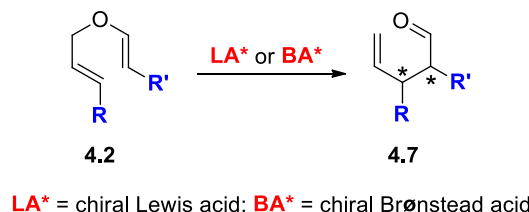
The two reaction categories under which variations of the asymmetric Claisen rearrangements have been characterized are depicted in **Scheme 4.2**. The first, and most extensively investigated, is the diastereoselective rearrangement. Asymmetric induction by this method requires that a chiral substituent come either from an ex-chiral pool (*i.e.*, using optically-active secondary or tertiary allylic alcohols to promote [1,3]- and/or [1,4]-chirality transfer from the C4—O3 bond across the pericyclic framework(246) or through incorporation of chiral substituents outside the pericyclic framework, **Scheme 4.2A**), or

from an externally sourced chiral auxiliary (**Scheme 4.2B**). The former approach necessitates the incorporation of the original chiral moiety into the body of the molecule during and beyond formation of the target compound while, in the latter, the auxiliary may be removed post-transformation (rendering the overall transformation an enantioselective one).⁽²⁴³⁾

Diastereoselective Claisen rearrangements



C: Enantioselective Claisen rearrangements



Scheme 4.2 Asymmetric versions of the Claisen rearrangement.

The second, and most desirable, method for asymmetric induction is the development of an enantioselective reaction to control both the absolute and relative configuration in the product (**Scheme 4.2C**). In this latter case, the stereochemical outcome of the sigmatropic rearrangement is controlled by an external Brønsted or Lewis acid with ligands that serve to function as the chiral auxiliary.⁽²⁴³⁾ These reagents function independent of the prochirality of the substrate and avoid the separate attachment and final removal of an external auxiliary that is implicit in the diastereoselective transformation, described earlier.⁽²⁴³⁾

The ultimate realisation for the Claisen rearrangement in asymmetric synthesis is the development of a catalysed process (*i.e.*, substoichiometric addition of a Lewis or Brønsted acid,(79, 247, 248) or organocatalyst(249, 250)) that can also affect the absolute configuration in the reaction. Truly catalytic variants of the Claisen rearrangement, proceeding with high enantioselectivity, continue to be relatively rare (particularly when establishing vicinal stereocenter relationships(79, 245, 248, 251-254)). Most protocols employing Lewis acids (*e.g.*, aluminum,(255-257) boron,(258, 259) magnesium(260)) require at least one equivalent of the chiral inductor to achieve adequate conversion, owing to the greater Lewis basicity of the product (and therefore poor catalyst turnover) or other competing background processes.(244, 261)

Furthermore, subtle interplay between substrate structure and rearrangement reactivity (in the presence of an electrophilic catalyst) renders the task of development of a general catalyst for the Claisen rearrangement particularly challenging.(241) For example, several *achiral* metal ion catalysts for the Claisen rearrangement have been identified (Pd^{II}-, (262-266) Cu^{II}-, (267) Bi^{III}-, (268) Sc^{III}-, (269) and Ln^{III}-complexes(182, 267, 270) and TiCl₄(271)), but only scandium,(272) palladium(253, 273) and copper(251, 252, 273, 274) complexes have shown any real capacity for asymmetric induction. Engagement of the prochiral substrate (in a constructive fashion) with a sufficient σ - or π -electrophilic catalyst is heavily dependent on the substitution off the allyl vinyl ether scaffold. Those substrates with significantly lengthened C4—O3 bonds are likely to be more susceptible to heterolytic decomposition while substrates with additional points of coordination (*e.g.*, Gostelli-type

allyl vinyl ethers(79, 247, 252)) to a chiral catalyst afford the necessary conformational restriction required for greater stereocontrol.(260)

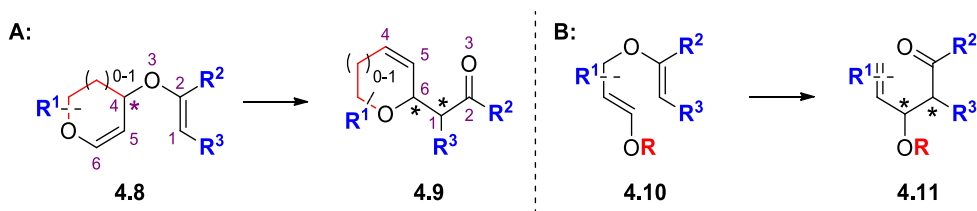
Extensive reviews of the pertinent literature for asymmetric induction in the Claisen rearrangement have been published by Nubbemeyer,(243) Taguchi,(261) Enders,(239) Hiersemann(241, 269) and others.(182, 187) We therefore feel it is beyond the scope of this dissertation to include an exhaustive description of the advancements in this research area. Being that each substrate will behave according to the substitution off the pericyclic scaffold, we have chosen to focus solely on the literature known for the rearrangement of C6 alkoxy-substituted allyl vinyl ethers as these bear the most resemblance to our own system.

4.2 Diastereoselective Claisen Rearrangement of Bis-Vinyl Ethers

It is surprising to find that little work has been done in the way of investigating asymmetric variants of the Claisen rearrangement of allyl vinyl ethers that possess a γ -allylic oxygen. These substrates, by virtue of their bond connectivity, have the potential to produce highly-substituted aldol-type products, **Scheme 4.3**, which are important structural subunits found in many biologically active natural products.(275) We recognised this gap in the pre-existing literature as an opportunity to further exploit the chemistry of our bis-vinyl ether substrates.

4.2.1 Early Diastereoselective Claisen Rearrangements of γ -Allyloxy Vinyl Ethers

The most extensively investigated class of C6 alkoxy-substituted allyl vinyl ethers, in this regard, are those resulting from cyclic furanoid ($n = 0$) or pyranoid ($n = 1$) glycols of type **4.8** (Scheme 4.3A). Stereocontrol during the course of the reaction is derived from the chiral information encoded in the C4—O3 bond of the parent structure which, when passing through a boat-type transition state, is transmitted to pro-chiral atoms C1 and C6.



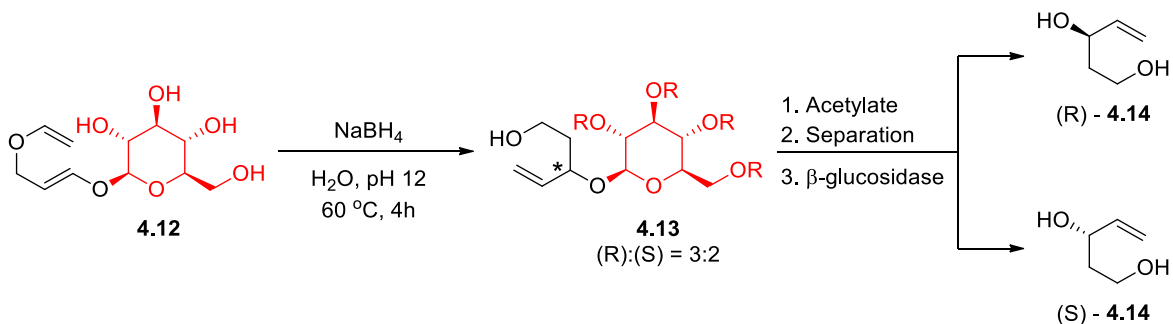
Scheme 4.3 Claisen rearrangement of cyclic (A) and acyclic (B) γ -allyloxy vinyl ethers.

These cyclic substrates undoubtedly represent an important subset of reactions⁽²⁷⁶⁾ that have led to the development of new synthetic methodologies (*e.g.*, C-glycosides and C-glycosyl amino acids⁽²⁷⁷⁻²⁷⁹⁾) and the synthesis of a number of interesting natural products.^(50, 280-283) Despite this, we can draw few analogies from the reactivity of these systems to that of our own bis-vinyl ethers (*see* **Chapter 1** and **Chapter 3**). The incorporation of a stereogenic center within³⁵ the pericyclic framework, in addition to the

³⁵ External asymmetric induction requires extensive knowledge about the nature of transition-state structure. Successful reactions are generally achieved when a highly ordered transition state, with defined orientation of the remote chiral element, is attainable. For the Claisen rearrangement, best results are often observed when stereodirecting subunits are placed adjacent to the nascent σ -bond formed during the course of the reaction (*i.e.*, C1 or C6).

added conformational restriction afforded by the glycal, enables better stereocontrol in the reaction when compared with their acyclic counterparts.

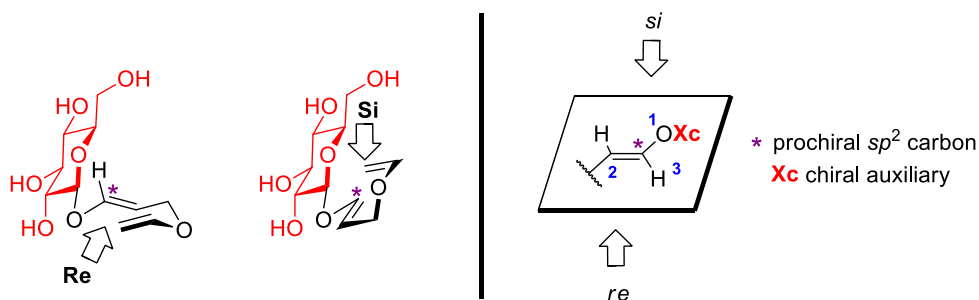
Reports of asymmetric transformations of allyl vinyl ethers of the type **4.10**, that better map onto the structure of our bis-vinyl ethers, are relatively sparse (**Scheme 4.3B**). To the best of our knowledge, the first asymmetric Claisen rearrangement described in this context was reported by Augé in 1990.⁽⁷⁶⁾ In this seminal work, Augé examined the accelerating effect of water on the rate of Claisen rearrangement for glyco-organic compound **4.12**, pictured in **Scheme 4.4**. The β -D-glucose moiety (in red), appended to the reactive allyl vinyl ether through the anomeric oxygen, permitted water solubility of the substrate (due to an extensive hydrogen bonding network) in addition to acting as a remote site of chirality that could be easily removed post-rearrangement.



Scheme 4.4 Auxiliary-controlled diastereoselective Claisen rearrangement of a γ -allyloxy allyl vinyl ether.

Reaction of **4.12** at 60 °C, in the presence of NaBH₄, afforded a 60:40 mixture of two diastereomers of **4.13**. These could be separated into their diastereomerically pure form *via* fractional crystallization (in diethyl ether) and then enzymatically cleaved to yield

enantiopure diols, **4.14**, with the major diastereomer giving rise to the R-enantiomer.³⁶ As a rationale for the preferential formation of (R)-**4.14**, the authors proposed a chair-type transition-state structure where the β -anomer of glucose is found to (slightly) bias attack towards the *re* face of the allyl vinyl ether in order to avoid unfavourable 1,3-syn diaxial interactions that result from approach at the *si* face, as depicted in **Scheme 4.5**.



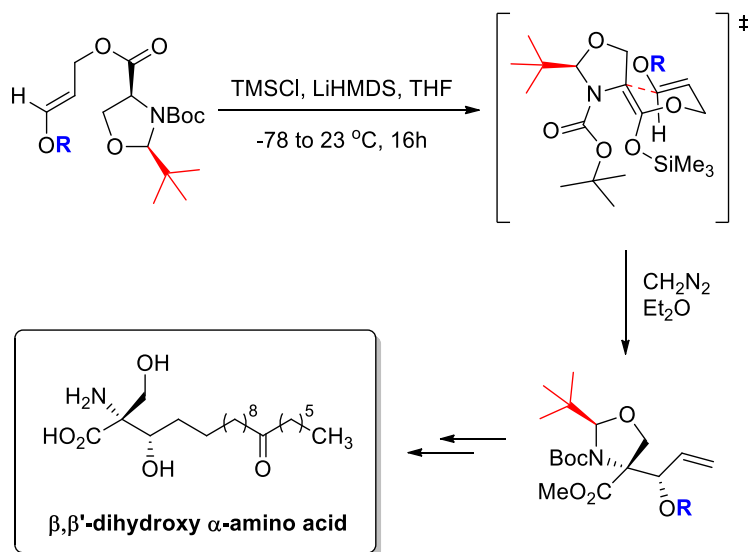
Scheme 4.5 Rationale for formation of (R)-4.14 as the major enantiomer.(76)

While the diastereoselectivity was rather poor for this reaction, its utility is exemplified in the ability to (a) successfully generate the Claisen product under mild conditions, (b) with some diastereofacial selectivity where (c) subsequent removal of the auxiliary affords enantiopure building blocks that can then be utilized in asymmetric synthesis.

In more recent years, Carbery(284) has reported the use of a serine-derived oxazolidinone “auxiliaries” in the Ireland Claisen rearrangement of β -alkoxy and β -aryloxy enol ethers leading to the formation of β,β' -dihydroxy α -amino acids (**Scheme 4.6**). The superb

³⁶ A reversal in the stereochemical outcome for this reaction is observed when α -D-glucose is used in place of the β -anomer, producing a 3:2 ratio of product **4.13** in favour of the S-enantiomer (after cleavage).

diastereoselectivity (*i.e.*, >98:2 dr) achieved using this method is the result of greater steric restraint within the transition state, with two of the pendant arms of the oxazolidinone becoming irreversibly ensconced in the final product.

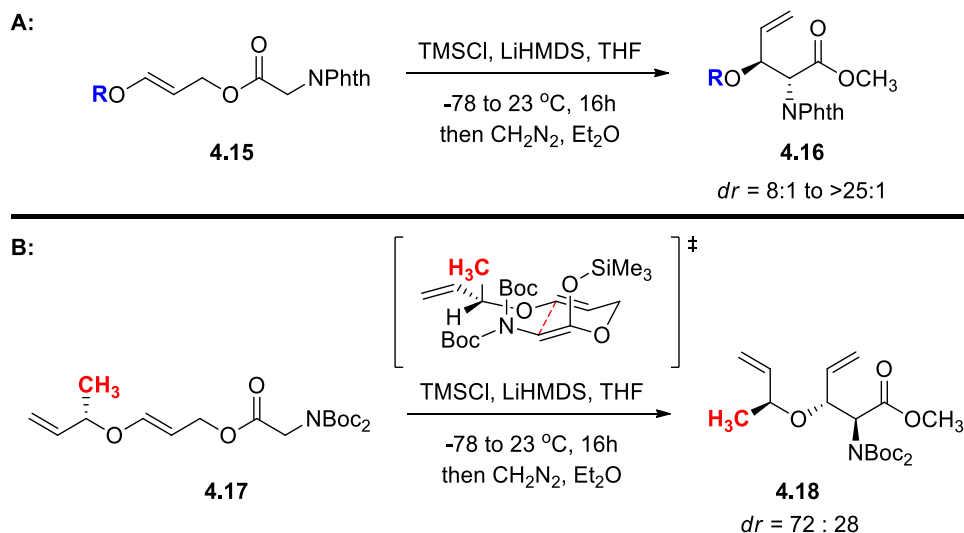


Scheme 4.6 Serine-derived oxazolidinone used to control the diastereoselectivity in the Ireland Claisen rearrangement of β -alkoxy and β -aryloxy enol ethers.

In 2011, Carbery extended his work on a related system(81) for the synthesis of β -alkoxy α -amino acids, derived from allyl glycinate **4.15** (Scheme 4.7A), by incorporating a chiral allylic enol ether as the remote stereocontrol element at position **R**, as shown in Scheme 4.7B.(285) It is particularly important to note that the reactivity of **4.15** (and by extension **4.17**) closely resembles that of our own system, where the electronic nature of an aryloxy substituent (**R**) was found to have profound effects on the rate of rearrangement.³⁷ Reaction

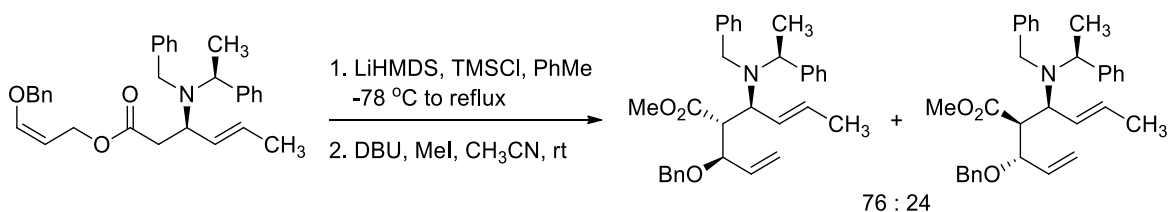
³⁷ Carbery notes that electron-withdrawing functionality on the aryloxy substituent at position **R** inhibits rearrangement of compound **4.15**, while electron-donating groups (which can stabilize carbocation formation) at this position resulted in complete conversion to **4.16**, but with significant by-product formation due to elimination of the aryloxy function. This reactivity profile matches closely to our own system and suggests a more dissociative transition state.

of **4.17**, using standard conditions for the ester-enolate Claisen rearrangement, afforded **4.18** as a mixture of two diastereomers in a *ca.* 2.5:1 ratio, suggesting that a more dissociative transition state can, evidently, still undergo rearrangement with some level of stereocontrol.



Scheme 4.7 Ireland Claisen rearrangement of alkoxyallyl glycinates.

The most recent report in this field comes from Davies' (286) work on the development of an Ireland Claisen rearrangement of enantiopure allyl β -amino esters to yield β -benzyloxy β' -amino acids that can be elaborated, in their enantiopure form, to C5-substituted transpentacins (**Scheme 4.8**).



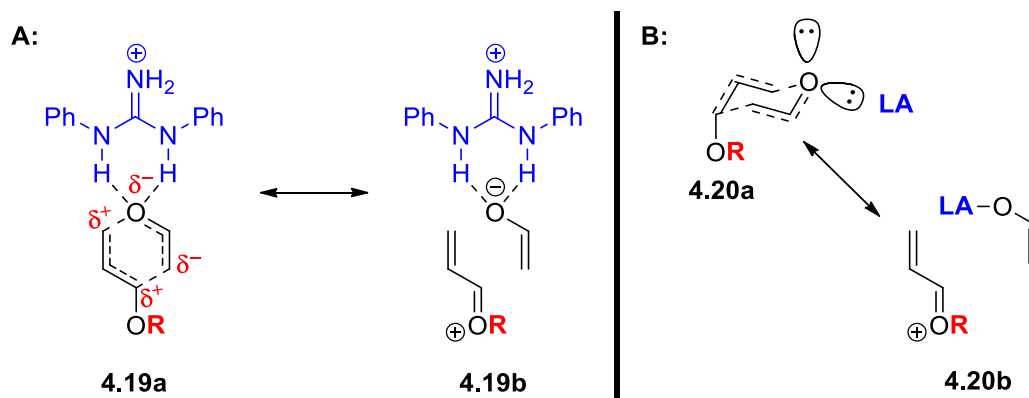
Scheme 4.8 Diastereocontrolled Ireland Claisen rearrangement of allyl β -amino esters.

One would have expected that the closer proximity of the chiral-directing element, in combination with the presumably more ordered transition-state structure (relative to **4.17**) would have resulted in a noticeable improvement in the stereoselectivity for the rearrangement, although this appears not to be the case.

It is not particularly surprising that so few examples for remote stereocontrol of allyl vinyl ethers of type **4.10** have been reported. The likely explanation is that lengthening of the C4–O3 bond, which accompanies alkoxy-substitution at C6, prevents remote auxiliaries from exerting their influence during the course of the reaction due to a higher degree of disorder in the transition-state structure.

This last point is particularly relevant, as Curran(78) found that dual hydrogen-bonding compounds (*i.e.*, diarylureas and, to a lesser extent, thioureas) could induce modest rate accelerations when used in stoichiometric quantities. Jacobsen(79) later reported that the presence of catalytic amounts of *N,N'*-diphenylguanidinium salts could also produce a similar rate enhancement for the Claisen rearrangement of compounds like **4.10**. However, attempts to extend this methodology to include asymmetric transformations using chiral guanidinium salts ultimately proved unsuccessful for these substrates.(79) This suggests that chiral, oxophilic Lewis acids (that presumably exert their influence by distinguishing between two enantiotopic lone pairs on the ether oxygen)(253) and hydrogen-bonding catalysts will likely not elicit any asymmetric control over the reaction unless they can also coordinate to some other heteroatom on the allyl fragment (**Scheme 4.9**). Increasing the coordination number in the allyl vinyl ether would (in theory) enable a sufficient decrease

(make more negative) in the entropy of activation (ΔS^\ddagger) so that the effect of a remote chiral environment could be transmitted through to the pericyclic framework during rearrangement.(287)

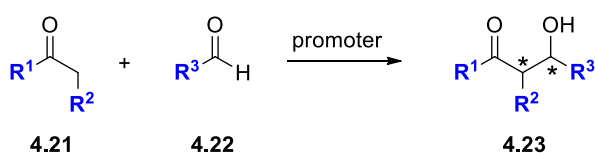


Scheme 4.9 Hydrogen-bonding catalysts (A) and oxophilic Lewis acids (B) may not be suitable stereocontrol agents. The extent of bond lengthening at C4–O3 makes the ethereal oxygen more accessible for coordination; this could result in fission of the vinyl ether, in which case [3,3]-rearranged products would be produced with poor diastereoselectivity, [1,3]-rearranged products could become possible, or the two fragments may fail to recombine entirely.

4.3 Accessing Aldol-Type Products Using the Claisen Rearrangement

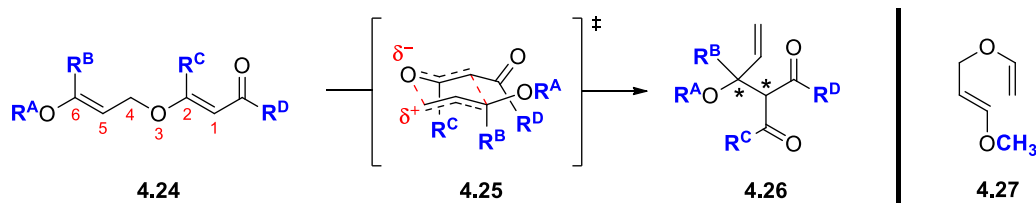
As was stated earlier, Claisen rearrangement of bis-vinyl ether substrates could provide an invaluable means to access highly substituted aldol-type products that are not easily synthesized using traditional methods.(35) That is to say, there are a limited number of strategies for generating such sterically encumbered systems in a single transformation.(245) The most widely utilized approach for accessing β -hydroxy products (*e.g.*, **4.23**) is the asymmetric aldol reaction. The inherent weakness in this methodology, however, is that variations of the aldol reaction primarily focus on formation of new

carbon-carbon bonds that produce secondary β -alcohols (**Scheme 4.10**).⁽²⁸⁸⁾ Stereoselective formation of β -hydroxy carbonyl compounds *via* aldol condensation of two different ketones continues to be a significant synthetic challenge.^(275, 289) In addition to being inherently less reactive than aldehydes, the decreased steric and electronic discrimination of ketones make it more difficult to differentiate between the two enantiotopic faces of the carbonyl.⁽²⁷⁵⁾



Scheme 4.10 A general aldol addition reaction.

An asymmetric variant of the Claisen rearrangement, using our bis-vinyl ethers (**4.24**) as the reactive substrate, could provide a unique approach to achieving the synthesis of these more sterically demanding structures (*e.g.*, **4.26** in **Scheme 4.11**).



Scheme 4.11 Transformation of bis-vinyl ether **4.24** into aldol-type product **4.26**.

Furthermore, the flexibility in choice of substituent at R^{B} (*i.e.*, C6 position), provides the opportunity to access both secondary (when $\text{R}^{\text{B}} = \text{H}$) or tertiary (when $\text{R}^{\text{B}} = \text{aryl or alkyl}$) alcohols, provided the functionality at R^{A} can be easily removed at a later stage.

4.4 Developing Conditions for an Asymmetric Claisen Rearrangement

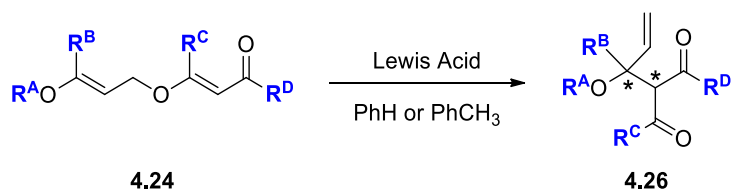
As was discussed at length in **Chapter 3**, the transition-state structure is considerably more polarized for elaborately substituted substrates like **4.24** than for the more modest system of **4.27**. This would initially suggest that bis-vinyl ether substrates of type **4.24** are weak candidates for asymmetric induction, either by remote stereocontrol (using an auxiliary or remote stereogenic center) or through use of a chiral Lewis or Brønsted acid. If this endeavor were to be fruitful, we would need to impose additional conformational restrictions within the transition-state structure during the course of rearrangement.

It was also demonstrated in **Chapter 3** that, even in the absence of an aryl substituent at **R^B**, the diastereoselectivity for thermal rearrangement of bis-vinyl ethers is rather poor. Furthermore, elevated temperatures can promote epimerization of β -keto esters, thereby negating any potential for control of the absolute configuration.

In an effort to address these issues simultaneously, we decided to employ an achiral Lewis acid to initiate the Claisen rearrangement under milder conditions.³⁸ To this end, we screened a number of Lewis acids that were known to lower the activation barrier to rearrangement in some context.³⁹

³⁸ A lower temperature for rearrangement would result in less conformational mobility, thereby improving the overall stereoselectivity of the transformation.

³⁹ Reactions were deliberately performed at, or below, ambient temperature in order to prevent the competing thermal reaction from being observed.

Table 4.1 Survey of Lewis acids.^c

| Entry | Lewis acid | Loading (mol%) | T (°C) | Time (hours) | %Conv. |
|-----------------|---|----------------|--------|--------------|------------------|
| 1 | Yb(OTf) ₃ | 10 | 23 | 18.5 | 0 |
| 2 | AlCl ₃ | 10 | 23 | 16 | — ^c |
| 3 | AlCl ₃ | 100 | 23 | 16 | — ^c |
| 4 | Et ₂ AlCl | 100 | -78 | 1.5 | — ^c |
| 5 | TiCl ₄ | 10 | -78 | 1.5 | — ^c |
| 6 | CuCl ₂ | 100 | 23 | 16 | — ^c |
| 7 | Zn(OTf) ₂ | 5 | 23 | 16 | — ^d |
| 8 ^b | IrCl ₃ | 10 | 23 | 18 | 0 |
| 9 ^b | RhCl ₃ | 10 | 23 | 18 | 0 |
| 10 ^b | Rh(PPh ₃) ₃ Cl | 10 | 23 | 18 | 0 |
| 11 ^b | Ru(PPh ₃) ₂ Cl ₂ | 10 | 23 | 18 | — ^c |
| 12 | Pd(PhCN) ₂ Cl ₂ | 10 | 23 | 1.5 | >99 ^e |
| 13 ^b | Pd(PPh ₃) ₂ Cl ₂ | 10 | 23 | 18 | 0 |
| 14 ^b | Pd(CH ₃ CN) ₂ Cl ₂ | 10 | 23 | 18 | >99 ^e |
| 15 ^b | Pd(COD)Cl ₂ | 10 | 23 | 18 | 0 |
| 16 ^b | Pd(OAc) ₂ | 10 | 23 | 18 | 12 |
| 17 ^b | Pd(PPh ₃) ₄ | 10 | 23 | 18 | 0 |
| 18 ^b | Pd ₂ (DBA) ₃ | 10 | 23 | 18 | 0 |

^aR^A = Bn or 1-phenylethyl; R^B = Me; R^C = Me or *n*Bu and R^D = Et or (S)-4-isopropylloxazolinin-2-one. ^bProgress of the reaction was monitored by ¹H NMR spectroscopy. ^cExtensive decomposition of **4.24** occurred. ^dComplete conversion of **4.24** into the hydrolysis product. ^eUnidentified side-products were observed in the ¹H NMR spectrum.

Not surprisingly, the use of most oxophilic Lewis acids (*i.e.*, Al³⁺, Ti⁴⁺ and Cu²⁺) was found to result in extensive decomposition of our bis-vinyl ether substrates (entry 2–6, **Table 4.1**). Both Hiersemann(267) and Sharma(290) have reported ytterbium(III) triflate as an effective catalyst for the rearrangement of (allyloxy)acrylates and allyl aryl ethers, respectively. It would appear that, despite the oxophilic nature of the lanthanide, Yb(III) is an ineffective catalyst for our system (entry 1, **Table 4.1**). Performing the reaction in

chlorinated solvents in the presence of pulverized 4Å molecular sieves or with gentle heating to 40 °C (data not shown) also failed to provide any Claisen rearranged product.

Palladium complexes, while largely known for their ability to catalyze rearrangements of *O*-allylimidates,(291-295) can also effect [3,3]-sigmatropic rearrangements in 3-oxo-1,5-dienes, provided certain structural demands are met.(262) Increasing the bulk of the vinyl ether functionality, through alkyl substitution at both the C1 and C2 position, appears to be a prerequisite for successful conversion to the corresponding δ,γ -unsaturated carbonyl compound. Lack of substitution at C1 is found to result in unproductive binding of the electrophilic metal to the electron rich vinyl ether, while α -unsubstituted allyl vinyl ethers (*i.e.*, C2) produce significant quantities of the allylic alcohol as result of enol ether cleavage.(262) Our substrates appear to satisfy these criteria (*i.e.*, substitution at C1 and C2) and so we decided to evaluate a number of palladium(0) and palladium(II) complexes for their ability to catalyze the Claisen rearrangement of bis-vinyl ethers **4.24** (entries 12–18, **Table 4.1**).⁴⁰

Palladium(0) complexes were found to provide no detectable reactivity with our bis-vinyl ether substrates (entries 17 and 18). In contrast, the more electrophilic palladium(II) catalysts were found to promote Claisen rearrangement, the extent of which was found to be dependent on the strength of the *trans*-effect and/or co-ordinating ability of the counter-

⁴⁰ Late transition-metals bind more strongly to soft Csp^2 - Csp^2 bonds, making palladium an attractive choice for Lewis acid catalysis of the Claisen rearrangement. Coordination to *both* the allylic and vinyl ether olefin would be expected to rigidify the transition-state structure, thereby increasing order within the system.

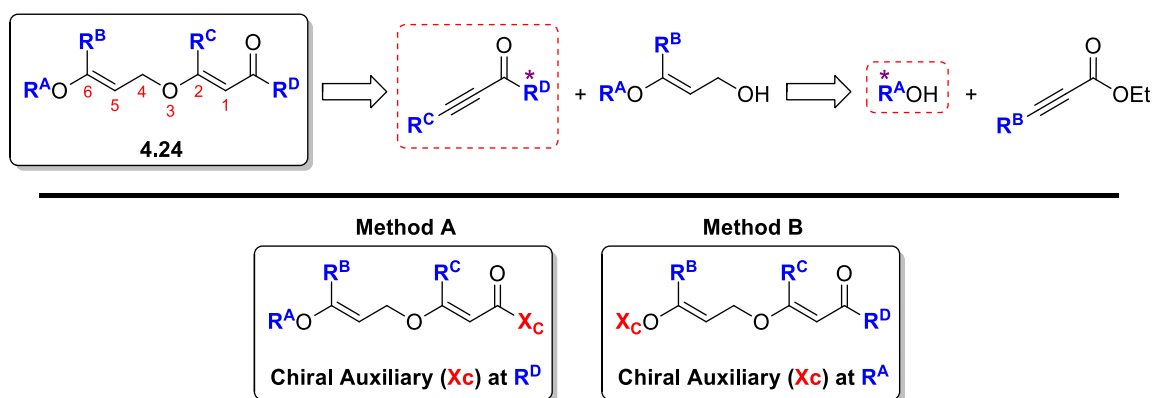
ion.⁴¹ For example, reaction of **4.24** in the presence of Pd(PhCN)₂Cl₂ (entry 12; unoptimized) results in >99% conversion after 1.5 h due to a stronger *trans*-effect when compared to Pd(PPh₃)₂Cl₂ (entry 13), which failed to produce any reaction after 18 h (although steric encumbrance of the triphenylphosphine ligands may also contribute to this lack of reactivity).

Having identified a suitable catalyst that would enable us to perform the reaction at lower temperatures, we now turned our attention to designing an appropriate scaffold that would enable chirality transfer to the two prochiral centers in our molecule. To accomplish this, we looked to identify a family of molecules where:

1. the stereodirecting element would be easily synthesized from non-racemic materials;
2. its incorporation would be compatible with our established methodology for the construction of bis-vinyl ethers of type **4.24**;
3. the placement of the chiral element, **Xc**, would impart a strong diastereofacial bias in the Claisen rearrangement; and
4. after reaction, the removal of **Xc** would be possible to ensure an overall enantioselective process; that is, **Xc** would not become permanently embedded in target molecule.

⁴¹ The *trans*-effect is the ability of a ligand to increase the rate of substitution of another ligand positioned *trans* to it. Good σ -donors and π -acceptors exert a strong *trans*-effect as they are better able to compete for donation into the same *d*-orbital, leading to a weakening of the bond *trans* to it, thus increasing its kinetic lability.

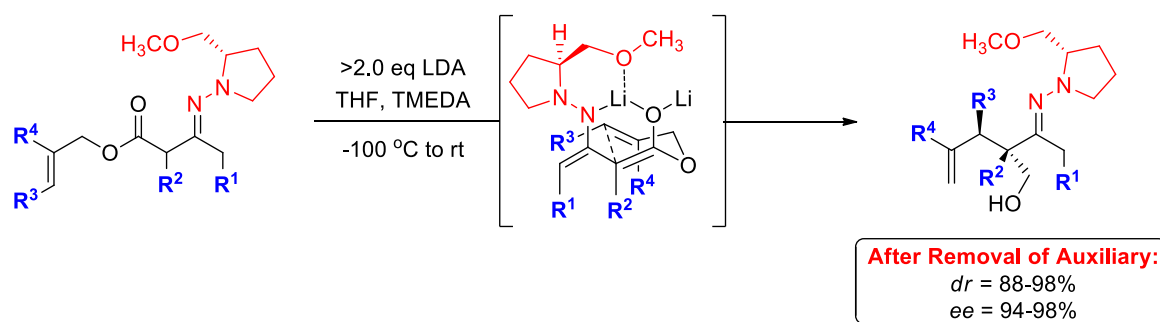
Remote stereocontrol is best achieved when a stereogenic element is placed near the site of new σ -bond formation (*i.e.*, C-1 or C-6).(243) Most fortuitously, the incorporation of enantiopure building blocks at sites R^A and R^D can be easily accomplished through judicious choice of starting alcohol (for R^A) to initiate the conjugate addition sequence *or* chiral alkynoates (at R^D) as the terminal coupling partner (**Scheme 4.12**).



Scheme 4.12 Incorporation of a remote chiral element into the bis-vinyl ether scaffold.

In order to limit the number of structural changes made to the scaffold, we wanted to choose a common motif at R^A that could be used in either approach (**Method A** or **Method B**) toward accessing enantiopure aldol-type products. In choosing this functionality, it was important that (a) it could be easily removed to reveal the latent β -alcohol post-rearrangement and (b) could be made available (as a structural analogue with one stereogenic carbon) in enantiopure form to evaluate the viability of **Method B**. With this in mind, we decided to incorporate benzyl-derived substituents at R^A since a number of these compounds are commercially available (*e.g.*, benzyl alcohol, (R)- or (S)-1-phenylethanol) while others can be readily synthesized *via* asymmetric reduction of the corresponding ketone.

Initial assessment for identification of a suitable chiral auxiliary at **R^D** (**Method A, Scheme 4.12**) proved to be a more difficult. Ideally, the chiral element — if it were to have any diastereofacial bias — should be no more than one atom removed from the pericyclic framework. A few examples in the literature demonstrate that this need not be the case(296, 297) (*e.g.*, Enders asymmetric Carroll rearrangement, shown in **Scheme 4.13**), but rearrangement of such substrates is known to also benefit from intramolecular chelation of a coordinated metal ion (thereby “reining in” the chiral element so that it can affect facial selectivity).

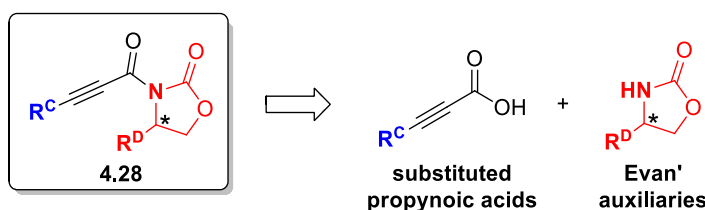


Scheme 4.13 Auxiliary-controlled diastereoselective Carroll rearrangement, using (S)-1-amino-2-methoxymethylpyrrolidine as the chiral auxiliary.

At this early stage in the investigation we still did not know how the catalytic addition of a palladium complex would affect the reaction trajectory for our substrates. Employing a Lewis acid can have a profound effect on the shape of the energy landscape for rearrangement,(241) the transition-state geometry(263) and even the nature of the transition-state structure, shifting the mechanistic pathway from a concerted rearrangement to a two-step, dissociative process.(267, 298, 299) Until experimental evidence was

accumulated, we had no way to predict how the proximity of the chiral element within the auxiliary would affect the [3,3]-sigmatropic process for our own molecules.

Experience had informed us that the activating group at R^D must be bonded to the carbonyl through a heteroatom-linkage, as ketones ($R^D = \text{alkyl}$) led to rapid, phosphine-mediated polymerization of the alkyne. This necessitated that chiral-element be at least two atoms removed from the pericyclic framework (C1–C6).



Scheme 4.14 Synthetic plan for incorporating oxazolidinone-auxiliaries into our alkyne building-blocks for the conjugate addition sequence.

Returning to our original objective, we decided to install oxazolidinone auxiliaries at R^D (**Xc, Method A**). Substrates of type **4.28** would immediately satisfy three of our four criteria as (1) Evans' auxiliaries could be easily synthesized from optically pure D- or L- α -amino acids(300) and then coupled to substituted propynoic acids of our choosing, **Scheme 4.14**; (2) incorporation of compounds like **4.28** into our existing synthetic protocol should be relatively straightforward; and (3) due to their prevalent use in the chemical literature, there are a multitude of ways to actuate their removal.

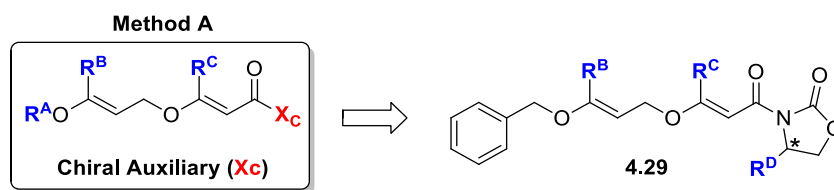
4.5 Evaluation of Auxiliary-Controlled Diastereoselective Claisen Rearrangements

For the purpose of providing a systematic division of the work in **Chapter 4**, evaluation of chiral auxiliaries at C1 (**R^D**, **Method A**) and C6 (**R^A**, **Method B**) will be addressed separately. It should be noted that both methods were examined in parallel, although optimization of conditions for the palladium-mediated Claisen rearrangement were performed solely on substrates where the chiral-auxiliary was placed at C6 (*i.e.*, substrates used in **Method B**). As such, optimization of conditions for this reaction will appear later in the Chapter in **Section 4.7.2**.

4.6 Method A: Incorporation of a Chiral Auxiliary at C1

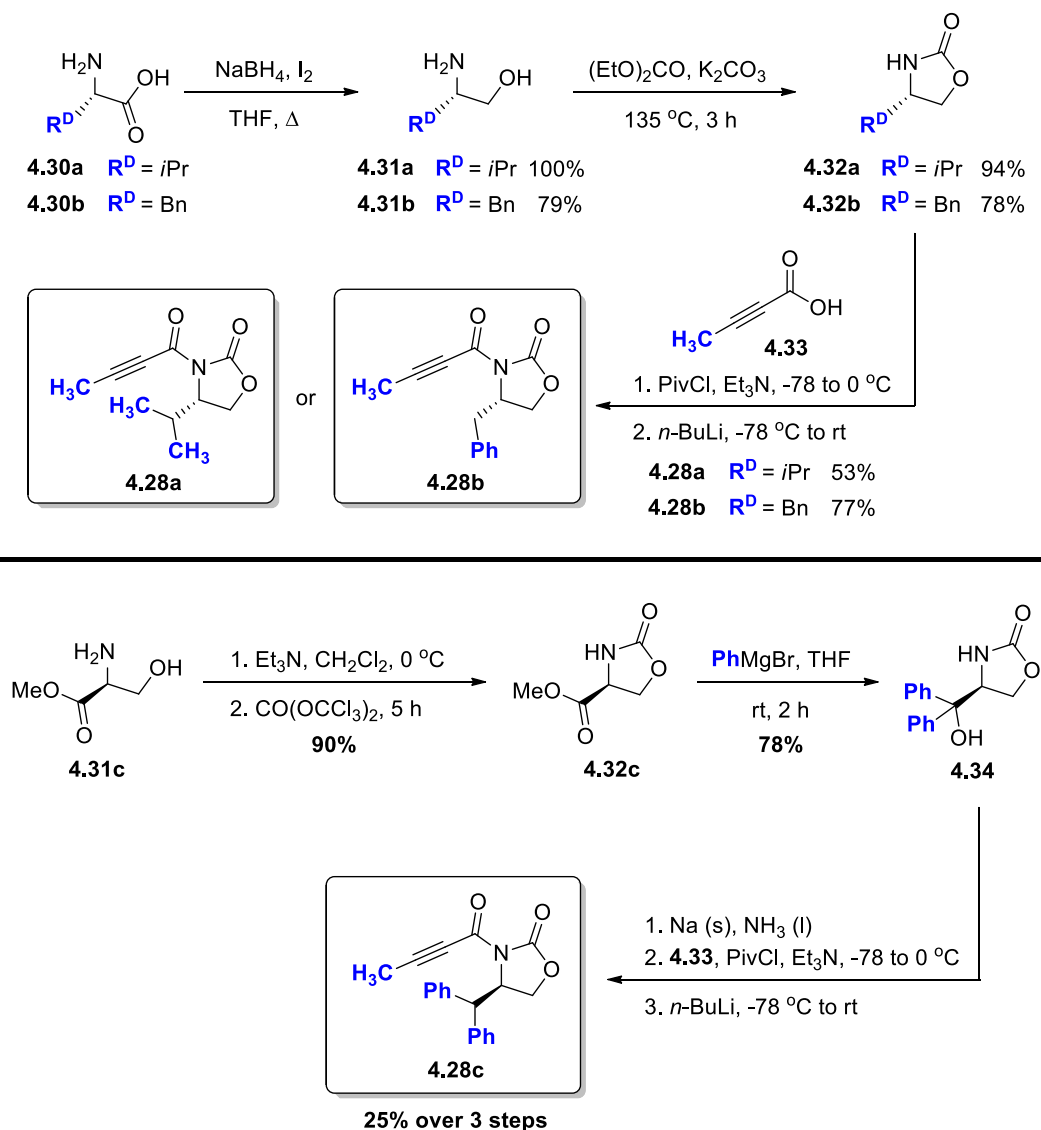
4.6.1 Synthesis of Oxazolidinone Building Blocks

Bis-vinyl ether **4.29** became our synthetic target for evaluating attachment of a distal chiral-element at C1 (**Scheme 4.15**). Preparation of the required building blocks (*i.e.*, oxazolidinone-based auxiliaries) was accomplished by following known literature procedures, as outlined in **Scheme 4.16**.



Scheme 4.15 Incorporation of a chiral auxiliary at C1.

Benzyl, isopropyl and diphenylmethyl substituents were installed at the stereogenic center in order to assess whether variations in steric encumbrance at R^D would affect the diastereofacial selectivity of the reaction.⁴²



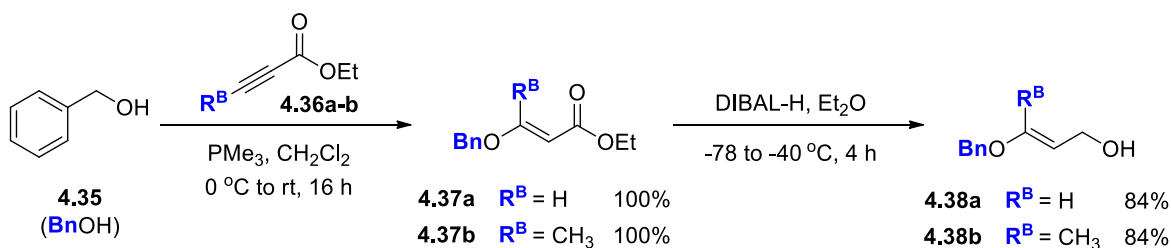
Scheme 4.16 Synthesis of chiral building blocks to act as a remote auxiliary off bis-vinyl ethers of type 4.29.

⁴² Compounds **4.31a** and **4.32a** were prepared by Dr. Caleb Bromba. Synthesis of 4(*S*)-isopropylloxazolidin-2-one, **4.32a**, was achieved by reacting the corresponding amino alcohol **4.31a** with diethyl carbonate in the presence of NaOEt (rather than K₂CO₃).

With compounds **4.28a–c** in hand, we now turned our attention to the preparation of a small series of molecules that would enable us to evaluate the viability of **Method A**.

4.6.2 Synthesis of Bis-Vinyl Ethers Containing Oxazolidinone-Based Chiral Auxiliaries

In keeping with our established iterative protocol, the synthesis of substrates **4.29** commenced with the conjugate addition of benzyl alcohol (**4.35**) to ethyl propiolate (**4.36a**) or ethyl-2-butynote (**4.36b**) in the presence of a catalytic amount (10 mol%) of triphenyl phosphine (**Scheme 4.17**). This first conjugate addition proceeded smoothly to afford mono-vinyl ethers **4.37a** and **4.37b** in quantitative yield as clear, colourless oils after purification by flash chromatography on silica gel treated with 1% triethylamine. DIBAL-H reduction of the vinylogous carbonate, **4.37**, was somewhat complicated by the propensity for these substrates to undergo elimination reactions under the conditions employed. Nonetheless, we were able to obtain the sensitive allylic alcohol, **4.38**, in yields comparable to that reported by Carbery (80% on *ca.* 2.0 g scale)(80) for the reduction of compounds of this type (**4.38a**) under a similar set of conditions.

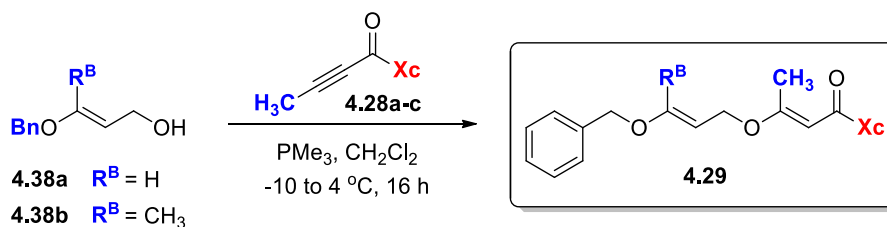


Scheme 4.17 Synthesis of allyl alcohol **4.38a** and **4.38b**.

In an attempt to employ our standard set of reaction conditions to the conjugate addition of alcohol **4.38** onto our chiral alkynyl-oxazolidinone building blocks (**4.28**), we discovered that the Claisen rearrangement for substrates of type **4.29** was particularly facile — occurring at temperatures as low as 25 °C.⁴³ To circumvent this background reaction, the conjugate addition was carried out at -10 °C, with warming to 4 °C overnight. The following morning, the reaction was concentrated on the pump, re-suspended in cold diethyl ether and quickly filtered over basic alumina with a minimal amount of solvent. Concentration of the filtrate under vacuum afforded compounds **4.29a–d** (Table 4.2) as colourless foam in good to excellent yields, with minimal amounts of the rearranged product.

⁴³ There is ample evidence to demonstrate that the Claisen rearrangement of substituted allyl vinyl ethers can be accelerated in the presence of polar, protic solvents such as water. Depending on the relative humidity within the lab on a given day, two consecutive trips to the NMR room could see >90% conversion of compounds **4.29** to the Claisen rearrangement product.

Table 4.2 Synthesis of bis-vinyl ethers 4.29.



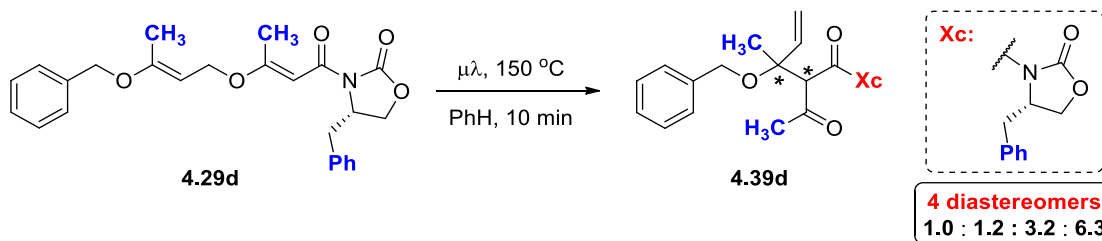
| Entry | R^B | Xc | Addition | Yield ^a |
|-------|--------|------|--------------|--------------------|
| 1 | H | | 4.29a | 99% |
| 2 | H | | 4.29b | 94% |
| 3 | H | | 4.29c | 100% |
| 4 | CH_3 | | 4.29d | 74% |

^aBased on isolation of the crude product.

4.6.3 [3,3]-Sigmatropic Rearrangements of Bis-Vinyl Ether 4.29d

As was indicated in **Section 4.4**, substrates bearing alkyl or aryl substitution at R^B (*i.e.*, position C6) would enable the construction of a new carbon-carbon σ -bond with a vicinal relationship between the newly formed quaternary and tertiary stereocenters in the rearrangement product. Few methodologies exist that can effectively execute such synthetic transformations. To this end, we chose to evaluate the thermal and palladium-mediated Claisen rearrangement of compound **4.29d**.

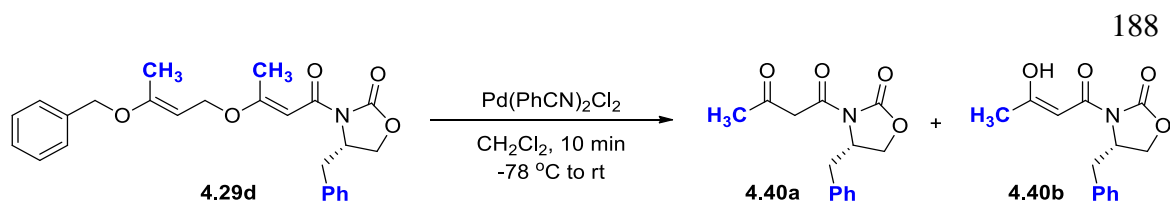
The thermal rearrangement of compound **4.29d** was achieved *via* microwave irradiation at 150 °C for 10 minutes in 2 mL of benzene.⁴⁴ Crude analysis by ¹H NMR spectroscopy revealed the formation of four diastereomers, the ratio of which is indicated in **Scheme 4.18**.



Scheme 4.18 Thermal induced Claisen rearrangement of **4.29d**.

This same substrate, **4.29d**, was then subjected to the conditions developed for our palladium-mediated rearrangement. To a 0.23 M solution of **4.29d** in dry dichloromethane at $-78\text{ }^\circ\text{C}$ was added 2.5 mol% Pd(PhCN)₂Cl₂ in one portion. The reaction was warmed to room temperature over 10–15 minutes, at which point the catalyst was precipitated by addition of a 1:1 mixture of diethyl ether:hexanes. The resulting suspension was filtered over a pad of silica gel and the filtrate removed under reduced pressure at 35 °C. Analysis of the crude reaction mixture by ¹H NMR spectroscopy revealed the unexpected formation of *ca.* 3.3:1.0 mixture of **4.40a** and its tautomer **4.40b** (**Scheme 4.19**).

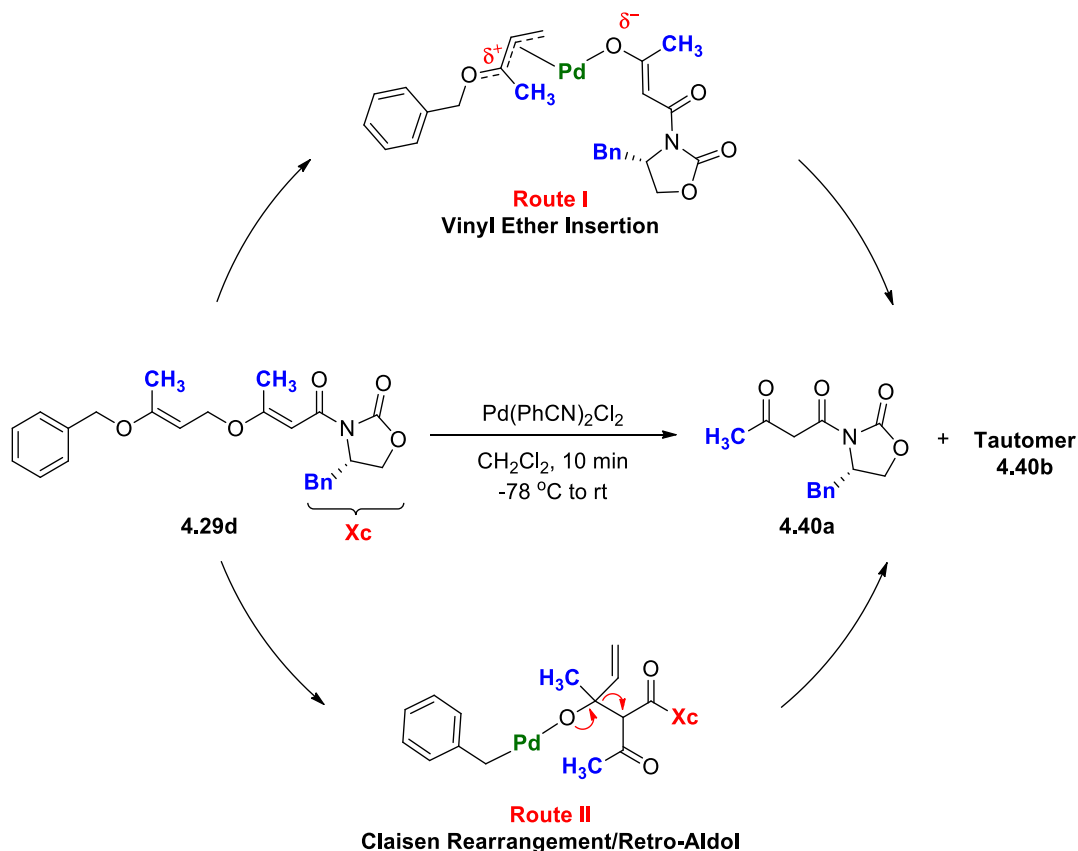
⁴⁴The thermal rearrangement of substrates **4.29** were performed under the described conditions in order to intentionally provide a mixture of all four diastereomers for analysis.



Scheme 4.19 Unexpected formation of oxazolidinone 4.40.

Palladium-induced enol ether cleavage is known to occur much more readily for the vinylogous ester than for the corresponding analogue where the electron-withdrawing functionality is absent.⁽³⁰¹⁾ Despite having substitution at both C1 and C2 (**R^C**) in our molecule, the presence of the conjugated carbonyl system may still promote an unproductive palladium insertion into the vinyl ether (**Route I**), resulting in formation of the putative hydrolysis product **4.40**, as shown in **Scheme 4.20**.

This reaction pathway, however, is not the only mechanistic option to explain the observed experimental result. A second possibility is that prolonged interaction of the Claisen product with the catalyst leads to C–O insertion at the benzyl alcohol (**Route II, Scheme 4.20**). In an effort to relieve some of the strain associated with having introduced a new quaternary stereocenter, a formal retro-aldol reaction occurs, giving rise to a similar distribution of by-products (**4.40**) as described for **Route I**.



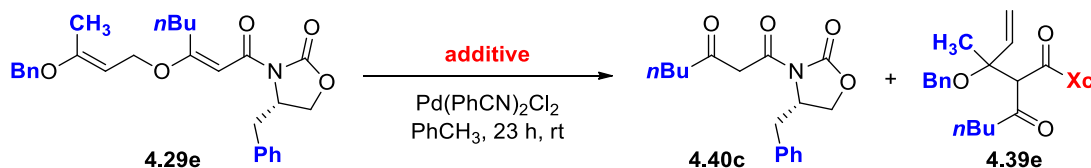
Scheme 4.20 Mechanistic possibilities for the unexpected chemical reactivity of 4.29d when treated with $\text{Pd}(\text{PhCN})_2\text{Cl}_2$.

4.6.4 Delineation of Mechanistic Possibilities for By-Product Formation

Nelson(302) reported that, for aliphatic allyl vinyl ethers lacking α -substitution (*i.e.*, substrates lacking a substituent at C2 – for which decomposition *via* **Route I** is found to predominate(262)), performing the reaction with nitrile additives having electronically- or sterically-diminished competency as ligands (relative to acetonitrile) can improve the reaction efficiency by decreasing the susceptibility of these substrates towards enol ether cleavage. Hoping to find a similar relationship between product distribution and ligand

addend with our own substrate, we subjected compound **4.29e** to Nelson's conditions for Claisen rearrangement. Results for this experiment are summarized in **Table 4.3**.

Table 4.3 Effect of ligand addend on product distribution.



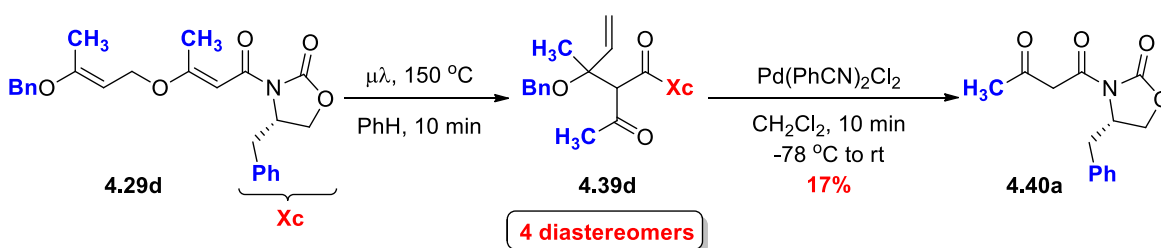
| Entry | Additive | Product |
|----------------|-------------------------------|----------------|
| 1 | None | 4.40c |
| 2 | <i>i</i> PrCN (500 mol%) | 4.40c |
| 3 | CH ₃ CN (500 mol%) | — ^a |
| 4 ^b | None | — ^a |

^aRecovered starting material. ^bAs a negative control, the reaction was performed without addition of the palladium catalyst.

Performing the reaction in the presence of 500 mol% CH₃CN (**entry 3**) over the course of 23 h was found to substantially retard the rearrangement to such an extent that only trace amounts of product **4.39e** were observed in the baseline of the ¹H NMR spectrum of the crude product. By contrast, when the reaction was carried out in the absence of additive (**entry 1**), or in the presence of 500 mol% *i*PrCN (**entry 2**), formation of **4.40** was observed. While this data can in no way identify the mechanistic pathway responsible for formation of **4.40** (*i.e.*, **Route I** or **Route II**, **Scheme 4.20**), it does confirm that interaction of the palladium-catalyst with either **4.29d** or **4.39d** is responsible for side product formation (refer also to entry 4).

To test the plausibility of the mechanistic hypothesis described by **Route II** in **Scheme 4.20**, substrate **4.29d** was thermally rearranged into the corresponding Claisen product

4.39d.⁴⁵ Subjecting this compound to further treatment with Pd(PhCN)₂Cl₂ at room temperature resulted in the formation of small quantities of the retro-aldol adduct **4.40a**. These results, pictured in **Scheme 4.21**, could not be consistently reproduced. We therefore chose to examine the reactivity of bis-vinyl ethers of type **4.29a–c**, lacking the methyl substituent at **R^B** (C-6), *in lieu* of the more sterically encumbered (unstable) substrate **4.29d**.



Scheme 4.21 Evaluation of a possible retro-aldol reaction with prolonged exposure to palladium.

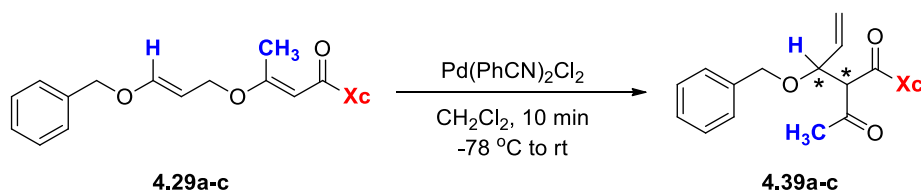
4.6.5 [3,3]-Sigmatropic Rearrangements of Bis-Vinyl Ether **4.29a–c**

We had returned to the less sterically encumbered substrates **4.29a–c** with the hope that, by reducing the steric burden at C6, we would be able to mitigate the competing (apparent) retro-aldol reaction, provided the palladium catalyst be removed immediately following [3,3]-sigmatropic rearrangement.

⁴⁵ Compound **4.39d** appears to be fairly robust (*i.e.*, bench-top stable), surviving purification by flash-column chromatography without any observable decomposition or epimerization of the acidic α -proton.

For comparative purposes, the thermal reaction was again performed on a representative sample, **4.29b**. Rearrangement provided a mixture of the four possible diastereomers, this time with reduced stereoselectivity compared to the more highly substituted congener (data not shown).

Table 4.4 Claisen rearrangement of bis-vinyl ethers **4.29a–c**.



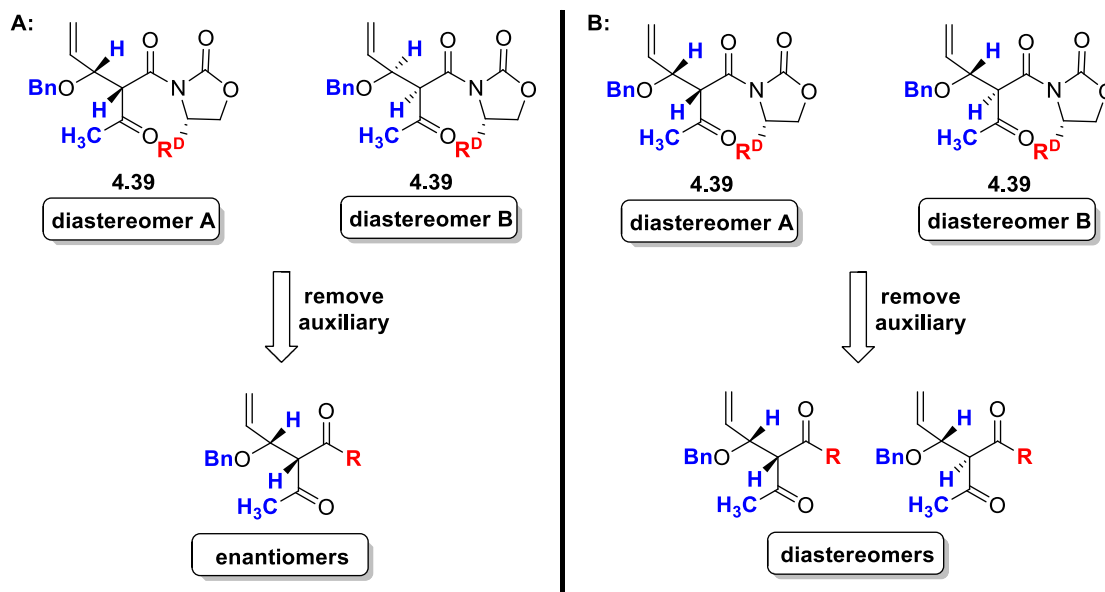
| Entry | Compound | Xc | dr ^b |
|-------|--------------|----|---|
| 1 | 4.29a | | 4.39a 2.0 : 1.0 (70%) ^a |
| 2 | 4.29b | | 4.39b 1.0 : 1.3 (68%) ^a |
| 3 | 4.29c | | 4.39c 1.5 : 1.0 |

^aYield after purification by flash column chromatography. ^bOnly two, of four possible, diastereomers were formed.

The palladium mediated-rearrangement had been executed with substrates **4.29a–c** in an identical manner as described for **4.29d**. We were pleased to discover that the reaction proceeded smoothly to the desired Claisen adduct, **4.39a–c**, without any apparent decomposition to **4.40**. As had been anticipated in **Section 4.4**, the mild conditions that accompany the use of a Lewis acid to catalyze the Claisen rearrangement led to an improvement in the overall diastereoselectivity of the reaction, relative to its thermal counterpart. Unfortunately, compounds **4.29a–c** afforded a near equimolar ratio of two

diastereomers with a presumed anti-configuration across the newly formed Csp^3-Csp^3 σ -bond.

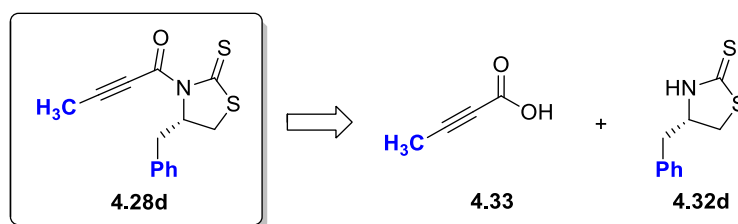
To eliminate the speculative nature of the above assignment, we opted to determine the relative stereochemical configuration of **4.39** from the above reaction. In either case, the mixture of diastereomers resulting from the rearrangement of **4.29a** or **4.29b** could be easily separated into their diastereomerically pure building blocks. Provided that the auxiliary could be easily removed, we would be able to determine the relationship between the two compounds (*i.e.*, diastereomers or enantiomers, **Scheme 4.22**) thereby providing some insight into the nature of the transition state for this reaction (*i.e.*, chair *versus* boat). This information would be an invaluable resource that would aid in future experimental design of remote stereodirecting elements for our bis-vinyl ethers.



Scheme 4.22 Product distribution, after removal of the chiral auxiliary, can determine whether the rearrangement is diastereoselective (A) or whether competing transition-state geometries lead to good overall enantioselectivity but poor diastereoselectivity (B).

We decided that the most expedient method for determining the stereochemical relationship between the given mixture of diastereomers (*e.g.*, 2:1 mixture of diastereomers for **4.39a**) was to remove the auxiliary to permit elaboration of the molecule into: (a) a known compound where the optical rotation could be compared to literature values for an established stereochemical configuration, (b) a rigidified or functionalized substrate that could be studied by NMR spectroscopy, or (c) through incorporation of a chiral element that would aid in crystal formation for determination of relative configuration *via* X-ray structural analysis.

It was most unfortunate to discover that removal of the Evans oxazolidinone was associated with a number of unforeseen difficulties resulting in the decomposition of our substrates. Thiazolidinethione auxiliaries, on the other hand, are readily cleaved under more mild reaction conditions, providing a means to alleviate the aforementioned problem.⁽³⁰³⁾ We thus elected to target isostere **4.28d** to use in place of the analogous compound **4.28b** in our conjugate addition/reduction sequence (**Scheme 4.23**).



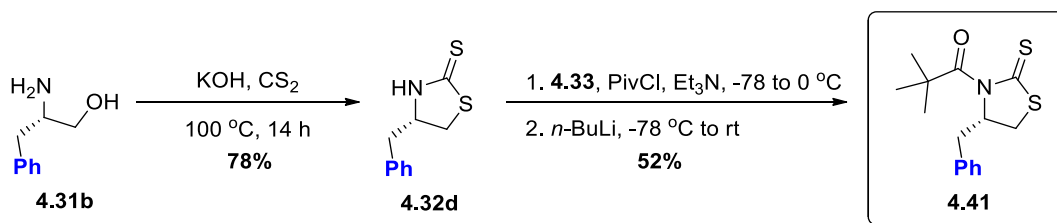
Scheme 4.23 Retrosynthetic plan for the synthesis of thiazolidinethione **4.28d**.

Unlike its cousin, oxazolidinone **4.28b**, there were no literature reports detailing the attachment of an alkyne derivative (such as **4.33**) to the Crimmins' auxiliary, **4.32d**. The

reason for this apparent hole in the chemical literature became clear as we began to investigate a number of ways to synthesize our target compound (**4.28d**).

4.6.6 Synthesis of Thiazolidinethione Building-Block **4.28d**

In keeping with the synthetic route that appeared earlier in this work (**Scheme 4.16**) we decided to first access Crimmins' auxiliary **4.32d** from β -amino alcohol **4.31b** (**Scheme 4.24**) following a known literature procedure.⁽³⁰⁴⁾ Reaction of **4.31b** with an excess of carbon disulfide, in a heated solution of 1M aqueous potassium hydroxide, afforded thiazolidinethione **4.32d** in good overall yield as a white, crystalline solid after recrystallization from absolute ethanol.

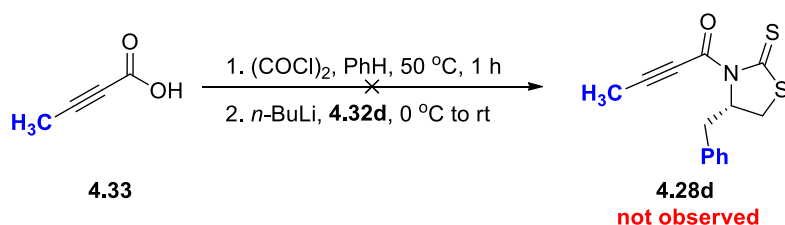


Scheme 4.24 Synthesis Crimmins' auxiliary **4.32d** and its use in an acylation reaction.

To access our proposed *N*-(2-alkynoyl)-derivative (**4.28d**) we attempted to react **4.32d** with the mixed anhydride generated from the reaction of tetrolic acid (**4.33**) with pivaloyl chloride. A gold-coloured, crystalline product was isolated from this reaction that was subsequently identified as **4.41**.⁽³⁰⁵⁾ This result was, at first, attributed to a failed attempt at generating the required anhydride. To ensure that formation of **4.41** was not due to a procedural or experimental error, the reaction was repeated and the generation of the mixed

anhydride was confirmed by infrared spectroscopy.⁴⁶ The results of this experiment were found to be consistent with our earlier observation, and so several alternate routes to access target compound **4.28d** were examined.

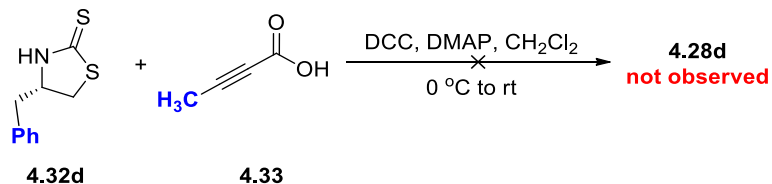
Since direct *N*-acylation of **4.32d**, from the corresponding acid chloride, is known,⁽³⁰⁵⁾ we decided to attempt such a reaction using 2-butyneoyl chloride (**Scheme 4.25**). While this reaction should have been straight forward, deprotonation of the thiazolidinethione resulted in the generation of a sulphur-based anion that launched an attack at the alkyne, leading to the formation of a number of (uncharacterized) by-products.



Scheme 4.25 Crimmins' auxiliary **4.32d** and its use in an acylation reaction.

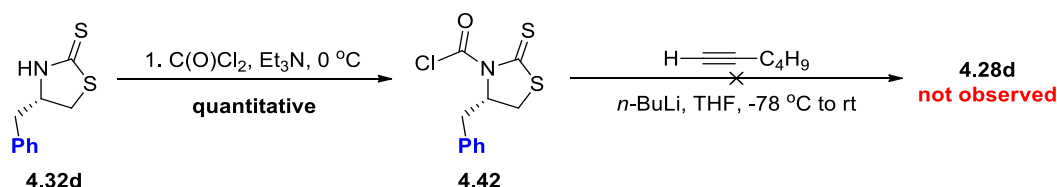
In an effort to bypass direct formation of an anionic-thiazolidinethione intermediate, a DCC-coupling between **4.32d** and tetrolic acid was performed (**Scheme 4.26**). This route also saw attack on the alkyne system, leading us to believe that this particular functionality (*i.e.*, the alkyne) was problematic when conjugated to an activating group.

⁴⁶ Dr. Fraser Hof was used in a blind control for confirmation that the anhydride had been formed successfully. I quote, "This infrared spectrum is cleaner than anything my students get out of a reaction after a column."



Scheme 4.26 DCC-coupling between tetrolic acid and Crimmins' auxiliary.

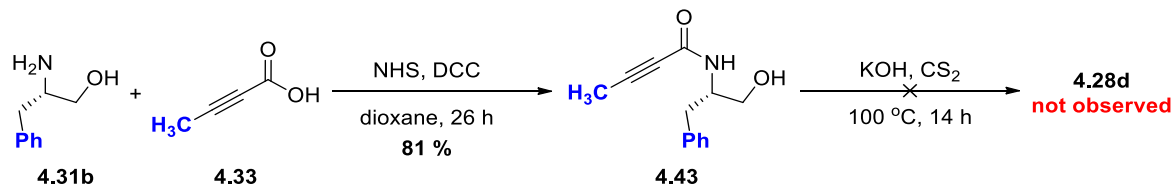
To avoid the use of the alkynoate, we reacted Crimmins' auxiliary **4.28d** with phosgene to generate dithiocarbamate **4.42** (Scheme 4.27). We proposed that the acid chloride would act as a hard electrophile when reacted with the anion of the terminal alkyne, thereby avoiding cross-reactivity with the thiocarbonyl.



Scheme 4.27 An attempt to take advantage of hard-soft acid-base concept to overcome unwanted reactivity of the thiocarbonyl.

Analysis of the product mixture from this reaction revealed, quite surprisingly, that the free auxiliary **4.32d** had been liberated from the “acyl” half of the molecule, thus stymying this approach.

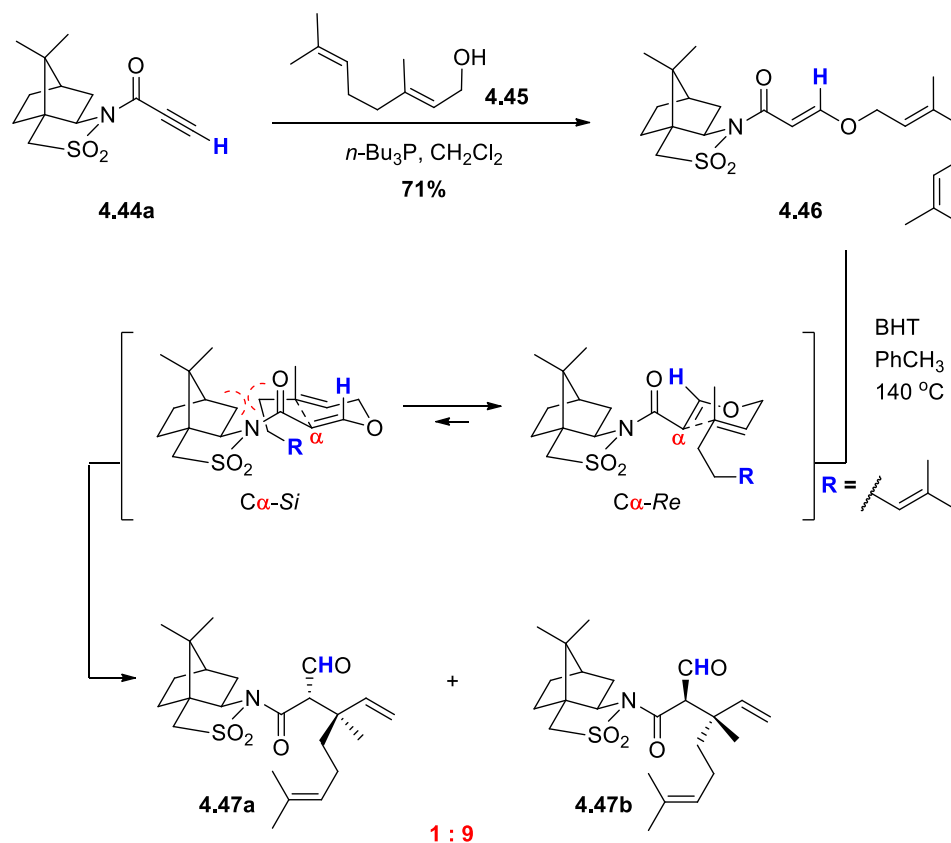
In a final attempt to access **4.28d** we performed a DCC-coupling between β-amino alcohol **4.31b** and 2-butynoic acid (**4.33**) to access ynamide **4.43**, using the procedure outlined by Moyano.⁽³⁰⁶⁾ Compound **4.43** was then subjected to our original conditions for formation of the thiazolidinethione core (Scheme 4.28). Unfortunately, the alkyne did not survive the reaction; no follow-up studies were performed.



Scheme 4.28 Alternate route to access compound **4.28d**.

4.6.7 Oppolzer's Camphorsultam Auxiliary at C1

Around this time, Takao and Tadano(307) reported the use of Oppolzer's camphorsultam as a remote auxiliary for the thermal [3,3]-sigmatropic rearrangement of geraniol-derived substrate **4.46** *en route* to monoterpene (+)-bakuchiol (**Scheme 4.29**). Accessed from the conjugate addition of alcohol **4.45** onto *N*-propioloyl camphorsultam, (**4.44a**), compound **4.46** was subjected to a thermally induced Claisen rearrangement to afford **4.47** with good diastereoselectivity (**4.47a**:**4.47b**, 1:9 *dr*) in 80% yield after column chromatography.

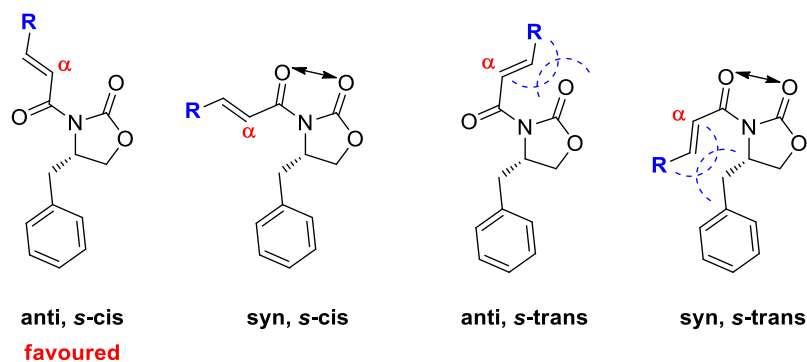


Scheme 4.29 An asymmetric Claisen rearrangement of allyl vinyl ether 4.46 using Oppolzer's camphorsultam as a remote chiral auxiliary at C1.

By contrast, performing the same reaction with Evans' 4-benzyl-2-oxazolidinone in place of the camphorsultam proved ineffective.⁴⁷ This may not be surprising, in light of the conformational behaviour of imides, as an *anti*, *s-cis* orientation is generally favoured (**Scheme 4.30**).⁴⁸ The chiral directing element, as consequence may be too far removed to impart any stereofacial selectivity (for interaction at C α) during the course of the reaction.⁽³⁰⁸⁾

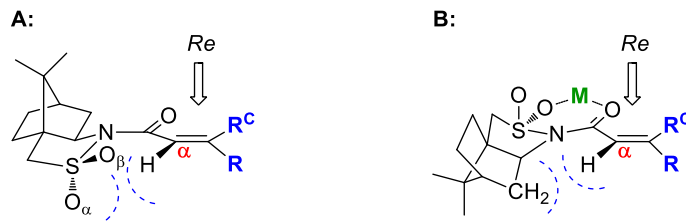
⁴⁷ The reaction using Evans' auxiliary failed to afford any stereoselectivity, yielding a 1.2:1 mixture of diastereomers.

⁴⁸ Addition of a chelation-metal can change the preferred rotamer conformation of imides from an *anti-s-cis* to a *syn s-cis* conformation.



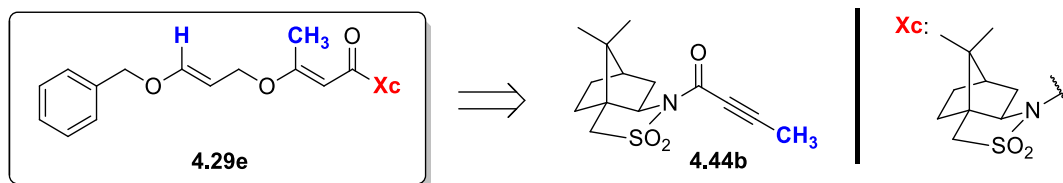
Scheme 4.30 Rotamers of oxazolidinone-based auxiliaries.

By contrast, camphor-derived auxiliaries have demonstrated superior selectivity for reactions where a coordinating Lewis acid is not available (*e.g.*, nitrile oxide cycloadditions,⁽³⁰⁹⁾ radical addition- or cyclization-reactions).⁽³¹⁰⁾ If good diastereoselectivity is to be observed, the rotameric preference of the acrylate needs to be highly controlled, and the functionality contributing to the facial selectivity of the reaction must also be proximate to the site of new-bond formation. This is satisfied in compound **4.46** since the more favourable conformation positions the carbonyl group *anti* to the sulfonyl while adopting an *s-cis* conformation with respect to the acrylate (**Scheme 4.31A**). Approach of the allyl-fragment must occur from the *C α -Re*-face as the *Si*-face is sufficiently shielded by *O α* .



Scheme 4.31 Attack of the preferred conformation for non-chelate (A) and chelate (B) reactions, with camphor-derived auxiliaries, occurs on the *Re*-face to produce the same stereoisomers under either set of conditions.

While we recognise that camphorsultam **4.44b** presents a similar obstacle for removal as those auxiliaries described previously, it would be interesting to note the difference (if any) in the diastereoselectivity for the reaction of bis-vinyl ether **4.29e** (Scheme 4.32). A dramatic improvement in facial selectivity for this reaction would undoubtedly prompt the search for (or design of) a similar auxiliary-motif that can be readily incorporated into (and just as readily cleaved from) our scaffold.



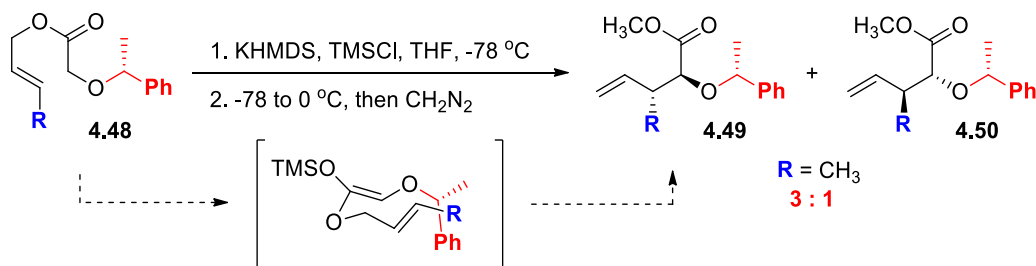
Scheme 4.32 Incorporation of Oppolzer's auxiliary into the bis-vinyl ether scaffold.

Preparation of **4.44b** is currently in progress. When the synthesis is complete, the chiral fragment (**4.44b**) will be incorporated into our standard protocol for accessing our vinyl ether substrates. Once in hand, **4.29e** will be subjected to our optimized set of reaction conditions for the palladium-mediated Claisen rearrangement.

4.7 Method B: Incorporation of a Chiral Auxiliary at C6

Owing to the inaccessibility of readily cleavable auxiliaries at C1, and the poor diastereoselectivity resulting from the palladium-mediated transformation of bis-vinyl ethers of type **4.29**, we chose to set aside this route in favour of those bis-vinyl ethers bearing a benzyl-derived auxiliary at **R^A** (**Method B**) as there was some literature precedent to suggest that these types of remote auxiliaries could exhibit improved diastereoselectivity, by comparison.

Kallmerten(311) reported modest stereocontrol for the rearrangement of allyl glycolates bearing phenethyl substitution at C1 (**Scheme 4.33**).

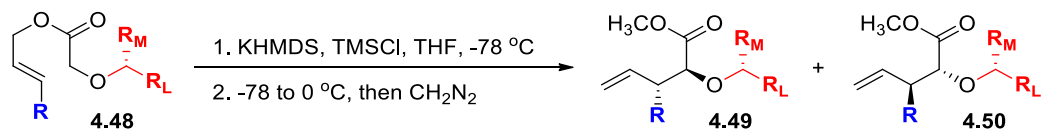


Scheme 4.33 Modest diastereoselectivity can be achieved in the Claisen rearrangement of allyl glycolates with use of 1-phenylethanol as a remote auxiliary at C1.(311)

Stereochemical induction in the glycolate system (**4.48**) was found to be relatively insensitive to substitution at C_γ while alteration of the degree of steric bulk at **R_L** resulted in a decrease in the diastereocontrol for the reaction (**Table 4.5**, entries 3–5).(311) It is particularly interesting to note that combinations of the phenethyl-auxiliary with aryl substituents at **R** result in a significant enhancement in diastereoselectivity, compared to

when **R** = alkyl (entry 2 and 7 *versus* entry 1). The authors speculate that this phenomenon may result from favourable π -stacking between the auxiliary and the C γ -aryl substituent.

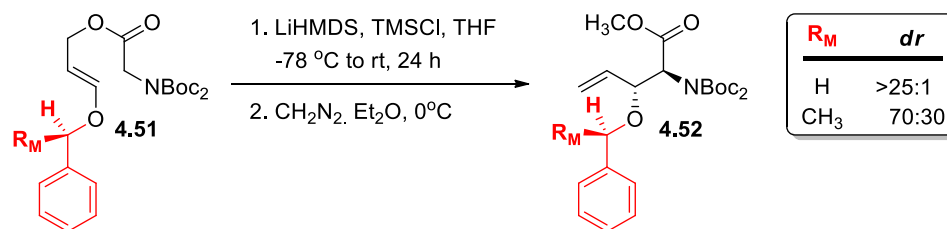
Table 4.5 Auxiliary-directed ester-enolate Claisen rearrangement of substituted allyl glycolates.(311)



| Entry | Glycolate | R | RL | RM | 4.49 : 4.50 |
|----------------|-----------|-----------------|--------------|-----------------|--------------------|
| 1 ^a | 4.48a | CH ₃ | Ph | CH ₃ | 3.0 : 1.0 |
| 2 ^b | 4.48b | Ph | Ph | CH ₃ | 6.1 : 1.0 |
| 3 ^a | 4.48c | CH ₃ | <i>t</i> -Bu | CH ₃ | 1.6 : 1.0 |
| 4 ^b | 4.48d | CH ₃ | mesityl | CH ₃ | 2.5 : 1.0 |
| 5 ^a | 4.48e | CH ₃ | Ph | Et | 2.3 : 1.0 |
| 6 ^b | 4.48f | <i>i</i> Pr | Ph | CH ₃ | 2.4 : 1.0 |
| 7 ^b | 4.48g | | Ph | CH ₃ | 4.2 : 1.0 |

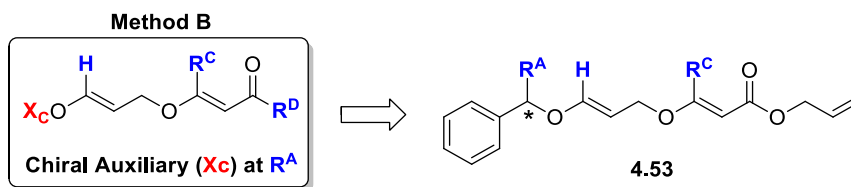
^aDiastereomeric ratio as determined by gas chromatography, or ^bHPLC analysis.

Carbery(80) also reported the use of a chiral benzyl enol-ether to control the relative facial selectivity in the Ireland-Claisen rearrangement of allyl glycinate **4.51**. In general, this reaction is seen to proceed with excellent diastereoselectivity (but as a mixture of enantiomers) in the absence of any remote chiral-directing element. Incorporation of (S)-1-phenylethanol at C6 was found to afford a *ca.* 2.3:1 ratio of diastereomers (**Scheme 4.34**, major diastereomer shown). The absolute stereochemistry for **4.52** was determined by converting the product of this reaction into the known β -hydroxy *N*-Boc α -amino ester, and comparing the optical rotation of the experimentally obtained mixture to that recorded for the enantiopure sample.(312)



Scheme 4.34 Ester-enolate Claisen rearrangement of substituted allyl glycinates.(80)

The result that Carbery reports for the rearrangement of **4.51**, when $R_M = \text{CH}_3$, provides sufficient evidence that this particular approach to stereinduction should work for our own system (**Scheme 4.35**). Our bis-vinyl ethers and Carbery's allyl glycinates both possess strong electron-donating benzyloxy substitution at C6, in addition to having electron-withdrawing functionality at C1. While the mechanism for rearrangement will inevitably differ between the two substrates, the close proximity of the chirality-directing element (with respect to the newly formed σ -bond) should provide better π -facial selectivity than was observed with our previously described work using Evans' oxazolidinone (**Method A**). Herein, we report our findings for the auxiliary-directed, palladium-mediated Claisen rearrangement of bis-vinyl ether substrates of type **4.53** using the approach illustrated for **Method B** (**Scheme 4.35**).

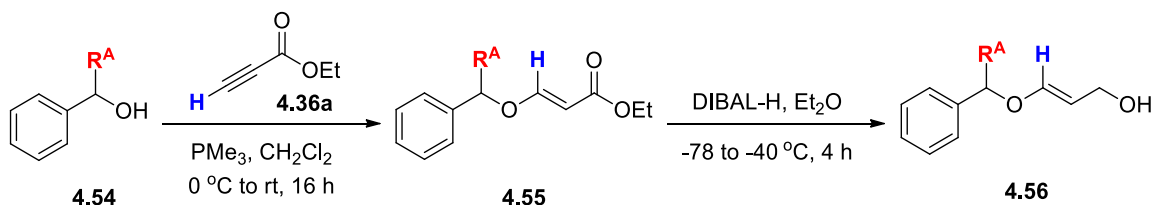


Scheme 4.35 Incorporation of a benzyl-derived auxiliary at C6.

4.7.1 Synthesis of Bis-Vinyl Ethers Containing Benzyl-Derived Chiral Auxiliaries

In order to evaluate the auxiliary-directed selectivity for benzyl-derivatized γ -alkoxyallyl vinyl ethers, we chose to target racemates of type **4.53** with a systematic increase in steric bulk at R^A . Synthesis of our target compounds commenced with phosphine-mediated conjugate addition of substituted benzyl alcohols **4.54a–d** onto ethyl propiolate. To achieve adequate conversion to acrylate **4.55**, catalyst loading had to be increased from the usual 1 mol% to 4 mol% for these more sterically encumbered (and slower to react) alcohols. Once this change was made, we could obtain quantitative yield of mono-vinyl ethers **4.55a–d** as clear, colourless oils at room temperature (Table 4.6). These substrates were used directly in the subsequent DIBAL-H reduction to afford allylic alcohols **4.56a–d** in moderate yield following chromatographic purification.

Table 4.6 Synthesis of allyl alcohols **4.56a–d**.



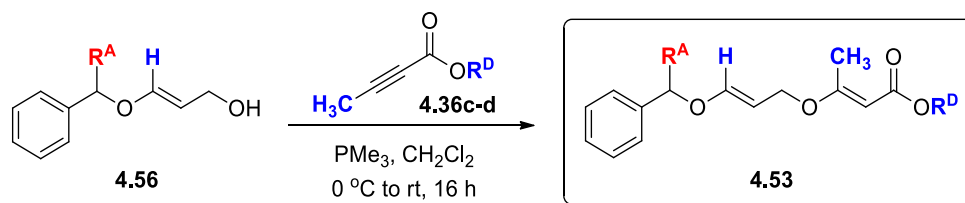
| Entry | R^A | 1 st Addition Yield (%) ^a | Reduction Yield (%) ^b |
|-------|--------------------------|---|----------------------------------|
| 1 | Me ^c | 4.55a 100 | 4.56a 58 |
| 2 | Et ^d | 4.55b ^e 100 | 4.56b 68 |
| 3 | <i>i</i> Pr ^d | 4.55c ^e 100 | 4.56c 62 |
| 4 | <i>t</i> Bu ^d | 4.55d 100 | 4.56d 70 |

^aYield of the crude isolate. ^bIsolated yield after chromatographic purification on triethylamine (1%) treated silica gel. ^cPhenethyl alcohol (**4.54a**) was purchased and used as received from Sigma-Aldrich. ^dAlcohols **4.54b–c** were prepared from the corresponding ketone, following reduction with sodium borohydride in methanol.(313, 314) ^eSubstrates were prepared as the methyl ester.

At this stage we had the liberty of exploring what effect varying the substitution at **R^D** would have on the selectivity of the rearrangement. With the aim of using removable protecting groups, we opted to compare alkyl (**R^D** = trimethylsilylethyl, **4.36d**) and allyl (**4.36c**) substitution at this position.⁴⁹ Compounds **4.36c**(315) and **4.36d**(316) were thus prepared following known literature procedure and reacted with alcohols **4.56a–d** using our original set of conditions for the conjugate addition reaction (*i.e.*, 10 mol% PMe_3). Quantitative conversion to the target compounds was achieved in all cases (**Table 4.7**). While the products of this reaction (**4.53a–e**) were amenable to purification by flash column chromatography, their propensity to undergo facile rearrangement with prolonged exposure to silica gel (even when treated with 1% triethylamine) proved somewhat problematic. In any event, the compounds were sufficiently clean that they could be used in the subsequent reaction without the need for chromatographic purification.

⁴⁹ A number of other functional groups were also examined (*e.g.*, **R^D** = ethyl, phenyl, benzyl), however we report only those that closely resemble the parent system (**4.53**) described here (*i.e.*, **R^B** = H and **R^C** = CH_3).

Table 4.7 Synthesis of bis-vinyl ethers 4.53.



| Entry | Alcohol | R ^A | R ^D | Addition Yield (%) ^a |
|-------|---------|----------------|----------------|---------------------------------|
| 1 | 4.56a | Me | 4.53a | >99 |
| 2 | 4.56a | Me | 4.53b | >99 |
| 3 | 4.56b | Et | 4.53c | >99 |
| 4 | 4.56c | <i>i</i> Pr | 4.53d | >99 |
| 5 | 4.56d | <i>t</i> Bu | 4.53e | >99 |

^aYield of the crude isolate.

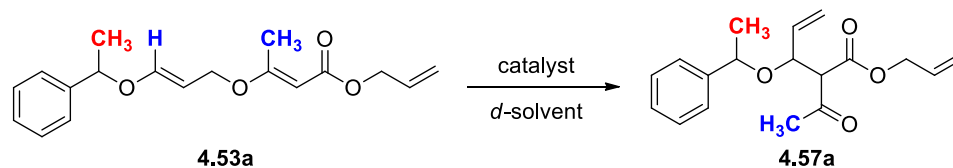
4.7.2 Optimization of the Palladium-Mediated Claisen Rearrangement

As was indicated in the prologue in **Section 4.5**, the conditions for Claisen rearrangement were identified and optimized using bis-vinyl ether **4.53a**. Compound **4.53a** was chosen as the model substrate primarily because its rearrangement provides *ca.* 3.1:1.0 mixture of diastereomeric products, *vide infra*, indicating that the stereogenic element is introducing some degree of π -facial selectivity during the course of the reaction. By contrast, the oxazolidinone auxiliary which appears in compounds of type **4.29** does not appear to influence the distribution of products to any significant extent, and so changes in selectivity for the reaction were likely not to be observed.

Bis(acetonitrile)palladium(II) dichloride and bis(benzonitrile)palladium(II) dichloride were identified in **Table 4.1** as potential Lewis acid catalysts for promoting the Claisen

rearrangement of bis-vinyl ethers at ambient temperature. A quantitative comparison of the product distribution resulting from the rearrangement of **4.53a** in the presence of either Lewis acid, in deuterated benzene, found Pd(PhCN)₂Cl₂ to be the superior choice of catalyst (**Table 4.8**, entry 1 and 2).

Table 4.8 Product distribution in the Claisen rearrangement of bis-vinyl ether **4.53a** using Pd(PhCN)₂Cl₂ or Pd(CH₃CN)₂Cl₂ as the Lewis acid catalyst.



| Entry | catalyst | <i>d</i> -solvent | <i>dr</i> ^{a,b,c} |
|----------|---|--|----------------------------|
| 1 | Pd(CH ₃ CN) ₂ Cl ₂ | benzene- <i>d</i> ₆ | 3.3 : 5.9 : 1.0 : 1.0 |
| 2 | Pd(PhCN) ₂ Cl ₂ | benzene- <i>d</i> ₆ | 2.0 : 1.0 |
| 3 | Pd(PhCN) ₂ Cl ₂ | dichloromethane- <i>d</i> ₂ | 2.5 : 1.0 |

^aDetermined by analysis of the crude ¹H NMR spectrum. ^bSignificant decomposition of the substrate was noted over time and is not accounted for in this value. ^cThe rate of decomposition differed between diastereomers, making accurate prediction of the diastereomeric ratio quite difficult.

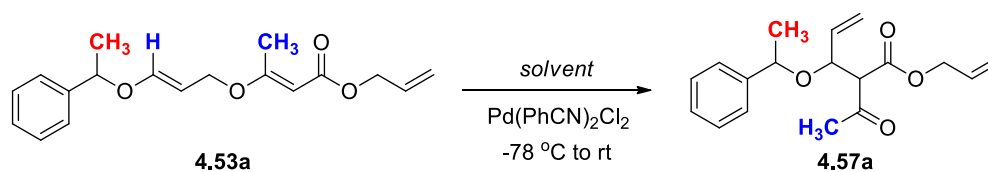
Changing the solvent to dichloromethane-*d*₂ (entry 3) led to a moderate improvement in the diastereoselectivity, prompting a further investigation on solvent effects. More immediate, however, was that the rearrangement of **4.53a** was plagued by a significant amount of decomposition product.

We had suspected that the prolonged contact of the substrate with the palladium catalyst at room temperature⁵⁰ was resulting in unwanted side product formation, either through *retro*-

⁵⁰ Precipitation of the catalyst was also performed at -78 and 0 °C. In either case, the γ -allyloxyvinyl ether, **4.53a**, was recovered unreacted.

aldol reaction or by other means. To limit unfavourable catalyst-product interaction we elected to precipitate the $\text{Pd}(\text{PhCN})_2\text{Cl}_2$ with a 50:50 mixture of hexanes-diethyl ether, and removed the orange solid by expedient filtration over a *ca.* 1.0 cm bed of silica gel. After evaporation of the filtrate under reduced pressure, the rearranged substrate (**4.57a**) could be stored at $-20\text{ }^\circ\text{C}$ for upwards of two weeks without any observable decomposition.

Using this new protocol, we followed up on our earlier result by screening a number of different solvents to determine whether the choice of medium could affect the selectivity of the [3,3]-rearrangement (**Table 4.9**). While no obvious relationship was observed, the best diastereoselectivity was noted when the reaction was performed in either dichloromethane (entry 3) or 1,2-dichloroethane (entry 5). Neither chlorinated solvent presented a significant advantage over the other so, for the sake of convenience, we chose to proceed with dichloromethane as the standard solvent for this reaction.

Table 4.9 Effect of solvent polarity on the Pd-mediated Claisen rearrangement.

| Entry | Solvent | ϵ | <i>dr</i> | 4.54a : 4.57a ^c |
|------------------|---|------------|-------------|----------------------------|
| 1 ^a | Et ₂ O | 4.33 | 2.35 : 1.00 | 0.36 : 1.00 |
| 2 ^a | CCl ₄ | 4.81 | 2.76 : 1.00 | 0.27 : 1.00 |
| 3 | CH ₂ Cl ₂ | 8.93 | 3.10 : 1.00 | 0.11 : 1.00 |
| 4 ^b | CH ₂ Cl ₂ | 8.93 | 3.14 : 1.00 | 0.17 : 1.00 |
| 5 | 1,2-(CH ₂) ₂ Cl ₂ | 10.36 | 3.19 : 1.00 | 0.11 : 1.00 |
| 6 ^{a,d} | CH ₃ CN | 37.5 | 2.60 : 1.00 | 0.19 : 1.00 |

^aA significant amount of decomposition was observed for this substrate when analyzed by ¹H NMR spectroscopy. ^bReaction was run in “wet” dichloromethane. ^cThe ratio of **4.54a**:**4.57a** is a qualitative indicator for decomposition across the different solvent conditions employed and does not reflect the true extent of decomposition in the sample. ^dPerforming the reaction in acetonitrile significantly decreases the rate of reaction due to coordination to the Pd-metal.

4.7.3 [3,3]-Sigmatropic Rearrangements of Bis-Vinyl Ethers 4.53

Having identified a suitable set of reaction conditions, we resumed our investigation of the palladium-mediated, auxiliary-controlled Claisen rearrangement of substrates **4.53**. Our first objective was to determine whether the stereoselectivity of the reaction was impacted by alkyl or allyl substitution at **R^D**. To this end, we compared the product distribution for both the thermal and the Lewis acid catalyzed rearrangement of **4.53a** and **4.53b**.

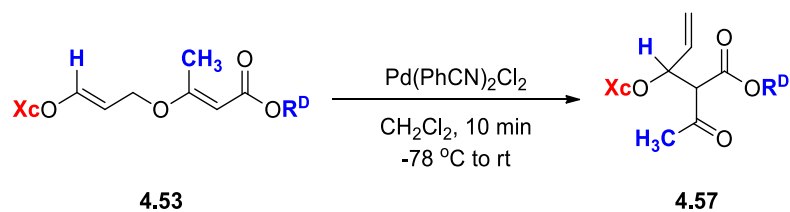
Thermal rearrangement of substrates **4.53a** and **4.53b** was achieved by microwave irradiation at 150 °C for 10 minutes. Spectral analysis of the crude reaction mixture revealed formation of all four possible diastereomeric products for either substrate (**Table 4.10**). The diastereomeric ratio for **4.57a** (**R^D** = allyl, entry 1) was significantly improved,

relative to **4.57b** ($R^D = (\text{CH}_2)_2\text{Si}(\text{CH}_3)_3$, entry 2), a result that is found to be in good agreement with Kallmerten's earlier observation for the ester-enolate Claisen rearrangement of allyl glycolates bearing a phenethyl auxiliary at C1.(311)

Application of our conditions for the palladium-mediated rearrangement to **4.53a** yielded two major products in a 3.10:1.00 ratio (**Table 4.10**, entry 1). As was the case with the thermal rearrangement, transformation of **4.53b** under the same conditions, afforded a similar distribution of products (to **4.53a**), but with lower overall stereoselectivity (*i.e.*, 2.33:1.00 dr).

We next examined the palladium-induced reaction for analogues **4.53a,c-e**. The Claisen rearrangement was found to proceed smoothly to afford **4.57a,c-e** with diastereoselectivity being proportional to the steric burden at R^A . As illustrated in **Table 4.10**, when $R^A = \text{Me}$ the diastereomeric ratio is *ca.* 3:1; this value increases to *ca.* 5:1 when $R^A = t\text{-Bu}$. These results are opposite the trend reported by Kallmerten,(311) listed in **Table 4.5** (*see* entry 1 and 5). While we are unable to predict the nature of the transition state, at the present time, we can envision improving upon these results through optimization of the substituent at C6 (**Xc**), C1 (R^D) and the nitrile ligand on the Pd-metal.

Table 4.10 Claisen rearrangement of bis-vinyl ethers 4.53a–d.



| Entry | Compound | Xc^{d} | R^{D} | $\text{dr}^{\text{a,e}}$ |
|-------|----------|------------------------|-----------------------|--|
| 1 | 4.53a | | | 4.57a 3.1 : 1.0 (2.5 : 1.0 : 4.8 : 1.1) ^{b,c} |
| 2 | 4.53b | | | 4.57b 2.3 : 1.0 (3.0 : 1.8 : 1.6 : 1.0) ^b |
| 3 | 4.53c | | | 4.57c 3.7 : 1.0 |
| 4 | 4.53d | | | 4.57d 4.7 : 1.0 |
| 5 | 4.53e | | | 4.57e 5.1 : 1.0 |

^aDiastereomeric ratio was determined from analysis of the crude reaction mixture by ¹H NMR spectroscopy. ^bRatio for the thermal reaction. Conditions: $\mu\lambda$, 150 °C, PhH, 10 minutes. ^cRatio for the thermal reaction was taken from the rearrangement of the analogous compound where Xc is derived from 1-(4-methoxyphenyl)ethanol. ^d" R^{A} " portion of auxiliary Xc is highlighted in red. ^eGreater than 99% conversion was observed for the rearrangement of substrates of type 4.53.

4.8 Summary

Our efforts toward the development of an asymmetric Claisen rearrangement of bis-vinyl ethers of type 4.24 have been described. The thermal rearrangement of such substrates at 150 °C was found to result in formation of all four possible diastereomeric products. Conversely, by employing an achiral Lewis acid catalyst, $\text{Pd(PhCN)}_2\text{Cl}_2$, we were able to

lower the temperature for reaction (thus decreasing the conformational mobility of these substrates) and impose additional conformational rigidity (through coordination of the γ -allyloxy and vinyl ether olefins to the transition metal center) resulting in the formation of only two diastereomers with unknown configuration at the newly generated stereogenic centers.

Remote chirality transfer in this system (*i.e.*, **4.24**) was investigated through incorporation of a stereogenic element at either C1 or C6. Poor diastereocontrol was observed for those bis-vinyl ethers of type **4.29**, containing an oxazolidinone-based auxiliary at C1, which we attributed to a preferential *anti*, *s-cis* orientation of the imide (**Scheme 4.30**). As consequence, the chiral directing element was far too removed to impart any stereofacial selectivity for interaction at **C α** . We believe that it should be possible to significantly improve the stereoselectivity of this transformation through use of an auxiliary that possesses fewer degrees of conformational freedom. As a proof of concept, alkyne **4.44b**, containing Oppolzer's camphor-sultam as the chiral directing-element, is being prepared for its eventual evaluation against those substrates which bear Evans' oxazolidinone at C1.

By contrast, bis-vinyl ethers of type **4.53** with benzyl-derived auxiliaries at C6 were found to improve the diastereoselectivity of the reaction proportional to the degree of steric burden placed on the benzylic carbon. When **R^A** = *tert*-butyl, β -alkoxy- γ,δ -unsaturated- β -keto ester **4.57e** was formed with a product ratio of 84:16, one of the highest diastereoselectivities to ever be reported for the rearrangement of bis-vinyl ethers of similar construction.

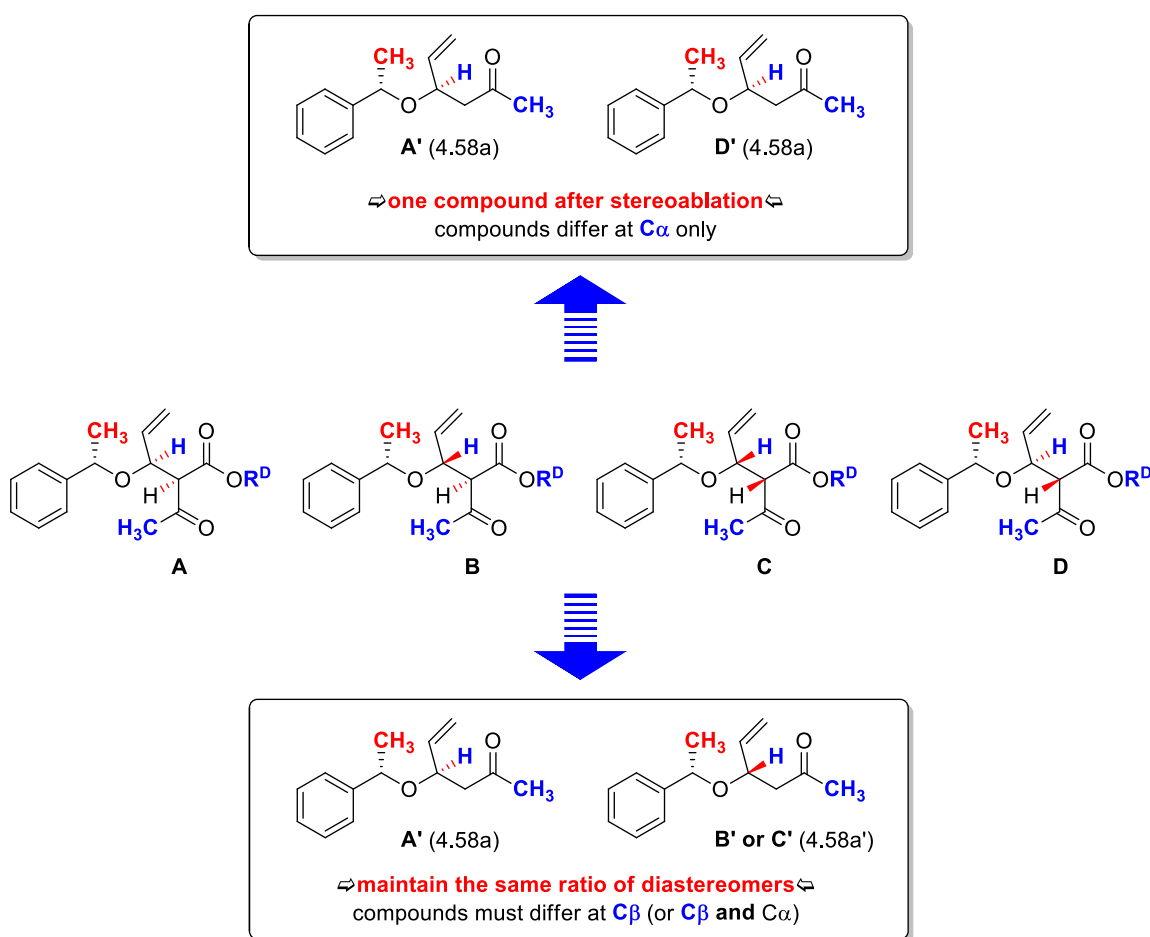
4.9 Future Work

The next stage of this investment will be to determine the absolute configuration at the newly generated stereogenic carbons (originating from C1 and C6) from the rearrangement of bis-vinyl ethers of type **4.53**. Unlike Claisen products of type **4.39**, these ester-bearing substrates (**4.57**) can not be subjected to purification by flash-column chromatography. Attempts to separate the two diastereomers using this method have led to epimerization at C α , creating a complex mixture of all four diastereomeric products. This necessitates that the crude reaction mixture be carried forward for all subsequent transformations and that the use of acidic or basic reagents be avoided.

Given that our progress for determining the relative configuration of our Claisen products will be hindered by the inherently sensitive nature of the β -ketoester functionality, we propose that ablating the stereochemistry at this position (through removal of the ester) will enable us to (potentially) determine (a) which stereocenter rendered the products diastereomeric, (b) if the products of the Claisen rearrangement were *syn*- or *anti*, and (c) additionally permit removal of the chiral auxiliary (with reduced probability of having an undesirable elimination reaction occur) which would (d) allow us to evaluate the stereochemistry at the carbon bearing the secondary alcohol.

Each of the above points are not, in themselves, straight forward. To illustrate this concept, the four possible diastereomers that could result from the rearrangement of either **4.57a** or **4.57b** are shown in **Scheme 4.36**. If the ^1H NMR spectrum were to show one compound after removal of the stereogenic center at C α (*e.g.*, **A'** and **D'**), then we can say that the two

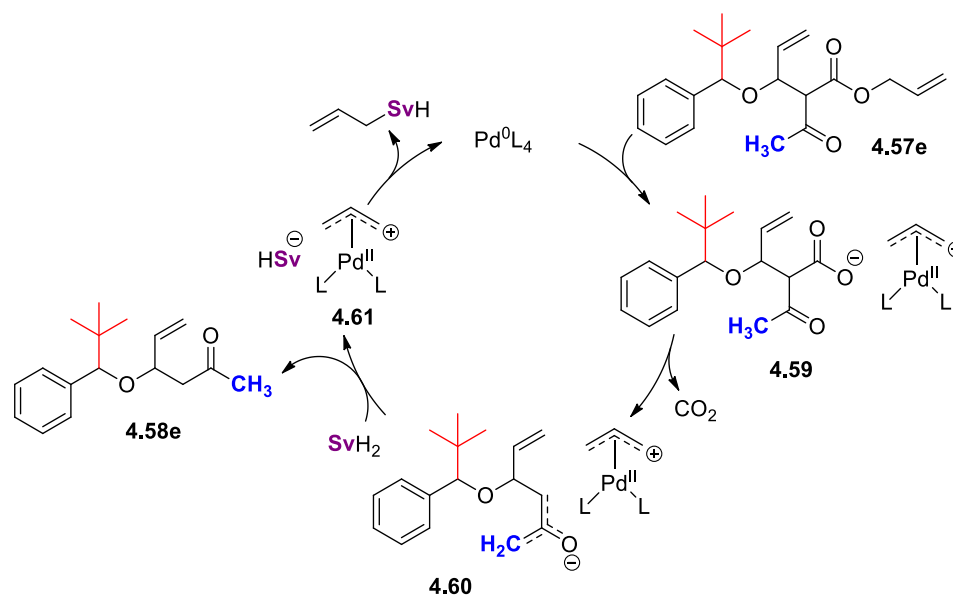
diastereomers must differ by the stereochemistry at $C\alpha$. This implies that one compound must be oriented *syn*- with respect to the two hydrogen substituents (*e.g.*, **A**) while the other must be derived from the diastereomer where the two hydrogen atoms are oriented *anti*- with respect to one another (*e.g.*, **D**). While the absolute stereochemical assignment at the secondary alcohol can be determined thereafter, we would still need to compare the parent molecule to a known compound in order to determine absolute configuration at $C\alpha$.



Scheme 4.36 Determination of relative stereochemistry by stereoablation at $C\alpha$, where each result is arbitrarily referenced to compound “A”.

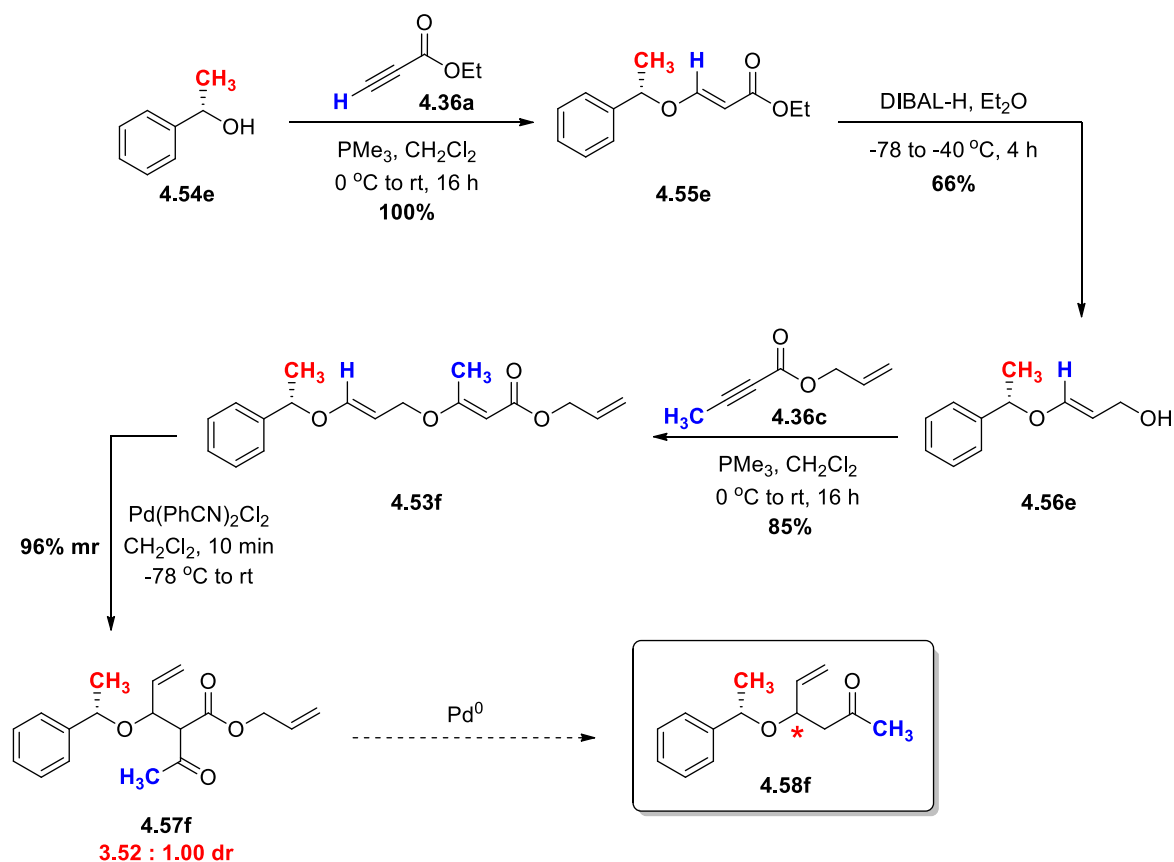
Should two diastereomers persist after removal of the ester, the stereochemical assignment at the secondary alcohol would remain trivial, however we will now be unable to make any assumptions as to whether the two hydrogens are oriented *syn* or *anti* with respect to one another. Comparison of the parent structure to a known compound would again be required to determine the absolute stereochemistry at C α . Nevertheless, we are keenly interested in determining the absolute stereochemical assignment at the secondary alcohol.

One strategy that we have envisioned for invoking the (above) described transformation is to perform a Pd⁰-mediated deallylation/decarboxylation to access compound **4.58**, provided that we can effectively circumvent the π -allyl intermediate from recombining with the α -carbanion prior to dissociation from the metal complex (**Scheme 4.37**).



Scheme 4.37 Including an allyl scavenger (*e.g.*, SvH₂) as a reagent in the deallylcarbonylation reaction may circumvent the competing decarboxylative allylation of **4.57**.

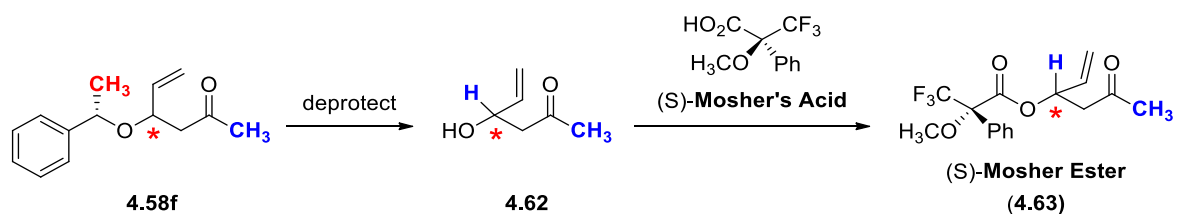
Recent work by Rawal(317) suggests that this decarboxylative allylation may not be the result of an intramolecular process, but rather an intermolecular transfer of the π -allyl system. Therefore, it should be possible to intercept the reductive elimination that would lead to the unproductive formation of allylated-products through optimization of the reaction conditions in the presence of an allyl scavenger (**Scheme 4.37**). Palladium-catalyzed decarboxylative protonation of β -carbonyl esters have been successfully accomplished with superstoichiometric triethylamine,(318, 319) formic acid(320, 321) or morpholine(322-326) additives. As such, our first goal will be to optimize this reaction using substrate **4.57a** (from *rac*-**4.54a**). Once a set of experimental conditions have been identified, they will be applied to substrate **4.57f**, derived from the enantiopure alcohol (*S*)-(-)-phenylethanol (**4.54e**), whose synthesis is shown in **Scheme 4.38**.



Scheme 4.38 Asymmetric synthesis of bis-vinyl ether **4.53f** and its subsequent transformations.

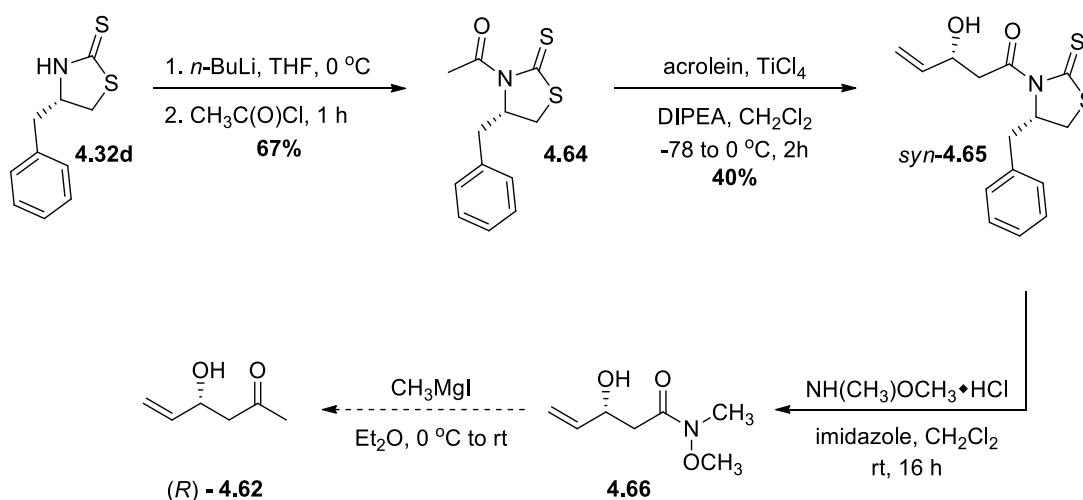
At this stage, we would have several options for determining the absolute stereochemistry at the allylic position. The first would be to remove the phenethyl auxiliary⁵¹ to permit synthesis to Mosher ester(327) **4.63**, allowing assignment of the stereochemical configuration at the carbinol carbon (**Scheme 4.39**).

⁵¹ Removal of the auxiliary in the presence of TiCl_4 would prevent reduction of the olefin that would likely occur under conditions used for hydrogenolysis.



Scheme 4.39 Proposed synthesis of Mosher ester for determination of absolute configuration at the stereogenic carbinol.

A second option would be to achieve the asymmetric synthesis of alcohol **4.62** (with known configuration about the chiral center) following the procedure of Nagaiah (**Scheme 4.40**).⁽³²⁸⁾ Comparison of the optical rotation for (*R*)-(+)-**4.62** against **4.62** would permit assignment of the carbinol carbon. In addition, (*R*)-(+)-**4.62** would be a useful control for Mosher ester analysis of **4.63** to ensure that the results from this experiment had been properly interpreted.



Scheme 4.40 Synthesis of (*R*)-**4.62**.

Chapter 5 Experimental

5.1 General Experimental Remarks

All reactions were performed in oven- or flame-dried glassware, under a positive pressure of argon, unless otherwise indicated. Liquid reagents and all solvents were transferred *via* glass syringe with a stainless steel needle, or by cannula. Organic solutions were concentrated between 35–40 °C by rotary evaporation under vacuum. Analytical thin-layer chromatography (TLC) was performed using aluminum plates pre-coated with silica gel (0.20mm, 60 Å pore-size, 230-400 mesh, Macherey-Nagel) impregnated with a fluorescent indicator (254 nm). TLC plates were visualized by exposure to ultraviolet light followed by staining with potassium permanganate or *p*-anisaldehyde. Flash-column chromatography was performed over silica gel 60 (Caledon, 63-200 µM).

5.2 Materials

All reagents were used as received from Sigma Aldrich, unless otherwise indicated. Bis(cyclopentadienyl)zirconium(IV) chloride hydride was purchased from Strem Chemicals, stored in a glovebox and used without further purification. Commercial solvents were used as received with the following exceptions. Anhydrous tetrahydrofuran was distilled from sodium/benzophenone prior to use. Acetonitrile, dichloromethane and toluene were dried by passage through a column of alumina in a commercial solvent purification system (SPS). Benzene and triethylamine were distilled over calcium hydride and degassed by freeze-pump-thaw prior to use.

5.3 Instrumentation

Nuclear magnetic resonance (NMR) spectra were recorded on either a Bruker AV300 (300 MHz) or Bruker Avance 500 (500 MHz) spectrometer as indicated. Proton (^1H) chemical shifts are reported in parts per million (ppm, δ scale) downfield from tetramethylsilane, and are referenced to residual protium in the NMR solvent (CDCl_3 : δ 7.26; $\text{CD}_3\text{C}(\text{O})\text{CD}_3$: δ 2.05; C_6D_6 : δ 7.16; CD_2Cl_2 : δ 5.32). Data are represented as follows: chemical shift, multiplicity (s = singlet, d = doublet, t = triplet, q = quartet, m = multiplet and/or multiple resonances, br = broad, app = apparent), coupling constant in Hertz (Hz), and integration. Likewise, carbon (^{13}C) chemical shifts are reported in parts per million downfield from tetramethylsilane and are referenced to the carbon resonances of the solvent (CDCl_3 : δ 77.22; $\text{CD}_3\text{C}(\text{O})\text{CD}_3$: δ 29.85; C_6D_6 : δ 128.06). Infrared spectra were collected using a Perkin Elmer 1000 FT-IR spectrometer. Data are represented as follows: frequency of absorption (cm^{-1}) and intensity of absorption (s = strong, m = medium, w = weak, br = broad). LR-ESI-MS data was collected on a Finnigan Mat LQC mass spectrometer while HR-ESI-MS data was obtained using a ThermoFisher Orbitrap Executive mass spectrometer at the University of Victoria Mass Spectrometry Facility and Proteomics Centre.

5.4 General Experimental Procedures for Chapter 2

5.4.1 General Procedure for Conjugate Addition

Alkyne **2.10c** (1.00 mmol) was added dropwise to a stirred solution of alcohol **2.32** (1.00 mmol) and trimethylphosphine (1.0 M in THF, 0.10 mmol) in dry dichloromethane (5 mL). The reaction mixture was stirred at room temperature for 18 h. The solvent was then removed under vacuum, and the residue was resuspended in diethyl ether (~ 10 mL). The resulting suspension was filtered through a thin layer of basic alumina. The filtrate was concentrated *in vacuo* and purified by flash column chromatography using silica gel pretreated with 1% triethylamine to afford the conjugate addition product, **2.33a**, as a clear, colourless oil.

5.4.2 General Procedure for LiAlH₄/LiAlD₄ Reduction

Lithium aluminum hydride (or lithium aluminum deuteride; 2.00 mmol) was added in one portion to a stirred solution of ester **2.33a** (1.00 mmol) in anhydrous diethyl ether (10 mL) maintained at 0 °C. After 1.5 h the reaction was quenched with 10% KOH (aq.). The two phases were separated and the aqueous layer was extracted twice with diethyl ether. The organic extracts were dried over anhydrous sodium sulfate, filtered, concentrated *in vacuo*, and purified by flash column chromatography using silica gel pretreated with 1% triethylamine to afford alcohol **2.35a** as a clear, colourless oil.

5.4.3 General Procedure for Methylation

Iodomethane (3.00 mmol) was added dropwise *via* syringe to a stirred mixture of alcohol **2.35c** (1.00 mmol) in dry tetrahydrofuran at 0 °C. Sodium hydride (60% w/w in mineral

oil, 2.00 mmol) was added in one portion to the reaction mixture, and the resulting slurry was warmed to ambient temperature overnight (~ 18 h). The reaction was quenched with a solution of saturated NH_4Cl (aq.) and 10% KOH (aq.) and extracted twice with diethyl ether. The organic extracts were dried over anhydrous sodium sulfate, filtered, concentrated *in vacuo*, and purified by flash column chromatography using silica gel pretreated with 1% triethylamine, to afford methyl ether **2.61** as a clear, colourless oil.

5.4.4 General Procedure for IBX Oxidation

2-Iodobenzoic acid (1.20 mmol) was added in one portion to a stirred solution of alcohol **2.35a** (1.00 mmol) in dry acetonitrile (3.0 mL) at ambient temperature. The progress of the reaction was monitored by TLC. Upon consumption of the alcohol (~3 h), the reaction was quenched with a saturated solution of NaCl (aq.) and the solids were removed by filtration through a fritted-glass funnel. The two phases were separated, and the aqueous layer was extracted twice with dichloromethane. The combined organic layers were dried over anhydrous sodium sulfate, filtered, concentrated *in vacuo*, and purified by flash column chromatography using silica gel pretreated with 1% triethylamine, to afford the corresponding aldehyde **2.69**.

5.4.5 General Procedure for the Wittig Olefination

n-Butyllithium (2.0 M in hexanes, 1.10 mmol) was added dropwise to a stirred solution of methyltriphenylphosphonium bromide (1.10 mmol) in anhydrous tetrahydrofuran (6 mL) at $-15\text{ }^\circ\text{C}$ for 15 minutes. A solution of aldehyde (**2.69**, 1.00 mmol) in anhydrous tetrahydrofuran (2 mL) was added dropwise, *via* cannula, and the resultant slurry was

gradually warmed from -15 °C to room temperature over 2.5 h. The reaction mixture was quenched with water and extracted twice with diethyl ether. The organic extracts were dried over anhydrous sodium sulfate, filtered, concentrated *in vacuo*, and purified by flash column chromatography using silica gel pretreated with 1% triethylamine, to afford diene **2.70** as a clear, colourless oil.

5.4.6 General Procedure for Cyclopropanation Reaction

Diene **2.82a** (0.58 mmol) was dissolved in anhydrous diethyl ether (10 mL) and cooled to 0 °C. Palladium(II) acetylacetonate (0.0069 mmol) was added to the reaction vessel, followed by 6 mL of diazomethane in ether (~20 mg of diazomethane/mL of ether). The resulting mixture was warmed to room temperature for 45 minutes and then cooled to 0 °C. The addition of palladium(II) acetylacetonate followed by diazomethane was repeated a total of six times, while cycling through from 0 °C to room temperature after each set of additions. After the sixth addition of reagents, the reaction vessel was gradually warmed to room temperature and the reaction mixture was stirred overnight (~14 h). The reaction contents were filtered through a plug of Celite, concentrated *in vacuo*, and then purified by flash column chromatography using silica gel pretreated with 1% triethylamine, to afford cyclopropane **2.83a** (with 8-14% of **2.82a** as a contaminant).

5.4.7 General Procedure for the Sonogashira Coupling

To a two-neck round bottom flask containing bis-(triphenylphosphine)palladium(II) dichloride (0.02 mmol), copper(I) iodide (0.01 mmol), aryl halide **2.109a** (1.00 mmol) and 3-butyne-1-ol (**2.32**, 1.20 mmol) were dissolved in ~6 mL of dry triethylamine and

subsequently heated to reflux. After 2.5 h, the reaction mixture was cooled and then partitioned between ethyl acetate and water (1:1, 25 mL) and the aqueous and organic phases were separated. The combined organic extracts were washed with water and then a saturated solution of NaCl (aq), dried over anhydrous sodium sulfate, filtered, concentrated *in vacuo*, and purified by flash column chromatography on silica gel to afford **2.110a** as a clear, orange oil.

5.4.8 General Procedure for the Hydrozirconation Reaction

A solution of **2.110** (1.00 mmol) in dry dichloromethane (2.5 mL) was added, via cannula, to a stirred suspension of bis(cyclopentadienyl)zirconium(IV) chloride hydride (3.00 mmol) in dry dichloromethane (3.8 mL) at ambient temperature, followed by rinsing with dichloromethane (2.5 mL). The mixture was stirred in the absence of light for 3 h, forming a clear yellow to orange solution. *N*-Bromosuccinimide (2.00 mmol) in anhydrous tetrahydrofuran (4 mL) was added dropwise to the reaction mixture, which was stirred for an additional 0.5 h. The reaction mixture was quenched by addition of a mixed aqueous solution of saturated Na₂S₂O₃ and saturates NaHCO₃ (1:1, 20 mL) and diluted with diethyl ether. The aqueous and organic layers were separated and the aqueous layer was extracted twice with diethyl ether. The combined organic extracts were dried over anhydrous sodium sulfate, filtered, concentrated *in vacuo*, and purified by flash column chromatography to afford **2.111** as a single regio- and stereoisomer.

5.4.9 Procedure for Acetal Protection of **2.110c**

p-Toluenesulfonic acid (0.0710 mmol), **2.110c** (1.541 mmol) and ethylene glycol (3.96 mmol) in 30 mL of benzene were heated to reflux with a Dean–Stark apparatus for 25 h. The reaction mixture was cooled to room temperature and washed once with a saturated solution of NaHCO₃ (aq.) and twice with brine. The organic layer was dried over anhydrous sodium sulfate, filtered, concentrated *in vacuo*, and purified by flash column chromatography on silica gel to afford **2.110d** as a clear, pale yellow oil.

5.4.10 Procedure for the Acetal Deprotection of **2.111c**

Hydrochloric acid (1.0 M, 0.45 mL) was added to a stirred solution of **2.111c** (0.0974 mmol) in methanol (7.5 mL) at room temperature. After 1 h the solution was diluted with water and methanol was removed by concentration under reduced pressure. The aqueous mixture was extracted twice with diethyl ether, and the organic extracts were washed with a saturated solution of NaCl (aq.), dried over anhydrous sodium sulfate, filtered, and concentrated *in vacuo* to afford **2.111d** as a clear, yellow oil.

5.4.11 General Procedure for the Radical-Mediated Cyclization Reaction

A solution of triphenyltin hydride (1.50 mmol) and azobisisobutyronitrile (0.10 mmol) in deoxygenated benzene (10 mL) was added, *via* syringe pump, to a refluxing solution of enyne **2.33b** (1.00 mmol) in deoxygenated benzene (115 mL) over 6.25 h. The reaction mixture was maintained at reflux for an additional 1.5 h, cooled to room temperature, concentrated *in vacuo*, and then purified by flash column chromatography to afford **2.46b** as a clear, colourless oil.

5.5 General Experimental Procedures for Chapter 3

5.5.1 General Procedure for the Sonogashira Coupling(329)

To a two-neck round bottom flask containing bis-(triphenylphosphine)palladium(II) dichloride (0.02 mmol), copper(I) iodide (0.04 mmol) and 1.8 mL of dry, degassed triethylamine, kept under an atmosphere of argon, was added 4-iodoanisole (1.00 mmol) followed by trimethylsilylacetylene (1.20 mmol). The reaction mixture was stirred at 60 °C for 5 hours before being partitioned between ethyl acetate and water (1:1, 25 mL). The aqueous and organic phases were separated the aqueous layer extracted twice with ethyl acetate. The combined organic extracts were washed with a saturated solution of NaCl (aq), dried over anhydrous magnesium sulfate, filtered, concentrated *in vacuo*, and purified by flash column chromatography on silica gel to afford the corresponding alkynylsilane **3.2a** as a yellow oil.

5.5.2 General Procedure for TBAF Deprotection

Tetrabutylammonium fluoride (1.10 mmol) was added dropwise to a solution of trimethyl(phenylethynyl)silane **3.2b** (1.00 mmol) in anhydrous tetrahydrofuran (2.4 mL) at 0 °C. After 20 minutes the reaction was quenched with a saturated solution of NH₄Cl (aq.) and extracted three times with diethyl ether. The organic extracts were dried over anhydrous sodium sulfate, filtered, concentrated *in vacuo*, and then purified by flash column chromatography to afford **3.3b** as a clear, yellow oil.

5.5.3 General Procedure for Acylation of Aryl Alkynes(207)

n-BuLi (1.05 mmol, 2.5 M in hexanes) was added dropwise to a stirred solution of ethynylarene (1.00 mmol) in 1 mL of dry tetrahydrofuran at -78 °C. The mixture was reacted at -78 °C for 1.5 h followed by addition of ethyl chloroformate (1.20 mmol) and subsequently warmed to ambient temperature overnight (19 h). The reaction was quenched with a saturated solution of NH_4Cl (aq.) and extracted twice with ethyl acetate. The combined organic extracts were dried over anhydrous sodium sulfate, filtered, concentrated *in vacuo* and purified by flash column chromatography on silica gel to afford known alkynoates **3.4a–g**.

5.5.4 General Procedure for Conjugate Addition

Alkyne **3.4** (1.00 mmol) was added dropwise to a stirred solution of alcohol **3.5** (1.00 mmol) and trimethylphosphine (1.0 M in THF, 0.10 mmol) in dry dichloromethane (5 mL) at 0 °C and then warmed to room temperature overnight (18 h). The solvent was then removed under vacuum, and the residue was resuspended in diethyl ether (~5 mL). The resulting suspension was filtered through a thin layer of basic alumina, the filtrate was concentrated *in vacuo* and purified by flash column chromatography using silica gel pretreated with 1% triethylamine to afford the conjugate addition product, **3.6**, as clear, colourless to yellow oils.

5.5.5 General Procedure for DIBAL-H Reduction

Diisobutylaluminum hydride (1.0 M in hexanes, 2.20 mmol) was added dropwise to a stirred solution of ester **3.6** (1.00 mmol) in diethyl ether (15 mL) at -78 °C. After 1 h the

reaction flask was moved to a $-40\text{ }^{\circ}\text{C}$ bath for an additional 2 h. The reaction mixture was poured into a vigorously stirred mixture of Rochelle's salt (0.5 M, 100 mL), diethyl ether (100 mL) and glycerol (0.2 mL mmol^{-1} DIBAL-H). Vigorous stirring was maintained until the phases became clear, at which point the aqueous and organic layers were separated. The aqueous layer was extracted with diethyl ether ($2 \times 30\text{ mL}$) and the combined organic layers were dried over anhydrous sodium sulfate, filtered, concentrated *in vacuo* and purified by flash column chromatography using silica gel pretreated with 1% triethylamine to afford alcohol **3.7** as clear, colourless to yellow oils.

5.5.6 Procedure for the Methylation of Alcohol **3.17**

Iodomethane (3.00 mmol) was added dropwise *via* syringe to a stirred mixture of alcohol **3.17** (1.00 mmol) in dry tetrahydrofuran (3.5 mL) at $0\text{ }^{\circ}\text{C}$. Sodium hydride (60% w/w in mineral oil, 3.00 mmol) was added in one portion to the reaction mixture, and the resulting slurry was warmed to ambient temperature overnight ($\sim 18\text{ h}$). The reaction was quenched with a solution of saturated NH_4Cl (aq.) and 10% KOH (aq.) and extracted twice with diethyl ether. The organic extracts were dried over anhydrous sodium sulfate, filtered, concentrated *in vacuo*, and purified by flash column chromatography using silica gel pretreated with 1% triethylamine, to afford methyl ether **3.18** as a clear, colourless oil.

5.5.7 Procedure for the Preparation of **3.21b(221)**

To a stirred solution of 4-methylacetophenone dimethylacetal (1.00 mmol)(330) and pyridine (2.00 mmol) in chloroform (1.0 mL) at $0\text{ }^{\circ}\text{C}$ was added trifluoroacetic anhydride (2.00 mmol) dropwise. The resulting reaction mixture was warmed to ambient temperature

and then heated at 45 °C overnight (16 h). The reaction mixture was cooled and then quenched by addition of 0.1 M HCl (~2 mL). The aqueous and organic phases were separated. The organic layer was washed with 0.1 M HCl (2 × 2.5 mL), then water (5 mL), dried over anhydrous sodium sulfate, filtered and concentrated *in vacuo*. Purification was achieved through filtration through a plug of basic alumina to afford **3.21b** as a bright yellow solid.

5.5.8 Synthesis of 1,1,1-trifluoro-4-methoxy-4-(4-methylphenyl)-3-butene-2-ol

(3.22b)

Lithium aluminum hydride (1.50 mmol) was added in one portion to a stirred solution of **3.21b** (1.00 mmol) in anhydrous diethyl ether (20 mL) maintained at 0 °C. After 20 min the reaction was quenched with 10% KOH (aq.) and then extracted with diethyl ether (2 × 15 mL). The combined organic extracts were washed with a saturated solution of NaCl (aq.), dried over anhydrous sodium sulfate, filtered, concentrated *in vacuo*, and purified by flash column chromatography using silica gel pretreated with 1% triethylamine to afford alcohol **3.22b** as a clear, colourless oil.

5.5.9 General Procedure for Kinetic Measurements

A solution of bis-vinyl ether **3.8** (0.01 mmol) in the specified solvent (0.5 mL) spiked with an internal standard (0.005M hexamethylbenzene or 0.010 M 1,4-dioxane for R^A = aryl or alkyl, respectively) was added to a 5 mm NMR tube and the progress of the reaction was monitored by ^1H NMR spectroscopy over time at 500 MHz in an instrument pre-equilibrated to the temperature indicated (± 1 °C). Plots of $[A]/[A]_0$ vs. t were obtained for

3.8, where $[A]_t$ is the integral for the observed protons in the starting bis-vinyl ether (the average of the $\sum(\text{vinyl ether olefins})$) normalized to the internal standard, and $[A]_o$ is the sum of the normalized integrals for the starting bis-vinyl ether and rearrangement product (using the $\sum(\alpha\text{-protons})$ for both diastereomers produced). By-products produced in the reaction (*i.e.*, elimination products) were also accounted for in the calculation of $[A]_o$, based on normalized signals for the terminal olefin. First-order rate constants, k , were obtained by fitting the data to equation $[A]_t = [A]_o e^{-kt} + B$ using linear least squares analysis. The activation energy was calculated directly from k using the Eyring equation, $\Delta G^\ddagger = RT[\ln(k_B/h) - \ln(k/T)]$. Eyring and Arrhenius parameters were also generated from the resulting k values, and associated error in thermodynamic properties determined on the basis of error associated with the slope and intercept for the data set were obtained using the XLfit statistical analysis package.

5.6 General Experimental Procedures for Chapter 4

5.6.1 General Procedure for Conjugate Addition (Method A)

Alkyne **4.36** (1.00 mmol) was added dropwise to a stirred solution of alcohol **4.35** (1.00 mmol) and trimethylphosphine (1.0 M in THF, 0.10 mmol) in dry dichloromethane (10 mL) at 0 °C and then warmed to room temperature overnight (18 h). The solvent was then removed under vacuum, and the residue was resuspended in diethyl ether (~5 mL). The resulting suspension was filtered through a thin layer of basic alumina, the filtrate was concentrated *in vacuo* and purified by flash column chromatography using silica gel pretreated with 1% triethylamine to afford the conjugate addition product, **4.37**, as clear, colourless oil.

5.6.2 General Procedure for Conjugate Addition (Method B)

A solution of alkyne **4.28** (1.00 mmol) in 4 mL of dry dichloromethane was added dropwise to a stirred solution of alcohol **4.38** (1.00 mmol) and trimethylphosphine (1.0 M in THF, 0.10 mmol) in dry dichloromethane (16 mL) at -10 °C. The reaction mixture was stirred at 4 °C for 18 h. The solvent was then removed under vacuum, and the residue was resuspended in diethyl ether (~ 10 mL). The resulting suspension was filtered through a thin layer of basic alumina and the filtrate was concentrated *in vacuo* to yield the conjugate addition product **4.29** as a clear, colourless oil.

5.6.3 General Procedure for Conjugate Addition (Method C)

Alkyne **4.36** (1.20 mmol) was added dropwise to a stirred solution of alcohol **4.54** (1.00 mmol) and trimethylphosphine (1.0 M in THF, 0.40 mmol) in dry dichloromethane (5 mL)

at 0 °C and subsequently warmed to room temperature overnight (~18 h). The solvent was then removed under vacuum, and the residue was resuspended in diethyl ether (~10 mL). The resulting suspension was filtered through a thin layer of basic alumina. The filtrate was concentrated *in vacuo* and purified by flash column chromatography using silica gel pretreated with 1% triethylamine, to afford the conjugate addition product, **4.55**, as a clear, colourless oil.

5.6.4 General Procedure for DIBAL-H Reduction

Diisobutylaluminum hydride (1.0 M in hexanes, 2.20 mmol) was added dropwise to a stirred solution of ester **4.37** (1.00 mmol) in diethyl ether (15 mL) at -78 °C. After 2 h the reaction flask was moved to a -40 °C bath for an additional 2 h. The reaction mixture was poured into a vigorously stirred mixture of Rochelle's salt (0.5 M, 100 mL), diethyl ether (100 mL) and glycerol (0.2 mL mmol⁻¹ DIBAL-H). Vigorous stirring was maintained until the phases became clear, at which point the aqueous and organic layers were separated. The aqueous layer was extracted with diethyl ether (2× 30 mL) and the combined organic layers were dried over anhydrous sodium sulfate, filtered, concentrated *in vacuo* and purified by flash column chromatography using silica gel pretreated with 1% triethylamine to afford alcohol **4.38** as a clear, colourless oil.

5.6.5 General Procedure for the Microwave-Promoted Claisen Rearrangement

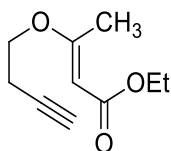
A solution of bis-vinyl ether **4.29d** (1.00 mmol) in 5 mL of benzene was heated in a microwave reactor at 150 °C for 10 minutes. Once the reaction was complete, the solvent

was removed under vacuum and the ratio of the diastereomeric products (**4.39**) was determined by ^1H NMR analysis of the crude sample.

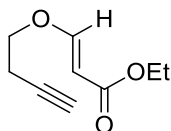
5.6.6 General Procedure for Palladium-Mediated Claisen Rearrangements

Bis(benzonitrile)palladium(II) dichloride (0.0025 mmol) was added in one portion to a stirring solution of bis-vinyl ether **4.27** (1.00 mmol) in dry dichloromethane (0.23 M) at -78 °C. The reaction was warmed, briefly, to room temperature over 10-15 min. The palladium was precipitated by addition of a 1:1 mixture of hexanes and diethyl ether and removed by filtration through a pad of silica gel. The filtrate was concentrated *in vacuo* and the diastereomeric ratio of the crude product **4.37** was analyzed by ^1H NMR spectroscopy.

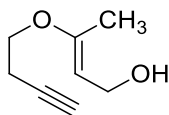
5.7 Compounds Pertaining to Chapter 2



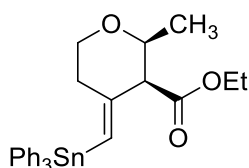
2.33a. Clear, light yellow oil (100% yield, 1.00:0.03 *E:Z*); ^1H NMR (300 MHz, $(\text{CD}_3)_2\text{CO}$) δ 5.05 (s, 1H), 4.07 (q, $J = 7.1$ Hz, 2H), 3.94 (t, $J = 6.3$ Hz, 2H), 2.63 (td, $J = 6.5, 2.7$ Hz, 2H), 2.44 (t, $J = 2.6$ Hz, 1H), 2.25 (s, 3H), 1.21 (t, $J = 7.2$ Hz, 3H); ^{13}C NMR (75 MHz, $(\text{CD}_3)_2\text{CO}$) δ 172.1 (C), 167.9 (C), 92.4 (CH), 81.2 (C), 71.2 (CH), 67.1 (CH_2), 59.6 (CH_2), 19.4 (CH_2), 18.8 (CH_3), 14.7 (CH_3); IR (neat, cm^{-1}) 3295 (s), 3094 (w), 2980 (m), 2123 (w), 1709 (s), 1623 (s), 1143 (s); HRMS (ESI) calcd for $\text{C}_{10}\text{H}_{14}\text{O}_3 + \text{H}^+$ 183.1021, found 183.1024.



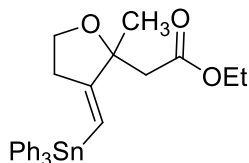
2.33b. Clear, colourless oil (93% yield, 1.00:0.06 *E:Z*); $R_f = 0.54$ (hexanes-dichloromethane-diethyl ether, 5:5:1); ^1H NMR (300 MHz, $(\text{CD}_3)_2\text{CO}$) δ 7.59 (d, $J = 12.6$ Hz, 1H), 5.25 (d, $J = 12.6$ Hz, 1H), 4.10 (q, $J = 7.1$ Hz, 2H), 4.06 (t, $J = 6.6$ Hz, 2H), 2.62 (td, $J = 6.5, 2.8$ Hz, 2H), 2.46 (t, $J = 2.8$ Hz, 1H), 1.21 (t, $J = 7.2$ Hz, 3H); ^{13}C NMR (75 MHz, $(\text{CD}_3)_2\text{CO}$) δ 167.6 (C), 162.8 (CH), 97.7 (CH), 80.9 (C), 71.5 (CH), 70.1 (CH_2), 60.0 (CH_2), 19.7 (CH_2), 14.7 (CH_3); IR (neat, cm^{-1}) 3296 (s), 3093 (m), 2982 (s), 2951 (s), 2896 (s), 2124 (w), 1708 (s), 1628 (s), 1468 (s), 1045 (s), 970 (s), 825 (s), 646 (s); HRMS (ESI) calcd for $\text{C}_9\text{H}_{12}\text{O}_3 + \text{Na}^+$ 191.0679, found 191.0697.



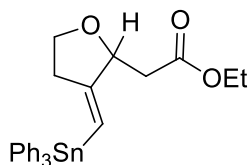
2.35a. Clear, light yellow oil (99% yield, 1.00:0.04 *E:Z*); ^1H NMR (300 MHz, $(\text{CD}_3)_2\text{CO}$) δ 4.69 (t, $J = 7.5$ Hz, 1H), 4.05 (dd, $J = 7.5, 5.6$ Hz, 2H), 3.75 (t, $J = 6.7$ Hz, 2H), 3.27 (t, $J = 5.5$ Hz, 1H), 2.54 (td, $J = 6.7, 2.7$ Hz, 2H), 2.40 (t, $J = 2.6$ Hz, 1H), 1.79 (s, 3H); ^{13}C NMR (75 MHz, $(\text{CD}_3)_2\text{CO}$) δ 155.8 (C), 99.1 (CH), 81.8 (C), 70.9 (CH), 65.5 (CH₂), 58.8 (CH₂), 19.6 (CH₂), 16.3 (CH₃); IR (neat, cm^{-1}) 3372 (br, s), 3298 (s), 3071 (w), 2927 (s), 2121 (m), 1661 (s); LRMS (ESI) calcd for $\text{C}_8\text{H}_{12}\text{O}_2 + \text{Na}^+$ 163.1, found 163.1.



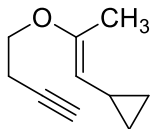
2.45. Clear, colourless oil (49% yield); $R_f = 0.23$ (hexanes-dichloromethane-diethyl ether, 10:4:1); ^1H NMR (300 MHz, CDCl_3) δ 7.62-7.52 (m, 5H), 7.44-7.32 (m, 10H), 6.02 (d, $J = 1.5$ Hz, 1H), 4.27 (dq, $J = 10.8, 7.1$ Hz, 1H), 4.17 (dq, $J = 10.8, 7.1$ Hz, 1H), 4.01 (ddd, $J = 10.8, 6.1, 1.2$ Hz, 1H), 3.68 (qd, $J = 6.5, 3.4$ Hz, 1H), 3.37 (d, $J = 3.2$ Hz, 1H), 3.31 (ddd, $J = 12.5, 10.8, 2.4$ Hz, 1H), 3.03 (dddd, $J = 13.9, 12.4, 6.0, 1.4$ Hz, 1H), 2.12 (ddt, $J = 14.0, 2.3, 1.2$ Hz, 1H), 1.32 (d, $J = 6.4$ Hz, 3H), 1.32 (t, $J = 7.0$ Hz, 3H); ^{13}C NMR (75 MHz, CDCl_3) δ 170.6 (C), 154.4 (C), 138.8 (C), 137.0 (CH), 129.3 (CH), 128.8 (CH), 122.4 (CH), 75.8 (CH), 68.8 (CH₂), 60.7 (CH₂), 59.1 (CH), 34.9 (CH₂), 19.3 (CH₃), 14.5 (CH₃); IR (neat, cm^{-1}) 3064 (m), 2978 (m), 1732 (s), 1609 (m), 1091 (s), 729 (s), 699 (s); HRMS (ESI) calcd for $\text{C}_{28}\text{H}_{30}\text{O}_3\text{Sn} + \text{H}^+$ 535.1290, found 535.1301.



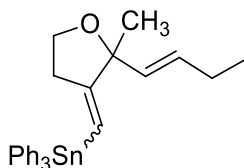
2.46a. Clear, colourless oil (46% yield); $R_f = 0.19$ (hexanes-dichloromethane-diethyl ether, 10:4:1); $^1\text{H NMR}$ (300 MHz, CDCl_3) δ 7.63-7.54 (m, 5H), 7.44-7.34 (m, 10 H), 5.96 (t, $J = 2.3$ Hz, 1H), 4.14 (q, $J = 7.2$ Hz, 2H), 3.95-3.78 (m, 2H), 2.72 (d, $J = 18.1$ Hz, 1H), 2.68 (d, $J = 18.1$ Hz, 1H), 2.66-2.43 (m, 2H), 1.49 (s, 3H), 1.23 (t, $J = 7.2$ Hz, 3H); $^{13}\text{C NMR}$ (75 MHz, CDCl_3) δ 170.5 (C), 168.2 (C), 138.5 (C), 137.1 (CH), 129.3 (CH), 128.9 (CH), 113.1 (CH), 83.4 (C), 65.1 (CH_2), 60.5 (CH_2), 45.5 (CH_2), 35.6 (CH_2), 26.6 (CH_3), 14.4 (CH_3); IR (neat, cm^{-1}) 3064 (m), 2978 (m), 1733 (s), 1622 (w), 1075 (m), 729 (s), 700 (s); HRMS (ESI) calcd for $\text{C}_{28}\text{H}_{30}\text{O}_3\text{Sn} + \text{Na}^+$ 557.1109, found 557.1117.



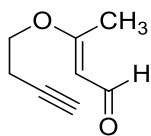
2.46b. Clear, colourless oil (83% yield); $R_f = 0.54$ (hexanes-dichloromethane-diethyl ether, 5:5:1); $^1\text{H NMR}$ (500 MHz, CDCl_3) δ 7.59-7.54 (m, 5H), 7.44-7.34 (m, 10H), 6.02 (app q, $J = 2.1$ Hz, 1H), 4.82-4.74 (m, 1H), 4.19 (q, $J = 7.2$ Hz, 2H), 3.94 (ddd, $J = 8.5, 7.6, 5.3$ Hz, 1H), 3.75 (app dt, $J = 8.3, 7.7$ Hz, 1H), 2.75 (dd, $J = 15.5, 4.0$ Hz, 1H), 2.63 (dd, $J = 15.5, 8.7$ Hz, 1H), 2.54-2.38 (m, 2H), 1.27 (t, $J = 7.2$ Hz, 3H); $^{13}\text{C NMR}$ (75 MHz, CDCl_3) δ 171.2 (C), 163.9 (C), 138.3 (C), 137.0 (CH), 129.3 (CH), 128.9 (CH), 113.8 (CH), 79.0 (CH), 67.2 (CH_2), 60.8 (CH_2), 40.7 (CH_2), 35.4 (CH_2), 14.3 (CH_3); IR (neat, cm^{-1}) 3064 (s), 3047 (s), 2980 (s), 2863 (s), 1735 (s), 1625 (m), 1480 (m), 1429 (s), 1163 (s), 1075 (s), 729 (s), 699 (s); HRMS (ESI) calcd for $\text{C}_{27}\text{H}_{28}\text{O}_3\text{Sn} + \text{Na}^+$ 543.0953, found 543.0955.



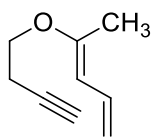
2.65. Clear, pale yellow oil (100% yield, 1.00:0.09 **2.65:2.70**); $R_f = 0.55$ (hexanes-diethyl ether, 20:1); $^1\text{H NMR}$ (300 MHz, $(\text{CD}_3)_2\text{CO}$) δ 4.03 (d, $J = 7.9$ Hz, 1H), 3.65 (t, $J = 6.7$ Hz, 2H), 2.49 (td, $J = 6.8, 2.8$ Hz, 2H), 2.38 (t, $J = 2.6$ Hz, 1H), 1.84 (s, 3H), 1.35-1.30 (m, 1H), 0.64 (ddd, $J = 8.1, 6.1, 4.0$ Hz, 2H), 0.20 (ddd, $J = 6.1, 4.7, 4.1$ Hz, 2H); $^{13}\text{C NMR}$ (75 MHz, $(\text{CD}_3)_2\text{CO}$) δ 153.2 (C), 102.6 (CH), 81.9 (C), 70.8 (CH), 65.5 (CH_2), 19.7 (CH_2), 16.8 (CH_3), 9.4 (CH), 7.1 (CH_2); IR (neat, cm^{-1}) 3313 (m), 3079 (m), 3002 (s), 2925 (s), 2856 (m), 1663 (m), 1219 (s), 1151 (s), 1079 (s), 837 (s); HRMS (ESI) calcd for $\text{C}_{10}\text{H}_{14}\text{O} + \text{Na}^+$ 173.0937, found 173.0946.



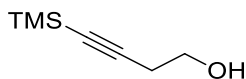
2.68. Clear, colourless oil (46% yield, 1.00:0.10 **2.68:2.90**); $R_f = 0.39$ (hexanes-dichloromethane-diethyl ether, 20:4:1); $^1\text{H NMR}$ (300 MHz, CDCl_3) δ 7.63-7.56 (m, 5H), 7.43-7.35 (m, 10H), 5.95 (t, $J = 2.3$ Hz, 1H), 5.75 (dt, $J = 15.5, 6.3$ Hz, 1H), 5.51 (dt, $J = 15.5, 1.5$ Hz, 1H), 3.88- 3.71 (m, 2H), 2.55- 2.46 (m, 2H), 2.10 (qdd, $J = 7.6, 6.1, 1.4$ Hz, 2H), 1.46 (s, 3H), 1.03 (t, $J = 7.5$ Hz, 3H); $^{13}\text{C NMR}$ (75 MHz, CDCl_3) δ 167.6 (C), 138.7 (C), 137.1 (CH), 132.8 (CH), 131.1 (CH), 129.2 (CH), 128.8 (CH), 113.4 (CH), 85.3 (C), 64.4 (CH_2), 35.7 (CH_2), 26.4 (CH_3), 25.4 (CH_2), 13.9 (CH_3); IR (neat, cm^{-1}) 3063 (m), 2970 (m), 2870 (m), 1616 (w), 1480 (w), 1429 (s), 1075 (s), 1059 (m), 971 (m), 728 (s), 699 (s); HRMS (ESI) calc for $\text{C}_{28}\text{H}_{30}\text{O}_3\text{Sn} + \text{Na}^+$ 525.1211, found 525.1214.



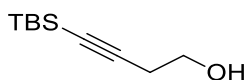
2.69. Clear, light yellow oil (76% yield); $R_f = 0.25$ (hexanes-diethyl ether, 1:2); $^1\text{H NMR}$ (300 MHz, $(\text{CD}_3)_2\text{CO}$) δ 9.80 (d, $J = 7.4$ Hz, 1H), 5.36 (d, $J = 7.4$ Hz, 1H), 3.99 (t, $J = 6.6$ Hz, 2H), 2.65 (td, $J = 6.5, 2.7$ Hz, 2H), 2.46 (t, $J = 2.7$ Hz, 1H), 2.27 (s, 3H); $^{13}\text{C NMR}$ (75 MHz, $(\text{CD}_3)_2\text{CO}$) δ 190.4 (CH), 176.0 (C), 105.7 (CH), 81.1 (C), 71.4 (CH), 67.5 (CH_2), 19.4 (CH_2), 17.7 (CH_3); IR (neat, cm^{-1}) 3304 (m), 3057 (m), 2958 (m), 2124 (w), 1703 (s), 1138 (m), 1060 (m); HRMS (ESI) calcd for $\text{C}_8\text{H}_{10}\text{O}_2 + \text{H}^+$ 139.0759, found 139.0759.



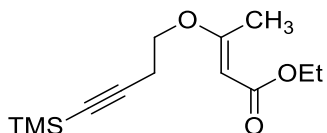
2.70. Clear, colourless oil (70% yield); $^1\text{H NMR}$ (300 MHz, $(\text{CD}_3)_2\text{CO}$) δ 6.44 (dt, $J = 16.7, 10.4$ Hz, 1H), 5.36 (d, $J = 10.7$ Hz, 1H), 4.96 (dd, $J = 16.7, 2.1$ Hz, 1H), 4.76 (dd, $J = 10.2, 2.1$ Hz, 1H), 3.83 (t, $J = 6.7$ Hz, 2H), 2.56 (td, $J = 6.7, 2.7$ Hz, 2H), 2.40 (t, $J = 2.7$ Hz, 1H), 1.89 (s, 3H); $^{13}\text{C NMR}$ (75 MHz, $(\text{CD}_3)_2\text{CO}$) δ 156.6 (C), 134.0 (CH), 111.4 (CH_2), 102.2 (CH), 81.6 (C), 71.0 (CH), 65.9 (CH_2), 19.7 (CH_2), 16.7 (CH_3); IR (neat, cm^{-1}) 3304 (s), 3086 (w), 3053 (m), 2977 (s), 2123 (w), 1644 (s), 1113 (s), 1073 (s); HRMS (ESI) calcd for $\text{C}_9\text{H}_{12}\text{O} + \text{H}^+$ 137.0966, found 137.0963.



2.78a. Clear, colourless oil (82% yield); $R_f = 0.39$ (hexanes-ethyl acetate, 4:1); $^1\text{H NMR}$ (300 MHz, CDCl_3) δ 3.70 (q, $J = 6.1$ Hz, 2H), 2.49 (t, $J = 6.3$ Hz, 2H), 1.94 (t, $J = 6.3$ Hz, 1H), 0.15 (s, 9H); $^{13}\text{C NMR}$ (75 MHz, CDCl_3) δ 103.5 (C), 87.2 (C), 61.1 (CH_2), 24.4 (CH_2), 0.3 (CH_3); IR (neat, cm^{-1}) 3350 (br, s), 2960 (s), 2900 (s), 2178 (s), 1410 (m), 1250 (s), 1055 (s), 1030 (s), 894 (s), 840 (s), 760 (s), 699 (s), 639 (s); HRMS (ESI) calcd for $\text{C}_7\text{H}_{14}\text{OSi} + \text{Na}^+$ 165.0706, found 165.0707.

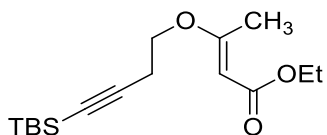


2.78b. Clear, yellow oil (15% yield); $^1\text{H NMR}$ (300 MHz, CDCl_3) δ 3.71 (t, $J = 6.3$ Hz, 2H), 2.51 (t, $J = 6.3$ Hz, 2H), 1.88 (br s, 1H), 0.92 (s, 9H), 0.09 (s, 6H); $^{13}\text{C NMR}$ (75 MHz, CDCl_3) δ 104.0 (C), 85.4 (C), 61.2 (CH_2), 26.3 (CH_3), 24.5 (CH_2), 16.7 (C), -4.3 (CH_3); IR (neat, cm^{-1}) 3338 (br, m), 2954 (s), 2930 (s), 2858 (s), 2176 (s), 1472 (m), 1250 (s), 1053 (m), 1030 (s), 838 (s), 776 (s), 682 (m); HRMS (ESI) calcd for $\text{C}_{10}\text{H}_{20}\text{OSi} + \text{Na}^+$ 207.1176, found 207.1176.

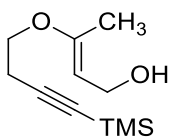


2.79a. Clear, colourless oil (96% yield); $^1\text{H NMR}$ (300 MHz, $(\text{CD}_3)_2\text{CO}$) δ 5.05 (s, 1H), 4.07 (q, $J = 7.1$ Hz, 2H), 3.93 (t, $J = 6.6$ Hz, 2H), 2.66 (t, $J = 6.7$ Hz, 2H), 2.25 (s, 3H), 1.21 (t, $J = 7.0$ Hz, 3H), 0.12 (s, 9H); $^{13}\text{C NMR}$ (75 MHz, $(\text{CD}_3)_2\text{CO}$) δ 172.1 (C), 167.8 (C), 103.9 (C), 92.4 (CH), 86.4 (C), 67.0 (CH_2), 59.5 (CH_2), 20.8 (CH_2), 18.8 (CH_3), 14.8

(CH₃), 0.1 (CH₃); IR (neat, cm⁻¹) 2960 (s), 2901 (s), 2181 (s), 1716 (s), 1634 (s), 1271 (s), 1141 (s), 1053 (s), 843 (s), 761 (s), 700 (m); HRMS (ESI) calcd for C₁₃H₂₂O₃Si + H⁺ 255.1411, found 255.1411.

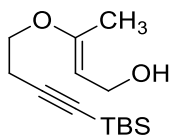


2.79b. Clear, pale yellow oil (100% yield, 1.00:0.04 E:Z); ¹H NMR (300 MHz, (CD₃)₂CO) δ 5.05 (s, 1H), 4.06 (q, *J* = 7.0 Hz, 2H), 3.95 (t, *J* = 6.6 Hz, 2H), 2.68 (t, *J* = 6.6 Hz, 2H), 2.25 (s, 3H), 1.21 (t, *J* = 7.2 Hz, 3H), 0.93 (s, 9H), 0.08 (s, 6H); ¹³C NMR (75 MHz, (CD₃)₂CO) δ 172.2 (C), 167.9 (C), 104.8 (C), 92.4 (CH), 84.5 (C), 67.2 (CH₂), 59.6 (CH₂), 26.4 (CH₃), 20.8 (CH₂), 18.9 (CH₃), 17.0 (C), 14.8 (CH₃), -4.4 (CH₃); IR (neat, cm⁻¹) 2954 (s), 2930 (s), 2858 (s), 2180 (s), 1714 (s), 1627 (s), 1275 (s), 1251 (s), 1142 (s), 1053 (s), 839 (s), 776 (s), 681 (m); HRMS (ESI) calcd for C₁₆H₂₈O₃Si + H⁺ 297.1881, found 297.1880.

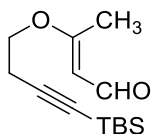


2.80a. Clear, colourless oil (70% yield); *R*_f = 0.29 (hexanes-ethyl acetate, 2:1); ¹H NMR (300 MHz, (CD₃)₂CO) δ 4.68 (t, *J* = 7.4 Hz, 1H), 4.04 (dd, *J* = 7.4, 5.5 Hz, 2H), 3.74 (t, *J* = 6.8 Hz, 2H), 3.28 (t, *J* = 5.5 Hz, 1H), 2.58 (t, *J* = 6.9 Hz, 2H), 1.79 (s, 3H), 0.12 (s, 9H); ¹³C NMR (75 MHz, (CD₃)₂CO) δ 155.8 (C), 104.6 (C), 99.2 (CH), 85.9 (C), 65.5 (CH₂), 58.8 (CH₂), 21.0 (CH₂), 16.3 (CH₃), 0.2 (CH₃); IR (neat, cm⁻¹) 3331 (br, s), 2959 (s), 2980

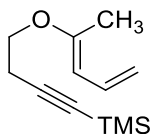
(m), 2180 (s), 1665 (s), 1250 (s), 842 (s); HRMS (ESI) calcd for $C_{11}H_{20}O_2Si + Na^+$ 235.1125, found 235.1125.



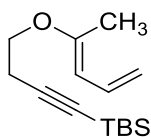
2.80b. Clear, colourless oil (71% yield); 1H NMR (300 MHz, $(CD_3)_2CO$) δ 4.68 (t, $J = 7.4$ Hz, 1H), 4.05 (dd, $J = 7.3, 5.5$ Hz, 2H), 3.76 (t, $J = 6.7$ Hz, 2H), 3.26 (t, $J = 5.5$ Hz, 1H), 2.60 (t, $J = 6.7$ Hz, 2H), 1.79 (s, 3H), 0.93 (s, 9H), 0.07 (s, 6H); ^{13}C NMR (75 MHz, $(CD_3)_2CO$) δ 155.8 (C), 105.5 (C), 99.1 (CH), 84.0 (C), 65.6 (CH_2), 58.9 (CH_2), 26.4 (CH_3), 21.0 (CH_2), 17.0 (C), 16.3 (CH_3), -4.3 (CH_3); IR (neat, cm^{-1}) 3332 (s), 2954 (s), 2929 (s), 2857 (s), 2179 (s), 1667 (s), 1472 (m), 1249 (s), 1079 (s), 838 (s); HRMS (ESI) calcd for $C_{14}H_{26}O_2Si + Na^+$ 277.1594, found 277.1594.



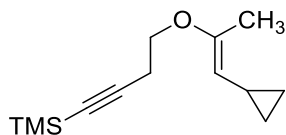
2.81b. Clear, pale yellow oil (26% yield); $R_f = 0.61$ (hexanes-diethyl ether, 1:3); 1H NMR (300 MHz, $(CD_3)_2CO$) δ 9.81 (d, $J = 7.6$ Hz, 1H), 5.35 (d, $J = 7.4$ Hz, 1H), 4.00 (t, $J = 6.5$ Hz, 2H), 2.72 (t, $J = 6.5$ Hz, 2H), 2.27 (s, 3H), 0.93 (s, 9H), 0.08 (s, 6H); ^{13}C NMR (75 MHz, $(CD_3)_2CO$) δ 190.2 (CH), 175.8 (C), 105.7 (CH), 104.6 (C), 84.6 (C), 67.5 (CH_2), 26.4 (CH_3), 20.8 (CH_2), 17.6 (CH_3), 17.0 (C), -4.4 (CH_3); IR (neat, cm^{-1}) 3453 (w), 2954 (s), 2929 (s), 2857 (s), 1667 (s), 1619 (s), 1226 (s), 1060 (m), 839 (s); HRMS (ESI) calcd for $C_{14}H_{24}O_2Si + H^+$ 253.1619, found 253.1619.



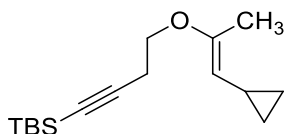
2.82a. Clear, colourless oil (36% yield); $R_f = 0.74$ (hexanes-ethyl acetate, 9:1); $^1\text{H NMR}$ (300 MHz, $(\text{CD}_3)_2\text{CO}$) δ 6.44 (dt, $J = 16.7, 10.4$ Hz, 1H), 5.36 (d, $J = 10.5$ Hz, 1H), 4.96 (dd, $J = 16.7, 2.2$ Hz, 1H), 4.75 (dd, $J = 10.2, 2.1$ Hz, 1H), 3.82 (t, $J = 6.9$ Hz, 2H), 2.60 (t, $J = 6.9$ Hz, 2H), 1.88 (s, 3H), 0.12 (s, 9H); $^{13}\text{C NMR}$ (75 MHz, $(\text{CD}_3)_2\text{CO}$) δ 156.6 (C), 134.0 (CH), 111.4 (CH_2), 104.6 (C), 102.3 (CH), 65.9 (CH_2), 21.1 (CH_2), 16.7 (CH_3), 0.2 (CH_3); IR (neat, cm^{-1}) 3086 (w), 2960 (s), 2925 (s), 2181 (s), 1651 (s), 1250 (s), 1073 (s), 844 (s), 760 (s); HRMS (ESI) calcd for $\text{C}_{12}\text{H}_{20}\text{OSi} + \text{H}^+$ 209.1356, found 209.1352.



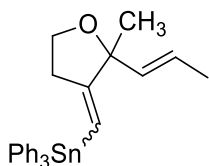
2.82b. Clear, pale yellow oil (67% yield); $R_f = 0.69$ (hexanes-ethyl acetate, 9:1); $^1\text{H NMR}$ (300 MHz, $(\text{CD}_3)_2\text{CO}$) δ 6.44 (dt, $J = 16.7, 10.4$ Hz, 1H), 5.35 (d, $J = 10.6$ Hz, 1H), 4.95 (dd, $J = 16.7, 2.2$ Hz, 1H), 4.75 (dd, $J = 10.3, 2.2$ Hz, 1H), 3.84 (t, $J = 6.7$ Hz, 2H), 2.62 (t, $J = 6.7$ Hz, 2H), 1.88 (s, 3H), 0.93 (s, 9H), 0.07 (s, 6H); $^{13}\text{C NMR}$ (75 MHz, $(\text{CD}_3)_2\text{CO}$) δ 156.6 (C), 134.0 (CH), 111.3 (CH_2), 105.2 (C), 102.2 (CH), 84.1 (C), 65.9 (CH_2), 26.4 (CH_3), 21.1 (CH_2), 17.0 (C), 16.7 (CH_3), -4.3 (CH_3); IR (neat, cm^{-1}) 2954 (s), 2929 (s), 2857 (s), 2179 (s), 1648 (s), 1472 (m), 1218 (s), 838 (s), 776 (s); HRMS (ESI) calcd for $\text{C}_{15}\text{H}_{26}\text{OSi} + \text{H}^+$ 251.1826, found 251.1828.



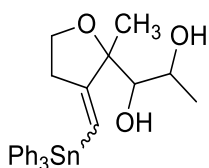
2.83a. Clear, colourless oil (87% yield; 1.00:0.14 **2.83a**:**2.82a**); $R_f = 0.80$ (hexanes-ethyl acetate, 9:1); $^1\text{H NMR}$ (300 MHz, CD_2Cl_2) δ 3.97 (d, $J = 7.8$ Hz, 1H), 3.64 (t, $J = 7.1$ Hz, 2H), 2.54 (t, $J = 7.1$ Hz, 2H), 1.86 (s, 3H), 1.36-1.21 (m, 1H), 0.64 (ddd, $J = 8.2, 6.0, 4.0$ Hz, 2H), 0.21 (ddd, $J = 6.0, 4.8, 4.0$ Hz, 2H), 0.13 (s, 9H); $^{13}\text{C NMR}$ (75 MHz, $(\text{CD}_3)_2\text{CO}$) δ 153.1 (C), 104.7 (C), 102.6 (CH), 85.6 (C), 65.5 (CH_2), 21.1 (CH_2), 16.8 (CH_3), 9.4 (CH), 7.1 (CH_2), 0.2 (CH_3); IR (neat, cm^{-1}) 3079 (m), 2958 (s), 2925 (s), 2872 (m), 2180 (s), 1664 (s), 1250 (s), 1151 (s), 843 (s); HRMS (ESI) calcd for $\text{C}_{13}\text{H}_{22}\text{OSi} + \text{H}^+$ 223.1513, found 223.1507.



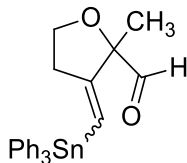
2.83b. Clear, colourless oil (76% yield; 1.00:0.09 **2.83b**:**2.82b**); $^1\text{H NMR}$ (300 MHz, $(\text{CD}_3)_2\text{CO}$) δ 4.02 (d, $J = 7.8$ Hz, 1H), 3.65 (t, $J = 6.8$ Hz, 2H), 2.56 (t, $J = 6.8$ Hz, 2H), 1.84 (s, 3H), 1.34-1.26 (m, 1H), 0.93 (s, 9H), 0.63 (ddd, $J = 8.2, 6.1, 3.8$ Hz, 2H), 0.23-0.18 (m, 2H), 0.07 (s, 6H); $^{13}\text{C NMR}$ (75 MHz, $(\text{CD}_3)_2\text{CO}$) δ 153.2 (C), 105.5 (C), 102.6 (CH), 83.8 (C), 65.5 (CH_2), 26.6 (CH_3), 21.2 (CH_2), 17.0 (C), 16.8 (CH_3), 9.4 (CH), 7.1 (CH_2), -4.3 (CH_3); IR (neat, cm^{-1}) 3079 (w), 2954 (s), 2928 (s), 2857 (s), 2179 (m), 1665 (m), 1250 (m), 1152 (m), 1079 (m), 838 (s), 825 (s); HRMS (ESI) calcd for $\text{C}_{16}\text{H}_{28}\text{OSi} + \text{H}^+$ 265.1982, found 265.1980.



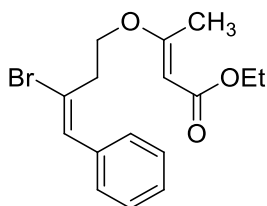
2.90. Clear, colourless oil (61% yield, 1.00:0.10 **2.90:2.91**); $R_f = 0.52$ (hexanes-dichloromethane-diethyl ether, 20:4:1); $^1\text{H NMR}$ (500 MHz, CDCl_3) δ 7.61-7.55 (m, 5H), 7.42-7.36 (m, 10H), 5.92 (t, $J = 2.4$ Hz, 1H), 5.69 (dq, $J = 15.3, 6.4$ Hz, 1H), 5.52 (dq, $J = 15.5, 1.6$ Hz, 1H); 3.81 (ddd, $J = 8.3, 7.9, 5.6$ Hz, 1H), 3.74 (dt, $J = 8.3, 7.5$ Hz, 1H), 2.56-2.40 (m, 2H), 1.72 (dd, $J = 6.4, 1.6$ Hz, 3H), 1.43 (s, 3H); $^{13}\text{C NMR}$ (75 MHz, CDCl_3) δ 167.6 (C), 138.7 (C), 137.1 (CH), 135.0 (CH), 129.2 (CH), 128.8 (CH), 124.2 (CH), 113.4 (CH), 85.2 (C), 64.5 (CH_2), 35.7 (CH_2), 26.4 (CH_3), 17.9 (CH_3); IR (neat, cm^{-1}) 3063 (m), 2974 (m), 2926 (w), 2858 (w), 1620 (w), 1429 (s), 1075 (s), 1057 (m), 728 (s), 699 (s); HRMS (ESI) calcd for $\text{C}_{27}\text{H}_{28}\text{OSn} + \text{Na}^+$ 511.1054, found 511.1058.



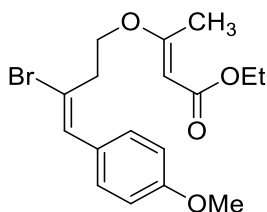
2.97. Clear, yellow oil (25% yield); $R_f = 0.15$ (hexanes-ethyl acetate, 3:1); $^1\text{H NMR}$ (300 MHz, CDCl_3) δ 7.63 – 7.55 (m, 5H), 7.44 – 7.34 (m, 10H), 5.96 (t, $J = 2.2$ Hz, 1H), 4.32 (q, $J = 6.4$ Hz, 1H), 3.97 (td, $J = 8.4, 4.4$ Hz, 1H), 3.78 (dt, $J = 7.2, 4.2$ Hz, 1H), 3.41 (t, $J = 4.4$ Hz, 1H), 2.63 (ddd, $J = 15.7, 8.5, 2.8$ Hz, 1H), 2.58 (d, $J = 9.6$ Hz, 1H), 2.46 (dddd, $J = 15.8, 6.8, 4.6, 2.0$ Hz, 1H), 1.37 (s, 3H), 1.29 (d, $J = 6.4$ Hz, 3H); $^{13}\text{C NMR}$ (75 MHz, CDCl_3) δ 167.3 (C), 138.5 (C), 137.1 (CH), 129.3 (CH), 128.5 (CH), 113.3 (CH), 89.2 (C), 77.8 (CH), 66.8 (CH), 66.6 (CH_2), 36.5 (CH_2), 23.7 (CH_3), 20.1 (CH_3); IR (neat, cm^{-1}) 3467 (m), 3064 (m), 2974 (m), 2928 (m), 2863 (m), 1429 (s), 1075 (m), 729 (s), 699 (s); HRMS (ESI) calc for $\text{C}_{27}\text{H}_{30}\text{O}_3\text{Sn} + \text{Na}^+$ 545.1109, found 545.1106.



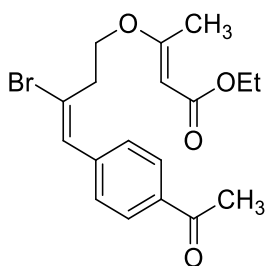
2.98. Clear, colourless oil (27% yield); $R_f = 0.36$ (hexanes-dichloromethane-diethyl ether, 10:4:1); $^1\text{H NMR}$ (300 MHz, CDCl_3) δ 9.53 (s, 1H), 7.57 – 7.52 (m, 5H), 7.42 – 7.35 (m, 10H), 6.18 (t, $J = 2.34$, 1H), 4.05-3.91 (m, 2H), 2.55 (app ddd, $J = 15.9, 7.4, 2.4$, 1H), 2.45 (dddd, $J = 15.8, 7.3, 5.8, 2.3$ Hz, 1H), 1.48 (s, 3H); $^{13}\text{C NMR}$ (125 MHz, CDCl_3) δ 199.4 (CH), 161.1 (C), 137.9 (C), 137.1 (CH), 129.5 (CH), 129.0 (CH), 119.6 (CH), 89.8 (C), 67.2 (CH_2), 35.3 (CH_2), 21.7 (CH_3); IR (neat, cm^{-1}) 3064 (m), 2958 (m), 2929 (m), 1732 (s), 1616 (m), 1122 (m), 1075 (s), 729 (s), 699 (s).



2.104a. Colourless solid (99% yield); $R_f = 0.38$ (hexanes-ethyl acetate, 9:1); $^1\text{H NMR}$ (300 MHz, $(\text{CD}_3)_2\text{CO}$) δ 7.44-7.29 (m, 5H), 7.20 (s, 1H), 5.12 (s, 1H), 4.14 (t, $J = 6.1$ Hz, 2H), 4.08 (q, $J = 7.1$ Hz, 2H), 3.07 (td, $J = 6.2, 0.9$ Hz, 2H), 2.25 (s, 3H), 1.22 (t, $J = 7.2$ Hz, 3H); $^{13}\text{C NMR}$ (75 MHz, $(\text{CD}_3)_2\text{CO}$) δ 172.2 (C), 167.8 (C), 136.9 (C), 135.9 (CH), 129.4 (CH), 129.2 (CH), 128.5 (CH), 126.0 (C), 92.5 (CH), 66.5 (CH_2), 59.6 (CH_2), 36.3 (CH_2), 18.9 (CH_3), 14.8 (CH_3); IR (thin film in CH_2Cl_2 , cm^{-1}) 3058 (w), 3026 (w), 2979 (m), 2935 (m), 1711 (s), 1627 (s), 1274 (m), 1142 (s), 1055 (s), 817 (m), 755 (m), 705 (m); HRMS (ESI) calcd for $\text{C}_{16}\text{H}_{19}\text{BrO}_3 + \text{Na}^+$ 361.0410, found 361.0410.

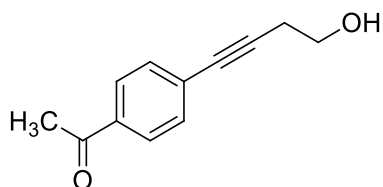


2.104b. Clear, pale yellow oil (99% yield); $R_f = 0.29$ (hexanes-ethyl acetate, 9:1); $^1\text{H NMR}$ (300 MHz, $(\text{CD}_3)_2\text{CO}$) δ 7.35 (d, $J = 8.2$ Hz, 2H), 7.11 (s, 1H), 6.95 (d, $J = 8.8$ Hz, 2H), 5.12 (s, 1H), 4.13 (t, $J = 6.1$ Hz, 2H), 4.08 (q, $J = 7.1$ Hz, 2H), 3.81 (s, 3H), 3.07 (td, $J = 6.1, 0.6$ Hz, 2H), 2.25 (s, 3H), 1.22 (t, $J = 7.0$ Hz, 3H); $^{13}\text{C NMR}$ (75 MHz, $(\text{CD}_3)_2\text{CO}$) δ 172.2 (C), 167.8 (C), 160.2 (C), 135.5 (CH), 130.5 (CH), 129.2 (C), 124.3 (C), 114.8 (CH), 92.5 (CH), 66.6 (CH_2), 59.6 (CH_2), 55.5 (CH_3), 36.4 (CH_2), 18.9 (CH_3), 14.8 (CH_3); IR (neat, cm^{-1}) 2977 (w), 2952 (w), 2836 (w), 1710 (s), 1625 (s), 1511 (s), 1251 (s), 1141 (s), 1055 (s), 819 (m); HRMS (ESI) calcd for $\text{C}_{17}\text{H}_{21}\text{BrO}_4 + \text{H}^+$ 369.0696, found 369.0696.

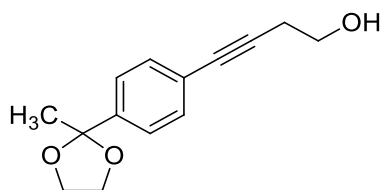


2.104c. Clear, colourless oil (79% yield); $R_f = 0.11$ (hexanes-ethyl acetate, 9:1); $^1\text{H NMR}$ (300 MHz, $(\text{CD}_3)_2\text{CO}$) δ 8.01 (d, $J = 8.5$ Hz, 2H), 7.57 (d, $J = 8.2$ Hz, 2H), 7.26 (s, 1H), 5.12 (s, 1H), 4.16 (t, $J = 5.9$ Hz, 2H), 4.07 (q, $J = 7.1$ Hz, 2H), 3.10 (td, $J = 5.9, 0.6$ Hz, 2H); 2.59 (s, 3H), 2.25 (s, 3H), 1.21 (t, $J = 7.0$ Hz, 3H); $^{13}\text{C NMR}$ (75 MHz, $(\text{CD}_3)_2\text{CO}$) δ 197.4 (C), 172.1 (C), 167.8 (C), 141.3 (C), 137.2 (C), 135.2 (CH), 129.4 (CH), 129.3 (CH), 128.0 (C), 92.6 (CH), 66.4 (CH_2), 59.6 (CH_2), 36.5 (CH_2), 26.7 (CH_3), 18.9 (CH_3), 14.8 (CH_3); IR (neat, cm^{-1}) 2979 (w), 2936 (w), 2895 (w), 1710 (s), 1685 (s), 1626 (s), 1268 (s),

1143 (s), 1055 (s), 818 (m), 665 (m); HRMS (ESI) calcd for $C_{18}H_{21}BrO_4 + Na^+$ 403.0515, found 403.0515.

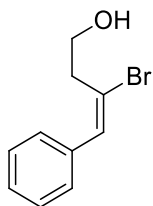


2.110c. Orange-yellow solid (92% yield); $R_f = 0.28$ (hexanes-ethyl acetate, 1:1); 1H NMR (300 MHz, $CDCl_3$) δ 7.89 (d, $J = 8.5$ Hz, 2H), 7.49 (d, $J = 8.5$ Hz, 2H), 3.84 (q, $J = 6.2$ Hz, 2H), 2.73 (t, $J = 6.2$ Hz, 2H), 2.60 (s, 3H), 1.76 (t, $J = 6.2$ Hz, 1H); ^{13}C NMR (75 MHz, $CDCl_3$) δ 197.6 (C), 136.1 (C), 132.0 (CH), 128.6 (C), 128.4 (CH), 90.5 (C), 81.9 (C), 61.2 (CH₂), 26.8 (CH₃), 24.1 (CH₂); IR (KBr, cm^{-1}) 3220 (m), 2952 (w), 2917 (w), 2885 (w), 1680 (s), 1602 (m), 1270 (m), 1045 (m), 834 (s), 594 (m); HRMS (ESI) calcd for $C_{12}H_{12}O_2 + H^+$ 189.0910, found 189.0910.

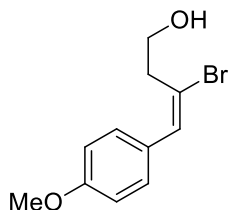


2.110d. Clear, pale yellow oil (62% yield); $R_f = 0.54$ (hexanes-ethyl acetate, 1:1); 1H NMR (300 MHz, $CDCl_3$) δ 7.43–7.36 (m, 4H), 4.08–3.97 (m, 2H), 3.81 (q, $J = 6.2$ Hz, 2H), 3.83–3.69 (m, 2H), 2.69 (t, $J = 6.3$ Hz, 2H), 1.88 (t, $J = 6.3$ Hz, 1H), 1.63 (s, 3H); ^{13}C NMR (75 MHz, $CDCl_3$) δ 143.3 (C), 131.7 (CH), 125.5 (CH), 123.0 (C), 108.8 (C), 86.7 (C), 82.5 (C), 64.7 (CH₂), 61.4 (CH₂), 27.6 (CH₃), 24.0 (CH₂); IR (neat, cm^{-1}) 3413 (br, s), 2987 (s),

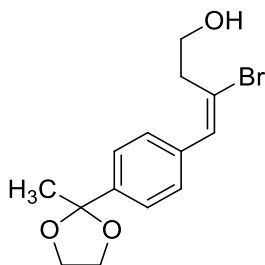
2958 (s), 2889 (s), 1506 (m), 1374 (s), 1248 (s), 1199 (s), 1039 (s), 839 (s); HRMS (ESI) calcd for $C_{14}H_{16}O_3 + H^+$ 233.1172, found 233.1172.



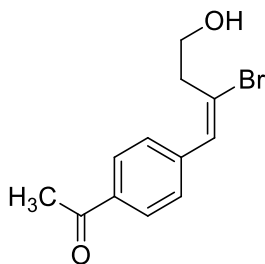
2.111a. Clear, colourless oil (77% yield); $R_f = 0.52$ (hexanes-ethyl acetate, 2:1); 1H NMR (300 MHz, $CDCl_3$) δ 7.30–7.17 (m, 5H), 7.08 (s, 1H), 3.85 (t, $J = 6.1$ Hz, 2H), 2.82 (td, $J = 6.1, 0.6$ Hz, 2H), 1.62 (s, 1H); ^{13}C NMR (75 MHz, $CDCl_3$) δ 136.2 (C), 135.4 (CH), 128.7 (CH), 128.5 (CH), 127.7 (CH), 126.2 (C), 60.9 (CH_2), 39.3 (CH_2); IR (neat, cm^{-1}) 3350 (br, s), 3057 (m), 3025 (m), 2954 (m), 2884 (m), 1633 (m), 1494 (m), 1446 (m), 1211 (w), 1047 (s), 753 (s), 701 (s).



2.111b. Clear, pale yellow oil (79% yield); $R_f = 0.20$ (hexanes-ethyl acetate, 4:1); 1H NMR (300 MHz, $CDCl_3$) δ 7.26 (d, $J = 8.5$ Hz, 2H), 7.10 (s, 1H), 6.87 (d, $J = 8.8$ Hz, 2H), 3.94 (q, $J = 6.0$ Hz, 2H), 3.81 (s, 3H), 2.91 (td, $J = 6.1, 0.6$ Hz, 2H), 1.55 (t, $J = 5.9$ Hz, 1H); ^{13}C NMR (75 MHz, $CDCl_3$) δ 159.2 (C), 135.0 (CH), 129.8 (CH), 128.8 (C), 124.7 (C), 114.1 (CH), 61.0 (CH_2), 55.5 (CH_3), 39.3 (CH_2); IR (neat, cm^{-1}) 3413 (br, s), 2955 (w), 2828 (w), 1606 (m), 1511 (s), 1250 (s), 1035 (m), 822 (w); HRMS (ESI) calcd for $C_{11}H_{13}BrO_2 + Na^+$ 278.9991, found 278.9981.



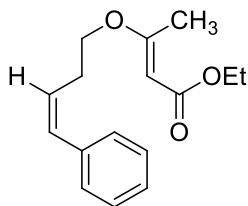
2.111c. Clear, orange oil (44% yield); $R_f = 0.50$ (hexanes-ethyl acetate, 1:1); ^1H NMR (300 MHz, CDCl_3) δ 7.43 (d, $J = 8.2$ Hz, 2H), 7.26 (d, $J = 7.9$ Hz, 2H), 7.11 (s, 1H), 4.04–3.98 (m, 2H), 3.91 (q, $J = 6.0$ Hz, 2H), 3.78–3.72 (m, 2H), 2.88 (td, $J = 6.1, 0.6$ Hz, 2H), 1.83 (t, $J = 6.2$ Hz, 1H); 1.62 (s, 3H); ^{13}C NMR (75 MHz, CDCl_3) δ 142.9 (C), 135.8 (C), 135.1 (CH), 128.4 (CH), 126.3 (C), 125.7 (CH), 108.9 (C), 64.7 (CH_2), 61.0 (CH_2), 39.4 (CH_2), 27.7 (CH_3); IR (neat, cm^{-1}) 3433 (m), 2977 (m), 2916 (m), 2885 (m), 1251 (m), 1198 (m), 1039 (s), 871 (m); HRMS (ESI) calcd for $\text{C}_{14}\text{H}_{17}\text{BrO}_3 + \text{Na}^+$ 335.0253, found 335.0253.



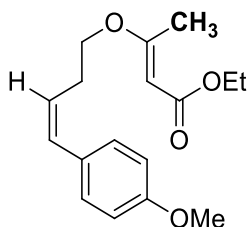
2.111d. Clear, orange-yellow oil (82% yield); $R_f = 0.50$ (hexanes-ethyl acetate, 1:1); ^1H NMR (300 MHz, CDCl_3) δ 7.92 (d, $J = 8.5$ Hz, 2H), 7.43 (d, $J = 8.5$ Hz, 2H), 7.17 (br s, 1H), 3.96 (t, $J = 6.2$ Hz, 2H), 2.89 (td, $J = 6.1, 0.6$ Hz, 2H), 2.59 (s, 3H); ^{13}C NMR (75 MHz, CDCl_3) δ 197.8 (C), 140.9 (C), 136.1 (C), 134.4 (CH), 128.8 (CH), 128.8 (CH), 128.5 (C), 60.7 (CH_2), 39.5 (CH_2), 26.8 (CH_3); IR (neat, cm^{-1}) 3426 (br, m), 2960 (m),

2917 (m), 2881 (m), 1680 (s), 1602 (s), 1407 (m), 1359 (m), 1268 (s), 1049 (m), 874 (m);

HRMS (ESI) calcd for $C_{12}H_{13}BrO_2 + Na^+$ 290.9991, found 290.9992.

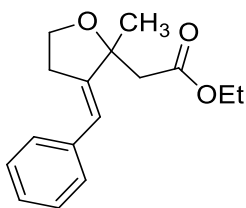


2.113a. Clear, colourless oil (20% yield); $R_f = 0.47$ (hexanes-dichloromethane-diethyl ether, 10:4:1); 1H NMR (300 MHz, $(CD_3)_2CO$) δ 7.45–7.19 (m, 5H), 6.56 (dt, $J = 15.8, 1.5$ Hz, 1H), 6.34 (dt, $J = 15.9, 6.8$ Hz, 1H), 5.08 (s, 1H), 4.07 (q, $J = 7.1$ Hz, 2H), 3.97 (t, $J = 6.6$ Hz, 2H), 2.64 (qd, $J = 6.6, 1.5$ Hz, 2H), 2.26 (s, 3H), 1.21 (t, $J = 7.0$ Hz, 3H); ^{13}C NMR (75 MHz, $(CD_3)_2CO$) δ 172.6 (C), 168.0 (C), 138.4 (C), 133.0 (CH), 129.4 (CH), 128.1 (CH), 126.9 (CH), 126.8 (CH), 92.1 (CH), 68.4 (CH₂), 59.5 (CH₂), 33.0 (CH₂), 19.0 (CH₃), 14.8 (CH₃); IR (neat, cm^{-1}) 3060 (w), 3028 (w), 2979 (m), 2933 (m), 1710 (s), 1624 (s), 1275 (m), 1141 (s), 1053 (s), 965 (m), 818 (m), 730 (m), 694 (m); HRMS (ESI) calcd for $C_{16}H_{20}O_3 + Na^+$ 283.1305, found 283.1305.

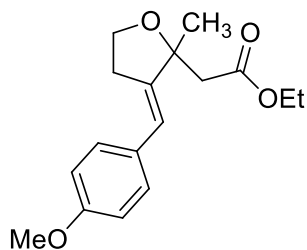


2.113b. Clear, colourless oil (25% yield); $R_f = 0.63$ (hexanes-dichloromethane-diethyl ether, 5:5:1); 1H NMR (300 MHz, $(CD_3)_2CO$) δ 7.34 (d, $J = 8.5$ Hz, 2H), 6.87 (d, $J = 8.8$ Hz, 2H), 6.49 (dt, $J = 15.8, 1.5$ Hz, 1H), 6.17 (dt, $J = 15.8, 6.9$ Hz, 1H), 5.07 (s, 1H), 4.07

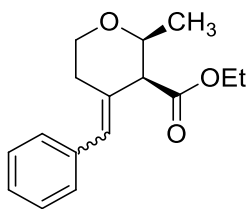
(q, $J = 7.1$ Hz, 2H), 3.94 (t, $J = 6.6$ Hz, 2H), 3.78 (s, 3H), 2.60 (qd, $J = 6.7, 1.5$ Hz, 2H), 2.25 (s, 3H), 1.21 (t, $J = 7.0$ Hz, 3H); ^{13}C NMR (75 MHz, $(\text{CD}_3)_2\text{CO}$) δ 172.6 (C), 168.0 (C), 160.1 (C), 132.5 (CH), 131.1 (C), 128.1 (CH), 124.3 (CH), 114.8 (CH), 92.1 (CH), 68.6 (CH_2), 59.5 (CH_2), 55.5 (CH_3), 33.0 (CH_2), 19.0 (CH_3), 14.8 (CH_3); IR (neat, cm^{-1}) 2980 (w), 2952 (m), 2934 (m), 2835 (w), 1709 (s), 1622 (s), 1512 (s), 1276 (s), 1249 (s), 1141 (s), 1052 (s), 967 (m), 821 (m); HRMS (ESI) calcd for $\text{C}_{17}\text{H}_{22}\text{O}_4 + \text{H}^+$ 291.1591, found 291.1592.



2.114a. Clear, colourless oil (35% yield); $R_f = 0.17$ (hexanes-dichloromethane-diethyl ether, 10:4:1); ^1H NMR (500 MHz, CDCl_3) δ 7.37–7.30 (m, 4H), 7.25–7.20 (m, 1H), 6.23 (t, $J = 2.4$ Hz, 1H), 4.13 (q, $J = 7.2$ Hz, 2H), 4.06 (ddd, $J = 8.3, 7.6, 6.0$ Hz, 1H), 3.96 (ddd, $J = 8.7, 7.5, 6.8$ Hz, 1H), 3.01–2.86 (m, 2H), 2.70 (d, $J = 19.1$ Hz, 1H), 2.68 (d, $J = 19.5$ Hz, 1H), 1.51 (s, 3H), 1.24 (t, $J = 7.2$ Hz, 3H); ^{13}C NMR (125 MHz, CDCl_3) δ 170.4 (C), 147.4 (C), 137.7 (C), 128.6 (CH), 128.4 (CH), 126.9 (CH), 120.7 (CH), 83.2 (C), 65.8 (CH_2), 60.5 (CH_2), 45.6 (CH_2), 31.8 (CH_2), 26.4 (CH_3), 14.5 (CH_3); IR (neat, cm^{-1}) 2979 (m), 2921 (m), 2860 (w), 1733 (s), 1448 (w), 1180 (m), 1034 (m), 695 (s); HRMS (ESI) calcd for $\text{C}_{16}\text{H}_{20}\text{O}_3 + \text{Na}^+$ 283.1305, found 283.1303.

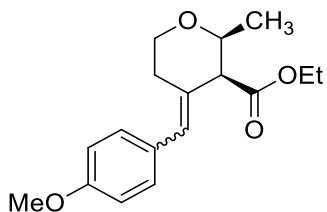


2.114b. Clear, colourless oil (33% yield); $R_f = 0.33$ (hexanes-dichloromethane-diethyl ether, 5:5:1); $^1\text{H NMR}$ (500 MHz, CDCl_3) δ 7.23 (d, $J = 8.7$ Hz, 2H), 6.87 (d, $J = 8.7$ Hz, 2H), 6.15 (t, $J = 2.4$ Hz, 1H), 4.10 (q, $J = 7.2$ Hz, 2H), 4.03 (ddd, $J = 8.7, 7.9, 6.0$ Hz, 1H), 3.97–3.91 (m, 1H), 3.79 (s, 3H), 2.95–2.81 (m, 2H), 2.66 (d, $J = 20.3$ Hz, 1H), 2.64 (d, $J = 20.3$ Hz, 1H), 1.48 (s, 3H), 1.21 (t, $J = 7.2$ Hz, 3H); $^{13}\text{C NMR}$ (125 MHz, CDCl_3) δ 170.5 (C), 158.6 (C), 145.0 (C), 130.5 (C), 129.6 (CH), 120.1 (CH), 114.0 (CH), 83.2 (C), 65.8 (CH₂), 60.5 (CH₂), 55.5 (CH₃), 45.7 (CH₂), 31.7 (CH₂), 26.3 (CH₃), 14.5 (CH₃); IR (neat, cm^{-1}) 2799 (m), 2917 (m), 1735 (s), 1608 (m), 1512 (s), 1250 (s), 1177 (m), 1033 (m), 826 (w); HRMS (ESI) calcd for $\text{C}_{17}\text{H}_{22}\text{O}_4 + \text{H}^+$ 291.1591, found 291.1590.



2.115a. Clear, colourless oil (34% yield, 1.00:1.00 dr); $R_f = 0.22$ (hexanes-dichloromethane-diethyl ether, 10:4:1); $^1\text{H NMR}$ (500 MHz, CDCl_3) δ 7.37–7.30 (m, 4H), 7.27–7.20 (m, 6H), 6.49 (d, $J = 1.2$ Hz, 1H), 6.46 (d, $J = 1.2$ Hz, 1H), 4.27 (q, $J = 7.0$ Hz, 2H), 4.25–4.13 (m, 3H), 4.10 (dd, $J = 11.1, 6.0$ Hz, 1H), 3.70 (qd, $J = 6.5, 3.6$ Hz, 1H), 3.59–3.52 (m, 1H), 3.54 (d, $J = 3.2$ Hz, 1H), 3.50 (qd, $J = 6.4, 3.4$ Hz, 1H), 3.38 (ddd, $J = 12.3, 11.1, 2.8$ Hz, 1H), 3.24–3.12 (m, 1H), 3.17 (d, $J = 3.2$ Hz, 1H), 2.91 (dddd, $J = 14.3,$

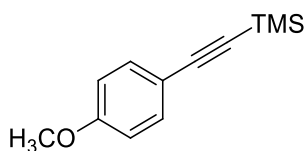
12.3, 6.3, 2.0 Hz, 1H), 2.66 (dt, $J = 14.3, 1.2$ Hz, 1H), 2.14 (d, $J = 13.6, 1.2$ Hz, 1H), 1.34 (t, $J = 7.2$ Hz, 3H), 1.31 (d, $J = 6.4$ Hz, 3H), 1.30 (t, $J = 7.2$ Hz, 3H), 1.23 (d, $J = 6.4$ Hz, 3H); ^{13}C NMR (125 MHz, CDCl_3) δ 171.2 (C), 171.0 (C), 136.9 (C), 136.6 (C), 135.6 (CH), 135.4 (CH), 129.2 (CH), 128.9 (CH), 128.5 (CH), 128.4 (CH), 127.5 (CH), 127.2 (CH), 127.0 (CH), 126.9 (CH), 75.4 (CH), 75.0 (CH), 69.5 (CH_2), 68.3 (CH_2), 60.7 (CH_2), 60.5 (CH_2), 56.0 (CH), 50.1 (CH), 33.9 (CH_2), 27.3 (CH_2), 19.4 (CH_3), 14.5 (CH_3), 14.5 (CH_3); IR (neat, cm^{-1}) 2978 (m), 2849 (m), 1735 (s), 1447 (m), 1262 (m), 1150 (s), 1092 (s), 1059 (m), 749 (m), 700 (s); HRMS (ESI) calcd for $\text{C}_{16}\text{H}_{20}\text{O}_3 + \text{H}^+$ 261.1485, found 261.1484.



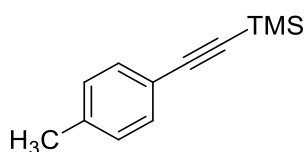
2.115b. Clear, colourless oil (16% yield, 1.00:0.62 dr); $R_f = 0.44$ (hexanes-dichloromethane-diethyl ether, 5:5:1); ^1H NMR (500 MHz, CDCl_3) δ 7.21 (d, $J = 8.7$ Hz, 2H, major), 7.16 (d, $J = 8.7$ Hz, 2H, minor), 6.88 (d, $J = 8.7$ Hz, 2H, major), 6.86 (d, $J = 8.7$ Hz, 2H, minor), 6.42 (d, $J = 1.2$ Hz, 1H, major), 6.39 (d, $J = 1.2$ Hz, 1H, minor), 4.26 (q, $J = 7.2$ Hz, 2H, major), 4.23 (q, $J = 7.2$ Hz, 2H, minor), 4.20–4.12 (m, 1H, major), 4.09 (dd, $J = 10.9, 5.8$ Hz, 1H, minor), 3.82 (s, 3H, major), 3.81 (s, 3H, minor), 3.69 (qd, $J = 6.4, 3.4$ Hz, 1H, minor), 3.58–3.52 (m, 2H, major), 3.49 (qd, $J = 6.4, 3.4$ Hz, 1H, major), 3.37 (ddd, $J = 12.7, 11.1, 2.8$ Hz, 1H, minor), 3.17–3.08 (m, 1H, major), 3.14 (d, $J = 3.2$ Hz, 1H, minor), 2.90 (dddd, $J = 14.3, 12.3, 6.0, 2.0$ Hz, 1H, minor), 2.64 (d, $J = 14.3$ Hz, 1H, minor), 2.11 (d, $J = 13.9$ Hz, 1H, major), 1.34 (t, $J = 7.2$ Hz, 3H, major), 1.30 (d, $J = 6.8$

Hz, 3H, minor), 1.29 (t, $J = 7.2$ Hz, 3H, minor), 1.23 (d, $J = 6.8$ Hz, 3H, major); ^{13}C NMR (125 MHz, CDCl_3) δ 171.4 (C, minor), 171.2 (C, major), 158.7 (C, major), 158.6 (C, minor), 134.1 (C, minor), 133.9 (C, major), 130.4 (CH, minor), 130.2 (CH, major), 129.4 (C, minor), 129.1 (C, major), 127.1 (CH, minor), 126.8 (CH, major), 114.0 (CH, major), 113.8 (CH, minor), 75.4 (CH, minor), 74.9 (CH, major), 69.5 (CH_2 , major), 68.3 (CH_2 , minor), 60.8 (CH_2 , major), 60.6 (CH_2 , minor), 56.0 (CH_3 , minor), 55.5 (CH_3 , major), 50.1 (CH), 33.9 (CH_2 , major), 27.3 (CH_2 , minor), 19.5 (CH_3 , minor), 19.45 (CH_3 , major), 14.6 (CH_3 , major), 14.6 (CH_3 , minor); IR (neat, cm^{-1}) 2975 (m), 2957 (m), 2917 (m), 2849 (m), 1732 (s), 1607 (s), 1511(s), 1296 (m), 1249 (s), 1177 (s), 1149 (s), 1091 (s), 1031 (s), 832 (m), 666 (m); HRMS (ESI) calcd for $\text{C}_{17}\text{H}_{22}\text{O}_4 + \text{H}^+$ 291.1591, found 291.1590.

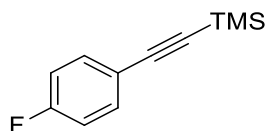
5.8 Compounds Pertaining to Chapter 3



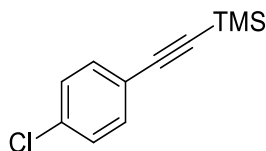
3.2a. Clear, yellow oil (98% yield); $R_f = 0.08$ (hexanes); $^1\text{H NMR}$ (300 MHz, CDCl_3) δ 7.41 (d, $J = 8.8$ Hz, 2H), 6.82 (d, $J = 8.8$ Hz, 2H), 3.80 (s, 3H), 0.26 (s, 9H); $^{13}\text{C NMR}$ (75 MHz, CDCl_3) δ 159.9 (C), 133.7 (CH), 115.5 (C), 114.0 (CH), 105.4 (C), 92.6 (C), 55.4 (CH₃), 0.26 (CH₃).



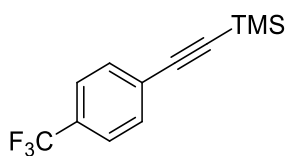
3.2b. Clear, yellow oil (99% yield); $R_f = 0.48$ (hexanes); $^1\text{H NMR}$ (300 MHz, CDCl_3) δ 7.36 (d, $J = 8.2$ Hz, 2H), 7.10 (d, $J = 8.2$ Hz, 2H), 2.34 (s, 3H), 0.25 (s, 9H); $^{13}\text{C NMR}$ (75 MHz, CDCl_3) δ 138.8 (C), 132.1 (CH), 129.1 (CH), 120.3 (C), 105.6 (C), 93.4 (C), 21.7 (CH₃), 0.2 (CH₃).



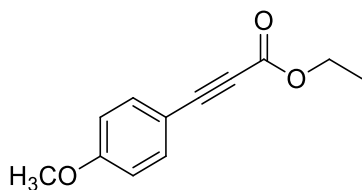
3.2e. Clear, yellow oil (99% yield); $R_f = 0.57$ (hexanes); $^1\text{H NMR}$ (300 MHz, CDCl_3) δ 7.44 (dd, $J = 8.9, 5.4$ Hz, 2H), 6.99 (t, $J = 8.8$ Hz, 2H), 0.24 (s, 9H); $^{13}\text{C NMR}$ (75 MHz, CDCl_3) δ 162.8 (d, $J_{\text{C-F}} = 249.8$ Hz, C), 134.1 (d, $J_{\text{C-F}} = 8.4$ Hz, CH), 119.5 (d, $J_{\text{C-F}} = 3.3$ Hz, C), 115.7 (d, $J_{\text{C-F}} = 22.1$, CH), 104.2 (C), 94.1 (C), 0.1 (CH₃).



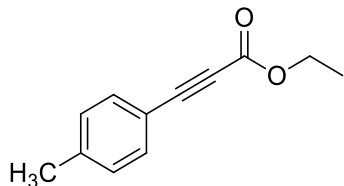
3.2f. Pale yellow solid (84% yield); $R_f = 0.48$ (hexanes); $^1\text{H NMR}$ (300 MHz, CDCl_3) δ 7.39 (d, $J = 8.5$ Hz, 2H), 7.27 (d, $J = 8.5$ Hz, 2H), 0.25 (s, 9H); $^{13}\text{C NMR}$ (75 MHz, CDCl_3) δ 134.7 (C), 133.4 (CH), 128.8 (CH), 121.8 (C), 104.0 (C), 95.6 (C), 0.1 (CH_3).



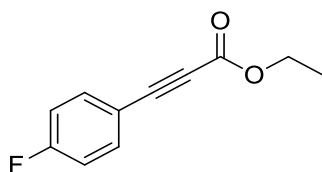
3.2g. Clear, pale yellow oil (99% yield); $R_f = 0.65$ (hexanes); $^1\text{H NMR}$ (300 MHz, CDCl_3) δ 7.55 (s, 4H), 0.26 (s, 9H); $^{13}\text{C NMR}$ (75 MHz, (CDCl_3) δ 132.2 (CH), 130.4 (q, $J_{\text{C-F}} = 34.2$ Hz, C), 127.1 (C), 125.3 (q, $J_{\text{C-F}} = 3.7$ Hz, CH), 124.1 (q, $J_{\text{C-F}} = 272.0$ Hz, CF_3), 103.6 (C), 97.4 (C), 0.0 (CH_3).



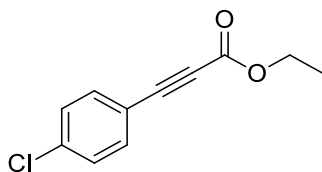
3.4a. Clear, colorless oil (93% yield); $R_f = 0.53$ (hexanes-ethyl acetate, 4:1); $^1\text{H NMR}$ (300 MHz, CDCl_3) δ 7.54 (d, $J = 9.1$ Hz, 2H), 6.88 (d, $J = 9.1$ Hz, 2H), 4.29 (q, $J = 7.2$ Hz, 2H), 3.84 (s, 3H), 1.35 (t, $J = 7.0$ Hz, 3H); $^{13}\text{C NMR}$ (75 MHz, CDCl_3) δ 161.7 (C), 154.6 (C), 135.1 (CH), 114.5 (CH), 111.6 (C), 87.1 (C), 80.4 (C), 62.1 (CH_2), 55.6 (CH_3), 14.3 (CH_3).



3.4b. Clear, yellow oil (2.2982 g, 95% yield); $R_f = 0.57$ (hexanes-ethyl acetate, 4:1); ^1H NMR (300 MHz, CDCl_3) δ 7.48 (d, $J = 8.2$ Hz, 2H), 7.17 (d, $J = 7.9$ Hz, 2H), 4.29 (q, $J = 7.1$ Hz, 2H), 2.37 (s, 3H), 1.35 (t, $J = 7.2$ Hz, 3H); ^{13}C NMR (75 MHz, CDCl_3) δ 154.4 (C), 141.5 (C), 133.2 (CH), 129.5 (CH), 116.7 (C), 86.8 (C), 80.6 (C), 62.2 (CH_2), 21.9 (CH_3), 14.3 (CH_3).

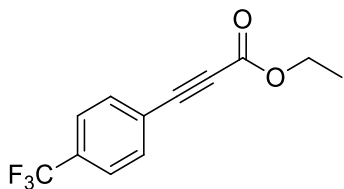


3.4e. Orange solid (96% yield); $R_f = 0.52$ (hexanes); ^1H NMR (300 MHz, CDCl_3) δ 7.59 (dd, $J = 9.1, 5.3$ Hz, 2H), 7.07 (t, $J = 8.6$ Hz, 2H), 4.30 (q, $J = 7.1$ Hz, 2H), 1.35 (t, $J = 7.2$ Hz, 3H); ^{13}C NMR (75 MHz, CDCl_3) δ 164.1 (d, $J_{\text{C-F}} = 254.0$ Hz, CF), 154.2 (C), 135.4 (d, $J_{\text{C-F}} = 8.8$ Hz, CH), 116.3 (d, $J_{\text{C-F}} = 22.2$ Hz, CH), 116.0 (d, $J_{\text{C-F}} = 3.3$ Hz, C), 85.2 (C), 80.8 (C), 62.4 (CH_2), 14.3 (CH_3).

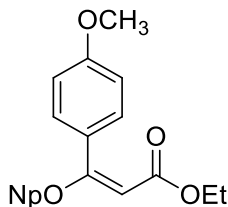


3.4f. Orange solid (80% yield); $R_f = 0.59$ (hexanes); ^1H NMR (300 MHz, CDCl_3) δ 7.51 (d, $J = 8.5$ Hz, 2H), 7.36 (d, $J = 8.5$ Hz, 2H), 4.31 (q, $J = 7.1$ Hz, 2H), 1.36 (t, $J = 7.0$ Hz,

3H); ^{13}C NMR (75 MHz, CDCl_3) δ 153.9 (C), 137.1 (C), 134.2 (CH), 129.1 (CH), 118.2 (C), 84.7 (C), 81.6 (C), 62.3 (CH_2), 14.2 (CH_3).

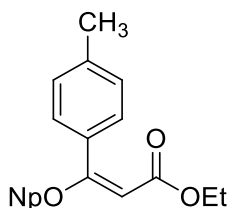


3.4g. Brown-orange oil (84% yield); $R_f = 0.61$ (10:4:1 hexanes-dichloromethane-diethyl ether); ^1H NMR (300 MHz, $(\text{CD}_3)_2\text{CO}$) δ 7.70 (d, $J = 8.5$ Hz, 2H), 7.64 (d, $J = 8.5$ Hz, 2H), 4.32 (q, $J = 7.1$ Hz, 2H), 1.37 (t, $J = 7.2$ Hz, 3H); ^{13}C NMR (75 MHz, $(\text{CD}_3)_2\text{CO}$) δ 153.8 (C), 133.3 (CH), 132.6 (C), 125.7 (q, $J = 3.7$ Hz, CH), 123.7 (C), 123.4 (q, $J = 272.7$ Hz, CF_3), 84.0 (C), 82.5 (C), 62.6 (CH_2), 14.3 (CH_3).

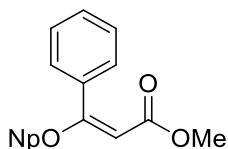


3.6a. Clear, pale yellow oil (94% yield, 15:1 E:Z); $R_f = 0.52$ (hexanes-ethyl acetate, 4:1); ^1H NMR (300 MHz, $(\text{CD}_3)_2\text{CO}$) δ 7.58 (d, $J = 9.1$ Hz, 2H, major), 7.45 (d, $J = 9.1$ Hz, 2H, minor), 7.00 (d, $J = 8.8$ Hz, 2H, major), 6.92 (d, $J = 9.1$ Hz, 2H, minor), 5.44 (s, 1H, major), 5.19 (s, 1H, minor), 4.12 (q, $J = 7.1$ Hz, 2H, major), 3.98 (q, $J = 7.1$ Hz, 2H, minor), 3.86 (s, 3H, major), 3.84 (s, 3H, minor), 3.69 (s, 2H, major), 3.65 (s, 2H, minor), 1.25 (t, $J = 7.0$ Hz, 3H, major), 1.13 (t, $J = 7.0$ Hz, 3H, minor), 1.03 (s, 9H); ^{13}C NMR (75 MHz, $(\text{CD}_3)_2\text{CO}$) δ 168.6 (C), 165.4 (C), 162.4 (C), 129.8 (CH), 128.7 (C), 114.8 (CH), 98.5 (CH), 83.2 (CH_2), 59.8 (CH_2), 55.8 (CH_3), 33.3 (C), 26.8 (CH_3), 14.8 (CH_3); IR (neat, cm^{-1}

¹) 2957 (m), 2904 (w), 2870 (w), 2839 (w), 1716 (s), 1606 (s), 1512 (s), 1253 (s), 1156 (s), 1098 (s), 1032 (m), 836 (m), 666 (w); HRMS (ESI) calcd for C₁₇H₂₄O₄ + Na⁺ 315.1567, found 315.1564.

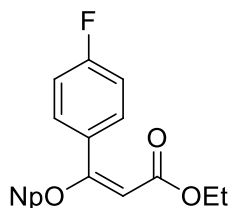


3.6b. Clear, yellow oil (99% yield, 17:1 E:Z); R_f = 0.63 (hexanes-ethyl acetate, 4:1); ¹H NMR (300 MHz, (CD₃)₂CO) δ 7.51 (d, *J* = 8.2 Hz, 2H), 7.27 (d, *J* = 7.9 Hz, 2H), 5.45 (s, 1H), 4.13 (q, *J* = 7.1 Hz, 2H), 3.67 (s, 2H), 2.37 (s, 3H), 1.25 (t, *J* = 7.2 Hz, 3H), 1.02 (s, 9H); ¹³C NMR (75 MHz, (CD₃)₂CO) δ 168.7 (C), 165.3 (C), 141.3 (C), 133.7 (C), 130.1 (CH), 128.2 (CH), 99.4 (CH), 83.1 (CH₂), 59.8 (CH₂), 33.3 (C), 26.8 (CH₃), 21.3 (CH₃), 14.8 (CH₃); IR (neat, cm⁻¹) 3030 (w), 2957 (s), 2870 (s), 1713 (s), 1621 (s), 1273 (s), 1154 (s), 1097 (s), 1040 (s), 820 (s), 727 (w); HRMS (ESI) calcd for C₁₇H₂₄O₃ + Na⁺ 299.1618, found 299.1615.

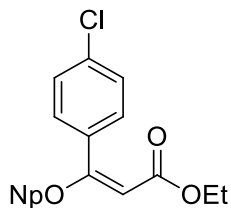


3.6d. Clear, pale yellow oil (94% yield, >20:1 E:Z); R_f = 0.42 (hexanes-ethyl acetate, 9:1); ¹H NMR (300 MHz, (CD₃)₂CO) δ 7.64–7.59 (m, 2H), 7.49–7.44 (m, 3H), 5.50 (s, 1H), 3.67 (s, 2H), 3.66 (s, 3H), 1.02 (s, 9H); ¹³C NMR (75 MHz, (CD₃)₂CO) δ 168.7 (C), 165.6 (C), 136.4 (C), 131.1 (CH), 129.5 (CH), 128.2 (CH), 99.7 (CH), 83.1 (CH₂), 51.0 (CH₃), 33.3 (C), 26.7 (CH₃); IR (neat, cm⁻¹) 3056 (w), 2955 (s), 2870 (m), 1722 (s), 1622 (s), 1275

(s), 1156 (s), 1099 (s), 1015 (m), 777 (m), 699 (m); HRMS (ESI) calcd for $C_{15}H_{20}O_3 + Na^+$ 271.1305, found 271.1305.

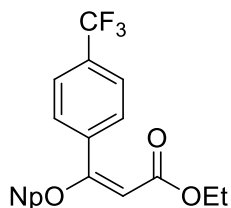


3.6e. Clear, orange oil (82% yield, 13:1 E:Z); $R_f = 0.72$ (hexanes-ethyl acetate, 4:1); 1H NMR (300 MHz, $(CD_3)_2CO$) δ 7.69 (dd, $J = 9.1, 5.3$ Hz, 2H), 7.22 (t, $J = 8.9$ Hz, 2H), 5.49 (s, 1H), 4.13 (q, $J = 7.1$ Hz, 2H), 3.68 (s, 2H), 1.25 (t, $J = 7.2$ Hz, 3H), 1.02 (s, 9H); ^{13}C NMR (75 MHz, $(CD_3)_2CO$) δ 167.2 (C), 165.2 (C), 164.7 (d, $J_{C-F} = 248.6$ Hz, CF), 132.9 (d, $J_{C-F} = 3.3$ Hz, C), 130.5 (d, $J_{C-F} = 8.3$ Hz, CH), 116.4 (d, $J_{C-F} = 22.1$ Hz, CH), 100.0 (CH), 83.3 (CH_2), 60.0 (CH_2), 33.3 (C), 26.8 (CH_3), 14.8 (CH_3); IR (neat, cm^{-1}) 2958 (s), 2871 (m), 1716 (s), 1621 (s), 1508 (s), 1261 (m), 1157 (s), 1097 (m), 1040 (w), 842 (m); HRMS (ESI) calcd for $C_{16}H_{21}FO_3 + Na^+$ 303.1367, found 303.1366.

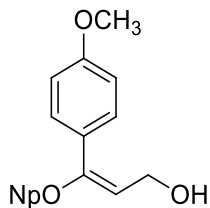


3.6f. Clear, orange oil (89% yield, 13:1 E:Z); $R_f = 0.65$ (hexanes-ethyl acetate, 4:1); 1H NMR (300 MHz, $(CD_3)_2CO$) δ 7.66 (d, $J = 8.5$ Hz, 2H), 7.49 (d, $J = 8.5$ Hz, 2H), 5.54 (s, 1H), 4.14 (q, $J = 7.1$ Hz, 2H), 3.69 (s, 2H), 1.26 (t, $J = 7.1$ Hz, 3H), 1.26 (s, 9H); ^{13}C NMR (75 MHz, $(CD_3)_2CO$) δ 166.8 (C), 165.1 (C), 136.5 (C), 135.3 (C), 129.8 (CH), 129.7 (CH), 100.5 (CH), 83.4 (CH_2), 60.1 (CH_2), 33.3 (C), 26.8 (CH_3), 14.7 (CH_3); IR (neat, cm^{-1}) 2957

(s), 2870 (m), 1716 (s), 1621 (s), 1489 (s), 1260 (s), 1161 (s), 1092 (s), 836 (s); HRMS (ESI) calcd for $C_{16}H_{21}ClO_3 + Na^+$ 319.1071, found 319.1070.

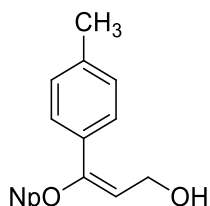


3.6g. Clear, orange oil (78% yield, >20:1 E:Z); $R_f = 0.50$ (hexanes-diethyl ether, 4:1); 1H NMR (300 MHz, $(CD_3)_2CO$) δ 7.88 (d, $J = 8.5$ Hz, 2H), 7.81 (d, $J = 8.5$ Hz, 2H), 5.65 (s, 1H), 4.16 (q, $J = 7.1$ Hz, 2H), 3.71 (s, 2H), 1.27 (t, $J = 7.0$ Hz, 3H), 1.03 (s, 9H); ^{13}C NMR (75 MHz, $(CD_3)_2CO$) δ 166.1 (C), 165.1 (C), 140.5 (C), 132.0 (q, $J_{C-F} = 32.4$ Hz, C), 128.9 (CH), 126.4 (q, $J_{C-F} = 3.7$ Hz, CH), 125.1 (q, $J_{C-F} = 271.1$ Hz, CF_3), 101.8 (CH), 83.5 (CH_2), 60.2 (CH_2), 33.3 (C), 26.7 (CH_3), 14.7 (CH_3); IR (neat, cm^{-1}) 2960 (m), 2904 (w), 2872 (w), 1717 (s), 1616 (s), 1324 (s), 1169 (s), 1130 (s), 1067 (s), 848 (w), 666 (w); HRMS (ESI) calcd for $C_{17}H_{21}F_3O_3 + Na^+$ 353.1335, found 353.1336.

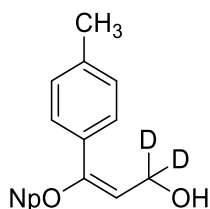


3.7a. Clear, colourless oil (97% yield, 18:1 E:Z); $R_f = 0.22$ (hexanes-ethyl acetate, 4:1); 1H NMR (300 MHz, $(CD_3)_2CO$) δ 7.41 (d, $J = 8.8$ Hz, 2H), 6.93 (d, $J = 8.8$ Hz, 2H), 5.38 (t, $J = 6.7$ Hz, 1H), 4.33 (dd, $J = 6.6, 5.7$ Hz, 2H), 3.81 (s, 3H), 3.52 (t, $J = 5.6$ Hz, 1H), 3.28 (s, 2H), 1.01 (s, 9H); ^{13}C NMR (75 MHz, $(CD_3)_2CO$) δ 160.7 (C), 155.2 (C), 129.3 (C), 128.3 (CH), 114.6 (CH), 113.6 (CH), 81.6 (CH_2), 57.3 (CH_2), 55.6 (CH_3), 33.0 (C), 26.9

(CH₃); IR (neat, cm⁻¹) 3367 (br, m), 2955 (s), 2901 (m), 2868 (m), 2825 (w), 1655 (w), 1608 (s), 1510 (s), 1249 (s), 1173 (s), 1033 (s), 967 (w), 837 (m); HRMS (ESI) calcd for C₁₅H₂₂O₃ + Na⁺ 273.1461, found 273.1462.

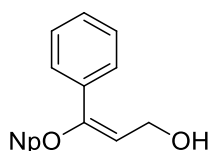


3.7b. Clear, colourless oil (82% yield, 20:1 E:Z); R_f = 0.33 (hexanes-ethyl acetate, 4:1); ¹H NMR (300 MHz, (CD₃)₂CO) δ 7.37 (d, *J* = 8.2 Hz, 2H), 7.18 (d, *J* = 7.9 Hz, 2H), 5.44 (t, *J* = 6.6 Hz, 1H), 4.34 (d, *J* = 6.7 Hz, 2H), 3.56 (br s, 1H), 3.28 (s, 2H), 2.33 (s, 3H), 1.01 (s, 9H); ¹³C NMR (75 MHz, (CD₃)₂CO) δ 155.4 (C), 138.7 (C), 134.2 (C), 129.9 (CH), 126.9 (CH), 114.6 (CH), 81.6 (CH₂), 57.3 (CH₂), 33.0 (C), 26.9 (CH₃), 21.2 (CH₃); IR (neat, cm⁻¹) 3325 (br, s), 3027 (w), 2955 (s), 2868 (s), 1652 (s), 1511 (s), 1057 (s), 1019 (s), 968 (s), 825 (s), 803 (w), 770 (w), 722 (w); HRMS (ESI) calcd for C₁₅H₂₂O₂ + Na⁺ 257.1512, found 257.1513.

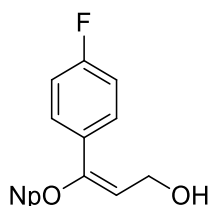


3.7b-d₂. Clear, pale yellow oil (75% yield, 14:1 E:Z); R_f = 0.30 (hexanes-dichloromethane-diethyl ether, 5:5:1); ¹H NMR (300 MHz, (CD₃)₂CO) δ 7.37 (d, *J* = 8.2 Hz, 2H), 7.18 (d, *J* = 7.9 Hz, 2H), 5.43 (s, 1H), 3.51 (br s, 1H), 3.28 (s, 2H), 2.33 (s, 3H), 1.01 (s, 9H); ¹³C NMR (75 MHz, (CD₃)₂CO) δ 155.6 (C), 138.7 (C), 134.2 (C), 129.9 (CH), 126.9 (CH),

114.4 (CH), 81.6 (CH₂), 33.0 (C), 27.0 (CH₃), 21.2 (CH₃); IR (neat, cm⁻¹) 3344 (br, s), 3027 (w), 2955 (s), 2918 (m), 2968 (m), 1651 (m), 1510 (m), 1316 (m), 1062 (m), 1019 (w), 823 (m); HRMS (ESI) calcd for C₁₅H₂₀D₂O₂ + Na⁺ 259.1637, found 259.1636.

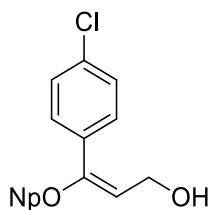


3.7d. Clear, colorless oil (98% yield, >20:1 E:Z); R_f = 0.60 (hexanes-ethyl acetate, 2:1); ¹H NMR (300 MHz, (CD₃)₂CO) δ 7.51–7.46 (m, 2H), 7.41–7.31 (m, 3H), 5.50 (t, *J* = 6.7 Hz, 1H), 4.36 (dd, *J* = 6.7, 5.6 Hz, 2H), 3.60 (t, *J* = 5.6 Hz, 1H), 3.29 (s, 2H), 1.02 (s, 9H); ¹³C NMR (75 MHz, (CD₃)₂CO) δ 155.3 (C), 137.0 (C), 129.3 (CH), 129.0 (CH), 126.9 (CH), 115.4 (CH), 81.6 (CH₂), 57.3 (CH₂), 33.0 (C), 26.9 (CH₃); IR (neat, cm⁻¹) 3338 (m, br), 3059 (w), 2956 (s), 2899 (s), 2868 (s), 1652 (m), 1363 (m), 1057 (s), 1028 (s), 755 (m), 698 (m); HRMS (ESI) calcd for C₁₄H₂₀O₂ + Na⁺ 243.1355, found 243.1355.

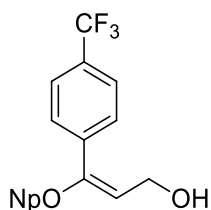


3.7e. Clear, orange-yellow oil (88% yield, 14:1 E:Z); R_f = 0.21 (hexanes-ethyl acetate, 4:1); ¹H NMR (300 MHz, (CD₃)₂CO) δ 7.52 (dd, *J* = 8.8, 5.6 Hz, 2H), 7.14 (t, *J* = 8.9 Hz, 2H), 5.48 (t, *J* = 6.6 Hz, 1H), 4.35 (dd, *J* = 6.4, 5.6 Hz, 2H), 3.63 (t, *J* = 5.6 Hz, 1H), 3.29 (s, 2H), 1.01 (s, 9H); ¹³C NMR (75 MHz, (CD₃)₂CO) δ 163.5 (d, *J*_{C-F} = 245.4 Hz, CF), 154.3 (C), 133.4 (d, *J*_{C-F} = 3.3 Hz, C), 128.9 (d, *J*_{C-F} = 8.5 Hz, CH), 116.1 (d, *J*_{C-F} = 21.4 Hz, CH), 115.4 (CH), 81.7 (CH₂), 57.3 (CH₂), 33.0 (C), 26.9 (CH₃); IR (neat, cm⁻¹) 3335 (br, s),

3048 (w), 2956 (s), 2904 (s), 2869 (s), 1652 (s), 1604 (s), 1507 (s), 1055 (s), 842 (s); HRMS (ESI) calcd for $C_{14}H_{19}FO_2 + Na^+$ 261.1261, found 261.1260.

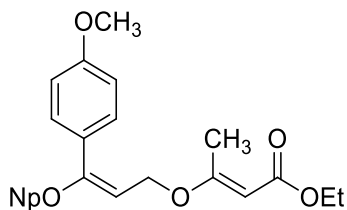


3.7f. Clear, yellow oil (99% yield, 15:1 E:Z); $R_f = 0.31$ (hexanes-ethyl acetate, 4:1); 1H NMR (300 MHz, $(CD_3)_2CO$) δ 7.51 (d, $J = 8.8$ Hz, 2H), 7.41 (d, $J = 8.8$ Hz, 2H), 5.56 (t, $J = 6.7$ Hz, 1H), 4.35 (dd, $J = 6.4, 5.6$ Hz, 2H), 3.65 (t, $J = 5.6$ Hz, 1H), 3.30 (s, 2H), 1.02 (s, 9H); ^{13}C NMR (75 MHz, $(CD_3)_2CO$) δ 154.1 (C), 135.8 (C), 134.2 (C), 129.4 (CH), 128.4 (CH), 116.2 (CH), 81.8 (CH_2), 57.2 (CH_2), 33.0 (C), 26.9 (CH_3); IR (neat, cm^{-1}) 3325 (br, m), 2956 (s), 2868 (m), 1652 (m), 1488 (s), 1092 (s), 1054 (s), 1014 (s), 966 (m), 836 (m), 789 (w); HRMS (ESI) calcd for $C_{14}H_{19}ClO_2 + Na^+$ 277.0966, found 277.0965.

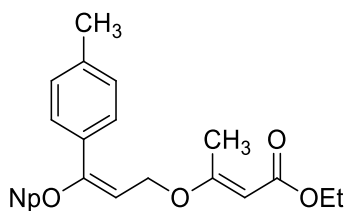


3.7g. Clear, pale yellow oil (86% yield, >20:1 E:Z); $R_f = 0.24$ (hexanes - ethyl acetate, 4:1); 1H NMR (300 MHz, $(CD_3)_2CO$) δ 7.72 (s, 4H), 5.71 (t, $J = 6.6$ Hz, 1H), 4.39 (dd, $J = 6.4, 5.6$ Hz, 2H), 3.73 (t, $J = 5.7$ Hz, 1H), 3.32 (s, 2H), 1.03 (s, 9H); ^{13}C NMR (75 MHz, $(CD_3)_2CO$) δ 153.7 (C), 140.9 (C), 130.2 (q, $J_{C-F} = 32.4$ Hz, C), 127.3 (CH), 126.2 (q, $J_{C-F} = 4.1$ Hz, CH), 125.3 (q, $J_{C-F} = 271.2$ Hz, CF_3), 118.1 (CH), 82.0 (CH_2), 57.3 (CH_2), 33.0 (C), 26.9 (CH_3); IR (neat, cm^{-1}) 3325 (br, m), 2959 (m), 2906 (m), 2871 (m), 1651 (w),

1618 (w), 1327 (s), 1128 (s), 1069 (s), 967 (w), 852 (m); LRMS (ESI) calcd for $2(\text{C}_{15}\text{H}_{19}\text{F}_3\text{O}_2) + \text{K}^+$ 615.23, found 615.33.

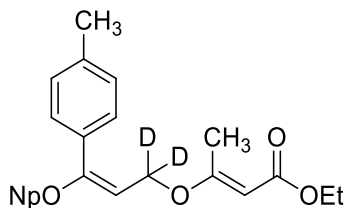


3.8a. Clear, colourless oil (99% yield, 9:1 E:Z); ^1H NMR (300 MHz, $(\text{CD}_3)_2\text{CO}$) δ 7.44 (d, $J = 8.8$ Hz, 2H), 6.96 (d, $J = 8.8$ Hz, 2H), 5.36 (t, $J = 7.0$ Hz, 1H), 5.20 (s, 1H), 4.64 (d, $J = 7.0$ Hz, 2H), 4.07 (q, $J = 7.1$ Hz, 2H), 3.83 (s, 3H), 3.34 (s, 2H), 2.27 (s, 3H), 1.22 (t, $J = 7.0$ Hz, 3H), 1.03 (s, 9H); ^{13}C NMR (75 MHz, $(\text{CD}_3)_2\text{CO}$) δ 172.4 (C), 168.1 (C), 161.2 (C), 158.9 (C), 128.8 (CH), 128.4 (C), 114.8 (CH), 106.3 (CH), 92.0 (CH), 81.6 (CH₂), 63.8 (CH₂), 59.5 (CH₂), 55.6 (CH₃), 33.0 (C), 26.9 (CH₃), 19.2 (CH₃), 14.8 (CH₃); IR (neat, cm^{-1}) 2956 (s), 2901 (m), 2869 (w), 2838 (w), 1711 (s), 1621 (s), 1511 (s), 1250 (s), 1141 (s), 1055 (s), 838 (m), 818 (m); HRMS (ESI) calcd for $\text{C}_{21}\text{H}_{30}\text{O}_5 + \text{Na}^+$ 385.1985, found 385.1984.

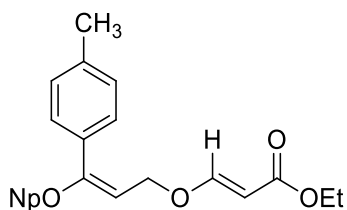


3.8b. Clear, colourless oil (100% yield, 9:1 E:Z); ^1H NMR (300 MHz, $(\text{CD}_3)_2\text{CO}$) δ 7.40 (d, $J = 8.2$ Hz, 2H), 7.22 (d, $J = 7.9$ Hz, 2H), 5.41 (t, $J = 6.9$ Hz, 1H), 5.20 (s, 1H), 4.66 (d, $J = 7.0$ Hz, 2H), 4.08 (q, $J = 7.1$ Hz, 2H), 3.34 (s, 2H), 2.35 (s, 3H), 2.27 (s, 3H), 1.22 (t, $J = 7.2$ Hz, 3H), 1.03 (s, 9H); ^{13}C NMR (75 MHz, $(\text{CD}_3)_2\text{CO}$) δ 172.3 (C), 168.1 (C), 159.0

(C), 139.6 (C), 133.3 (C), 130.0 (CH), 127.4 (CH), 107.2 (CH), 92.1 (CH), 81.6 (CH₂), 63.8 (CH₂), 59.5 (CH₂), 33.1 (C), 26.9 (CH₃), 21.2 (CH₃), 19.2 (CH₃), 14.8 (CH₃); IR (neat, cm⁻¹) 2956 (m), 2898 (m), 2869 (m), 1712 (s), 1621 (s), 1274 (m), 1142 (s), 1056 (s), 825 (m); HRMS (ESI) calcd for C₂₁H₃₀O₄ + Na⁺ 369.2036, found 369.2034.

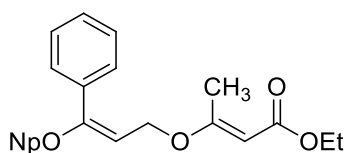


3.8b-dz. Clear, pale yellow oil (97% yield, 8:1 E:Z); ¹H NMR (500 MHz, (CD₃)₂CO) δ 7.39 (d, *J* = 8.5 Hz, 2H), 7.22 (d, *J* = 7.9 Hz, 2H), 5.41 (s, 1H), 5.20 (s, 1H), 4.07 (q, *J* = 7.1 Hz, 2H), 3.35 (s, 2H), 2.35 (s, 3H), 2.26 (s, 3H), 1.22 (t, *J* = 7.0 Hz, 3H), 1.03 (s, 9H); ¹³C NMR (125 MHz, (CD₃)₂CO) δ 172.4 (C), 168.1 (C), 159.1 (C), 139.6 (C), 133.3 (C), 130.1 (CH), 127.4 (CH), 107.1 (CH), 92.1 (CH), 81.6 (CH₂), 59.5 (CH₂), 33.1 (C), 26.9 (CH₃), 21.2 (CH₃), 19.2 (CH₃), 14.8 (CH₃); IR (neat, cm⁻¹) 2956 (m), 2869 (m), 1712 (s), 1621 (s), 1279 (m), 1144 (s), 1069 (s), 824 (m); HRMS (ESI) calcd for 2(C₂₁H₂₈D₂O₄) + Na⁺ 719.4431, found 719.4432.

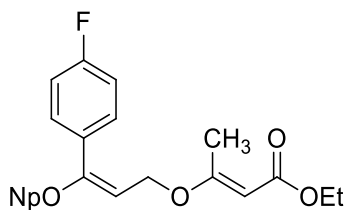


3.8c. Clear, pale yellow oil (100% yield, 9:1 E:Z); ¹H NMR (300 MHz, (CD₃)₂CO) δ 7.65 (d, *J* = 12.6 Hz, 1H), 7.40 (d, *J* = 8.2 Hz, 2H), 7.23 (d, *J* = 7.9 Hz, 2H), 5.43 (t, *J* = 7.3 Hz, 1H), 5.31 (d, *J* = 12.6 Hz, 1H), 4.72 (d, *J* = 7.3 Hz, 2H), 4.10 (q, *J* = 7.1 Hz, 2H), 3.34 (s,

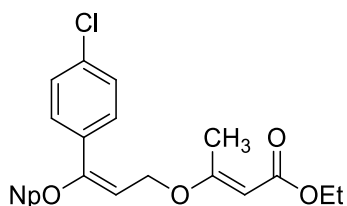
2H), 2.35 (s, 3H), 1.22 (t, $J = 7.0$ Hz, 3H), 1.03 (s, 9H); ^{13}C NMR (75 MHz, $(\text{CD}_3)_2\text{CO}$) δ 167.7 (C), 163.0 (CH), 159.8 (C), 139.7 (C), 133.1 (C), 130.1 (CH), 127.5 (CH), 106.9 (CH), 97.5 (CH), 81.7 (CH₂), 66.4 (CH₂), 59.9 (CH₂), 33.0 (C), 26.9 (CH₃), 21.2 (CH₃), 14.7 (CH₃); IR (neat, cm^{-1}) 2957 (m), 2869 (m), 1712 (s), 1639 (m), 1623 (s), 1130 (s), 1056 (s), 827 (m), 666 (m); HRMS (ESI) calcd for $\text{C}_{20}\text{H}_{28}\text{O}_4 + \text{Na}^+$ 355.1880, found 355.1880.



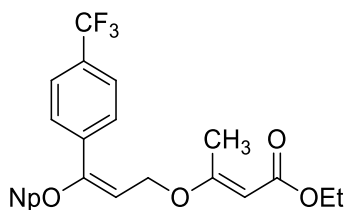
3.8d. Clear, colorless oil (98% yield, 9:1 E:Z); ^1H NMR (300 MHz, $(\text{CD}_3)_2\text{CO}$) δ 7.54–7.49 (m, 2H), 7.46–7.37 (m, 3H), 5.48 (t, $J = 7.0$ Hz, 1H), 5.21 (s, 1H), 4.68 (d, $J = 7.0$ Hz, 2H), 4.07 (q, $J = 7.1$ Hz, 2H), 3.36 (s, 2H), 2.27 (s, 3H), 1.22 (t, $J = 7.0$ Hz, 3H), 1.03 (s, 9H); ^{13}C NMR (75 MHz, $(\text{CD}_3)_2\text{CO}$) δ 172.3 (C), 168.1 (C), 158.9 (C), 136.1 (C), 129.7 (CH), 129.4 (CH), 127.4 (CH), 108.1 (CH), 92.1 (CH), 81.7 (CH₂), 63.8 (CH₂), 59.5 (CH₂), 33.1 (C), 26.9 (CH₃), 19.1 (CH₃), 14.8 (CH₃); IR (neat, cm^{-1}) 2957 (s), 2905 (m), 2869 (m), 1712 (s), 1621 (s), 1273 (s), 1141 (s), 1056 (s), 818 (m), 767 (m), 699 (m); HRMS (ESI) calcd for $\text{C}_{20}\text{H}_{28}\text{O}_4 + \text{Na}^+$ 355.1880, found 355.1878.



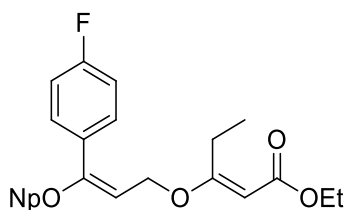
3.8e. Clear, pale yellow oil (65.5 mg, 87% yield, 7:1 E:Z); ^1H NMR (300 MHz, $(\text{CD}_3)_2\text{CO}$) δ 7.56 (dd, $J = 8.9, 5.4$ Hz, 2H), 7.18 (t, $J = 8.8$ Hz, 2H), 5.47 (t, $J = 7.0$ Hz, 1H), 5.20 (s, 1H), 4.66 (d, $J = 6.7$ Hz, 2H), 4.08 (q, $J = 7.1$ Hz, 2H), 3.35 (s, 2H), 2.27 (s, 3H), 1.22 (t, $J = 7.0$ Hz, 3H), 1.03 (s, 9H); ^{13}C NMR (75 MHz, $(\text{CD}_3)_2\text{CO}$) δ 172.9 (C), 168.1 (C), 163.9 (d, $J_{\text{C-F}} = 245.4$ Hz, CF), 157.9 (C), 132.5 (d, $J_{\text{C-F}} = 3.2$ Hz, C), 129.5 (d, $J_{\text{C-F}} = 8.6$ Hz, CH), 116.3 (d, $J_{\text{C-F}} = 22.1$ Hz, CH), 108.2 (CH), 92.2 (CH), 81.8 (CH_2), 63.7 (CH_2), 59.5 (CH_2), 33.1 (C), 26.9 (CH_3), 19.1 (CH_3), 14.8 (CH_3); IR (neat, cm^{-1}) 2958 (m), 2905 (w), 2871 (w), 1711 (s), 1622 (s), 1507 (m), 1271 (m), 1229 (m), 1141 (s), 1053 (s), 953 (w), 843 (m), 818 (m); HRMS (ESI) calcd for $\text{C}_{20}\text{H}_{27}\text{FO}_4 + \text{Na}^+$ 373.1786, found 373.1783.



3.8f. Clear, pale yellow oil (82% yield, 8:1 E:Z); ^1H NMR (300 MHz, $(\text{CD}_3)_2\text{CO}$) δ 7.53 (d, $J = 8.8$ Hz, 2H), 7.44 (d, $J = 8.8$ Hz, 2H), 5.54 (t, $J = 7.0$ Hz, 1H), 5.20 (s, 1H), 4.67 (d, $J = 7.0$ Hz, 2H), 4.08 (q, $J = 7.1$ Hz, 2H), 3.36 (s, 2H), 2.27 (s, 3H), 1.22 (t, $J = 7.0$ Hz, 3H), 1.03 (s, 9H); ^{13}C NMR (75 MHz, $(\text{CD}_3)_2\text{CO}$) δ 172.2 (C), 168.0 (C), 157.6 (C), 135.0 (C), 134.9 (C), 129.6 (CH), 128.9 (CH), 109.0 (CH), 92.2 (CH), 81.9 (CH_2), 63.6 (CH_2), 59.5 (CH_2), 33.0 (C), 26.8 (CH_3), 19.1 (CH_3), 14.8 (CH_3); IR (neat, cm^{-1}) 2957 (m), 2869 (w), 1711 (s), 1621 (s), 1272 (m), 1142 (s), 1054 (s), 839 (w), 818 (w); HRMS (ESI) calcd for $\text{C}_{20}\text{H}_{27}\text{ClO}_4 + \text{Na}^+$ 389.1490, found 389.1486.

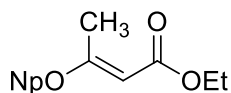


3.8g. Clear, colourless oil (99% yield, 11:1 E:Z); ^1H NMR (500 MHz, $(\text{CD}_3)_2\text{CO}$) δ 7.76 (s, 4H), 5.69 (t, $J = 6.8$ Hz, 1H), 5.21 (s, 1H), 4.71 (d, $J = 7.2$ Hz, 2H), 4.08 (q, $J = 7.2$ Hz, 2H), 3.39 (s, 2H), 2.28 (s, 3H), 1.22 (t, $J = 7.2$ Hz, 3H), 1.05 (s, 9H); ^{13}C NMR (125 MHz, $(\text{CD}_3)_2\text{CO}$) δ 172.2 (C), 168.0 (C), 157.2 (C), 140.1 (C), 130.9 (q, $J_{\text{C-F}} = 32.4$ Hz, C), 127.9 (CH), 126.4 (q, $J_{\text{C-F}} = 3.8$ Hz, CH), 125.2 (q, $J_{\text{C-F}} = 271.3$ Hz, CF_3), 110.8 (CH), 92.3 (CH), 82.0 (CH_2), 63.6 (CH_2), 59.6 (CH_2), 33.1 (C), 26.8 (CH_3), 19.1 (CH_3), 14.8 (CH_3); IR (neat, cm^{-1}) 2959 (s), 2866 (m), 1713 (s), 1622 (s), 1326 (s), 1273 (m), 1141 (s), 1068 (s), 1017 (m), 852 (w), 819 (w); HRMS (ESI) calcd for $\text{C}_{20}\text{H}_{25}\text{F}_3\text{O}_4 + \text{Na}^+$ 409.1597, found 409.1600.

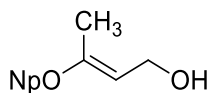


3.8h. Clear, yellow oil (88% yield, 6:1 E:Z); ^1H NMR (300 MHz, $(\text{CD}_3)_2\text{CO}$) δ 7.57 (dd, $J = 8.9, 5.4$ Hz, 2H), 7.19 (t, $J = 8.9$ Hz, 2H), 5.49 (t, $J = 6.9$ Hz, 1H), 5.14 (s, 1H), 4.66 (d, $J = 7.0$ Hz, 2H), 4.08 (q, $J = 7.0$ Hz, 2H), 3.36 (s, 2H), 2.75 (q, $J = 7.4$ Hz, 2H), 1.22 (t, $J = 7.2$ Hz, 3H), 1.09 (t, $J = 7.5$ Hz, 3H), 1.03 (s, 9H); ^{13}C NMR (75 MHz, $(\text{CD}_3)_2\text{CO}$) δ 177.1 (C), 167.8 (C), 163.9 (d, $J_{\text{C-F}} = 246.5$ Hz, CF), 158.0 (C), 132.6 (d, $J_{\text{C-F}} = 3.3$ Hz, C), 129.5 (d, $J_{\text{C-F}} = 8.0$ Hz, CH), 116.3 (d, $J_{\text{C-F}} = 22.0$ Hz, CH), 108.2 (CH), 91.3 (CH), 81.9 (CH_2), 63.7 (CH_2), 59.6 (CH_2), 33.1 (C), 26.9 (CH_3), 26.1 (CH_2), 14.8 (CH_3), 12.3 (CH_3); IR (neat, cm^{-1}) 2971 (m), 2958 (m), 2904 (w), 2870 (w), 1712 (s), 1620 (s), 1508 (s), 1377

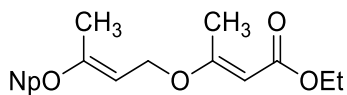
(m), 1228 (m), 1141 (s), 1053 (s), 843 (m), 822 (m); HRMS (ESI) calcd for $2(\text{C}_{21}\text{H}_{29}\text{FO}_4) + \text{Na}^+$ 751.3992, found 751.3991.



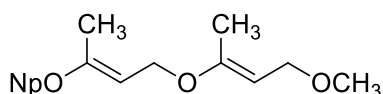
3.14. Clear, colorless oil (92% yield, >20:1 E:Z); $R_f = 0.56$ (hexanes-diethyl ether, 9:1); ^1H NMR (300 MHz, $(\text{CD}_3)_2\text{CO}$) δ 5.02 (s, 1H), 4.06 (q, $J = 7.0$ Hz, 2H), 3.48 (s, 2H), 2.27 (s, 3H), 1.20 (t, $J = 7.0$ Hz, 3H), 0.99 (s, 9H); ^{13}C NMR (75 MHz, $(\text{CD}_3)_2\text{CO}$) δ 172.8 (C), 168.1 (C), 91.8 (CH), 78.5 (CH_2), 59.5 (CH_2), 31.9 (C), 26.7 (CH_3), 18.9 (CH_3), 14.8 (CH_3); IR (neat, cm^{-1}) 2959 (m), 2871 (w), 1713 (s), 1623 (s), 1281 (m), 1139 (s), 1056 (s), 817 (w); HRMS (ESI) calcd for $\text{C}_{11}\text{H}_{20}\text{O}_3 + \text{H}^+$ 201.1485, found 201.1486.



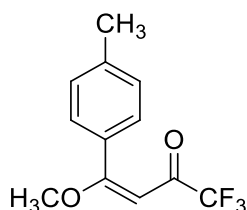
3.15. Clear, colorless oil (79% yield, >20:1 E:Z); $R_f = 0.32$ (hexanes-diethyl ether, 1:1); ^1H NMR (300 MHz, $(\text{CD}_3)_2\text{CO}$) δ 4.65 (t, $J = 7.3$ Hz, 1H), 4.04 (dd, $J = 7.3, 5.6$ Hz, 2H), 3.29 (s, 2H), 3.19 (t, $J = 5.6$ Hz, 1H), 1.80 (s, 3H), 0.95 (s, 9H); ^{13}C NMR (75 MHz, $(\text{CD}_3)_2\text{CO}$) δ 156.5 (C), 98.5 (CH), 77.1 (CH_2), 59.0 (CH_2), 31.9 (C), 26.9 (CH_3), 16.3 (CH_3); IR (neat, cm^{-1}) 3330 (br, s), 2956 (s), 2902 (s), 2870 (s), 1661 (s), 1245 (s), 1080 (s), 986 (s), 841 (w), 792 (m); HRMS (ESI) calcd for $\text{C}_9\text{H}_{18}\text{O}_2 + \text{Na}^+$ 181.1199, found 181.1201.



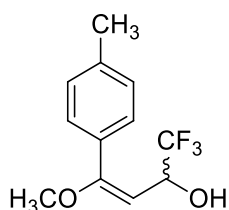
3.16. Clear, colourless oil (96% yield containing 10% Claisen rearrangement product, >20:1 E:Z); ^1H NMR (300 MHz, $(\text{CD}_3)_2\text{CO}$) δ 5.08 (s, 1H), 4.72 (t, $J = 7.6$ Hz, 1H), 4.40 (d, $J = 7.6$ Hz, 2H), 4.08 (q, $J = 7.1$ Hz, 2H), 3.38 (s, 2H), 2.25 (s, 3H), 1.88 (s, 3H), 1.23 (t, $J = 7.2$ Hz, 3H), 0.99 (s, 9H); ^{13}C NMR (75 MHz, $(\text{CD}_3)_2\text{CO}$) δ 172.6 (C), 168.1 (C), 160.0 (C), 92.3 (CH), 91.9 (CH), 77.5 (CH_2), 66.2 (CH_2), 59.4 (CH_2), 32.0 (C), 26.9 (CH_3), 19.2 (CH_3), 16.6 (CH_3), 14.8 (CH_3); IR (neat, cm^{-1}) 2957 (s), 2904 (m), 2870 (m), 1712 (s), 1664 (m), 1619 (s), 1390 (m), 1272 (m), 1212 (m), 1132 (s), 1035 (s), 939 (w), 815 (w); HRMS (ESI) calcd for $\text{C}_{15}\text{H}_{26}\text{O}_4 + \text{Na}^+$ 293.1723, found 293.1719.



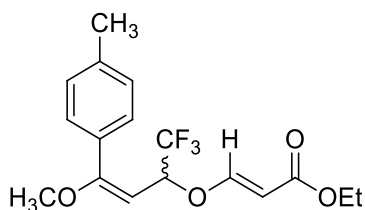
3.18. Clear, colourless oil (70% yield, >20:1 E:Z); $R_f = 0.54$ (hexanes-ethyl acetate, 4:1); ^1H NMR (300 MHz, $(\text{CD}_3)_2\text{CO}$) δ 4.67 (t, $J = 7.2$ Hz, 1H), 4.62 (t, $J = 7.2$ Hz, 1H), 4.21 (d, $J = 7.3$ Hz, 2H), 3.88 (d, $J = 7.3$ Hz, 2H), 3.34 (s, 2H), 3.21 (s, 3H), 1.83 (s, 3H), 1.78 (s, 3H), 0.96 (s, 9H); ^{13}C NMR (75 MHz, $(\text{CD}_3)_2\text{CO}$) δ 158.6 (C), 157.8 (C), 94.9 (CH), 93.5 (CH), 77.3 (CH_2), 69.2 (CH_2), 64.4 (CH_2), 56.9 (CH_3), 32.0 (C), 26.9 (CH_3), 16.8 (CH_3), 16.6 (CH_3); IR (neat, cm^{-1}) 2956 (s), 2923 (s), 2892 (s), 2869 (s), 2813 (w), 1661 (s), 1479 (m), 1389 (s), 1207 (s), 1070 (s), 1048 (s), 946 (w), 901 (w), 782 (w); HRMS (ESI) calcd for $\text{C}_{14}\text{H}_{26}\text{O}_3 + \text{Na}^+$ 265.1774, found 265.1774.



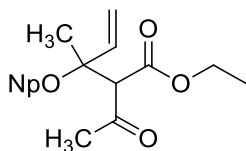
3.21b. Yellow solid (71% yield, 9:1 E:Z); ^1H NMR (300 MHz, $(\text{CD}_3)_2\text{CO}$) δ 7.68 (d, $J = 8.2$ Hz, 2H, minor), 7.43 (d, $J = 8.2$ Hz, 2H, major), 7.34 (d, $J = 7.9$ Hz, 2H, minor), 7.24 (d, $J = 8.2$ Hz, 2H, major), 6.20 (s, 1H, minor), 5.97 (s, 1H, major), 4.09 (s, 3H, minor), 4.04 (s, 3H, major), 2.41 (s, 3H, minor), 2.38 (s, 3H, major); ^{13}C NMR (75 MHz, $(\text{CD}_3)_2\text{CO}$) δ 179.6 (C), 177.6 (q, $J_{\text{C-F}} = 32.8$ Hz, C), 144.0 (C), 132.2 (C), 130.4 (CH, minor), 130.0 (CH, major), 129.4 (CH, major), 129.3 (CH, minor), 117.9 (q, $J_{\text{C-F}} = 292.6$ Hz, CF_3), 95.7 (CH, minor), 92.3 (CH, major), 63.3 (CH_3 , minor), 58.3 (CH_3 , major), 21.5 (CH_3).



3.22b. Clear, colourless oil (93% yield, 14:1 E:Z); $R_f = 0.15$ (hexanes-dichloromethane-diethyl ether, 10:4:1); ^1H NMR (300 MHz, $(\text{CD}_3)_2\text{CO}$) δ 7.40 (d, $J = 8.2$ Hz, 2H, minor), 7.34 (d, $J = 8.2$ Hz, 2H, major), 7.24 (d, $J = 7.9$ Hz, 2H, major), 7.11 (d, $J = 7.9$ Hz, 2H, minor), 5.12 (d, $J = 6.2$ Hz, 1H), 4.88 (d, $J = 10.2$ Hz, 1H), 4.51–4.38 (m, 1H), 3.72 (s, 3H, major), 3.54 (s, 3H, minor), 2.36 (s, 3H, major, minor); ^{13}C NMR (75 MHz, $(\text{CD}_3)_2\text{CO}$) δ 163.7 (C), 140.0 (C), 133.2 (C), 129.7 (CH), 129.4 (CH), 126.6 (q, $J_{\text{C-F}} = 281.2$ Hz, CF_3), 94.1 (q, $J_{\text{C-F}} = 2.2$ Hz, CH), 69.2 (q, $J_{\text{C-F}} = 31.6$ Hz, CF_3), 55.8 (CH_3), 21.3 (CH_3); IR (neat, cm^{-1}) 3391 (br, s), 3009 (w), 2942 (m), 2839 (w), 1652 (s), 1355 (s), 1270 (s), 1171 (s), 1128 (s), 1106 (s), 1038 (s), 977 (w), 857 (m), 827 (m), 743 (m), 695 (s), 668 (w); LRMS (ESI) calcd for $\text{C}_{12}\text{H}_{13}\text{F}_3\text{O}_2 + \text{H}^+$ 247.09, found 247.07.



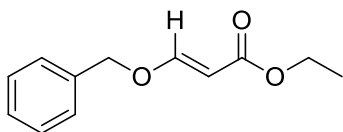
3.27. Clear, pale yellow oil (100% yield, 4:1 E:Z); $R_f = 0.35$ (hexanes-dichloromethane-diethyl ether, 10:4:1); $^1\text{H NMR}$ (300 MHz, $(\text{CD}_3)_2\text{CO}$) δ 7.38 (d, $J = 12.0$ Hz, 1H), 7.34–7.35 (m, 4H), 5.16 (d, $J = 12.3$ Hz, 1H), 5.02 (dq, $J = 10.2, 6.0$ Hz, 1H), 4.98 (d, $J = 10.2$ Hz, 1H), 4.08 (qd, $J = 7.1, 0.7$ Hz, 2H), 3.81 (s, 3H), 2.39 (s, 3H), 1.21 (t, $J = 7.2$ Hz, 3H); $^{13}\text{C NMR}$ (75 MHz, $(\text{CD}_3)_2\text{CO}$) δ 167.3 (C), 167.0 (C), 160.2 (CH), 140.7 (C), 132.4 (C), 130.2 (CH), 129.5 (CH), 124.9 (q, $J_{\text{C-F}} = 279.0$ Hz, CF_3), 100.8 (CH), 89.9 (CH), 78.6 (q, $J_{\text{C-F}} = 32.4$ Hz, CH), 60.2 (CH_2), 56.5 (CH_3), 21.3 (CH_3), 14.6 (CH_3); IR (neat, cm^{-1}) 3031 (w), 2982 (m), 2941 (m), 2841 (w), 1714 (s), 1645 (s), 1370 (m), 1322 (m), 1274 (s), 1179 (s), 1128 (s), 1043 (m), 1022 (m), 947 (m), 887 (w), 827 (m), 696 (m); HRMS (ESI) calcd for $\text{C}_{17}\text{H}_{19}\text{F}_3\text{O}_4 + \text{Na}^+$ 367.1128, found 367.1124.



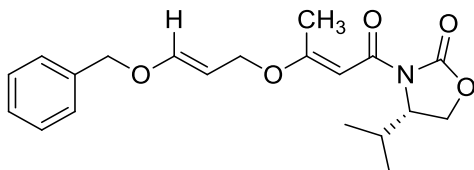
Representative Claisen Product from 3.16. Clear, colourless oil (1.00:1.74 dr⁵²); $R_f = 0.35$ (hexanes-dichloromethane-diethyl ether, 10:4:1); $^1\text{H NMR}$ (300 MHz, C_6D_6) δ 6.13 (dd, $J = 17.6, 10.8$ Hz, 1H, major), 5.91 (dd, $J = 17.9, 10.8$ Hz, 1H, minor), 5.15 (dd, $J = 17.6, 1.5$ Hz, 1H, major), 5.15 (dd, $J = 17.9, 1.3$ Hz, 1H, minor), 5.11 (dd, $J = 10.1, 1.3$ Hz, 1H, major), 5.09 (dd, $J = 10.8, 1.2$ Hz, 1H, minor), 3.91 (m, 2H major, 2H minor), 3.82 (s, 1H, minor), 3.77 (s, 1H, major), 2.89 (d, $J = 10.2$ Hz, 1H, major), 2.86 (d, $J = 10.8$ Hz, 1H, major), 2.86 (d, $J = 10.8$ Hz, 1H, minor), 2.83 (d, $J = 11.1$ Hz, 1H, minor), 2.17 (s, 3H, minor), 2.11 (s, 3H, major), 1.56 (s, 3H, minor), 1.47 (s, 3H, major), 0.92 (t, $J = 7.1$ Hz, 3H, major), 0.92 (t, $J = 7.1$ Hz, 3H, minor), 0.89 (s, 9H, major), 0.86 (s, 9H, minor); $^{13}\text{C NMR}$ (75 MHz, C_6D_6) δ 201.3 (C, minor), 200.6 (C, major), 167.5 (C, major), 167.4 (C, minor), 140.9 (CH, minor), 140.5 (CH, major), 117.0 (CH_2 , minor), 116.6 (CH_2 , major), 78.4 (C, minor), 77.9 (C, major), 72.0 (CH_2 , minor), 71.9 (CH_2 , major), 68.7 (CH, major), 68.1 (CH, minor), 60.8 (CH_2 , major), 60.7 (CH_2 , minor), 32.4 (CH_3 , minor), 31.9 (C, major), 31.7 (C, minor), 31.5 (CH_3 , major), 27.0 (CH_3), 19.9 (CH_3 , major), 18.2 (CH_3 , minor), 14.1 (CH_3); IR (neat, cm^{-1}) 2975 (m), 2955 (s), 2903 (m), 2869 (m), 1733 (s), 1716 (s), 1143 (s), 1071 (s), 927 (w); LRMS (ESI) calcd for $\text{C}_{15}\text{H}_{26}\text{O}_4 + \text{Na}^+$ 293.17, found 292.87.

⁵² Claisen rearrangement was induced at 40 °C in MeOH for a representative sample of the Claisen adduct from compound 3.16. Flash chromatography on silica gel, pretreated with 1% triethylamine, afforded a mixture of two diastereomers (1.00:1.74). The dr is not representative of the product ratio of the crude reaction mixture prior to purification.

5.9 Compounds Pertaining to Chapter 4

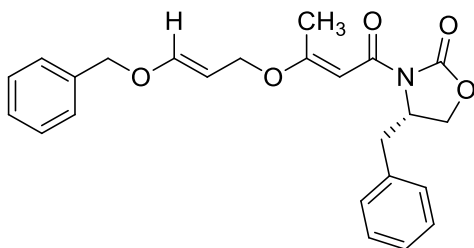


4.37a. Clear, colourless oil (100% yield); ^1H NMR (300 MHz, $(\text{CD}_3)_2\text{C}(\text{O})$) δ 7.69 (d, $J = 12.6$ Hz, 1H), 7.45–7.32 (m, 5H), 5.35 (d, $J = 12.6$ Hz, 1H), 5.01 (s, 1H), 4.11 (q, $J = 7.1$ Hz, 2H), 1.22 (t, $J = 7.2$ Hz, 3H); ^{13}C NMR (75 MHz, $(\text{CD}_3)_2\text{C}(\text{O})$) δ 167.6 (C), 162.8 (CH), 136.9 (C), 129.4 (CH), 129.1 (CH), 128.7 (CH), 98.1 (CH), 73.6 (CH_2), 60.0 (CH_2), 14.7 (CH_3); IR (neat, cm^{-1}) 3092 (w), 3066 (w), 3035 (w), 2981 (m), 2938 (w), 2905 (w), 1709 (s), 1644 (s), 1629 (s), 1455 (m), 1326 (m), 1216 (s), 1200 (s), 1132 (s), 1047 (s), 966 (m), 824 (m), 740 (m), 697 (m).

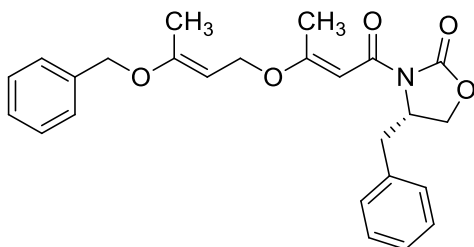


4.29a. Clear, colourless oil (99 % yield); ^1H NMR (300 MHz, C_6D_6) δ 7.16–7.04 (m, 5H), 6.38 (d, $J = 12.6$ Hz, 1H), 4.98 (dt, $J = 12.6, 7.6$ Hz, 1H), 4.41 (s, 2H), 4.22 (t, $J = 8.0$ Hz, 2H), 4.19–4.11 (m, 1H), 3.43 (dd, $J = 8.8, 2.9$ Hz, 1H), 3.25 (app t, $J = 8.6$ Hz, 1H), 2.54 (s, 3H), 2.30 (sept d, $J = 7.0, 4.5$ Hz, 1H), 0.63 (d, $J = 7.0$ Hz, 3H), 0.48 (d, $J = 7.0$ Hz, 3H); ^{13}C NMR (75 MHz, C_6D_6) δ 174.5 (C), 165.4 (C), 154.6 (C), 152.4 (CH), 137.2 (C), 128.7 (CH), 128.1 (CH), 127.8 (CH), 98.5 (CH), 92.2 (CH), 71.5 (CH_2), 67.1 (CH_2), 62.5 (CH_2), 58.4 (CH), 29.0 (CH), 20.8 (CH_3), 17.8 (CH_3), 14.7 (CH_3); IR (neat, cm^{-1}) 3127 (w), 3066 (w), 3033 (w), 2964 (m), 2930 (m), 2875 (w), 1769 (s), 1677 (s), 1656 (s), 1598 (s), 1386 (s), 1362 (s), 1299 (s), 1186 (s), 1077 (m), 1051 (m), 1032 (m), 982 (m), 938 (m),

877 (w), 717 (m), 699 (m); HRMS (ESI) calcd for $C_{20}H_{25}NO_5 + Na^+$ 382.1625, found 382.1624.

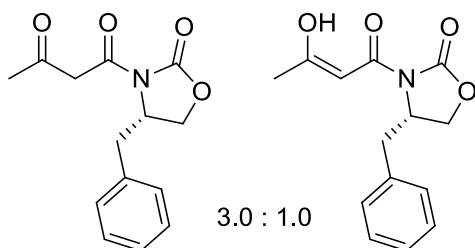


4.29b. Clear, colourless foam (94% yield); 1H NMR (300 MHz, C_6D_6) δ 7.15–6.92 (m, 10H), 6.40 (d, $J = 12.6$ Hz, 1H), 5.00 (dt, $J = 12.6, 7.6$ Hz, 1H), 4.43 (s, 2H), 4.40–4.31 (m, 1H), 4.25 (d, $J = 7.6$ Hz, 2H), 3.49 (dd, $J = 8.8, 2.9$ Hz, 1H), 3.17 (app t, $J = 8.8$ Hz, 1H), 3.12 (dd, $J = 13.2, 2.9$ Hz, 1H), 2.58 (s, 3H), 2.41 (dd, $J = 13.3, 9.5$ Hz, 1H); ^{13}C NMR (75 MHz, C_6D_6) δ 174.8 (C), 165.4 (C), 154.0 (C), 152.5 (CH), 137.1 (C), 136.5 (C), 129.7 (CH), 129.0 (CH), 128.7 (CH), 128.1 (CH), 127.8 (CH), 127.2 (CH), 98.5 (CH), 92.3 (CH), 71.5 (CH_2), 67.2 (CH_2), 65.3 (CH_2), 55.5 (CH), 38.3 (CH_2), 20.9 (CH_3); IR (neat, cm^{-1}) 3064 (w), 3030 (w), 2925 (w), 2873 (w), 1769 (s), 1674 (m), 1657 (m), 1596 (s), 1386 (m), 1349 (m), 1288 (m), 1184 (s), 1030 (m), 938 (w), 828 (w), 700 (m); HRMS (ESI) calcd for $C_{24}H_{25}NO_5 + Na^+$ 430.1625, found 430.1622.

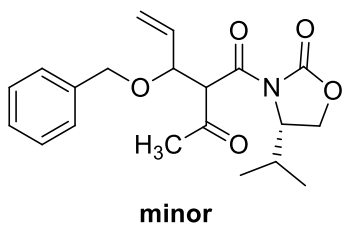


4.29d. Clear, colourless oil (74% yield, 10% Claisen); 1H NMR (300 MHz, $(CD_3)_2C(O)$) δ 7.45–7.22 (m, 10H), 6.69 (s, 1H), 4.96 (t, $J = 7.8$ Hz, 1H), 4.82 (s, 2H), 4.81–4.74 (m, 1H),

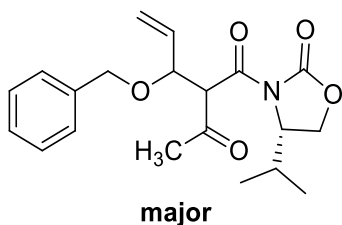
4.50 (d, $J = 7.6$ Hz, 2H), 4.30 (t, $J = 8.3$ Hz, 1H), 4.18 (dd, $J = 8.8, 2.9$ Hz, 1H), 3.23 (dd, $J = 13.3, 3.1$ Hz, 1H), 2.95 (dd, $J = 13.5, 8.8$ Hz, 1H), 2.35 (s, 3H), 1.93 (s, 3H); ^{13}C NMR (75 MHz, $(\text{CD}_3)_2\text{C}(\text{O})$) δ 174.6 (C), 166.0 (C), 159.8 (C), 154.5 (C), 138.0 (C), 137.2 (C), 130.4 (CH), 129.5 (CH), 129.2 (CH), 128.6 (CH), 128.5 (CH), 127.7 (CH), 93.1 (CH), 92.6 (CH), 69.8 (CH_2), 66.3 (CH_2), 55.8 (CH), 38.5 (CH_2), 20.6 (CH_3), 16.8 (CH_3).



4.40. Clear, yellow oil (**4.40a**:**4.40b**, 3.0:1.0); ^1H NMR (500 MHz, C_6D_6) δ 14.18 (s, 1H, minor), 7.20–6.82 (m, 5H major, 5 H minor), 4.33 (s, 1H, minor), 4.20–4.14 (m, 1H, major), 4.15–4.10 (m, 1H, minor), 3.67 (s, 2H, major), 3.43 (dd, $J = 9.3, 2.9$ Hz, 1H, minor), 3.40 (dd, $J = 9.3, 2.9$ Hz, 1H, major), 3.13 (app t, $J = 8.5$ Hz, 1H, major), 3.10–3.08 (m, 1H, minor), 3.08 (dd, $J = 13.4, 3.7$ Hz, 1H, major), 2.91 (dd, $J = 13.4, 3.2$ Hz, 1H, minor), 2.38 (dd, $J = 13.7, 9.3$ Hz, 1H, major), 2.28 (dd, $J = 13.2, 9.3$ Hz, 1H, minor), 1.78 (s, 3H, major), 1.65 (s, 3H, minor); ^{13}C NMR (125 MHz, C_6D_6) δ 200.2 (C, major), 180.7 (C, major), 171.1 (C, minor), 166.5 (C, major), 153.8 (C, major), 152.8 (C, minor), 135.9 (C, minor), 135.8 (C, major), 129.7 (CH, major), 129.6 (CH, minor), 129.0 (CH, minor), 129.0 (CH, major), 127.3 (CH, major), 127.0 (CH, minor), 90.3 (CH, minor), 66.0 (CH_2 , major), 65.5 (CH_2 , minor), 55.0 (CH, major), 54.6 (CH, minor), 51.4 (CH_2 , major), 37.9 (CH_2 , minor), 37.7 (CH_2 , major), 29.5 (CH_3 , major), 21.7 (CH_3 , minor); HRMS (ESI) calcd for $\text{C}_{14}\text{H}_{15}\text{NO}_4 + \text{Na}^+$ 284.0893, found 284.0891.

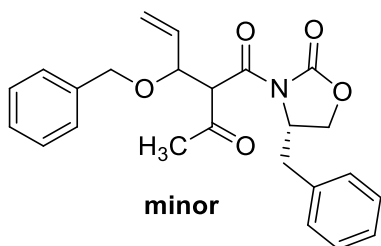


4.39a. Clear, colourless oil; $R_f = 0.45$ (hexanes-dichloromethane-diethyl ether, 4:4:1); ^1H NMR (300 MHz, C_6D_6) δ 7.24–7.03 (m, 5H), 5.88 (ddd, $J = 17.3, 10.2, 7.0$ Hz, 1H), 5.42 (ddd, $J = 17.3, 1.8, 0.9$ Hz, 1H), 5.14 (ddd, $J = 10.4, 1.9, 0.9$ Hz, 1H), 5.10 (s, 1H), 4.80 (ddt, $J = 8.5, 7.0, 0.9$ Hz, 1H), 4.46 (d, $J = 11.4$ Hz, 1H), 4.18 (d, $J = 11.4$ Hz, 1H), 3.83 (ddd, $J = 8.5, 3.8, 2.9$ Hz, 1H), 3.31 (dd, $J = 9.1, 2.9$ Hz, 1H), 3.07 (app t, $J = 8.8$ Hz, 1H), 2.47 (s, 3H), 2.27 (sept d, $J = 6.9, 4.1$ Hz, 1H), 0.62 (d, $J = 7.0$ Hz, 3H), 0.37 (d, $J = 7.0$ Hz, 3H); ^{13}C NMR (75 MHz, C_6D_6) δ 202.4 (C), 166.8 (C), 154.2 (C), 138.5 (C), 137.2 (CH), 128.6 (CH), 128.0 (CH), 127.7 (CH), 119.0 (CH_2), 79.4 (CH), 71.3 (CH_2), 63.5 (CH), 63.1 (CH_2), 58.5 (CH), 32.7 (CH), 28.4 (CH_3), 17.5 (CH_3), 14.5 (CH_3); HRMS (ESI) calcd for $\text{C}_{20}\text{H}_{25}\text{NO}_5 + \text{Na}^+$ 382.1625, found 382.1628.

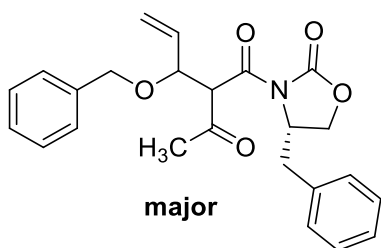


4.39a. Clear, colourless oil; $R_f = 0.30$ (hexanes-dichloromethane-diethyl ether, 4:4:1); ^1H NMR (300 MHz, C_6D_6) δ 7.24–7.04 (m, 5H), 5.78 (ddd, $J = 17.3, 10.2, 7.2$ Hz, 1H), 5.32 (ddd, $J = 17.6, 1.5, 0.9$ Hz, 1H), 5.30 (s, 1H), 5.06 (ddd, $J = 10.5, 1.8, 0.9$ Hz, 1H), 4.79 (ddt, $J = 8.6, 7.2, 0.9$ Hz, 1H), 4.44 (d, $J = 11.7$ Hz, 1H), 4.17 (d, $J = 11.7$ Hz, 1H), 3.90 (dt, $J = 8.5, 3.7$ Hz, 1H), 3.28 (dd, $J = 9.1, 3.2$ Hz, 1H), 3.12 (app t, $J = 8.8$ Hz, 1H), 2.44

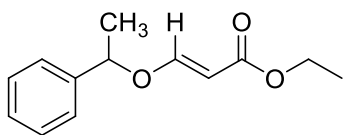
(s, 3H), 2.07 (sept d, $J = 7.0, 3.8$ Hz, 1H), 0.47 (d, $J = 6.7$ Hz, 3H), 0.34 (d, $J = 7.0$ Hz, 3H); ^{13}C NMR (75 MHz, C_6D_6) δ 202.1 (C), 166.9 (C), 154.4 (C), 138.5 (C), 136.9 (CH), 128.6 (CH), 128.0 (CH), 127.7 (CH), 119.2 (CH_2), 80.0 (CH), 71.3 (CH_2), 63.6 (CH), 63.0 (CH_2), 58.5 (CH), 32.4 (CH), 28.4 (CH_3), 17.4 (CH_3), 14.5 (CH_3); HRMS (ESI) calcd for $\text{C}_{20}\text{H}_{25}\text{NO}_5 + \text{Na}^+$ 382.1625, found 382.1628.



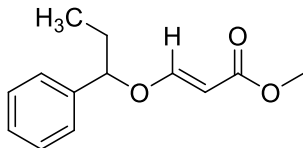
4.39b. Clear, colourless oil; $R_f = 0.40$ (hexanes-dichloromethane-diethyl ether, 4:4:1); ^1H NMR (300 MHz, C_6D_6) δ 7.26–6.94 (m, 8H), 6.87–6.82 (m, 2H), 5.90 (ddd, $J = 17.3, 10.2, 7.0$ Hz, 1H), 5.44 (ddd, $J = 17.3, 1.8, 0.9$ Hz, 1H), 5.19–5.14 (m, 1H), 5.13 (d, $J = 8.5$ Hz, 1H), 4.88–4.81 (m, 1H), 4.48 (d, $J = 11.4$ Hz, 1H), 4.21 (d, $J = 11.4$ Hz, 1H), 4.08 (ddt, $J = 9.4, 7.9, 2.9$ Hz, 1H), 3.38 (dd, $J = 8.8, 2.6$ Hz, 1H), 3.08 (dd, $J = 13.5, 3.2$ Hz, 1H), 3.00 (app t, $J = 8.5$ Hz, 1H), 2.49 (s, 3H), 2.35 (dd, $J = 13.5, 9.4$ Hz, 1H); ^{13}C NMR (75 MHz, C_6D_6) δ 202.1 (C), 166.7 (C), 153.6 (C), 138.4 (C), 137.0 (CH), 135.8 (C), 129.8 (CH), 129.0 (CH), 128.6 (CH), 128.1 (CH), 127.9 (CH), 127.3 (CH), 119.2 (CH_2), 79.6 (CH), 71.3 (CH_2), 65.9 (CH_2), 63.4 (CH), 55.3 (CH), 37.4 (CH_2), 32.7 (CH_3); HRMS (ESI) calcd for $\text{C}_{24}\text{H}_{25}\text{NO}_5 + \text{Na}^+$ 430.1625, found 430.1621.



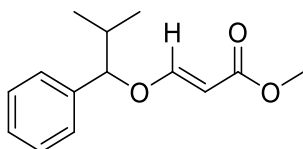
4.39b. Clear, colourless oil; $R_f = 0.28$ (hexanes-dichloromethane-diethyl ether, 4:4:1); ^1H NMR (300 MHz, C_6D_6) δ 7.22–6.94 (m, 8H), 6.82–6.76 (m, 2H), 5.85 (ddd, $J = 17.4, 10.2, 7.2$ Hz, 1H), 5.34 (ddd, $J = 17.3, 1.8, 0.9$ Hz, 1H), 5.23 (d, $J = 8.8$ Hz, 1H), 5.09 (ddd, $J = 10.2, 1.8, 0.9$ Hz, 1H), 4.80 (ddt, $J = 8.5, 7.0, 0.9$ Hz, 1H), 4.44 (d, $J = 11.7$ Hz, 1H), 4.17 (d, $J = 11.4$ Hz, 1H), 4.17–4.10 (m, 1H), 3.31 (dd, $J = 9.1, 3.2$ Hz, 1H), 3.05 (app t, $J = 8.6$ Hz, 1H), 2.81 (dd, $J = 13.5, 3.2$ Hz, 1H), 2.40 (s, 3H), 2.25 (dd, $J = 13.5, 9.1$ Hz, 1H); ^{13}C NMR (75 MHz, C_6D_6) δ 202.1 (C), 167.1 (C), 153.8 (C), 138.4 (C), 137.0 (CH), 135.6 (C), 129.6 (CH), 129.0 (CH), 128.6 (CH), 128.1 (CH), 127.9 (CH), 127.4 (CH), 119.3 (CH_2), 79.9 (CH), 71.3 (CH_2), 65.9 (CH_2), 63.7 (CH), 55.0 (CH), 37.5 (CH_2), 32.5 (CH_3); HRMS (ESI) calcd for $\text{C}_{24}\text{H}_{25}\text{NO}_5 + \text{Na}^+$ 430.1625, found 430.1621.



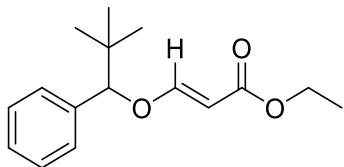
4.55a. Clear, pale yellow oil; $R_f = 0.38$ (hexanes-ethyl acetate, 9:1); ^1H NMR (300 MHz, $(\text{CD}_3)_2\text{CO}$) δ 7.53 (d, $J = 12.3$ Hz, 1H), 7.42–7.28 (m, 5H), 5.28 (q, $J = 6.4$ Hz, 1H), 5.20 (d, $J = 12.3$ Hz, 1H), 4.04 (qd, $J = 7.1, 1.2$ Hz, 2H), 1.57 (d, $J = 6.4$ Hz, 3H), 1.17 (t, $J = 7.0$ Hz, 3H); ^{13}C NMR (75 MHz, $(\text{CD}_3)_2\text{CO}$) δ 167.6 (C), 162.2 (CH), 142.8 (C), 129.6 (CH), 128.9 (CH), 126.8 (CH), 98.9 (CH), 81.0 (CH), 59.9 (CH_2), 23.6 (CH_3), 14.7 (CH_3).



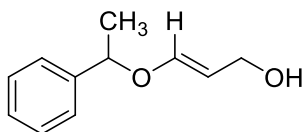
4.55b. Clear, colorless oil; ^1H NMR (300 MHz, $(\text{CD}_3)_2\text{CO}$) δ 7.53 (d, $J = 12.3$ Hz, 1H), 7.44-7.29 (m, 5H), 5.20 (d, $J = 12.3$ Hz, 1H), 5.03 (dd, $J = 7.2, 6.0$ Hz, 1H), 3.56 (s, 3H), 2.03-1.76 (m, 2H), 0.92 (t, $J = 7.3$ Hz, 3H); ^{13}C NMR (75 MHz, $(\text{CD}_3)_2\text{CO}$) δ 168.1 (C), 162.7 (CH), 141.4 (C), 129.5 (CH), 129.0 (CH), 127.3 (CH), 98.5 (CH), 86.5 (CH), 51.0 (CH₃), 31.1 (CH₂), 10.1 (CH₃); IR (neat, cm^{-1}) 3034 (w), 2971 (m), 2942 (m), 2876 (w), 1714 (s), 1644 (s), 1625 (s), 1436 (w), 1289 (w), 1196 (s), 1141 (s), 1049 (w), 833 (w), 752 (w), 701 (s); HRMS (ESI) calcd for $\text{C}_{13}\text{H}_{16}\text{O}_3 + \text{Na}^+$ 243.0992, found 243.0989.



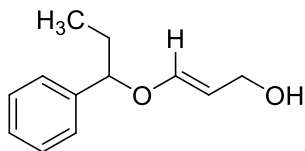
4.55c. Clear, colorless oil; $R_f = 0.38$ (hexanes-ethyl acetate, 4:1); ^1H NMR (300 MHz, $(\text{CD}_3)_2\text{CO}$) δ 7.52 (d, $J = 12.6$ Hz, 1H), 7.43-7.29 (m, 5H), 5.19 (d, $J = 12.3$ Hz, 1H), 4.81 (d, $J = 7.0$ Hz, 1H), 3.55 (s, 3H), 2.12 (octet, $J = 6.8$ Hz, 1H), 1.01 (d, $J = 6.7$ Hz, 3H), 0.82 (d, $J = 6.7$ Hz, 3H); ^{13}C NMR (75 MHz, $(\text{CD}_3)_2\text{CO}$) δ 168.1 (C), 162.9 (CH), 140.3 (C), 129.3 (CH), 128.9 (CH), 127.9 (CH), 98.4 (CH), 90.3 (CH), 51.0 (CH₃), 35.2 (CH), 18.9 (CH₃), 18.5 (CH₃); IR (neat, cm^{-1}) 3031 (m), 2964 (s), 2876 (m), 1713 (s), 1645 (s), 1455 (m), 1436 (m), 1285 (m), 1198 (s), 1134 (s), 1049 (m), 988 (m), 832 (m), 756 (m), 702 (s); HRMS (ESI) calcd for $\text{C}_{14}\text{H}_{18}\text{O}_3 + \text{Na}^+$ 257.1148, found 257.1154.



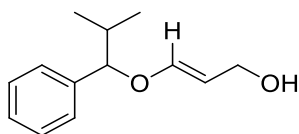
4.55d. Clear, colorless oil (100 % yield); $R_f = 0.32$ (hexanes-ethyl acetate, 2:1); $^1\text{H NMR}$ (300 MHz, $(\text{CD}_3)_2\text{CO}$) δ 7.50 (d, $J = 12.6$ Hz, 1H), 7.41-7.28 (m, 5H), 5.14 (d, $J = 12.3$ Hz, 1H), 4.83 (s, 1H), 4.02 (q, $J = 7.1$ Hz, 1H), 4.01 (q, $J = 7.1$ Hz, 1H), 1.15 (t, $J = 7.0$ Hz, 3H), 0.96 (s, 9H); $^{13}\text{C NMR}$ (75 MHz, $(\text{CD}_3)_2\text{CO}$) δ 167.6 (C), 162.8 (CH), 138.7 (C), 128.9 (CH), 128.8 (CH), 128.7 (CH), 98.8 (CH), 92.0 (CH), 59.9 (CH_2), 36.2 (C), 26.2 (CH_3), 14.6 (CH_3); IR (neat, cm^{-1}) 3031 (w), 2976 (s), 2901 (m), 2872 (m), 1711 (s), 1643 (s), 1624 (s), 1367 (m), 1132 (s), 1046 (m), 958 (m), 834 (m), 742 (m), 703 (s); HRMS (ESI) calcd for $\text{C}_{16}\text{H}_{22}\text{O}_3 + \text{Na}^+$ 285.1461, found 285.1460.



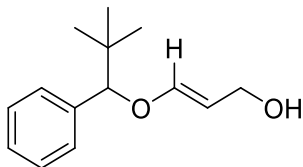
4.56a. Clear, colorless oil; $R_f = 0.33$ (hexanes-ethyl acetate, 9:1); $^1\text{H NMR}$ (300 MHz, $(\text{CD}_3)_2\text{CO}$) δ 7.40-7.23 (m, 5H), 6.37 (dt, $J = 12.3, 1.2$ Hz, 1H), 5.01 (dt, $J = 12.6, 7.1$ Hz, 1H), 4.92 (q, $J = 6.4$ Hz, 1H), 3.87 (ddd, $J = 7.0, 5.9, 1.2$ Hz, 2H), 3.30 (t, $J = 5.7$ Hz, 1H), 1.46 (d, $J = 6.4$ Hz, 3H); $^{13}\text{C NMR}$ (75 MHz, $(\text{CD}_3)_2\text{CO}$) δ 148.3 (CH), 144.2 (C), 129.3 (CH), 128.3 (CH), 126.7 (CH), 107.1 (CH), 78.6 (CH), 60.1 (CH_2), 24.0 (CH_3); IR (neat, cm^{-1}) 3356 (br, s), 3060 (w), 2978 (s), 2872 (s), 1671 (s), 1640 (s), 1450 (m), 1170 (s), 1069 (m), 997 (s), 726 (m), 701 (s); HRMS (ESI) calcd for $\text{C}_{11}\text{H}_{14}\text{O}_2 + \text{Na}^+$ 201.0886, found 201.0890.



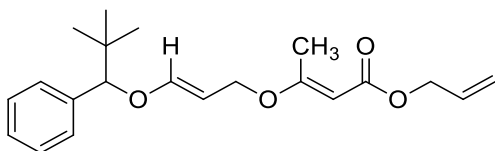
4.56b. Clear, colorless oil; ^1H NMR (300 MHz, $(\text{CD}_3)_2\text{CO}$) δ 7.40–7.24 (m, 5H), 6.36 (dt, $J = 12.6, 1.2$ Hz, 1H), 4.99 (dt, $J = 12.4, 7.1$ Hz, 1H), 4.68 (dd, $J = 7.0, 6.1$ Hz, 1H), 3.85 (ddd, $J = 6.9, 5.7, 1.2$ Hz, 2H), 3.27 (t, $J = 5.6$ Hz, 1H), 1.93–1.65 (m, 2H), 0.88 (t, $J = 7.3$ Hz, 3H); ^{13}C NMR (75 MHz, $(\text{CD}_3)_2\text{CO}$) δ 148.7 (CH), 142.9 (C), 129.2 (CH), 128.3 (CH), 127.3 (CH), 106.9 (CH), 84.1 (CH), 60.1 (CH_2), 31.5 (CH_2), 10.2 (CH_3); IR (neat, cm^{-1}) 3348 (br, s), 3066 (w), 3030 (w), 2967 (s), 2877 (s), 1671 (s), 1647 (s), 1453 (m), 1171 (s), 998 (s), 926 (s), 751 (m), 701 (s); HRMS (ESI) calcd for $\text{C}_{12}\text{H}_{16}\text{O}_2 + \text{Na}^+$ 215.1042, found 215.1044.



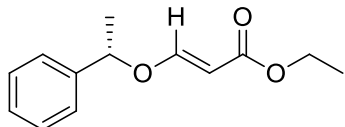
4.56c. Clear, colorless oil; $R_f = 0.45$ (hexanes-ethyl acetate, 2:1); ^1H NMR (300 MHz, $(\text{CD}_3)_2\text{CO}$) δ 7.40–7.24 (m, 5H), 6.34 (dt, $J = 12.6, 1.2$ Hz, 1H), 4.98 (dt, $J = 12.3, 7.0$ Hz, 1H), 4.46 (d, $J = 7.0$ Hz, 1H), 3.83 (ddd, $J = 7.0, 5.8, 1.1$ Hz, 2H), 3.26 (t, $J = 5.7$ Hz, 1H), 2.09–1.92 (m, 1H), 0.96 (d, $J = 6.7$ Hz, 3H), 0.79 (d, $J = 6.7$ Hz, 3H); ^{13}C NMR (75 MHz, $(\text{CD}_3)_2\text{CO}$) δ 149.0 (CH), 141.7 (C), 128.9 (CH), 128.3 (CH), 128.0 (CH), 106.8 (CH), 88.0 (CH), 60.1 (CH_2), 35.4 (CH), 19.1 (CH_3), 18.5 (CH_3); IR (neat, cm^{-1}) 3348 (br, s), 3030 (w), 2961 (s), 2873 (s), 1670 (s), 1652 (s), 1453 (m), 1169 (s), 1002 (s), 927 (s), 754 (m), 701 (s); HRMS (ESI) calcd for $\text{C}_{13}\text{H}_{18}\text{O}_2 + \text{Na}^+$ 229.1199, found 229.1199.



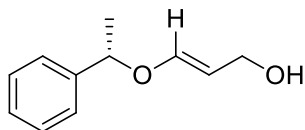
4.56d. Clear, pale yellow oil; ^1H NMR (300 MHz, $(\text{CD}_3)_2\text{CO}$) δ 7.37–7.24 (m, 5H), 6.31 (dt, $J = 12.3, 1.2$ Hz, 1H), 4.95 (dtd, $J = 12.3, 7.0, 0.6$ Hz, 1H), 4.46 (s, 1H), 3.82 (ddd, $J = 7.0, 5.6, 1.2$ Hz, 2H), 3.26 (t, $J = 5.6$ Hz, 1H), 0.92 (s, 9H); ^{13}C NMR (75 MHz, $(\text{CD}_3)_2\text{CO}$) δ 149.1 (CH), 140.0 (C), 129.0 (CH), 128.4 (CH), 128.2 (CH), 106.8 (CH), 90.3 (CH), 60.1 (CH_2), 36.1 (C), 26.4 (CH_3); IR (neat, cm^{-1}) 3348 (br, m), 3030 (w), 2956 (s), 2870 (s), 1670 (s), 1651 (s), 1453 (m), 1364 (m), 1164 (s), 1000 (s), 926 (m), 742 (s), 703 (s); HRMS (ESI) calcd for $\text{C}_{14}\text{H}_{20}\text{O}_2 + \text{Na}^+$ 243.1355, found 243.1356.



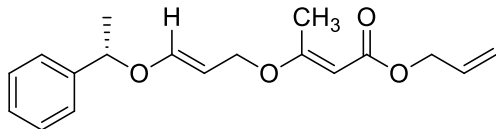
4.53d. Clear, colourless oil; ^1H NMR (300 MHz, C_6D_6) δ 7.23–7.09 (m, 5H), 6.13 (d, $J = 12.3$ Hz, 1H), 5.91 (ddt, $J = 17.3, 10.5, 5.6$ Hz, 1H), 5.25 (dq, $J = 17.0, 1.7$ Hz, 1H), 5.06 (dq, $J = 10.4, 1.5$ Hz, 1H), 5.04 (s, 1H), 5.00 (dt, $J = 12.4, 7.5$ Hz, 1H), 4.65 (dt, $J = 5.6, 1.5$ Hz, 2H), 4.18 (s, 1H), 3.69–3.56 (m, 2H), 2.40 (s, 3H), 0.94 (s, 9H); ^{13}C NMR (75 MHz, CDCl_3) δ 172.4 (C), 167.2 (C), 151.4 (CH), 138.8 (C), 133.8 (CH), 128.4 (CH), 128.0 (CH), 127.9 (CH), 117.1 (CH_2), 100.2 (CH), 91.5 (CH), 90.4 (CH), 66.4 (CH_2), 64.1 (CH_2), 35.6 (C), 26.1 (CH_3), 19.3 (CH_3); IR (neat, cm^{-1}) 3065 (w), 2956 (m), 2871 (m), 1712 (s), 1674 (m), 1651 (m), 1619 (s), 1453 (m), 1394 (m), 1364 (m), 1268 (m), 1141 (s), 1038 (s), 995 (m), 930 (m), 815 (m), 742 (m), 704 (m).



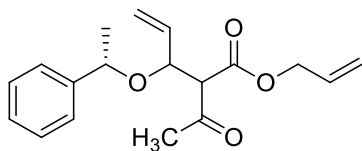
4.55e. Clear, colourless oil (100% yield; 18:1 *E:Z*); ^1H NMR (300 MHz, $(\text{CD}_3)_2\text{C}(\text{O})$) δ 7.54 (d, $J = 12.6$ Hz, 1H), 7.42–7.29 (m, 5H), 5.28 (q, $J = 6.5$ Hz, 1H), 5.20 (d, $J = 12.3$ Hz, 1H), 4.04 (q, $J = 7.1$ Hz, 1H), 4.04 (q, $J = 7.0$ Hz, 1H), 1.57 (d, $J = 6.7$ Hz, 3H), 1.17 (t, $J = 7.2$ Hz, 3H); ^{13}C NMR (75 MHz, $(\text{CD}_3)_2\text{C}(\text{O})$) δ 167.6 (C), 162.2 (CH), 142.8 (C), 129.6 (CH), 128.9 (CH), 126.8 (CH), 98.9 (CH), 81.1 (CH), 59.9 (CH_2), 23.6 (CH_3), 14.7 (CH_3); IR (neat, cm^{-1}) 3060 (w), 3034 (w), 2981 (m), 2934 (w), 1709 (s), 1643 (s), 1625 (s), 1451 (m), 1369 (m), 1324 (m), 1283 (m), 1196 (s), 1136 (s), 1069 (s), 833 (w), 762 (w), 700 (s); HRMS (ESI) calcd for $\text{C}_{13}\text{H}_{16}\text{O}_3 + \text{Na}^+$ 243.0992, found 243.0990.



4.56e. Clear, colourless oil (66% yield); ^1H NMR (300 MHz, $(\text{CD}_3)_2\text{C}(\text{O})$) δ 7.37–7.24 (m, 5H), 6.37 (dt, $J = 12.3, 1.2$ Hz, 1H), 5.01 (dt, $J = 12.4, 7.1$ Hz, 1H), 4.93 (q, $J = 6.5$ Hz, 1H), 3.87 (ddd, $J = 7.0, 5.9, 1.2$ Hz, 2H), 3.32 (t, $J = 5.6$ Hz, 1H), 1.45 (d, $J = 6.4$ Hz, 3H); ^{13}C NMR (75 MHz, $(\text{CD}_3)_2\text{C}(\text{O})$) δ 148.4 (CH), 144.2 (C), 129.2 (CH), 128.3 (CH), 126.7 (CH), 107.1 (CH), 178.6 (CH), 60.1 (CH_2), 24.0 (CH_3); IR (neat, cm^{-1}) 3357 (br, s), 3060 (m), 3032 (m), 2978 (s), 2930 (s), 2872 (s), 1671 (vs), 1651 (vs), 1495 (m), 1451 (s), 1375 (s), 1211 (s), 1170 (vs), 1069 (s), 997 (s), 929 (s), 762 (s), 701 (s), 666 (w); HRMS (ESI) calcd for $\text{C}_{11}\text{H}_{14}\text{O}_2 + \text{Na}^+$ 201.0886, found 201.0888.



4.53f. Clear, yellow oil (85% yield); ^1H NMR (500 MHz, $(\text{CD}_3)_2\text{CO}$) δ 7.39–7.27 (m, 5H), 6.62 (dt, $J = 12.3, 0.8$ Hz, 1H), 5.94 (ddt, $J = 17.3, 10.5, 5.5$ Hz, 1H), 5.28 (dq, $J = 17.5, 1.7$ Hz, 1H), 5.16 (dq, $J = 10.3, 1.5$ Hz, 1H), 5.08–5.01 (m, 2H), 5.04 (s, 1H), 4.53 (dt, $J = 5.6, 1.6$ Hz, 2H), 4.23 (d, $J = 7.5$ Hz, 2H), 2.19 (s, 3H), 1.50 (d, $J = 6.4$ Hz, 3H); ^{13}C NMR (125 MHz, $(\text{CD}_3)_2\text{CO}$) δ 127.8 (C), 167.7 (C), 152.0 (CH), 143.8 (C), 134.5 (CH), 129.4 (CH), 128.5 (CH), 126.7 (CH), 117.4 (CH_2), 100.6 (CH), 91.5 (CH), 79.2 (CH), 67.2 (CH_2), 64.3 (CH_2), 23.9 (CH_3), 19.2 (CH_3); IR (neat, cm^{-1}) 3065 (w), 3030 (w), 2980 (m), 2931 (m), 2881 (w), 1712 (s), 1674 (s), 1615 (s), 1451 (m), 1378 (m), 1268 (s), 1185 (s), 1129 (s), 1036 (s), 996 (s), 933 (s), 816 (m), 762 (m), 701 (s); HRMS (ESI) calcd for $\text{C}_{18}\text{H}_{22}\text{O}_4 + \text{Na}^+$ 325.1410, found 325.1404.



4.57f. Clear, yellow oil (96% mr; 3.52:1.00 dr; 13% alcohol elim.); ^1H NMR (300 MHz, CDCl_3) δ 7.41–7.18 (m, 5H, major; 5H, minor), 5.94–5.70 (m, 2H, minor), 5.87 (ddd, $J = 17.2, 10.3, 5.8$ Hz, 1H, major), 5.63 (ddd, $J = 17.3, 10.1, 7.3$ Hz, 1H, major), 5.40–5.08 (m, 4H, major; 4H, minor), 4.67–4.48 (m, 3H, minor), 4.58 (dt, $J = 5.7, 1.4$ Hz, 2H, major), 4.53 (q, $J = 6.3$ Hz, 1H, major), 3.79 (d, $J = 9.4$ Hz, 1H, major), 3.67 (d, $J = 9.4$ Hz, 1H, minor), 2.37 (s, 3H, major), 2.17 (s, 3H, minor), 1.39 (d, $J = 6.4$ Hz, 3H, minor), 1.38 (d, $J = 6.4$ Hz, 3H, major); ^{13}C NMR (75 MHz, CDCl_3) δ 201.5 (C, major), 201.4 (C, minor),

166.7 (C, minor), 166.6 (C, major), 144.3 (C, major), 142.3 (C, minor), 135.7 (CH, major), 135.5 (CH, minor), 131.6 (CH), 128.6 (CH, minor), 128.3 (CH, major), 127.4 (CH, major), 126.9 (CH, minor), 126.3 (CH, major), 125.5 (CH, minor), 120.4 (CH₂, minor), 119.2 (CH₂, major), 119.0 (CH₂, major), 118.9 (CH₂, minor), 78.0 (CH, major), 76.7 (CH, minor), 76.0 (CH, major), 74.9 (CH, minor), 66.0 (CH₂, major), 65.9 (CH₂, minor), 65.2 (CH, minor), 64.6 (CH, major), 31.4 (CH₃, major), 30.2 (CH₃, minor), 24.0 (CH₃, minor), 22.1 (CH₃, major); IR (neat, cm⁻¹) 3086 (w), 3065 (w), 3029 (w), 2976 (m), 2930 (w), 2892 (w), 1749 (s), 1716 (s), 1648 (w), 1454 (m), 1422 (m), 1358 (s), 1185 (s), 1081 (s), 1032 (s), 989 (s), 935 (s), 763 (s), 701 (s).

Bibliography

1. Lipinski CA (2004) Lead- and drug-like compounds: the rule-of-five revolution. *Drug Discovery Today: Technologies* 1(4):337-341.
2. Welsch ME, Snyder SA, & Stockwell BR (2010) Privileged scaffolds for library design and drug discovery. *Current Opinion in Chemical Biology* 14(3):347-361.
3. Lander ES (2004) *Nat Rev Drug Discov* 3(9):730-730.
4. Roughley SD & Jordan AM (2011) The Medicinal Chemist's Toolbox: An Analysis of Reactions Used in the Pursuit of Drug Candidates. *Journal of Medicinal Chemistry* 54(10):3451-3479.
5. Ritchie TJ & Macdonald SJF (2009) The impact of aromatic ring count on compound developability – are too many aromatic rings a liability in drug design? *Drug Discovery Today* 14(21–22):1011-1020.
6. Lipinski CA, Lombardo F, Dominy BW, & Feeney PJ (1997) Experimental and computational approaches to estimate solubility and permeability in drug discovery and development settings. *Advanced Drug Delivery Reviews* 23(1–3):3-25.
7. Veber DF, *et al.* (2002) Molecular Properties That Influence the Oral Bioavailability of Drug Candidates. *Journal of Medicinal Chemistry* 45(12):2615-2623.
8. Feher M & Schmidt JM (2002) Property Distributions: Differences between Drugs, Natural Products, and Molecules from Combinatorial Chemistry. *Journal of Chemical Information and Computer Sciences* 43(1):218-227.
9. Lovering F, Bikker J, & Humblet C (2009) Escape from Flatland: Increasing Saturation as an Approach to Improving Clinical Success. *Journal of Medicinal Chemistry* 52(21):6752-6756.
10. Ritchie TJ, Macdonald SJF, Young RJ, & Pickett SD (2011) The impact of aromatic ring count on compound developability: further insights by examining carbo- and hetero-aromatic and -aliphatic ring types. *Drug Discovery Today* 16(3–4):164-171.
11. Kombarov R, *et al.* (2010) BioCores: identification of a drug/natural product-based privileged structural motif for small-molecule lead discovery. *Mol Divers* 14(1):193-200.
12. Kirschning A & Hahn F (2012) Merging Chemical Synthesis and Biosynthesis: A New Chapter in the Total Synthesis of Natural Products and Natural Product Libraries. *Angewandte Chemie International Edition* 51(17):4012-4022.

13. Arya P, Joseph R, Gan Z, & Rakic B (2005) Exploring New Chemical Space by Stereocontrolled Diversity-Oriented Synthesis. *Chemistry & Biology* 12(2):163-180.
14. Dandapani S & Marcaurelle LA (2010) Current strategies for diversity-oriented synthesis. *Current Opinion in Chemical Biology* 14(3):362-370.
15. Rathke MW & Lindert A (1971) Reaction of lithium N-isopropylcyclohexylamide with esters. Method for the formation and alkylation of ester enolates. *Journal of the American Chemical Society* 93(9):2318-2320.
16. Ireland RE & Mueller RH (1972) Claisen rearrangement of allyl esters. *Journal of the American Chemical Society* 94(16):5897-5898.
17. Ireland RE, Wipf P, & Armstrong JD (1991) Stereochemical control in the ester enolate Claisen rearrangement. 1. Stereoselectivity in silyl ketene acetal formation. *The Journal of Organic Chemistry* 56(2):650-657.
18. Ireland RE & Vevert J-P (1981) Synthèse totale des acides (+) et (-) nonactique à partir de carbohydrates. *Canadian Journal of Chemistry* 59(3):572-583.
19. Ireland RE, Wuts PGM, & Ernst B (1981) 3-Acyltetramic acid antibiotics. 1. Synthesis of tirandamycic acid. *Journal of the American Chemical Society* 103(11):3205-3207.
20. Ireland RE & Daub JP (1981) The synthesis of chiral subunits for macrolide synthesis: the Prelog-Djerassi lactone and derivatives. *The Journal of Organic Chemistry* 46(3):479-485.
21. Ireland RE, Thaisrivongs S, & Wilcox CS (1980) Total synthesis of lasalocid A (X537A). *Journal of the American Chemical Society* 102(3):1155-1157.
22. Ireland RE, Wilcox CS, Thaisrivongs S, & Vanier NR (1979) The generation of C-glycosides through the enolate Claisen rearrangement. *Canadian Journal of Chemistry* 57(13):1743-1745.
23. Ireland RE, *et al.* (1983) The total synthesis of ionophore antibiotics. A convergent synthesis of lasalocid A (X537A). *Journal of the American Chemical Society* 105(7):1988-2006.
24. Becker D & Kazmaier U (2013) Synthesis of Tubuphenylalanines via Ireland–Claisen Rearrangement. *The Journal of Organic Chemistry* 78(1):59-65.
25. Ritter K (1990) Claisen rearrangement of organotin compounds. *Tetrahedron Letters* 31(6):869-872.

26. Sparks MA & Panek JS (1991) Claisen rearrangements of enantiomerically pure C3-(acyloxy)-(E)-vinylsilanes. *The Journal of Organic Chemistry* 56(10):3431-3438.
27. Ireland RE, Mueller RH, & Willard AK (1976) The ester enolate Claisen rearrangement. Stereochemical control through stereoselective enolate formation. *Journal of the American Chemical Society* 98(10):2868-2877.
28. Gül Ş, Schoenebeck F, Aviyente V, & Houk KN (2010) Computational Study of Factors Controlling the Boat and Chair Transition States of Ireland–Claisen Rearrangements. *The Journal of Organic Chemistry* 75(6):2115-2118.
29. Araoz R, *et al.* (2011) Total Synthesis of Pinnatoxins A and G and Revision of the Mode of Action of Pinnatoxin A. *Journal of the American Chemical Society* 133(27):10499-10511.
30. Feldman KS & Selfridge BR (2013) Synthesis Studies on the Lomaiviticin A Aglycone Core: Development of a Divergent, Two-Directional Strategy. *The Journal of Organic Chemistry* 78(9):4499-4511.
31. Akahori Y, Yamakoshi H, Sawayama Y, Hashimoto S, & Nakamura S (2014) Synthesis of Chiral Building Blocks for Oxygenated Terpenoids through a Simultaneous and Stereocontrolled Construction of Contiguous Quaternary Stereocenters by an Ireland–Claisen Rearrangement. *The Journal of Organic Chemistry* 79(2):720-735.
32. Penner M, Rauniyar V, Kaspar LT, & Hall DG (2009) Catalytic Asymmetric Synthesis of Palmerolide A via Organoboron Methodology. *Journal of the American Chemical Society* 131(40):14216-14217.
33. Faulkner DJ & Petersen MR (1969) A synthesis of trans-trisubstituted olefins using the claisen rearrangement. *Tetrahedron Letters* 10(38):3243-3246.
34. Johnson WS, *et al.* (1970) Simple stereoselective version of the Claisen rearrangement leading to trans-trisubstituted olefinic bonds. Synthesis of squalene. *Journal of the American Chemical Society* 92(3):741-743.
35. House HO, Crumrine DS, Teranishi AY, & Olmstead HD (1973) Chemistry of carbanions. XXIII. Use of metal complexes to control the aldol condensation. *Journal of the American Chemical Society* 95(10):3310-3324.
36. Ireland RE & Wilcox CS (1977) A stereoselective method for the generation of aldol-type systems. *Tetrahedron Letters* 18(33):2839-2842.

37. Ireland RE, Thaisrivongs S, Vanier N, & Wilcox CS (1980) Enolate Claisen rearrangement of esters from furanoid and pyranoid glycols. *The Journal of Organic Chemistry* 45(1):48-61.
38. Haga M & Ness RK (1965) Preparation and Properties of 3,5-Di-O-p-anisoyl-1,2-dideoxy-D-erythro-pentofuranos-1-ene. Various p-Anisoylated Derivatives of D-Ribofuranose 1a. *The Journal of Organic Chemistry* 30(1):158-162.
39. Kosower EM & Sorensen TS (1963) Some Unsaturated Imines. *The Journal of Organic Chemistry* 28(3):692-695.
40. Xiao Q, *et al.* (2013) Enantioselective synthesis of tatanans A–C and reinvestigation of their glucokinase-activating properties. *Nat Chem* 5(5):410-416.
41. Song Y, Hwang S, Gong P, Kim D, & Kim S (2007) Stereoselective Total Synthesis of (–)-Perrottetinene and Assignment of Its Absolute Configuration. *Organic Letters* 10(2):269-271.
42. Kesava Reddy N, Vijaykumar BVD, & Chandrasekhar S (2012) Formal Synthesis of Antiplatelet Drug, Beraprost. *Organic Letters* 14(1):299-301.
43. Davies SG, Fletcher AM, Roberts PM, Thomson JE, & Zammit CM (2013) Asymmetric syntheses of enantiopure C(5)-substituted transpentacins via diastereoselective Ireland-Claisen rearrangements. *Chemical Communications* 49(63):7037-7039.
44. Ko H, Kim E, Park JE, Kim D, & Kim S (2003) Total Synthesis of Pancratistatin Relying on the [3,3]-Sigmatropic Rearrangement. *The Journal of Organic Chemistry* 69(1):112-121.
45. Ireland RE, Wipf P, & Xiang JN (1991) Stereochemical control in the ester enolate Claisen rearrangement. 2. Chairlike vs boatlike transition-state selection. *The Journal of Organic Chemistry* 56(11):3572-3582.
46. Cave RJ, Lythgoe B, Metcalfe DA, & Waterhouse I (1977) Stereochemical aspects of some Claisen rearrangements with cyclic orthoesters. *Journal of the Chemical Society, Perkin Transactions 1* (10):1218-1228.
47. Ireland RE & Vevert JP (1980) A chiral total synthesis of (–)- and (+)-nonactic acids from carbohydrate precursors and the definition of the transition for the enolate claisen rearrangement in heterocyclic systems. *The Journal of Organic Chemistry* 45(21):4259-4260.
48. Gajewski JJ & Emrani J (1984) Origin of the rate acceleration in the Ireland-Claisen rearrangement. *Journal of the American Chemical Society* 106(19):5733-5734.

49. Curran DP & Young-Ger S (1984) Synthetic application of a substituent controlled claisen rearrangement. Preparation of advanced chiral intermediates for the synthesis of pseudomonic acids. *Tetrahedron Letters* 25(38):4179-4182.
50. Curran DP (1982) An approach to the enantiocontrolled synthesis of pseudomonic acids via a novel mono—claisen rearrangement. *Tetrahedron Letters* 23(42):4309-4310.
51. Curran DP & Suh Y-G (1987) Selective mono-claisen rearrangement of carbohydrate glycals. A chemical consequence of the vinylogous anomeric effect. *Carbohydrate Research* 171(1):161-191.
52. Burrows CJ & Carpenter BK (1981) Substituent effects on the aliphatic Claisen rearrangement. 1. Synthesis and rearrangement of cyano-substituted allyl vinyl ethers. *Journal of the American Chemical Society* 103(23):6983-6984.
53. Burrows C & Carpenter BK (1981) Substituent effects on the aliphatic Claisen rearrangements. 2. Theoretical analysis. *Journal of the American Chemical Society* 103(23):6984-6986.
54. Curran DP & Suh YG (1984) Substituent effects on the Claisen rearrangement. The accelerating effect of a 6-donor substituent. *Journal of the American Chemical Society* 106(17):5002-5004.
55. Denmark SE & Dappen MS (1984).alpha.-Chloro ketoximes as precursors of nitrosoalkenes: preparation, stereochemistry and conformation. *The Journal of Organic Chemistry* 49(5):798-806.
56. Gajewski JJ & Conrad ND (1979) Variable transition state structure in 3,3-sigmatropic shifts from .alpha.-secondary deuterium isotope effects. *Journal of the American Chemical Society* 101(22):6693-6704.
57. McMichael KD & Korver GL (1979) Secondary deuterium isotope effects and transition state structure in the aromatic Claisen rearrangement. *Journal of the American Chemical Society* 101(10):2746-2747.
58. Gajewski JJ & Conrad ND (1979) Aliphatic Claisen rearrangement transition state structure from secondary .alpha.-deuterium isotope effects. *Journal of the American Chemical Society* 101(10):2747-2748.
59. Vittorelli P, Winkler T, Hansen HJ, & Schmid H (1968) Stereochemie des Übergangszustandes aliphatischer CLAISEN-Umlagerungen. Vorläufige Mitteilung. *Helvetica Chimica Acta* 51(6):1457-1461.
60. Hansen HJ & Schmid H (1974) Stereochemie von [3.3]- und [5.5]-sigmatropischen umlagerungen. *Tetrahedron* 30(13):1959-1969.

61. Vance RL, *et al.* (1988) Transition structures for the Claisen rearrangement. *Journal of the American Chemical Society* 110(7):2314-2315.
62. Wiest O, Black KA, & Houk KN (1994) Density Functional Theory Isotope Effects and Activation Energies for the Cope and Claisen Rearrangements. *Journal of the American Chemical Society* 116(22):10336-10337.
63. Dewar MJS & Healy EF (1984) Ground states of molecules. 68. MNDO study of the Claisen rearrangement. *Journal of the American Chemical Society* 106(23):7127-7131.
64. Dewar MJS & Jie C (1989) Mechanism of the Claisen rearrangement of allyl vinyl ethers. *Journal of the American Chemical Society* 111(2):511-519.
65. Gajewski JJ, Gee KR, & Jurayj J (1990) Energetic and rate effects of the trifluoromethyl group at C-2 and C-4 on the aliphatic Claisen rearrangement. *The Journal of Organic Chemistry* 55(6):1813-1822.
66. Gajewski JJ & Brichford NL (1994) Secondary Deuterium Kinetic Isotope Effects in the Aqueous Claisen Rearrangement: evidence against an Ionic Transition State. *Journal of the American Chemical Society* 116(7):3165-3166.
67. Yoo HY & Houk KN (1994) Transition Structures and Kinetic Isotope Effects for the Claisen Rearrangement. *Journal of the American Chemical Society* 116(26):12047-12048.
68. Gajewski JJ, *et al.* (1987) The mechanism of rearrangement of chorismic acid and related compounds. *Journal of the American Chemical Society* 109(4):1170-1186.
69. Coates RM, Rogers BD, Hobbs SJ, Curran DP, & Peck DR (1987) Synthesis and Claisen rearrangement of alkoxyallyl enol ethers. Evidence for a dipolar transition state. *Journal of the American Chemical Society* 109(4):1160-1170.
70. Copley SD & Knowles JR (1987) The conformational equilibrium of chorismate in solution: implications for the mechanism of the non-enzymic and the enzyme-catalyzed rearrangement of chorismate to prephenate. *Journal of the American Chemical Society* 109(16):5008-5013.
71. Houk KN, Li Y, & Evanseck JD (1992) Transition Structures of Hydrocarbon Pericyclic Reactions. *Angewandte Chemie International Edition in English* 31(6):682-708.
72. Yoo HY & Houk KN (1997) Theory of Substituent Effects on Pericyclic Reaction Rates: Alkoxy Substituents in the Claisen Rearrangement. *Journal of the American Chemical Society* 119(12):2877-2884.

73. Sehgal A, Shao L, & Gao J (1995) Transition Structure and Substituent Effects on Aqueous Acceleration of the Claisen Rearrangement. *Journal of the American Chemical Society* 117(45):11337-11340.
74. Grieco PA, Brandes EB, McCann S, & Clark JD (1989) Water as a solvent for the Claisen rearrangement: practical implications for synthetic organic chemistry. *The Journal of Organic Chemistry* 54(25):5849-5851.
75. Severance DL & Jorgensen WL (1992) Effects of hydration on the Claisen rearrangement of allyl vinyl ether from computer simulations. *Journal of the American Chemical Society* 114(27):10966-10968.
76. Lubineau A, Augé J, Bellanger N, & Caillebourdin S (1990) Water-promoted claisen sigmatropic rearrangement using glyco-organic substrates. Chiral auxiliary-mediated induction. *Tetrahedron Letters* 31(29):4147-4150.
77. Cramer CJ & Truhlar DG (1992) What causes aqueous acceleration of the Claisen rearrangement? *Journal of the American Chemical Society* 114(23):8794-8799.
78. Curran DP & Kuo LH (1995) Acceleration of a dipolar Claisen rearrangement by Hydrogen bonding to a soluble diaryl¹urea. *Tetrahedron Letters* 36(37):6647-6650.
79. Uyeda C & Jacobsen EN (2008) Enantioselective Claisen Rearrangements with a Hydrogen-Bond Donor Catalyst. *Journal of the American Chemical Society* 130(29):9228-9229.
80. Tellam JP & Carbery DR (2010) Development of the Ireland–Claisen Rearrangement of Alkoxy- and Aryloxy-Substituted Allyl Glycinates. *The Journal of Organic Chemistry* 75(22):7809-7821.
81. Tellam JP, Kociok-Köhn G, & Carbery DR (2008) An Ireland–Claisen Approach to β -Alkoxy α -Amino Acids. *Organic Letters* 10(22):5199-5202.
82. Davies KA & Wulff JE (2011) Marrying Iterative Synthesis to Cascading Radical Cyclization: 6-endo/5-exo Radical Cascade across Bis-Vinyl Ethers. *Organic Letters* 13(20):5552-5555.
83. O'Rourke NF, Davies KA, & Wulff JE (2012) Cascading Radical Cyclization of Bis-Vinyl Ethers: Mechanistic Investigation Reveals a 5-exo/3-exo/retro-3-exo/5-exo Pathway. *The Journal of Organic Chemistry* 77(19):8634-8647.
84. O'Rourke NF & Wulff JE (2014) Investigation of quantitative structure-reactivity relationships in the aliphatic Claisen rearrangement of bis-vinyl ethers reveals a dipolar, dissociative mechanism. *Organic & Biomolecular Chemistry* 12(8):1292-1308.

85. Davies KA, Kou KGM, & Wulff JE (2011) Oxygen-containing analogues of juvenile hormone III. *Tetrahedron Letters* 52(18):2302-2305.
86. Felix RJ, Munro-Leighton C, & Gagné MR (2014) Electrophilic Pt(II) Complexes: Precision Instruments for the Initiation of Transformations Mediated by the Cation–Olefin Reaction. *Accounts of Chemical Research*.
87. Toullec PY, Blarre T, & Michelet V (2009) Mimicking Polyolefin Carbocyclization Reactions: Gold-Catalyzed Intramolecular Phenoxycyclization of 1,5-Enynes. *Organic Letters* 11(13):2888-2891.
88. Corey EJ & Wood HB (1996) A New Strategy for Stereocontrol of Cation–Olefin Cyclization. The First Chemical Emulation of the A/B-trans-9,10-syn-Folding Pathway of Steroid Biosynthesis from 2,3-Oxidosqualene. *Journal of the American Chemical Society* 118(47):11982-11983.
89. Rendler S & MacMillan DWC (2010) Enantioselective Polyene Cyclization via Organo-SOMO Catalysis. *Journal of the American Chemical Society* 132(14):5027-5029.
90. Lecker SH, Nguyen NH, & Vollhardt KPC (1986) Cobalt-catalyzed one-step assembly of B-ring aromatic steroids from acyclic precursors. *Journal of the American Chemical Society* 108(4):856-858.
91. Kotora M, Hessler F, & Eignerová B (2012) Transition-Metal-Mediated or -Catalyzed Syntheses of Steroids and Steroid-Like Compounds. *European Journal of Organic Chemistry* 2012(1):29-42.
92. Pattenden G, Stoker DA, & Thomson NM (2007) Cascade radical-mediated cyclisations with conjugated ynone electrophores. An approach to the synthesis of steroids and other novel ring-fused polycyclic carbocycles. *Organic & Biomolecular Chemistry* 5(11):1776-1788.
93. Urabe H & Kuwajima I (1986) A radical cyclization between enol silyl ethers and aryl or alkenyl bromide moieties. *Tetrahedron Letters* 27(12):1355-1358.
94. Walkup RD, Kane RR, & Obeyesekere NU (1990) An α -alkylation/reduction of ketones via radical cyclizations of β -chloroethylsilyl enol ethers. *Tetrahedron Letters* 31(11):1531-1534.
95. Zlotorzynska M, Zhai H, & Sammis GM (2008) Chemoselective Oxygen-Centered Radical Cyclizations onto Silyl Enol Ethers. *Organic Letters* 10(21):5083-5086.
96. Rueda-Becerril M, Leung JCT, Dunbar CR, & Sammis GM (2011) Alkoxy Radical Cyclizations onto Silyl Enol Ethers Relative to Alkene Cyclization, Hydrogen

Atom Transfer, and Fragmentation Reactions. *The Journal of Organic Chemistry* 76(19):7720-7729.

97. Zhai H, Zlotorzynska M, & Sammis G (2009) Construction of protected hydroxylated pyrrolidines using nitrogen-centered radical cyclizations. *Chemical Communications* (38):5716-5718.
98. Zlotorzynska M, Zhai H, & Sammis GM (2009) Unique Diastereoselectivity Trends in Aminyl Radical Cyclizations onto Silyl Enol Ethers. *The Journal of Organic Chemistry* 75(3):864-872.
99. Kim S, Kim KH, & Cho JR (1997) The effect of α -alkoxy group in radical-mediated β -fragmentation reactions. *Tetrahedron Letters* 38(22):3915-3918.
100. Baldwin JE (1976) Rules for ring closure. *Journal of the Chemical Society, Chemical Communications* (18):734-736.
101. Beckwith ALJ, Easton CJ, & Serelis AK (1980) Some guidelines for radical reactions. *Journal of the Chemical Society, Chemical Communications* (11):482-483.
102. Beckwith ALJ & Schiesser CH (1985) Regio- and stereo-selectivity of alkenyl radical ring closure: A theoretical study. *Tetrahedron* 41(19):3925-3941.
103. Spellmeyer DC & Houk KN (1987) Force-field model for intramolecular radical additions. *The Journal of Organic Chemistry* 52(6):959-974.
104. Tripp JC, Schiesser CH, & Curran DP (2005) Stereochemistry of Hexenyl Radical Cyclizations with tert-Butyl and Related Large Groups: Substituent and Temperature Effects. *Journal of the American Chemical Society* 127(15):5518-5527.
105. Handa S & Pattenden G (1999) Novel cascade of seven radical-mediated 6-endo-trig cyclisations leading to a unique all-trans, anti heptacycle. *Journal of the Chemical Society, Perkin Transactions 1* (8):843-846.
106. Boger DL & Mathvink RJ (1990) Tandem free-radical alkene addition reactions of acyl radicals. *Journal of the American Chemical Society* 112(10):4003-4008.
107. Batsanov A, Chen L, Gill GB, & Pattenden G (1996) Acyl radical-mediated polyene cyclisations directed towards steroid ring synthesis. *Journal of the Chemical Society, Perkin Transactions 1* (1):45-55.
108. Boehm HM, *et al.* (2000) Cascade radical cyclisations leading to steroid ring constructions. Regio- and stereo-chemical studies using ester- and fluoro-alkene

- substituted polyene acyl radical intermediates. *Journal of the Chemical Society, Perkin Transactions 1* (20):3522-3538.
109. Dess DB & Martin JC (1991) A useful 12-I-5 triacetoxypersulfonamide (the Dess-Martin persulfonamide) for the selective oxidation of primary or secondary alcohols and a variety of related 12-I-5 species. *Journal of the American Chemical Society* 113(19):7277-7287.
 110. Chen YK, Yoshida M, & MacMillan DWC (2006) Enantioselective Organocatalytic Amine Conjugate Addition. *Journal of the American Chemical Society* 128(29):9328-9329.
 111. Allin SM, Thomas CI, Doyle K, & Elsegood MRJ (2004) An Asymmetric Synthesis of Both Enantiomers of the Indole Alkaloid Deplancheine. *The Journal of Organic Chemistry* 70(1):357-359.
 112. Evans PA, Murthy VS, Roseman JD, & Rheingold AL (1999) Enantioselective Total Synthesis of the Nonisoprenoid Sesquiterpene (-)-Kumausallene. *Angewandte Chemie International Edition* 38(21):3175-3177.
 113. Evans PA, Raina S, & Ahsan K (2001) Intramolecular addition of acyl radicals to [small alpha]-substituted vinylogous carbonates: demonstrating the effect of ring size on acyclic stereocontrol. *Chemical Communications* (23):2504-2505.
 114. Chatgililoglu C, Crich D, Komatsu M, & Ryu I (1999) Chemistry of Acyl Radicals. *Chemical Reviews* 99(8):1991-2070.
 115. De Vleeschouwer F, Van Speybroeck V, Waroquier M, Geerlings P, & De Proft F (2007) Electrophilicity and Nucleophilicity Index for Radicals. *Organic Letters* 9(14):2721-2724.
 116. Handa S, Nair PS, & Pattenden G (2000) Novel Regio- and Stereoselective Cascade 6-endo-trig Cyclisations from Polyene Acyl Radical Intermediates Leading to Steroid-Like Pentacycles and Heptacycles. *Helvetica Chimica Acta* 83(9):2629-2643.
 117. Sato K & Sasaki M (2007) Convergent synthesis of the BCDEFGHIJ-ring polyether core of gambieric acids, potent antifungal polycyclic ethers. *Tetrahedron* 63(26):5977-6003.
 118. Yoshikai K, Hayama T, Nishimura K, Yamada K-i, & Tomioka K (2004) Thiol-Catalyzed Acyl Radical Cyclization of Alkenals. *The Journal of Organic Chemistry* 70(2):681-683.
 119. Carpenter AJ & Chadwick DJ (1985) Chemoselective protection of heteroaromatic aldehydes as imidazolidine derivatives : Preparation of 5-substituted furan- and

- thiophene-2-carboxaldehydes via metallo-imidazolidine intermediates. *Tetrahedron* 41(18):3803-3812.
120. Reece CA, Rodin JO, Brownlee RG, Duncan WG, & Silverstein RM (1968) Synthesis of the principal components of the sex attractant from male *Ips confusus* frass: 2-methyl-6-methylene-7-octen-4-ol, 2-methyl-6-methylene-2,7-octadien-4-ol, and (+)-cis-verbenol. *Tetrahedron* 24(11):4249-4256.
 121. Lillie BM & Avery MA (1994) The protection of ketones and aldehydes as 4-trimethylsilylmethyl-1,3-dioxolanes. *Tetrahedron Letters* 35(7):969-972.
 122. Wang P, *et al.* (2008) Sequential Removal of Photolabile Protecting Groups for Carbonyls with Controlled Wavelength. *The Journal of Organic Chemistry* 73(16):6152-6157.
 123. Wang P, Wang Y, Hu H, & Liang X (2009) Installation of Photolabile Carbonyl-Protecting Groups under Neutral Conditions without Using Any Other Chemical Reagents. *European Journal of Organic Chemistry* 2009(2):208-211.
 124. Ko HM, *et al.* (2009) Total Synthesis of (–)-Amphidinolide K. *Angewandte Chemie International Edition* 48(13):2364-2366.
 125. Leeuwenburgh MA, *et al.* (2000) Radical Cyclization of Sugar-Derived β -(Alkynyloxy)acrylates: Synthesis of Novel Fused Ethers. *Organic Letters* 2(9):1275-1277.
 126. J. Maguire R, P. Munt S, & J. Thomas E (1998) An approach to the C(10)-C(16) fragment of the bryostatins: stereoselective exocyclic double-bond formation by vinyl radical cyclization. *Journal of the Chemical Society, Perkin Transactions 1* (17):2853-2864.
 127. Munt SP & Thomas EJ (1989) Stereoselective exocyclic double bond formation via vinyl radical cyclization. *Journal of the Chemical Society, Chemical Communications* (8):480-482.
 128. Ghosh AK, *et al.* (2010) Design and Synthesis of Potent HIV-1 Protease Inhibitors Incorporating Hexahydrofuropyranol-Derived High Affinity P2 Ligands: Structure–Activity Studies and Biological Evaluation. *Journal of Medicinal Chemistry* 54(2):622-634.
 129. Stewart AM, Meier K, Schulz B, Steinert M, & Snider BB (2010) Synthesis and Biological Evaluation of (\pm)-Dinemasone C and Analogues. *The Journal of Organic Chemistry* 75(17):6057-6060.

130. Zhang C, *et al.* (2009) Discovery of okilactomycin and congeners from *Streptomyces scabrisporus* by antisense differential sensitivity assay targeting ribosomal protein S4. *J Antibiot* 62(2):55-61.
131. Dat NT, *et al.* (2008) Phenolic Constituents of *Amorpha fruticosa* That Inhibit NF- κ B Activation and Related Gene Expression. *Journal of Natural Products* 71(10):1696-1700.
132. Fathi AR, Krautheim A, Kaap S, Eger K, & Steinfelder HJ (2000) Michael adducts of ascorbic acid as inhibitors of protein phosphatase 2A and inducers of apoptosis. *Bioorganic & Medicinal Chemistry Letters* 10(14):1605-1608.
133. Zhang M, Liu N, & Tang W (2013) Stereoselective Total Synthesis of Hainanolidol and Harringtonolide via Oxidopyrylium-Based [5 + 2] Cycloaddition. *Journal of the American Chemical Society* 135(33):12434-12438.
134. Spence JTJ & George JH (2013) Biomimetic Total Synthesis of ent-Penilactone A and Penilactone B. *Organic Letters* 15(15):3891-3893.
135. Wu G, *et al.* (2012) Penilactones A and B, two novel polyketides from Antarctic deep-sea derived fungus *Penicillium crustosum* PRB-2. *Tetrahedron* 68(47):9745-9749.
136. El-Elimat T, *et al.* (2013) Waol A, trans-dihydrowaol A, and cis-dihydrowaol A: polyketide-derived γ -lactones from a *Volutella* species. *Tetrahedron Letters* 54(32):4300-4302.
137. Abdelkafi H, Herson P, & Nay B (2012) Asymmetric Synthesis of the Oxygenated Polycyclic System of (+)-Harringtonolide. *Organic Letters* 14(5):1270-1273.
138. Lu P, Gu Z, & Zakarian A (2013) Total Synthesis of Maoecrystal V: Early-Stage C-H Functionalization and Lactone Assembly by Radical Cyclization. *Journal of the American Chemical Society* 135(39):14552-14555.
139. Tenenbaum JM, Morris WJ, Custar DW, & Scheidt KA (2011) Synthesis of (-)-Okilactomycin by a Prins-Type Fragment-Assembly Strategy. *Angewandte Chemie International Edition* 50(26):5892-5895.
140. Qin S, *et al.* (2009) Two New Fusidilactones from the Fungal Endophyte *Fusidium* sp. *European Journal of Organic Chemistry* 2009(19):3279-3284.
141. Deshmukh SK, *et al.* (2009) Anti-Inflammatory and Anticancer Activity of Ergoflavin Isolated from an Endophytic Fungus. *Chemistry & Biodiversity* 6(5):784-789.

142. Seaforth CE, Mohammed S, Maxwell A, Tinto WF, & Reynolds WF (1992) Mabiocide A, a new saponin from *Colubrina elliptica*. *Tetrahedron Letters* 33(29):4111-4114.
143. Krohn K, *et al.* (2002) Fusidilactones, a New Group of Polycyclic Lactones from an Endophyte, *Fusidium* sp. *European Journal of Organic Chemistry* 2002(14):2331-2336.
144. Gao X, Nakadai M, & Snider BB (2003) Synthesis of (-)-TAN-2483A. Revision of the Structures and Syntheses of (±)-FD-211 (Waol A) and (±)-FD-212 (Waol B). *Organic Letters* 5(4):451-454.
145. Alvarez E, Candenas M-L, Perez R, Ravelo JL, & Delgado Martin J (1995) Useful Designs in the Synthesis of Trans-Fused Polyether Toxins. *Chemical Reviews* 95(6):1953-1980.
146. Handa S & Pattenden G (1998) A new approach to steroid ring construction based on a novel radical cascade sequence. *Chemical Communications* (3):311-312.
147. Shimizu N & Nishida S (1972) Reactions of carbene with 1,1-dicyclopropylethylene. A new tool to investigate radical cycloadditions. *Journal of the Chemical Society, Chemical Communications* (7):389-390.
148. Dopico PG & Finn MG (1999) Synthesis and cycloaromatization kinetics of aromatic allene enynes. *Tetrahedron* 55(1):29-62.
149. Cheng K-L & Wagner PJ (1994) Biradical Rearrangements during Intramolecular Cycloaddition of Double Bonds to Triplet Benzenes. *Journal of the American Chemical Society* 116(17):7945-7946.
150. Wagner PJ, Liu K-C, & Noguchi Y (1981) Monoradical rearrangements of the 1,4-biradicals involved in Norrish type II photoreactions. *Journal of the American Chemical Society* 103(13):3837-3841.
151. Bucher G, Mahajan AA, & Schmittel M (2009) The Photochemical C2–C6 Cyclization of Enyne–Allenes: Interception of the Fulvene Diradical with a Radical Clock Ring Opening. *The Journal of Organic Chemistry* 74(16):5850-5860.
152. Siebert MR, Osbourn JM, Brummond KM, & Tantillo DJ (2010) Differentiating Mechanistic Possibilities for the Thermal, Intramolecular [2 + 2] Cycloaddition of Allene–Ynes. *Journal of the American Chemical Society* 132(34):11952-11966.
153. Tomilov YV, Kostitsyn AB, Shulishov EV, & Nefedov OM (1990) Palladium(II)-Catalyzed Cyclopropanation of Simple Allyloxy and Allylamino Compounds and of 1-Oxy-1,3-butadienes with Diazomethane. *Synthesis* 1990(03):246-248.

154. Bernardi F, Bottoni A, & Miscione GP (2001) DFT Study of the Palladium-Catalyzed Cyclopropanation Reaction. *Organometallics* 20(13):2751-2758.
155. Lebel H, Marcoux J-F, Molinaro C, & Charette AB (2003) Stereoselective Cyclopropanation Reactions. *Chemical Reviews* 103(4):977-1050.
156. Lautens M, Klute W, & Tam W (1996) Transition Metal-Mediated Cycloaddition Reactions. *Chemical Reviews* 96(1):49-92.
157. Doyle MP, *et al.* (1984) Stereoselectivity of catalytic cyclopropanation reactions. Catalyst dependence in reactions of ethyl diazoacetate with alkenes. *Organometallics* 3(1):44-52.
158. Hahn Norbert D, Nieger M, & Dötz Karl H (2004) Highly Regio- and Diastereoselective Chromium(0)-Catalysed Cyclopropanation of 1-Alkoxy-1,3-dienes with Diazo Compounds. *European Journal of Organic Chemistry* 2004(5):1049-1056.
159. Denmark SE, Stavenger RA, Faucher A-M, & Edwards JP (1997) Cyclopropanation with Diazomethane and Bis(oxazoline)palladium(II) Complexes. *The Journal of Organic Chemistry* 62(10):3375-3389.
160. Paulissen R, Hubert AJ, & Teyssie P (1972) Transition metal catalysed cyclopropanation of olefin. *Tetrahedron Letters* 13(15):1465-1466.
161. Anciaux AJ, *et al.* (1983) Transition metal catalyzed reactions of diazoesters : Cyclopropanation of dienes and trienes. *Tetrahedron* 39(13):2169-2173.
162. Doyle MP (1986) Catalytic methods for metal carbene transformations. *Chemical Reviews* 86(5):919-939.
163. Suda M (1981) Cyclopropanation of Terminal Olefins Using Diazomethane/Palladium(II) Acetate. *Synthesis* 1981(09):714-714.
164. Markó IE, Giard T, Sumida S, & Gies A-E (2002) Regio- and stereoselective cyclopropanation of functionalised dienes. Novel methodology for the synthesis of vinyl- and divinyl-cyclopropanes. *Tetrahedron Letters* 43(12):2317-2320.
165. Mende U, Radüchel B, Skuballa V, & Vorbrüggen H (1975) A new simple conversion of α,β -unsaturated carbonyl compounds into their corresponding cyclopropyl ketones and esters. *Tetrahedron Letters* 16(9):629-632.
166. Chen S, Ma J, & Wang J (2008) Palladium-catalyzed cyclopropanation of electron-deficient olefins with aryldiazocarbonyl compounds. *Tetrahedron Letters* 49(48):6781-6783.

167. Hensarling RM, Doughty VA, Chan JW, & Patton DL (2009) "Clicking" Polymer Brushes with Thiol-yne Chemistry: Indoors and Out. *Journal of the American Chemical Society* 131(41):14673-14675.
168. Guseva Ekaterina V, Volchkov Nikolay V, Tomilov Yury V, & Nefedov Oleg M (2004) Catalytic Cyclopropanation of Fluorine-Containing Alkenes and Dienes with Diazomethane and Methyl Diazoacetate. *European Journal of Organic Chemistry* 2004(14):3136-3144.
169. Kuivila HG & Sommer R (1967) Reversibility of organotin radical attack on terminal olefins and 2-butenes. *Journal of the American Chemical Society* 89(22):5616-5619.
170. Stork G & Mook R (1987) Vinyl radical cyclizations mediated by the addition of stannyl radicals to triple bonds. *Journal of the American Chemical Society* 109(9):2829-2831.
171. Effio A, Griller D, Ingold KU, Beckwith ALJ, & Serelis AK (1980) Allylcarbinyl-cyclopropylcarbinyl rearrangement. *Journal of the American Chemical Society* 102(5):1734-1736.
172. Stork G & Mook Jr R (1986) Five vs six membered ring formation in the vinyl radical cyclization. *Tetrahedron Letters* 27(38):4529-4532.
173. Beckwith ALJ & O'Shea DM (1986) Kinetics and mechanism of some vinyl radical cyclisations. *Tetrahedron Letters* 27(38):4525-4528.
174. Wille U (2013) Radical Cascades Initiated by Intermolecular Radical Addition to Alkynes and Related Triple Bond Systems. *Chemical Reviews* 113(1):813-853.
175. Abeywickrema AN, Beckwith ALJ, & Gerba S (1987) Consecutive ring closure and neophyl rearrangement of some alkenylaryl radicals. *The Journal of Organic Chemistry* 52(18):4072-4078.
176. Cha JK & Cooke RJ (1987) Synthetic studies toward verrucosidin: Determination of the absolute configuration. *Tetrahedron Letters* 28(45):5473-5476.
177. VanRheenen V, Kelly RC, & Cha DY (1976) An improved catalytic OsO₄ oxidation of olefins to cis-1,2-glycols using tertiary amine oxides as the oxidant. *Tetrahedron Letters* 17(23):1973-1976.
178. Gómez AM, Company MaD, Uriel C, Valverde Sn, & López JC (2002) Six- versus five-membered ring formation in radical cyclization of 1-vinyl-5-methyl-5-hexenyl radicals. *Tetrahedron Letters* 43(28):4997-5000.

179. Toyota M, Yokota M, & Ihara M (1999) Construction of bicyclo[2.2.2]octane ring system via homoallyl-homoallyl radical rearrangement. *Tetrahedron Letters* 40(8):1551-1554.
180. Liu X & Ready JM (2008) Directed hydrozirconation of homopropargylic alcohols. *Tetrahedron* 64(29):6955-6960.
181. Keliher EJ, *et al.* (2006) Efficient syntheses of four stable-isotope labeled (1R)-menthyl (1S,2S)-(+)-2-phenylcyclopropanecarboxylates. *Organic & Biomolecular Chemistry* 4(14):2777-2784.
182. Majumdar KC, Alam S, & Chattopadhyay B (2008) Catalysis of the Claisen rearrangement. *Tetrahedron* 64(4):597-643.
183. Bennett GB (1977) The Claisen Rearrangement in Organic Synthesis; 1967 to January 1977. *Synthesis* 1977(09):589-606.
184. Ziegler FE (1977) Stereo- and regiochemistry of the Claisen rearrangement: applications to natural products synthesis. *Accounts of Chemical Research* 10(6):227-232.
185. Ziegler FE (1988) The thermal, aliphatic Claisen rearrangement. *Chemical Reviews* 88(8):1423-1452.
186. Ganem B (1996) The Mechanism of the Claisen Rearrangement: Déjà Vu All Over Again. *Angewandte Chemie International Edition in English* 35(9):936-945.
187. Martín Castro AM (2004) Claisen Rearrangement over the Past Nine Decades. *Chemical Reviews* 104(6):2939-3002.
188. Kupczyk-Subotkowska L, Saunders WH, Shine HJ, & Subotkowski W (1993) Thermal rearrangement of allyl vinyl ether: heavy-atom kinetic isotope effects and the transition structure. *Journal of the American Chemical Society* 115(14):5957-5961.
189. White WN & Fife WK (1961) The ortho-Claisen Rearrangement. IV. The Rearrangement of X-Cinnamyl p-Tolyl Ethers I. *Journal of the American Chemical Society* 83(18):3846-3853.
190. Frey HM & Montague DC (1968) Thermal unimolecular isomerization of 1-methylallyl vinyl ether in the gas phase and in solution. *Transactions of the Faraday Society* 64(0):2369-2374.
191. Denmark SE & Harmata MA (1982) Carbanion-accelerated Claisen rearrangements. *Journal of the American Chemical Society* 104(18):4972-4974.

192. Denmark SE & Harmata MA (1984) Carbanion-accelerated Claisen rearrangements 3. Vicinal quaternary centers. *Tetrahedron Letters* 25(15):1543-1546.
193. Barluenga J, Aznar F, Liz R, & Bayod M (1984) Synthesis of substituted 2-aminopent-4-enals and 2-amino-3-(2-furyl)propanals via [3,3]- and [1,3]-sigmatropic shifts of [small beta]-allyloxyenamines. *Journal of the Chemical Society, Chemical Communications* (21):1427-1428.
194. Welch JT & Samartino JS (1985) Facile diastereoselective ester enolate Claisen rearrangements of allyl fluoroacetates. *The Journal of Organic Chemistry* 50(19):3663-3665.
195. Koreeda M & Luengo JI (1985) The anionic oxy-claisen rearrangement of enolates of .alpha.-allyloxy ketones. A remarkable rate accelerating effect exhibited by the nature of the counterion. *Journal of the American Chemical Society* 107(19):5572-5573.
196. Wilcox CS & Babston RE (1986) Substituent effects in [3,3]-sigmatropic rearrangements. Alkyl group effects and transition-state syn-diaxial interactions. *Journal of the American Chemical Society* 108(21):6636-6642.
197. Aviyente V, Yoo HY, & Houk KN (1997) Analysis of Substituent Effects on the Claisen Rearrangement with Ab Initio and Density Functional Theory. *The Journal of Organic Chemistry* 62(18):6121-6128.
198. Wood JL & Moniz GA (1999) Rhodium Carbenoid-Initiated Claisen Rearrangement: Scope and Mechanistic Observations. *Organic Letters* 1(3):371-374.
199. Rehbein J, Leick S, & Hiersemann M (2009) Gosteli–Claisen Rearrangement: Substrate Synthesis, Simple Diastereoselectivity, and Kinetic Studies. *The Journal of Organic Chemistry* 74(4):1531-1540.
200. Craig D & Slavov NK (2008) A quantitative structure-reactivity relationship in decarboxylative Claisen rearrangement reactions of allylic tosylmalonate esters. *Chemical Communications* (45):6054-6056.
201. Aviyente V & Houk KN (2000) Cyano, Amino, and Trifluoromethyl Substituent Effects on the Claisen Rearrangement. *The Journal of Physical Chemistry A* 105(2):383-391.
202. Gao J (1994) Combined QM/MM Simulation Study of the Claisen Rearrangement of Allyl Vinyl Ether in Aqueous Solution. *Journal of the American Chemical Society* 116(4):1563-1564.

203. Lubineau A, Auge J, Bellanger N, & Caillebourdin S (1992) Water-promoted organic synthesis using glyco-organic substrates: the Claisen rearrangement. *Journal of the Chemical Society, Perkin Transactions 1* (13):1631-1636.
204. Wigfield DC, Feiner S, Malbacho G, & Taymaz K (1974) Investigations on the question of multiple mechanisms in the cope rearrangement. *Tetrahedron* 30(16):2949-2959.
205. Gajewski JJ & Gilbert KE (1984) Empirical approach to substituent effects in [3,3]-sigmatropic shifts utilizing the thermochemistry of coupled nonconcerted alternative paths. *The Journal of Organic Chemistry* 49(1):11-17.
206. Yukawa Y & Tsuno Y (1959) Resonance Effect in Hammett Relationship. III. The Modified Hammett Relationship for Electrophilic Reactions. *Bulletin of the Chemical Society of Japan* 32(9):971-981.
207. Gao H & Zhang J (2012) Cationic Rhodium(I)-Catalyzed Regioselective Tandem Heterocyclization/[3+2] Cycloaddition of 2-(1-Alkynyl)-2-alken-1-ones with Alkynes. *Chemistry – A European Journal* 18(10):2777-2782.
208. Dust JM & Arnold DR (1983) Substituent effects on benzyl radical ESR hyperfine coupling constants. The σ_{α} scale based upon spin delocalization. *Journal of the American Chemical Society* 105(5):1221-1227.
209. Creary X, Mehrsheikh-Mohammadi ME, & McDonald S (1987) Methylenecyclopropane rearrangement as a probe for free radical substituent effects. σ_{bul} Values for commonly encountered conjugating and organometallic groups. *The Journal of Organic Chemistry* 52(15):3254-3263.
210. Creary X (2006) Super Radical Stabilizers. *Accounts of Chemical Research* 39(10):761-771.
211. Jiang X & Ji G (1992) A self-consistent and cross-checked scale of spin-delocalization substituent constants, the σ_{JJ} scale. *The Journal of Organic Chemistry* 57(22):6051-6056.
212. Jiang X-K (1997) Establishment and Successful Application of the σ_{JJ} Scale of Spin-Delocalization Substituent Constants. *Accounts of Chemical Research* 30(7):283-289.
213. Hansch C, Leo A, & Taft RW (1991) A survey of Hammett substituent constants and resonance and field parameters. *Chemical Reviews* 91(2):165-195.
214. Brown HC & Okamoto Y (1958) Electrophilic Substituent Constants. *Journal of the American Chemical Society* 80(18):4979-4987.

215. Kim SS, Zhu Y, & Lee KH (2000) Thermal Isomerizations of Ketenimines to Nitriles: Evaluations of Sigma-Dot (σ^{\bullet}) Constants for Spin-Delocalizations. *The Journal of Organic Chemistry* 65(10):2919-2923.
216. de la Mare PBD (1954) Some observations concerning the theory of aromatic substitution. *Journal of the Chemical Society (Resumed)* (0):4450-4454.
217. Swain CG & Langsdorf WP (1951) Concerted Displacement Reactions. VI. m- and p-Substituent Effects as Evidence for a Unity of Mechanism in Organic Halide Reactions1. *Journal of the American Chemical Society* 73(6):2813-2819.
218. Okamoto Y & Brown HC (1957) A Quantitative Treatment for Electrophilic Reactions of Aromatic Derivatives1-3. *The Journal of Organic Chemistry* 22(5):485-494.
219. Gassman PG & Tidwell TT (1983) Electron-deficient carbocations. *Accounts of Chemical Research* 16(8):279-285.
220. Linderman RJ & Lonikar MS (1988) Addition of organocuprates to acetylenic di- and trifluoromethyl ketones. Regiospecific synthesis of .beta.,.beta.-disubstituted unsaturated fluoro ketones. *The Journal of Organic Chemistry* 53(26):6013-6022.
221. Bonacorso HG, *et al.* (2005) An efficient and regiospecific preparation of trifluoromethyl substituted 4-(1H-pyrazol-1-yl)-7-chloroquinolines. *Journal of Heterocyclic Chemistry* 42(6):1055-1061.
222. Christoffers J & Mann A (2001) Enantioselective Construction of Quaternary Stereocenters. *Angewandte Chemie International Edition* 40(24):4591-4597.
223. Cozzi PG, Hilgraf R, & Zimmermann N (2007) Enantioselective Catalytic Formation of Quaternary Stereogenic Centers. *European Journal of Organic Chemistry* 2007(36):5969-5994.
224. Ramon DJ & Yus M (2004) Enantioselective Synthesis of Oxygen-, Nitrogen- and Halogen-Substituted Quaternary Carbon Centers. *Current Organic Chemistry* 8(2):149-183.
225. Denissova I & Barriault L (2003) Stereoselective formation of quaternary carbon centers and related functions. *Tetrahedron* 59(51):10105-10146.
226. Liu W-B, Reeves CM, Virgil SC, & Stoltz BM (2013) Construction of Vicinal Tertiary and All-Carbon Quaternary Stereocenters via Ir-Catalyzed Regio-, Diastereo-, and Enantioselective Allylic Alkylation and Applications in Sequential Pd Catalysis. *Journal of the American Chemical Society* 135(29):10626-10629.

227. Ilardi EA, Stivala CE, & Zakarian A (2009) [3,3]-Sigmatropic rearrangements: recent applications in the total synthesis of natural products. *Chemical Society Reviews* 38(11):3133-3148.
228. Majumdar KC & Nandi RK (2013) The Claisen rearrangement in the syntheses of bioactive natural products. *Tetrahedron* 69(34):6921-6957.
229. Bourelle-Wargnier F, Vincent M, & Chucho J (1979) Thermally induced retro-Claisen rearrangement of formyl-ethynyl-cyclopropanes. *Journal of the Chemical Society, Chemical Communications* (13):584-585.
230. Baumann BC, Rey M, Markert J, Prinzbach H, & Dreiding AS (1971) Hexamethyl-2-oxabicyclo [3.2.0] hepta-3,6-dien. *Helvetica Chimica Acta* 54(6):1589-1599.
231. Rey M & Dreiding AS (1965) Reversible Umlagerung eines cis-2-Vinylcyclopropylformaldehydes zu einem Dihydrooxepin. Vorläufige Mitteilung. *Helvetica Chimica Acta* 48(8):1985-1987.
232. carbonylgruppen V, Maier G, & Wießler M (1969) Valenzisomerisierungen unter der beteiligung. *Tetrahedron Letters* 10(57):4987-4990.
233. Baxter AD, Roberts SM, Scheinmann F, Wakefield BJ, & Newton RF (1983) The norbornadiene route to prostaglandin I₂ and other prostaglandins: preparation and rearrangement of 7-substituted norbornadienes. *Journal of the Chemical Society, Chemical Communications* (17):932-933.
234. Heinrich N, *et al.* (2012) Reversible Cyclopropane Ring-Cleavage Reactions within Etheno-Bridged [4.3.1]Propelladiene Frameworks Leading to Aza- and Oxa-[5.6.5.6]fenestratetraenes. *Chemistry – A European Journal* 18(43):13585-13588.
235. Levin S, Nani RR, & Reisman SE (2011) Enantioselective Total Synthesis of (+)-Salvileucalin B. *Journal of the American Chemical Society* 133(4):774-776.
236. Boeckman RK, Zhang J, & Reeder MR (2002) Synthetic and Mechanistic Studies of the Retro-Claisen Rearrangement 4. An Application to the Total Synthesis of (+)-Laurenyne. *Organic Letters* 4(22):3891-3894.
237. Reeder MR (1997) Synthetic and Mechanistic Studies of the Retro-Claisen Rearrangement. 3. A Route to Enantiomerically Pure Vinyl Cyclobutane Diesters via a Highly Diastereoselective Syn SN₂^c Reaction and Their Rearrangement to Enantiomerically Pure Dihydrooxacenes. *The Journal of Organic Chemistry* 62(19):6456-6457.
238. Ponaras AA (1983) A new variant of the Claisen rearrangement capable of creating the bond between two quaternary centers. *The Journal of Organic Chemistry* 48(21):3866-3868.

239. Enders D, Knopp M, & Schiffers R (1996) Asymmetric [3,3]-sigmatropic rearrangements in organic synthesis. *Tetrahedron: Asymmetry* 7(7):1847-1882.
240. Nakazaki A & Kobayashi S (2012) Stereocontrolled Synthesis of Functionalized Spirocyclic Compounds Based on Claisen Rearrangement and its Application to the Synthesis of Spirocyclic Sesquiterpenes and Pyrrolidinoindoline Alkaloids. *Synlett* 23(10):1427-1445.
241. Rehbein J & Hiersemann M (2013) Claisen Rearrangement of Aliphatic Allyl Vinyl Ethers from 1912 to 2012: 100 Years of Electrophilic Catalysis. *Synthesis* 45(09):1121-1159.
242. Bartlett PA (1980) Stereocontrol in the synthesis of acyclic systems: applications to natural product synthesis. *Tetrahedron* 36(1):2-72.
243. Nubbemeyer U (2003) Recent Advances in Asymmetric [3,3]-Sigmatropic Rearrangements. *Synthesis* 2003(07):0961-1008.
244. Kazmaier U, Mues H, & Krebs A (2002) Asymmetric Chelated Claisen Rearrangements in the Presence of Chiral Ligands—Scope and Limitations. *Chemistry – A European Journal* 8(8):1850-1855.
245. Tan J, Cheon C-H, & Yamamoto H (2012) Catalytic Asymmetric Claisen Rearrangement of Enolphosphonates: Construction of Vicinal Tertiary and All-Carbon Quaternary Centers. *Angewandte Chemie International Edition* 51(33):8264-8267.
246. Stork G & Raucher S (1976) Chiral synthesis of prostaglandins from carbohydrates. Synthesis of (+)-15-(S)-prostaglandin A₂. *Journal of the American Chemical Society* 98(6):1583-1584.
247. Uyeda C & Jacobsen EN (2011) Transition-State Charge Stabilization through Multiple Non-covalent Interactions in the Guanidinium-Catalyzed Enantioselective Claisen Rearrangement. *Journal of the American Chemical Society* 133(13):5062-5075.
248. Uyeda C, Rötheli AR, & Jacobsen EN (2010) Catalytic Enantioselective Claisen Rearrangements of O-Allyl β -Ketoesters. *Angewandte Chemie International Edition* 49(50):9753-9756.
249. Kaebamrung J, Mahatthananchai J, Zheng P, & Bode JW (2010) An Enantioselective Claisen Rearrangement Catalyzed by N-Heterocyclic Carbenes. *Journal of the American Chemical Society* 132(26):8810-8812.

250. Mahatthananchai J, Kaeobamrung J, & Bode JW (2012) Chiral N-Heterocyclic Carbene-Catalyzed Annulations of Enals and Ynals with Stable Enols: A Highly Enantioselective Coates–Claisen Rearrangement. *ACS Catalysis* 2(4):494-503.
251. Abraham L, Czerwonka R, & Hiersemann M (2001) The Catalytic Enantioselective Claisen Rearrangement of an Allyl Vinyl Ether. *Angewandte Chemie International Edition* 40(24):4700-4703.
252. Abraham L, Körner M, Schwab P, & Hiersemann M (2004) The Catalytic Diastereo- and Enantioselective Claisen Rearrangement of 2-Alkoxy-carbonyl-Substituted Allyl Vinyl Ether. *Advanced Synthesis & Catalysis* 346(11):1281-1294.
253. Akiyama K & Mikami K (2004) Enantioselective catalysis of Claisen rearrangement by DABNTf–Pd(II) complex. *Tetrahedron Letters* 45(39):7217-7220.
254. Geherty ME, Dura RD, & Nelson SG (2010) Catalytic Asymmetric Claisen Rearrangement of Unactivated Allyl Vinyl Ethers. *Journal of the American Chemical Society* 132(34):11875-11877.
255. Maruoka K, Saito S, & Yamamoto H (1995) Molecular Design of a Chiral Lewis Acid for the Asymmetric Claisen Rearrangement. *Journal of the American Chemical Society* 117(3):1165-1166.
256. Tayama E, Saito A, Ooi T, & Maruoka K (2002) Activation of ether functionality of allyl vinyl ethers by chiral bis(organoaluminum) Lewis acids: application to asymmetric Claisen rearrangement. *Tetrahedron* 58(41):8307-8312.
257. Maruoka K, Banno H, & Yamamoto H (1991) Enantioselective activation of ethers by chiral organoaluminum reagents: Application to asymmetric Claisen rearrangement. *Tetrahedron: Asymmetry* 2(7):647-666.
258. Ito H, Sato A, Kobayashi T, & Taguchi T (1998) Enantioselective Claisen rearrangement of difluorovinyl allyl ethers. *Chemical Communications* (22):2441-2442.
259. Corey EJ & Lee DH (1991) Highly enantioselective and diastereoselective Ireland-Claisen rearrangement of achiral allylic esters. *Journal of the American Chemical Society* 113(10):4026-4028.
260. Yoon TP & MacMillan DWC (2001) Enantioselective Claisen Rearrangements: Development of a First Generation Asymmetric Acyl-Claisen Reaction. *Journal of the American Chemical Society* 123(12):2911-2912.
261. Ito H & Taguchi T (1999) Asymmetric Claisen rearrangement. *Chemical Society Reviews* 28(1):43-50.

262. van der Baan JL & Bickelhaupt F (1986) Palladium(II)-catalyzed Claisen rearrangement of allyl vinyl ethers. *Tetrahedron Letters* 27(51):6267-6270.
263. Mikami K, Takahashi K, & Nakai T (1987) Diastereocontrol via the phenol- and palladium(II)-catalyzed Claisen rearrangement with cyclic enol ethers. *Tetrahedron Letters* 28(47):5879-5882.
264. Mikami K, Takahashi K, Nakai T, & Uchimaru T (1994) Asymmetric Tandem Claisen-Ene Strategy for Convergent Synthesis of (+)-9(11)-Dehydroestrone Methyl Ether: Stereochemical Studies on the Ene Cyclization and Cyclic Enol Ether Claisen Rearrangement for Steroid Total Synthesis. *Journal of the American Chemical Society* 116(24):10948-10954.
265. Sugiura M & Nakai T (1996) Regiochemical control in the Pd(II)-catalyzed Claisen rearrangement via in situ enol ether exchange. *Tetrahedron Letters* 37(44):7991-7994.
266. Hiersemann M (1999) The Pd(II)-Catalyzed and the Thermal Claisen Rearrangement of 2-Alkoxy carbonyl-Substituted Allyl Vinyl Ethers. *Synlett* 1999(11):1823-1825.
267. Hiersemann M & Abraham L (2001) The Cu(OTf)₂- and Yb(OTf)₃-Catalyzed Claisen Rearrangement of 2-Alkoxy carbonyl-Substituted Allyl Vinyl Ethers. *Organic Letters* 3(1):49-52.
268. Ollevier T & Mwene-Mbeja TM (2008) Diastereoselective bismuth triflate catalyzed Claisen rearrangement of 2-alkoxy carbonyl-substituted allyl vinyl ethers. *Canadian Journal of Chemistry* 86(3):209-212.
269. Hiersemann M & Abraham L (2002) Catalysis of the Claisen Rearrangement of Aliphatic Allyl Vinyl Ethers. *European Journal of Organic Chemistry* 2002(9):1461-1471.
270. Trost BM & Schroeder GM (2000) Cyclic 1,2-Diketones as Building Blocks for Asymmetric Synthesis of Cycloalkenones. *Journal of the American Chemical Society* 122(15):3785-3786.
271. Koch G, Janser P, Kottirsch G, & Romero-Giron E (2002) Highly diastereoselective Lewis acid promoted Claisen-Ireland rearrangement. *Tetrahedron Letters* 43(27):4837-4840.
272. Marié J-C, *et al.* (2010) Enantioselective Synthesis of 3,4-Chromanediones via Asymmetric Rearrangement of 3-Allyloxyflavones. *The Journal of Organic Chemistry* 75(13):4584-4590.

273. Cao T, Linton EC, Deitch J, Berritt S, & Kozlowski MC (2012) Copper(II)- and Palladium(II)-Catalyzed Enantioselective Claisen Rearrangement of Allyloxy- and Propargyloxy-Indoles to Quaternary Oxindoles and Spirocyclic Lactones. *The Journal of Organic Chemistry* 77(24):11034-11055.
274. Abraham L, Körner M, & Hiersemann M (2004) Highly enantioselective catalytic asymmetric Claisen rearrangement of 2-alkoxycarbonyl-substituted allyl vinyl ethers. *Tetrahedron Letters* 45(18):3647-3650.
275. Adachi S & Harada T (2009) Catalytic Enantioselective Aldol Additions to Ketones. *European Journal of Organic Chemistry* 2009(22):3661-3671.
276. Werschkun B & Thiem J (2001) Claisen Rearrangements in Carbohydrate Chemistry. *Glycoscience, Topics in Current Chemistry*, ed Stütz A (Springer Berlin Heidelberg), Vol 215, pp 293-325.
277. Chambers DJ, Evans GR, & Fairbanks AJ (2005) Synthesis of C-glycosyl amino acids: scope and limitations of the tandem Tebbe/Claisen approach. *Tetrahedron: Asymmetry* 16(1):45-55.
278. Godage HY, Chambers DJ, Evans GR, & Fairbanks AJ (2003) Stereoselective synthesis of C-glycosides from carboxylic acids: the tandem Tebbe-Claisen approach. *Organic & Biomolecular Chemistry* 1(21):3772-3786.
279. Chen C-L, Namba K, & Kishi Y (2009) Attempts To Improve the Overall Stereoselectivity of the Ireland-Claisen Rearrangement. *Organic Letters* 11(2):409-412.
280. Pazos G, Pérez M, Gándara Z, Gómez G, & Fall Y (2012) Enantiodivergent synthesis of (+)- and (-)-isolaurepan. *Tetrahedron* 68(44):8994-9003.
281. Zúñiga A, Pérez M, González M, Gómez G, & Fall Y (2011) Formal Synthesis of Aspergillide A from Tri-O-acetyl-d-glucal. *Synthesis* 2011(20):3301-3306.
282. Pazos G, Pérez M, Gándara Z, Gómez G, & Fall Y (2009) A new, enantioselective synthesis of (+)-isolaurepan. *Tetrahedron Letters* 50(37):5285-5287.
283. Wender PA, *et al.* (2002) The Practical Synthesis of a Novel and Highly Potent Analogue of Bryostatin. *Journal of the American Chemical Society* 124(46):13648-13649.
284. Fairhurst NWG, Mahon MF, Munday RH, & Carbery DR (2012) Remote Stereocontrol in [3,3]-Sigmatropic Rearrangements: Application to the Total Synthesis of the Immunosuppressant Mycestericin G. *Organic Letters* 14(3):756-759.

285. Tellam JP & Carbery DR (2011) Ireland-Claisen rearrangement of substrates bearing chiral enol ether units. *Tetrahedron Letters* 52(45):6027-6029.
286. Davies SG, *et al.* (2014) Diastereoselective Ireland-Claisen rearrangements of substituted allyl [small beta]-amino esters: applications in the asymmetric synthesis of C(5)-substituted transpentacins. *Organic & Biomolecular Chemistry* 12(17):2702-2728.
287. Johnson JS & Evans DA (2000) Chiral Bis(oxazoline) Copper(II) Complexes: Versatile Catalysts for Enantioselective Cycloaddition, Aldol, Michael, and Carbonyl Ene Reactions. *Accounts of Chemical Research* 33(6):325-335.
288. Palomo C, Oiarbide M, & Garcia JM (2004) Current progress in the asymmetric aldol addition reaction. *Chemical Society Reviews* 33(2):65-75.
289. Aoki S, Kotani S, Sugiura M, & Nakajima M (2012) Trichlorosilyl triflate-mediated enantioselective directed cross-aldol reaction between ketones using a chiral phosphine oxide as an organocatalyst. *Chemical Communications* 48(44):5524-5526.
290. Sharma GVM, Ilangovan A, Sreenivas P, & Mahalingam AK (2000) Alternative Lewis Acids to Effect Claisen Rearrangement. *Synlett* 2000(05):0615-0618.
291. Donde Y & Overman LE (1999) High Enantioselection in the Rearrangement of Allylic Imidates with Ferrocenyl Oxazoline Catalysts. *Journal of the American Chemical Society* 121(12):2933-2934.
292. Hollis TK & Overman LE (1997) Cyclopalladated ferrocenyl amines as enantioselective catalysts for the rearrangement of allylic imidates to allylic amides. *Tetrahedron Letters* 38(51):8837-8840.
293. Kang J, Yew KH, Kim TH, & Choi DH (2002) Preparation of bis[palladacycles] and application to asymmetric aza-Claisen rearrangement of allylic imidates. *Tetrahedron Letters* 43(52):9509-9512.
294. Jiang Y, Longmire JM, & Zhang X (1999) The first tridentate ligand for catalytic enantioselective aza-Claisen rearrangement of allylic imidates. *Tetrahedron Letters* 40(8):1449-1450.
295. Leung P-H, Ng K-H, Li Y, J. P. White A, & J. Williams D (1999) Designer cyclopalladated-amine catalysts for the asymmetric Claisen rearrangement. *Chemical Communications* (23):2435-2436.
296. Maier S & Kazmaier U (2000) Modifications of Peptides by Chelate Claisen Rearrangements of Manganese Enolates. *European Journal of Organic Chemistry* 2000(7):1241-1251.

297. Enders D, Knopp M, Runsink J, & Raabe G (1995) Diastereo- and Enantioselective Synthesis of Polyfunctional Ketones with Adjacent Quaternary and Tertiary Centers by Asymmetric Carroll Rearrangement. *Angewandte Chemie International Edition in English* 34(20):2278-2280.
298. Nonoshita K, Banno H, Maruoka K, & Yamamoto H (1990) Organoaluminum-promoted Claisen rearrangement of allyl vinyl ethers. *Journal of the American Chemical Society* 112(1):316-322.
299. Maruoka K, Nonoshita K, Banno H, & Yamamoto H (1988) Unprecedented stereochemical control in the Claisen rearrangement of allyl vinyl ethers using organoaluminum reagents. *Journal of the American Chemical Society* 110(23):7922-7924.
300. Sudharshan M & Hultin PG (1997) An Improved Preparation of Oxazolidin-2-one Chiral Auxiliaries. *Synlett* 1997(02):171-172.
301. Lutz RP (1984) Catalysis of the Cope and Claisen rearrangements. *Chemical Reviews* 84(3):205-247.
302. Kerrigan NJ, Bungard CJ, & Nelson SG (2008) Pd(II)-catalyzed aliphatic Claisen rearrangements of acyclic allyl vinyl ethers. *Tetrahedron* 64(29):6863-6869.
303. Crimmins MT & Chaudhary K (2000) Titanium Enolates of Thiazolidinethione Chiral Auxiliaries: Versatile Tools for Asymmetric Aldol Additions. *Organic Letters* 2(6):775-777.
304. Chen N, Jia W, & Xu J (2009) A Versatile Synthesis of Various Substituted Taurines from Vicinal Amino Alcohols and Aziridines. *European Journal of Organic Chemistry* 2009(33):5841-5846.
305. Yamada S & Katsumata H (1999) Asymmetric Acylation of sec-Alcohols with Twisted Amides Possessing Axial Chirality Induced by the Adjacent Asymmetric Center. *The Journal of Organic Chemistry* 64(26):9365-9373.
306. Cevallos A, Rios R, Moyano* A, Pericàs MA, & Riera A (2000) A convenient synthesis of chiral 2-alkynyl-1,3-oxazolines. *Tetrahedron: Asymmetry* 11(21):4407-4416.
307. Takao K-i, Sakamoto S, Touati M, Kusakawa Y, & Tadano K-i (2012) Asymmetric Construction of All-Carbon Quaternary Stereocenters by Chiral-Auxiliary-Mediated Claisen Rearrangement and Total Synthesis of (+)-Bakuchiol. *Molecules* 17(11):13330-13344.

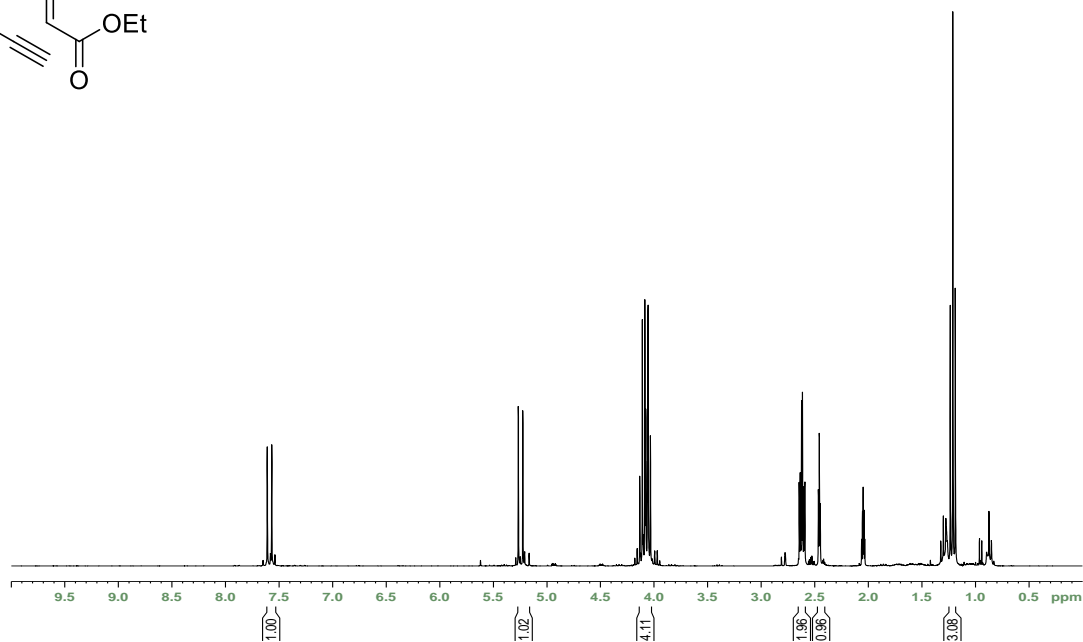
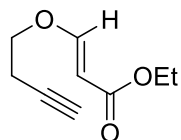
308. Fritz-Langhals E & Schu"tz G (1993) Simple synthesis of optically active 2-fluoropropanoic acid and analogs of high enantiomeric purity. *Tetrahedron Letters* 34(2):293-296.
309. Curran DP, Kim BH, Daugherty J, & Heffner TA (1988) The preparation of optically active δ^2 -isoxazolines. A model for asymmetric induction in the non lewis acid catalyzed reactions of oppolzer's chiral sultam. *Tetrahedron Letters* 29(29):3555-3558.
310. Curran DP, Shen W, Zhang J, & Heffner TA (1990) Asymmetric radical addition, cyclization, and annulation reactions with Oppolzer's camphor sultam. *Journal of the American Chemical Society* 112(18):6738-6740.
311. Kallmerten J & Gould TJ (1986) Auxiliary-directed diastereoselectivity in the Claisen rearrangement of glycolate esters. *The Journal of Organic Chemistry* 51(7):1152-1155.
312. Monache Gd, Giovanni MCD, Misiti D, & Zappia G (1997) An enantioselective, stereodivergent synthesis of threonine analogs. *Tetrahedron: Asymmetry* 8(2):231-243.
313. Cao L, *et al.* (2009) Novel and Direct Transformation of Methyl Ketones or Carbinols to Primary Amides by Employing Aqueous Ammonia. *Organic Letters* 11(17):3810-3813.
314. Deiters A, Chen K, Eary CT, & Martin SF (2003) Biomimetic Entry to the Sarpagan Family of Indole Alkaloids: Total Synthesis of (+)-Geissoschizine and (+)-N-Methylvellosimine. *Journal of the American Chemical Society* 125(15):4541-4550.
315. Feray L & Bertrand MP (2008) Dialkylzinc-Mediated Atom Transfer Sequential Radical Addition Cyclization. *European Journal of Organic Chemistry* 2008(18):3164-3170.
316. Booker JEM, *et al.* (2006) Approaches to the quaternary stereocentre and to the heterocyclic core in diazonamide A using the Heck reaction and related coupling reactions. *Organic & Biomolecular Chemistry* 4(22):4193-4205.
317. Montgomery TD, Zhu Y, Kagawa N, & Rawal VH (2013) Palladium-Catalyzed Decarboxylative Allylation and Benzylolation of N-Alloc and N-Cbz Indoles. *Organic Letters* 15(5):1140-1143.
318. Gowrisankar S, Kim KH, Kim SH, & Kim JN (2008) Synthesis of 1,5-dicarbonyl and related compounds from Baylis-Hillman adducts via Pd-mediated decarboxylative protonation protocol. *Tetrahedron Letters* 49(43):6241-6244.

319. Kim SH, Kim ES, Kim TH, & Kim JN (2009) Expedient synthesis of 3-substituted cycloalkanones via a Pd-catalyzed decarboxylative protonation protocol. *Tetrahedron Letters* 50(46):6256-6260.
320. Shimizu I, Makuta T, & Oshima M (1989) Facile Synthesis of α -Keto Acids and Esters by Palladium-Catalyzed Decarboxylation Reactions of Diallyl α -Oxalcarboxylates. *Chemistry Letters* 18(8):1457-1460.
321. Hanessian S, Griffin AM, & Rozema MJ (1997) Tricyclic β -lactams: Total synthesis and antibacterial activity of 5 α -methoxyethyl and 5 α -hydroxyethyl trinems. *Bioorganic & Medicinal Chemistry Letters* 7(14):1857-1862.
322. Hoffman RV & Tao J (1998) A Synthesis of d-erythro- and l-threo-Sphingosine and Sphinganine Diastereomers via the Biomimetic Precursor 3-Ketosphinganine. *The Journal of Organic Chemistry* 63(12):3979-3985.
323. Marigo M, Bertelsen S, Landa A, & Jørgensen KA (2006) One-Pot Organocatalytic Domino Michael-Aldol and Intramolecular SN2 Reactions. Asymmetric Synthesis of Highly Functionalized Epoxycyclohexanone Derivatives. *Journal of the American Chemical Society* 128(16):5475-5479.
324. Song J, Wang Y, & Deng L (2006) The Mannich Reaction of Malonates with Simple Imines Catalyzed by Bifunctional Cinchona Alkaloids: Enantioselective Synthesis of β -Amino Acids. *Journal of the American Chemical Society* 128(18):6048-6049.
325. Zhang H, Sridhar Reddy M, Phoenix S, & Deslongchamps P (2008) Total Synthesis of Ouabagenin and Ouabain. *Angewandte Chemie International Edition* 47(7):1272-1275.
326. Farmer RL, *et al.* (2010) Concise Syntheses of the Abyssinones and Discovery of New Inhibitors of Prostate Cancer and MMP-2 Expression. *ACS Medicinal Chemistry Letters* 1(8):400-405.
327. Hoye TR, Jeffrey CS, & Shao F (2007) Mosher ester analysis for the determination of absolute configuration of stereogenic (chiral) carbinol carbons. *Nat. Protocols* 2(10):2451-2458.
328. Venkatesham A & Nagaiah K (2012) Stereoselective total synthesis of stagonolide-C. *Tetrahedron: Asymmetry* 23(15-16):1186-1197.
329. Chang H-K, Liao Y-C, & Liu R-S (2007) Diversity in Platinum-Catalyzed Hydrative Cyclization of Trialkyne Substrates To Form Tetracyclic Ketones. *The Journal of Organic Chemistry* 72(21):8139-8141.

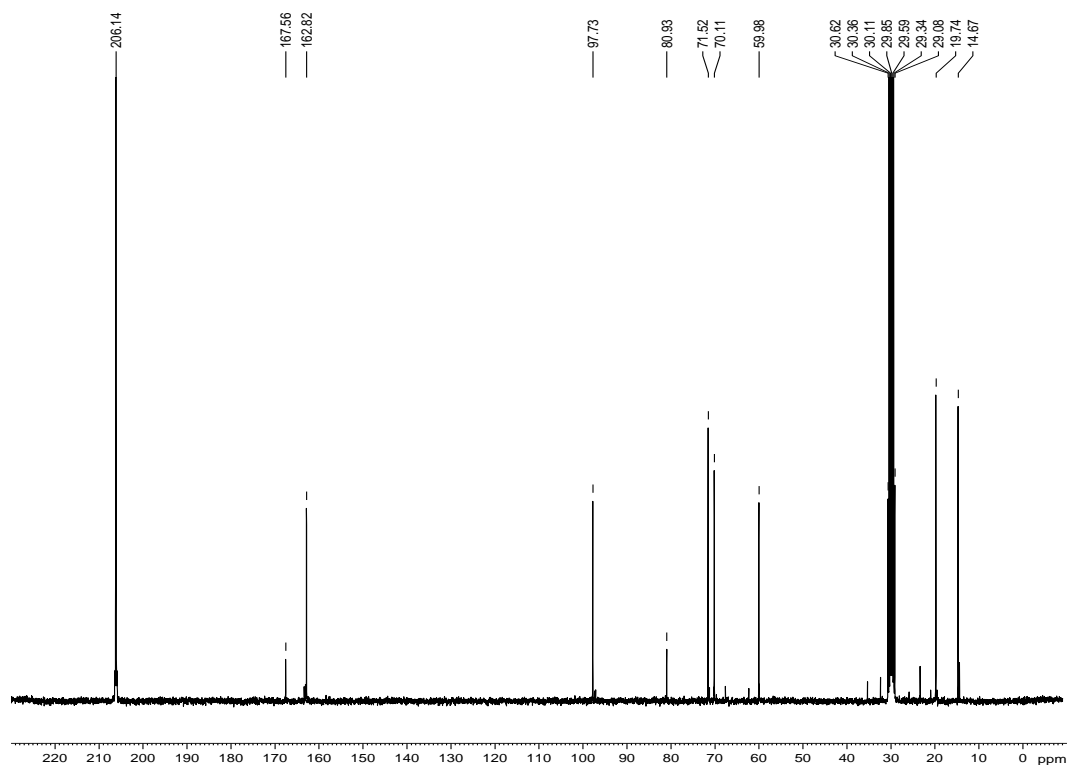
330. Thevenet D & Neier R (2011) An Efficient Photoinduced Deprotection of Aromatic Acetals and Ketals. *Helvetica Chimica Acta* 94(2):331-346.

Appendix A Chapter 2 Spectral Data

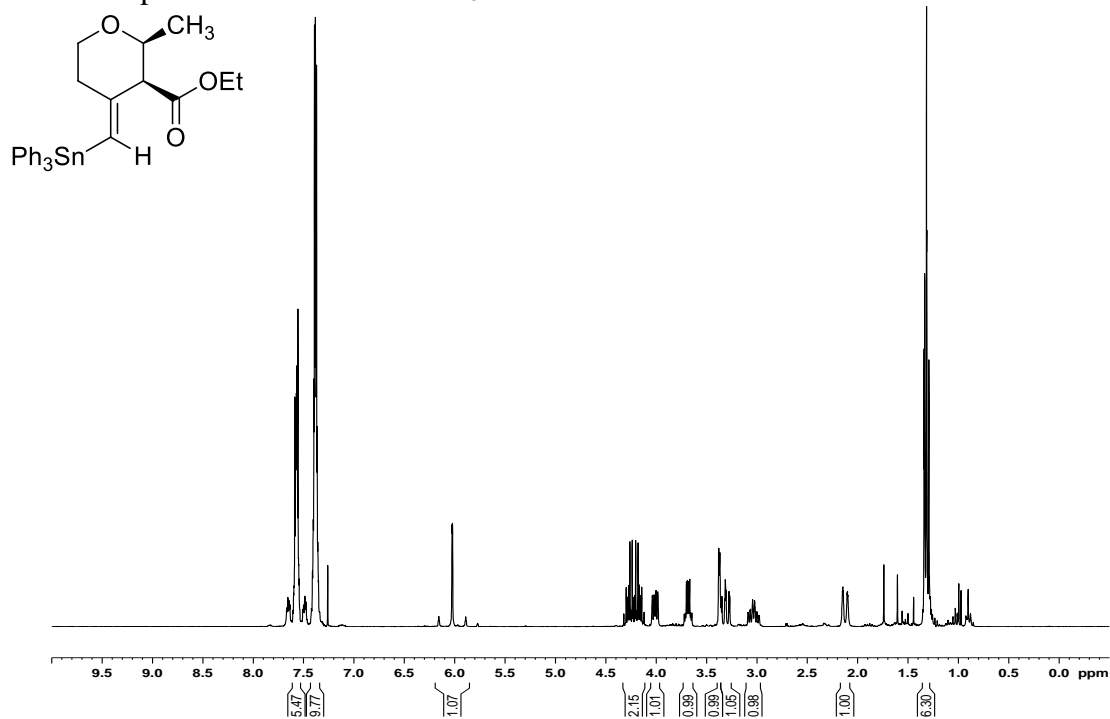
^1H NMR spectrum for 2.33b (1.00:0.06 E:Z) in $(\text{CD}_3)_2\text{CO}$



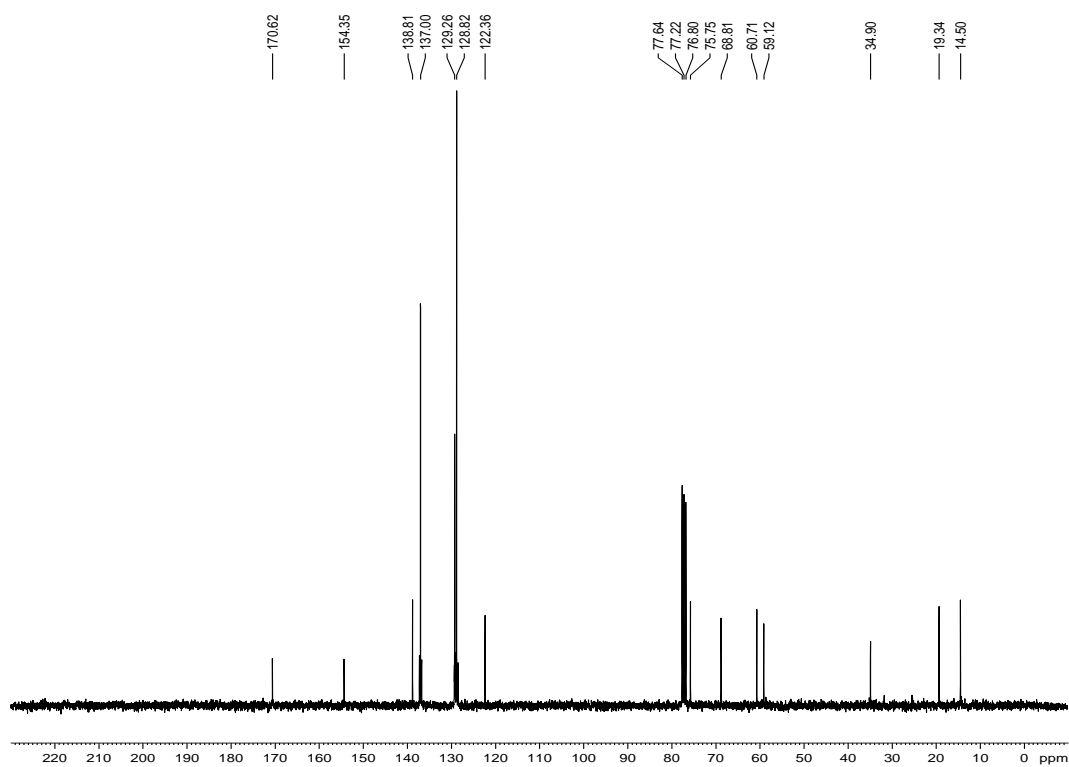
^{13}C NMR spectrum for 2.33b (1.00:0.06 E:Z) in $(\text{CD}_3)_2\text{CO}$



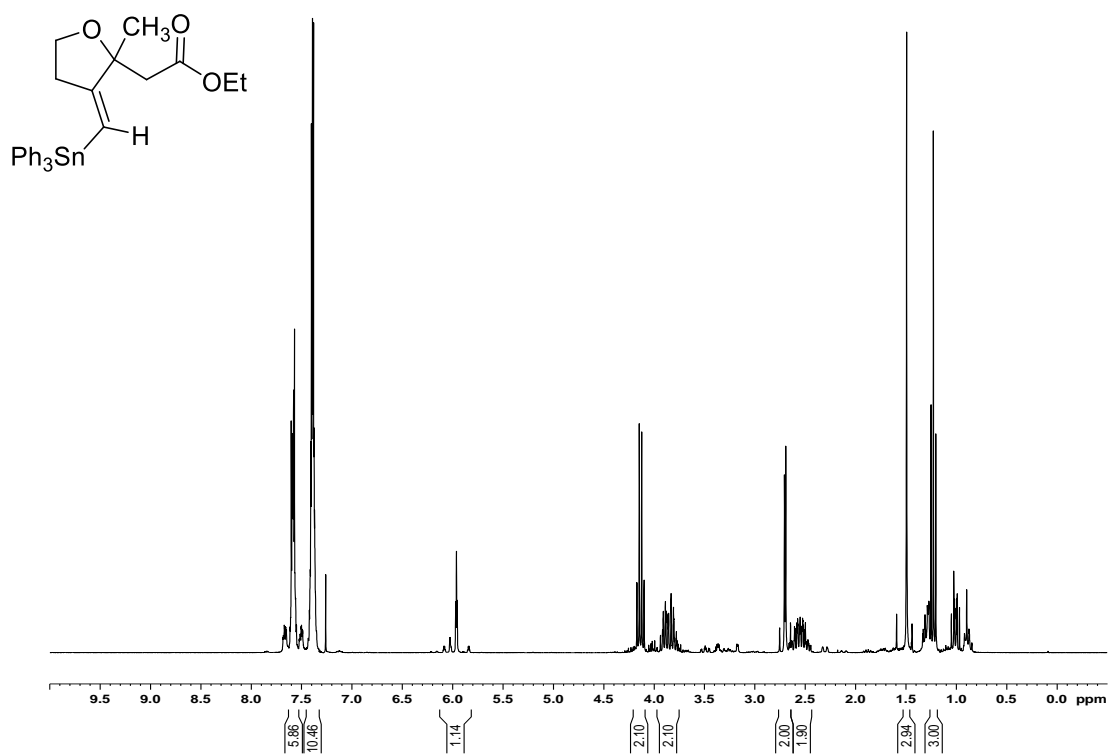
^1H NMR spectrum for 2.45 in CDCl_3



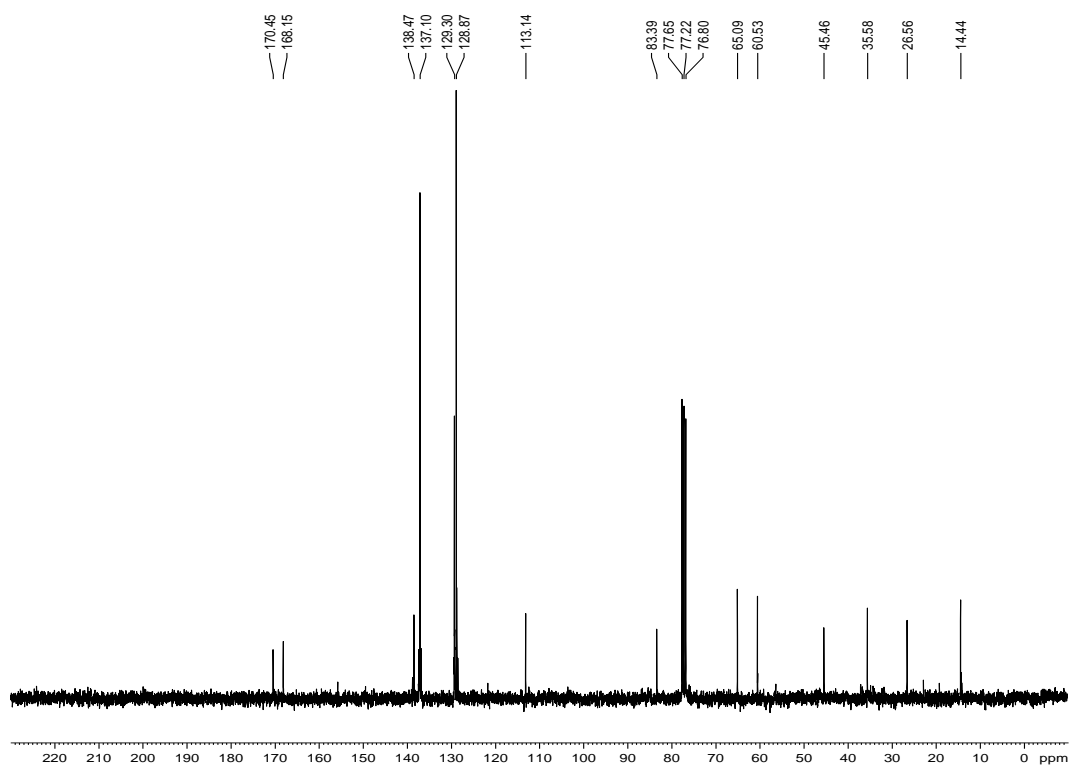
^{13}C NMR spectrum for 2.45 in CDCl_3



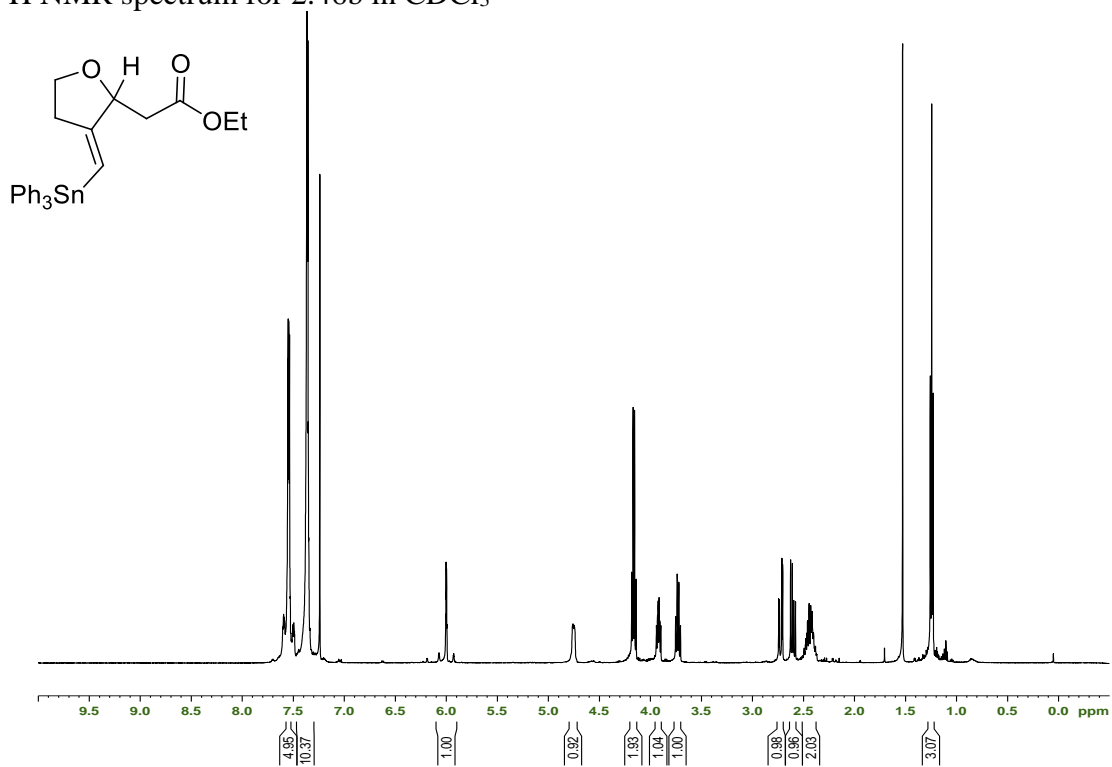
^1H NMR spectrum for 2.46a in CDCl_3



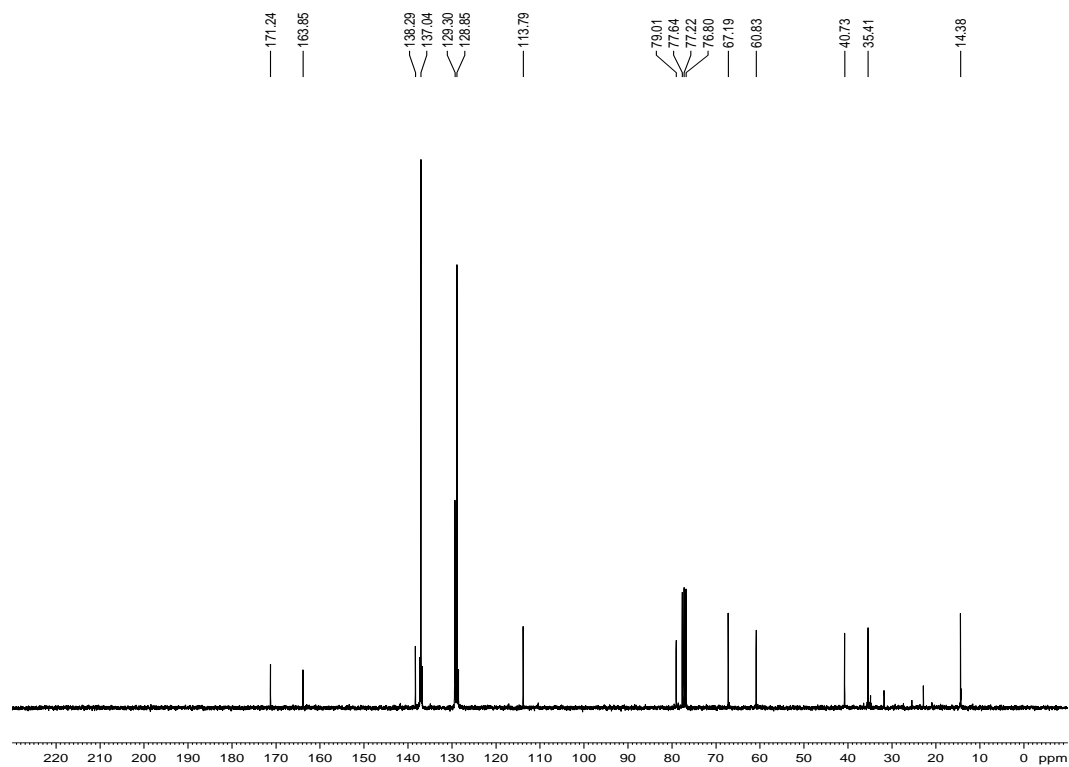
^{13}C NMR spectrum for 2.46a in CDCl_3



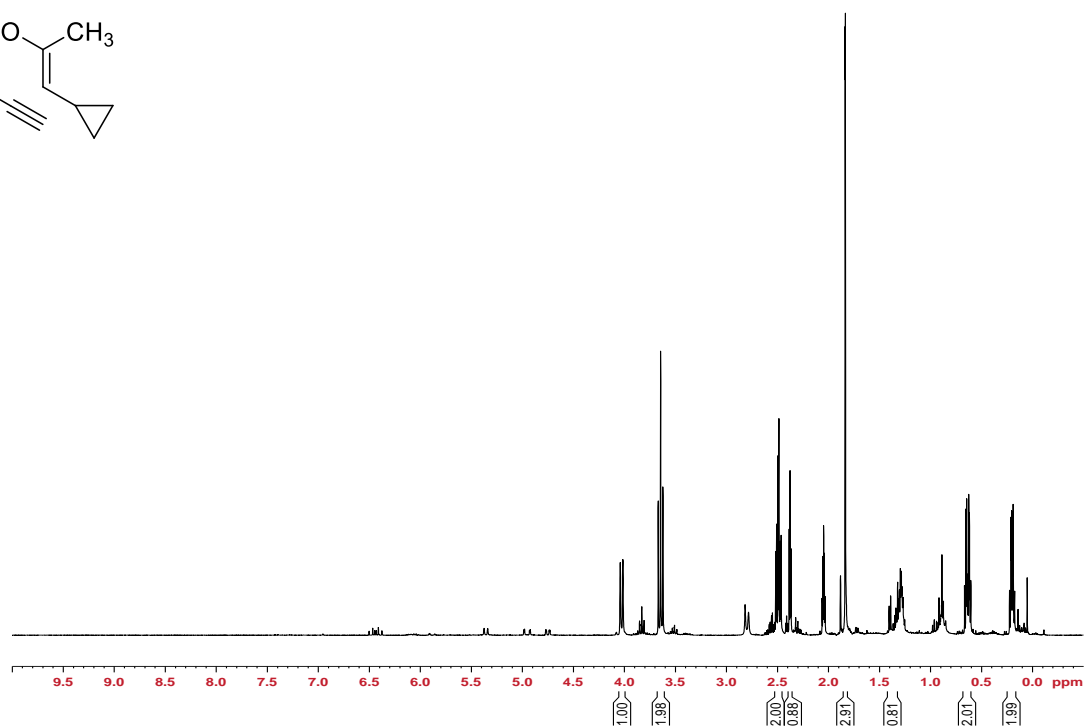
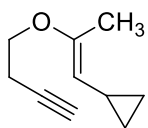
^1H NMR spectrum for 2.46b in CDCl_3



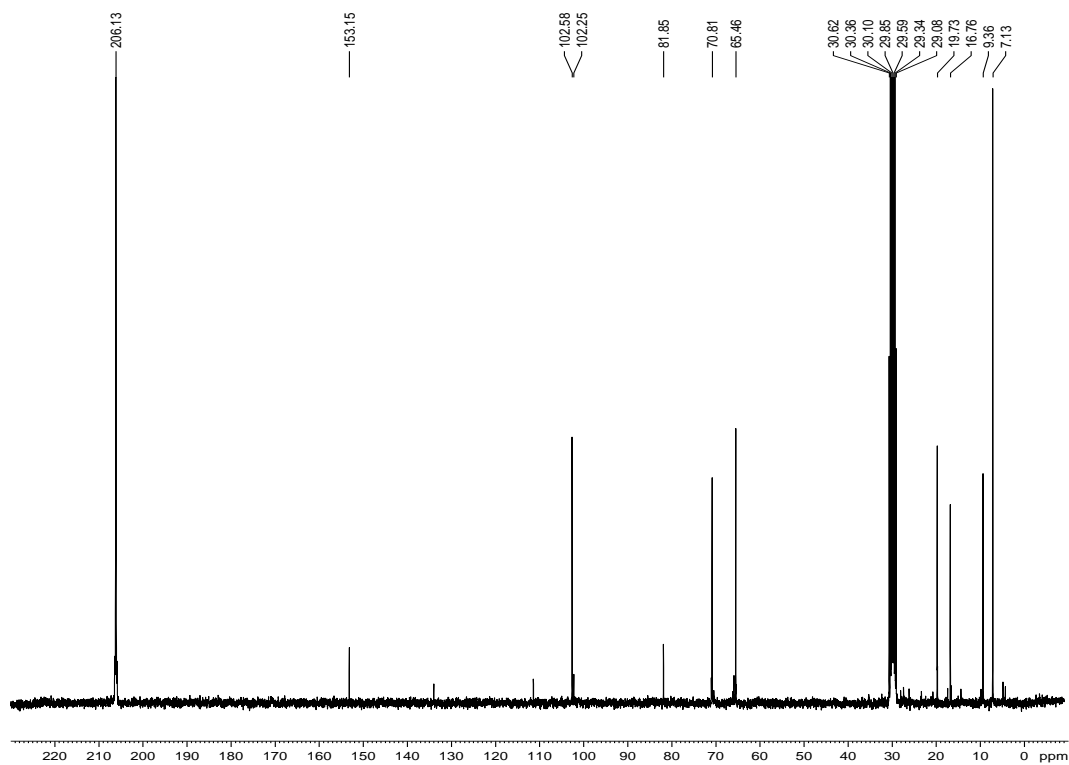
^{13}C NMR spectrum for 2.46b in CDCl_3



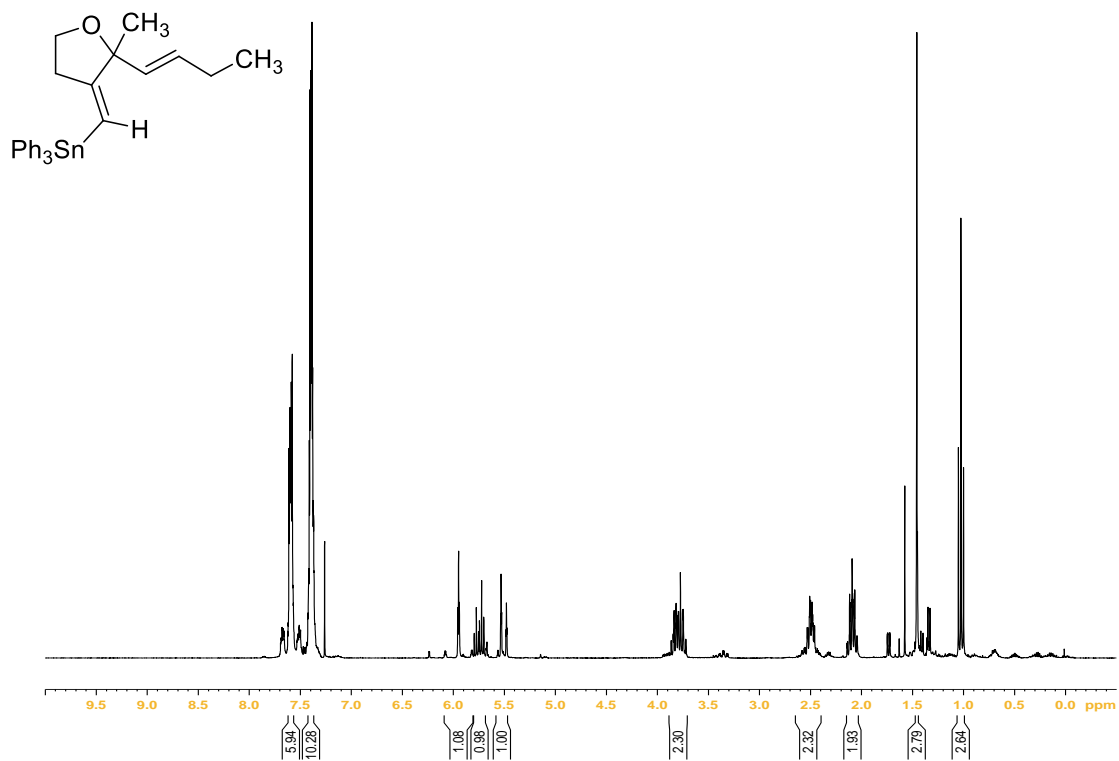
^1H NMR spectrum for 2.65 (1.00:0.09 2.65:2.70) in $(\text{CD}_3)_2\text{CO}$



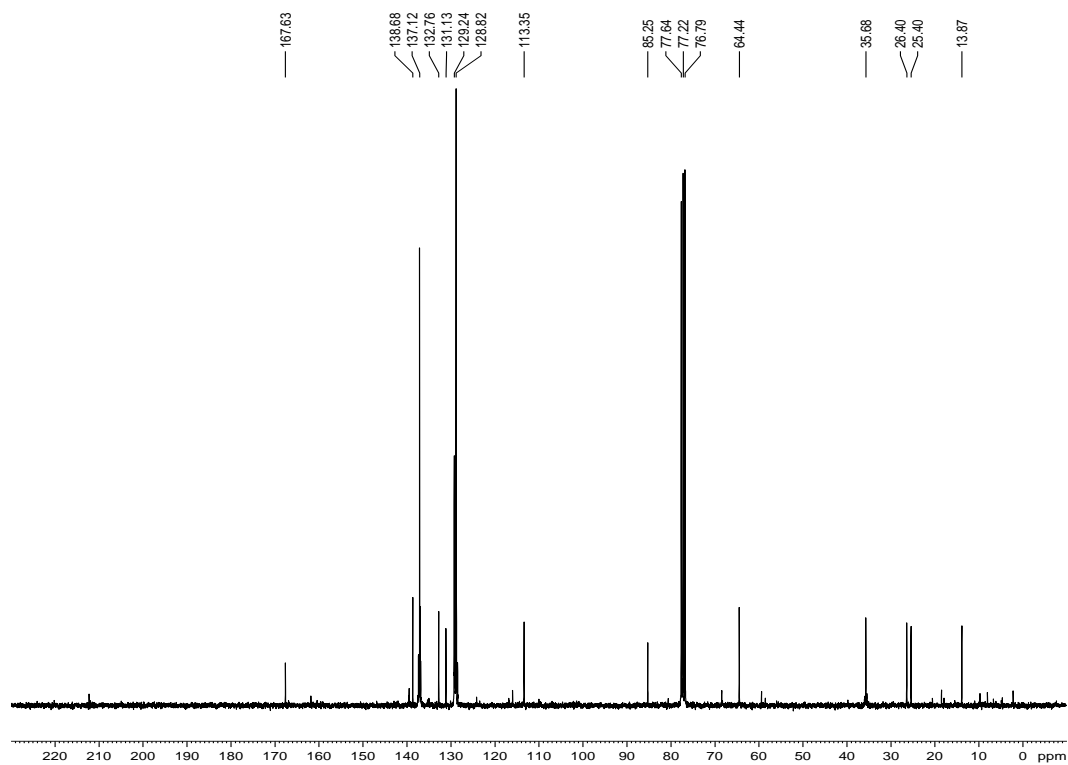
^{13}C NMR spectrum for 2.65 (1.00:0.09 2.65:2.70) in $(\text{CD}_3)_2\text{CO}$



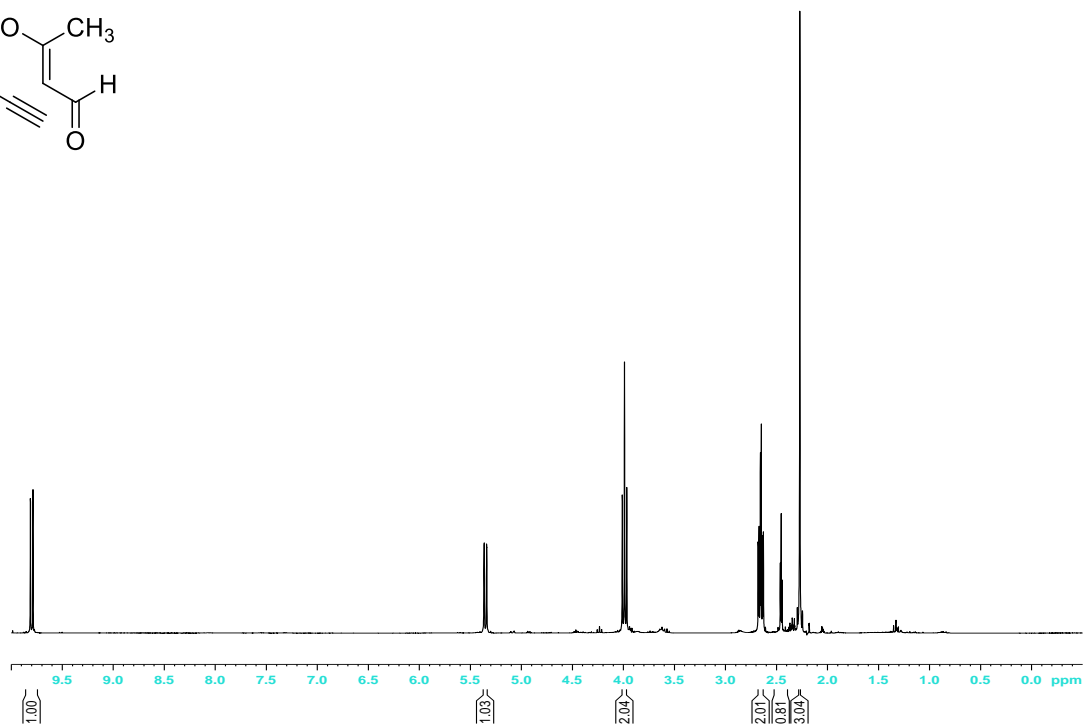
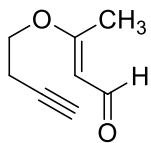
^1H NMR spectrum for 2.68 (1.00:0.10 2.68:2.90) in CDCl_3



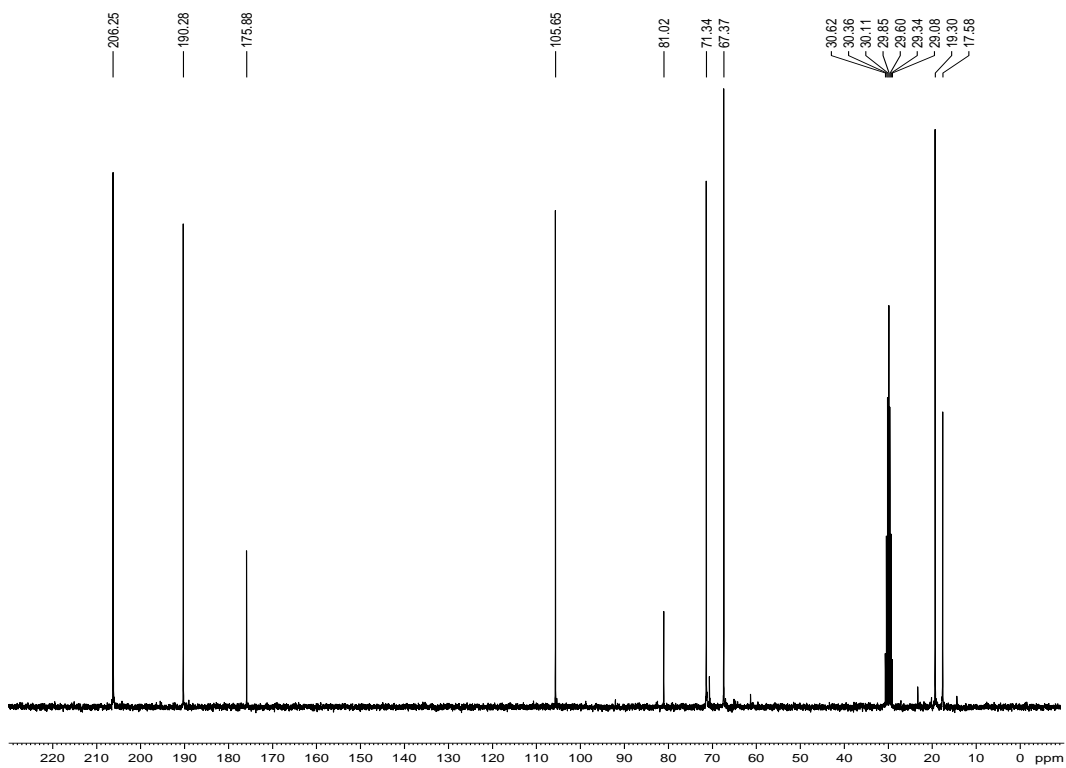
^{13}C NMR spectrum for 2.68 (1.00:0.10 2.68:2.90) in CDCl_3



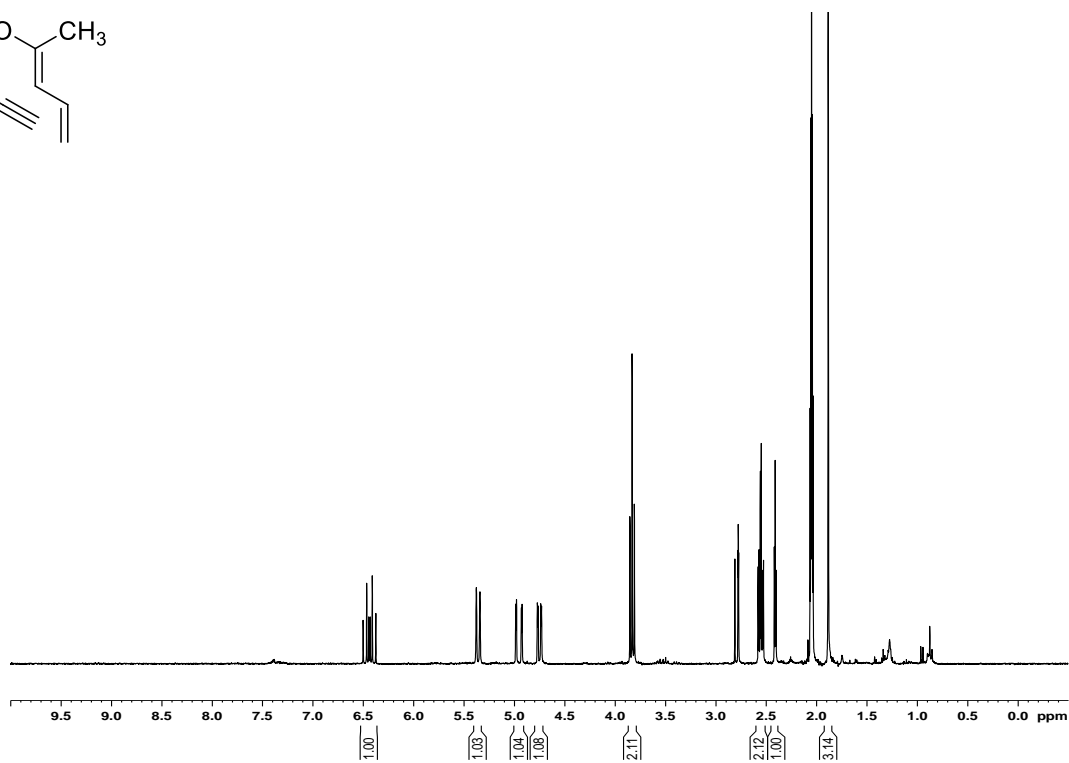
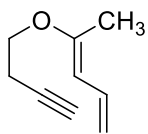
^1H NMR spectrum for 2.69 in $(\text{CD}_3)_2\text{CO}$



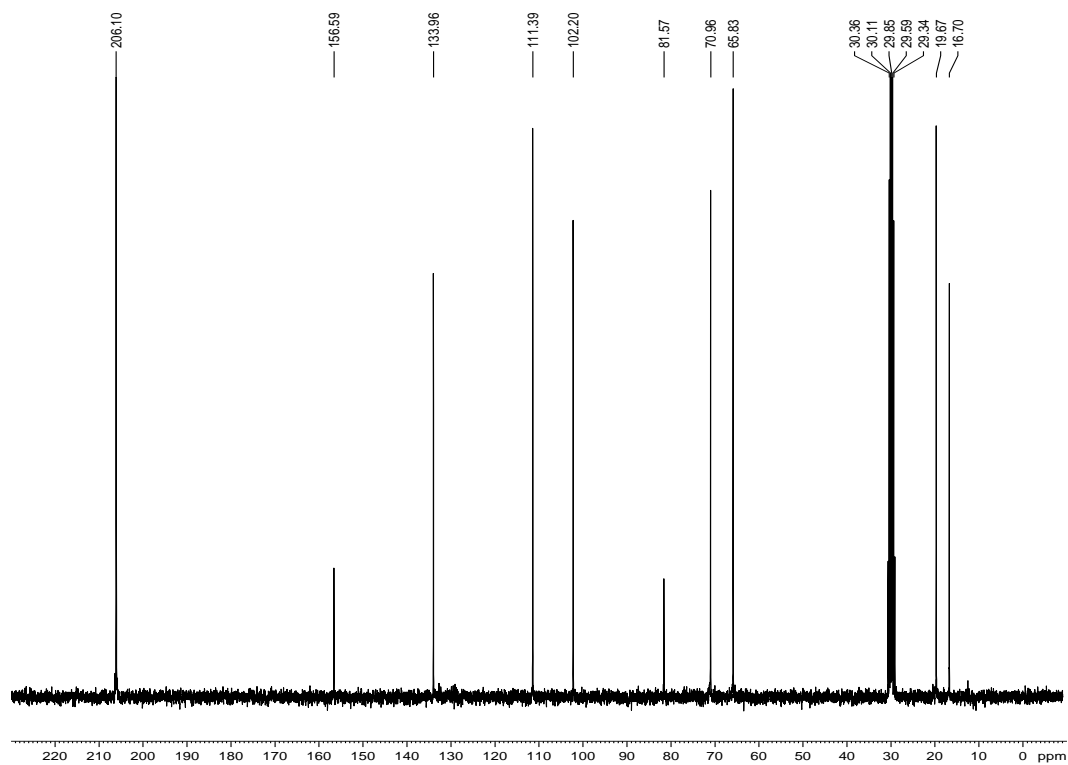
^{13}C NMR spectrum for 2.69 in $(\text{CD}_3)_2\text{CO}$



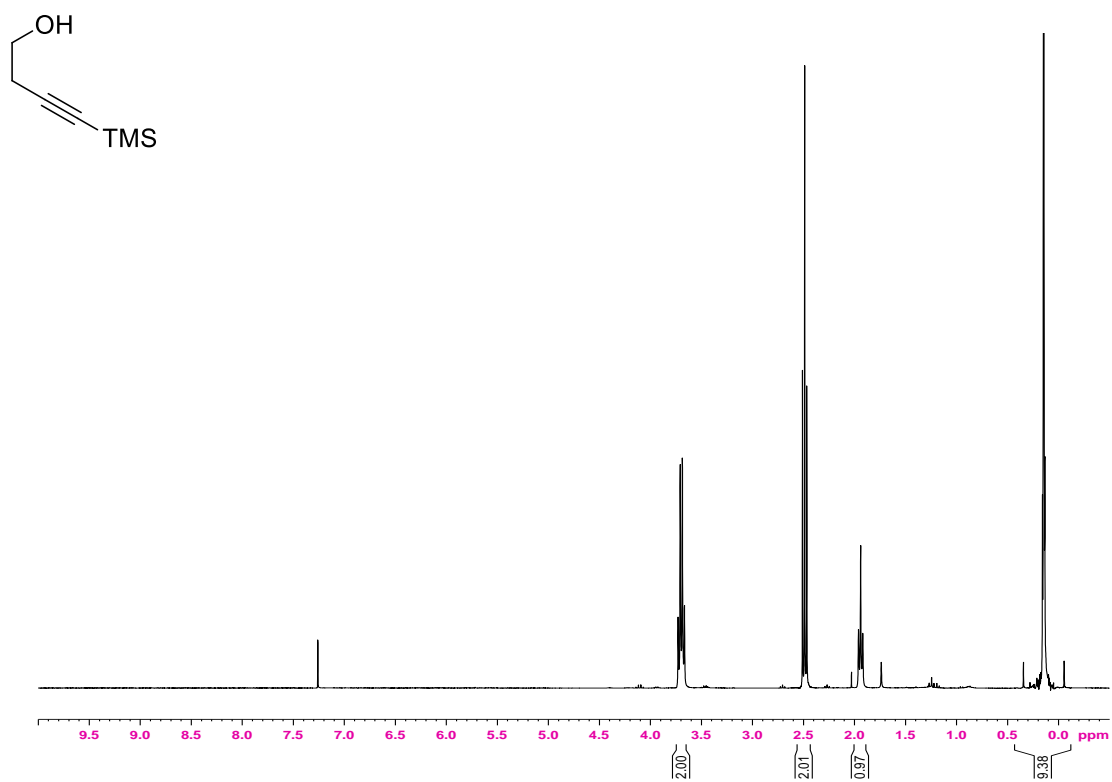
^1H NMR spectrum for 2.70 in $(\text{CD}_3)_2\text{CO}$



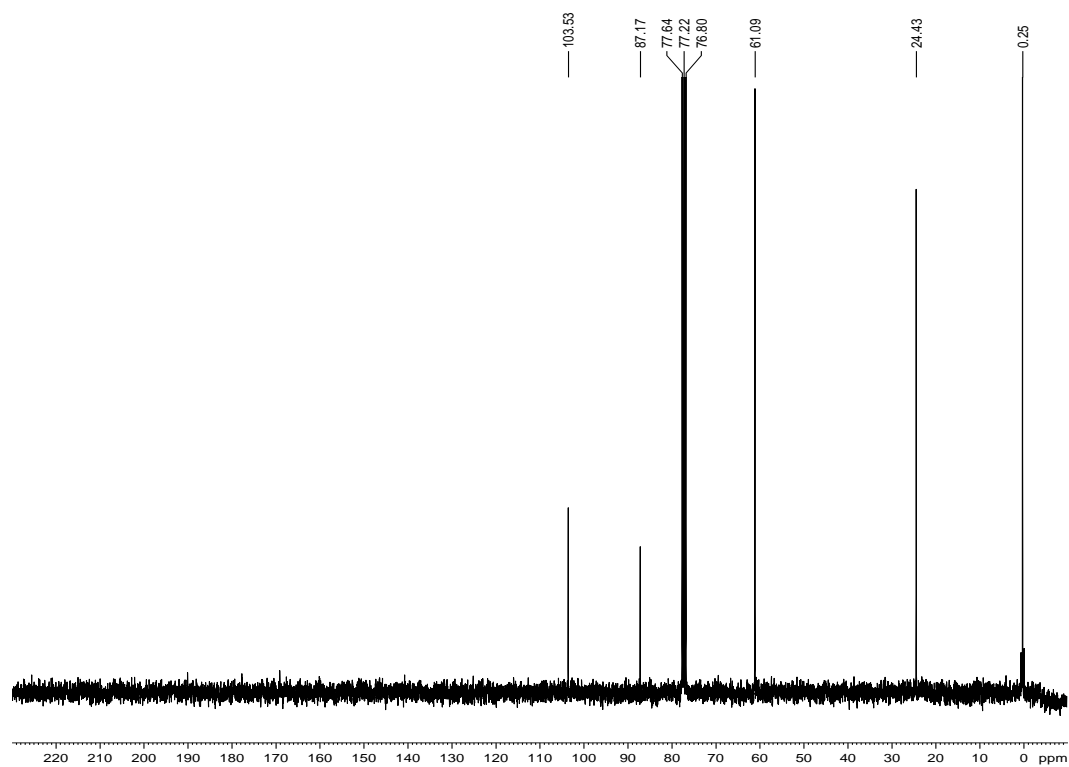
^{13}C NMR spectrum for 2.70 in $(\text{CD}_3)_2\text{CO}$



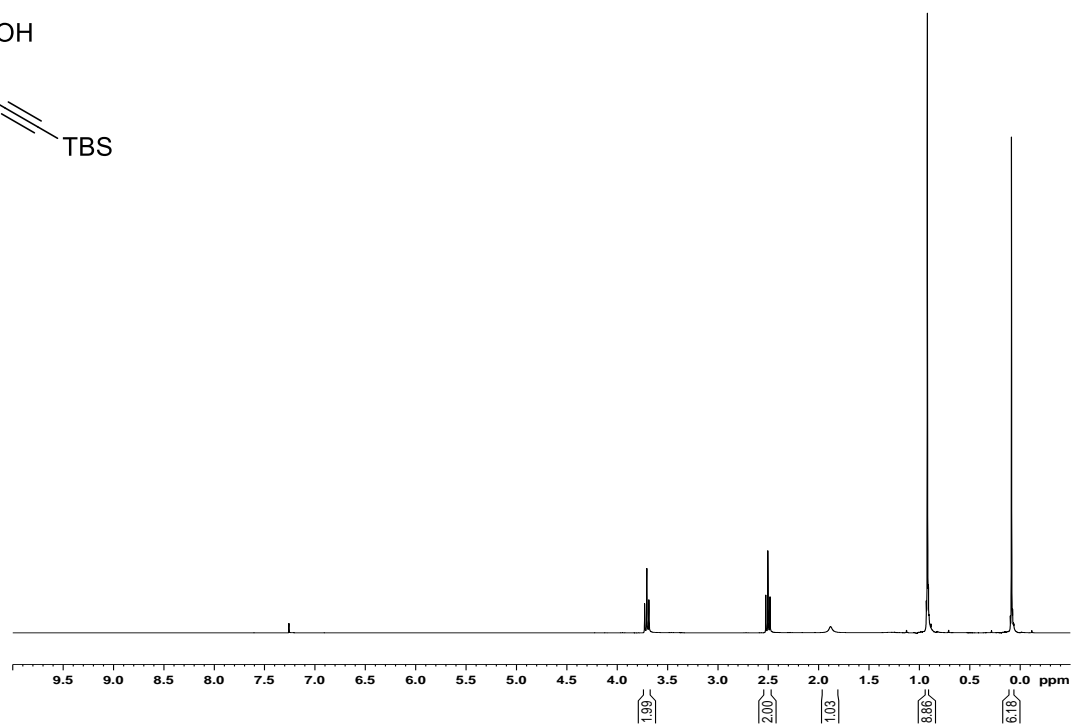
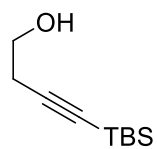
^1H NMR spectrum for 2.78a in CDCl_3



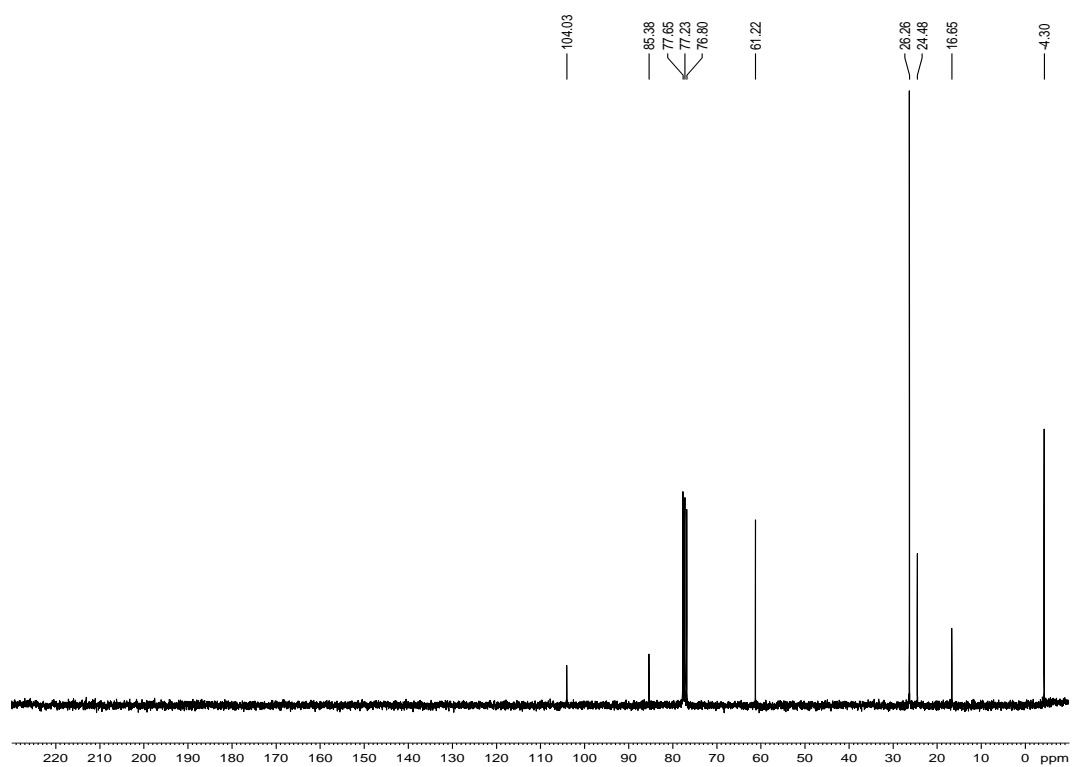
^{13}C NMR spectrum for 2.78a in CDCl_3



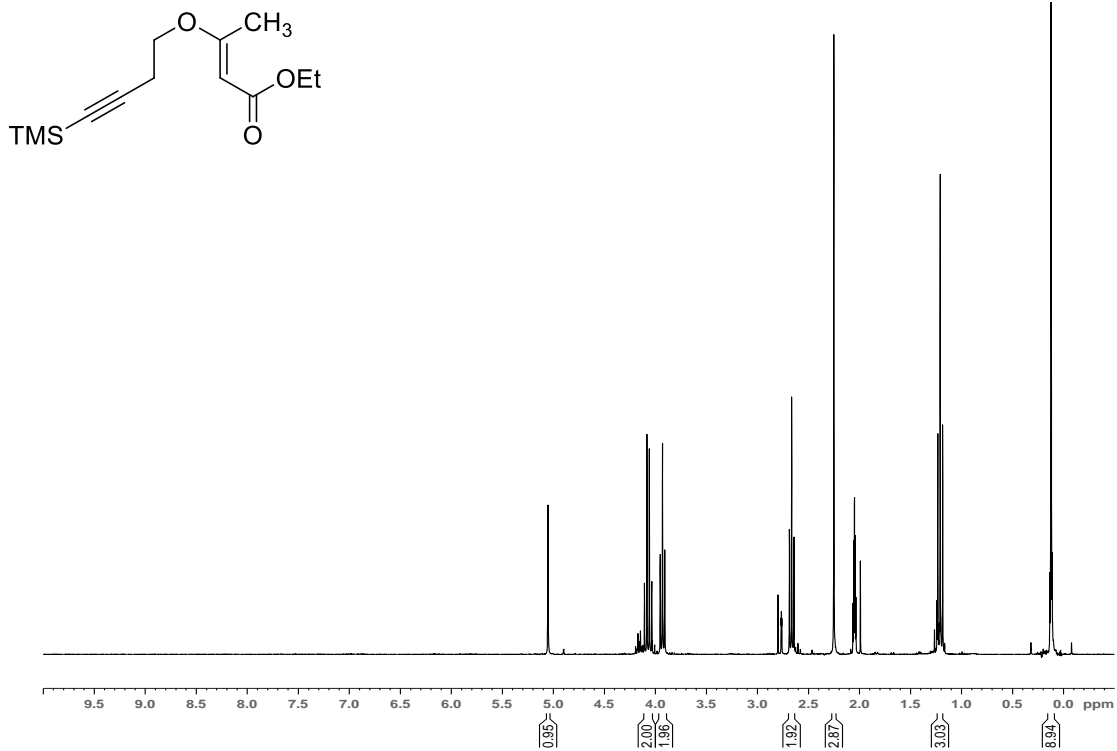
^1H NMR spectrum for 2.78b in CDCl_3



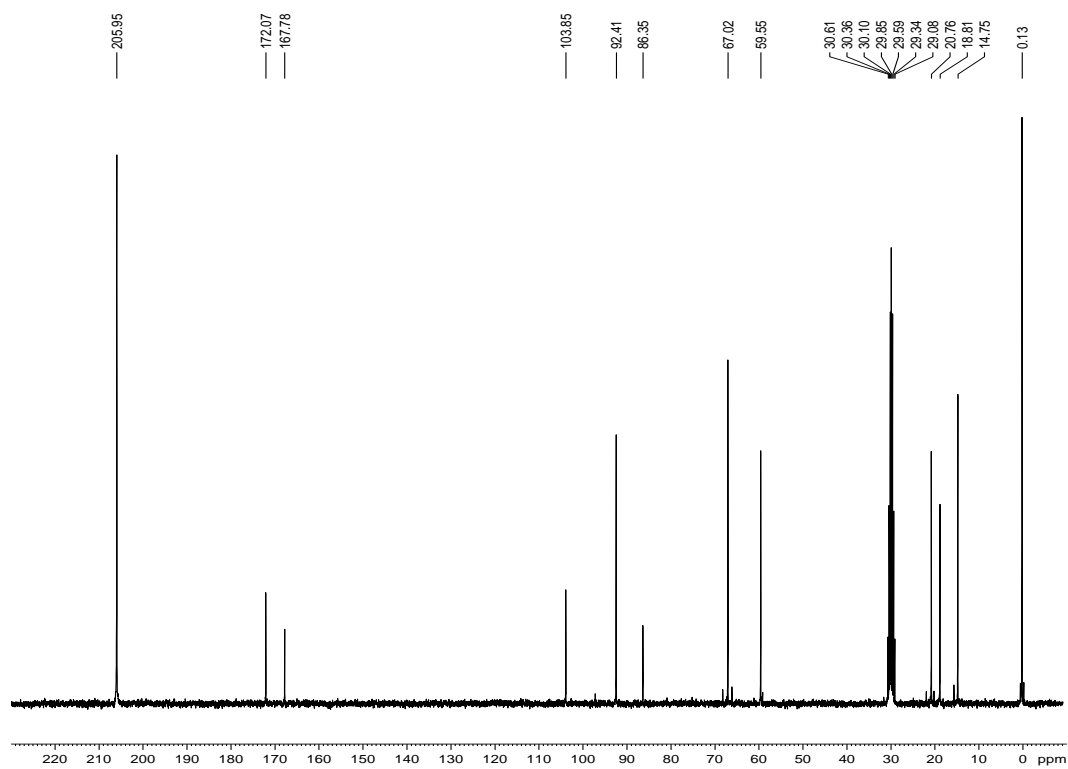
^{13}C NMR spectrum for 2.78b in CDCl_3



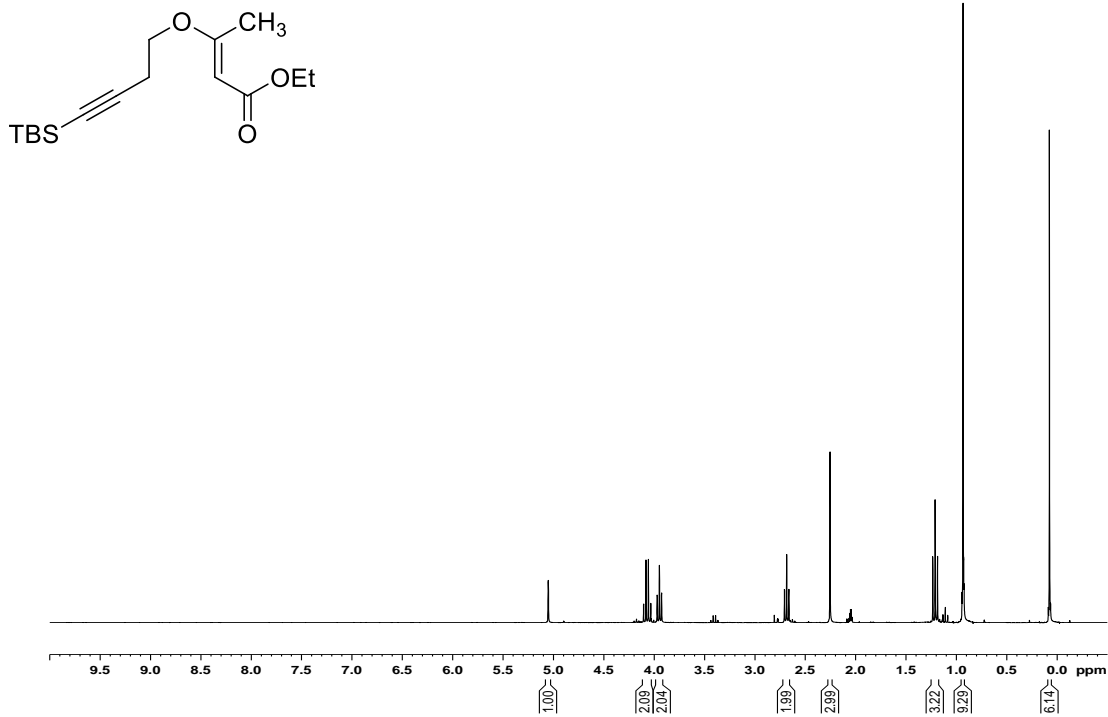
^1H NMR spectrum for 2.79a in $(\text{CD}_3)_2\text{CO}$



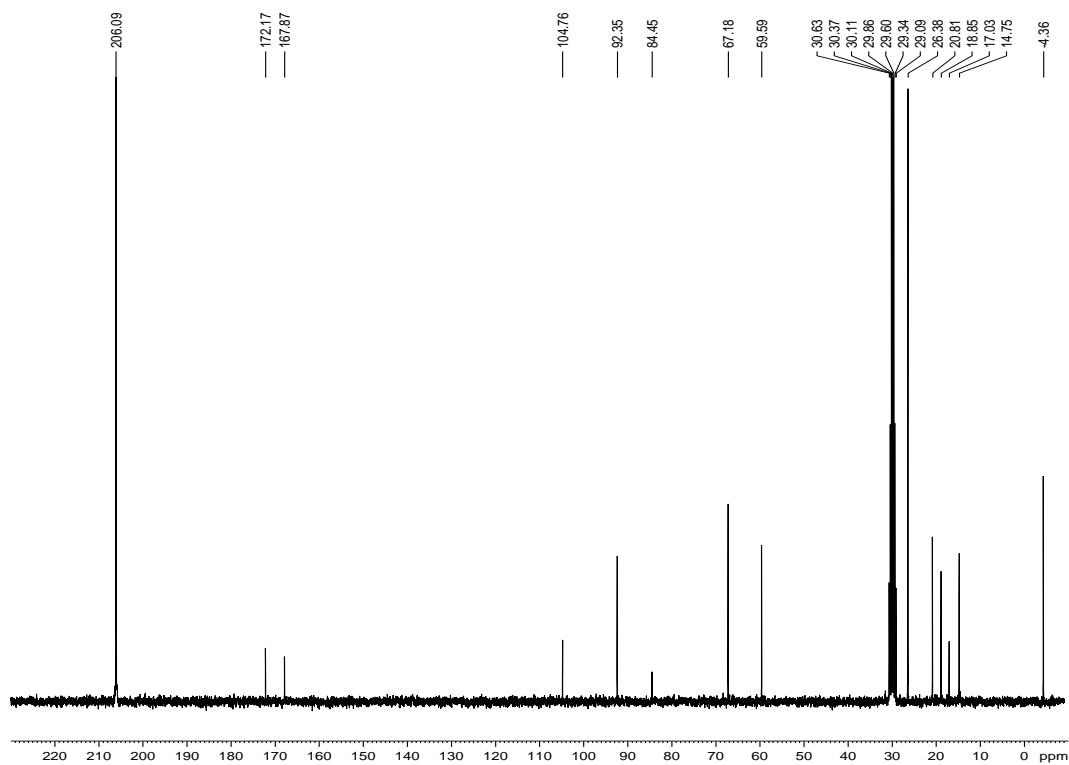
^{13}C NMR spectrum for 2.79a in $(\text{CD}_3)_2\text{CO}$



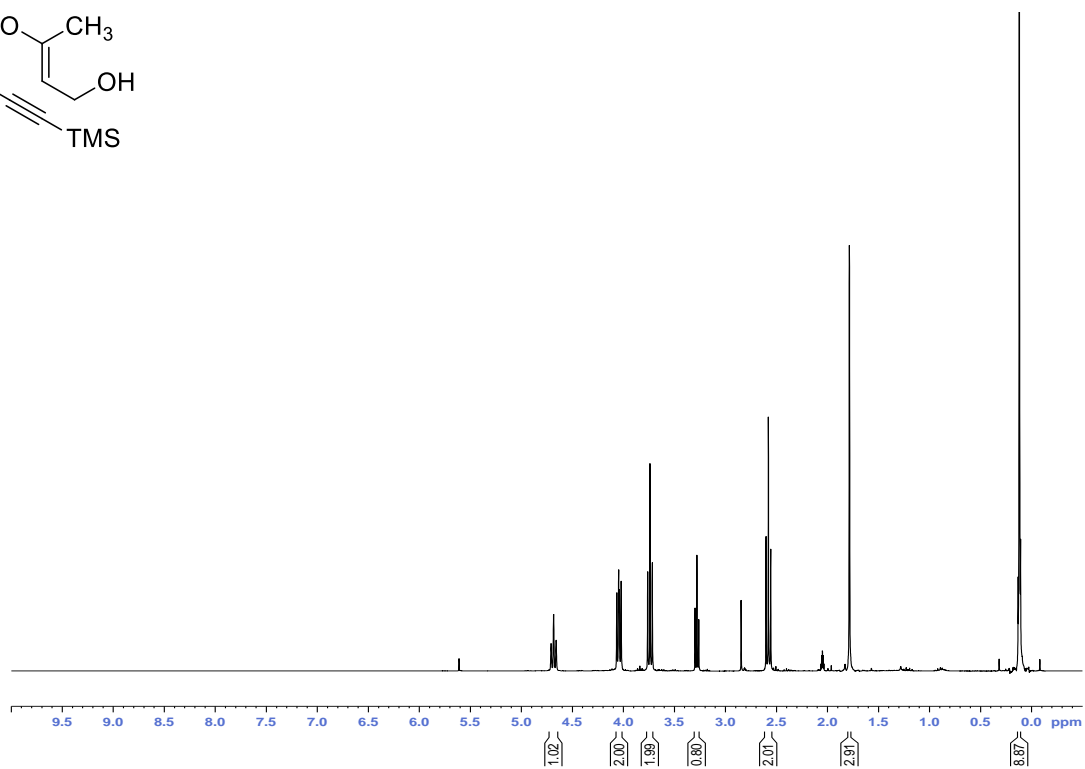
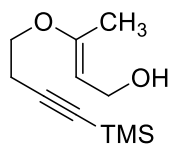
^1H NMR spectrum for 2.79b (1.00:0.04 E:Z) in $(\text{CD}_3)_2\text{CO}$



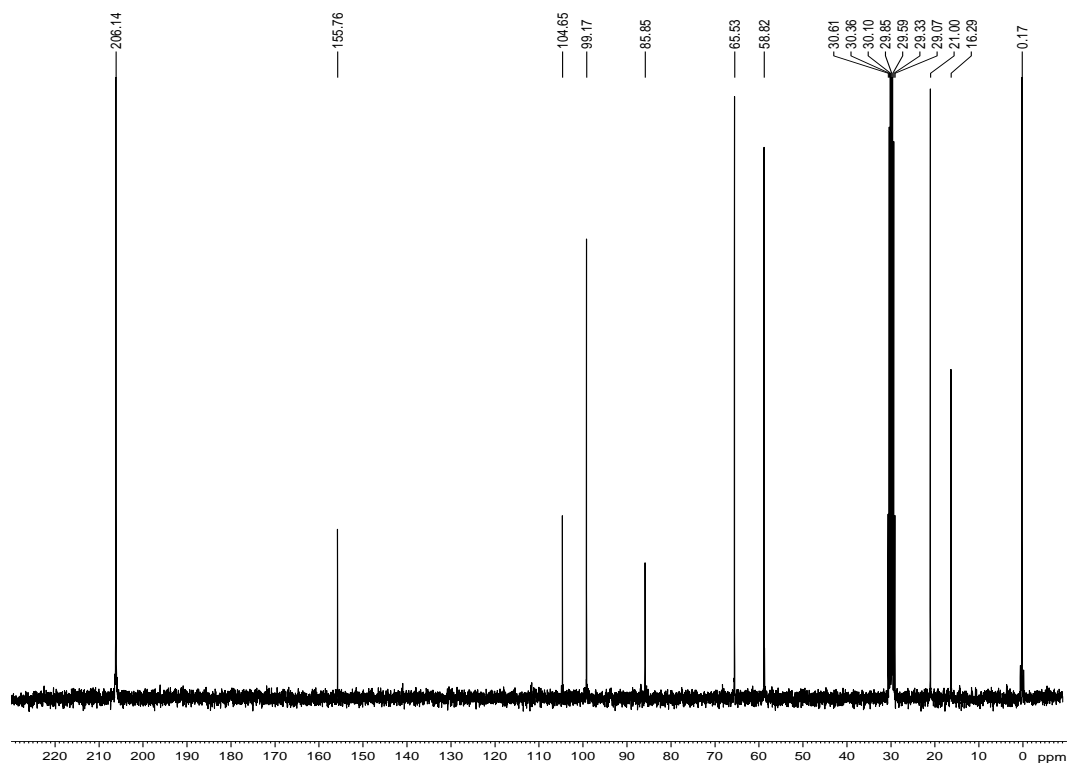
^{13}C NMR spectrum for 2.79b (1.00:0.04 E:Z) in $(\text{CD}_3)_2\text{CO}$



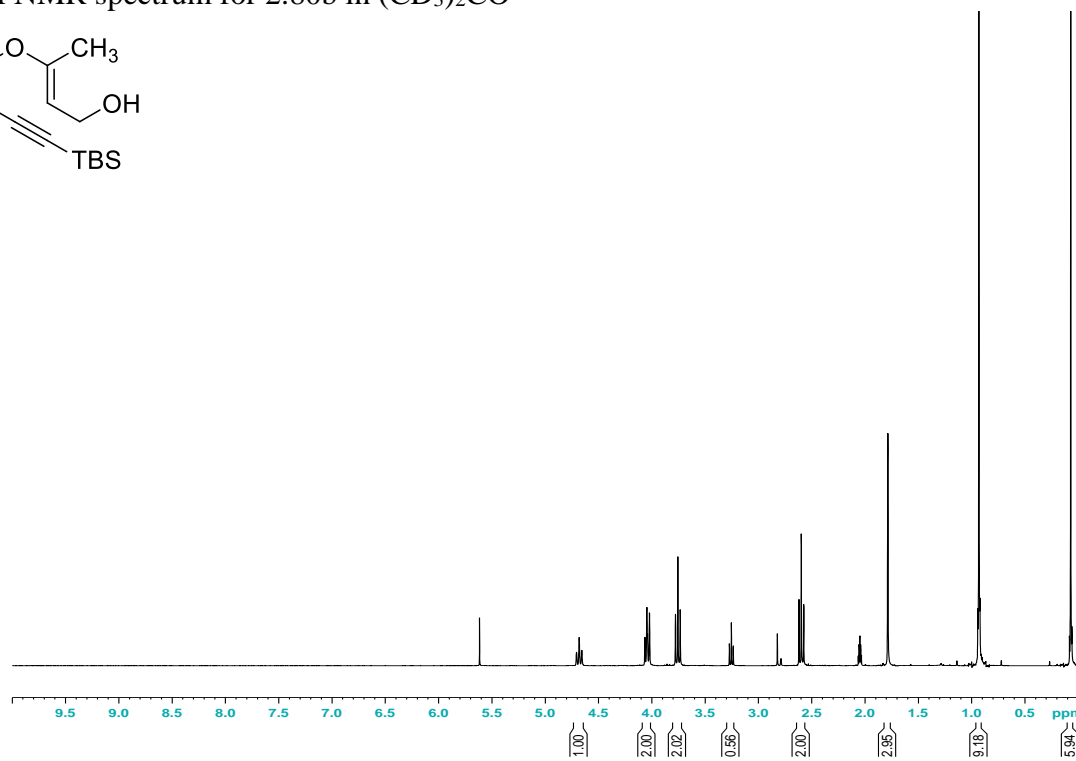
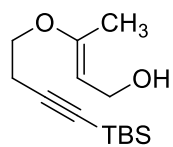
^1H NMR spectrum for 2.80a in $(\text{CD}_3)_2\text{CO}$



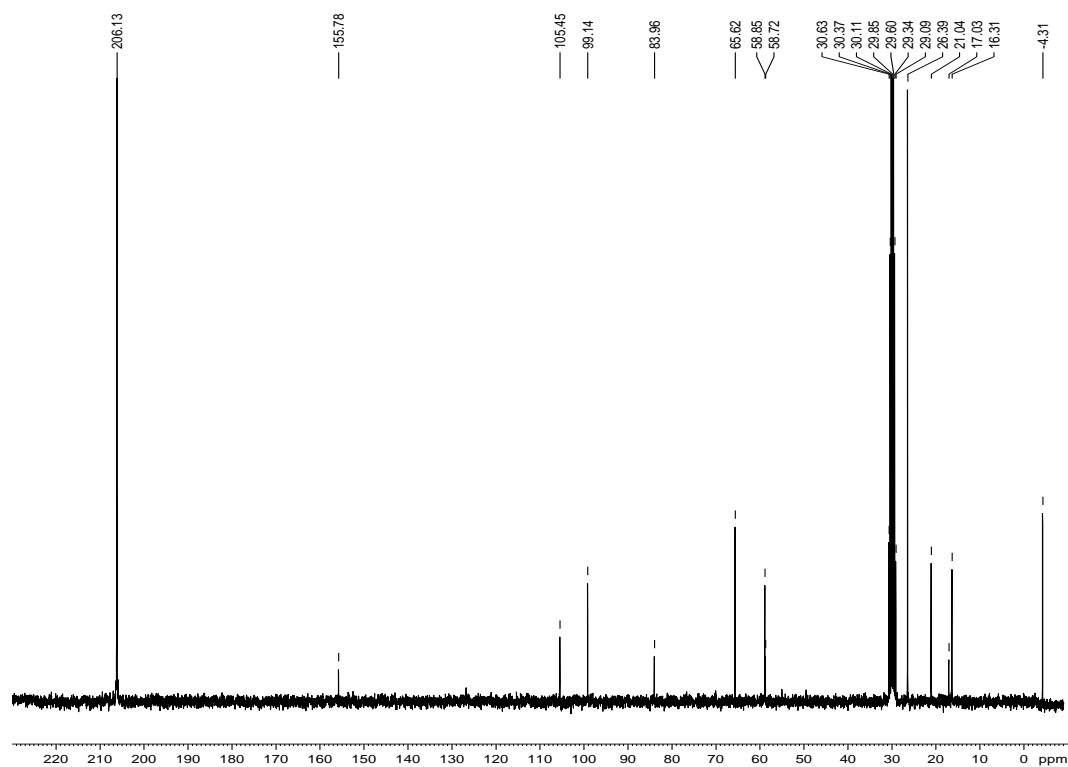
^{13}C NMR spectrum for 2.80a in $(\text{CD}_3)_2\text{CO}$



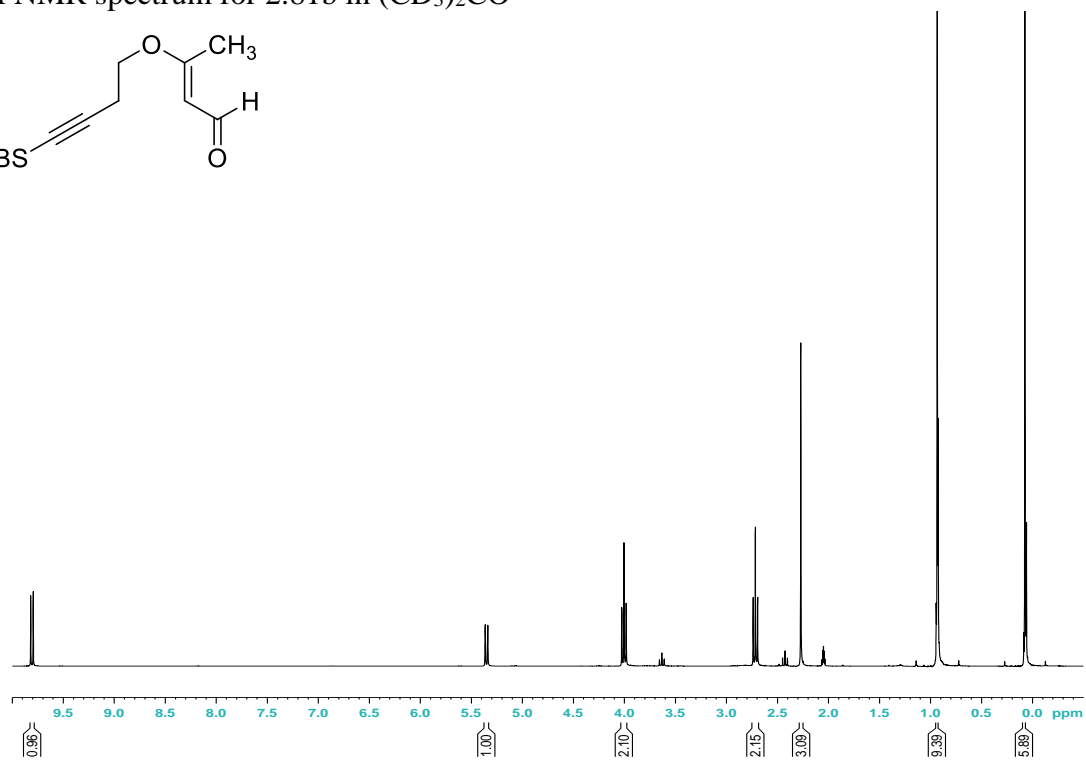
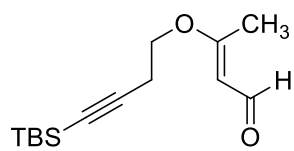
^1H NMR spectrum for 2.80b in $(\text{CD}_3)_2\text{CO}$



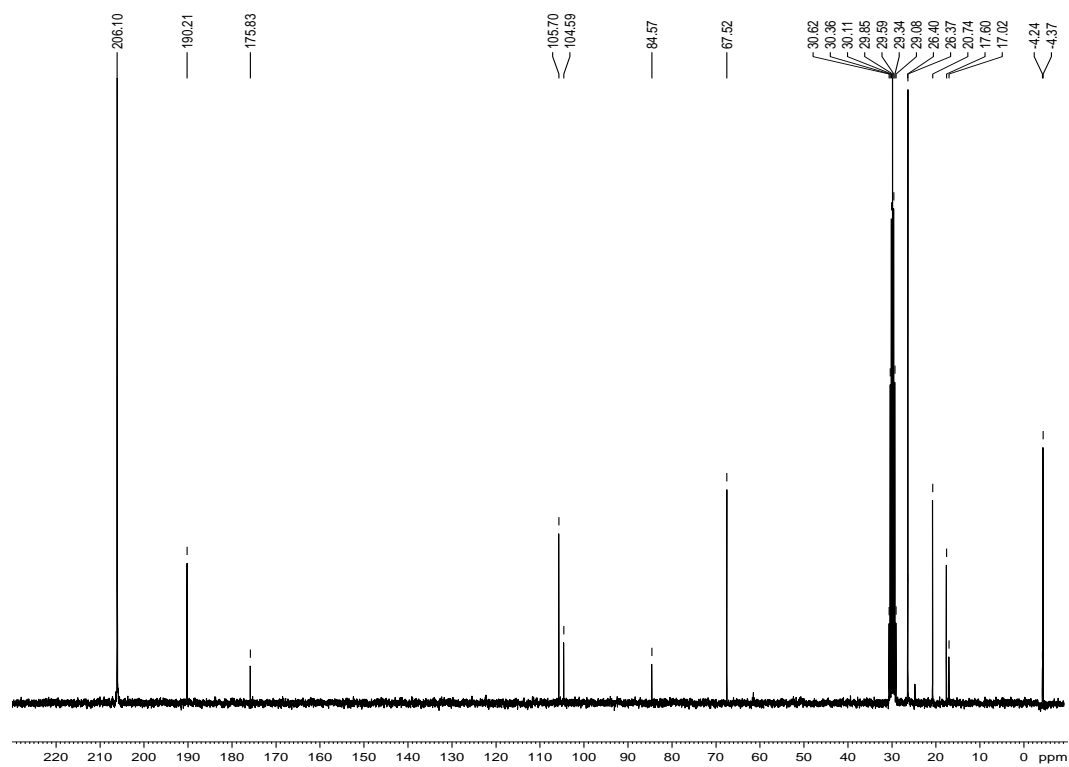
^{13}C NMR spectrum for 2.80b in $(\text{CD}_3)_2\text{CO}$



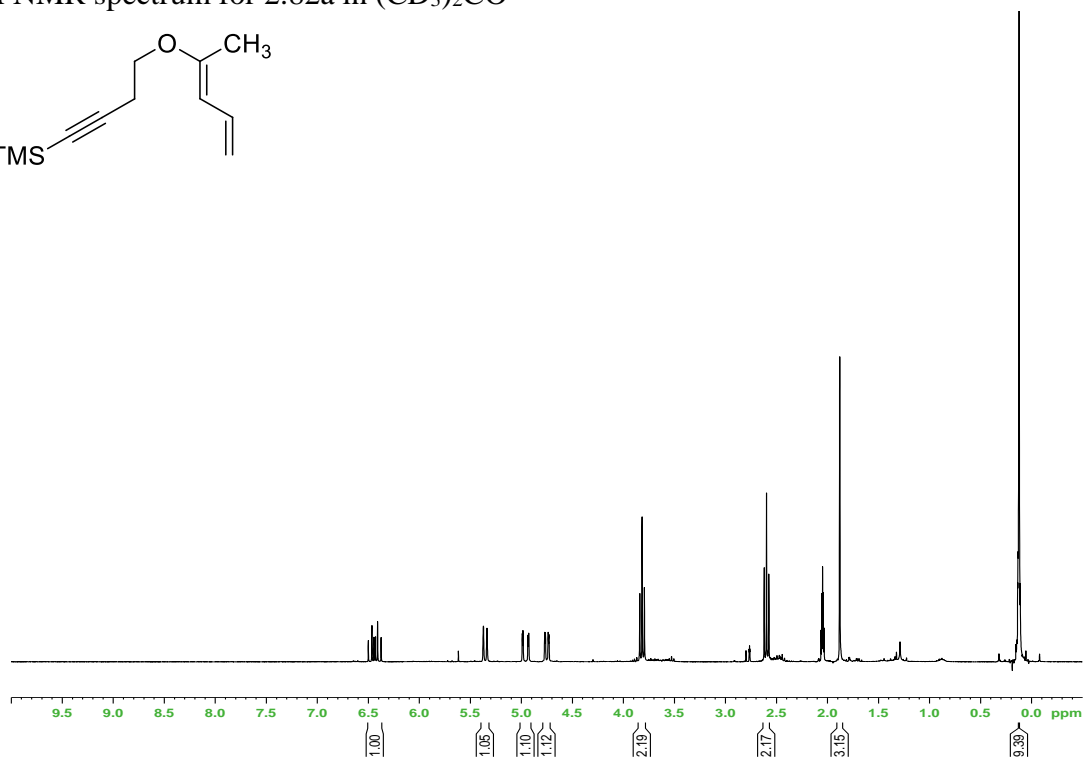
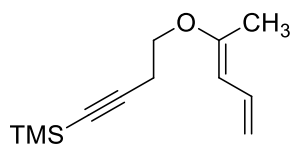
^1H NMR spectrum for 2.81b in $(\text{CD}_3)_2\text{CO}$



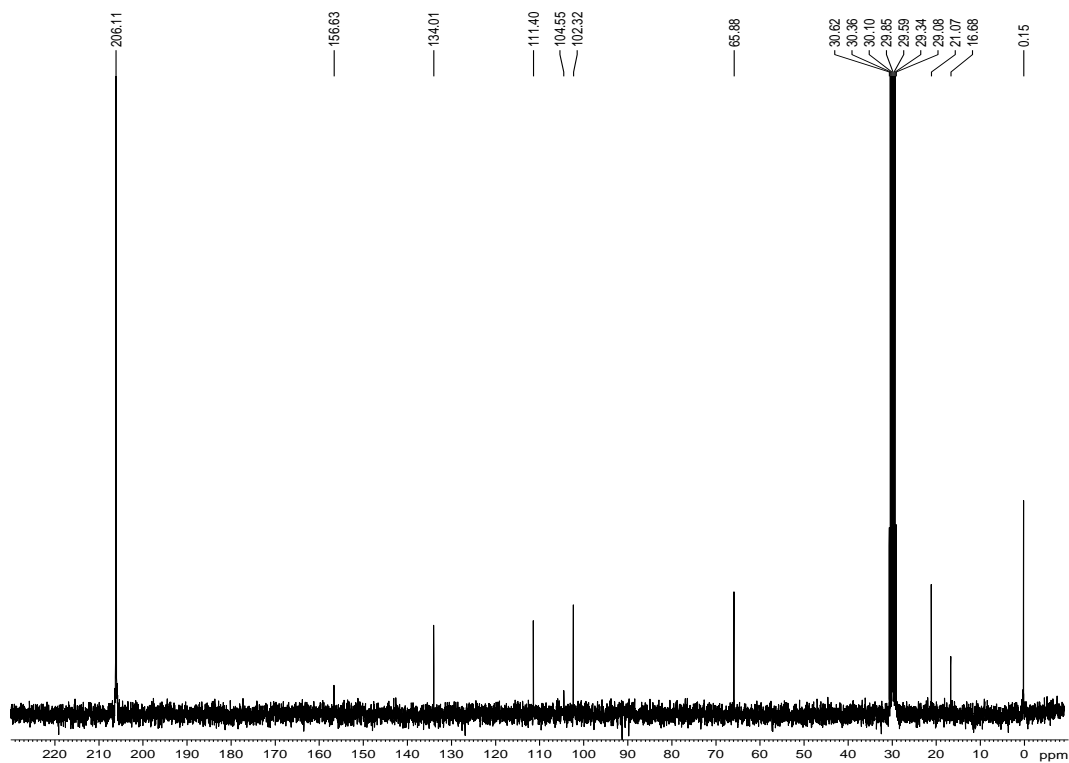
^{13}C NMR spectrum for 2.81b in $(\text{CD}_3)_2\text{CO}$



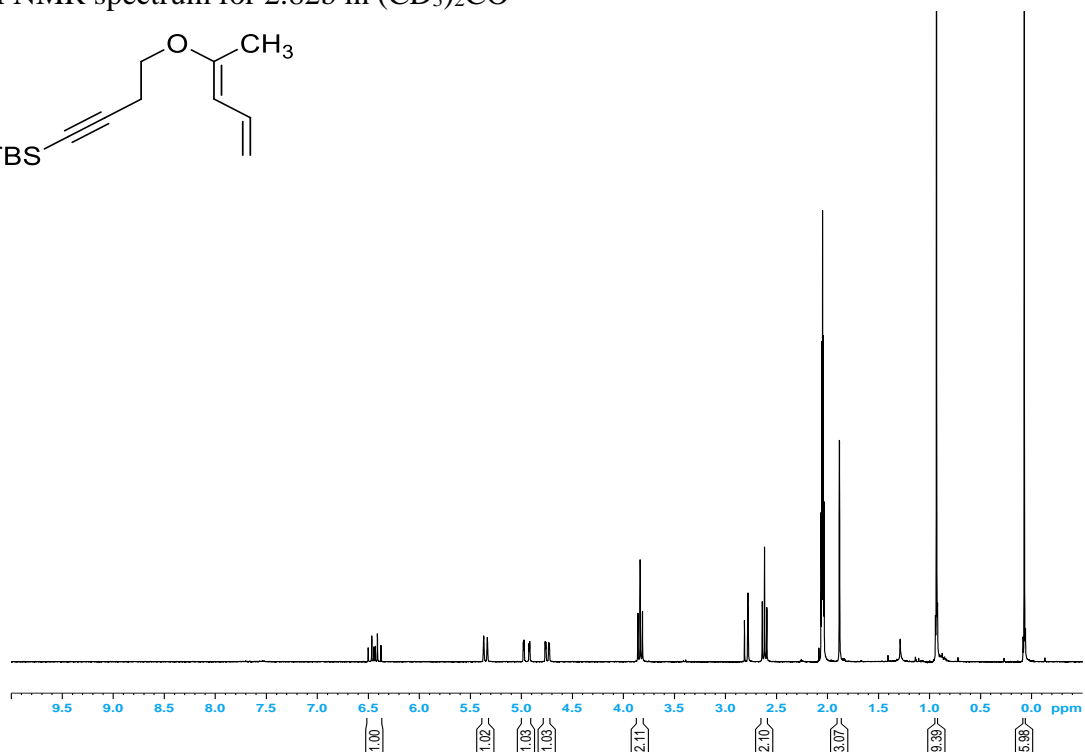
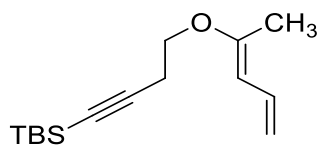
^1H NMR spectrum for 2.82a in $(\text{CD}_3)_2\text{CO}$



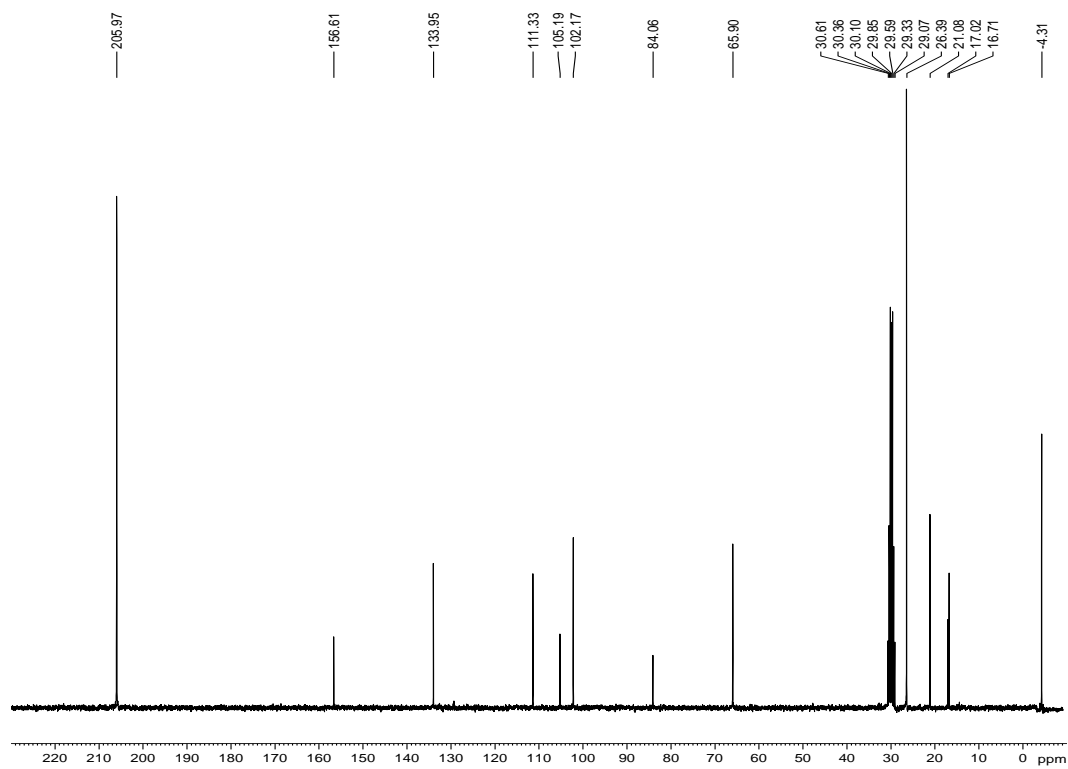
^{13}C NMR spectrum for 2.82a in $(\text{CD}_3)_2\text{CO}$



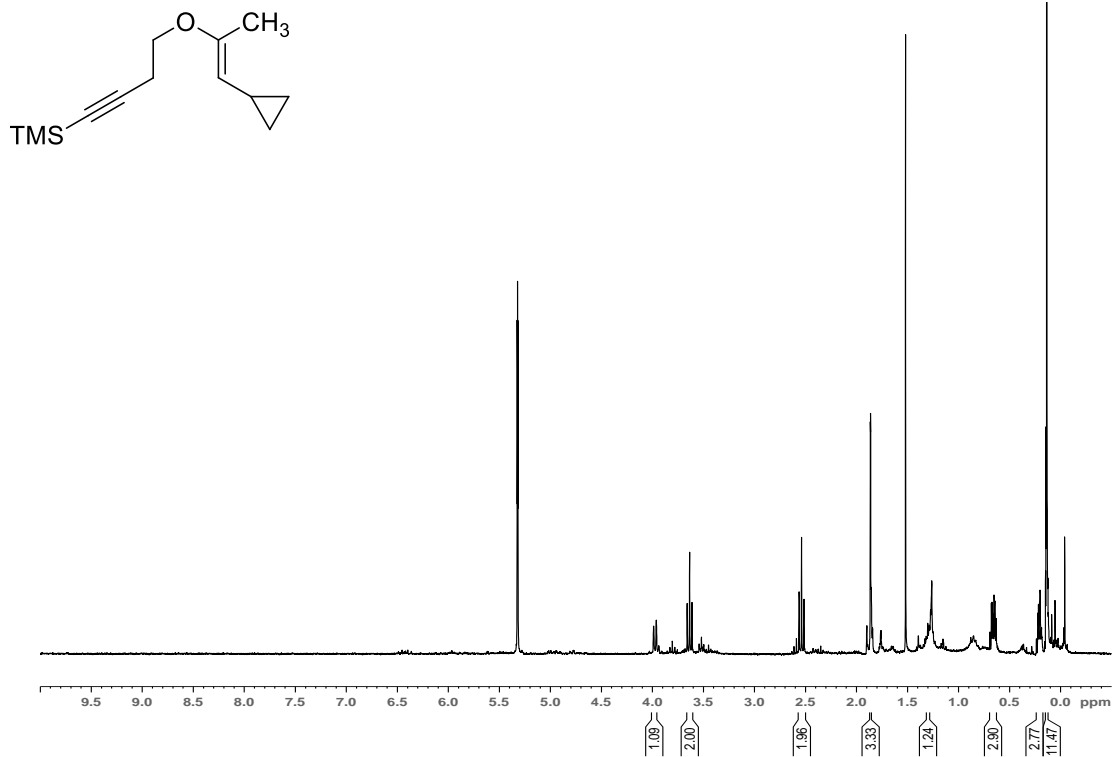
^1H NMR spectrum for 2.82b in $(\text{CD}_3)_2\text{CO}$



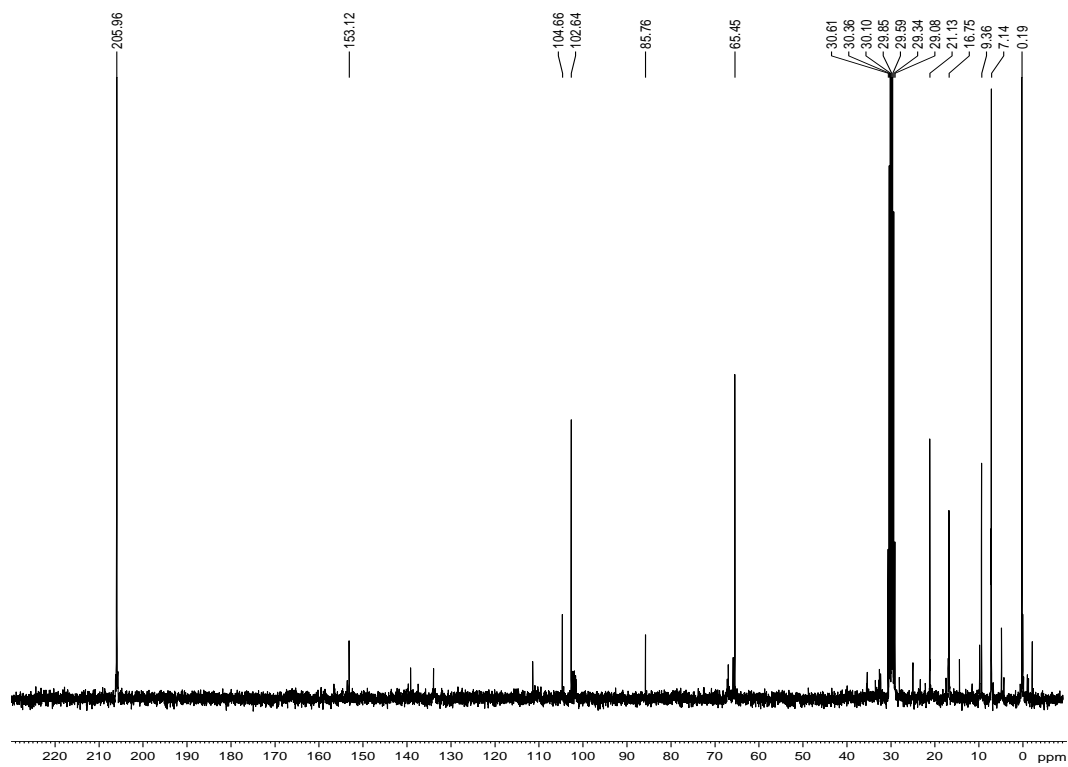
^{13}C NMR spectrum for 2.82b in $(\text{CD}_3)_2\text{CO}$



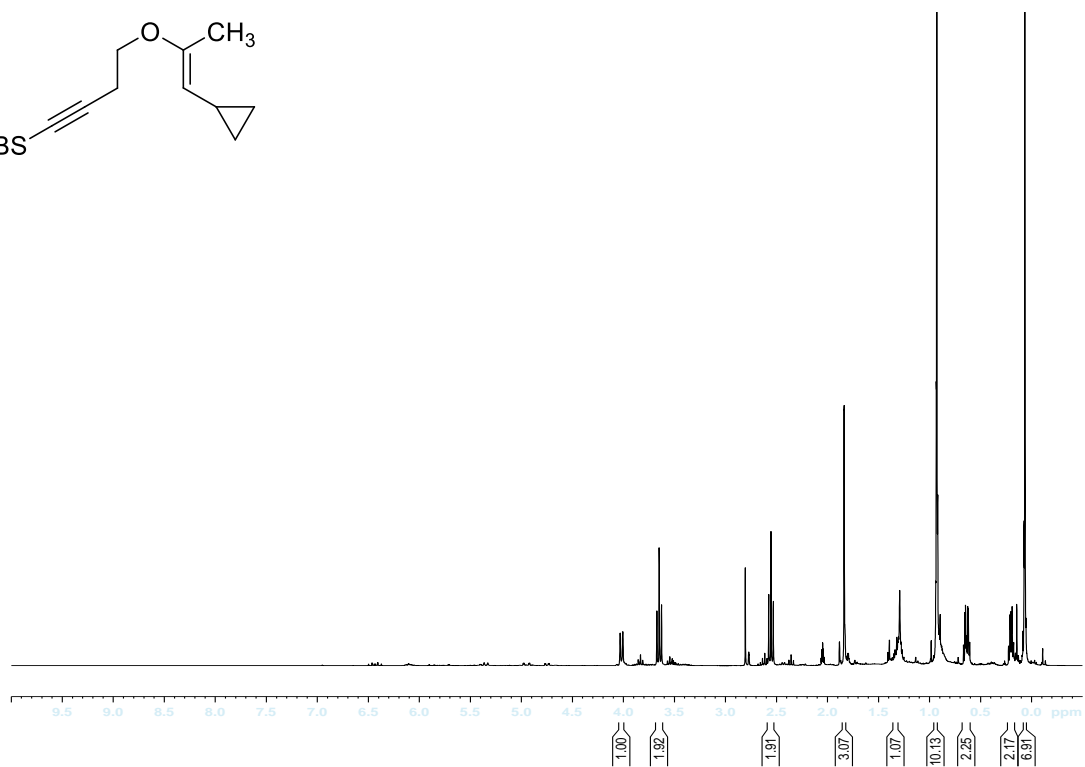
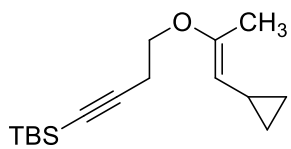
^1H NMR spectrum for 2.83a (1.00:0.14 2.83a:2.82a) in CD_2Cl_2



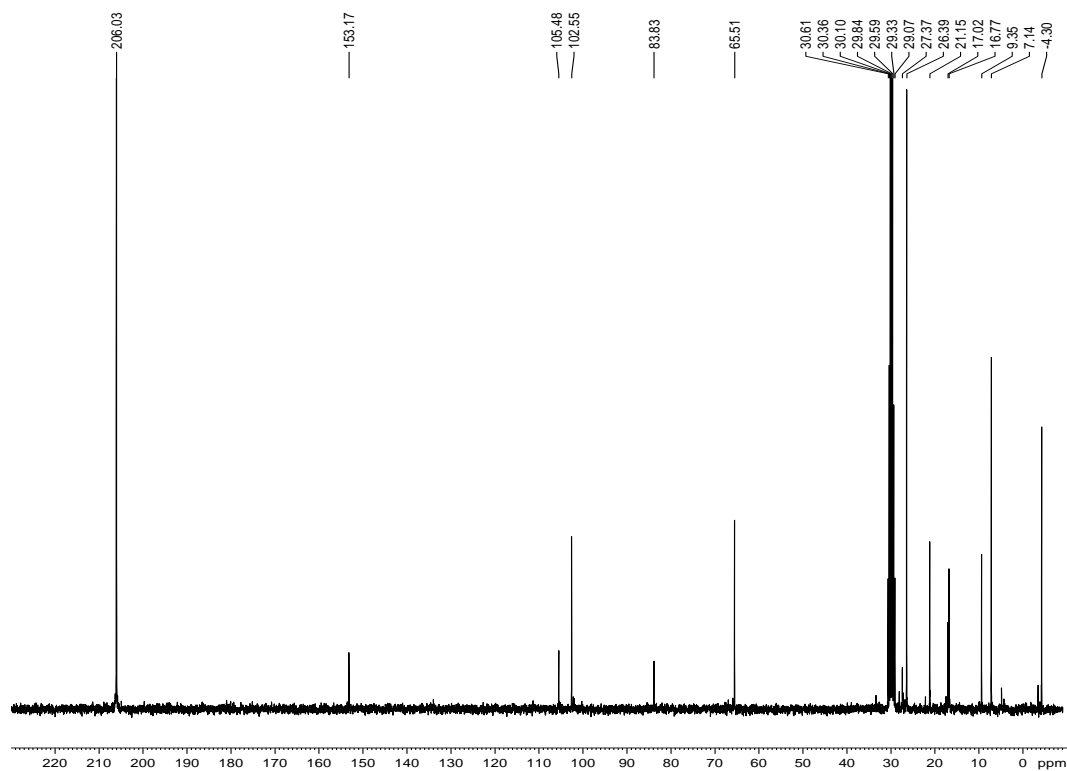
^{13}C NMR spectrum for 2.83a (1.00:0.14 2.83a:2.82a) in $(\text{CD}_3)_2\text{CO}$



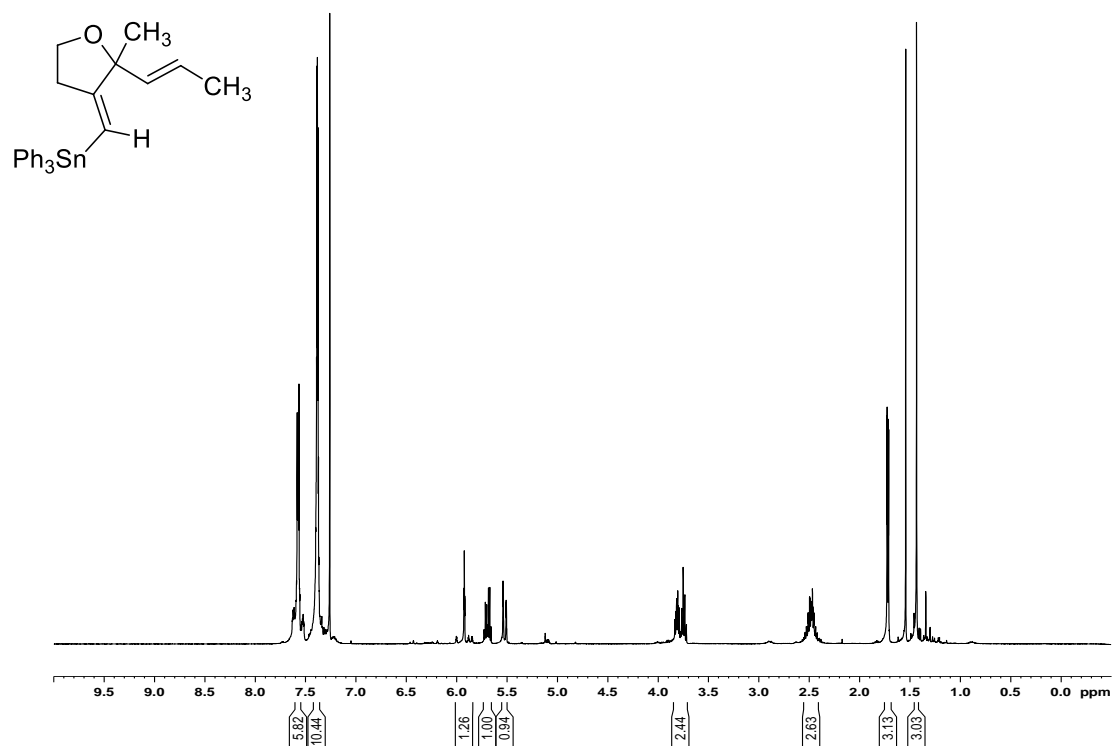
^1H NMR spectrum for 2.83b (1.00:0.09 2.83b:2.82b) in $(\text{CD}_3)_2\text{CO}$



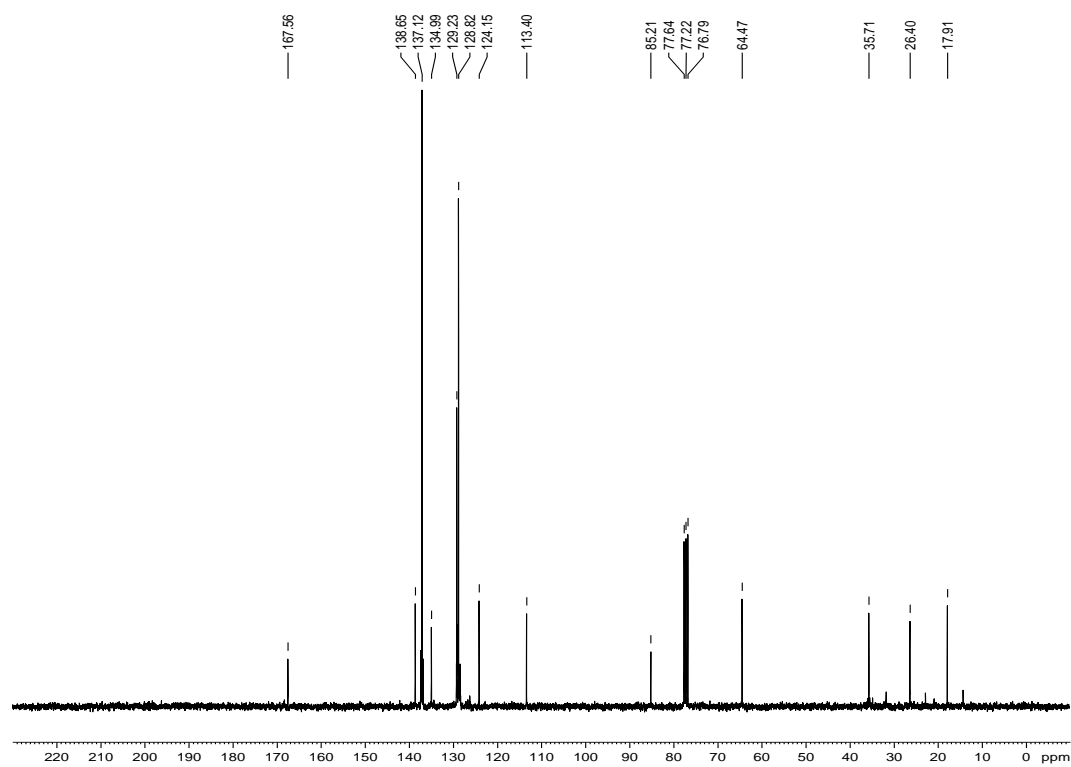
^{13}C NMR spectrum for 2.83b (1.00:0.09 2.83b:2.82b) in $(\text{CD}_3)_2\text{CO}$



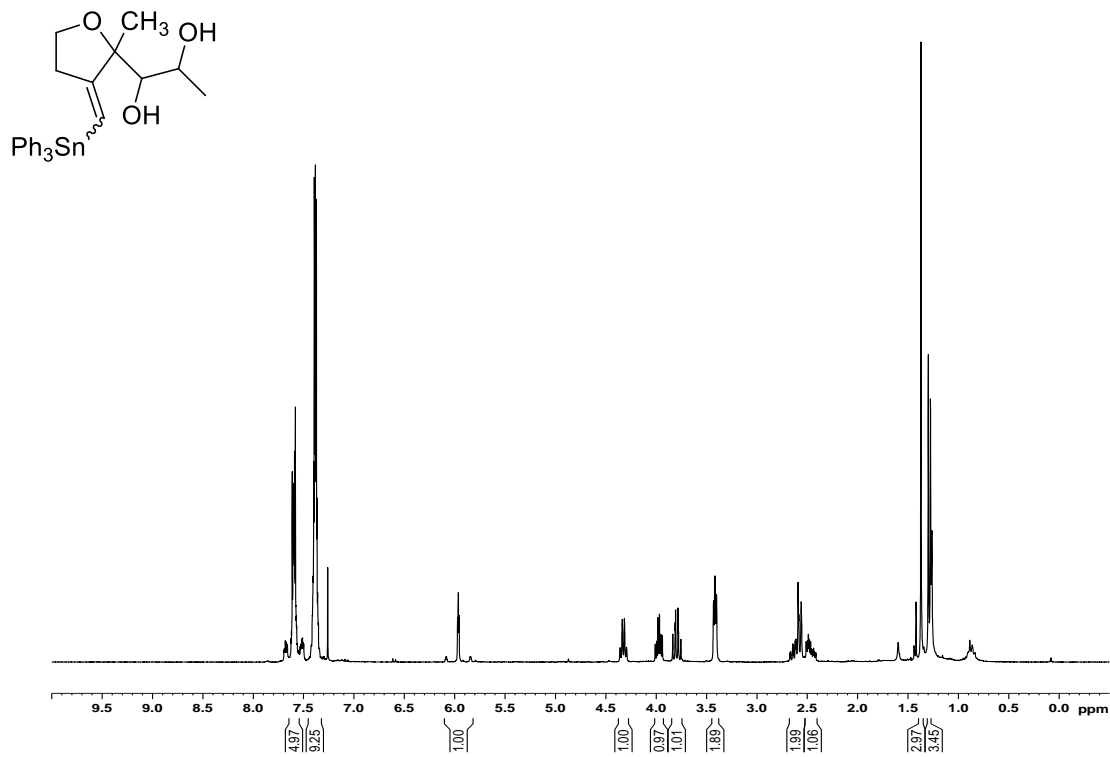
^1H NMR spectrum for 2.90 (1.00:0.10 2.90:2.91) in CDCl_3



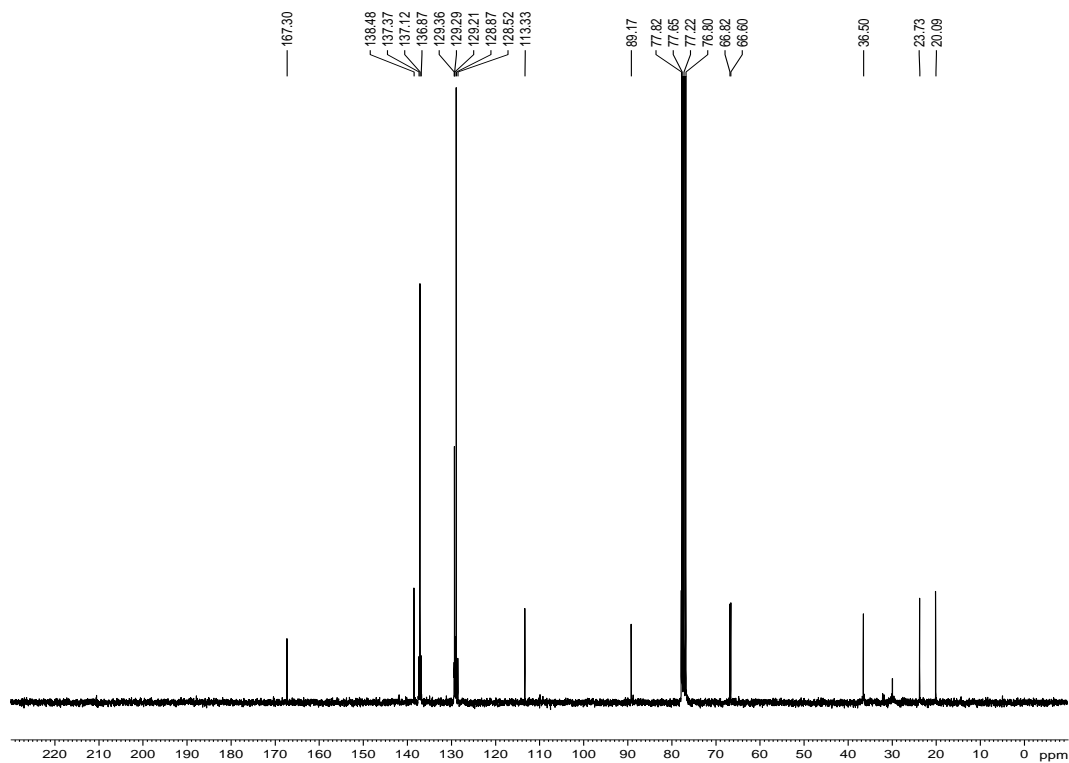
^{13}C NMR spectrum for 2.90 (1.00:0.10 2.90:2.91) in CDCl_3



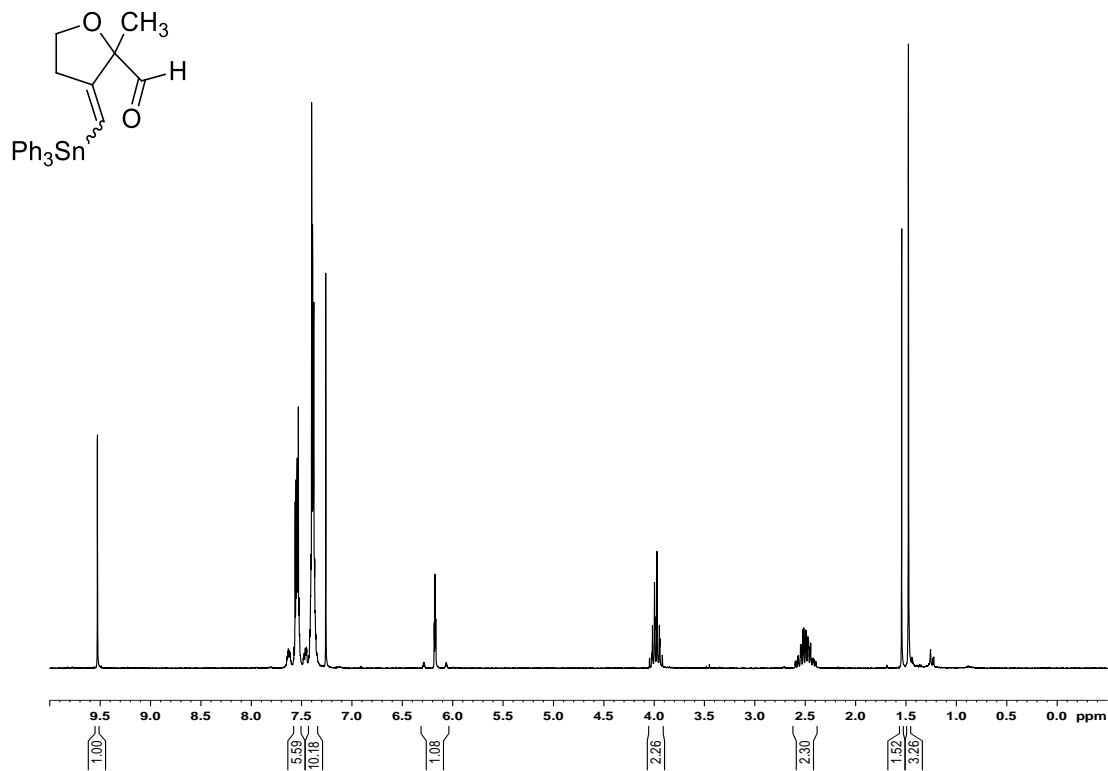
^1H NMR spectrum for 2.97 in CDCl_3



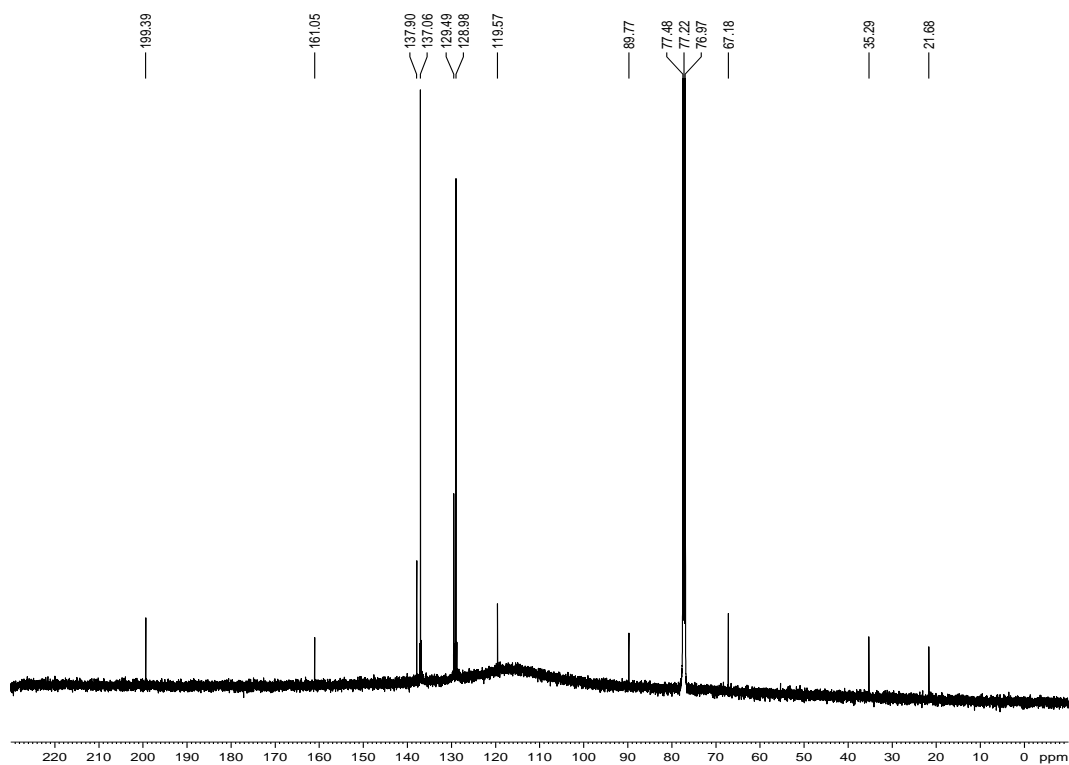
^{13}C NMR spectrum for 2.97 in CDCl_3



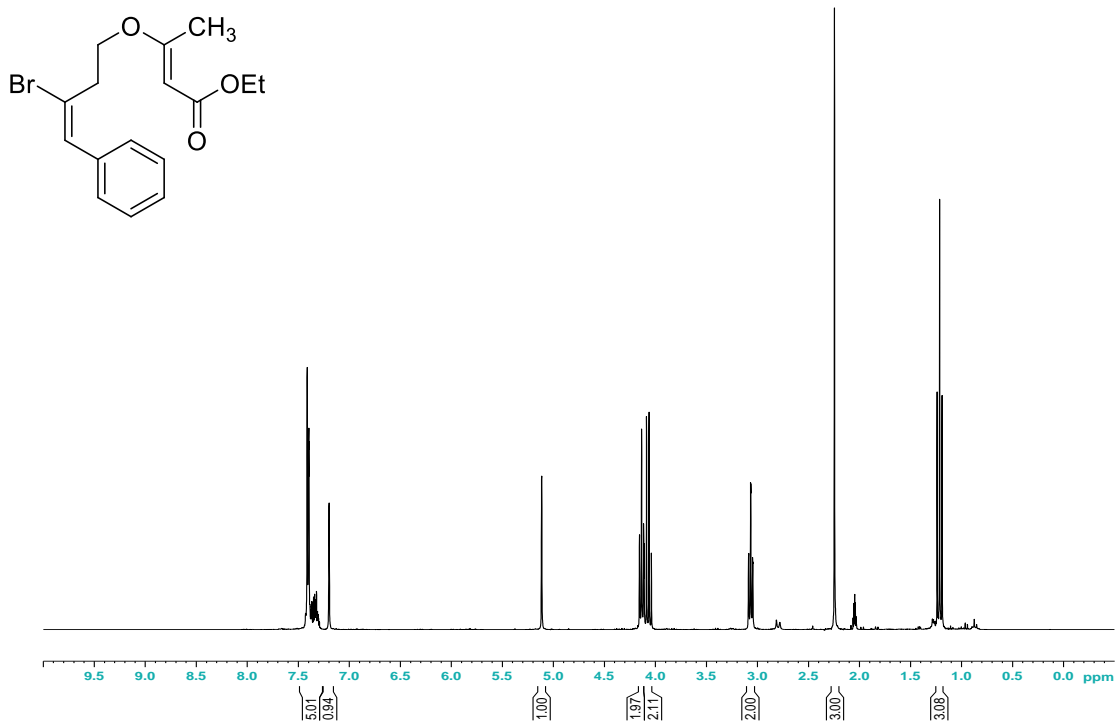
^1H NMR spectrum for 2.98 in CDCl_3



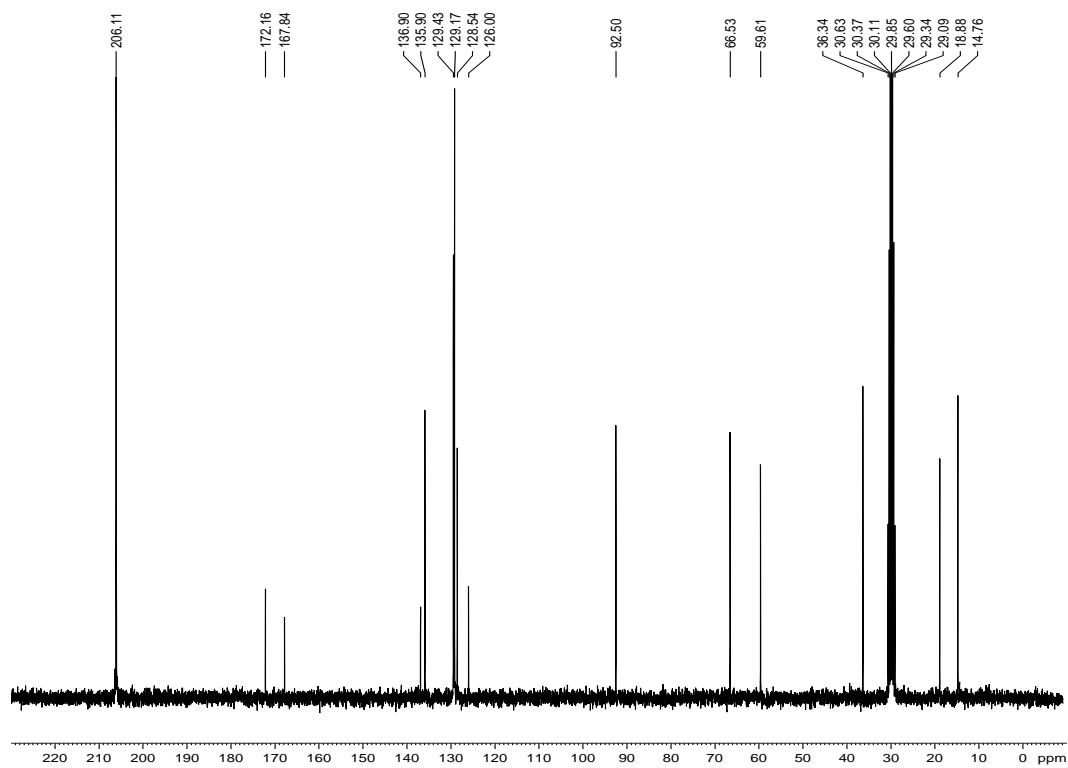
^{13}C NMR spectrum for 2.98 in CDCl_3



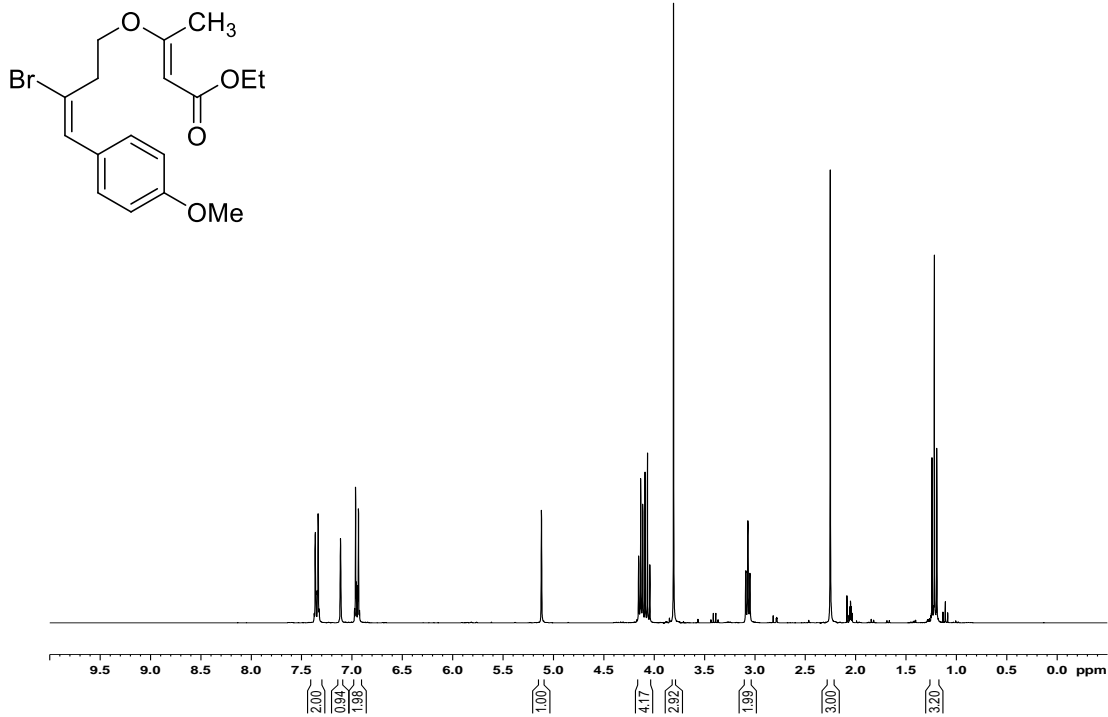
^1H NMR spectrum for 2.104a in $(\text{CD}_3)_2\text{CO}$



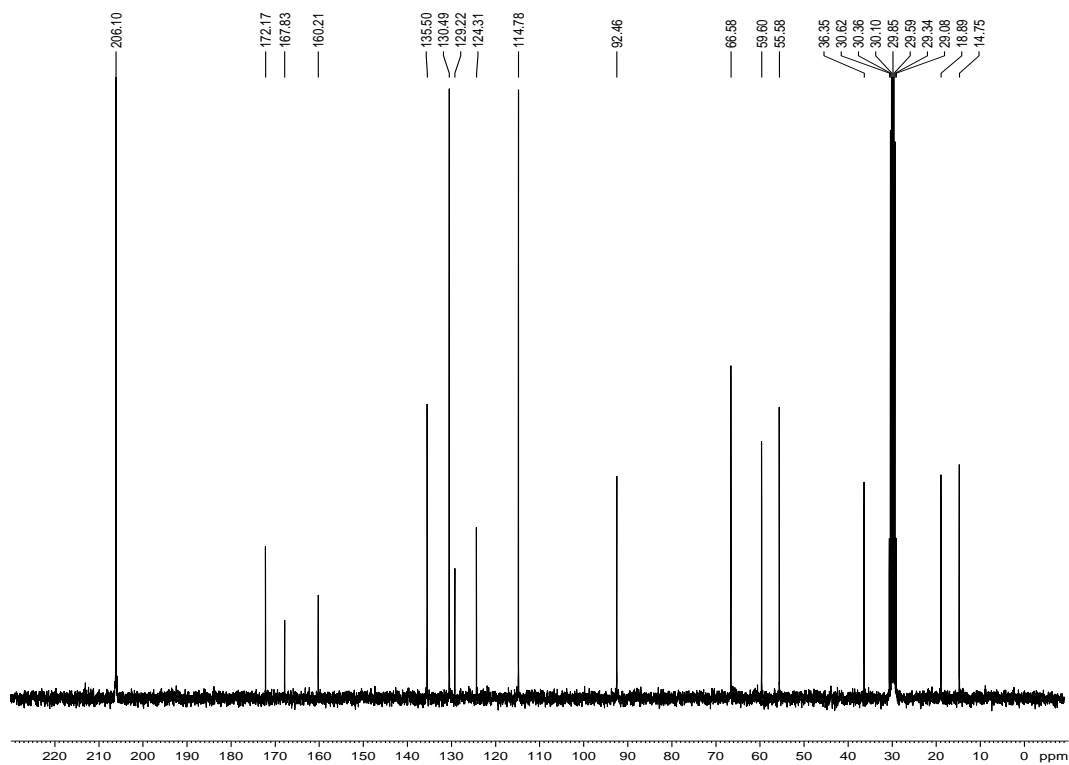
^{13}C NMR spectrum for 2.104a in $(\text{CD}_3)_2\text{CO}$



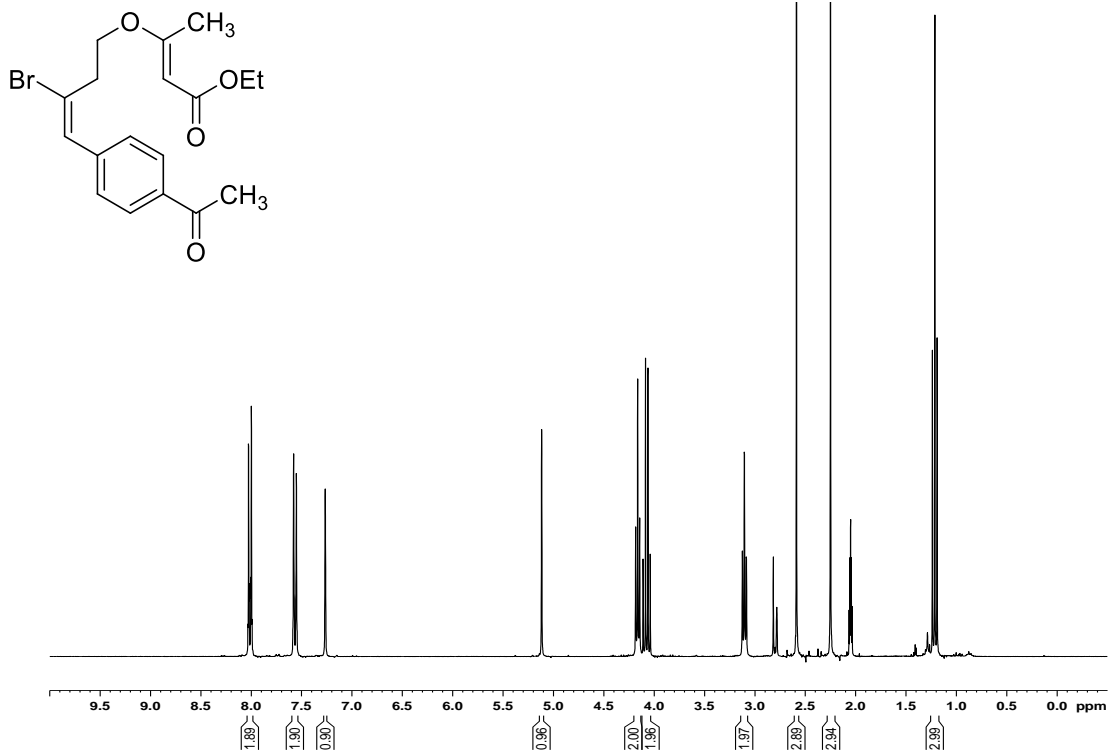
^1H NMR spectrum for 2.401b in $(\text{CD}_3)_2\text{CO}$



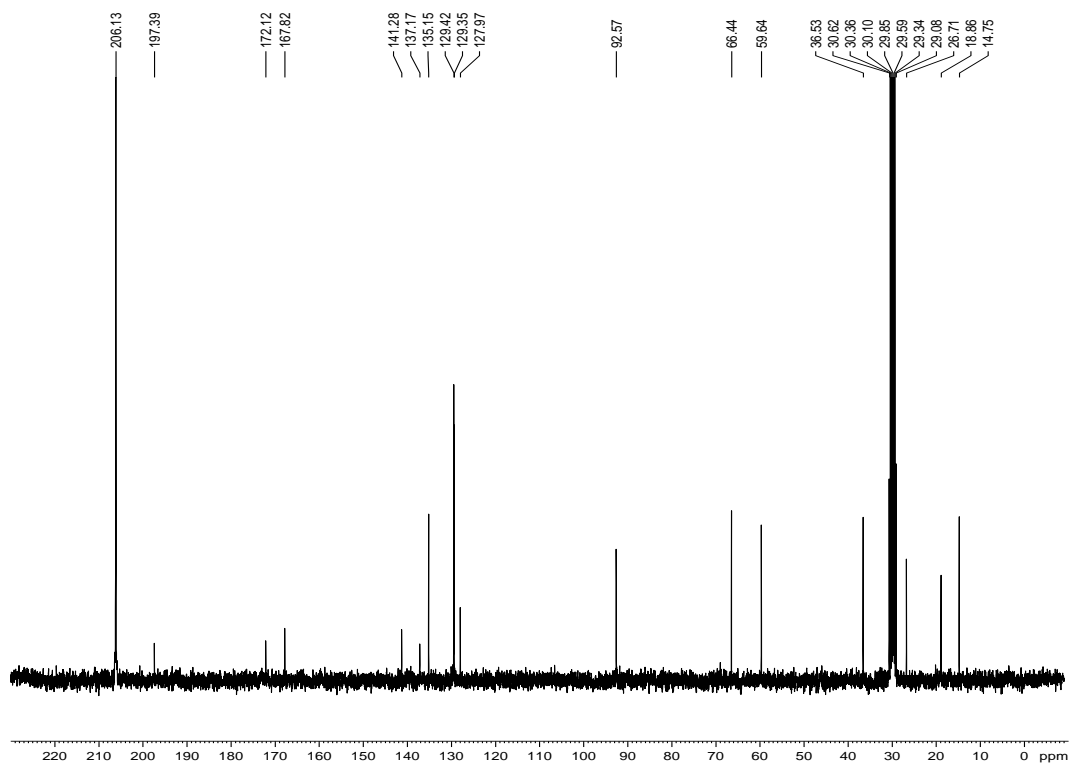
^{13}C NMR spectrum for 2.401b in $(\text{CD}_3)_2\text{CO}$



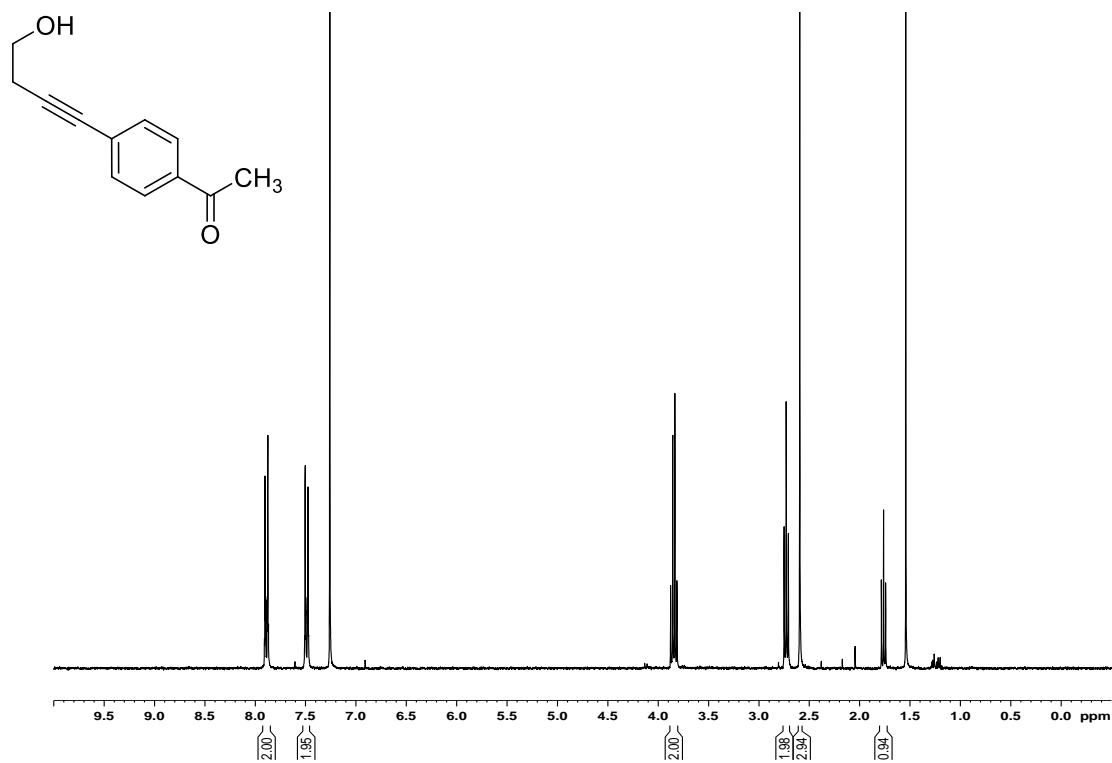
^1H NMR spectrum for 2.401c in $(\text{CD}_3)_2\text{CO}$



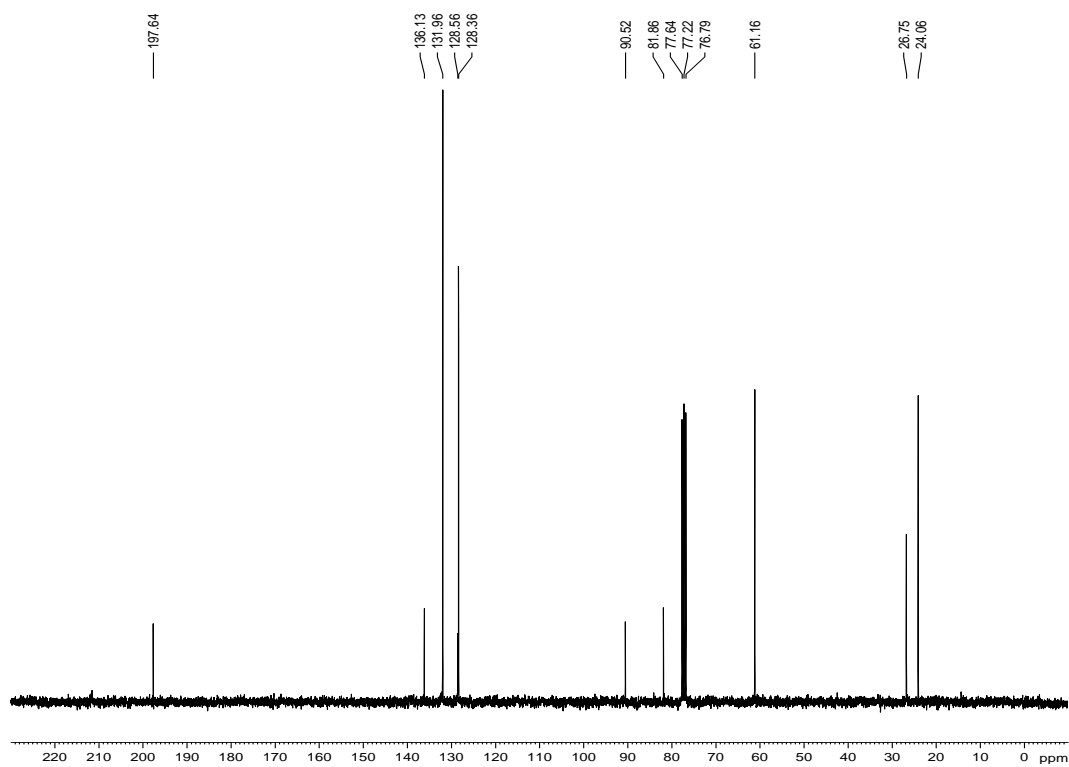
^{13}C NMR spectrum for 2.401c in $(\text{CD}_3)_2\text{CO}$



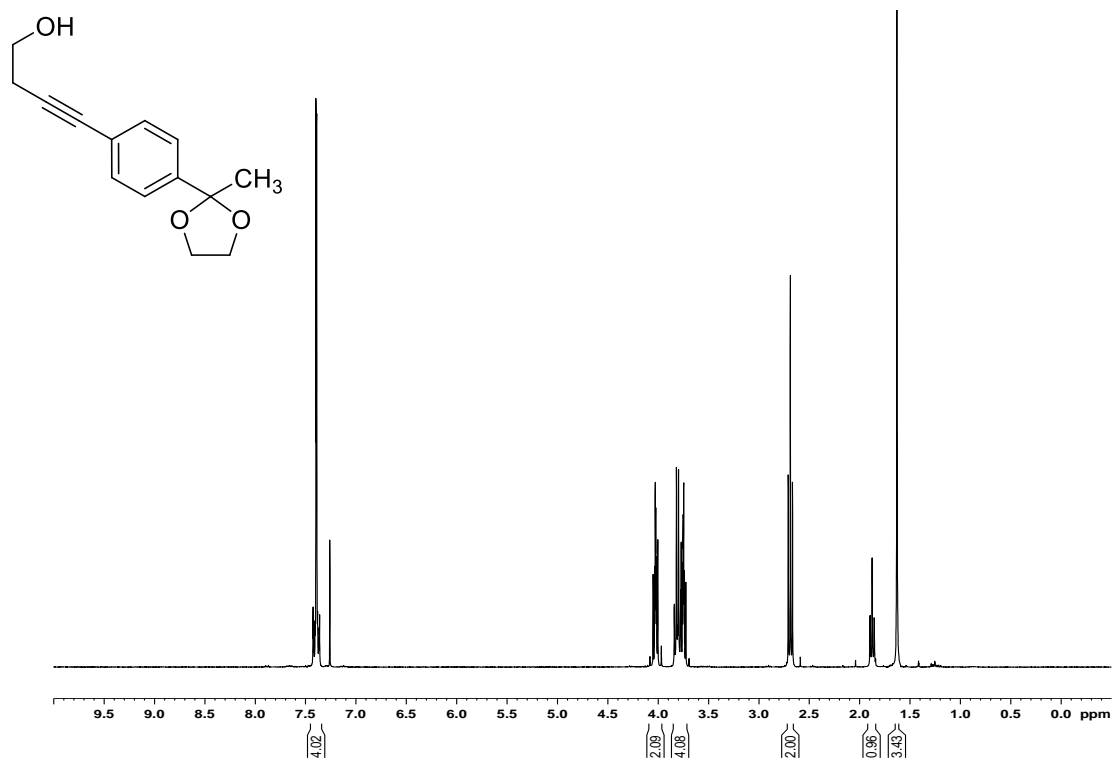
^1H NMR spectrum for 2.110c in CDCl_3



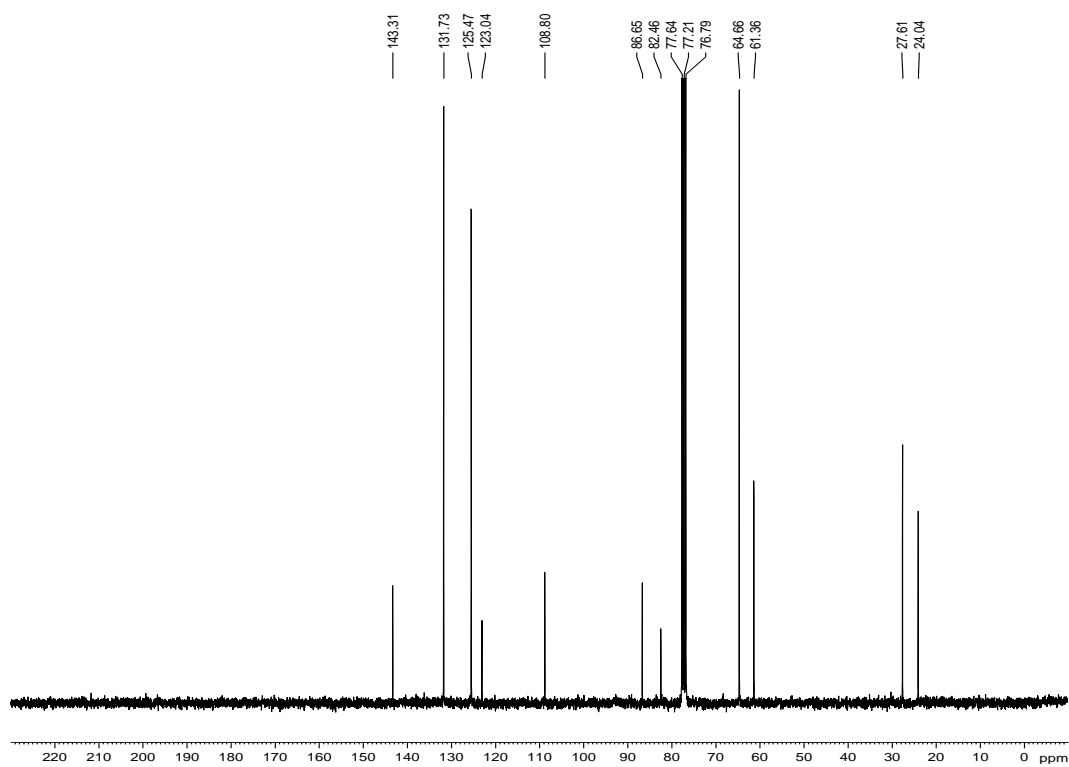
^{13}C NMR spectrum for 2.110c in CDCl_3



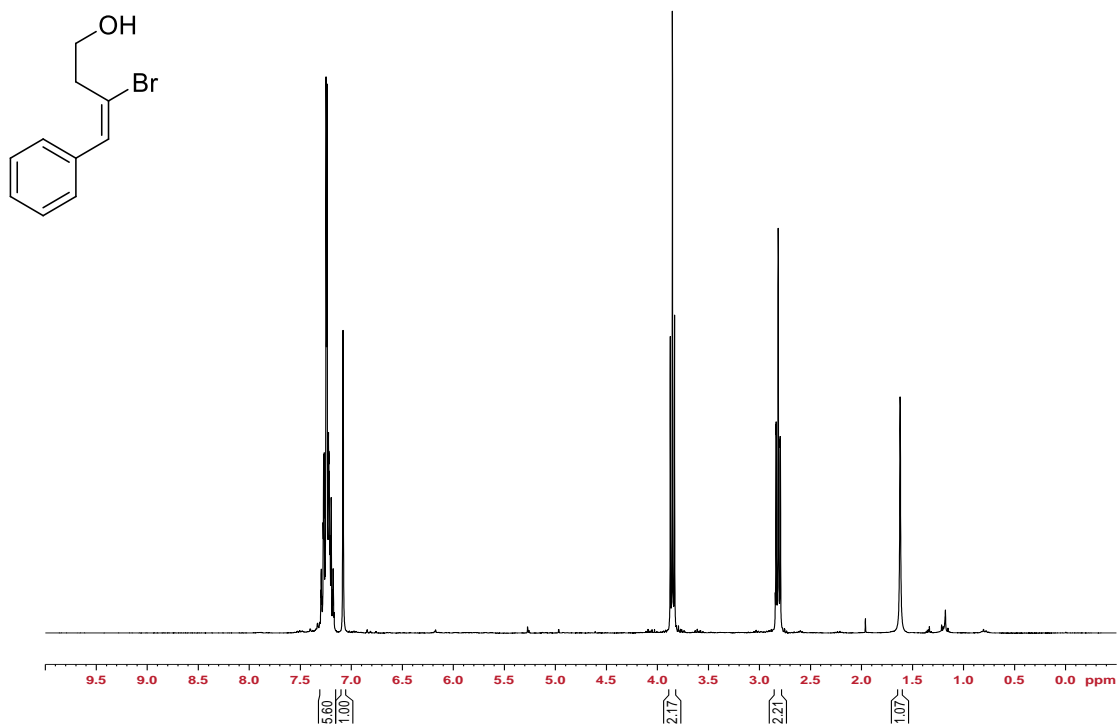
^1H NMR spectrum for 2.110d in CDCl_3



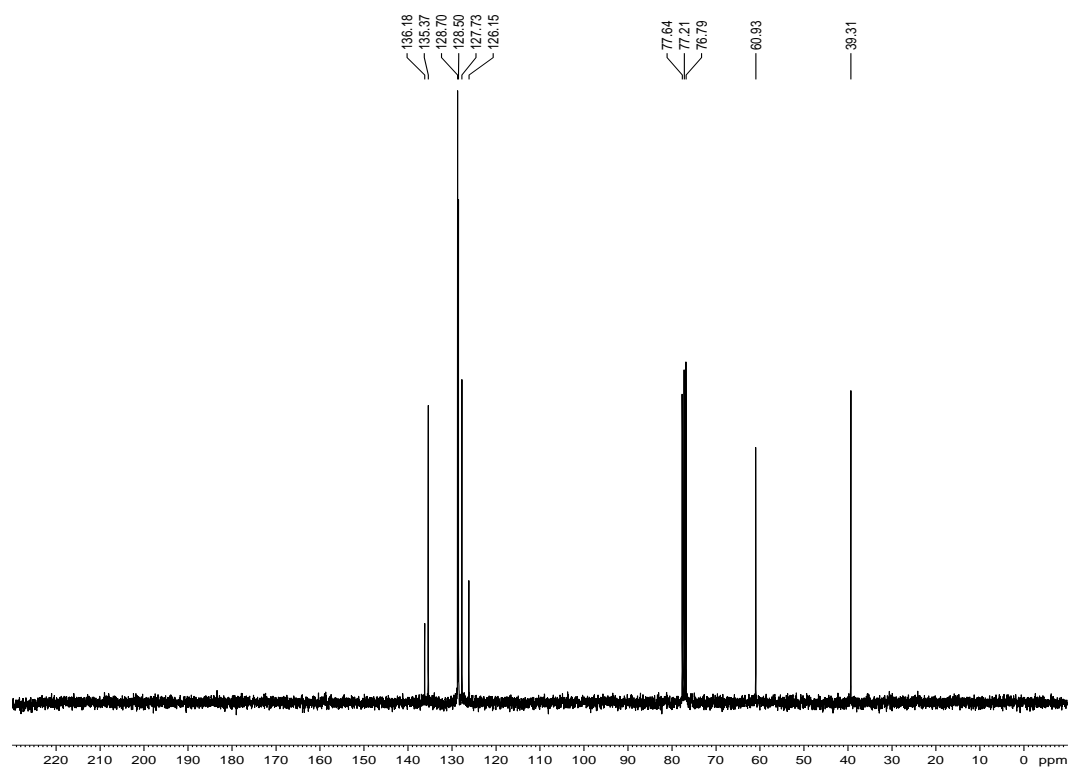
^{13}C NMR spectrum for 2.110d in CDCl_3



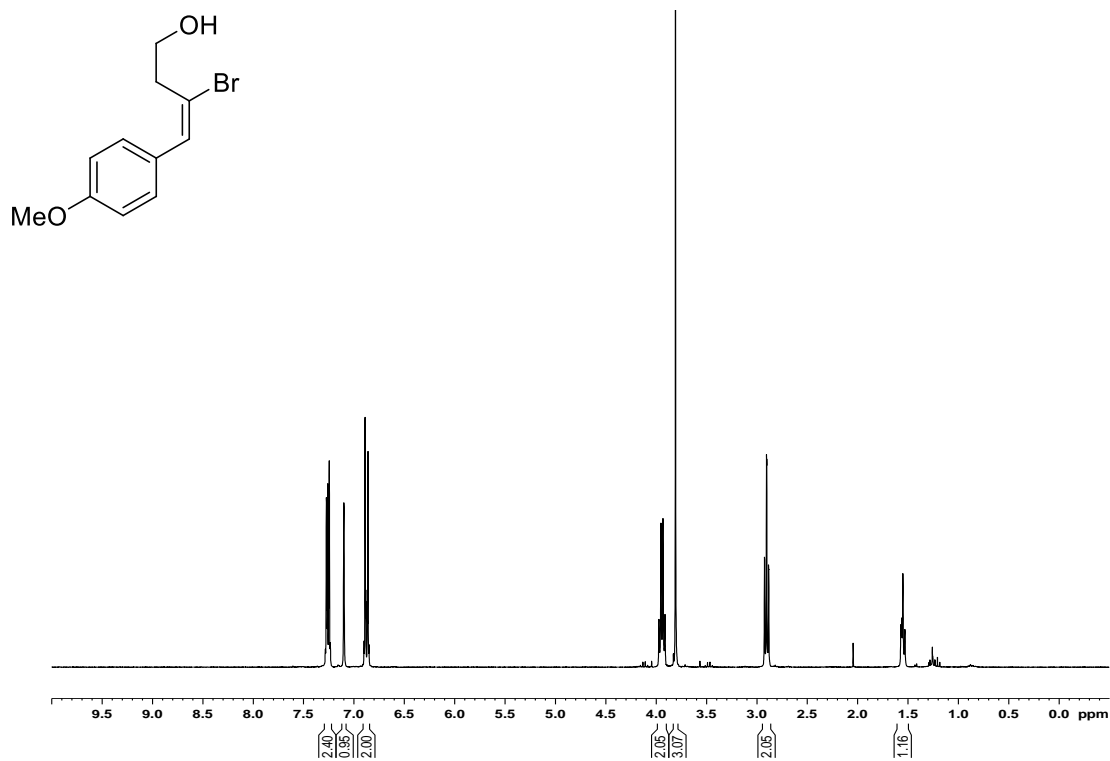
^1H NMR spectrum for 2.111a in CDCl_3



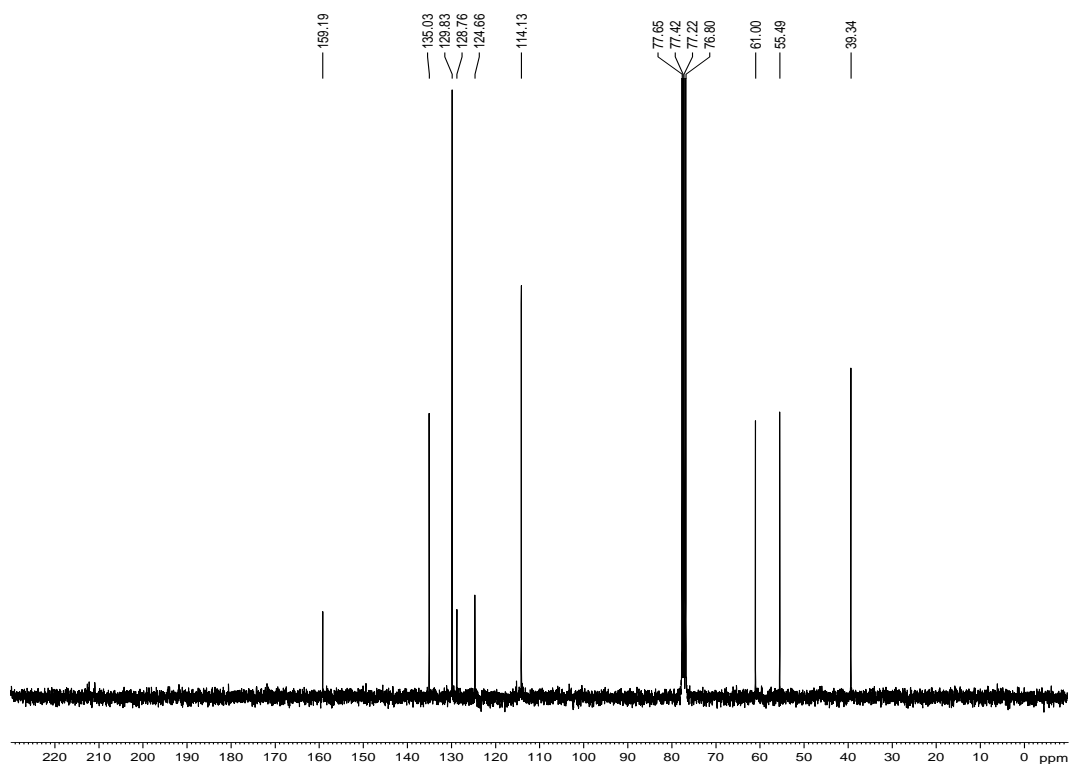
^{13}C NMR spectrum for 2.111a in CDCl_3



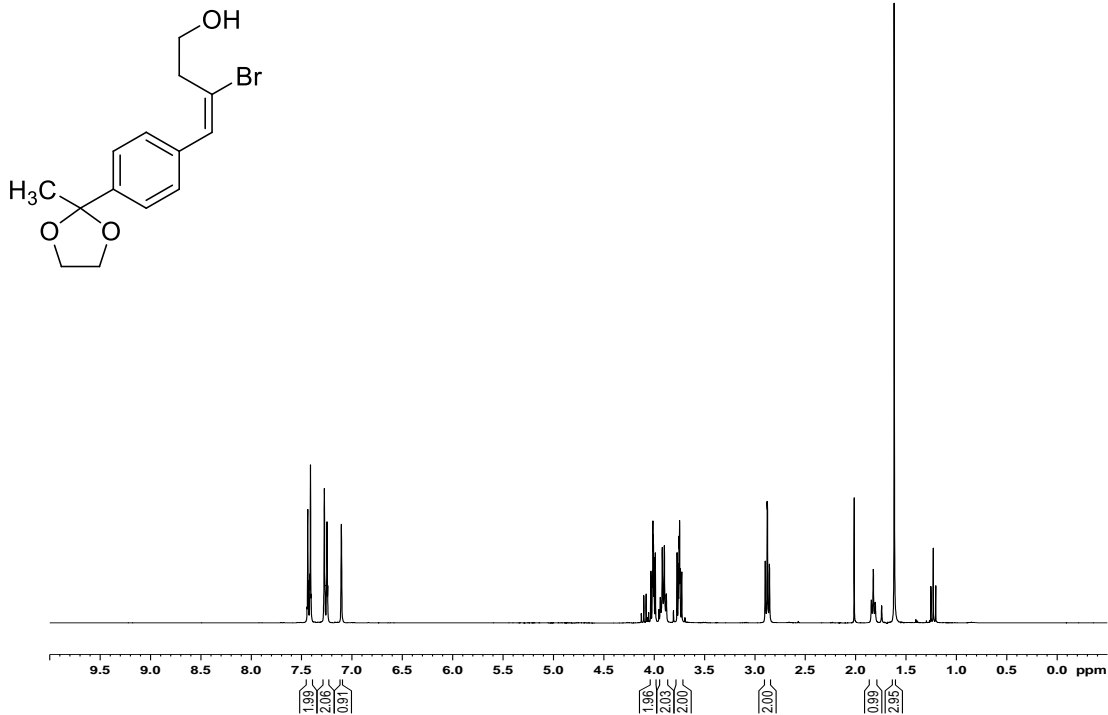
^1H NMR spectrum for 2.111b in CDCl_3



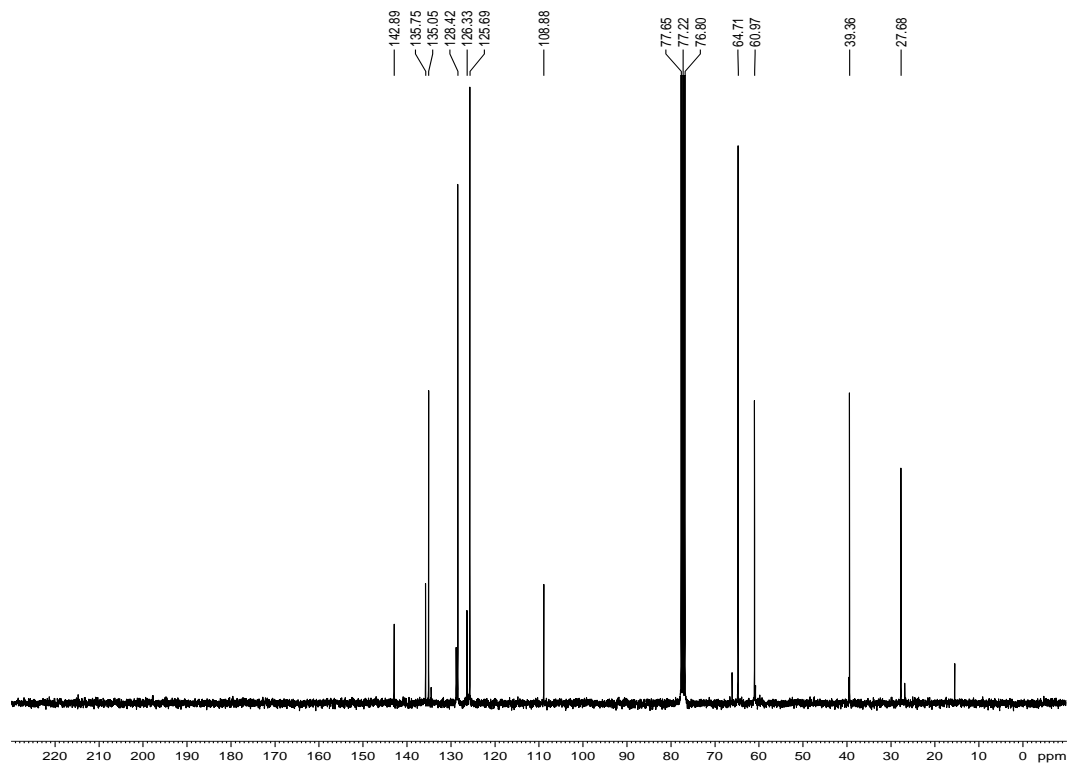
^{13}C NMR spectrum for 2.111b in CDCl_3



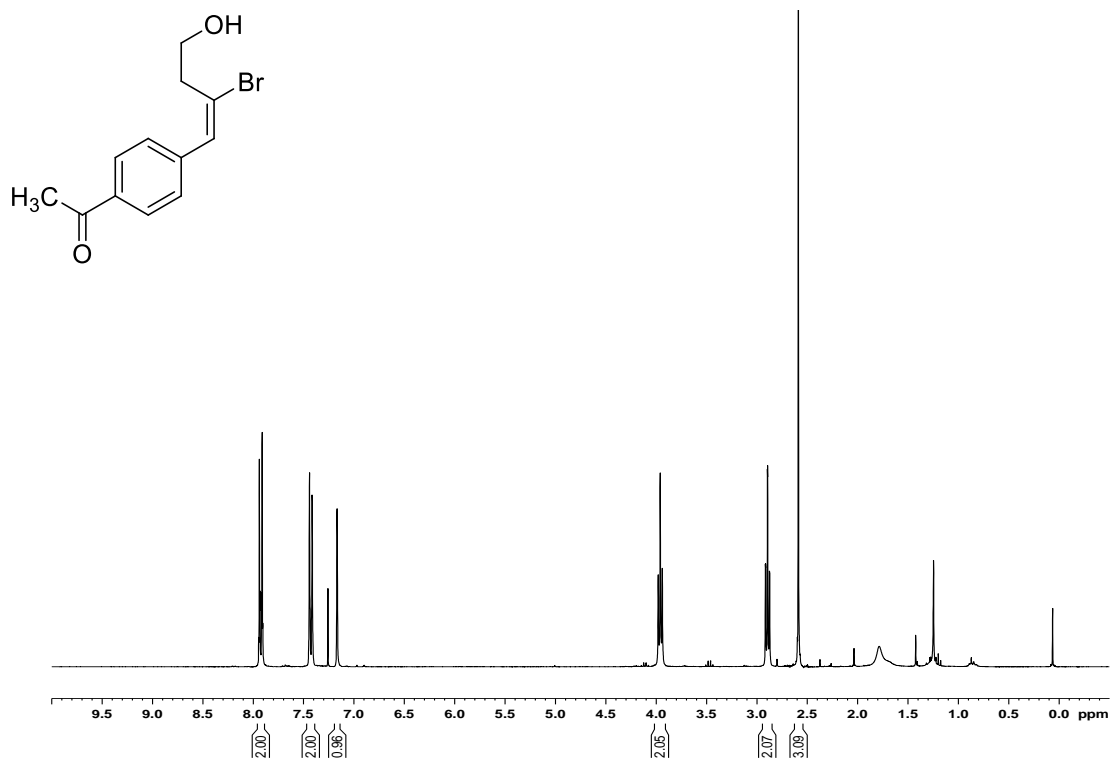
^1H NMR spectrum for 2.111c in CDCl_3 (with ethyl acetate impurity)



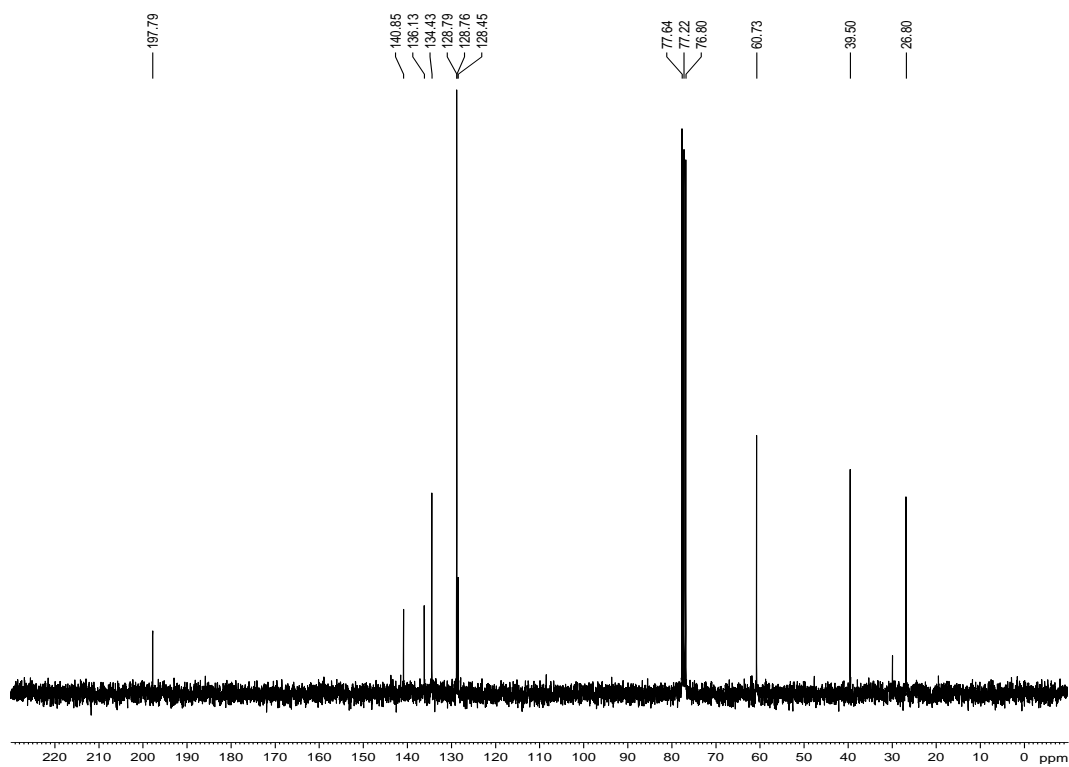
^{13}C NMR spectrum for 2.111c in CDCl_3 (with ethyl acetate impurity)



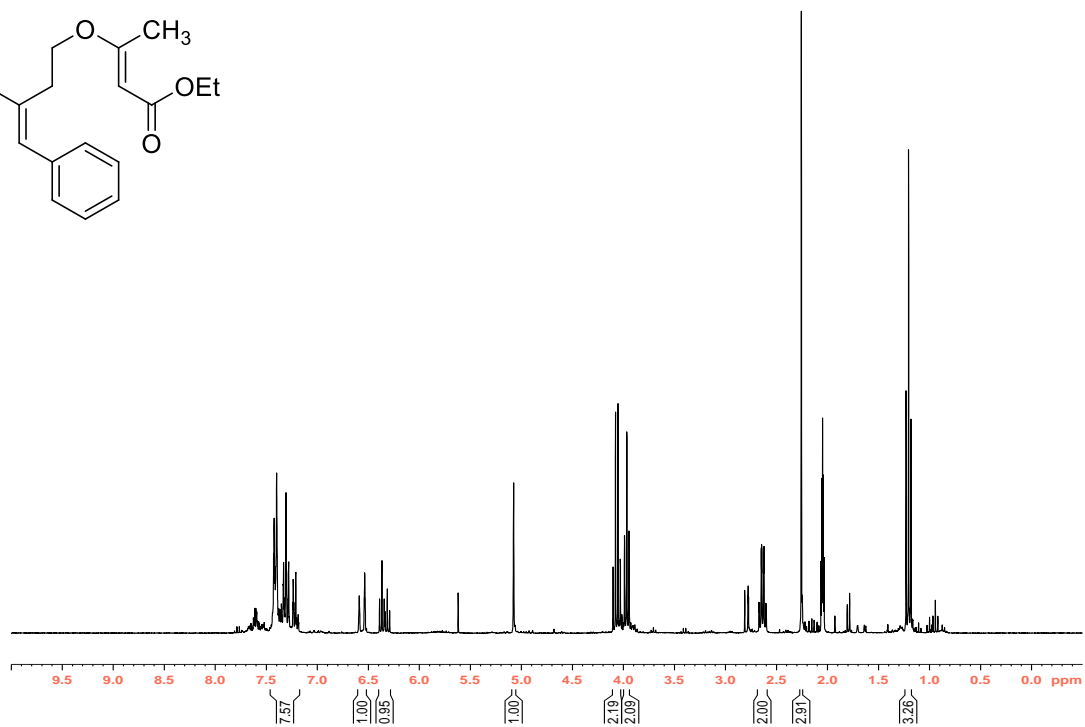
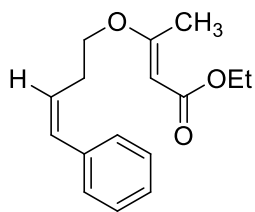
^1H NMR spectrum for 2.111d in CDCl_3



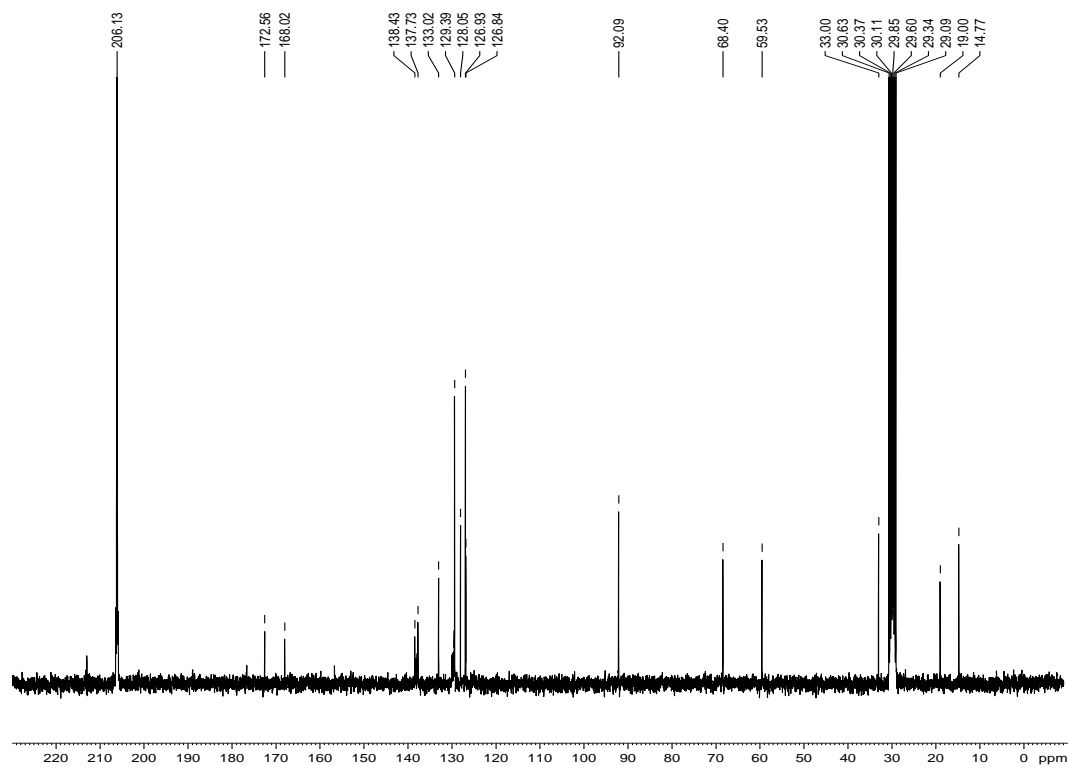
^{13}C NMR spectrum for 2.111d in CDCl_3



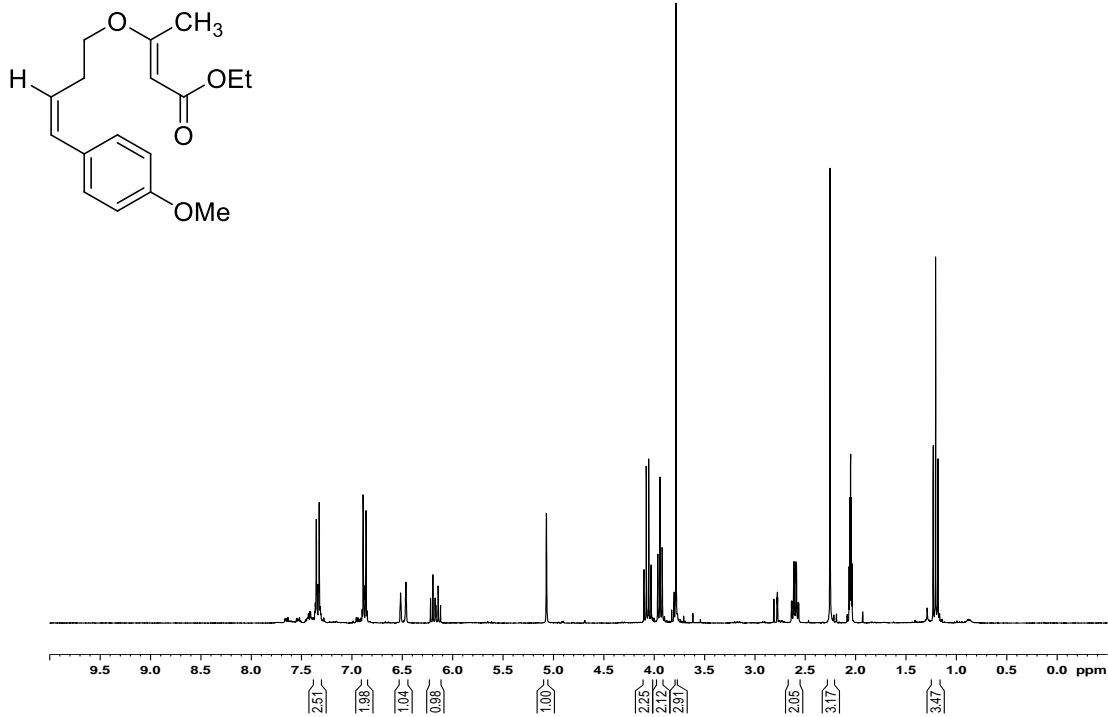
^1H NMR spectrum for 2.113a in $(\text{CD}_3)_2\text{CO}$



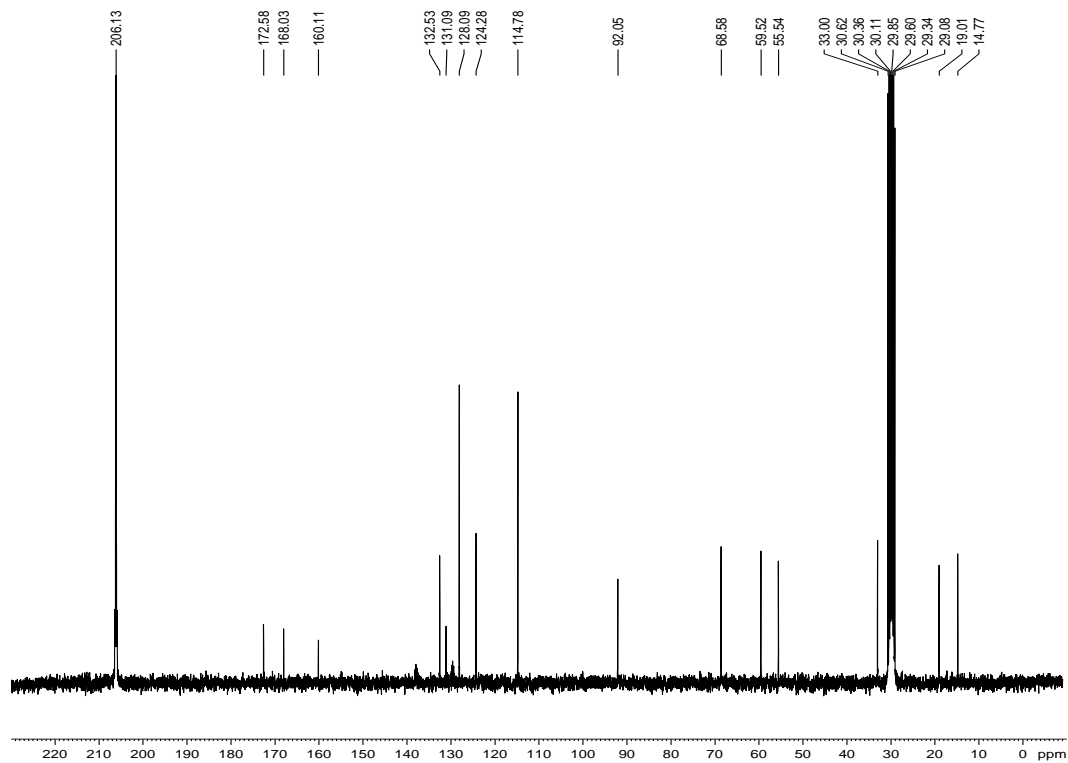
^{13}C NMR spectrum for 2.113a in $(\text{CD}_3)_2\text{CO}$



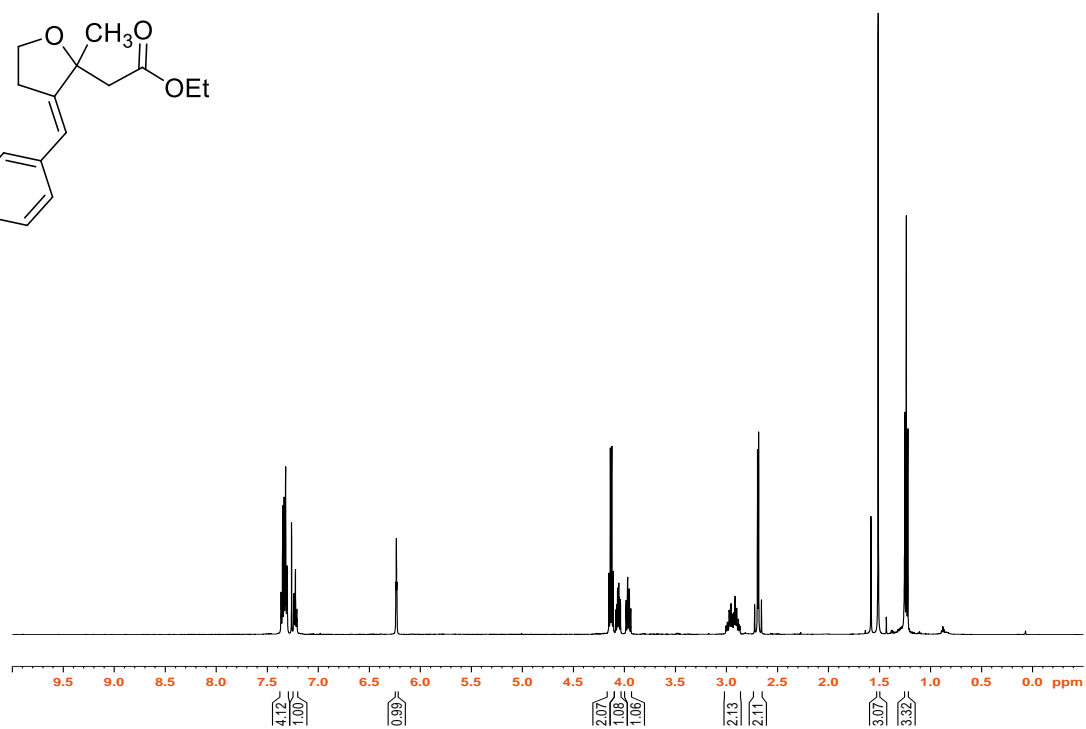
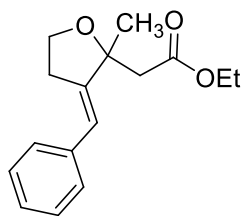
^1H NMR spectrum for 2.113b in $(\text{CD}_3)_2\text{CO}$



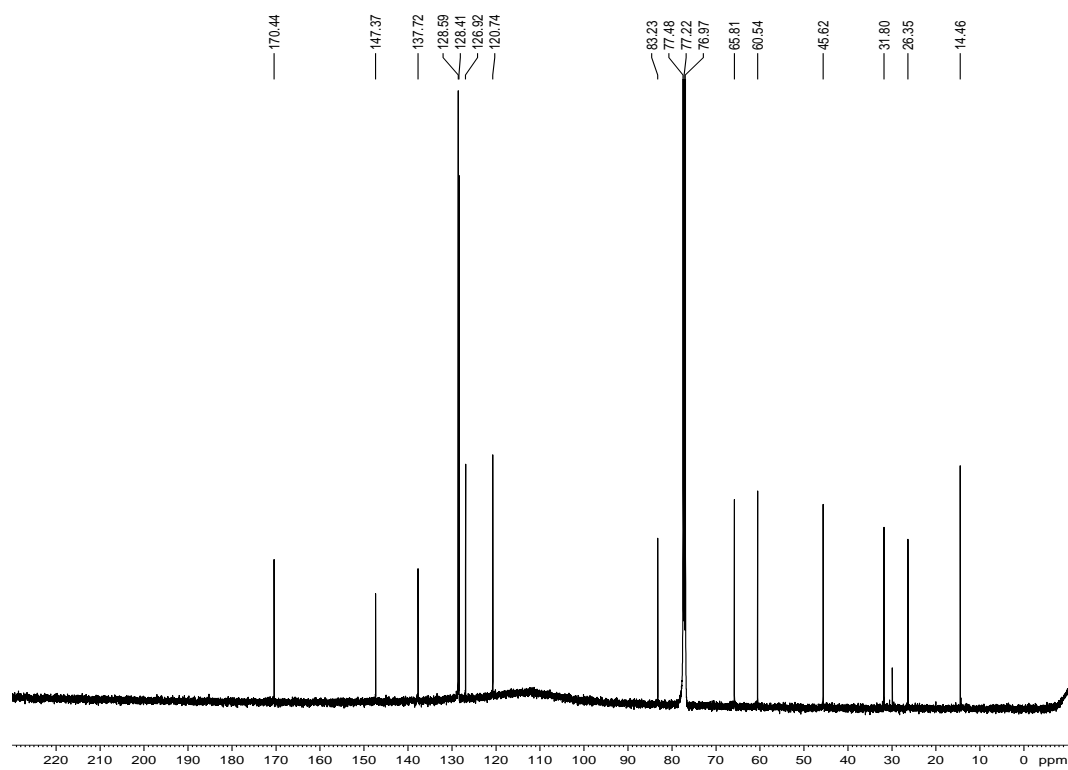
^{13}C NMR spectrum for 2.113b in $(\text{CD}_3)_2\text{CO}$



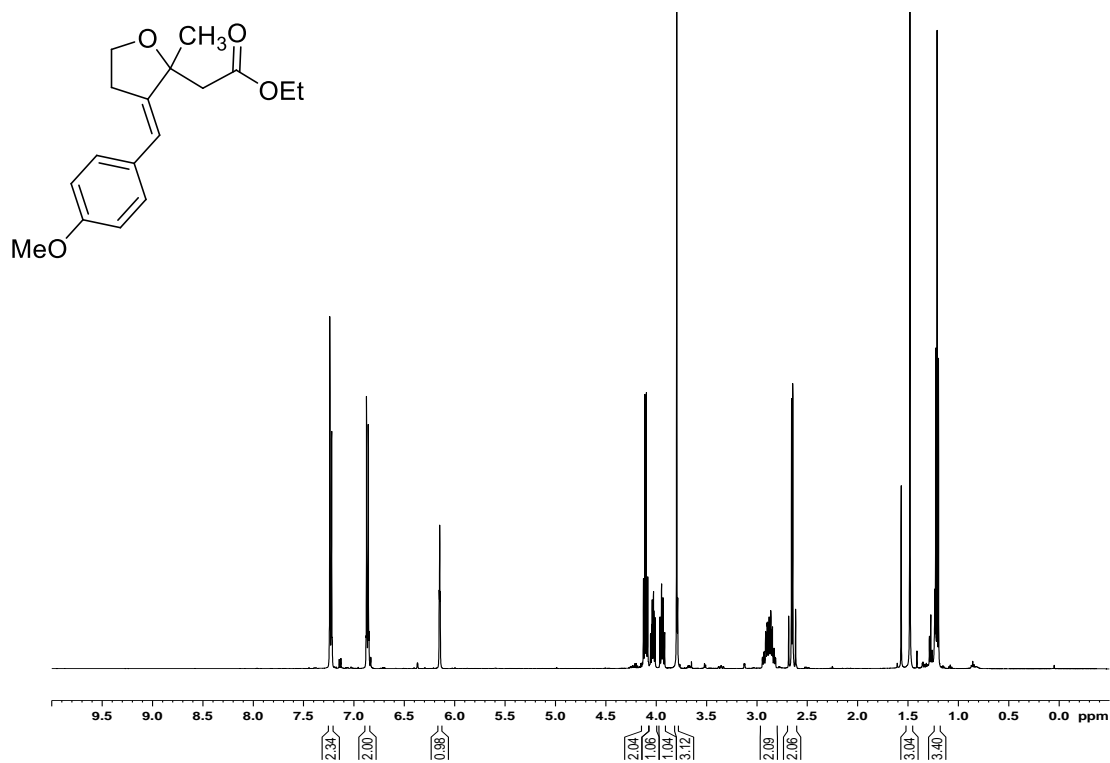
^1H NMR spectrum for 2.114a in CDCl_3



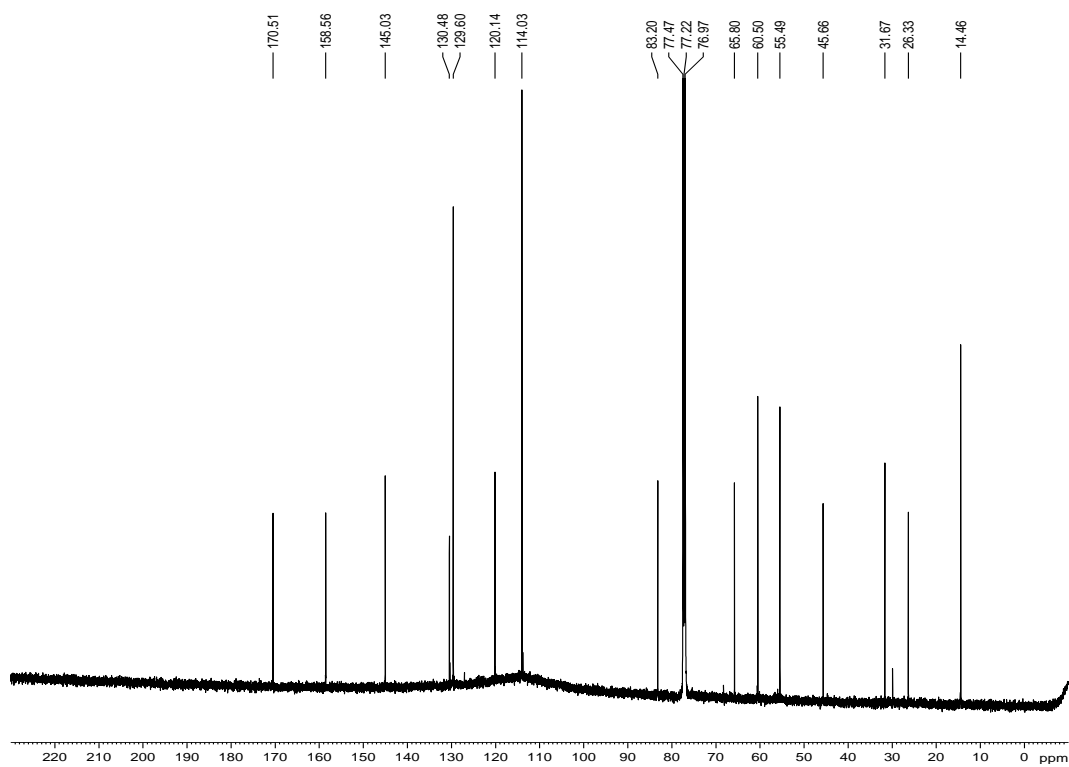
^{13}C NMR spectrum for 2.114a in CDCl_3



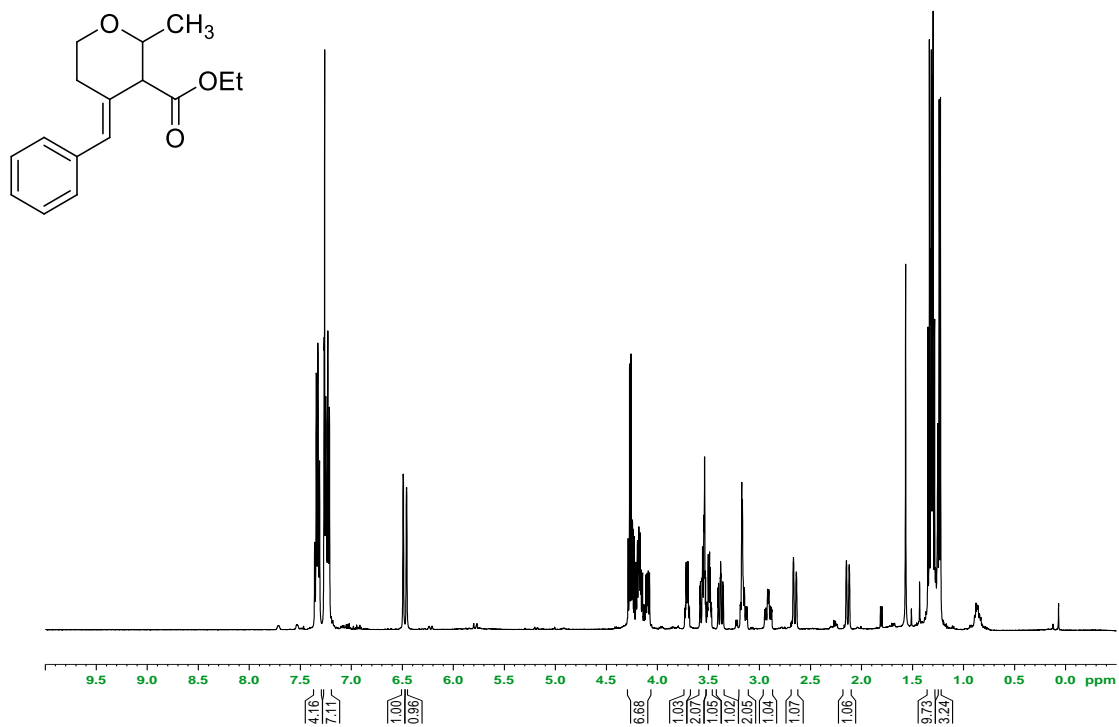
^1H NMR spectrum for 2.114b in CDCl_3



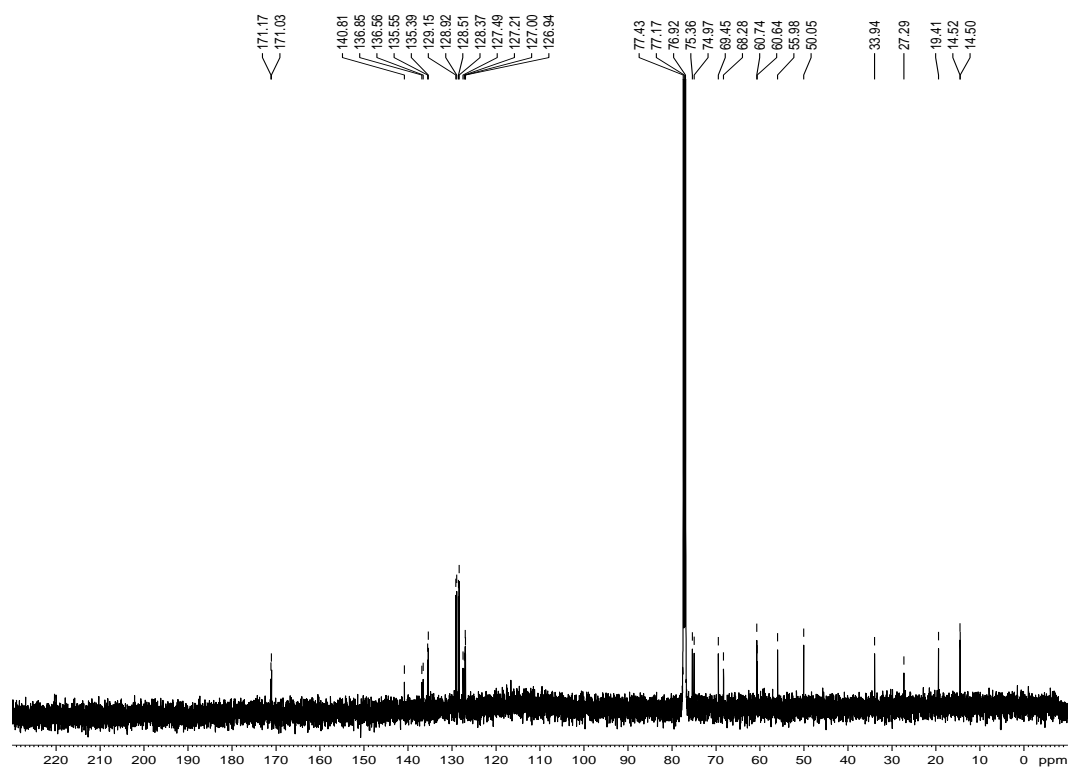
^{13}C NMR spectrum for 2.114b in CDCl_3



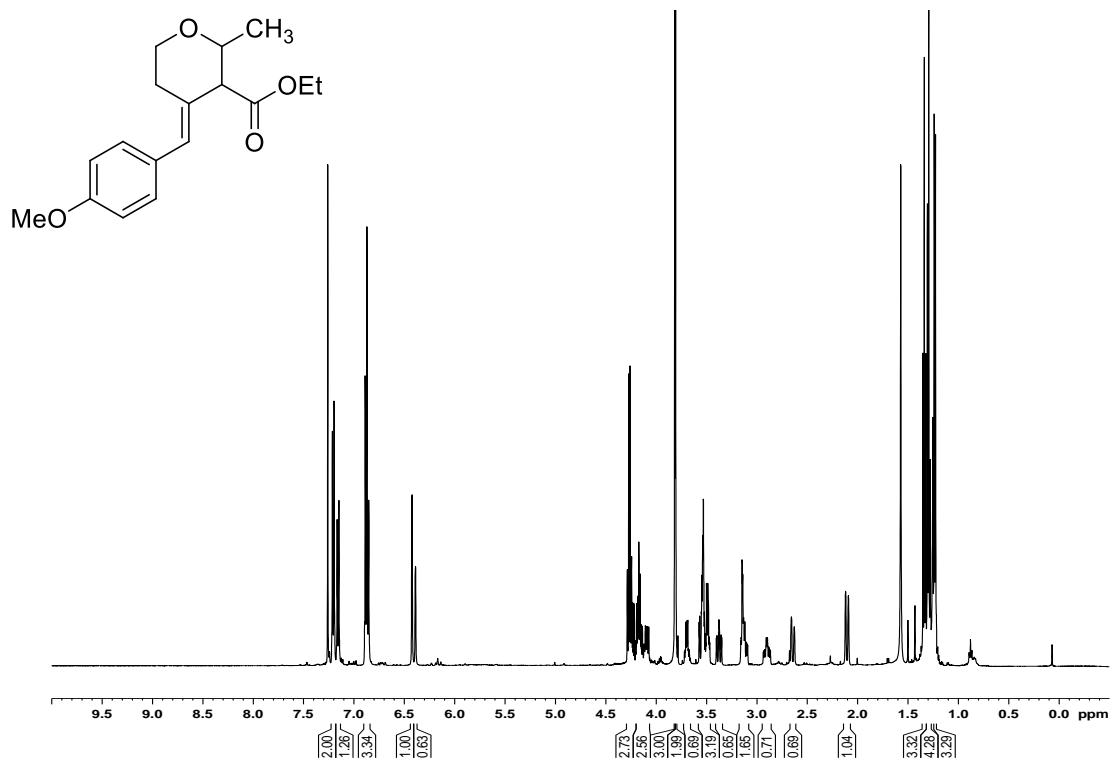
^1H NMR spectrum for 2.115a in CDCl_3



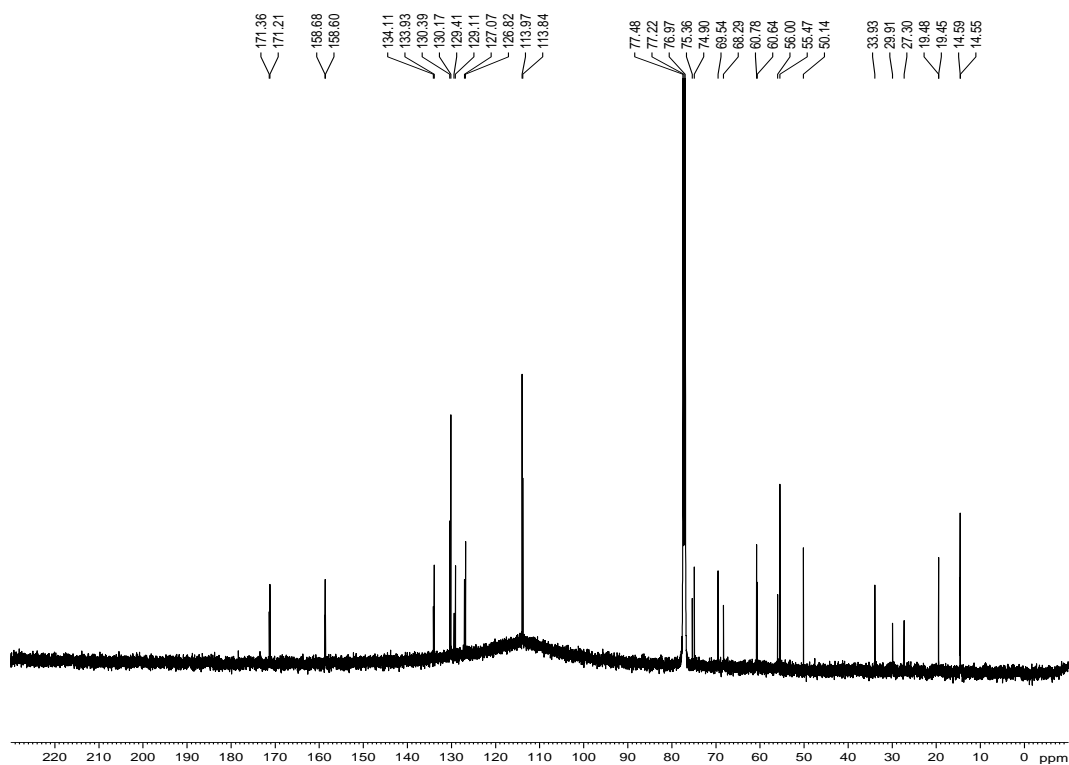
^{13}C NMR spectrum for 2.115a in CDCl_3



^1H NMR spectrum for 2.115b in CDCl_3



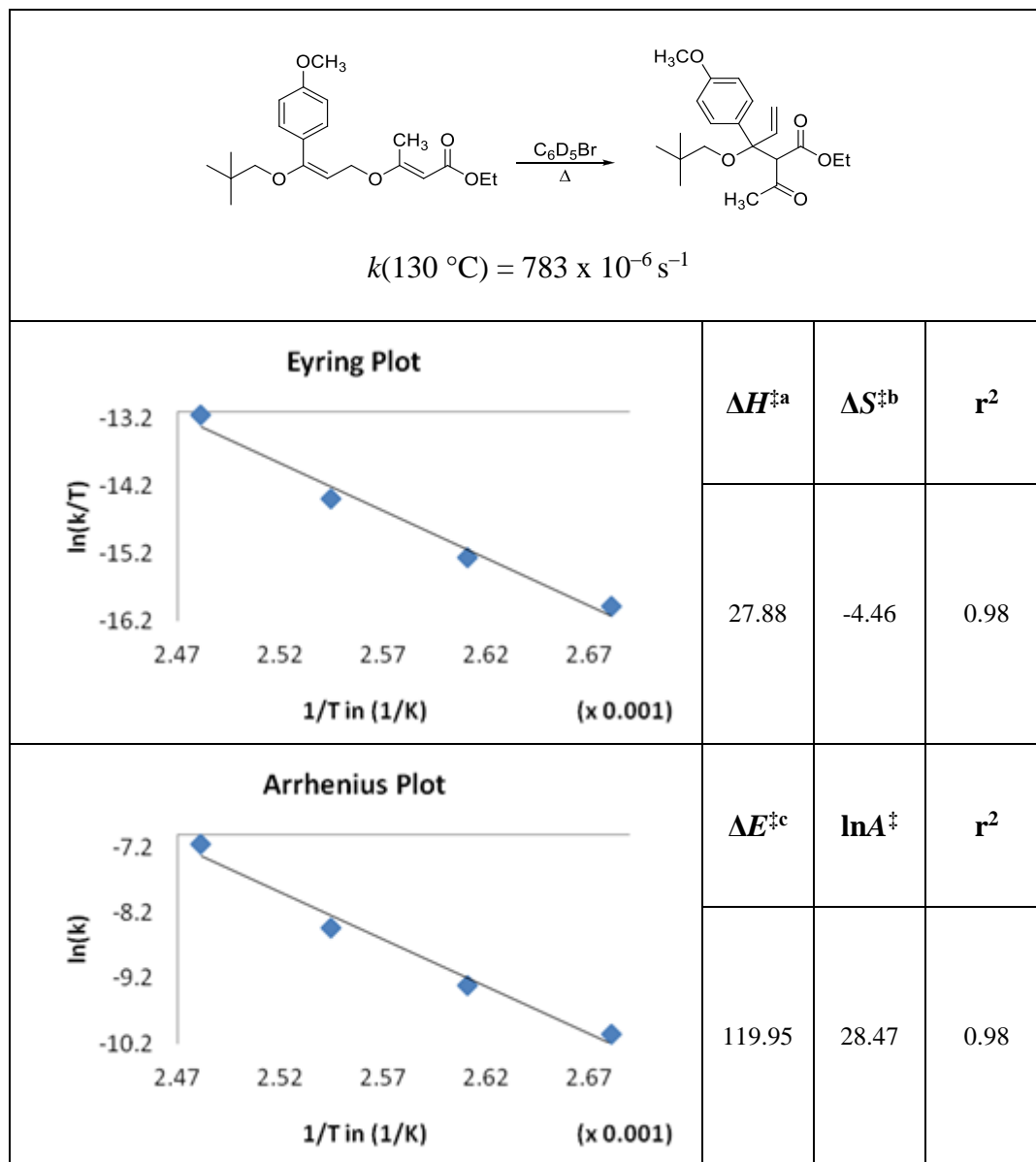
^{13}C NMR spectrum for 2.115b in CDCl_3



Appendix B

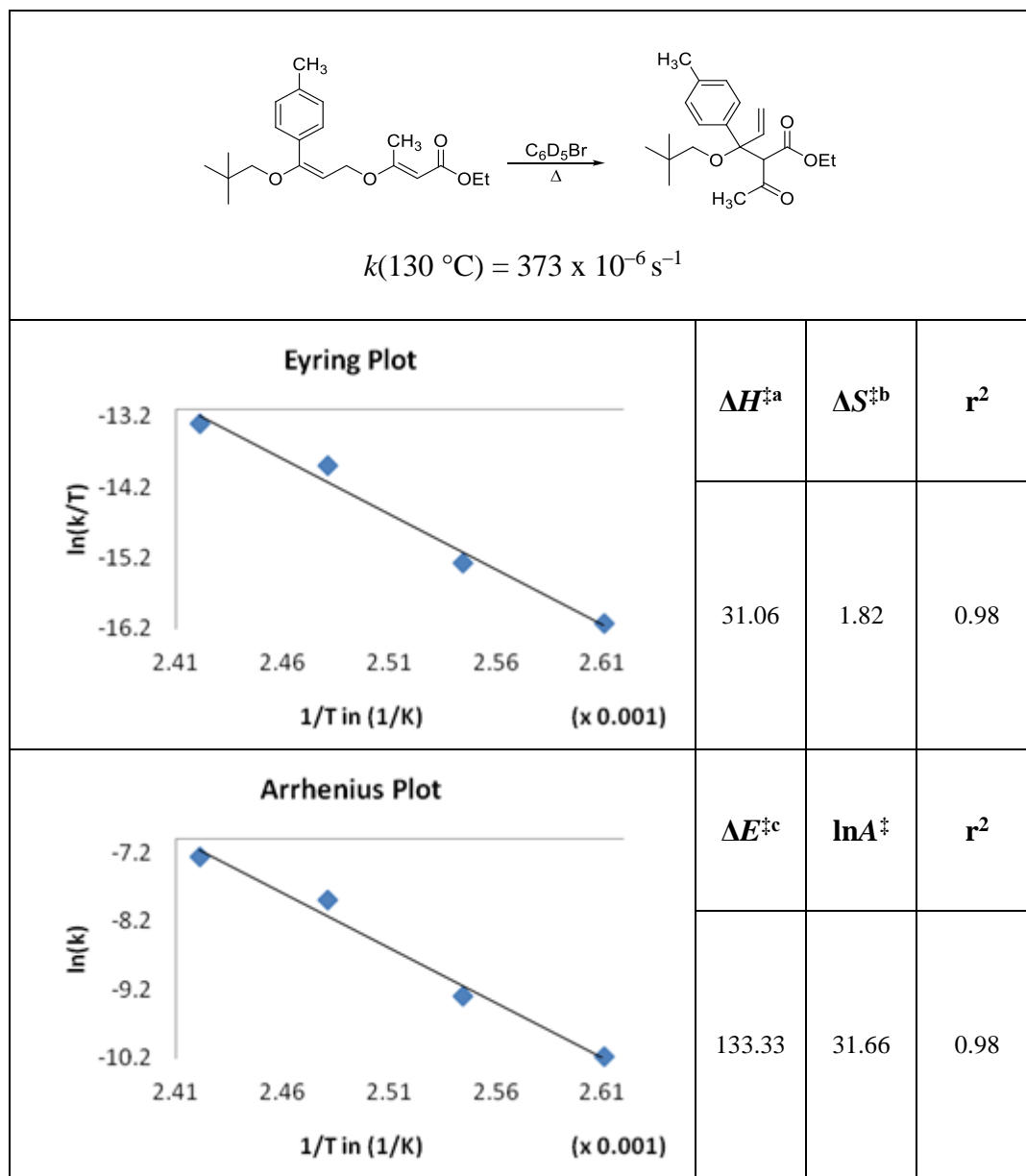
Chapter 3 Eyring and Arrhenius Plots

Eyring and Arrhenius Plots for Compound 3.8a



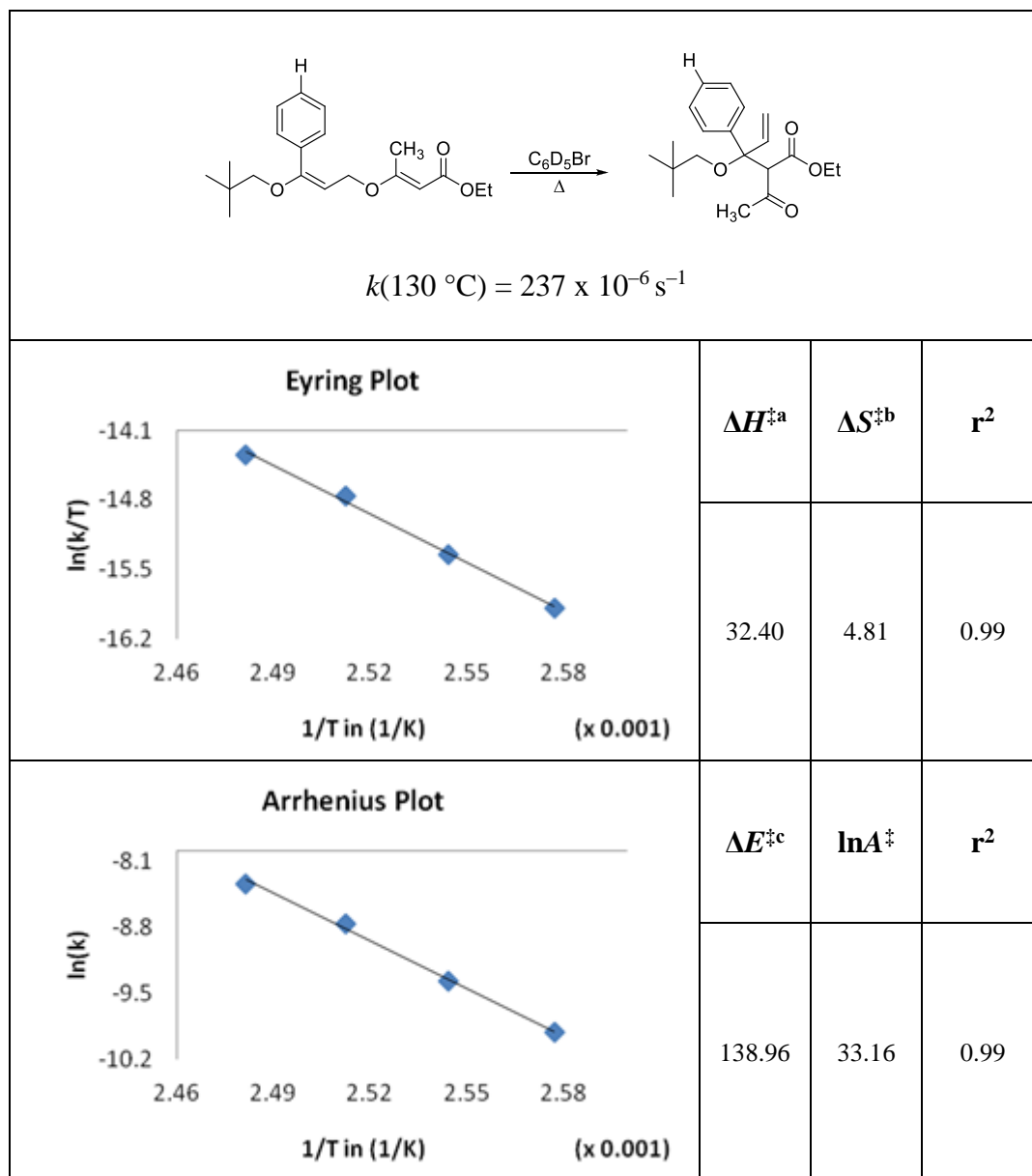
^a[kcal/mol]; ^b[cal/mol·K]; ^c[kJ/mol]

Eyring and Arrhenius Plots for Compound 3.8b



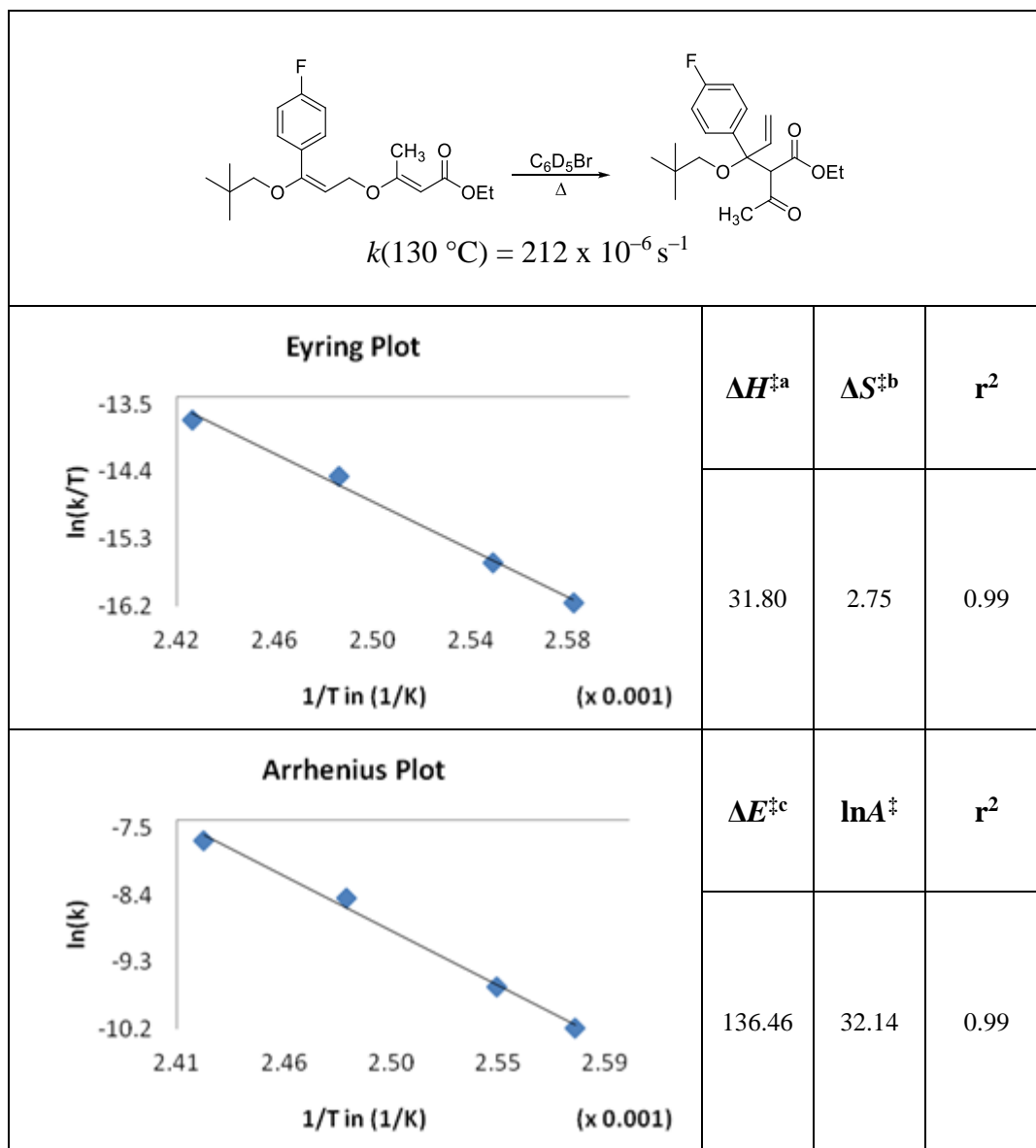
^a[kcal/mol]; ^b[cal/mol·K]; ^c[kJ/mol]

Eyring and Arrhenius Plots for Compound 3.8d



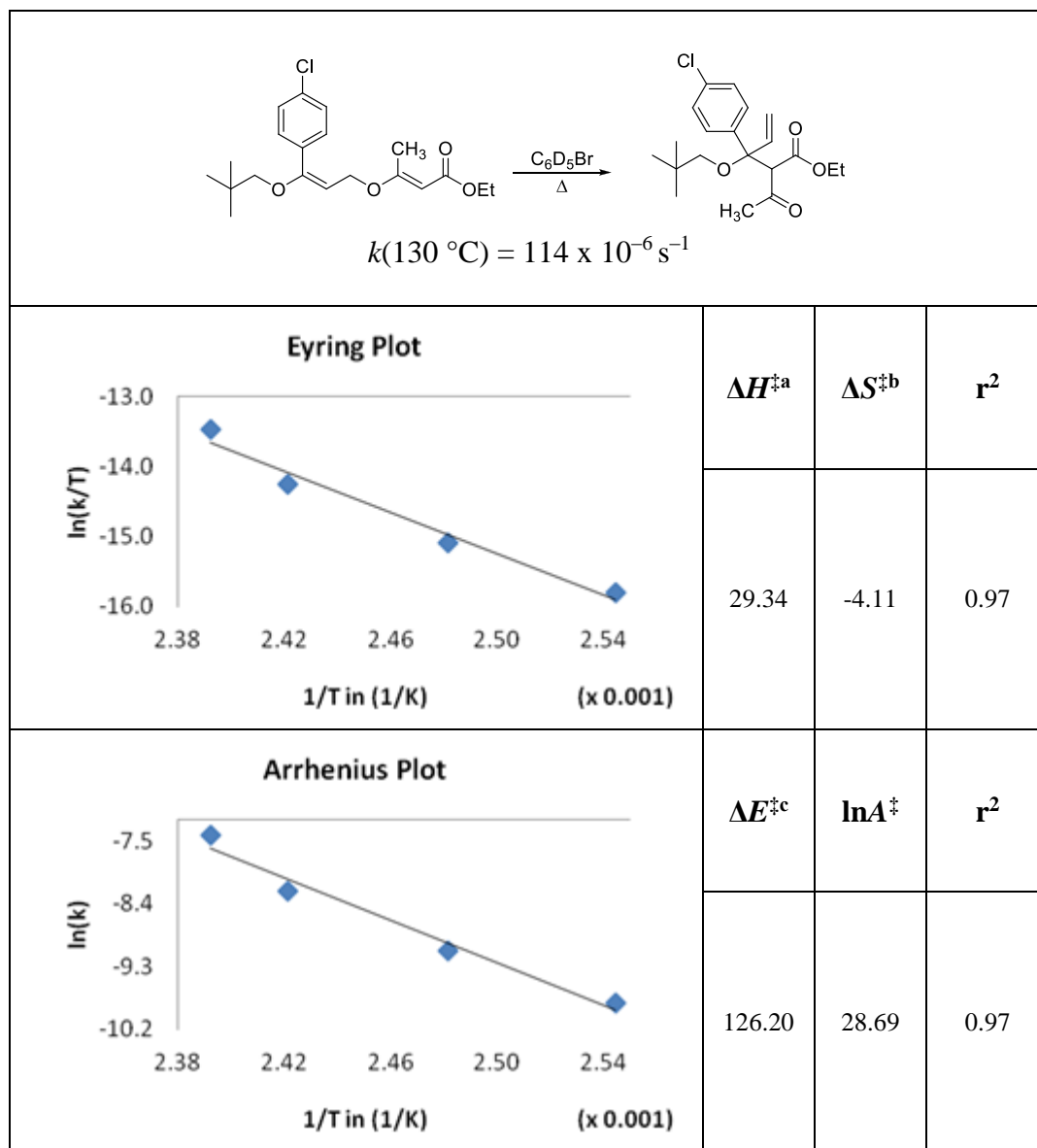
^a[kcal/mol]; ^b[cal/mol·K]; ^c[kJ/mol]

Eyring and Arrhenius Plots for Compound 3.8e



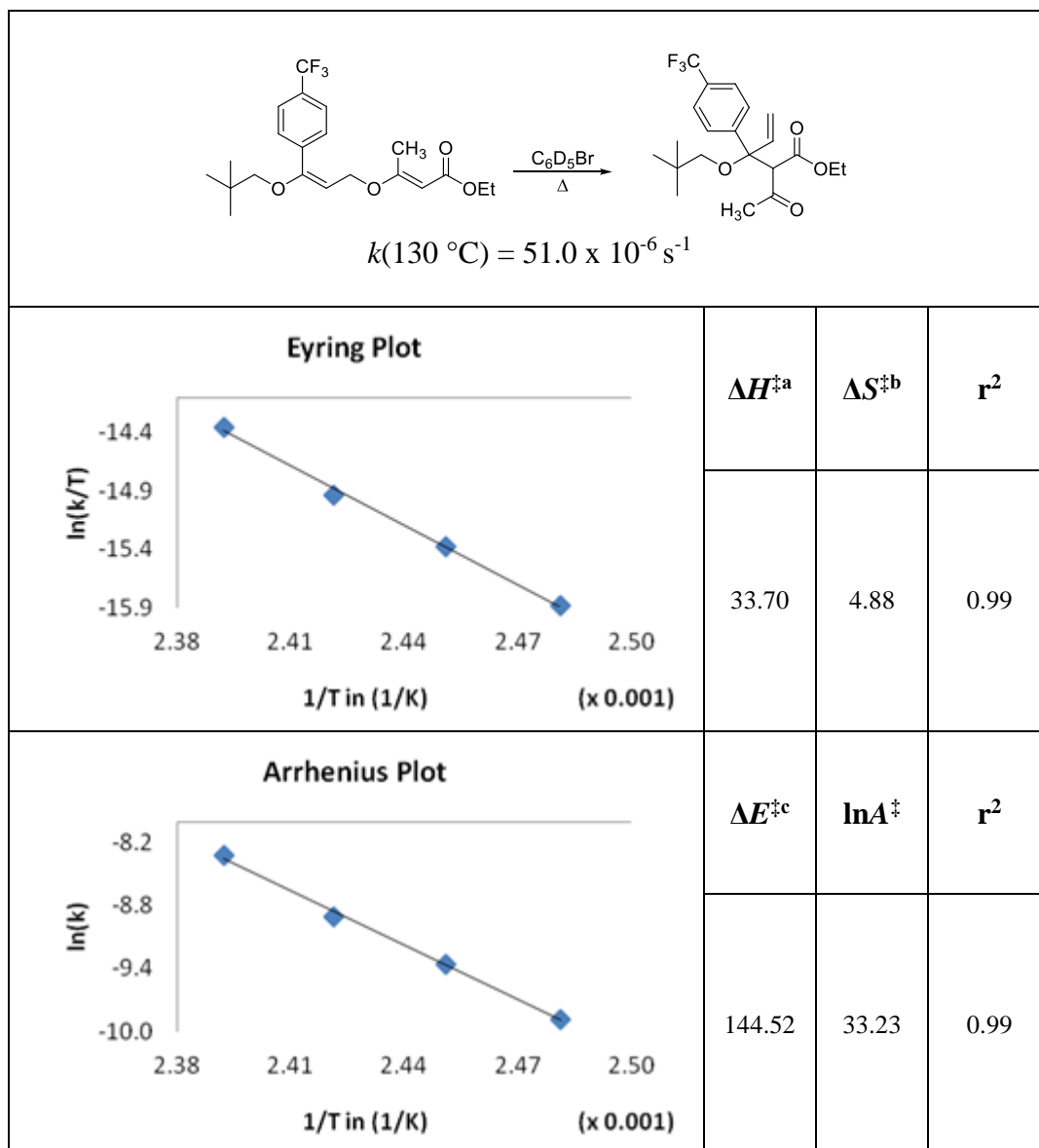
^a[kcal/mol]; ^b[cal/mol·K]; ^c[kJ/mol]

Eyring and Arrhenius Plots for Compound 3.8f



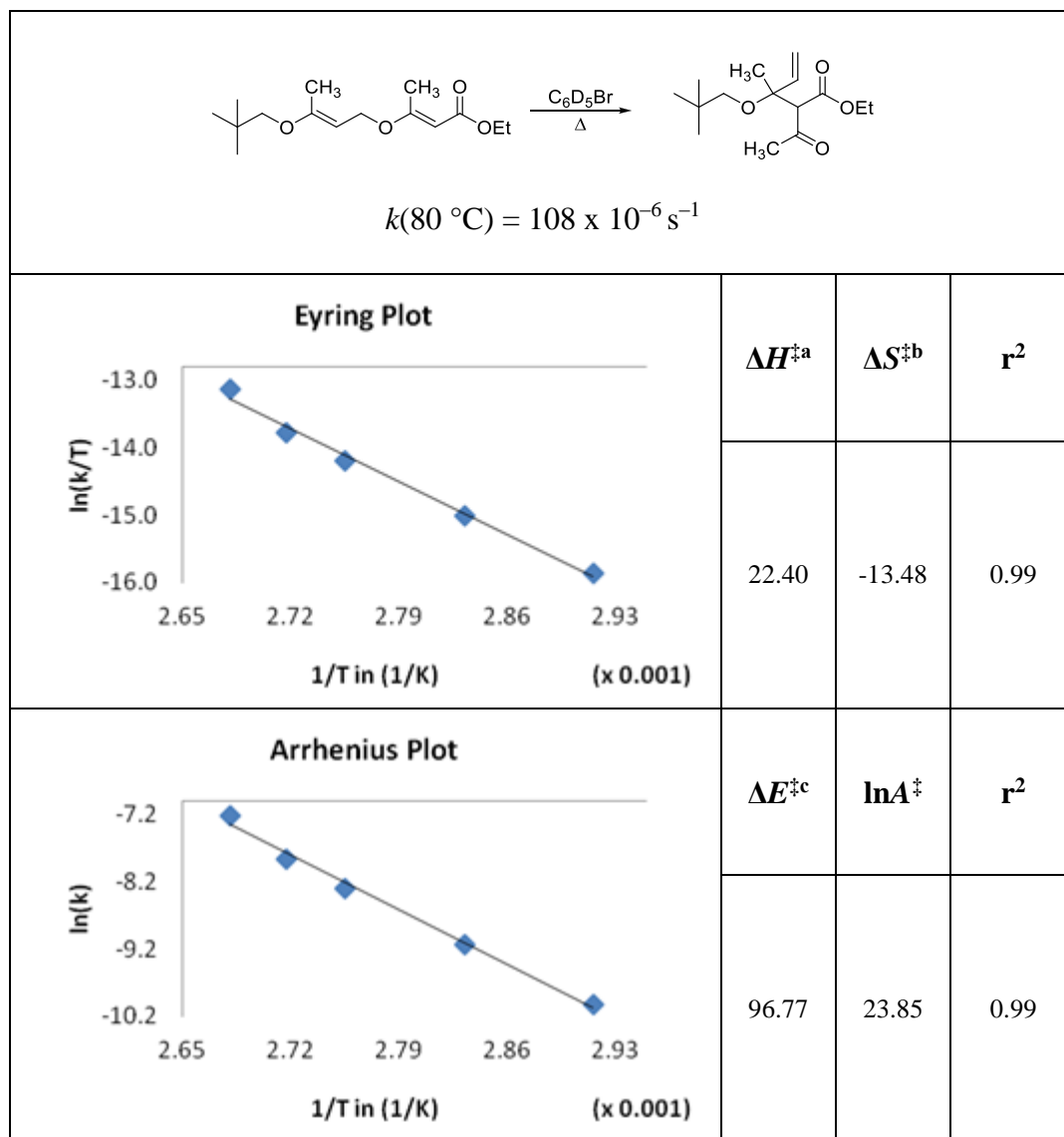
^a[kcal/mol]; ^b[cal/mol·K]; ^c[kJ/mol]

Eyring and Arrhenius Plots for Compound 3.8g



^a[kcal/mol]; ^b[cal/mol·K]; ^c[kJ/mol]

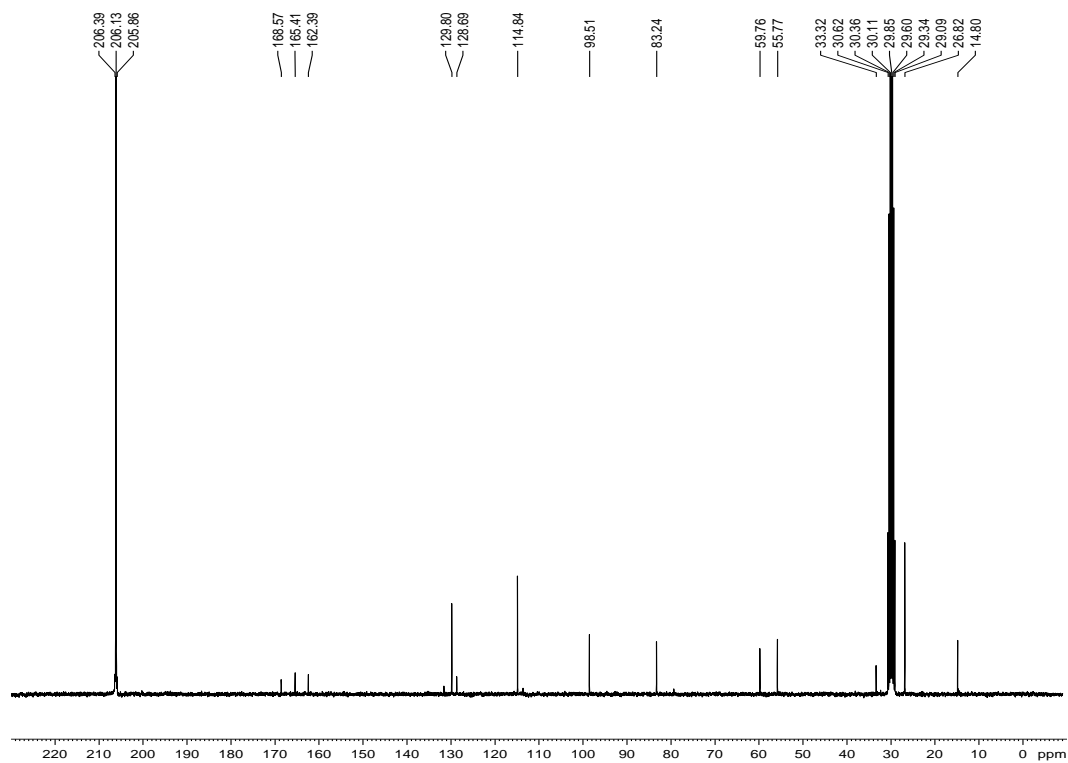
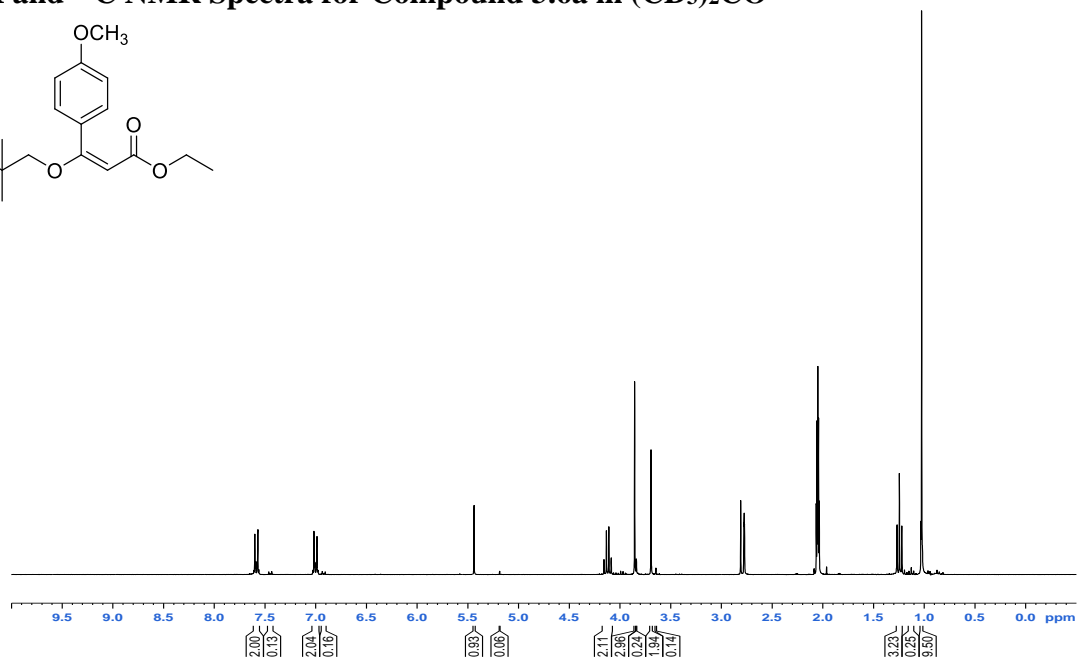
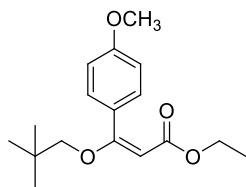
Eyring and Arrhenius Plots for Compound 3.16

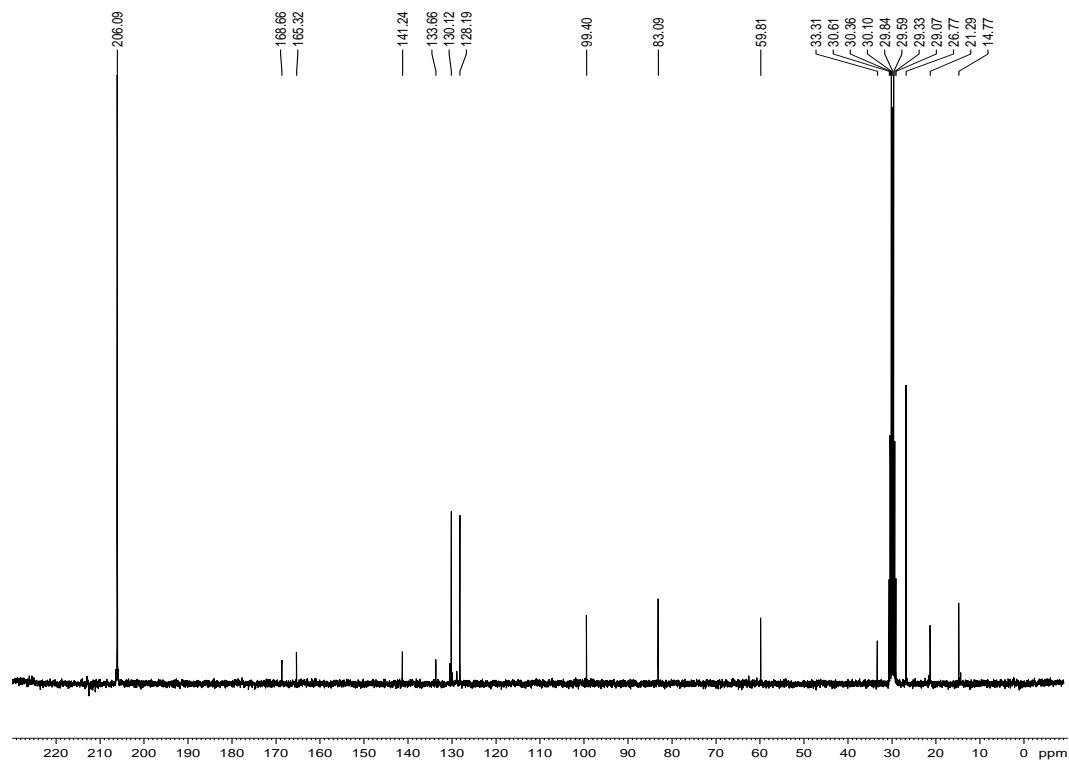
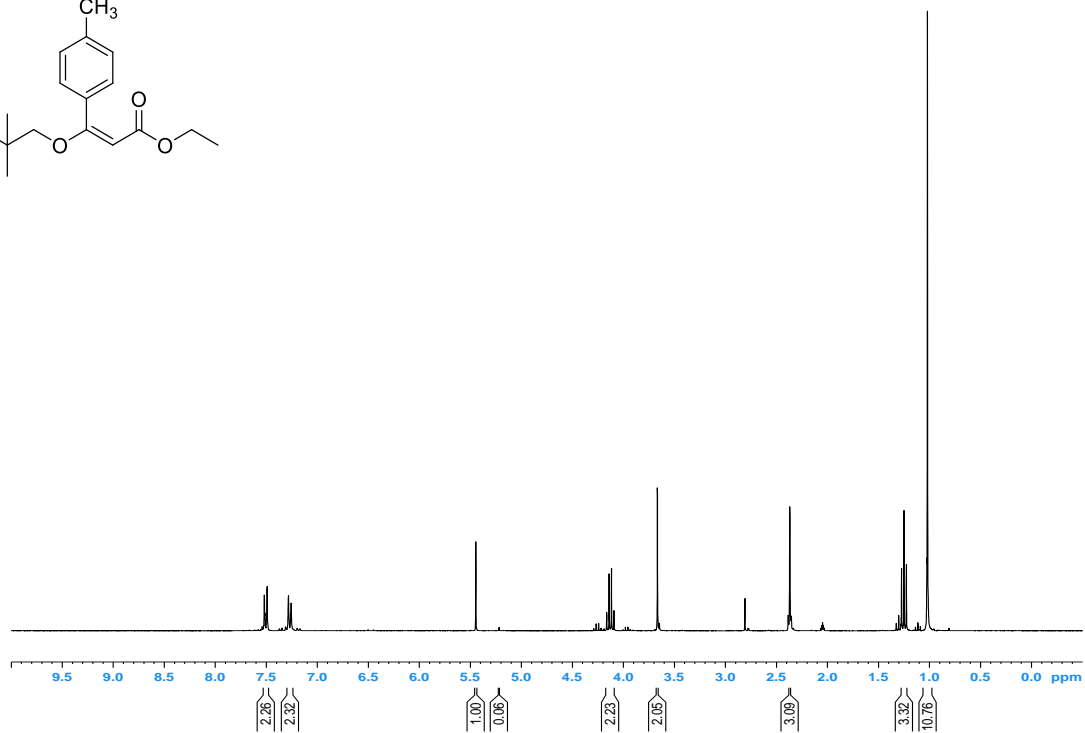
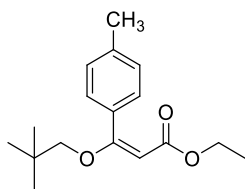


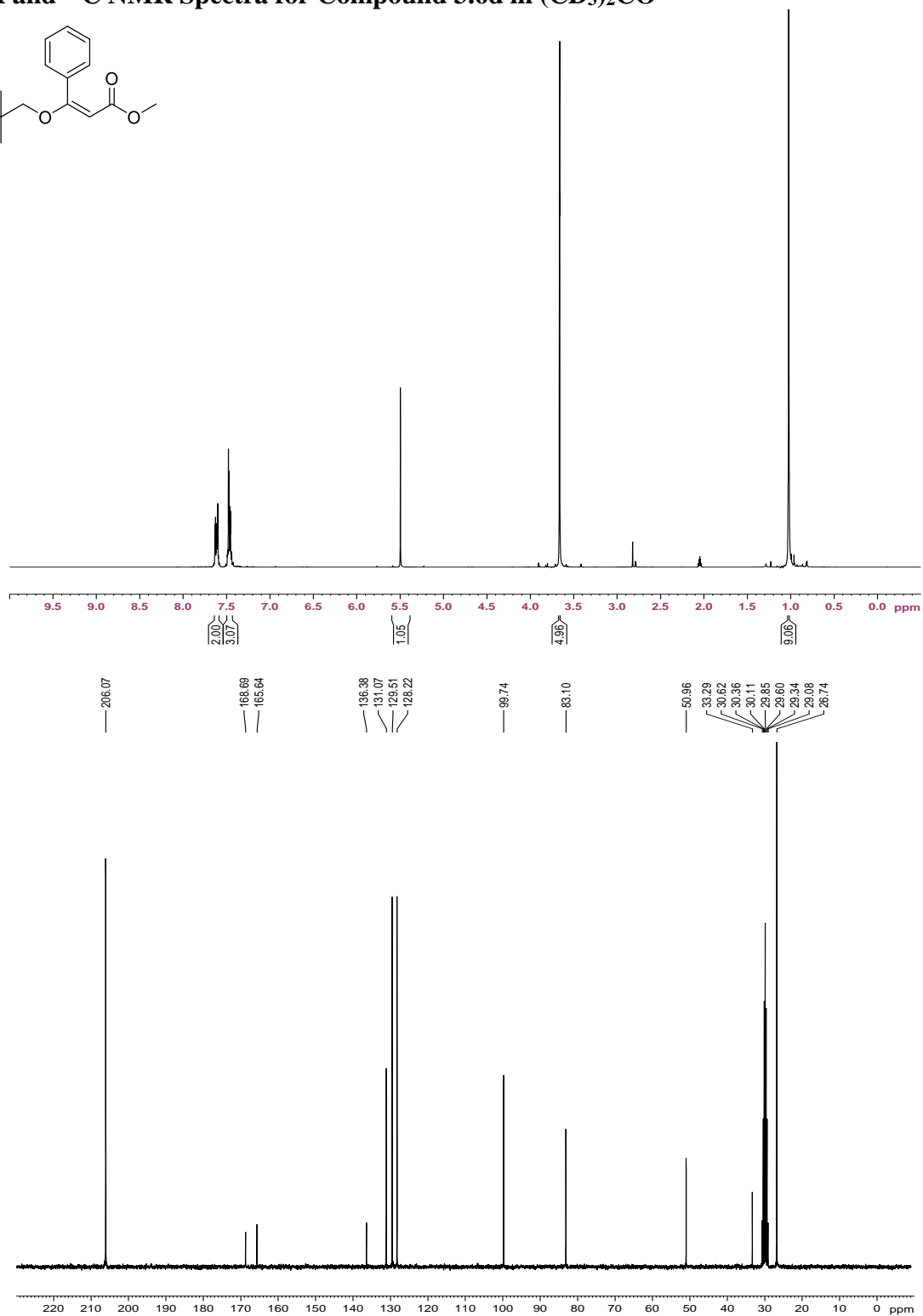
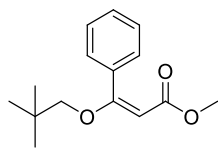
^a[kcal/mol]; ^b[cal/mol·K]; ^c[kJ/mol]

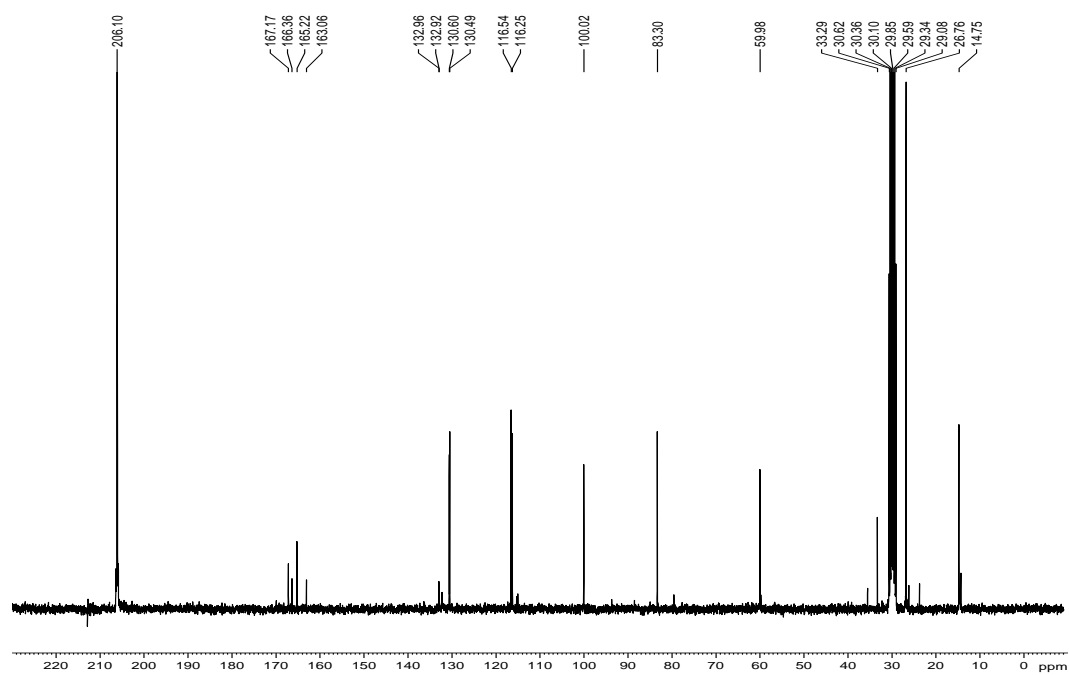
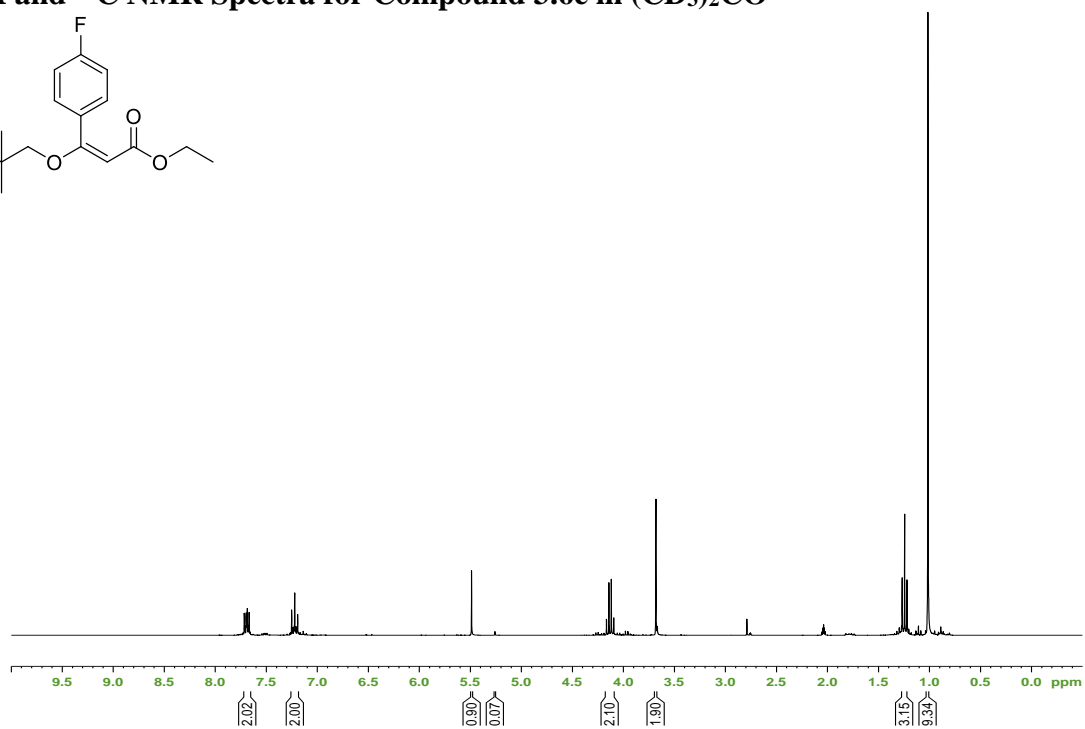
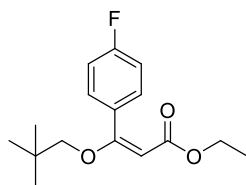
Appendix C Chapter 3 Spectral Data

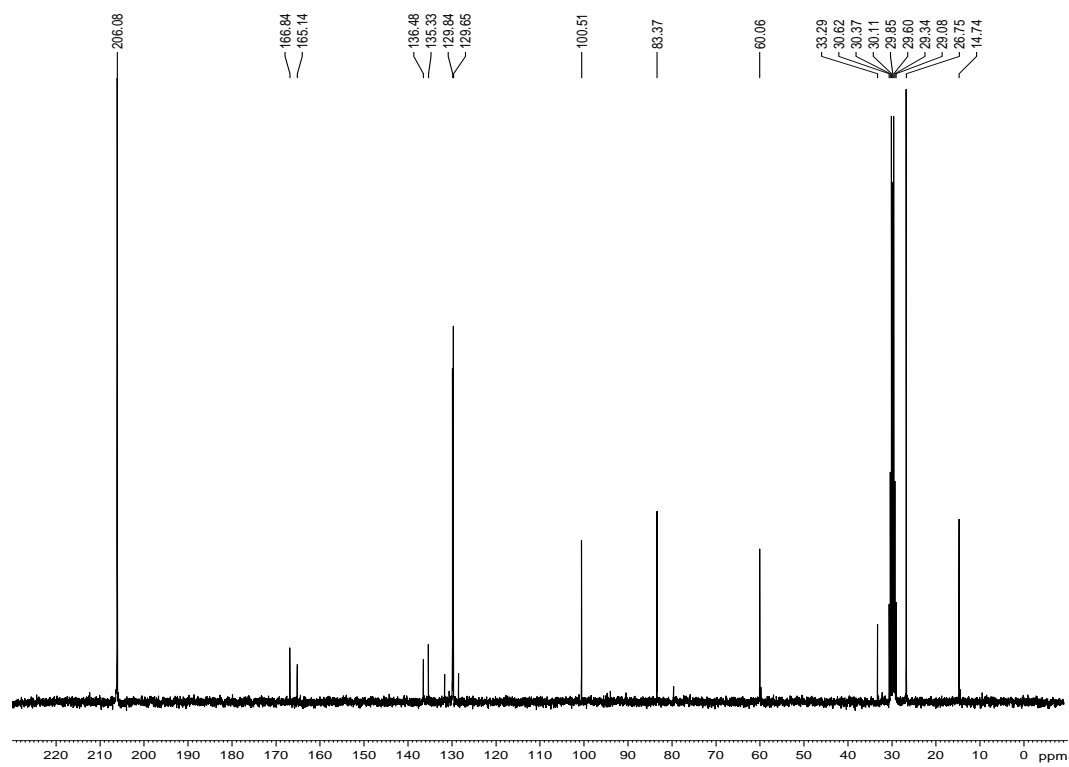
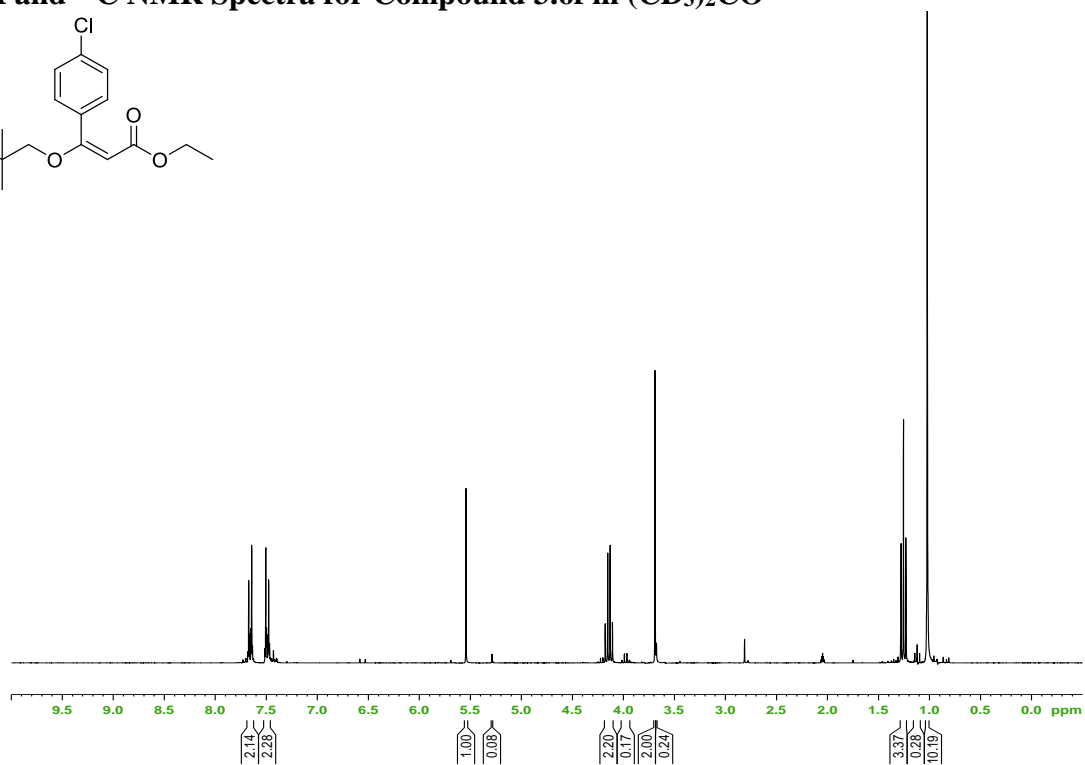
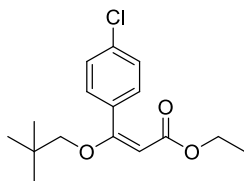
^1H and ^{13}C NMR Spectra for Compound 3.6a in $(\text{CD}_3)_2\text{CO}$

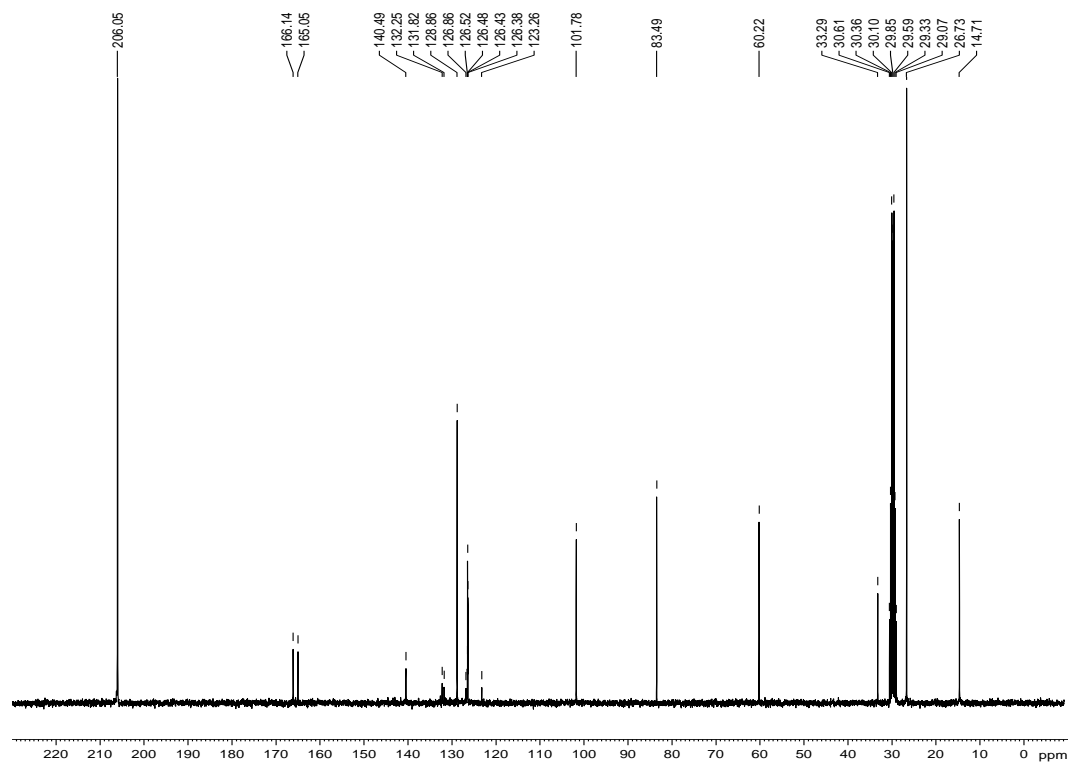
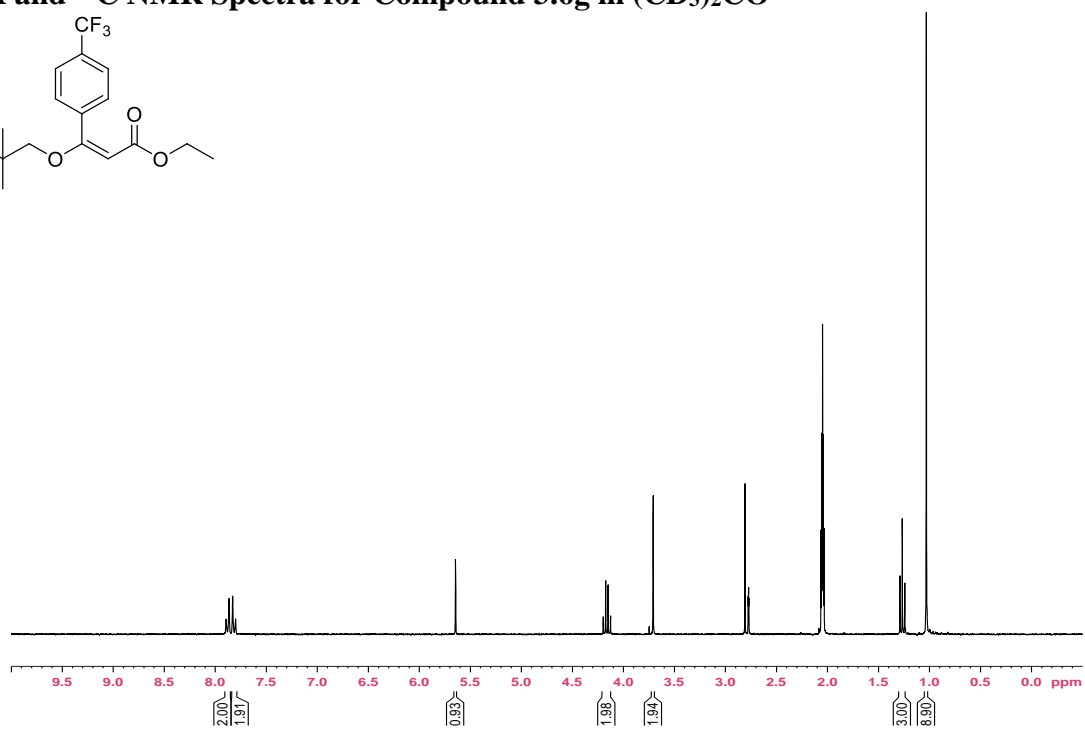
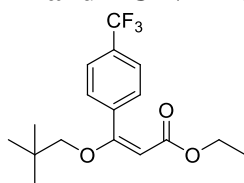


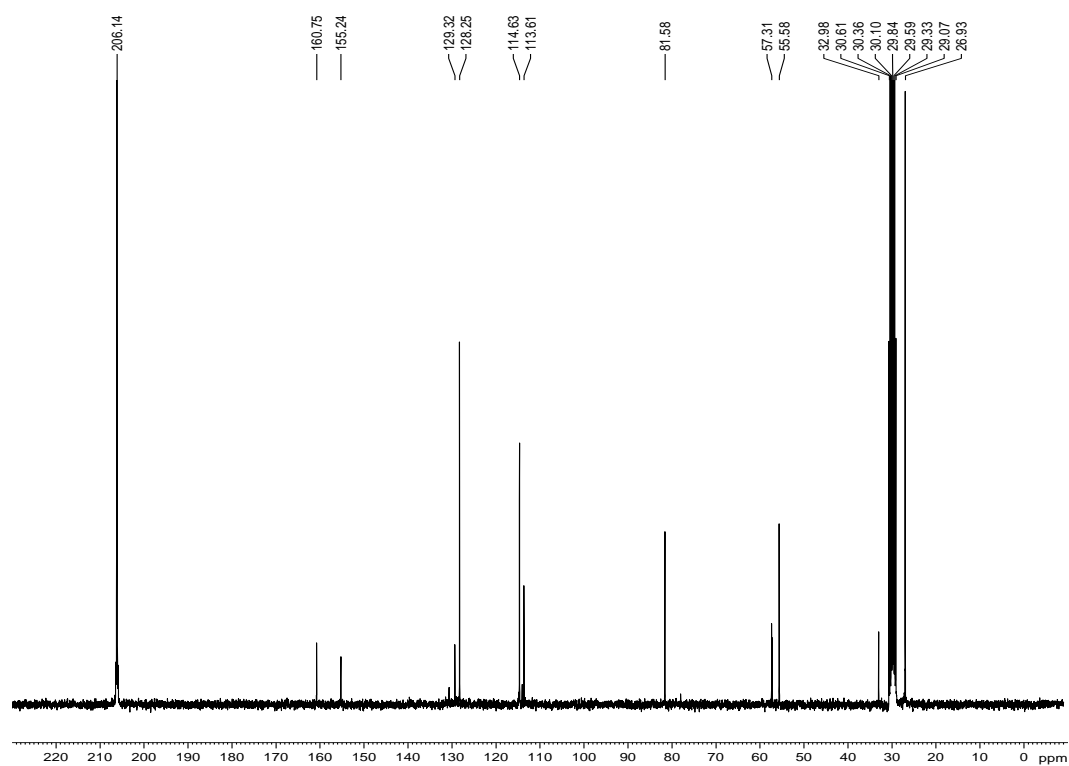
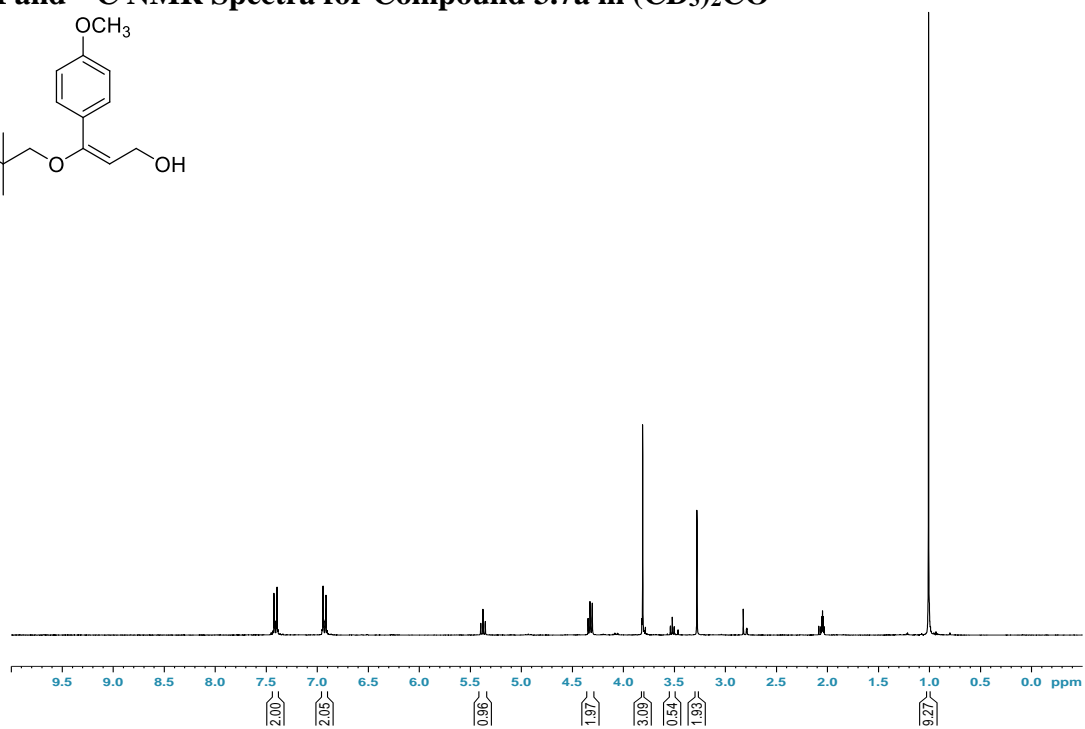
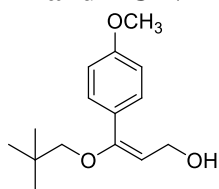
^1H and ^{13}C NMR Spectra for Compound 3.6b in $(\text{CD}_3)_2\text{CO}$ 

^1H and ^{13}C NMR Spectra for Compound 3.6d in $(\text{CD}_3)_2\text{CO}$ 

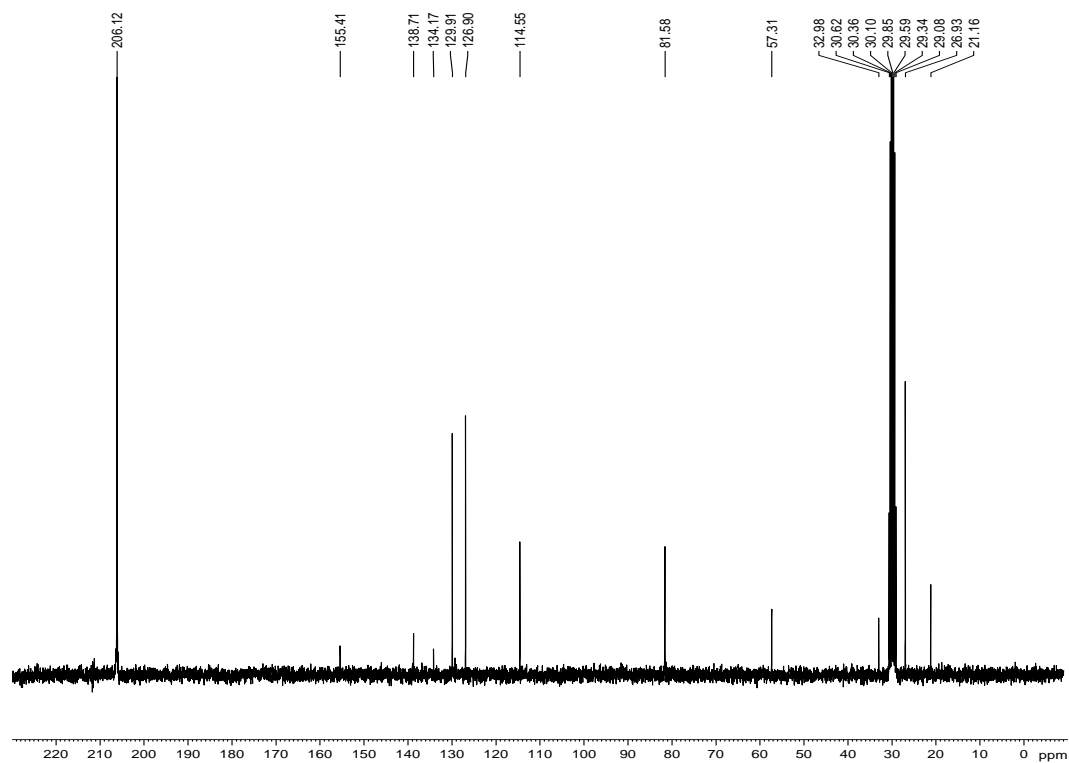
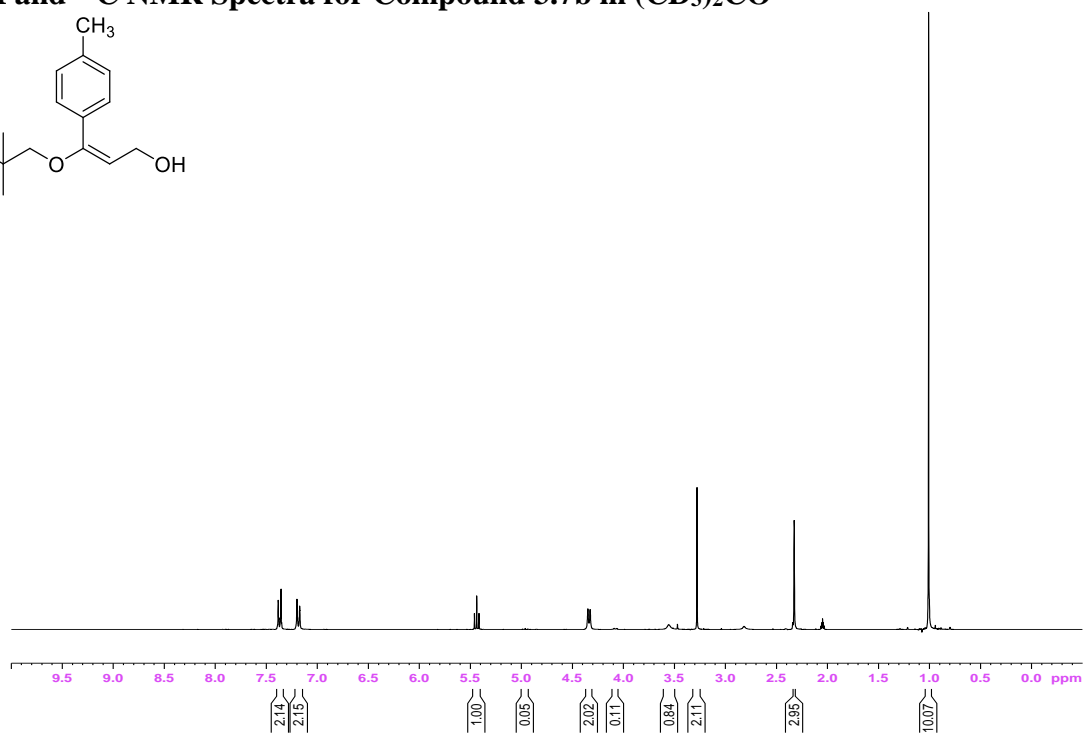
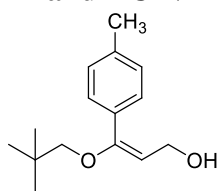
^1H and ^{13}C NMR Spectra for Compound 3.6e in $(\text{CD}_3)_2\text{CO}$ 

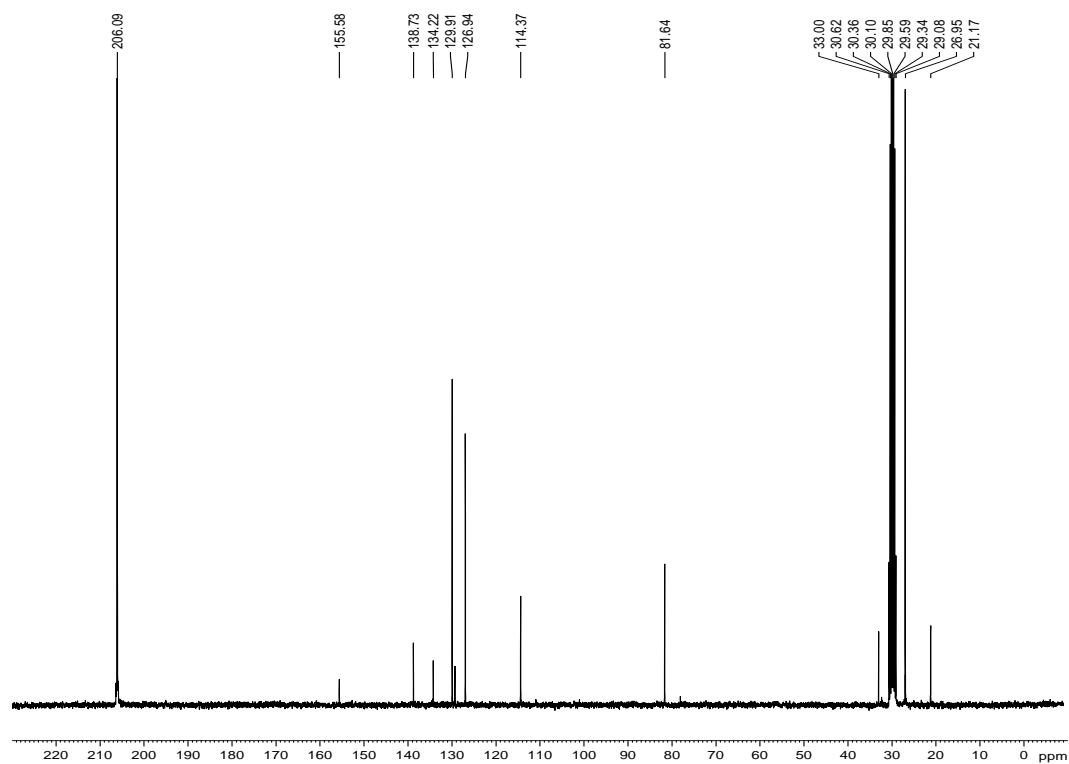
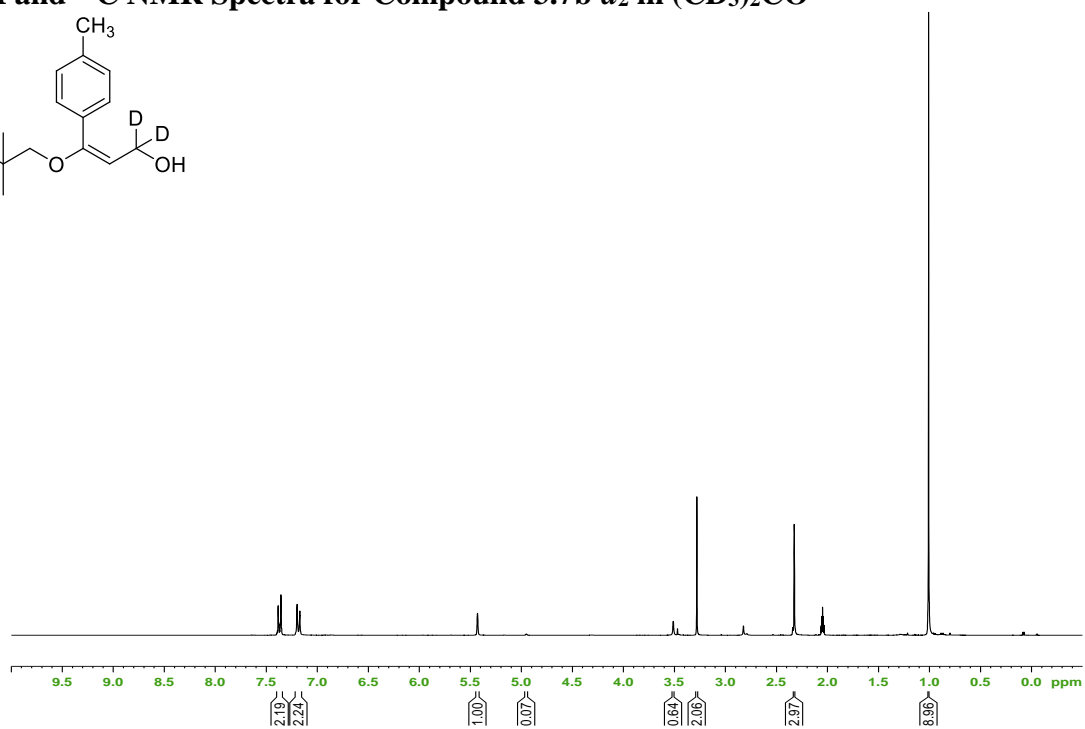
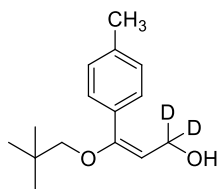
^1H and ^{13}C NMR Spectra for Compound 3.6f in $(\text{CD}_3)_2\text{CO}$ 

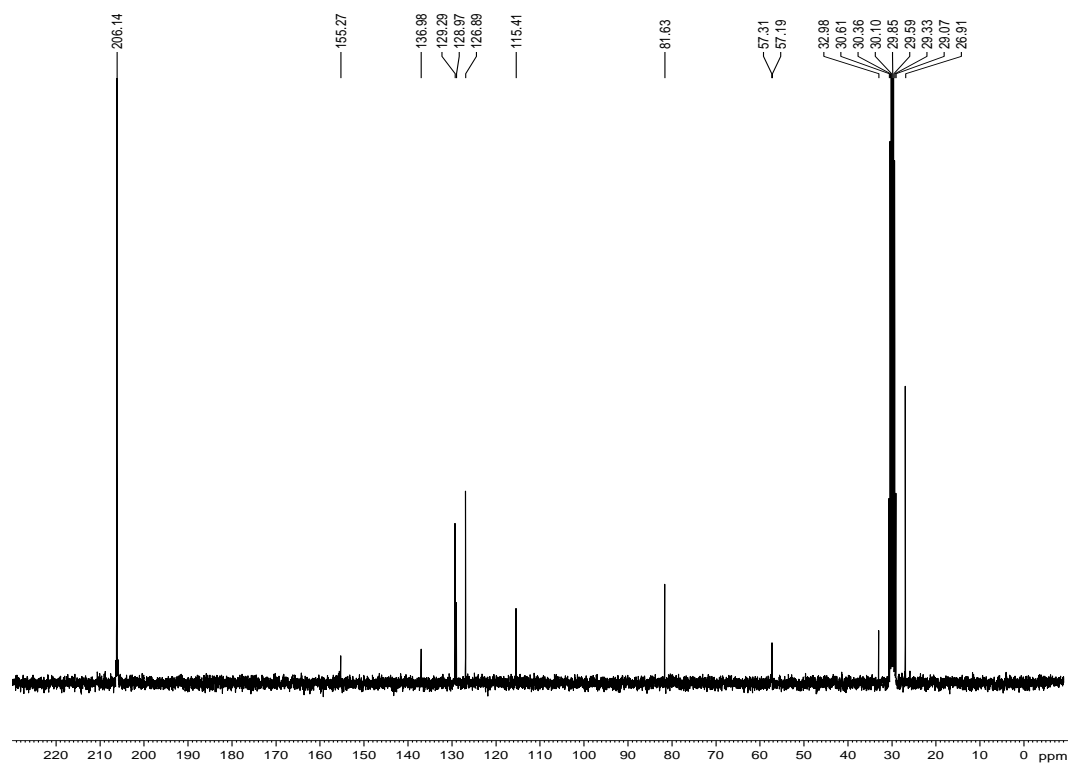
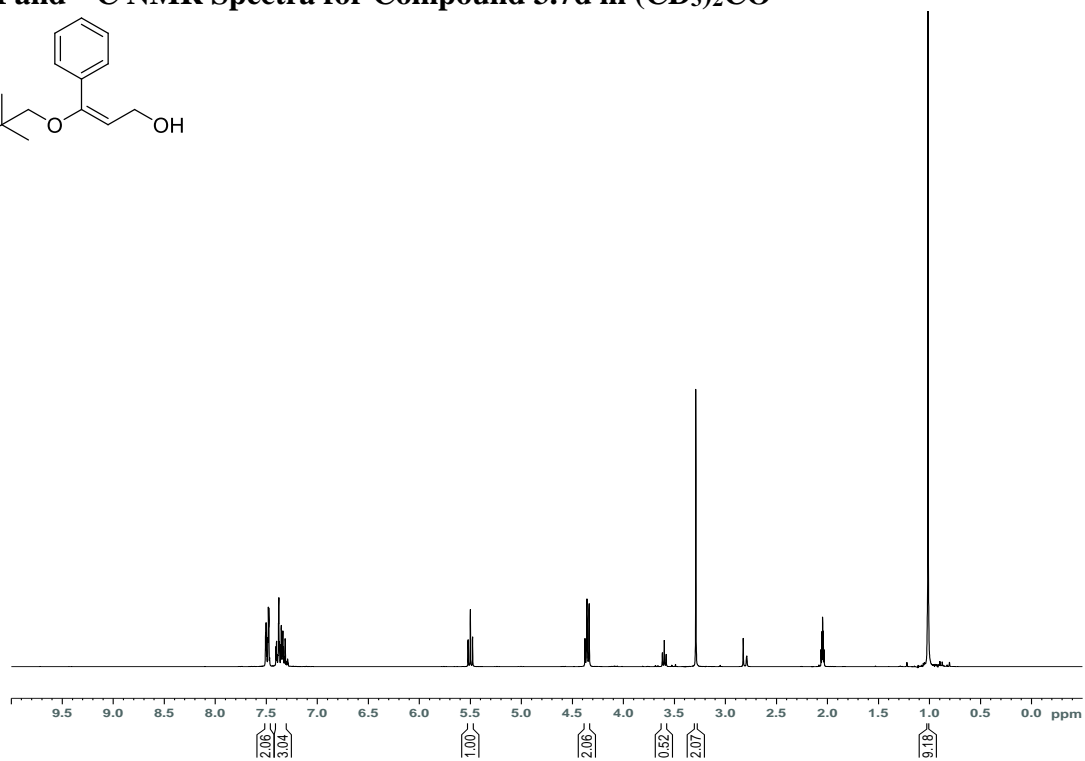
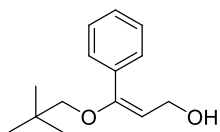
^1H and ^{13}C NMR Spectra for Compound 3.6g in $(\text{CD}_3)_2\text{CO}$ 

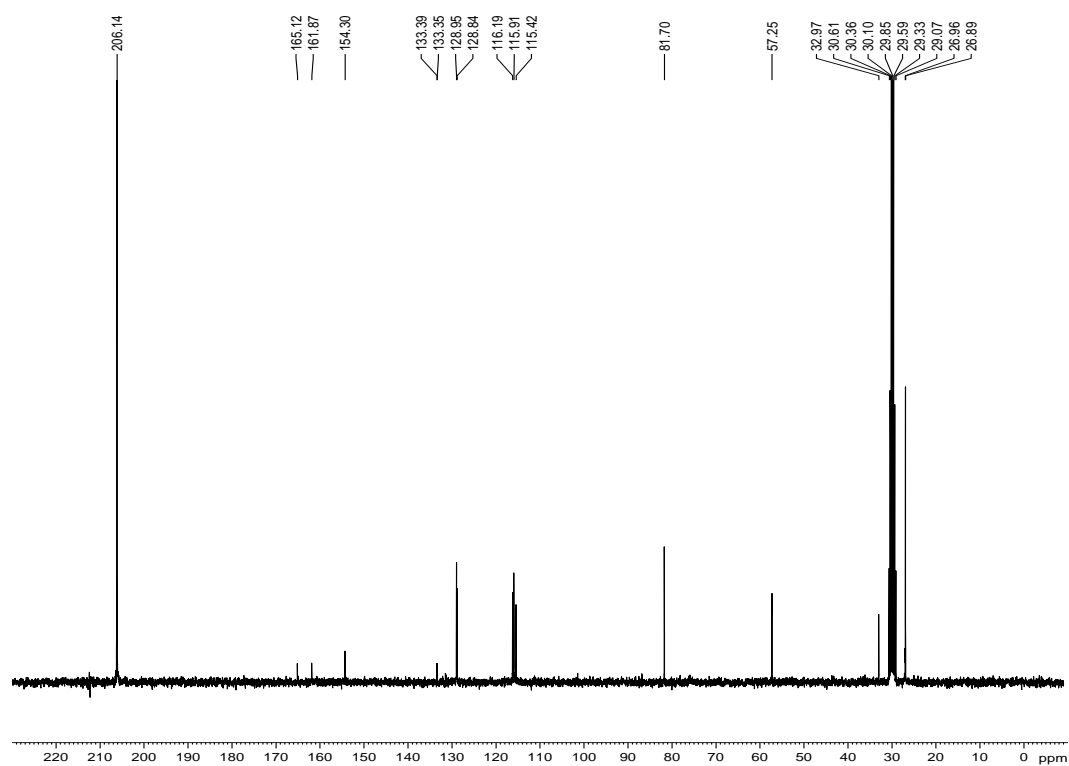
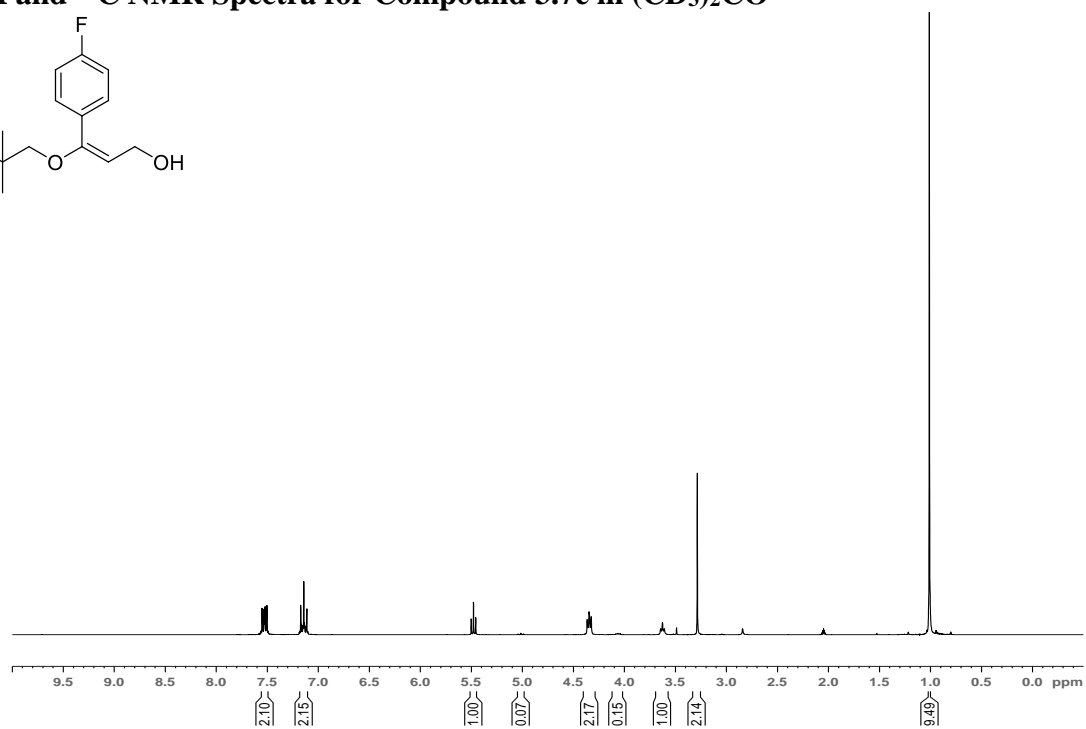
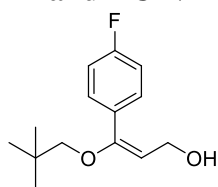
^1H and ^{13}C NMR Spectra for Compound 3.7a in $(\text{CD}_3)_2\text{CO}$ 

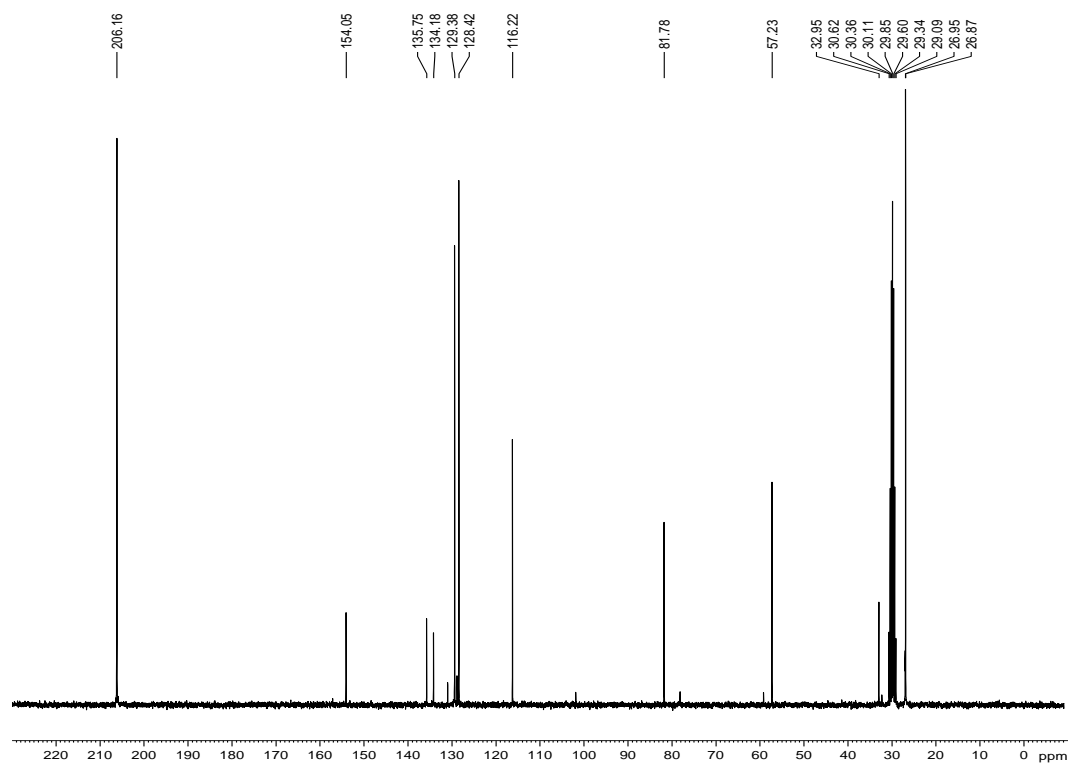
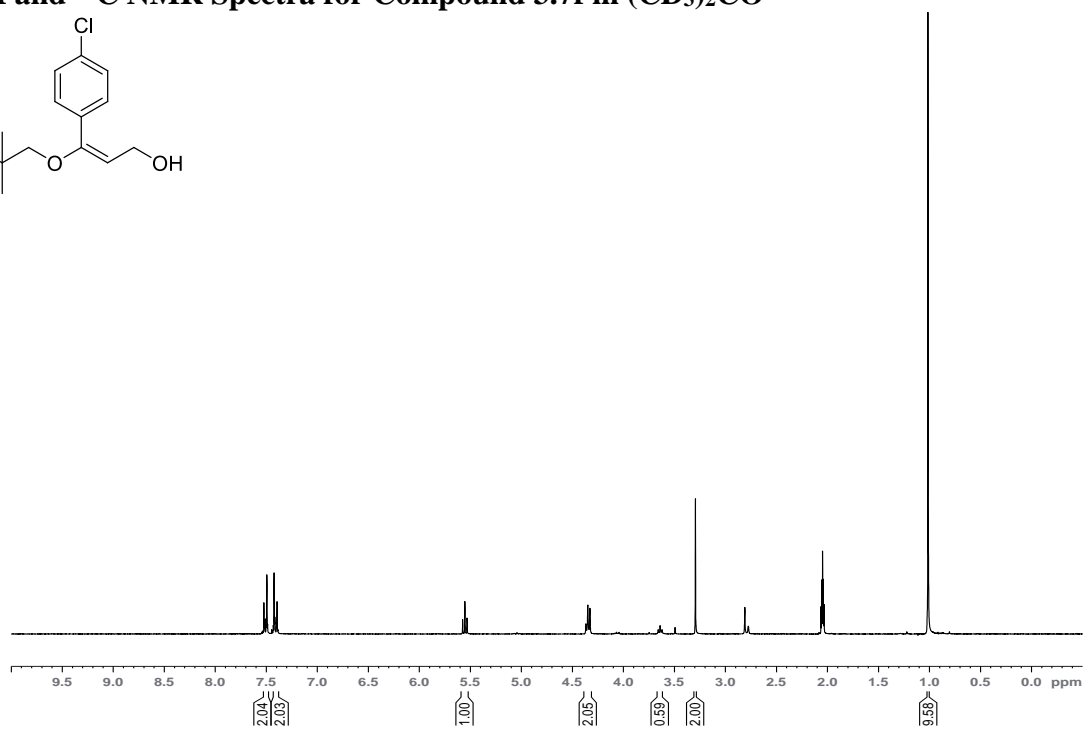
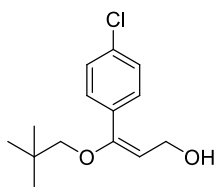
¹H and ¹³C NMR Spectra for Compound 3.7b in (CD₃)₂CO

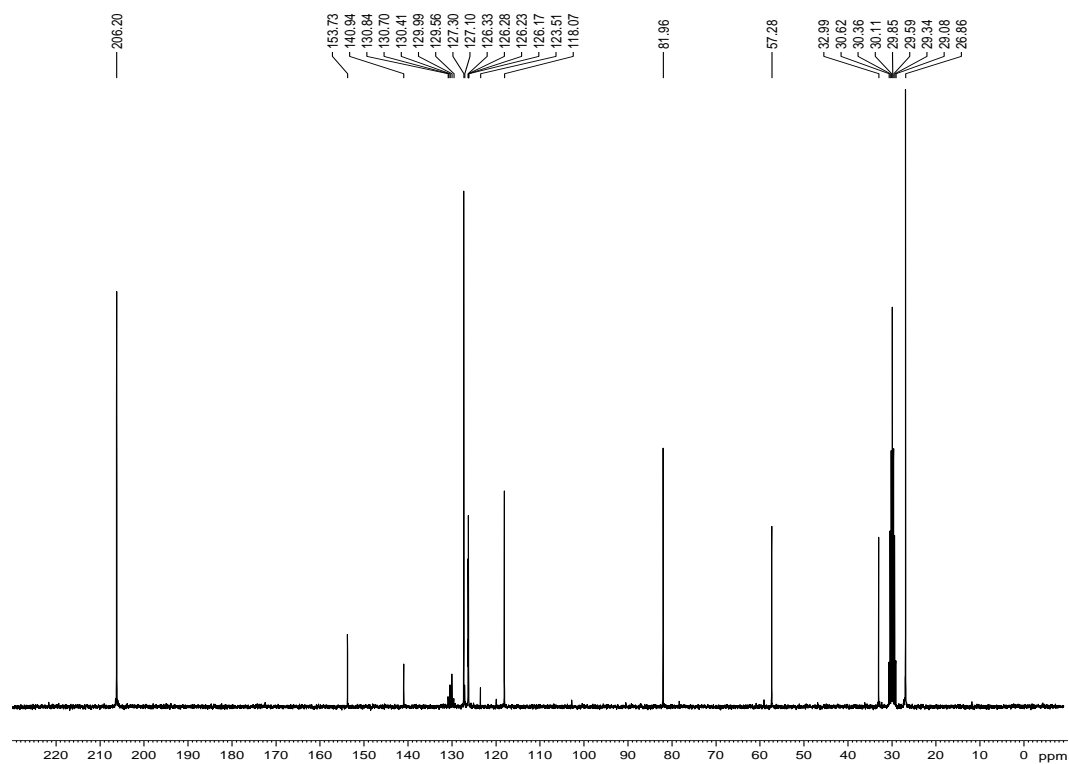
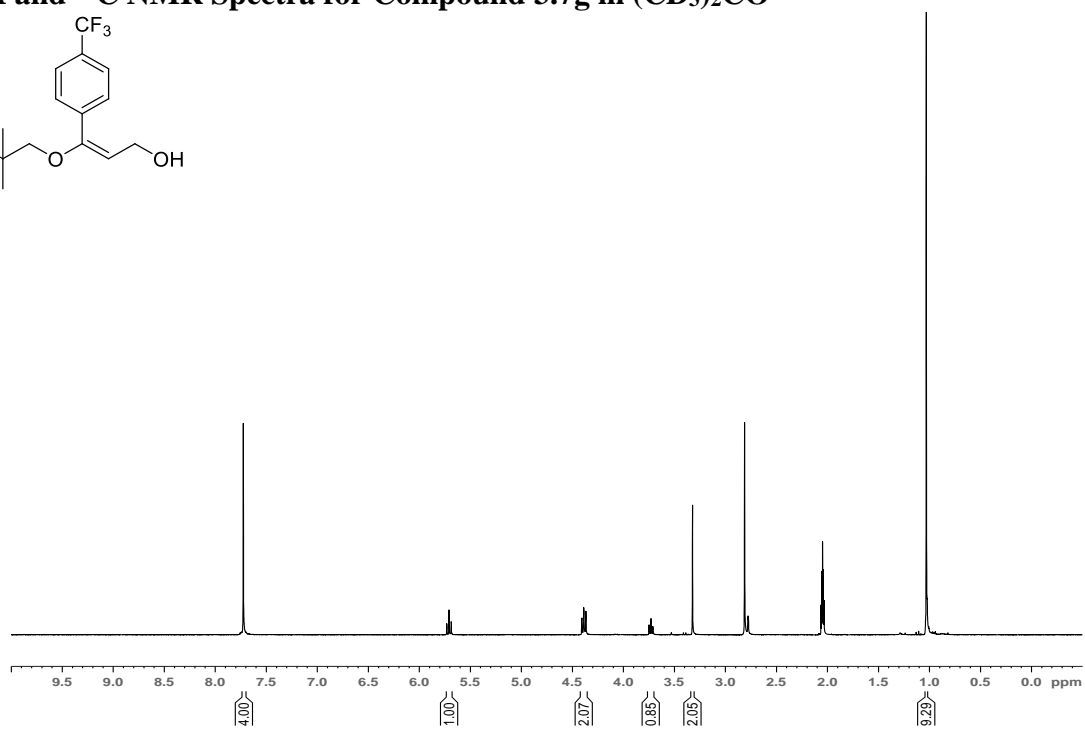
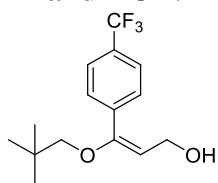


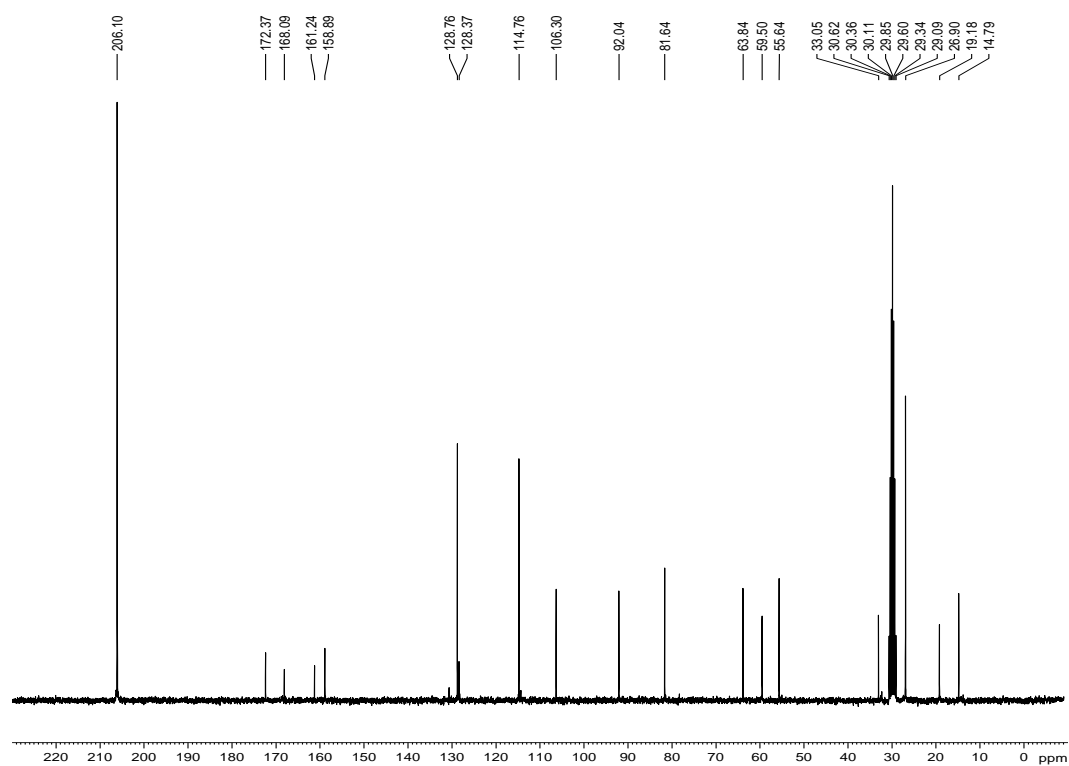
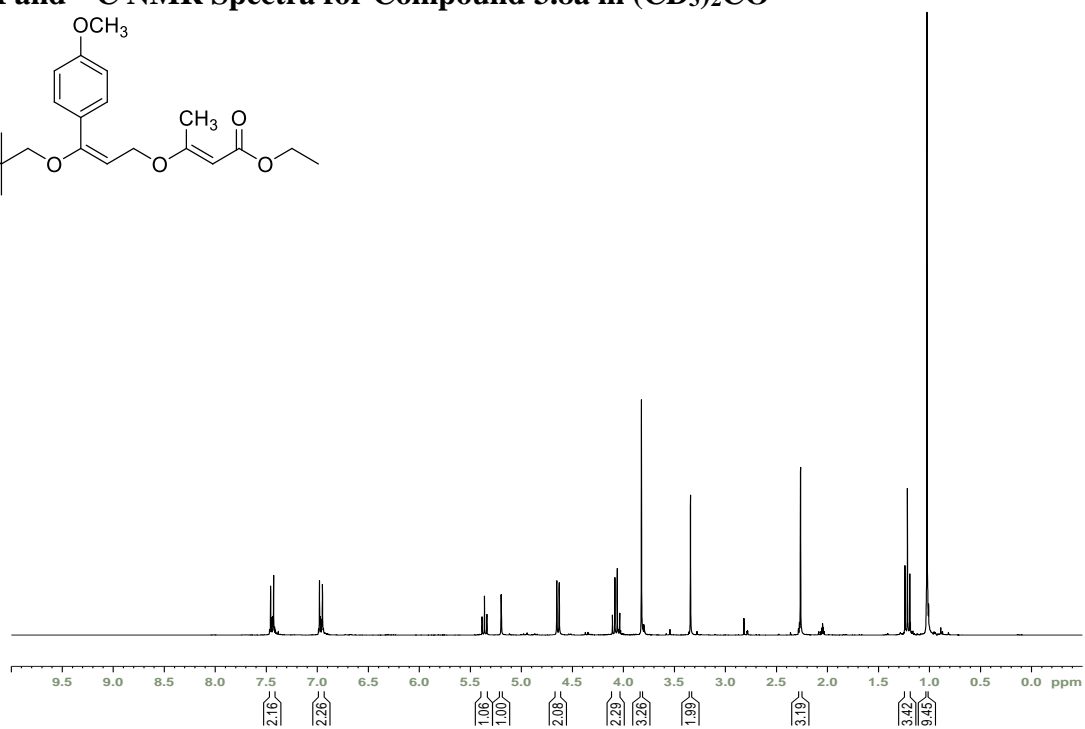
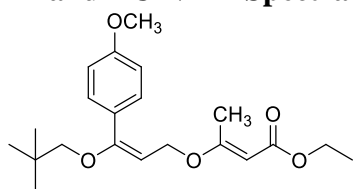
^1H and ^{13}C NMR Spectra for Compound 3.7b- d_2 in $(\text{CD}_3)_2\text{CO}$ 

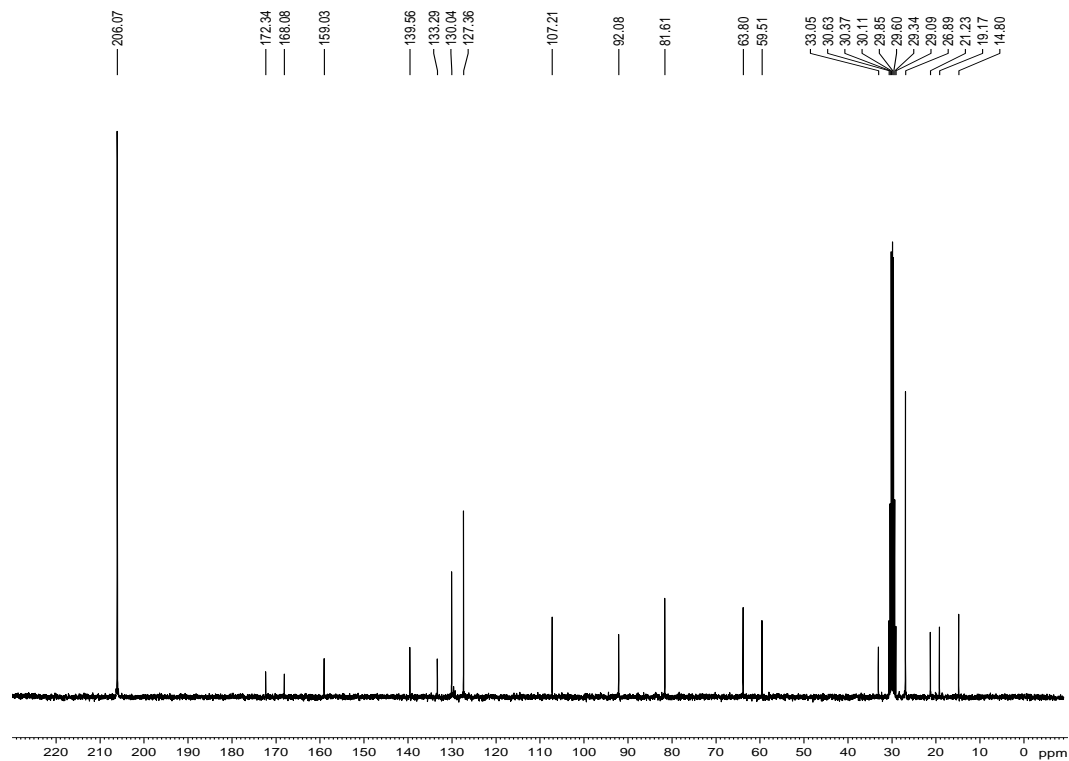
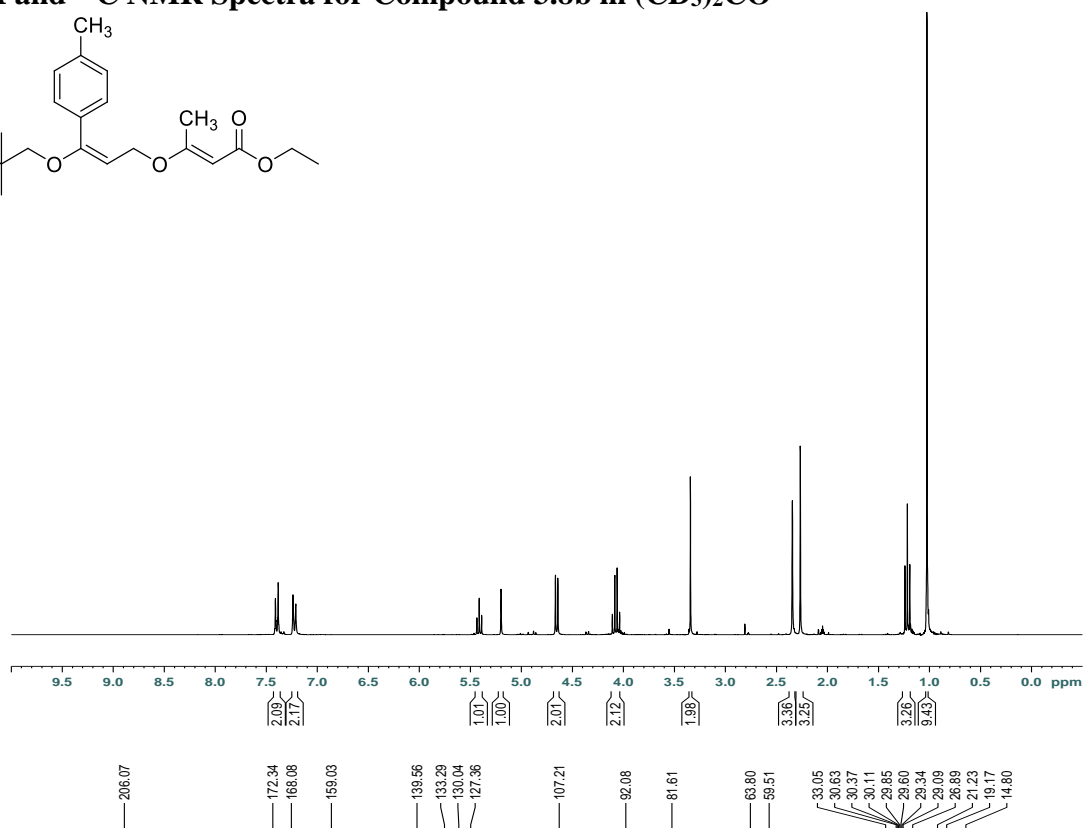
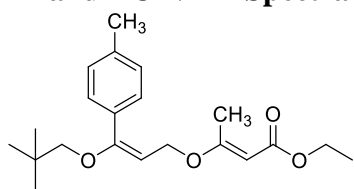
^1H and ^{13}C NMR Spectra for Compound 3.7d in $(\text{CD}_3)_2\text{CO}$ 

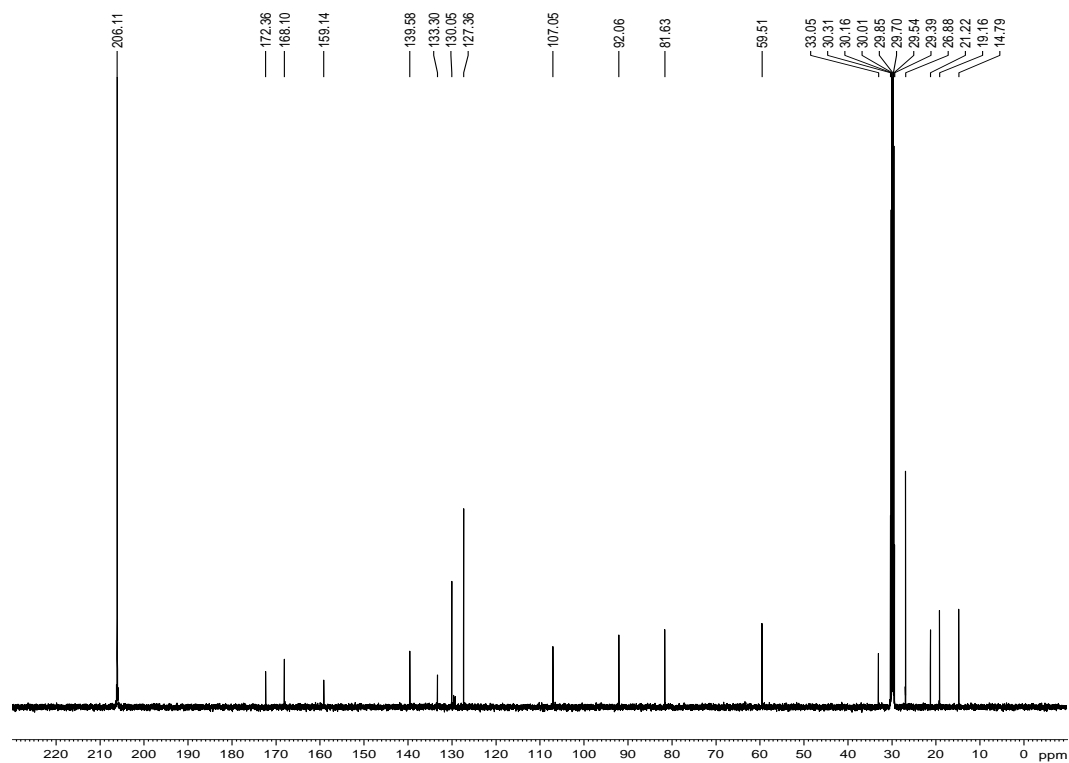
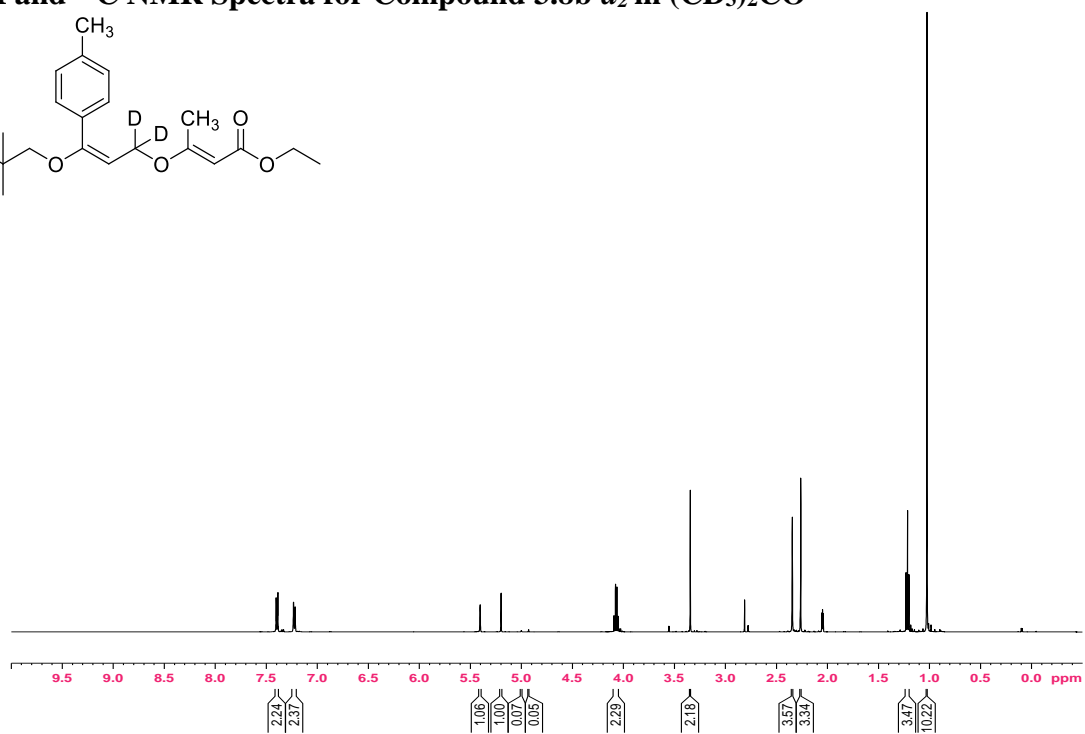
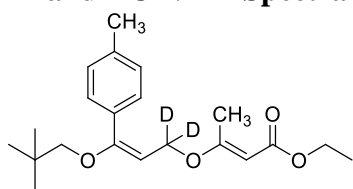
^1H and ^{13}C NMR Spectra for Compound 3.7e in $(\text{CD}_3)_2\text{CO}$ 

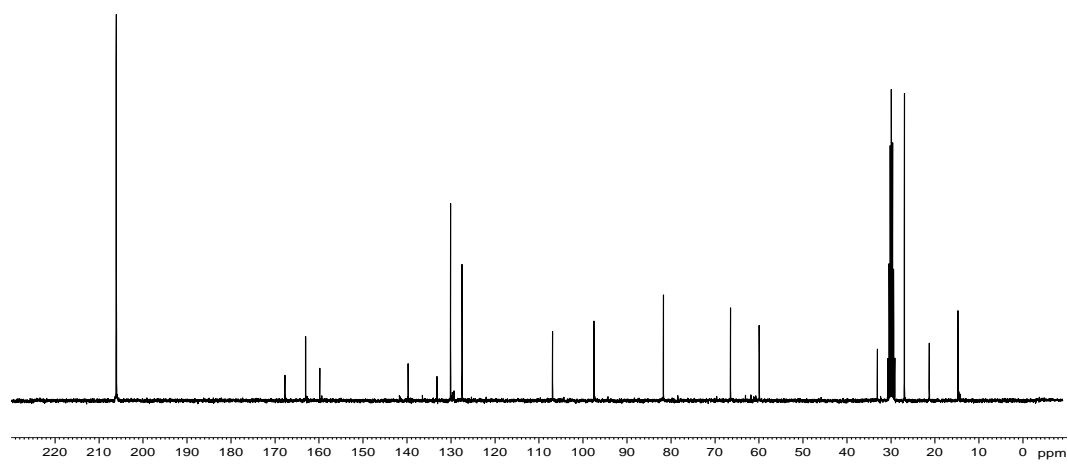
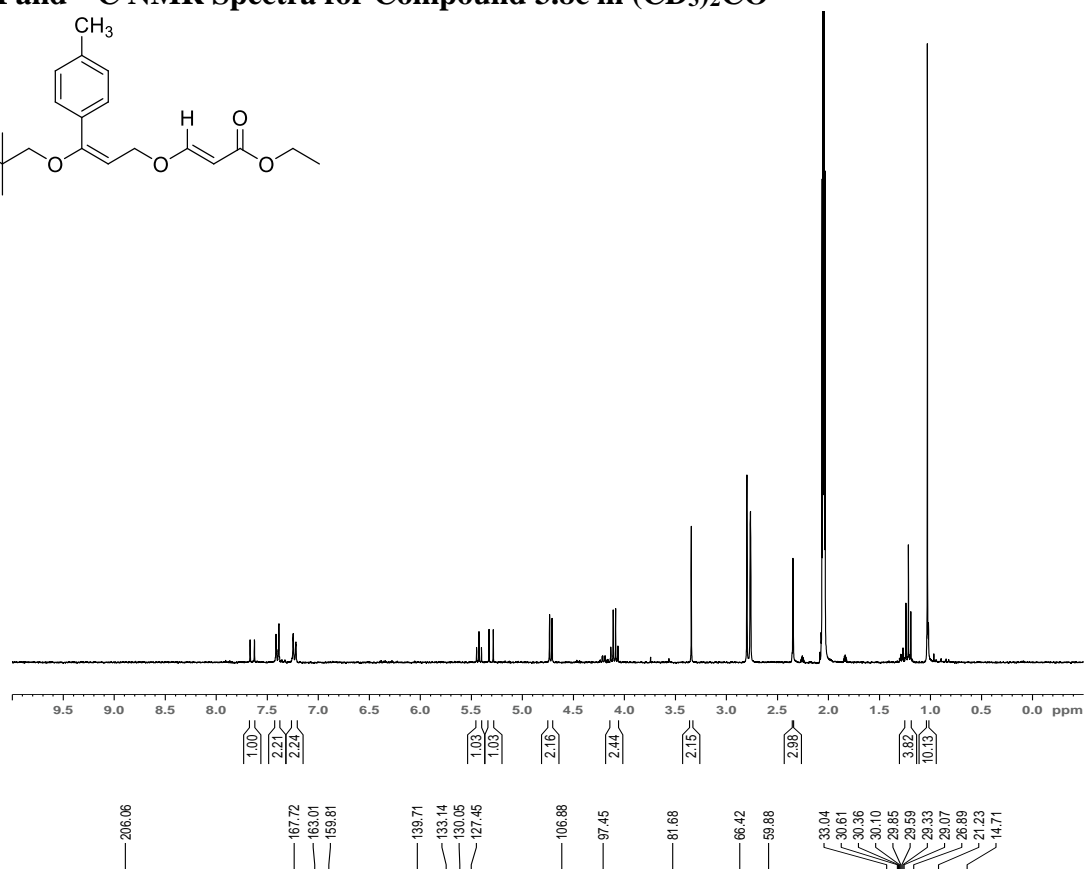
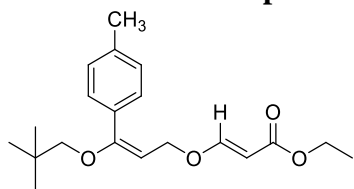
^1H and ^{13}C NMR Spectra for Compound 3.7f in $(\text{CD}_3)_2\text{CO}$ 

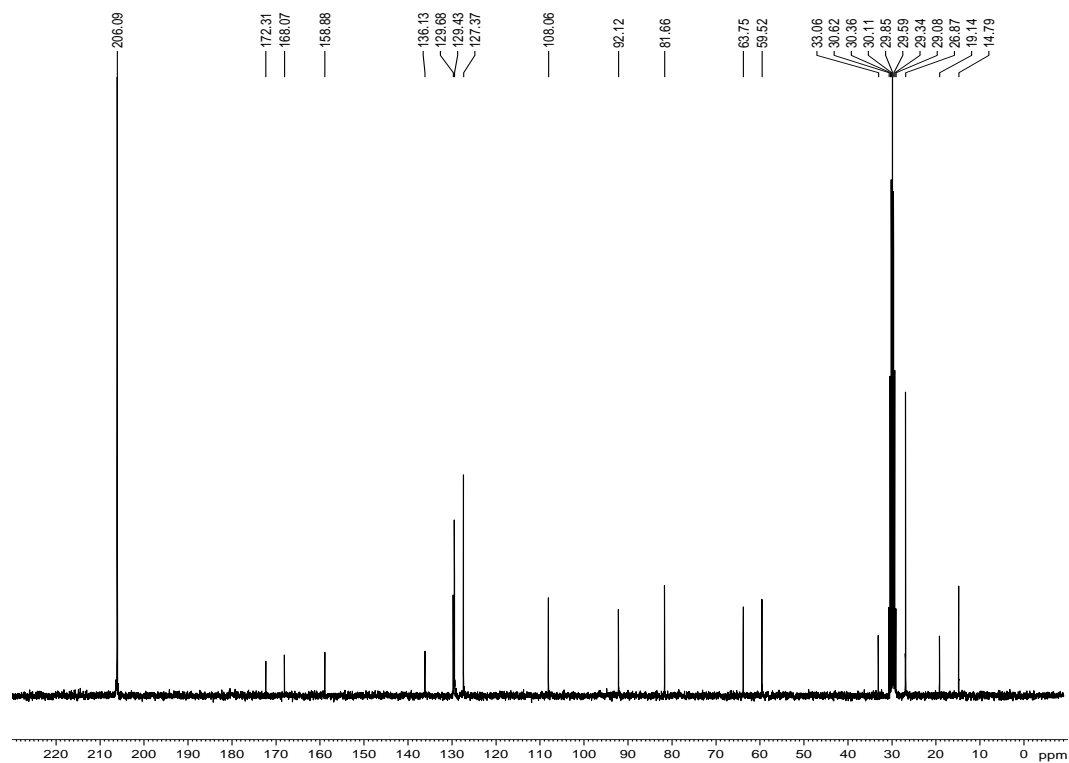
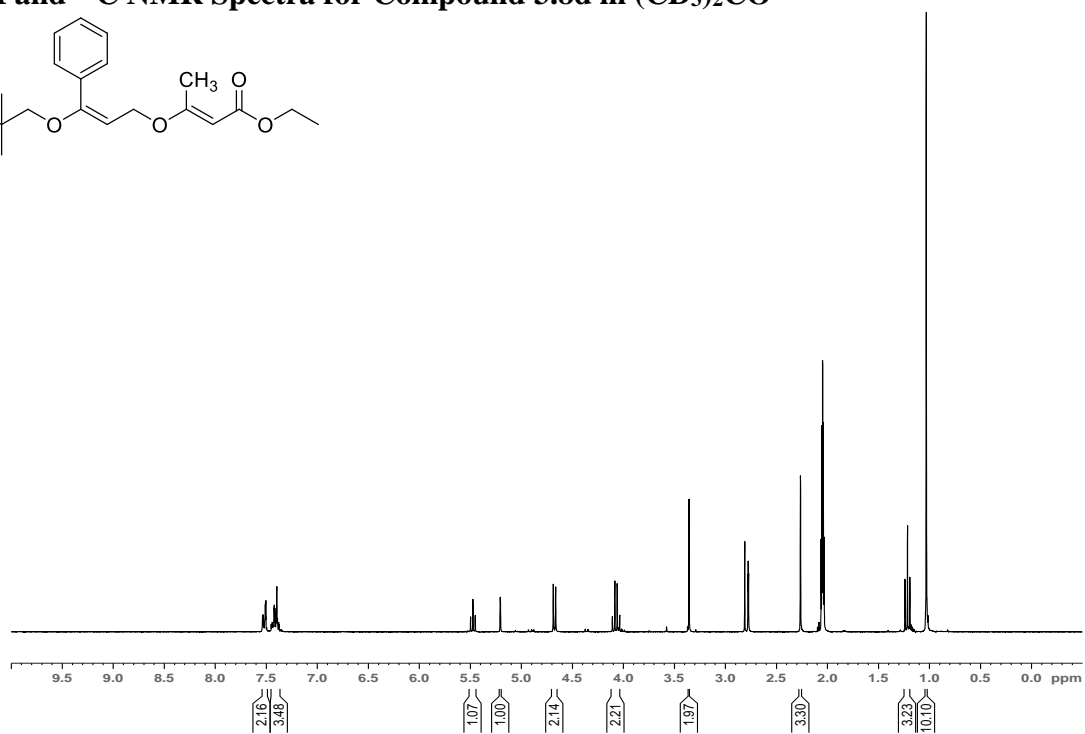
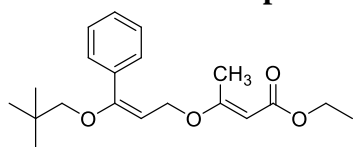
^1H and ^{13}C NMR Spectra for Compound 3.7g in $(\text{CD}_3)_2\text{CO}$ 

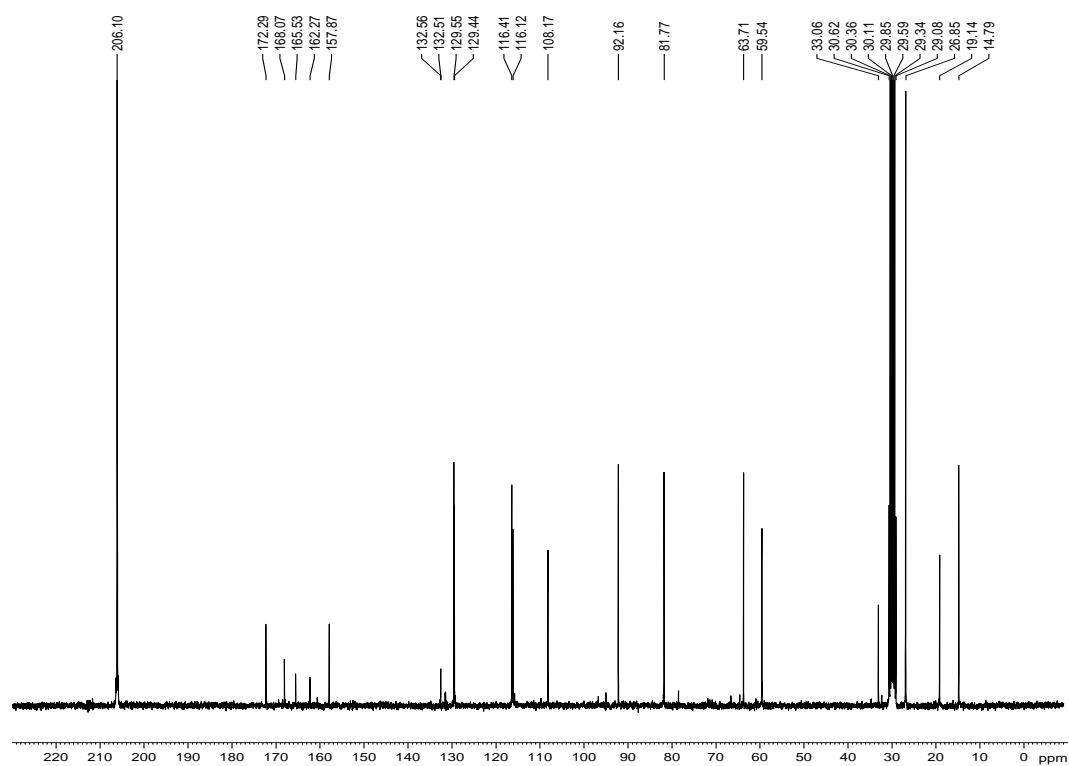
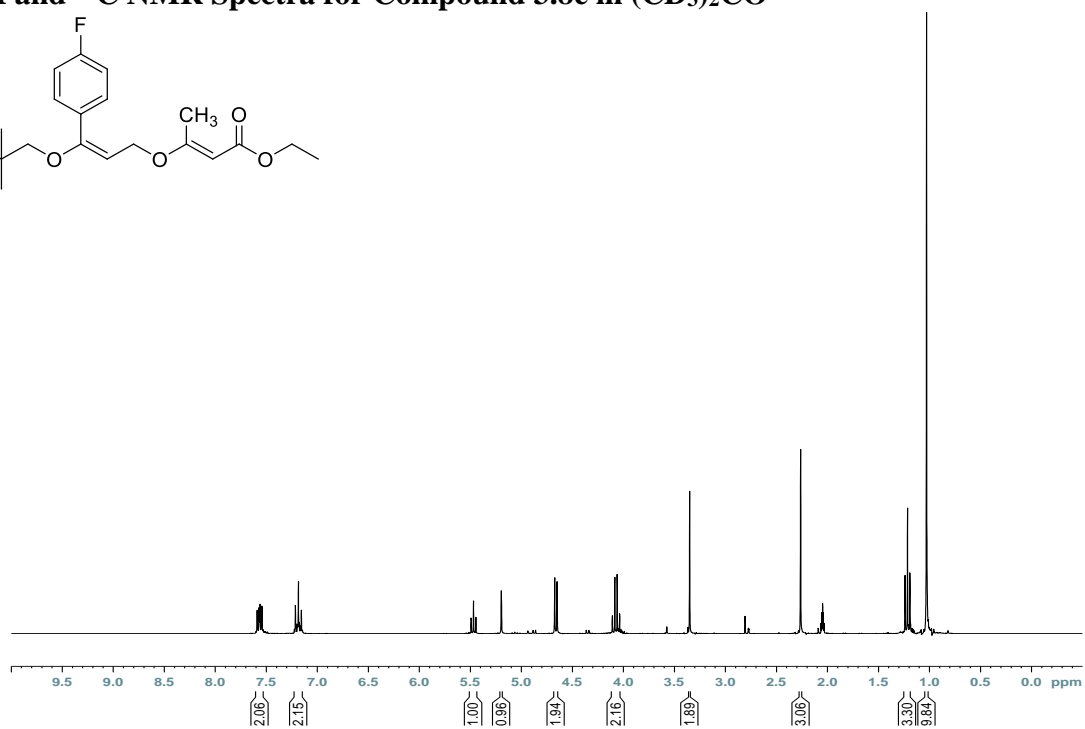
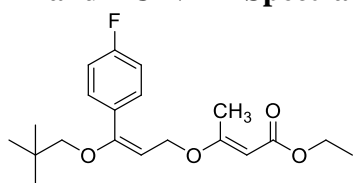
^1H and ^{13}C NMR Spectra for Compound 3.8a in $(\text{CD}_3)_2\text{CO}$ 

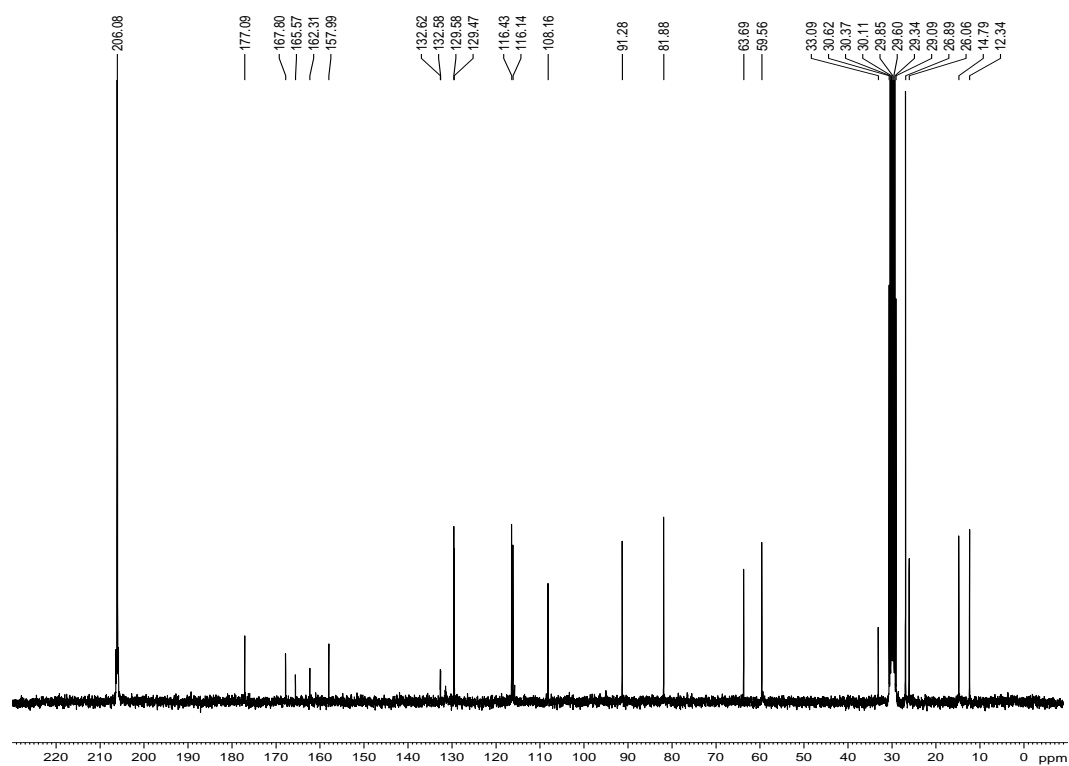
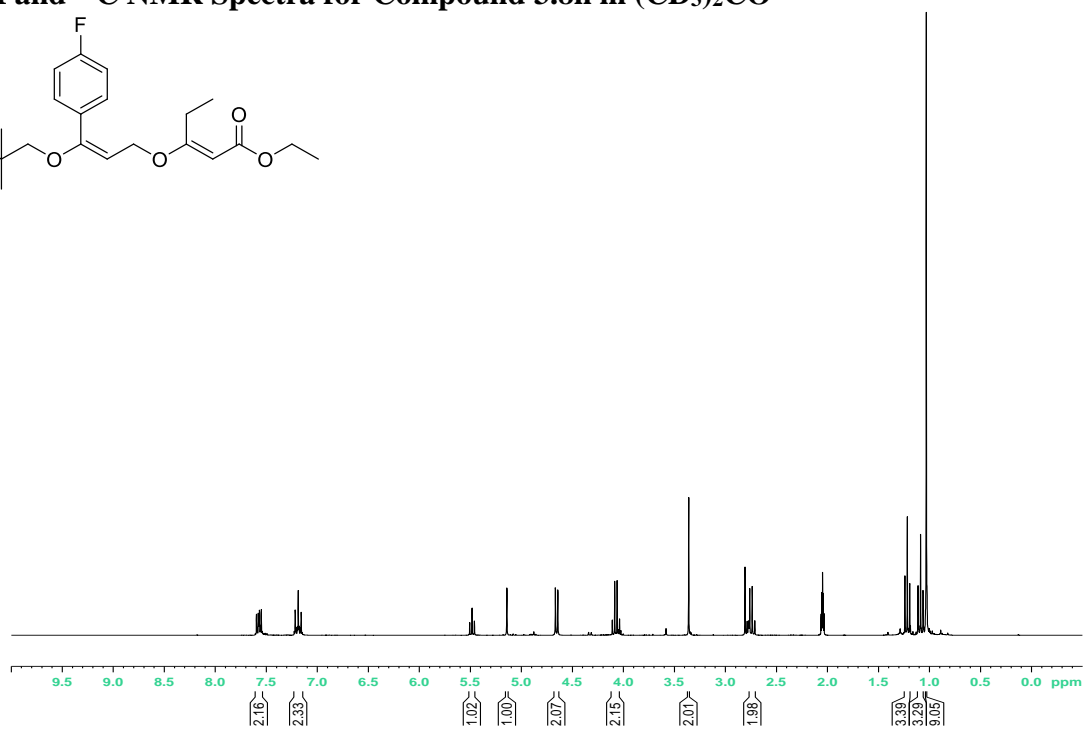
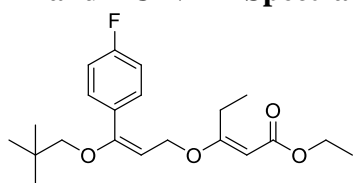
^1H and ^{13}C NMR Spectra for Compound 3.8b in $(\text{CD}_3)_2\text{CO}$ 

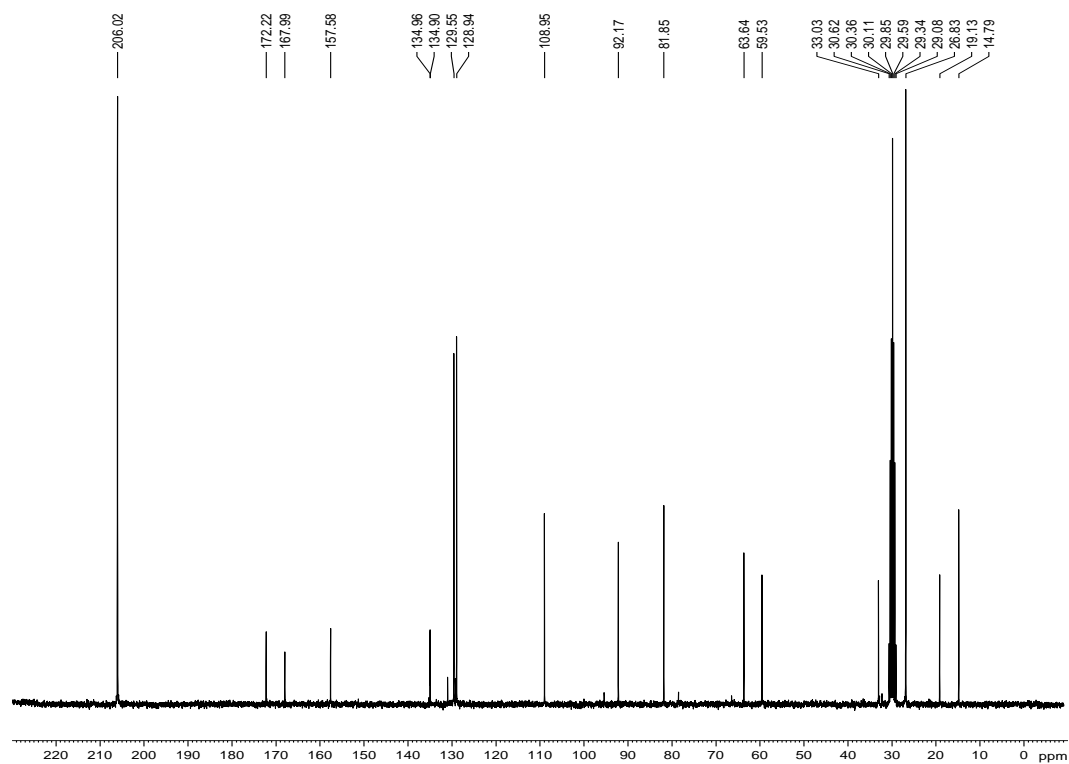
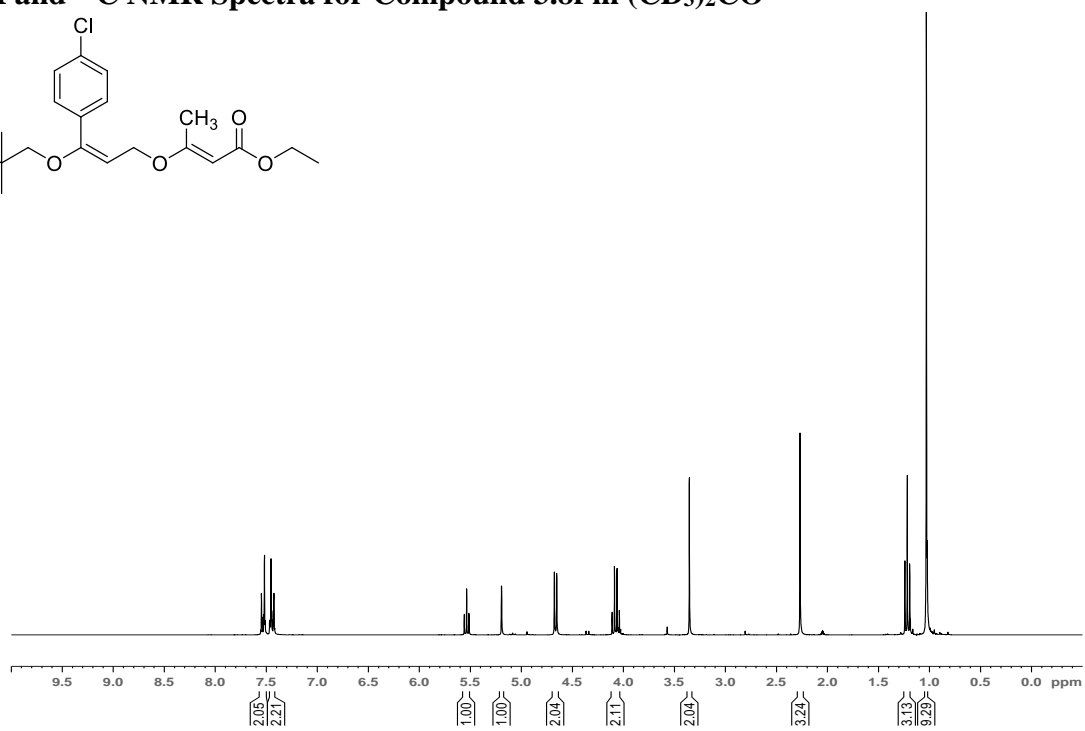
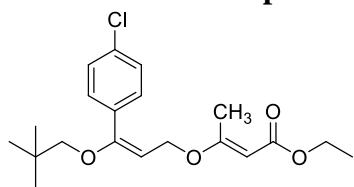
^1H and ^{13}C NMR Spectra for Compound 3.8b- d_2 in $(\text{CD}_3)_2\text{CO}$ 

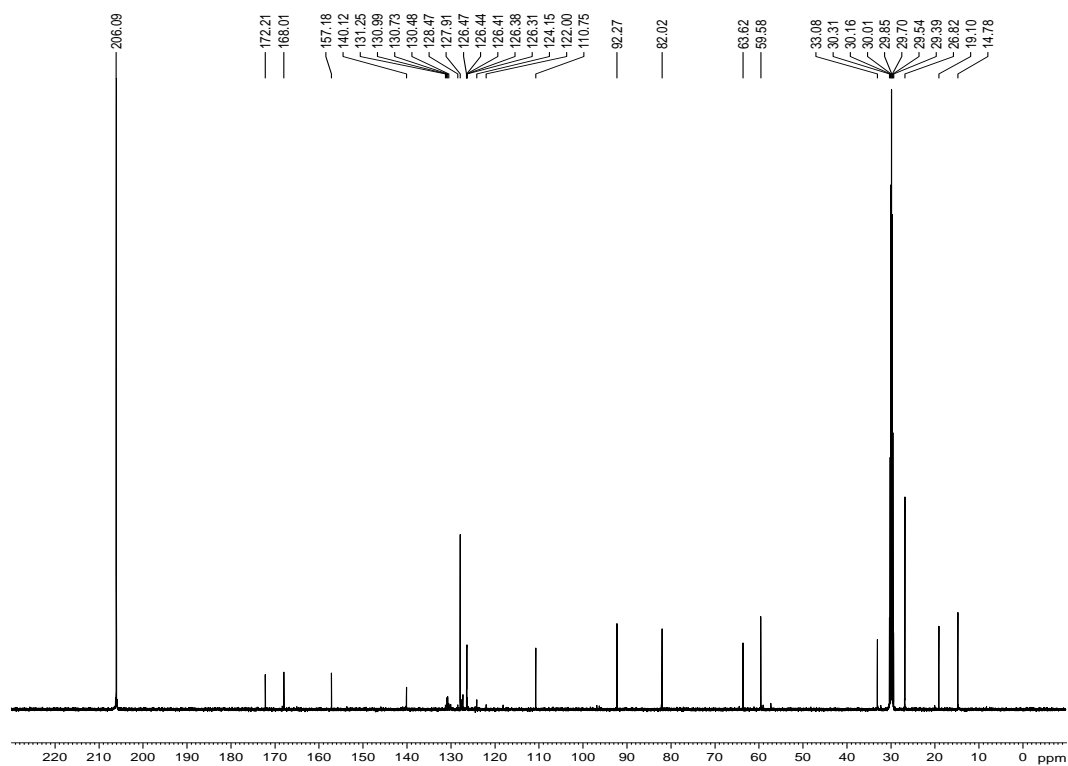
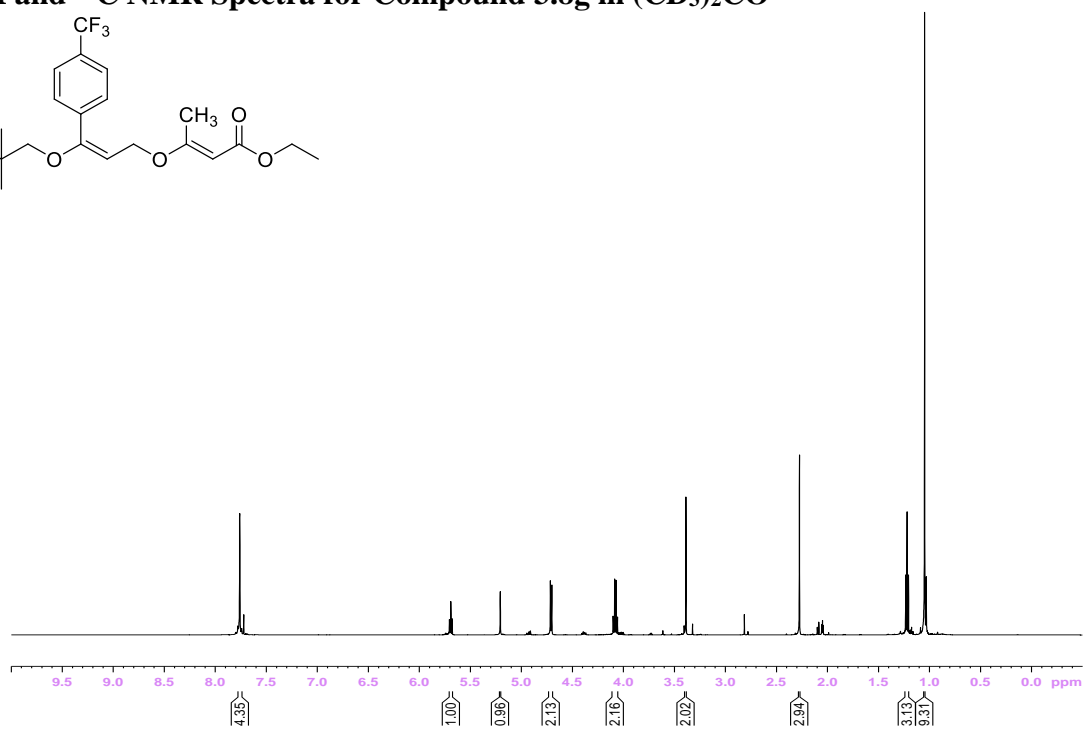
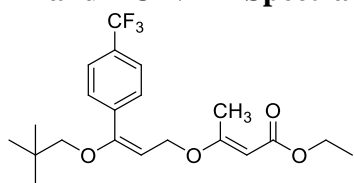
^1H and ^{13}C NMR Spectra for Compound 3.8c in $(\text{CD}_3)_2\text{CO}$ 

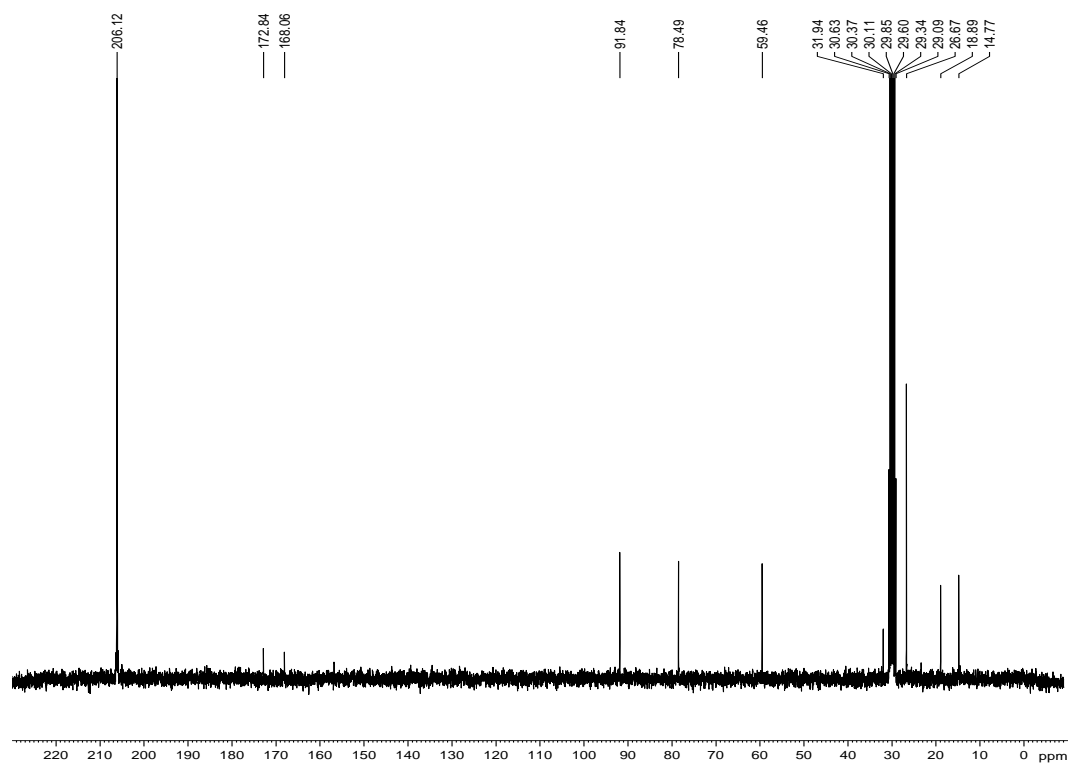
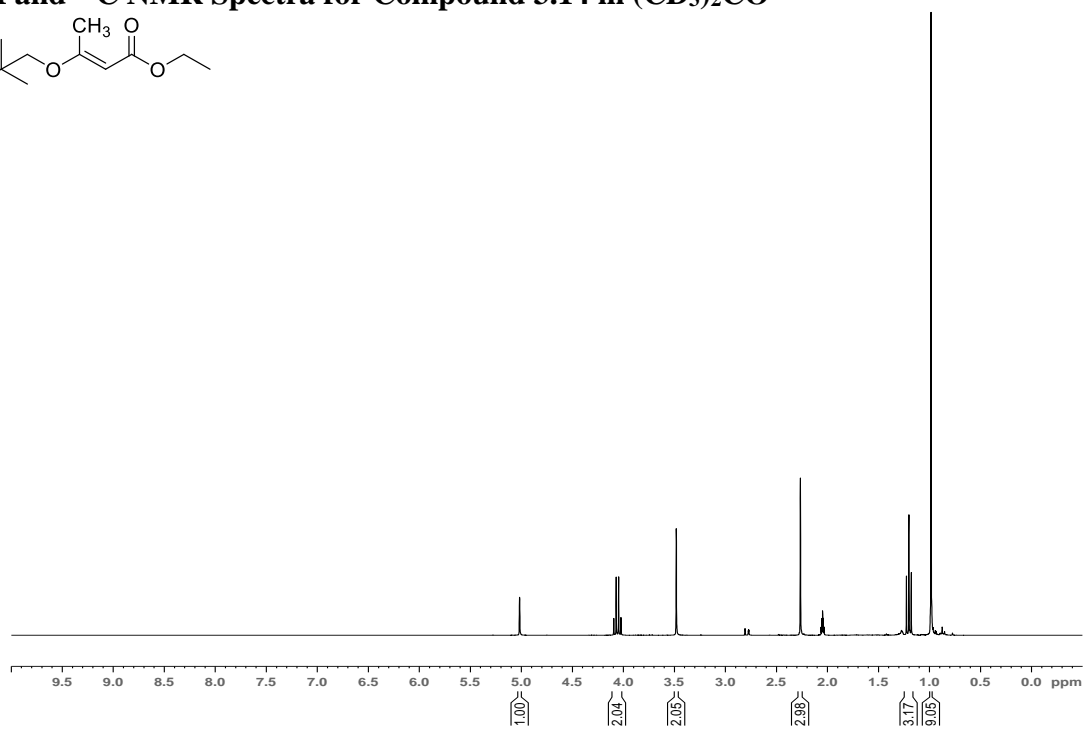
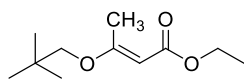
^1H and ^{13}C NMR Spectra for Compound 3.8d in $(\text{CD}_3)_2\text{CO}$ 

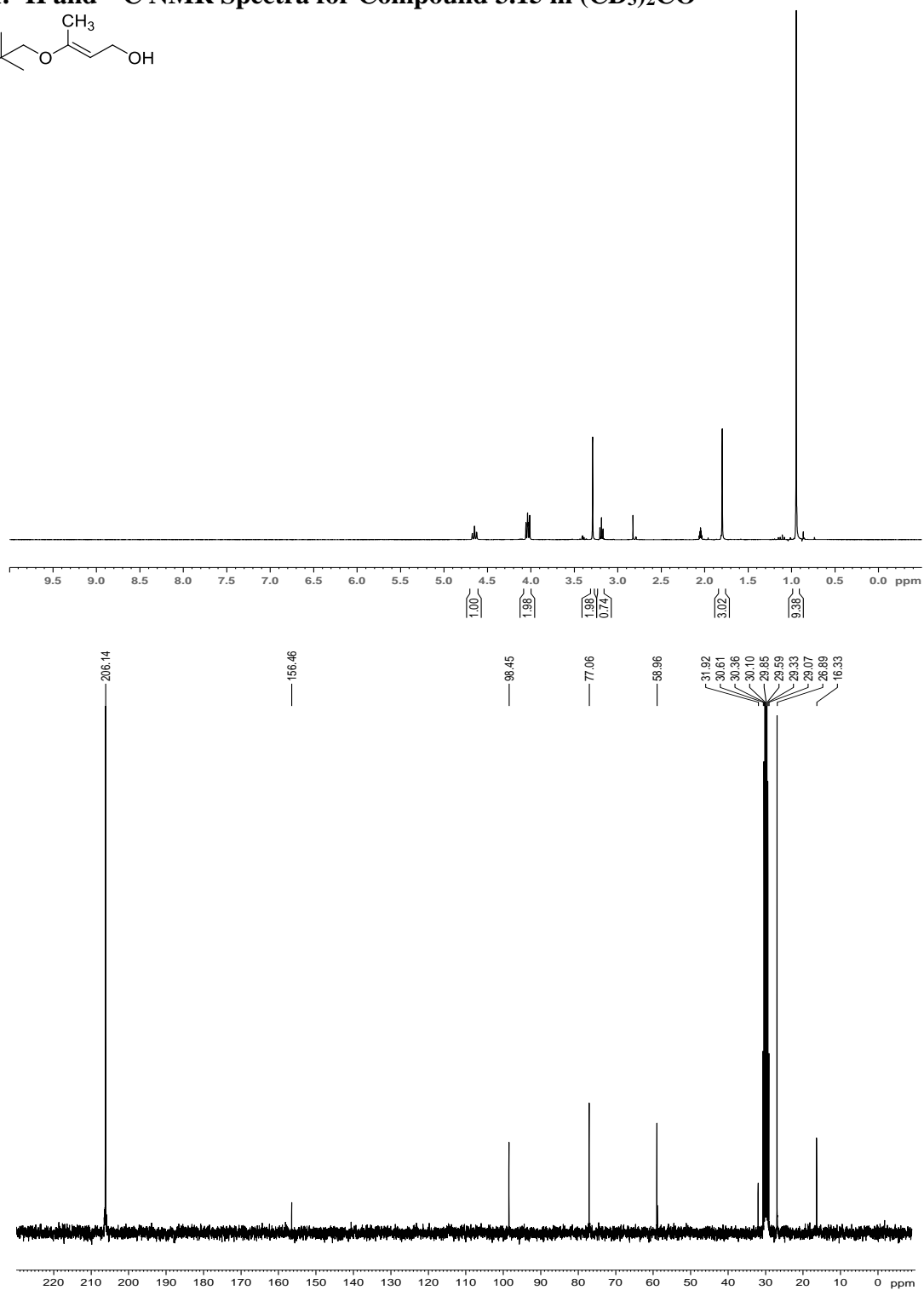
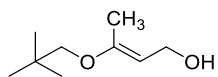
^1H and ^{13}C NMR Spectra for Compound 3.8e in $(\text{CD}_3)_2\text{CO}$ 

^1H and ^{13}C NMR Spectra for Compound 3.8h in $(\text{CD}_3)_2\text{CO}$ 

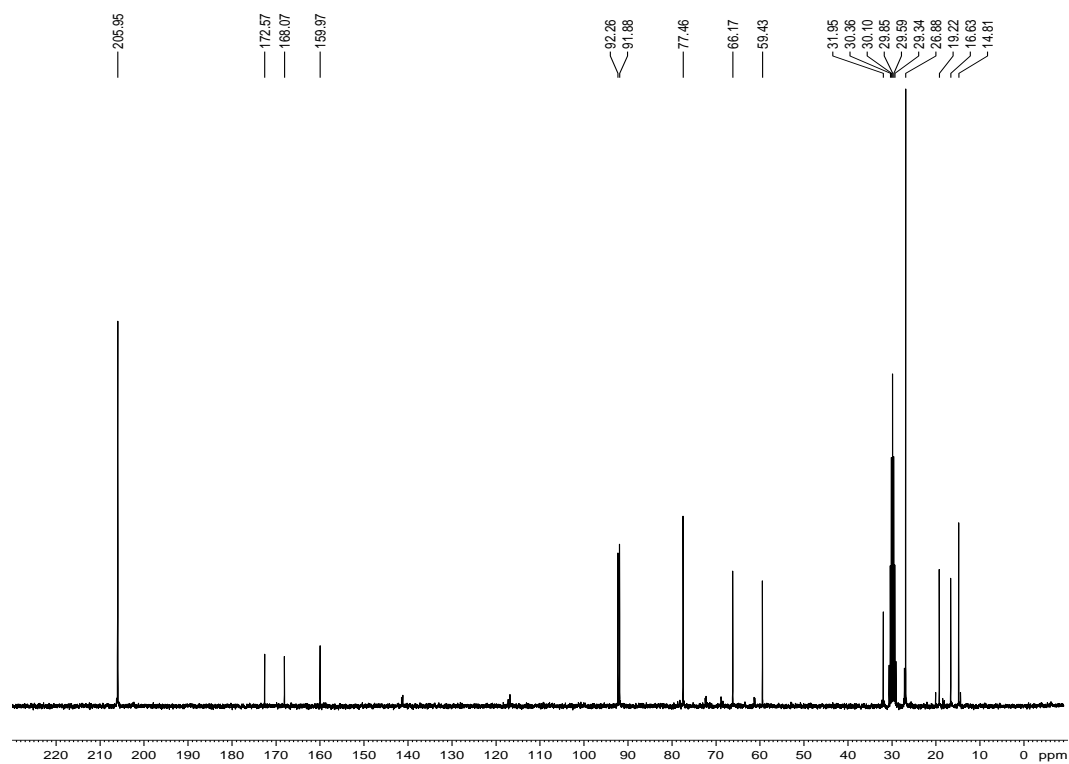
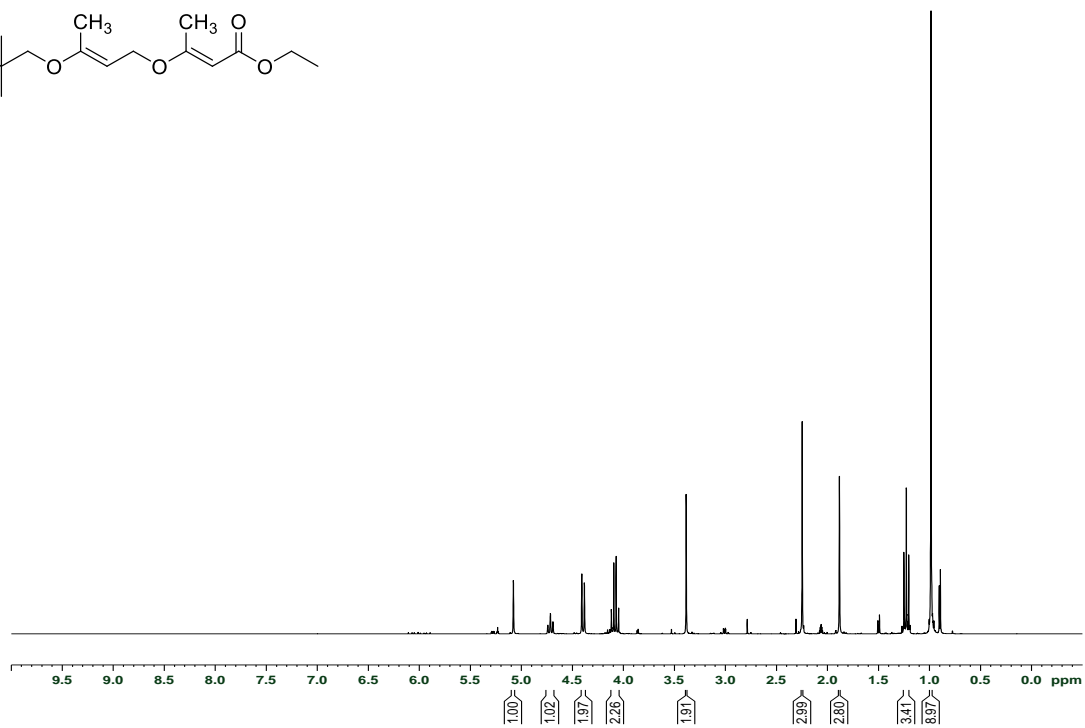
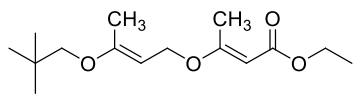
^1H and ^{13}C NMR Spectra for Compound 3.8f in $(\text{CD}_3)_2\text{CO}$ 

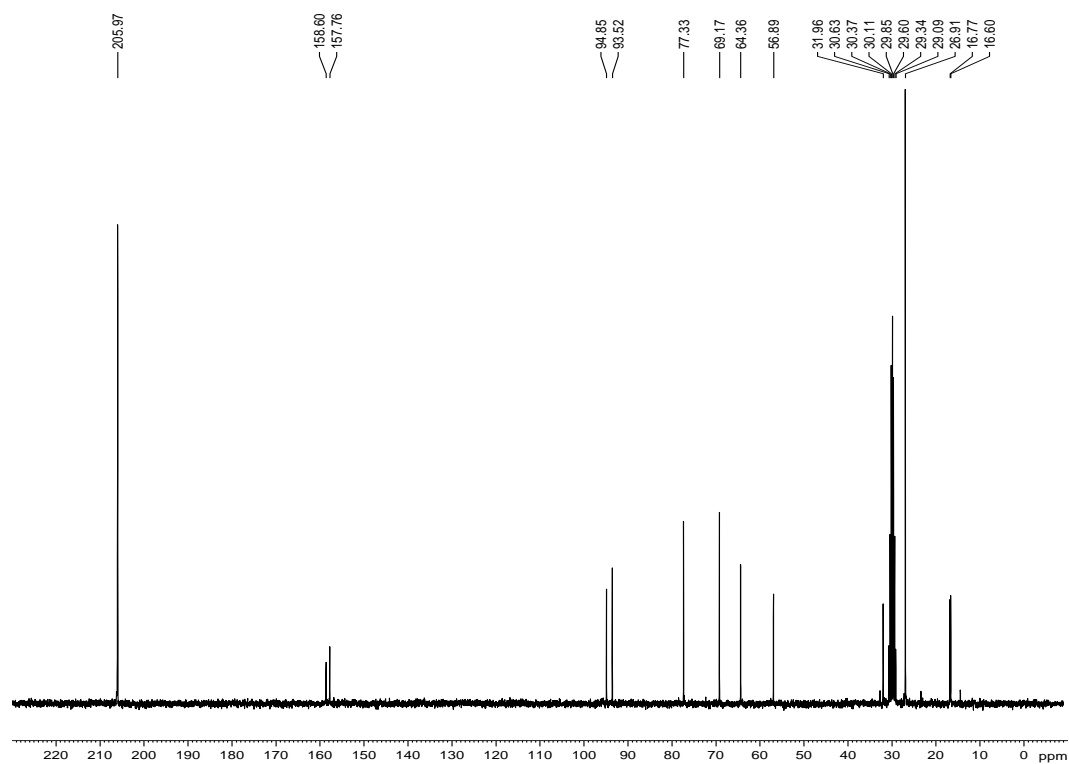
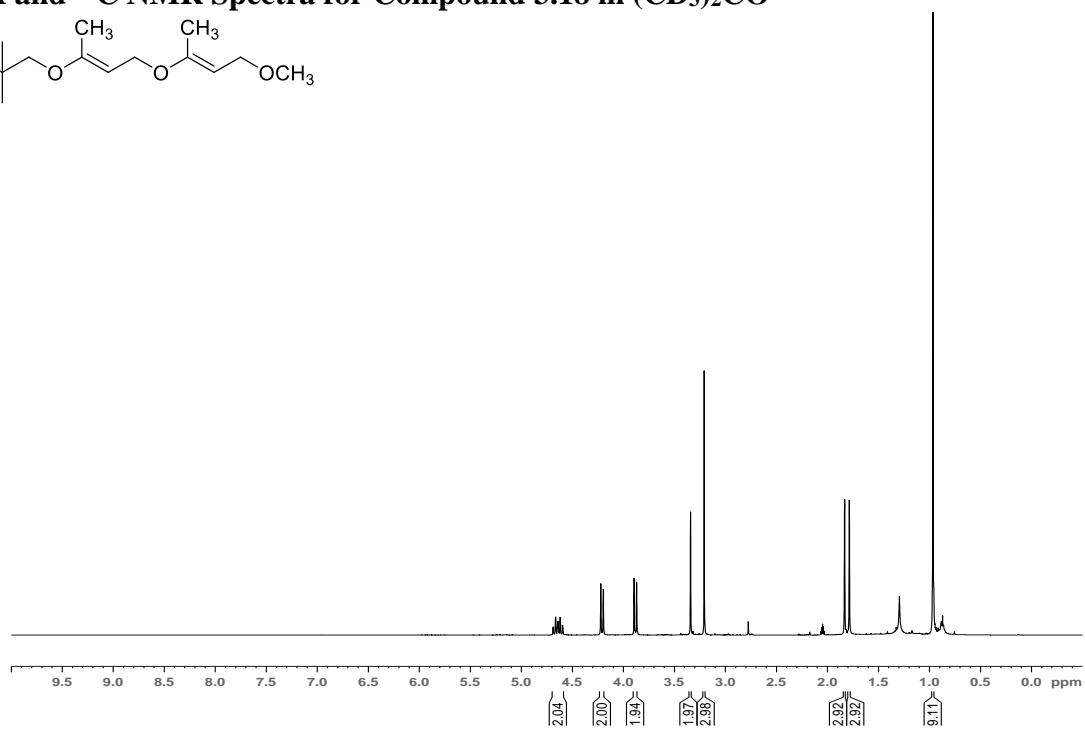
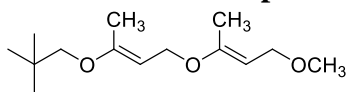
^1H and ^{13}C NMR Spectra for Compound 3.8g in $(\text{CD}_3)_2\text{CO}$ 

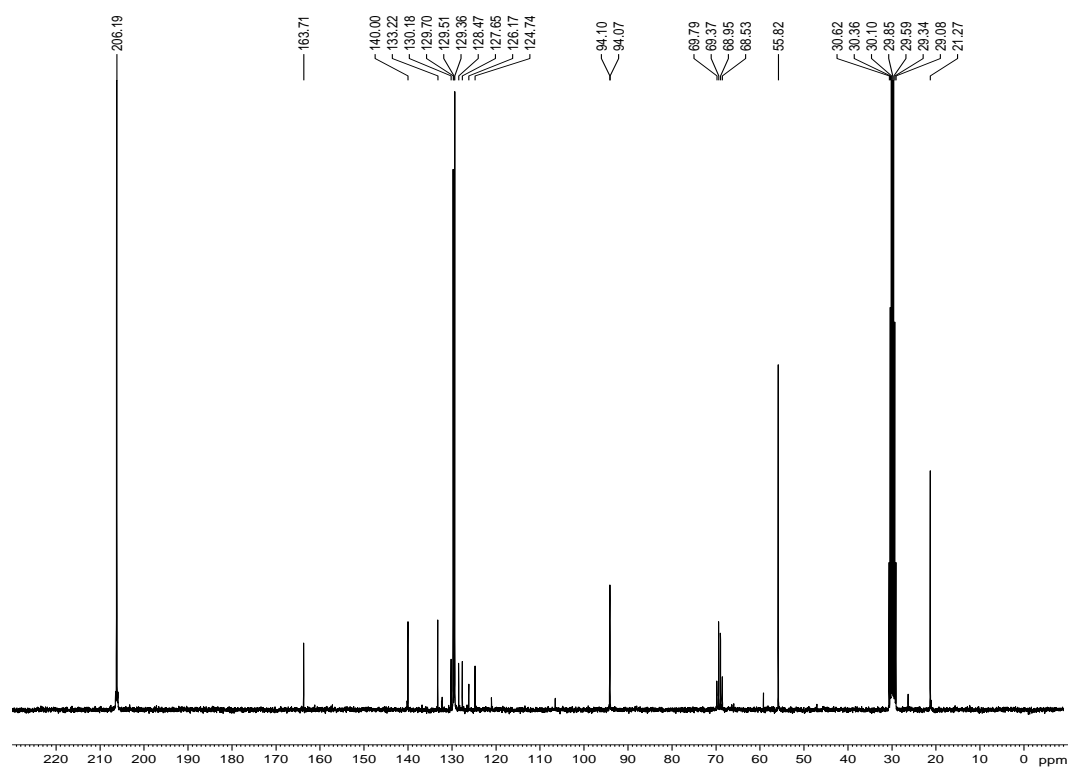
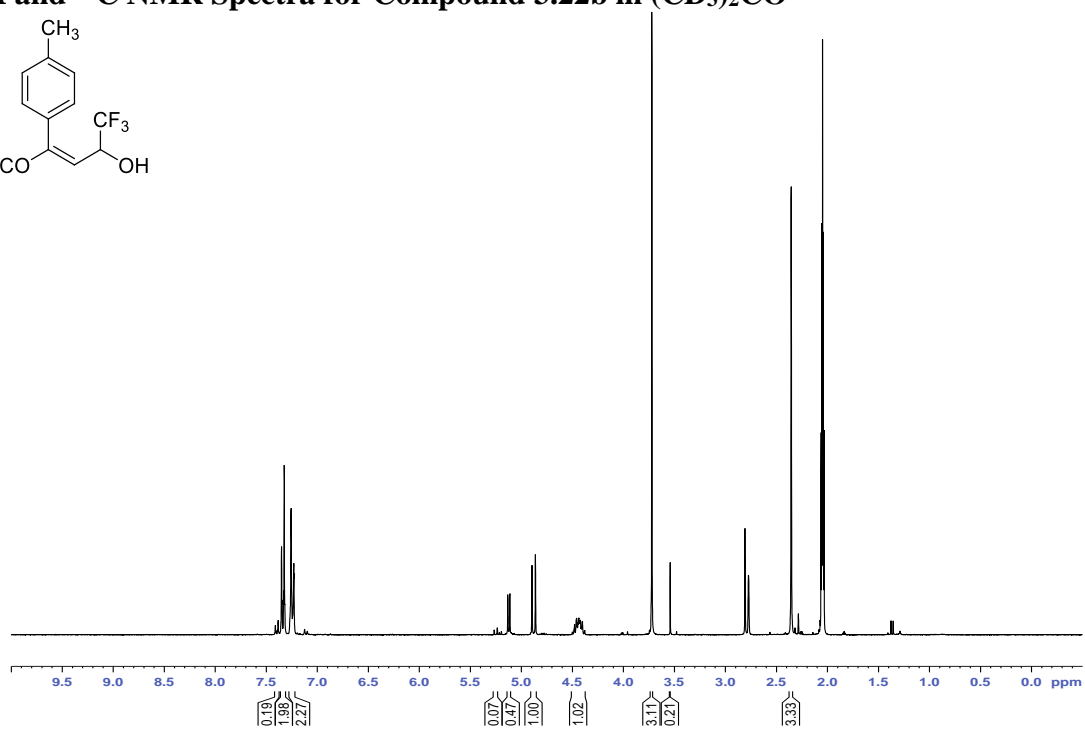
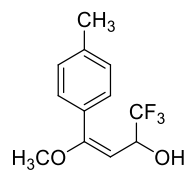
^1H and ^{13}C NMR Spectra for Compound 3.14 in $(\text{CD}_3)_2\text{CO}$ 

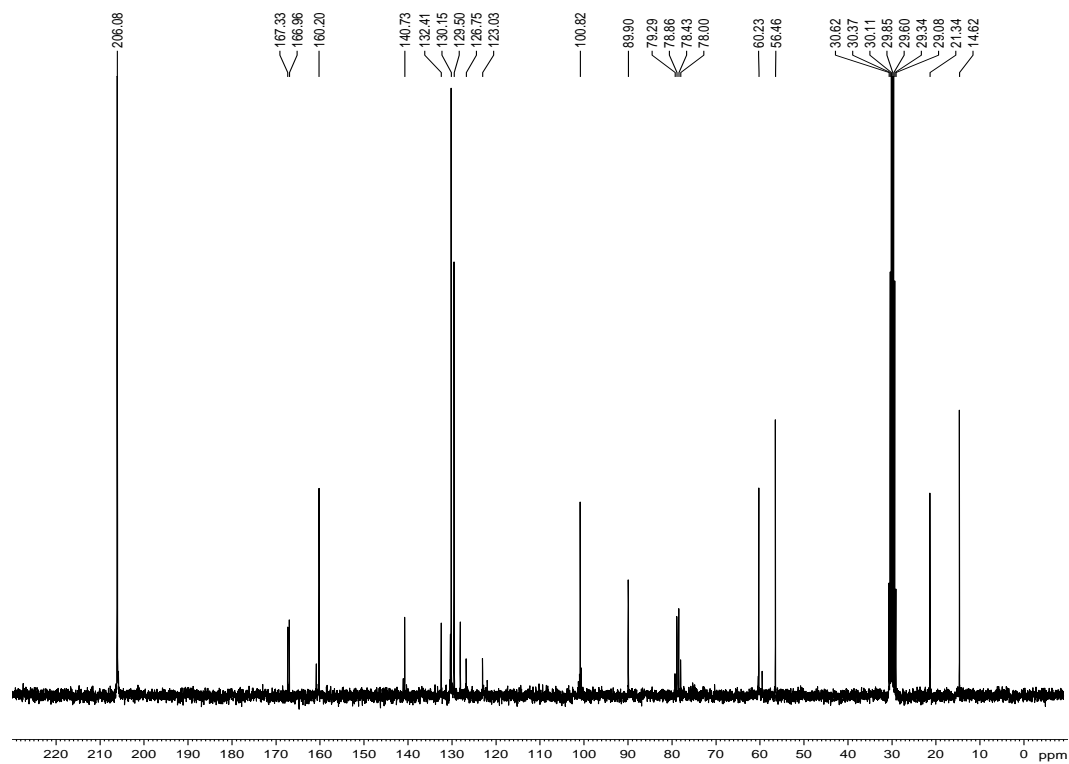
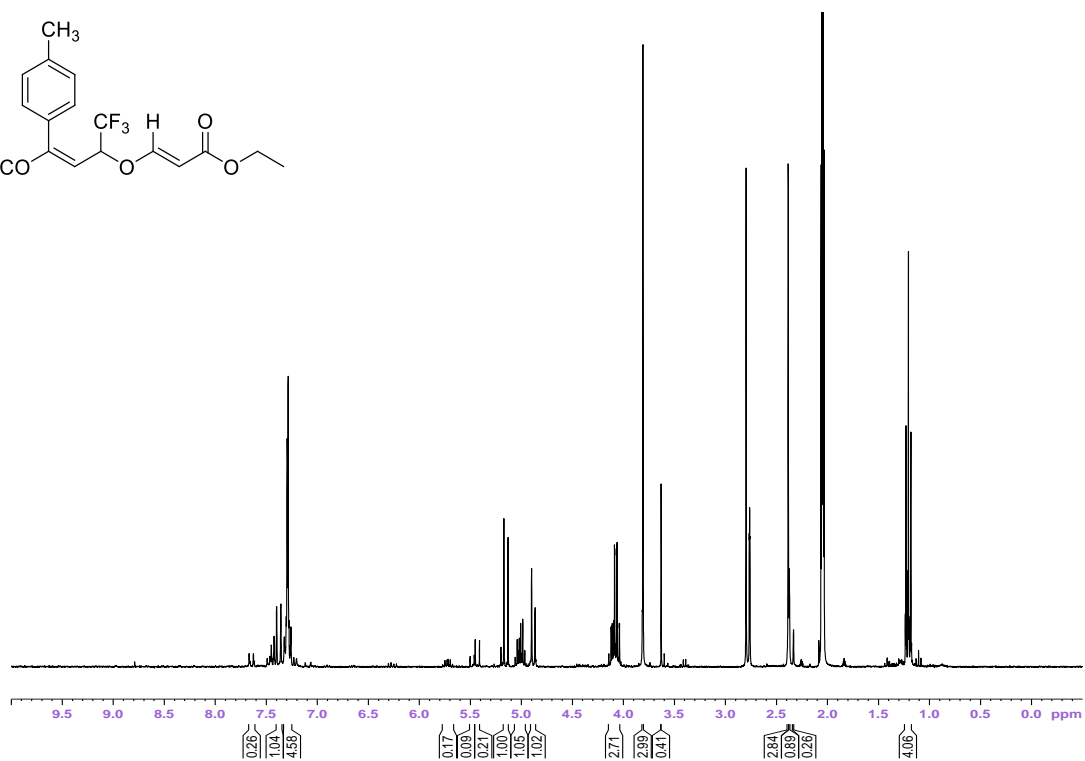
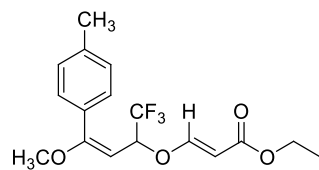
31. ^1H and ^{13}C NMR Spectra for Compound 3.15 in $(\text{CD}_3)_2\text{CO}$ 

^1H and ^{13}C NMR Spectra for Compound 3.16 in $(\text{CD}_3)_2\text{CO}$
(containing 10% Claisen Product)



^1H and ^{13}C NMR Spectra for Compound 3.18 in $(\text{CD}_3)_2\text{CO}$ 

^1H and ^{13}C NMR Spectra for Compound 3.22b in $(\text{CD}_3)_2\text{CO}$ 

^1H and ^{13}C NMR Spectra for Compound 3.27 in $(\text{CD}_3)_2\text{CO}$ (mixture of isomers)

^1H and ^{13}C NMR Spectra for the Claisen Rearrangement Product from 3.16, in C_6D_6 